

UNCLASSIFIED



National Aeronautics and
Space Administration

JSC 22471(U)

Lyndon B. Johnson Space Center
Houston, Texas 77058

HAZARD ANALYSIS FOR THE BREAKUP OF SATELLITES 16937 AND 16938

FEBRUARY 27, 1987

19980819 132

LEMSCO 23613

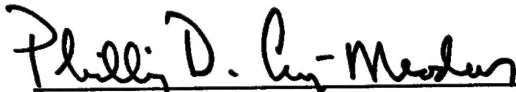
U00820

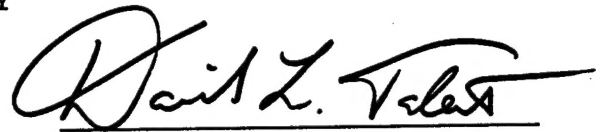
UNCLASSIFIED

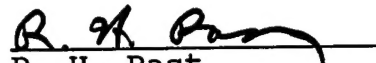
HAZARD ANALYSIS FOR THE BREAKUP
OF SATELLITES 16937 AND 16938

Job Order 68-240

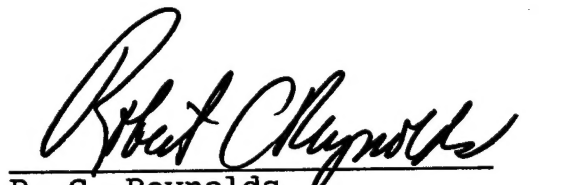
PREPARED BY

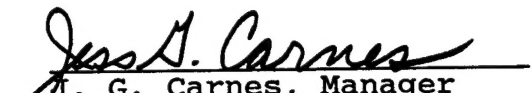

P. D. Anz-Meador
Scientist


D. L. Talent
Principal Scientist


R. H. Rast
Principal Scientist

APPROVED BY


R. C. Reynolds
Orbital Debris Project Leader


J. G. Carnes, Manager
Solar System Exploration
Department

Prepared By

Space Systems Section
Solar System Exploration Department
Lockheed Engineering and Management Services Co., Inc.

Contract NAS 9-15800

For

Space Science Branch

Solar System Exploration Division

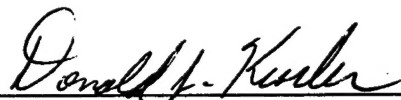
NATIONAL AERONAUTICS AND SPACE ADMINISTRATION
LYNDON B. JOHNSON SPACE CENTER
HOUSTON, TEXAS

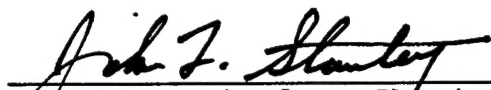
February 27, 1987

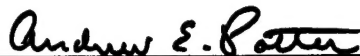
LEMSCO-23613

APPROVAL

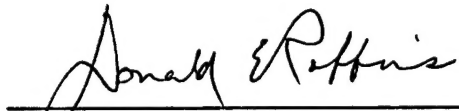

SN3/E. G. Stansbery
Space Sciences Branch



SN3/D. J. Kessler
Space Sciences Branch


SN3/J. F. Stanley, Deputy Chief
Space Sciences Branch


SN3/A. E. Potter, Chief
Space Sciences Branch

CONCURRENCE


SN/D. E. Robbins, Technical Monitor
Solar System Exploration
Division


SN/M. B. Duke, Chief
Solar System Exploration
Division

Space Science Branch

Solar System Exploration Division

NATIONAL AERONAUTICS AND SPACE ADMINISTRATION
LYNDON B. JOHNSON SPACE CENTER
HOUSTON, TEXAS

February 27, 1987

This study was
Performed for the Strategic Defense Initiative Organization
(SDIO) under the SDIO/NASA agreement for the
launch of the Delta 180 Mission

LEMSCO 23613

TABLE OF CONTENTS

Glossary of Acronyms and Abbreviations Executive Summary

1.0 Introduction1-1
1.1 The Delta-180 Mission1-2
1.2 The On-Orbit Safety Group1-3
1.3 Summary of NASA Involvement1-3
1.3.1 Goals.1-3
1.3.1.1 Pre-mission Hazard Prediction1-3
1.3.1.2 Post-mission Model Updates.1-4
1.3.2 Modeling1-4
1.3.2.1 Scenarios1-4
1.3.2.2 Velocity Distributions.1-5
1.3.2.3 Linear Momentum Transfer.1-5
1.3.3 Field Measurements1-7
1.3.3.1 DoD Radars.1-7
1.3.3.2 Meteor Radar.1-7
1.3.3.3 Ground-based Optical/IR1-7
1.3.3.4 Airborne Optical.1-8
2.0 Pre-mission Predictions.2-1
2.1 Flux in the LEO Environment2-14
2.1.1 Short-term Flux Predictions.2-18
2.1.2 Mid-term Flux Predictions.2-20
2.1.3 Long-term Flux Predictions2-20
2.2 Orbit Lifetimes2-22
2.3 Summary of Predictions.2-22

3.0 The Measurement Campaign3-1
3.1 DoD radars.3-3
3.1.1 Eglin.3-3
3.1.2 Kiernan Reentry Site (KREMS) Measurements. .3-10	
3.1.3 Other DoD Radar Measurements3-22
3.1.4 NAVSPASUR.3-27
3.2 Meteor Radar Measurements3-30
3.3 Optical/IR Ground-based Measurements.3-33
3.2.1 AMOS/MOTIF/GEODSS.3-33
3.4 Airbourne Optical Measurements.3-45
3.5 Summary of Optical/IR Data.3-49
4.0 Comparison of Pre- and Post-mission Data4-1
4.1 Piece Count and Size Distribution4-1
4.2 Linear Momentum Transfer.4-13
4.3 Velocity Distributions.4-13
4.4 Size vs. Optical Magnitudes of Debris4-15
4.5 Object Lifetimes.4-22
5.0 Conclusions.5-1

Appendix A. Pre-mission Modeling

Appendix B. Teledyne-Brown Report

Appendix C. Systems Planning Corporation/Remote
Sensing Report

Appendix D. Primary Distribution List for Delta-180 Final Report

LIST OF FIGURES

Figure 1-1	Fragmentation Velocity vs. Size Distribution1-6
Figure 1-2	Facility Identification, Maui, HI1-9
Figure 2-1	On-orbit Breakup Program Structure.2-2
Figure 2-2	Illustration of Overlap Area for Grazing Collision2-4
Figure 2-3	Debris Velocity Distribution.2-7
Figure 2-4	Gabbard Diagram: 100% Kinetic Energy Transfer Scenario2-8
Figure 2-5	Gabbard Diagram: 50% Kinetic Energy Transfer Scenario2-9
Figure 2-6	Number vs. Inclination: Head-on Collision.2-11
Figure 2-7	Number vs. Inclination: Grazing Collision.2-12
Figure 2-8	Number vs. Inclination: Explosion Scenario2-13
Figure 2-9	Flux vs. Altitude: head-on Collision post 1 year.2-15
Figure 2-10	Flux vs. Altitude: Head-on Collision post 1 year Compared to Meteoroid Background.2-16
Figure 2-11	Flux vs. Altitude: Grazing Collision post 1 year Compared to Meteoroid Background.2-17
Figure 2-12	Flux vs. Altitude: Head-on Collision at Breakup2-21
Figure 3-1	World-wide Observation Network -- Radar, Optical, IR.3-4
Figure 3-2	Number vs. Detection time -- DOY 249.3-5
Figure 3-3	Gabbard Diagram -- DOY 249 -- 23° Cloud3-6
Figure 3-4	Gabbard Diagram -- DOY 249 -- 38° Cloud3-7
Figure 3-5	Number vs. Inclination Distribution -- 23° Cloud3-9
Figure 3-6	Number vs. Inclination Distribution -- 39° Cloud3-11
Figure 3-7	Number vs. Period Distribution -- 23° Cloud3-12
Figure 3-8	Number vs. Period Distribution -- 39° Cloud3-13

Figure 3-9 Inclination vs. Period -- 39° Cloud3-14
Figure 3-10 Filtered ALTAIR Data -- DOY 249.3-19
Figure 3-11 ALTAIR Data -- DOY 2493-20
Figure 3-11a Kaena Point dBsm vs. time3-26
Figure 3-12 Debris Decay -- 23° Cloud.3-29
Figure 3-13 SRS Meteor Radar Array Deployment.3-31
Figure 3-14 Ground Tracks Superimposed on SRS Radar Radiation Pattern.3-32
Figure 3-15 Typical Meteor Radar RTI3-34
Figure 3-16 Mass Distribution Observed by Meteor Radar3-36
Figure 3-17 AMOS and MOTIF Instrument Plan Views3-39
Figure 3-18 AATS Optical Diagram3-40
Figure 3-19 Typical Maui "Fence" -- DOY 256.3-43
Figure 3-20 Optical Window Installation on Aeromet Learjet . .	.3-46
Figure 3-21 APS Equipment Layout on Aeromet Learjet.3-47
Figure 3-22 Learjet groundtracks DOY 249 and DOY 2503-50
Figure 3-23 Typical Optical Data Screening Form.3-52
Figure 4-1 Number vs. Diameter Distribution -- DOY 249, 23° Cloud Compared to Theoretical Distribution.4-3
Figure 4-2 Number vs. Diameter Distribution -- DOY 249, 39° Cloud Compared to Theoretical Distribution.4-4
Figure 4-3 Number vs. Diameter Distribution -- DOY 250, 23° Cloud Compared to Theoretical Distribution.4-5
Figure 4-4 Number vs. Diameter Distribution -- DOY 250, 39° Cloud Compared to Theoretical Distribution.4-6
Figure 4-5 Number vs. Diameter Distribution -- DOY 251, 23° Cloud Compared to Theoretical Distribution.4-7
Figure 4-6 Number vs. Diameter Distribution -- DOY 251, 39° Cloud Compared to Theoretical Distribution.4-8
Figure 4-7 Number vs. Diameter Distribution -- DOY 318 NSSC Catalogued Objects Compared to Theoretical Distribution.4-9
Figure 4-8 Number vs. Mass Distribution -- DOY 249 SRS Meteor Radar Data Compared to Theoretical Distribution.4-12

LIST OF TABLES

Table 3-1	Detector/Time Matrix3-2
Table 3-2	Summary of Surviving Objects3-17
Table 3-3	Summary of ALTAIR post-EOM Data.3-21
Table 3-4	Summary of ALTAIR UHF Data3-23
Table 3-5	NORAD's Delta-180 Related Objects.3-24
Table 3-6	Summary of NAVSPASUR Observations.3-28
Table 3-7	Debris Particle Mass Estimates3-35
Table 3-8	AMOS/MOTIF/GEODSS Sensors.3-37
Table 3-9	Learjet Optical Observing Site Optical Systems Specifications3-48
Table 3-10	Time-Ordered Event List -- Delta-180 Optical Observations3-53
Table 3-11	Delta-180 Fragments Identified from Optical Data.3-58
Table 4-1	Observed Cloud Mass.4-11

ACRONYMS AND ABBREVIATIONS

AATS	AMOS Acquisition Television System
ALCOR	ARPA Lincoln C-Band Observables Radar
ALTAIR	ARPA Long-Range Tracking and Instrumentation Radar
AMOS	DARPA Maui Optical Station
APS	Airbourne Pointing System
ARPA	Advanced Research Projects Agency
DARPA	Defense Advanced Research Projects Agency
DoD	Department of Defense
DOY	Day of year
EOM	End of mission
FOV	Field of view
GEODSS	Ground-based Electro-Optical Deep Space Surveillance
HOE	Homing Overlay Experiment
IBM	International Business Machines
IR	Infrared
IRIG-B	Inter-Range Instrumentation Group - B
ISIT	Intensified Silicon Intensifier Target
JSC	Lyndon B. Johnson Space Center
KREMS	Kiernan Reentry Site
KMR	Kwajalein Missile Range
LBD	Laser Beam Director
LEMSCO	Lockheed Engineering and Management Services Company
LEO	Low earth orbit
LLLTV	Low Light Level Television
LOS	Learjet Optical System
LWIR	Long-Wavelength Infrared
MMWR	Millimeter Wave Radar
MOTIF	Maui Optical Tracking and Identification Facility
NASA	National Aeronautics and Space Administration
NAVSPASUR	Naval Space Surveillance
NFOV	Narrow field of view
NORAD	North American Aerospace Defense Command
PAS	Payload Assist System
PARCS	Perimeter Acquisition Radar Characterization System
RCS	Radar cross section

RTI	Range-Time-Intensity
SAO	Smithsonian Astrophysical Observatory
SDI	Strategic Defense Initiative
SDIO	Strategic Defense Initiative Office
SIT	Silicon Intensifier Target
SLBM	Submarine-launched ballistic missile
SRS	SPC Remote Sensing Company
SSC	Space Surveillance Center
SSN	Space Surveillance Network
TBE	Teledyne Brown Engineering
TRADEX	Target Resolution and Discrimination Experiment
UHF	Ultra-High Frequency
USAF	United States Air Force
USASDC	United States Army Strategic Defense Command
USSC	United States Space Command
UT	Universal Time
VDAS	Video Digital Analysis System
VHF	Very High Frequency

EXECUTIVE SUMMARY

Satellites 16937 and 16938 were placed in orbit on September 5, 1986. Prior to the launch of these two satellites, the possibility was foreseen that a collision between them might occur. Consequently, the hazards to other spacecraft that might result from the orbital debris produced by such an event were assessed by modelling.

Because so little is known about the dynamics of collisions in space, three different collision scenarios were postulated and analyzed. These scenarios differed in the amount of momentum interchange between the colliding bodies. Results from the modelling efforts showed that in all cases, the debris resulting from a collision would reenter the atmosphere within a short time; within a few months the debris flux would be below background levels, and would not pose any significant hazard to other spacecraft.

Since so little is known about collisions in space, it was thought prudent to back up the modelling calculations with measurements, so that the predictions of the models could be verified if a collision occurred. For this purpose, DOD satellite tracking radars and telescopes were alerted to collect data, a sensitive airborne optical system was deployed to detect small debris, and a meteor radar was set up to detect debris that might reenter following a possible collision.

In fact, the satellites did collide on September 5 at 17:53 UT. An extensive array of radar and optical data was collected on the debris cloud resulting from the collision. The data were best fit by the model which postulated only a small amount of momentum transfer in the collision. The number of debris objects produced in the collision was in good

agreement with model predictions, but the rate of decay and reentry of the debris was slower by about 25% than predicted. The reflectivity of the debris was low, of the order of 10%, which hampered optical observations.

It was concluded that the models of the collision successfully predicted the potential hazard to other spacecraft, since the differences between the predicted and observed debris number, size distribution, and decay rate were not significant relative to the hazard assessment.

1.0 INTRODUCTION

On September 5, 1986 at 17:53 UT, satellites 16937 and 16938, the second stage and a scientific payload associated with Delta launch 180 (Delta-180) collided. The collision took place 217.5 km above a ground position of 14.82° N and 167.7° E. The impact speed was ~ 3 km/sec, and produced two clouds of debris, one at the 23° inclination of the second stage and one at the 39° inclination of the payload. This was the first known high velocity impact between comparably sized objects in orbit. The test provided an opportunity to observe a collisional breakup under controlled conditions. Since the role of collisions may be critical in determining future states of the man-made debris population, it was felt that as much information as possible should be extracted from the mission data.

The NASA/Johnson Space Center (JSC), as the lead NASA organization for studying orbital debris, was tasked to support range safety for any possible debris generated in the mission and for assisting in confirming that no severe long-term degradation of low Earth orbit (LEO) would result as a consequence of the proposed test. A conservative breakup model was agreed upon, and used to satisfy, to the extent possible, the requirement that any explosion or collision not pose a significant long-term hazard. These predictive calculations were made using the models available at JSC. A breakup model was developed based on laboratory tests, theoretical modeling, and the data extracted from the SOLWIND satellite breakup (P-78 test).

To verify the predictive calculations and to improve the breakup model, a coordinated observing campaign, consisting of optical, infrared (IR), and radar instruments was planned and executed by JSC. Data were taken for several weeks after the breakup.

This report documents all phases of the JSC activity, presenting the predictive modeling (Section 2), the observing campaign and the data acquired (Section 3), and the analysis of that data (Section 4). The conclusions of the project are presented in Section 5. The Space Science Branch of the Johnson Space Center was supported in this project by the on-site support contractor, Lockheed Engineering and Management Services Company (LEMSCO), and by three LEMSCO subcontractors, Teledyne-Brown Engineering (TBE) who analyzed the Eglin radar data and supported the end-of-mission radar data analysis, SPC Remote Sensing Company (SRS) who operated a modified meteor radar to detect reentry ionization trails, and the Aeromet Corporation who operated an aircraft used to observe the optical characteristics of the debris. Data from the TBE and SRS reports have been excerpted and included in the body of this report; the complete versions of their reports have been attached as Appendices B and C.

1.1 The Delta-180 Mission

Delta-180, a Delta 3920-class vehicle given the international designator 1986-069, lifted off from Cape Canaveral's Launch Pad 17B at 11:08 a.m. EST on September 5, 1986. Following a nominal flight, the Delta's second stage was placed in a near-circular orbit at an altitude of 220 km and an inclination of 28.5 degrees. Forty-five minutes later the 3rd stage separated from the 2nd stage while over the Indian Ocean. After a series of maneuvers, the two stages were in significantly different orbits: Delta 2nd stage, 210km x 550km, 23° inclination; Delta 3rd stage, 210km x 590km, 40° inclination. With these orbits, the two stages would cross one another with a relative velocity approaching 3 km/sec.

There was the possibility that the two stages would collide, generating a significant amount of orbiting debris. Since this debris could pose a hazard to other spacecraft, there were safety issues to address.

1.2 The On-Orbit Safety Group

To address any safety issues, the SDIO formed an on-orbit Safety Group. Membership in this group included the Johnson Space Center, The Aerospace Corporation, Johns Hopkins' Applied Physics Laboratory, the Eastern Test Range, Space Command, as well as operational and engineering elements associated with the Delta 180 mission. Members of the On-Orbit Safety Group were to predict and evaluate the potential hazard resulting from a possible Delta-180 breakup. The contributions JSC made were in the areas of computer modeling and data acquisition and analysis of any resulting debris.

1.3. JSC Involvement Summary

1.3.1 Goals

1.3.1.1 Pre-mission Hazard Prediction

Beginning in Spring, 1986, personnel of JSC's Space Science Branch began modeling orbital debris from various possible mission anomalies. These predictions were in the form of spatial densities and the cumulative flux of debris at altitudes up to 2500 km. Initial conditions were extracted from unclassified reports, while boundary conditions, such as debris velocity distribution, number vs. size distribution, and mass as a function of size, were established using published data from laboratory hypervelocity impact experiments, destructive testing of spacecraft components, and past on-orbit breakup events. Data produced by the modeling was presented at a series of meetings held in late Spring and early Summer.

1.3.1.2 Post-mission Model Update

Following the end-of-mission, the JSC tasks were to reduce selected data from various field sensors, analyze the data with respect to the pre-mission predictions, publish the findings, and update the on-orbit breakup event model. The latter goal included determining the number vs. size distribution of the breakup objects, and the correlation of object size (estimated from radar cross section) with the observed visual magnitude and albedo of the debris. Also to be examined were the velocity distribution of the debris resulting from the collision, an estimation of the debris lifetimes and, the question of linear momentum transfer. These quantities are of interest because of the unique nature of the Delta-180 mission.

Also, since the relative velocity of the collision was approximately 3 km/s, the extent of hypervelocity phenomenology was unknown. As regards the debris ejecta, parameters of interest were number, mass, and size distributions, velocity distributions, and other hypervelocity impact effects, such as albedo reduction.

1.3.2 Modeling

1.3.2.1 Scenarios

Three different impact scenarios were modeled: a head-on (or direct hit) collision, a grazing impact of the two satellites, and the proximity explosion of the satellites. In simulating a grazing impact, 10% of one object was used as a projectile on the second object; the roles were reversed and the debris produced in each event summed to give the total amount of debris generated. It was found that using this percentage of a satellite as a projectile, both satellites would be completely destroyed. Only in the case of a grazing

impact involving 2% or less of each satellite would a portion of the more massive satellite remain intact.

1.3.2.2 Velocity Distributions

Pre-mission generated data was most sensitive to the velocity distribution as a function of size of the debris. In early modeling efforts, several distributions were used. The curve derived from a hydro-code analysis of the 1984 Homing Overlay Experiment was considered but then discarded because it didn't accurately reflect the observed data from the P-78 test. Other curves were laboratory generated; these were functions of both size and kinetic energy transferred to target. The curve derived from observations of P-78 was also evaluated.

Characteristic of all velocity distribution functions was the small velocity perturbation given large objects and a velocity perturbation on the order of the impact velocity for small particles. This is depicted in Figure 1-1.

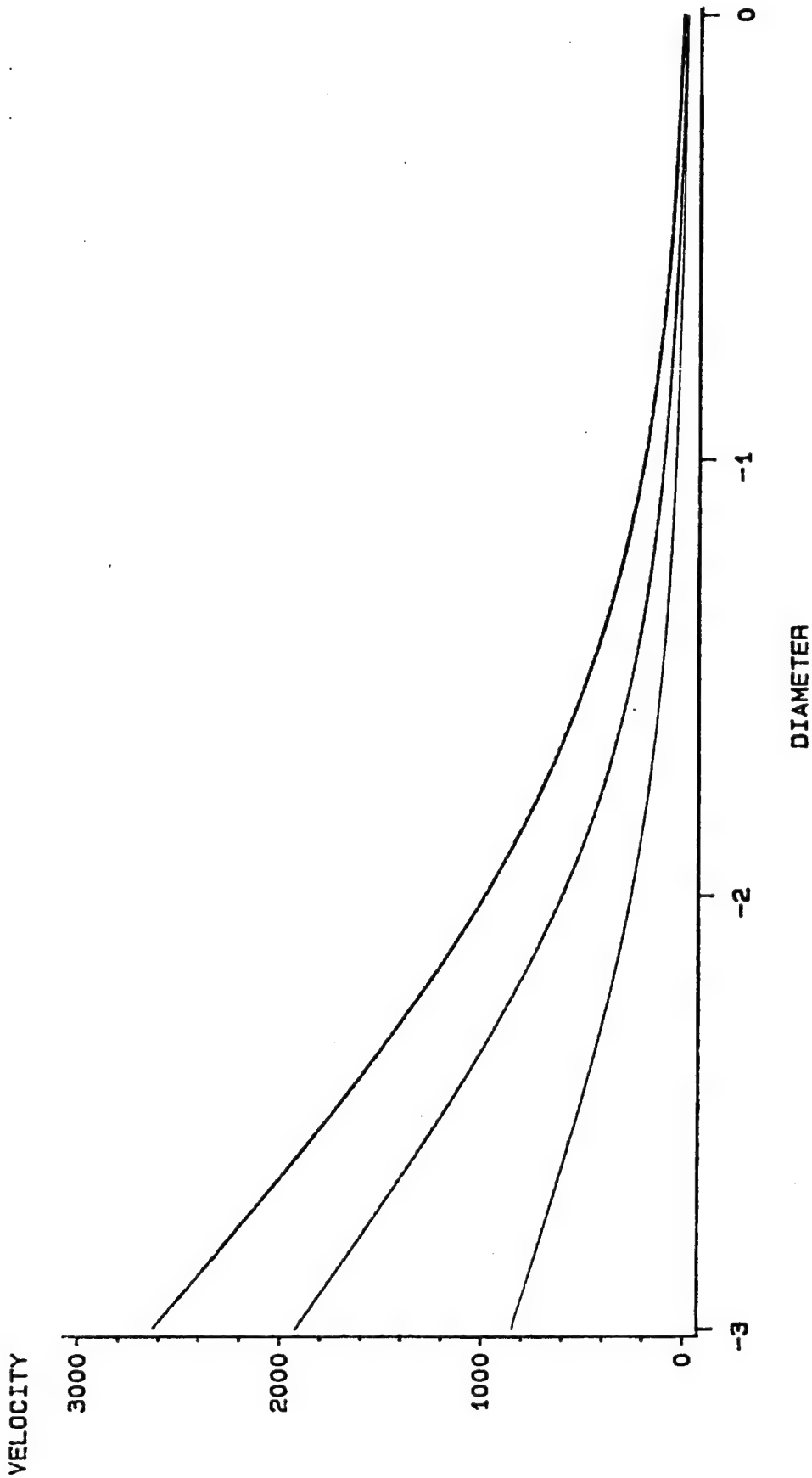
1.3.2.3 Linear Momentum Transfer

In previous work, the JSC breakup model had modeled a 100% transfer of linear momentum to the small debris, and no momentum transfer to the large fragments; this effect characterized the breakup of the SOLWIND satellite in the P-78 experiment. This resulted in the small objects being injected into one set of characteristic orbits, and the larger pieces remaining in the target's original orbit.

In the case of Delta-180, it was thought that three distinct debris clouds might be formed: one centered about the target's orbit, one centered about the projectile's orbit, and a third (the momentum exchange orbit) in a lower-energy orbit near an inclination equal to the mass-weighted mean of the

Velocity distribution (2.7 km/s impact)

velocity vs log10(diameter)
 Top to bottom: 100%, 50%, and 10% KE transfer



Units of velocity are [m/s]
 Units of diameter are [m]

target's and projectile's inclinations. For the Delta-180 predictions, the breakup model was modified in some scenarios to reflect the case in which not all the momentum was transferred to the small objects. This would allow some of the smaller particles to accompany the larger fragments in the target/projectile orbits.

1.3.3 Field Measurements

1.3.3.1 Department of Defense (DoD) Radars

Radars operationally controlled by or under contract with the North American Aerospace Defense Command (NORAD), the United States Space Command (USSPACECOM), and the United States Army Strategic Defense Command (USASDC) contributed both metric and signature observations of the Delta-180 objects. The metric observations (i.e., kinematic data only) defined the positions and velocities of the objects before, during, and after the breakup. Signature observations characterized the size, shape, and orientation of the fragments generated.

1.3.3.2 Meteor Radar

A very high frequency (VHF) backscatter radar system was erected in Hawaii to detect the ionization trails from Delta-180 objects entering the atmosphere after EOM. Both monostatic and interferometer radars were deployed to allow vector measurement of position and velocity. Operating at two frequencies allowed wavelength dependent studies of the return echo signatures.

1.3.3.3 Ground-based Optical/IR Instruments

The Defense Advanced Research Projects Agency (DARPA) operates the Maui Optical Station (AMOS) on the island of

Maui, Hawaii. The AMOS complex includes the Maui Optical Tracking and Identification Facility (MOTIF) which is operated as the primary sensor of the USAF SPACETRACK network. Also located at the Maui site is a complete Ground-based Electro-Optical Deep Space Surveillance (GEODSS) facility consisting of three primary instruments. Although GEODSS is operated by NORAD, it shares physical facilities with AMOS/MOTIF (Figure 1-2). All of these facilities were used during the Delta-180 measurement campaign.

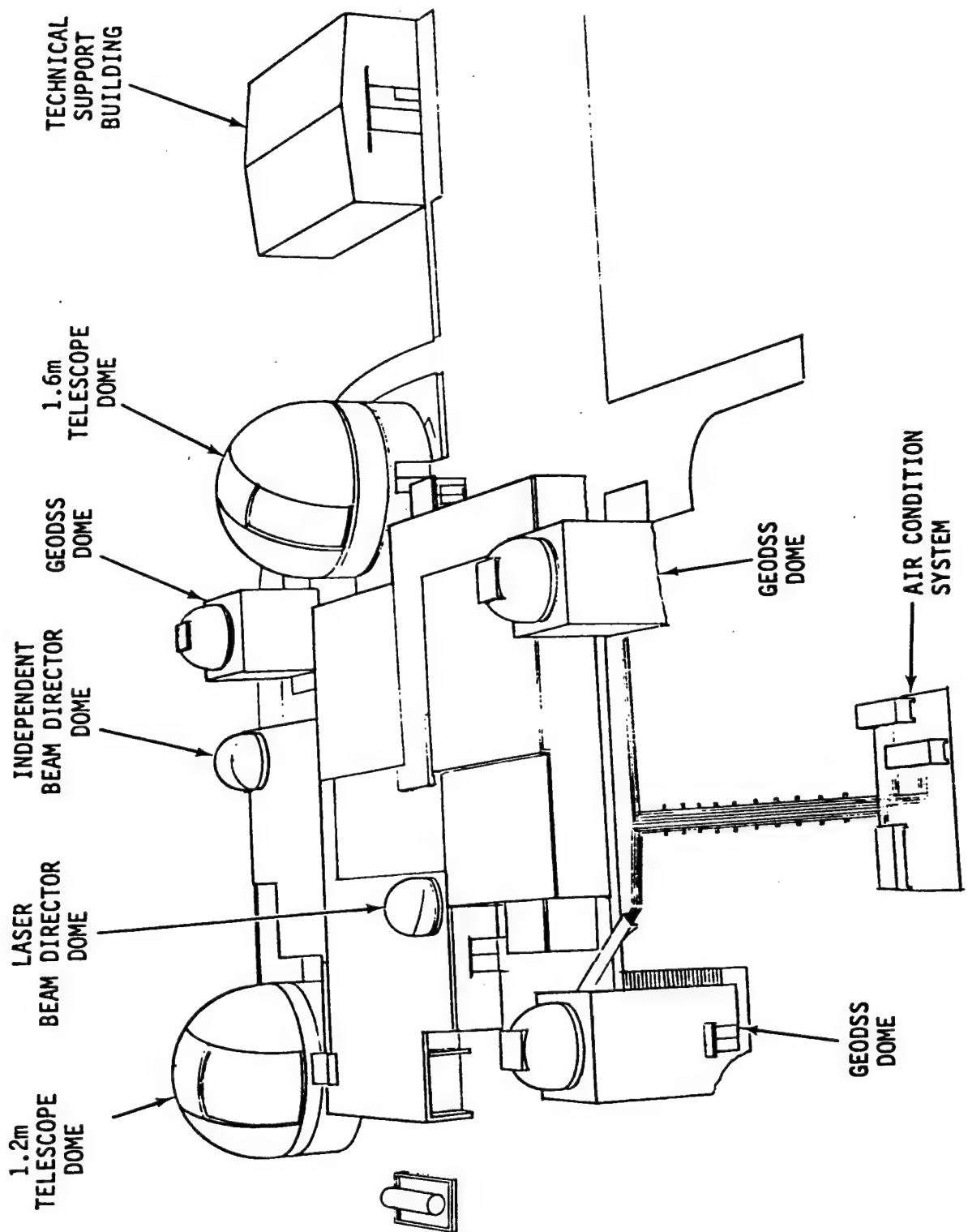
The telescopes of AMOS/MOTIF employed during the Delta-180 effort were a 1.6m telescope, twin 1.2m telescopes and two acquisition telescopes systems -- one on each of the larger instruments. In addition, the three GEODSS instruments, two with apertures of 1.0m and one of 0.4m were also used.

The measurement effort extended from September 6, 1986 (DOY 249) through September 15, 1986 (DOY 258), and occupied about 1 hour each night. These ground-based optical efforts were conducted coincidentally with radar operations, in particular with the radar at Kaena Point.

1.3.3.4 Airborne Optical Instruments

On September 6, 1986 (DOY 249), and September 7, 1986 (DOY 250), a specially equipped Learjet was flown from the Kwajalein Atoll for the purposes of obtaining optical image data on the Delta-180 fragments. A Lenzar Low Light Level TV was positioned at a right side forward station, while a Wide Field of View (WFOV) and Narrow Field of View (NFOV) system shared a right aft platform. All three of these were SIT type video detectors.

Figure 1-2 Facility identification, Maui, HI.



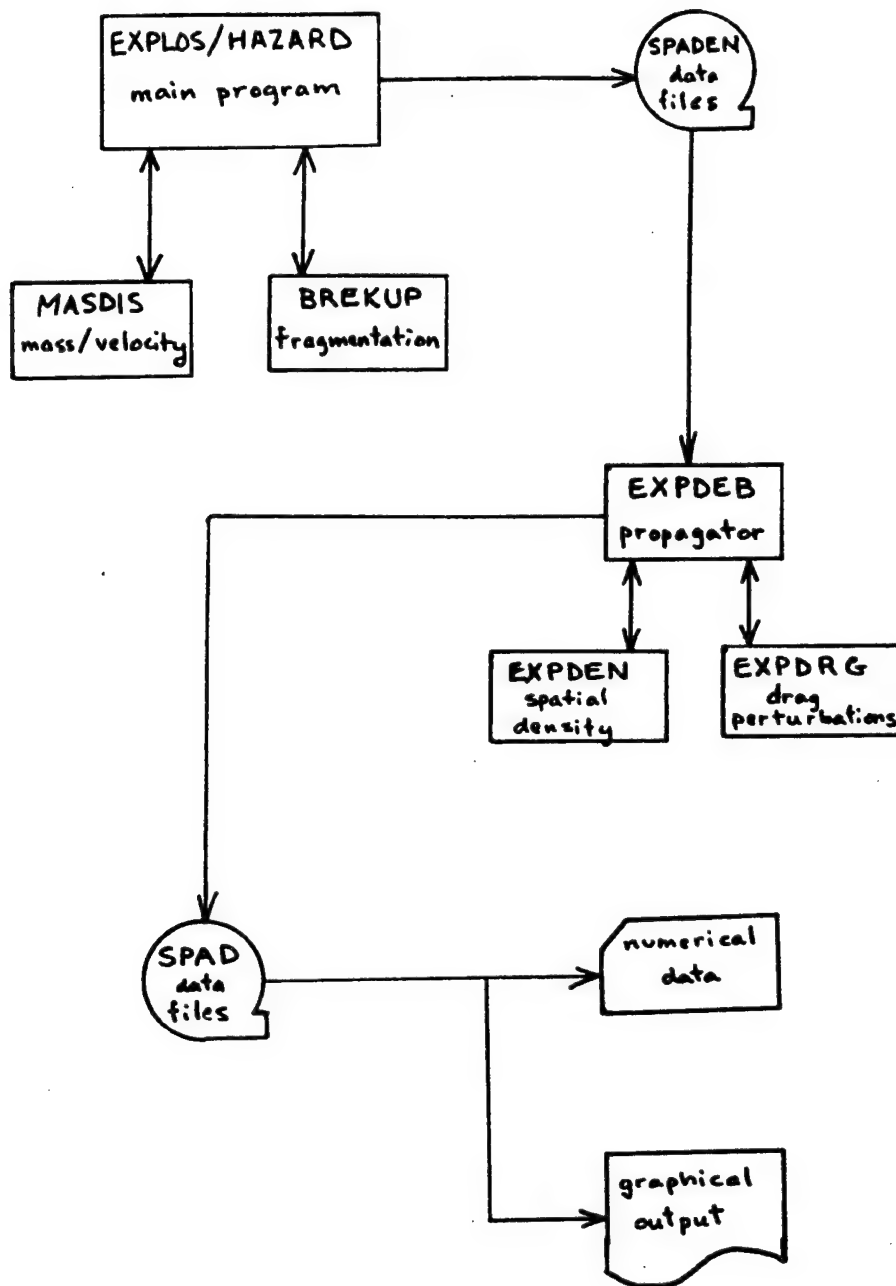
2.0 PRE-MISSION PREDICTIONS

Predictive modeling of the debris generated by the Delta-180 test event was tasked to JSC by the Delta-180 program office. Given inputs of satellite (target) and projectile orbital elements and mass, the program EXPLOS/HAZARD was used to produce output data in the form of tables of resulting debris, reentering debris, Gabbard plots, and state vectors/orbital elements for several collision and explosion scenarios. These data were used to predict the environmental hazard arising from the Delta-180 mission, and to provide coordinates for planning radar and optical observations for the measurement campaign. Orbital lifetimes were also predicted.

A block diagram of the program is shown in Figure 2-1. Program module MASDIS calculates object mass as a function of size (diameter) and the delta-velocity distribution as a function of size. These power-law distributions have been developed from laboratory simulations and past on-orbit breakup events. Two extrapolations must be made with respect to hypervelocity impact data obtained in the laboratory: first, the data from the laboratory case of low mass projectiles/high mass targets must be scaled to the case of projectiles and targets of similar mass -- this scaling is not well-understood and there is a resulting uncertainty in the models; second, a flat plate or "semi-infinite" target composed of aluminum or basalt under 1g in a laboratory, may not react as would a typical spacecraft structure of similar dimensions. In particular, at distances far removed from the impact site, the breakup characteristics of a large laboratory test article may not mimic well the breakup of its on-orbit counterpart. Hence the breakup characteristics for the larger fragments must come primarily from on-orbit breakups.

The software module BREKUP determines whether the event was catastrophic (that is, whether the target fragments completely)

Figure 2-1 On-orbit breakup program structure.



On-Orbit Breakup Program Structure

or not, and computes the total mass (or number of objects) produced per size bin. An object (target) is subject to catastrophic breakup if the ejecta mass, defined as the projectile mass multiplied $(V_1/V_{\text{norm}})^2$ ($V_{\text{norm}}=1$ km/sec), is greater than 10% of the object mass. For the Delta-180 experiment, the mass ratio of the second stage to the SDI/PAS payload was 0.6, so a head-on collision would have been catastrophic to both structures. If the impact was not head-on, only the overlap mass was considered as participating in the collision as shown in Figure 2-2, and in that case the collision would still be catastrophic if more than about 2% of the mass overlapped.

Superimposed on the number or mass per size bin for the Delta-180 experiment were a number of objects from the three scientific modules. Some of these objects could have remained intact after the event, resulting in a divergence from the power-law distributions of the explosion model. It was therefore expected that the observed fragment distribution might deviate from the predicted distribution by having more large fragments. In fact, the number of objects was observed to be much smaller per size bin than that predicted by the collisional breakup model.

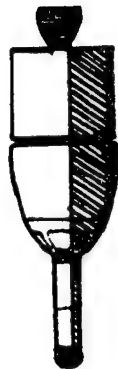
Debris arising from a collision process is categorized in the model as either fragments or ejecta. Ejecta are those particles to which momentum is transferred and come from material near the impact site. Fragments will not be involved in the exchange of momentum, thus retaining the original orbital characteristics of the structure, and come from material farther away from the impact site. For a catastrophic event, in which both target and projectile are completely disrupted, both ejecta and fragments are produced. The number vs. mass distribution is given by:

$$N = 1.7069 \times 10^{-4} m_T e^{-0.02056 m^{0.5}}, m > 1936\text{gm}$$

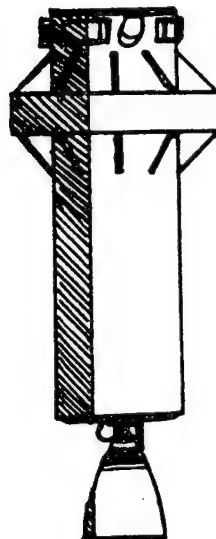
$$N = 8.6921 \times 10^{-4} m_T e^{-0.05756 m^{0.5}}, m < 1936\text{gm}$$

Figure 2-2 Illustration of overlap area for grazing collision.

Illustration of Overlap Area for Grazing Collision



Projectile material



Target material



where N is the cumulative number of pieces produced with a mass greater than m [gm], and m_T [gm] is the mass of the target. These equations, from Time Evolution of the Near-Earth Man-Made Orbital Debris Environment by S.Y. Su and D.J. Kessler, may be expressed in terms of debris object diameter by making the substitution:

$$m = 4.72 \times 10^4 d^{2.26} ,$$

where m [gm] is object mass and d [m] is the object's diameter. This equation is based on measurements of payloads, rocket motors, and debris. In the case of non-catastrophic events, only ejecta are produced. Ejecta follow a power-law distribution given by:

$$N = 0.4478 \left(\frac{m}{m_p v^2} \right)^{-0.7496} ,$$

in which N is again the cumulative number of objects with mass greater than m [gm]. m_p is the projectile mass, in grams, and v is the projectile velocity, in km/sec. In some cases for the Delta-180 analysis, ejecta type material was distributed with little momentum transfer.

The driver program, EXPLOS, and later HAZARD, models a collision by distributing the objects evenly among 525 equal-area tiles on the surface of a sphere centered on the target. Thus, the objects are distributed isotropically by vectorally adding the delta-velocity given by the mass vs velocity distribution to the target's initial velocity vector. State vectors, and the classical orbital elements may then be calculated for each tile's contribution to the total number of objects. Mass is conserved.

Three different breakup scenarios were modeled to support the Delta-180 predictions: a direct hit (100% mass overlap), a grazing impact (10% mass overlap), and an explosion. Given spacecraft masses of 873kg for the Delta

stage and 1455kg for the SDI/PAS payload, no scenario examined would have left a substantial part of either structure intact. Some software modifications were developed to model the explosion case. The program output data, debris flux as a function of altitude and debris size, were sensitive to the velocity distribution used and the amount of linear momentum transferred.

The models were run utilizing several velocity distributions, as shown in Figure 2-3. The upper-most curve represents the results of a hydro-code analysis of the Homing Overlay Experiment (HOE) exoatmospheric interception tests carried out in 1984. The remaining curves represent the velocity distribution for different sizes and amount of kinetic energy transferred to the target. The Delta-180 experiment provided an opportunity to assess the kinetic energy transfer manifested in the delta-velocity delivered to the resultant pieces of debris. The effect of kinetic energy transfer may be seen by comparing Figure 2-4 and Figure 2-5; both are Gabbard plots of the objects greater than 10cm in diameter and were produced by HAZARD. The former utilizes the high velocity distribution (100% kinetic energy transfer) while the latter was run using the nominal distribution (50% kinetic energy transfer). The high energy curve deposits the larger, radar-observable debris over a substantially larger volume of space.

Linear momentum transfer between the Delta stage and the SDI satellite displays itself as a size vs. orbital plane distribution: those pieces undergoing momentum transfer will be injected into center-of-mass orbits, creating a debris cloud whose inclination lies at the mass-weighted mean of the original satellites inclinations.

The hypervelocity impact scenarios assuming 100% momentum transfer to the ejecta predicted that there would be

Fragment Velocity vs Diameter

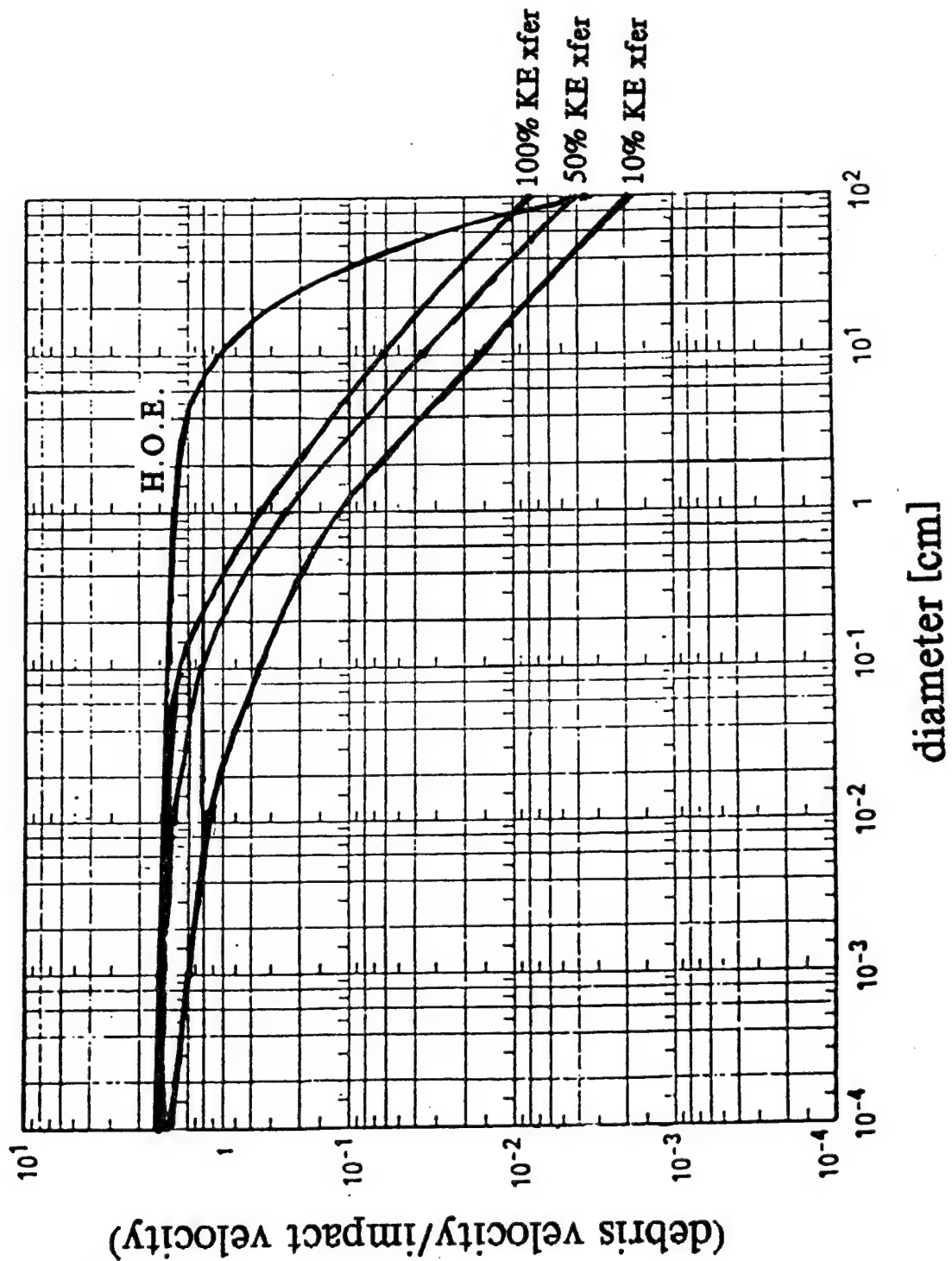
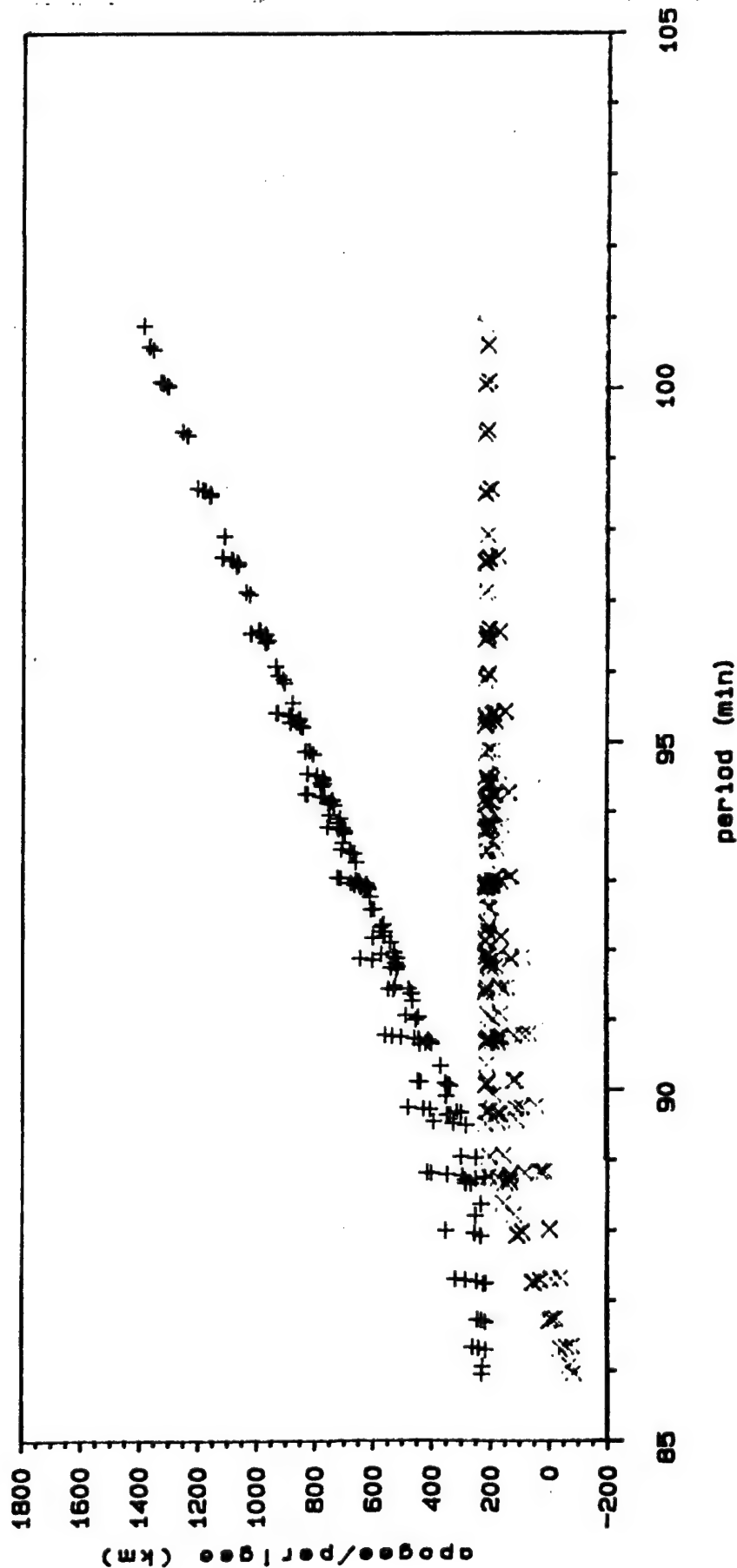


Figure 2-3 Debris velocity distributions.

Hazard Analysis Project

head-on (100%) scenario: diam. > 10cm

Figure 2-4 Gabbard diagram: 100% KE transfer scenario.



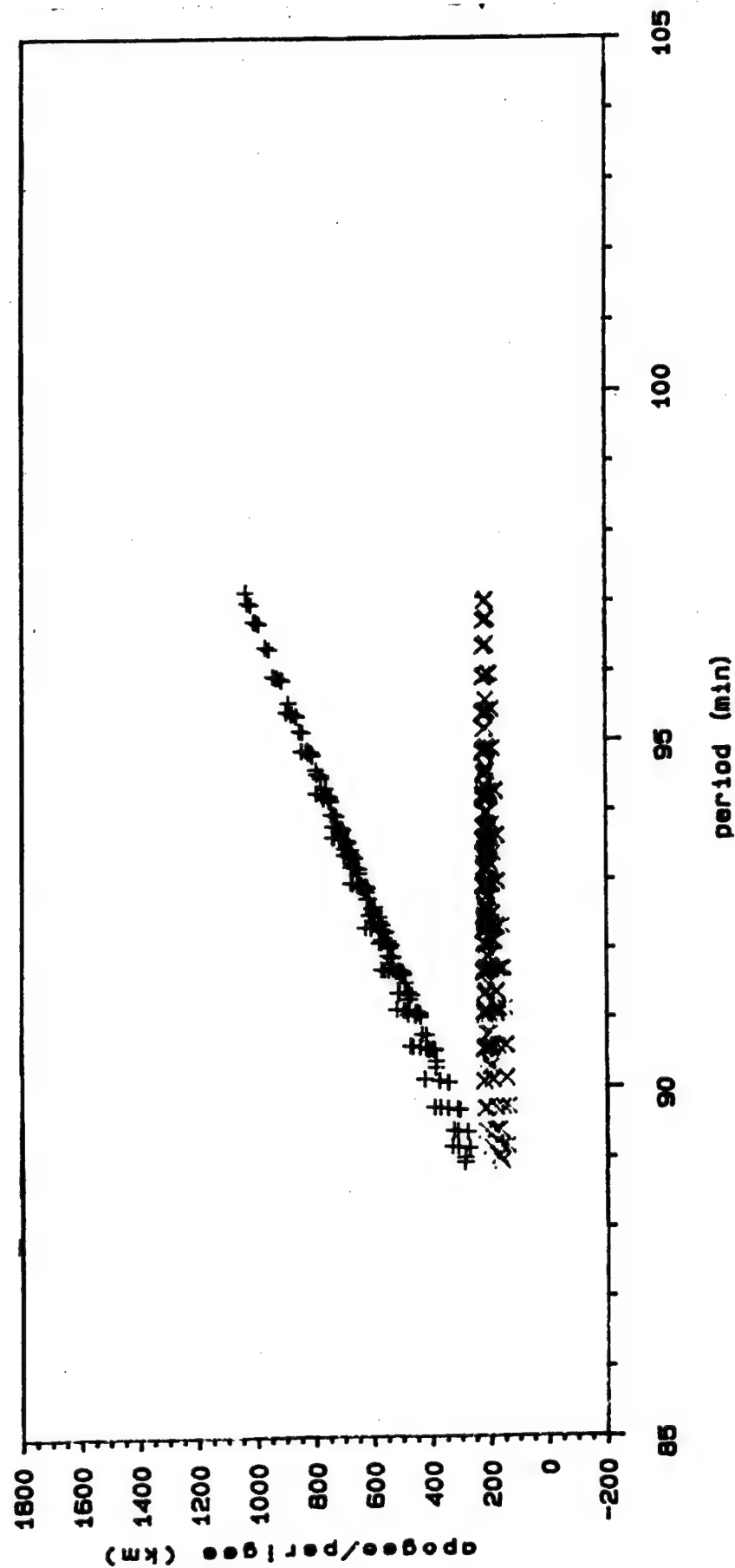
delta second stage

high velocity distribution

Hazard Analysis Project

head-on (100%) scenario: diam. > 10cm

Figure 2-5 Gabbard diagram: 50% KE transfer scenario.



delta second stage

nominal velocity distribution

three debris clouds: one composed of fragments at an inclination of 22.9° (Delta fragments), one composed of fragments at inclinations around 40.1° (satellite fragments), and the center-of-mass cloud composed entirely of ejecta around an inclination of 33.7° . The values used for the inclinations above are based on pre-mission planning. In accordance with observations, the Delta cloud shall be referred to as the 23° cloud, and the PAS/satellite cloud as the 39° cloud. An alternative scenario was defined which transferred only 50% of the momentum to the ejecta, so that the 23° and 39° clouds included ejecta as well as fragments.

The explosion case differed in that proximity explosions of both the Delta stage and the SDI/PAS spacecraft would transfer no momentum; hence, there would exist only two debris clouds, each conforming to the parent body's orbital characteristics. This scenario was interpreted as having the spacecraft fragment before collision and having the debris clouds pass through one another with little momentum transfer. Initial debris orbital characteristics for each case are given in Figures 2-6 through 2-8.

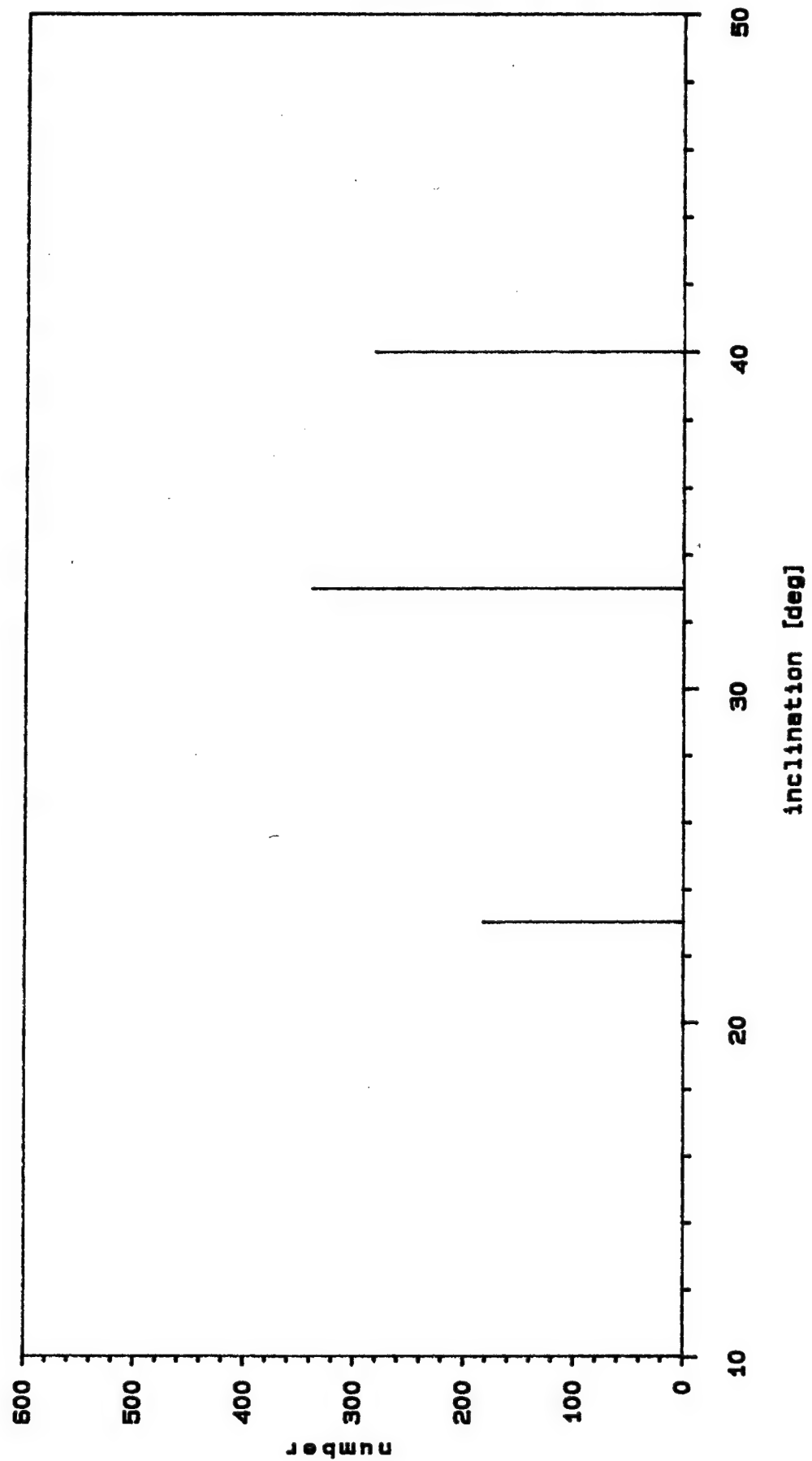
Perturbations on, and orbital decay of, the resulting objects were modeled using analytical King-Hele expressions for the decay of a satellite in an atmosphere. A modified version of the Jacchia 71 model atmosphere was used as the reference atmosphere. The exospheric temperature, a function of solar flux and geomagnetic index, was assumed to be constant over the lifetimes of the objects under investigation. All diurnal, seasonal, latitudinal, and semi-annual variations were neglected. In general, this program provides values within ~25% of the actual decay time.

For reporting purposes, the following nomenclature was adopted: short term effects refer to those effects occurring immediately post-EOM to several hours post-EOM; mid-

Hazard Analysis Project

head-on (100%) collision scenario: diam. > 10cm

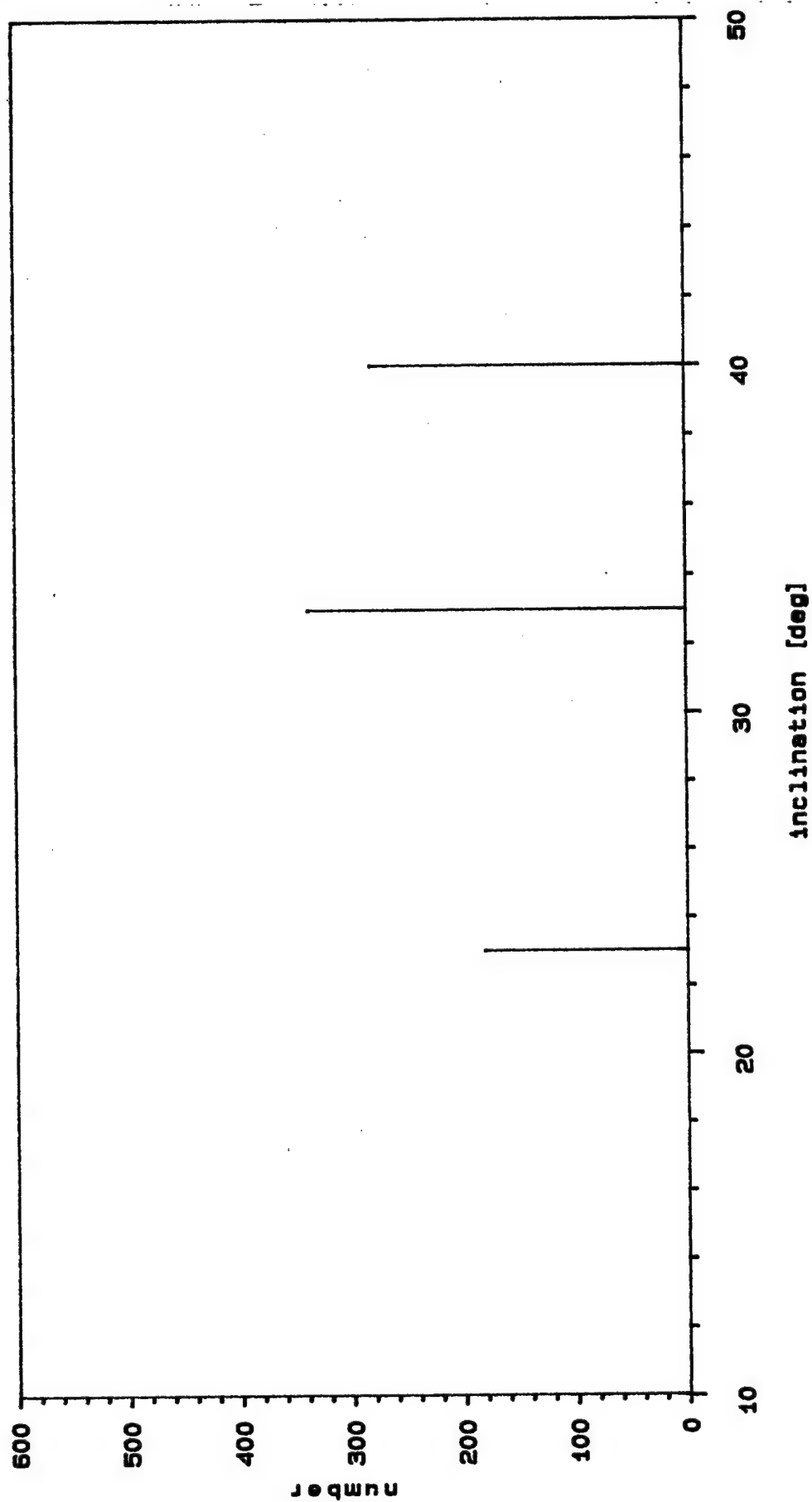
Figure 2-6 Number vs. inclination: head-on collision.



Hazard Analysis Project

grazing (10%) collision scenario: diam. > 10cm

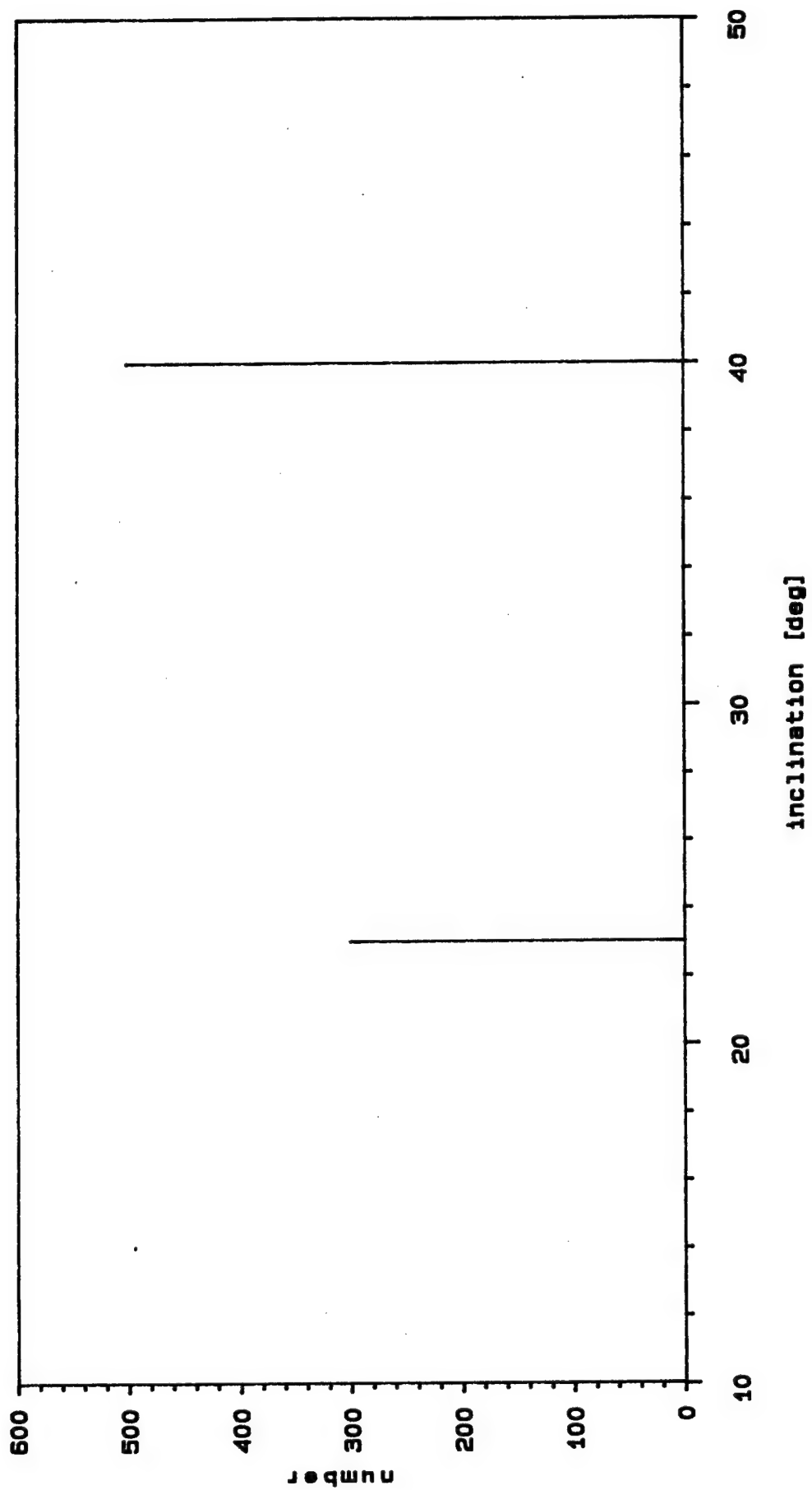
Figure 2-7 Number vs. inclination: grazing collision.



Hazard Analysis Project

explosion scenario; diam. > 10cm

Figure 2-8 Number vs. inclination: explosion scenario.



term refers to several hours post-EOM to a week post-EOM, and long term refers to the ensuing debris cloud evolution. In most cases, analysis stopped at an elapsed time of 1 year; however, in some cases, the debris cloud evolution was followed for up to 5 years. Throughout the analysis, the natural meteoroid background was used as a point of reference. The natural background has never necessitated significant constraints on a space program.

2.1 Flux in the LEO Environment

From the number of objects in orbit at any time, one may calculate spatial densities and the cumulative object flux as a function of altitude and size. Figure 2-9 shows a typical plot of this cumulative flux, in this case the flux for a direct hit collision, with the debris receiving 50% of the kinetic energy, after an elapsed time of 1 year. Figure 2-10 shows the same case, but with the natural meteoroid background included. In the Figure 2-9, the cumulative flux for debris greater than 4cm in diameter is less than 10^{-9} impacts/m²/yr after 1 year, while in the Figure 2-10, only the 1cm flux exceeds the natural background after 1 year. By contrast, Figure 2-11 displays the effect of the kinetic energy transfer to the debris. In this case, a glancing blow is modeled; the high energy velocity distribution curve is used, however, with the result that the cumulative flux for debris greater than 4cm in diameter exceeds the natural environment by over a factor of 2 around breakup altitude, and by a lesser extent out to an altitude of 1000km. Appendix A contains a catalog of debris flux evolution plots for various impact and explosion scenarios.

Caution must be applied in viewing plots such as these, for the spatial densities and attendant cumulative flux calculated and presented here are actually averaged over the entire volume of an altitude shell 50km thick. While this

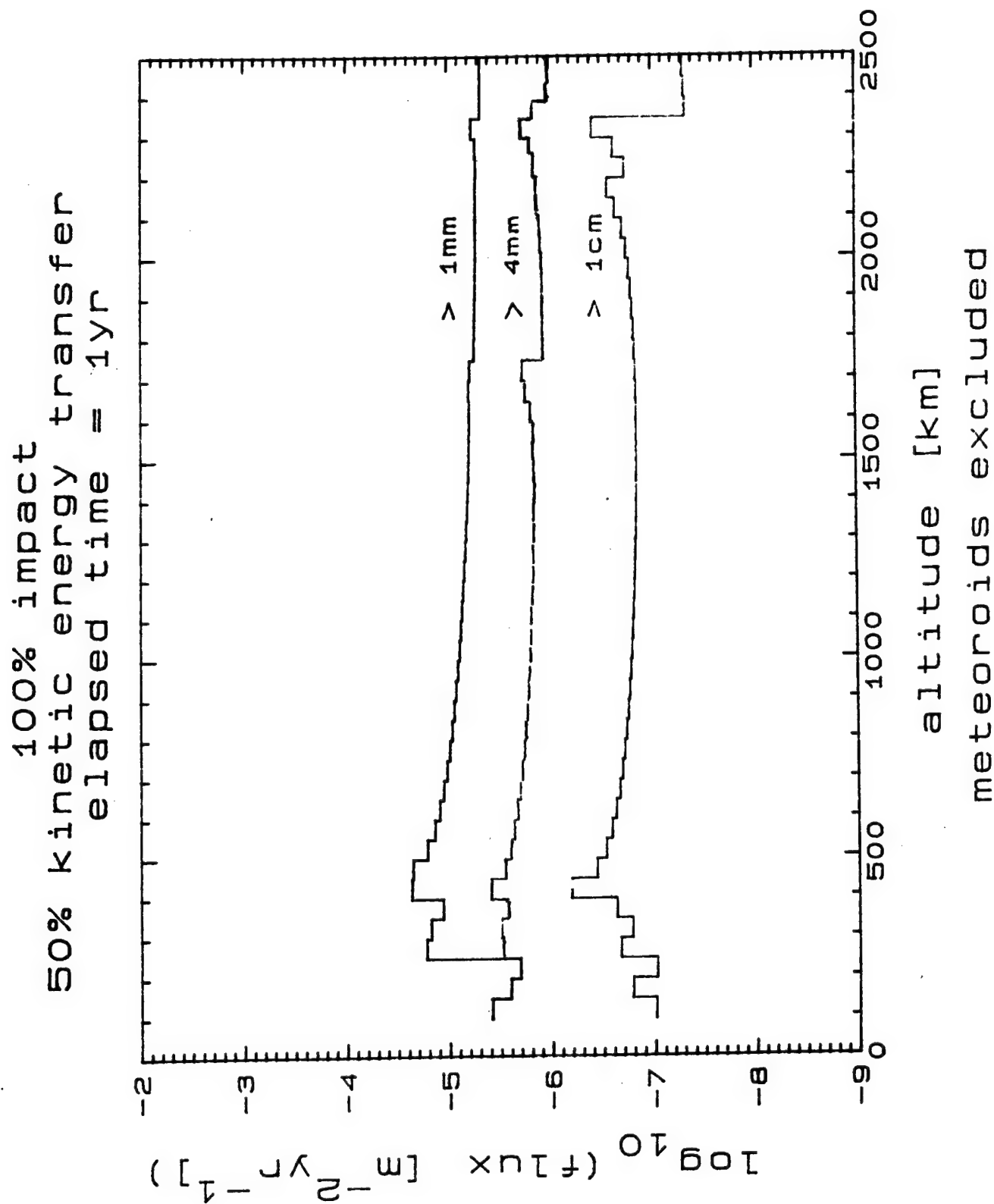


Figure 2-9 Flux vs. altitude: head-on collision post 1 year.

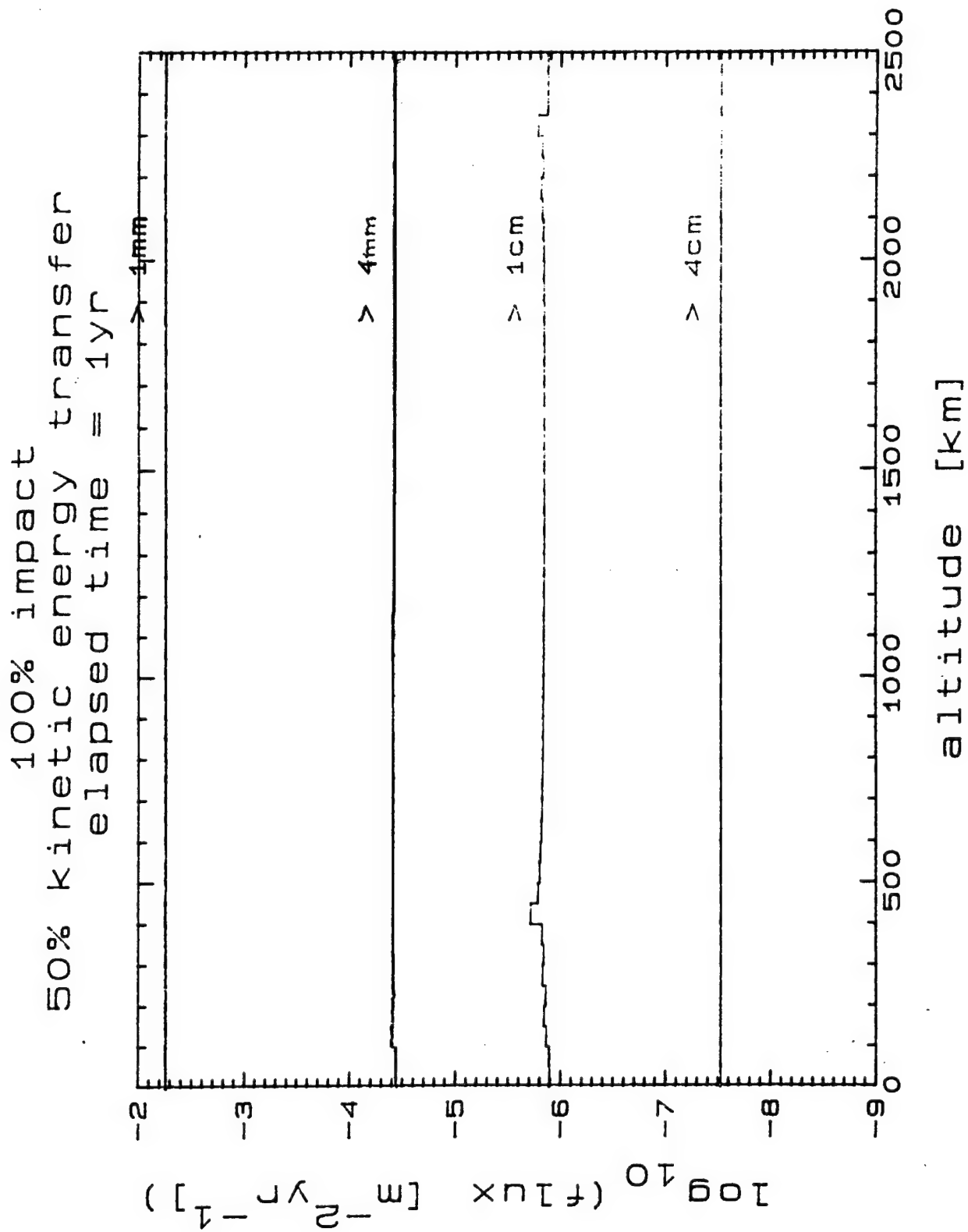


Figure 2-10 Flux vs. altitude: head-on collision post 1 year compared to meteoroid background.

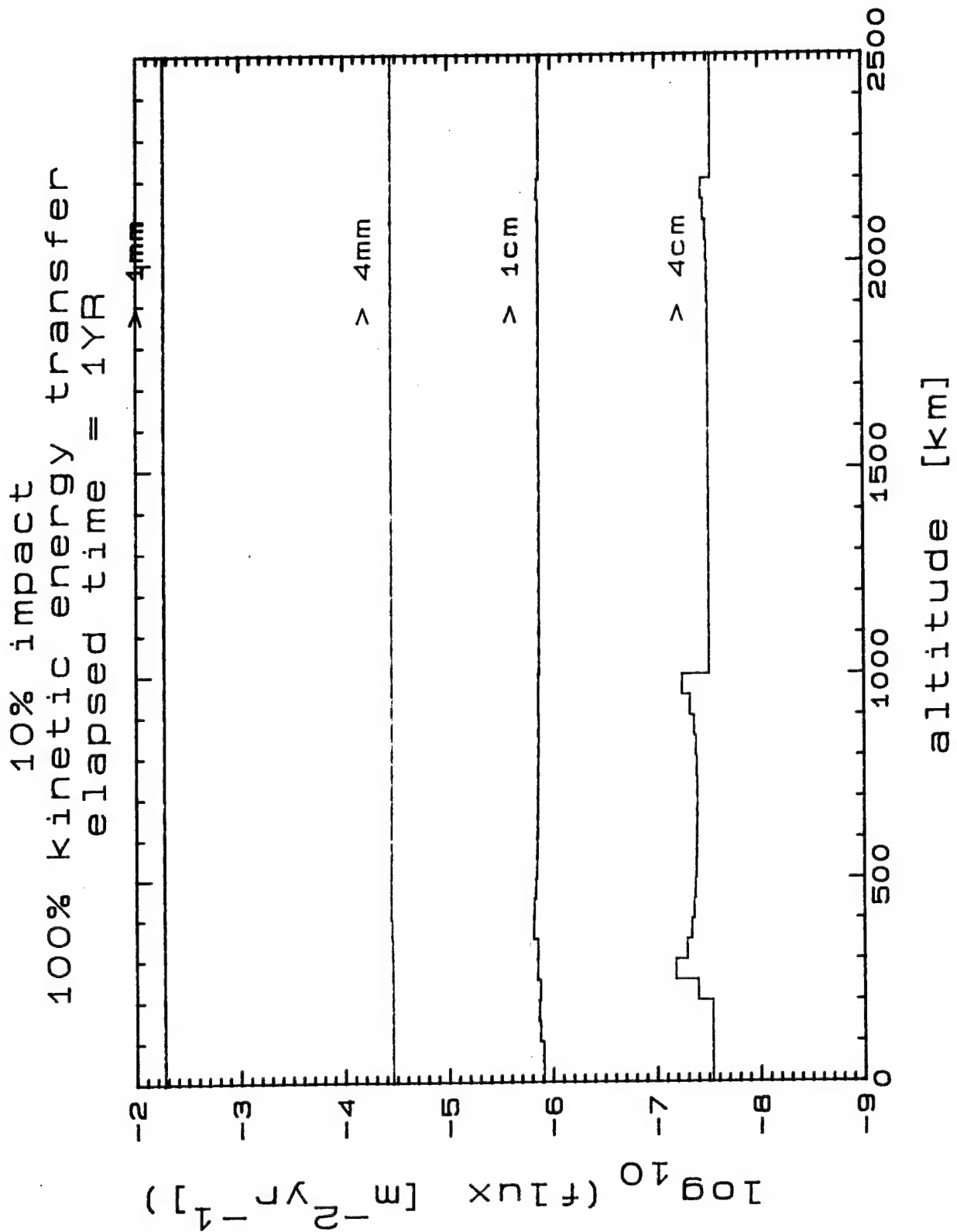


Figure 2-11 Flux vs. altitude: grazing collision post 1 year compared to meteoroid background.

is adequate in gauging the environmental impact of the debris after it has evolved into a shell-like structure, the short term environment is much different.

Shortly after breakup, the debris will appear (as modeled) as a sphere in a co-moving reference frame; in an external inertial reference frame, it will appear as a double cone. As drag and perturbations alter the orbits of the debris pieces, their period will vary; thus, the cone-like structure will evolve into a torus girdling the Earth. Eventually, as the right ascensions of the ascending nodes precess, this torus will smear itself into a debris shell about the Earth.

2.1.1 Short Term Effects

Of considerable importance in an on-orbit test such as Delta 180 is the possible effect of the debris cloud on U.S. or foreign satellites in the path of the cloud. The United States Space Command and the Aerospace Corporation performed analyses of the cloud interaction with other space vehicles and the debris flux generated shortly after the event, especially during the first day when the debris flux was at its greatest. These analyses assured conditions in which the probability of damage to other spacecraft as a result of the on-orbit test was minimal.

The JSC debris model available at the time the Delta-180 predictions were made assumes the orbital planes of the debris objects are randomly distributed in calculating debris fluxes. Therefore, the fluxes produced must be viewed as "average" values. This average corresponds to actual fluxes once the debris cloud evolves to a shell configuration, which occurs in the long term, i.e. months post-EOM. Before that time, while the orbital planes have correlated position and the debris cloud is in a

pseudo-toroidal state, the average flux will be less than the true flux inside the debris cloud. However, the hazard to a spacecraft in the region of space spanned by the cloud is the product of the flux times the exposure time, and for all LEO orbits, the average flux times 100% exposure time will be essentially the same as the true flux times the transit time through the toroid. Therefore, while the average fluxes do not directly relate to the true fluxes inside the toroid, they do provide an accurate indicator of the hazard level relative to the meteoroid population and to the background orbital debris at all times post-EOM.

Due to the low altitude at which the test was conducted, a large portion of the debris produced was predicted to reenter immediately after breakup -- within the first day. The number distribution used predicted approximately 800 large (>10cm diameter) particles would be created; if half of these reentered shortly after EOM, as would be suggested by a symmetrical distribution of debris about the target, about 400 objects should have been seen by the Eglin radar. In fact, the Eglin AN/FPS-85 phased array radar observed 381 particles several days after breakup.

For each scenario, the cumulative flux for particles greater than 1cm and 4cm exceeded the natural meteoroid background over some portion of the volume of interest. For 4cm objects, the collision fragments dominated the meteoroid environment by up to a factor of 50. In some cases the total flux was increased over the background out to an altitude of over 2000km. The 1cm and larger objects also dominated the meteoroid background, but generally only by a factor of 10; however, the background was exceeded to higher altitudes, in most cases. The cumulative flux for objects greater than or equal to 4mm exceeded the meteoroids by only a factor of 2 to 3 at breakup altitude. Fragments as small as 1mm were produced in the collision, yet their contribution to the total

flux was negligible in all cases. A typical example of these data are provided in Figure 2-12.

2.1.2 Mid Term Effects

The mid-term period covers that time interval in which the debris clouds forms pseudo-toroids about the Earth. Thus, the actual flux rates will again be higher inside the toroids than that predicted by computer, and lower outside. As regards the graphics in Appendix A, the fluxes predicted for the mid-term period are typically about a factor of two less than the short term flux, and about a factor of two greater than the predicted flux after an elapsed time of one month.

2.1.3 Long Term Effects

The long-term consequences cover the time from the formation of the pseudo-toroid cloud a few days post-EOM until the reentry of all debris created during the Delta-180 mission. During this period, the pre-mission predictions most closely match the actual environment, since the impact of mission/model uncertainties become of decreasing importance with the passage of time. Although some long-life orbits, of up to five years, were populated in the breakup, the cumulative flux arising from this event began to fall below the meteoroid flux within three months to one year in every case investigated. This was primarily due to the perigee altitudes of the debris. Large objects, which receive small delta-velocities, remained in orbits similar to those of the parent body. Small objects which received large forward delta-velocities, began with perigee altitudes around breakup altitude (modeled as 217.5km altitude), but because of their larger area-to-mass ratio, these objects decayed quickly as drag forces decreased their orbital energy.

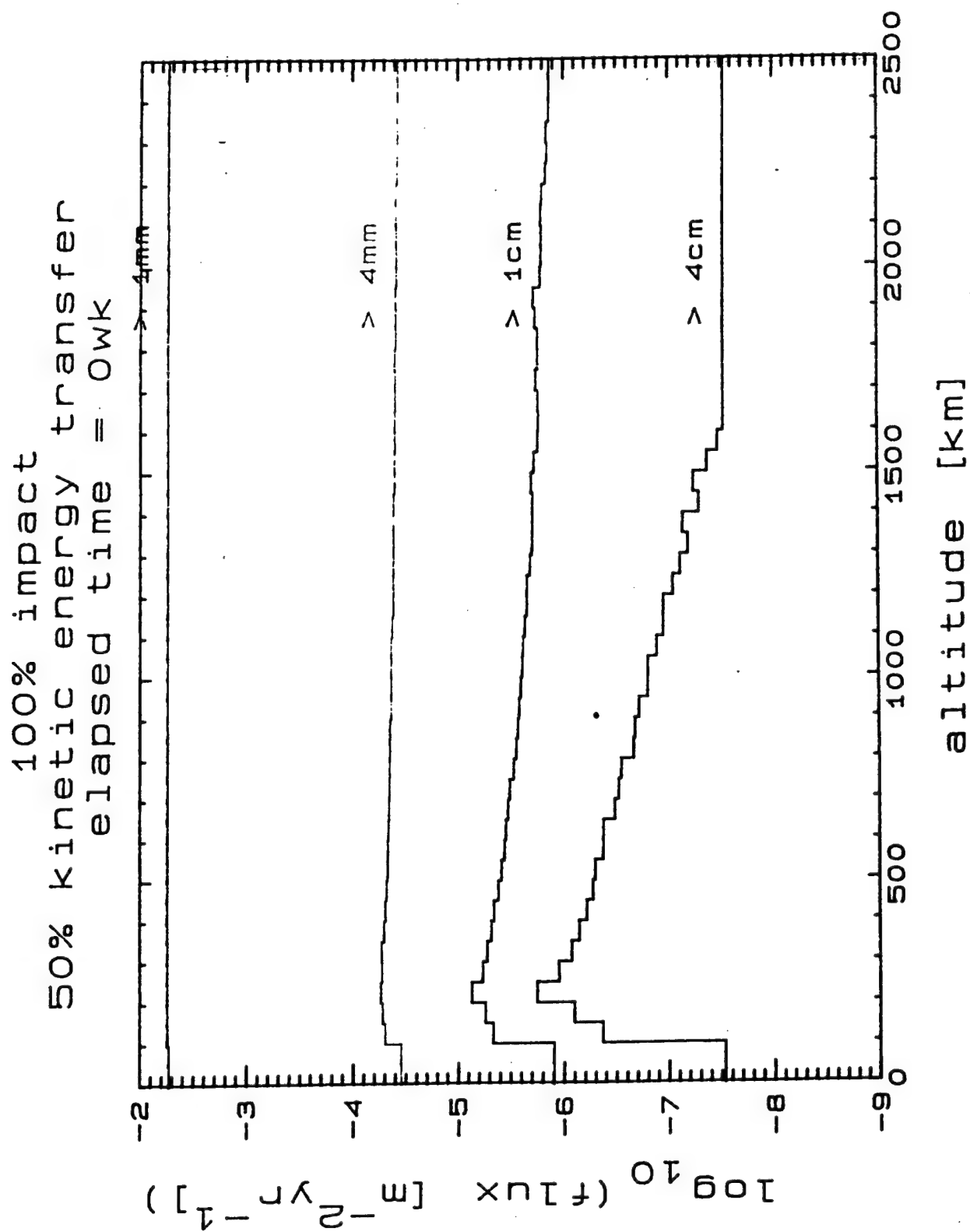


Figure 2-12 Flux vs. altitude: head-on collision at breakup.

2.2 Object Lifetimes

Estimates of the average object lifetimes were made to support the assessment of long-term impacts of the test on space operations in LEO. These estimates were very sensitive to the velocity distribution and event scenario. In general the impact scenarios produced longer lived objects than the explosion scenario. In nearly all cases, objects larger than 4cm were removed from orbit in 1 year; smaller particles showed a persistence of up to several years, but not significantly contributing to the environment. The explosion case and the low kinetic energy transfer, grazing impact case deposited the debris objects in a smaller region of space. In these scenarios, large particles re-entered the atmosphere in approximately six months, with the smaller particles remaining in orbit up to several years. This is due chiefly to the high apogees of the particles; reentry did not occur until perturbations brought these apogees down to an altitude comparable to the perigee altitude, i.e., the altitude of the Delta-180 breakup.

2.3 Summary of Predictions

In summary of Appendix A, the cumulative flux for objects greater than or equal to 4cm were predicted to exceed the meteoroid background, albeit by only a factor of 10 or less at three months, decreasing to the background threshold in roughly 6 months. The 1cm flux curve displayed similar behavior, in all cases falling below the background at about 6 months elapsed time. The 4mm fluxes were predicted to fall below the background in, at most, 1 month post-EOM. No significant contribution was made to the total flux by the 1mm cumulative flux. Thus, in all cases surveyed, the potential hazard presented by the Delta-180 breakup event was predicted to be below that of the natural meteoroid background in 1 year or less.

3.0 THE MEASUREMENT CAMPAIGN

The measurement campaign involved a variety of radar and optical detectors in an effort to provide maximum coverage of the creation and subsequent evolution of the Delta-180 debris clouds.

At EOM, DoD radars with favorable passes were the Advanced Research Projects Agency (ARPA) Lincoln C-Band Observables Radar (ALCOR), the ARPA Long-Range Tracking and Instrumentation Radar (ALTAIR), the Millimeter Wave Radar (MMWR), and the Target Resolution and Discrimination Experiment radar (TRADEX). Additional post-EOM radars with good passes were Antigua, Kaena Point, Ascension, Beale, Eglin, Naval Space Surveillance (NAVSPASUR), and San Miguel. Other DoD radars were located at latitudes too high for good passes.

From one day before EOM to four days after, the JSC meteor radar on the island of Kauai collected metric observations of range and velocity, as well as signature observations to provide order-of-magnitude mass determinations. Details of all radar observations are included in this section.

Both ground-based and airborne optical observations were obtained for the post-EOM phase of the Delta-180 test. The airborne observations obtained data on two days, while the ground-based optical measurement campaign covered ten days with a variety of detectors. Specifics of both modes of data acquisition will be described in the following sections.

One objective of using multiple detectors was to obtain simultaneous observations using radar, IR, and optical systems to correlate radar cross-section, geometric size, and albedo. Table 3-1 presents the times of activity for all of the

TABLE 3-1
Detector/Time Matrix

DOY	KWAJ (WFOV)	KWAJ (NFOV)	KWAJ (LENZAR)	GEODSS (1)	GEODSS (2)	GEODSS (3)	AMOS (AATS)	AMOS (ASR)	AMOS (IRCCD)	MOTIF (AATS)	MOTIF (LLTV)	LBD (HAW.)	ALTAIR (KWAJ)	KAENA POINT
249	18:22 	18:11 	18:11 	14:45 	14:45 	14:45 	14:11 	X	14:50 	14:11 	14:41 	X	16:22 	X
	18:36 	18:36 	18:22 	15:30 	15:30 	15:30 	15:32 		15:31 	15:33 	15:35 		18:08 ^a 	
250	17:40 	17:02 	17:02 	14:44 	14:44 	15:02 	X	X	X	14:11 	14:33 	X	16:10 	X
	18:00 	18:00 	18:00 	15:23 	15:23 	15:22 				15:33 	15:21 		18:00 ^b 	
251	X	X	X	15:03 	15:03 	15:03 	X	15:05 	X	15:03 	14:36 	X	15:40 	X
				15:28 	15:28 	15:28 		15:29 		15:28 	15:00 		17:26 ^c 	
252	X	X	X	X	X	X	X	X	X	X	X	X	X	15:02
														*
253	X	X	X	X	X	X	X	X	X	X	X	X	X	15:19
														*
254	X	X	X	15:00 	15:00 	15:00 	X	X	X	X	15:04 	X	X	X
				15:28 	15:28 	15:28 					15:30 			
255	X	X	X	14:50 	14:50 	14:50 	X	X	X	X	15:30 	*	X	X
				15:30 	15:30 	15:30 					X	*		
256	X	X	X	14:50 	14:50 	14:50 	14:56 	15:23 		15:05 	15:04 	X	X	14:50
				15:30 	15:30 	15:30 			X		15:30 			15:25
257	X	X	X	14:57 	14:57 	14:57 	14:56 	14:55 		14:40 	14:40 	X	X	14:45
				15:30 	15:30 	15:30 			X		15:30 			16:25
258	X	X	X	14:57 	14:57 	14:44 	15:00 	14:47 	X	15:00 	14:57 	X	X	X
				15:42 	15:42 	15:35 	15:35 	15:28 		15:35 	15:42 			

^a ALTAIR additional times (249): 00:21-01:10, 01:59-02:07, 03:35-04:11, 05:22-05:44, 22:50-23:43

^b ALTAIR additional times (250): 00:41-00:53, 03:00-03:25, 04:50-05:11, 22:50-23:22

^c ALTAIR additional times (251): 00:50-01:30, 02:25-03:15

X=No observations.

*=Time not available.

All times are UT.

detectors. Figure 3-1 shows the location of these sensors on a world map.

3.1 DoD Radar Measurements

3.1.1 Eglin Radar

The electronically-steered phased-array radar located at Eglin Air Force Base was originally designed with a primary unclassified mission of space surveillance. With the emergence of a submarine-launched ballistic missile (SLBM) threat, however, Eglin is now a "collateral" sensor with a different primary mission. Lowering the SLBM fence allows Eglin to operate as a sensitive space surveillance radar. Since the inclinations of Delta-180 objects prevented detection by the north-facing Perimeter Acquisition Radar Characterization System (PARCS) in North Dakota, Eglin was chosen as the primary sensor for long-term debris data collection.

One day post-EOM, passes of both 23° and 39° inclination objects from Delta-180 occurred. Figure 3-2 shows the spread of the debris cloud on day 249 (September 6, 1986) as the number of debris objects tracked as a function of the time interval (90 minutes total observing time) during which Eglin acquired a particular object. Despite the low elevation for Eglin's 31° latitude, 190 objects were positively identified from the 23° cloud. From the higher pass elevation and larger mass SDI/PAS payload, one would have anticipated detecting more objects from the 39° inclination cloud. Eglin data, however, revealed only 191 objects. Gabbard plots for the 23° and 39° clouds during day 249 are shown in Figures 3-3 and 3-4 respectively. The 39° clouds lack of large objects could be explained by unknown additional Delta second stage mass which would have caused more fragmentation, differing fragment densities, unusual impact conditions, or increased

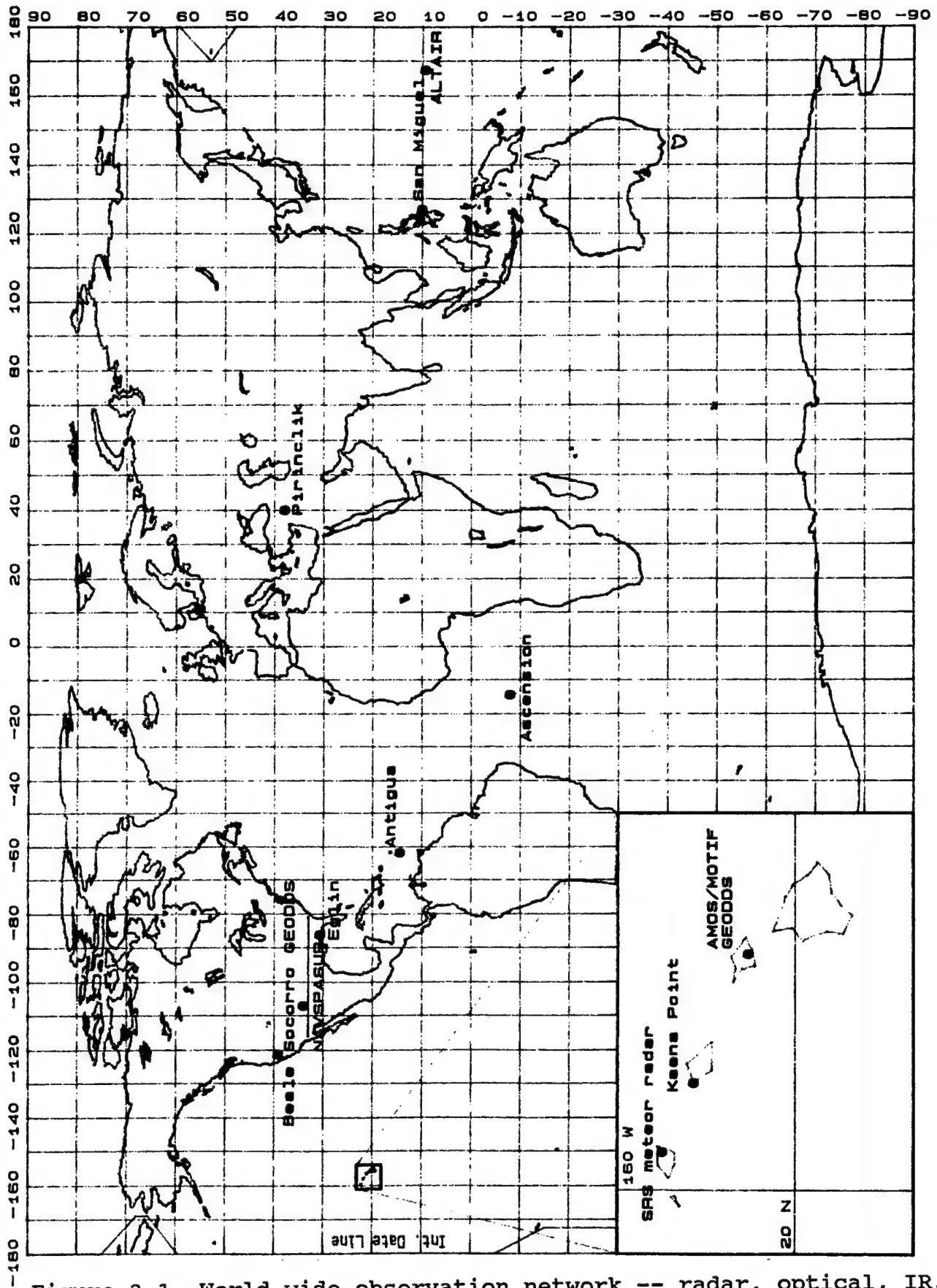
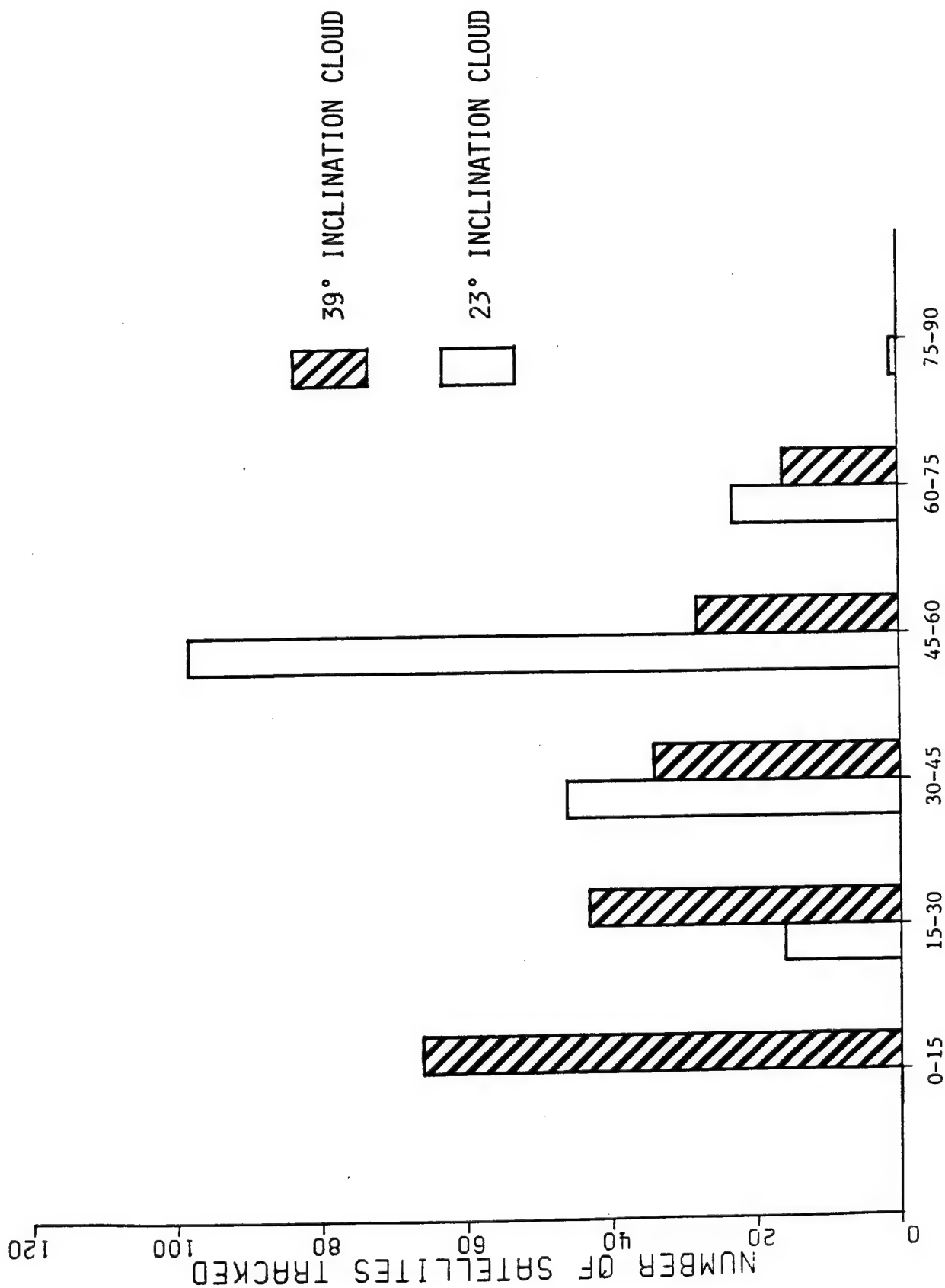


Figure 3-1 World wide observation network -- radar, optical, IR.

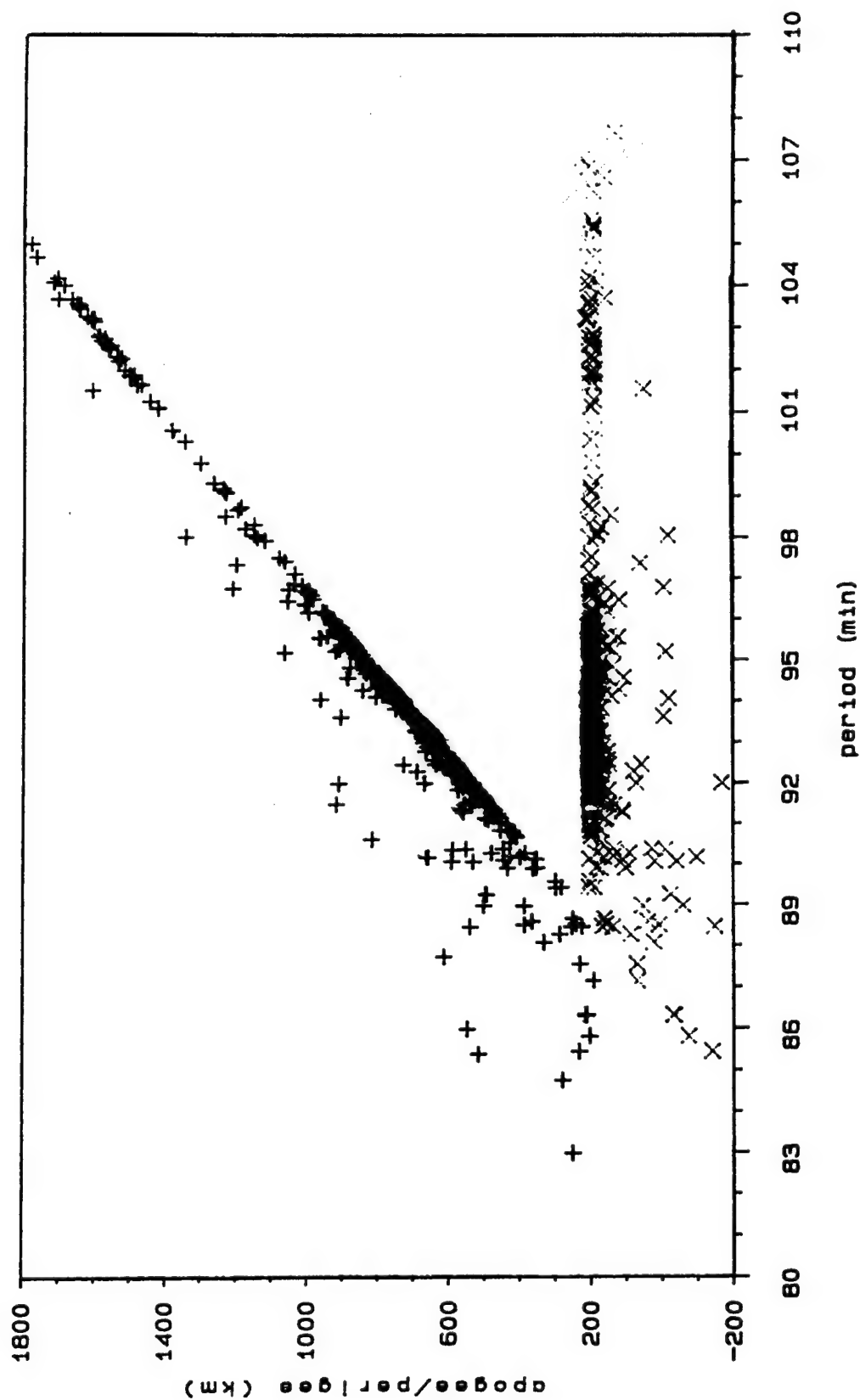
Figure 3-2 Number vs. detection time, DOY 249.



Hazard Analysis Project

Eglin data for day: 249_23

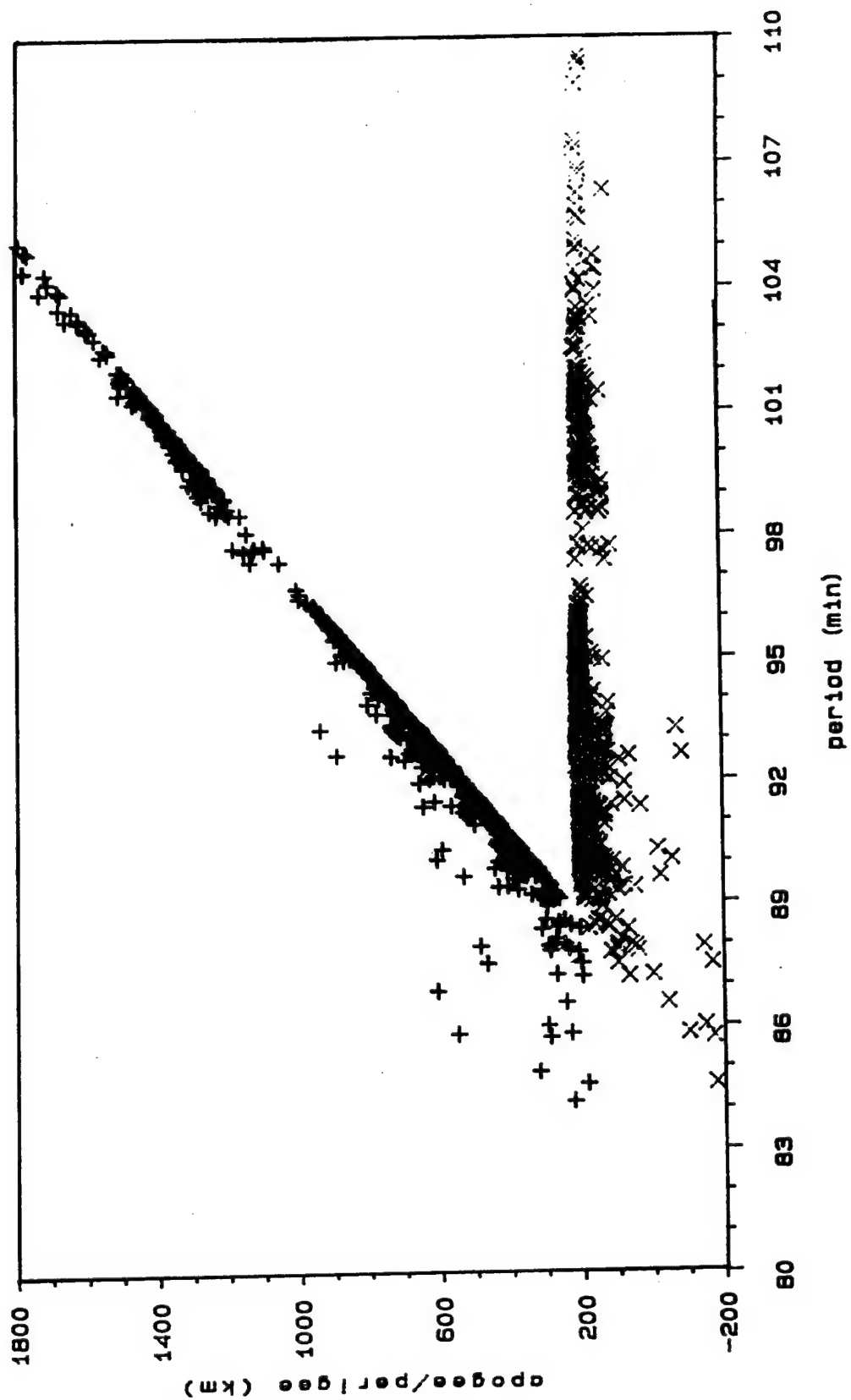
Figure 3-3 Gabbard diagram: DOY 249 -- 23° cloud.



Hazard Analysis Project

Eglin data for day: 249_38

Figure 3-4 Gabbard diagram: DOY 249 -- 38° cloud.



fragmentation caused by the range destruct package onboard the SDI/PAS.

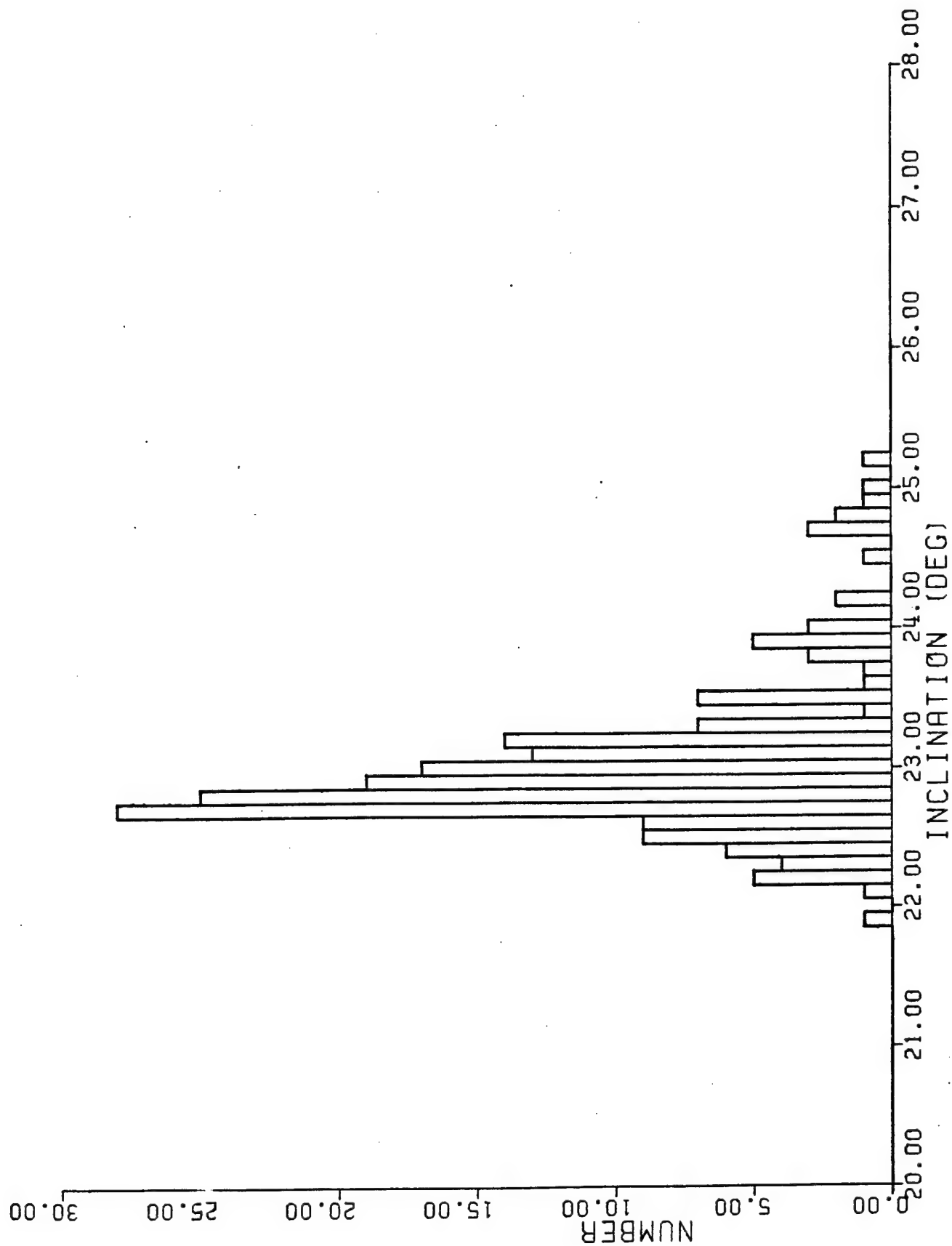
As Figure 3-3 shows, the 23° cloud periods range from 79 minutes to 116 minutes. Included in the objects plotted are several pieces in highly elliptical deorbit trajectories. About 20% were in fact in trajectories of this nature. A surprise in the data were several pieces of debris in very high apogee orbits; the data imply an increase in velocity of about 1km/s, which is a sizable fraction of the impact velocity. As was seen in the predictions (section 2), even for 100% kinetic energy transfer, a particle receiving this large a delta-velocity would be on the order of a centimeter in diameter. The Eglin sensors are not able to detect objects this small even at the perigee altitude of these pieces, so there is some inconsistency between the predictions and these observations.

The inclination distribution of the 23° cloud ranged from 21.95° to 25.25°. There was an inclination bias away from the initial inclination and towards higher inclination, as shown in Figure 3-5. This would imply some degree of momentum transfer to the large objects coming from the second stage.

The 39° cloud Gabbard plot, shown in Figure 3-4, demonstrates many similarities to the 23° cloud. Roughly 15% of the objects are in deorbit trajectories, and there are several anomalous objects with high apogee altitudes, including one with a period of 518 minutes. An orbit such as this would have been populated by an object experiencing a velocity change on the order of 2km/s, which would indicate an object of ~5mm diameter from the breakup model and is, of course, much too small to have been seen by the Eglin radar.

The inclination distribution exhibits a greater range than that of the 23° cloud, 34.7° to 41.4°, as would be expected

Figure 3-5 Number vs. inclination distribution: 23° cloud.



for similar plane change angles from a higher initial inclination. The inclination distribution is depicted in Figure 3-6, and shows a weighting toward higher inclinations, which is not the expected case.

A careful examination of the Gabbard plots presented thus far will disclose a clustering of objects in the 39° cloud between approximately 98 and 103 minutes of period. Plotting a number vs. period distribution for the 23° and 39° clouds yields Figures 3-7 and 3-8 respectively. Discounting "noise" due to reentering objects with 84 to 89 minute periods, each cloud is fairly symmetric about a period of 92 minutes. However, the 39° cloud shows a group of objects in long period orbits. Correlation with Figure 3-9, debris inclination vs. period, shows that between the periods of 98 and 104 minutes there is a general trend towards inclinations greater than the mean. The cause of this clustering is at present unknown, though it may be a residual effect of the maneuvers conducted immediately prior to EOM.

Efforts to obtain object size information from the Eglin data has been hampered by the use of default values for radar cross section in the NORAD two-line element sets derived from Intercept 205 of the Eglin "Log R" Intercepts 1, 15, and 224 also contain size information in the form of signal to noise ratios. Unfortunately, the calibration factors necessary to convert these ratios to radar cross sections are classified, and no action has at this time been taken to obtain them for direct or contracted processing. Eglin "Log S" tapes, currently undergoing analysis by Xontech, Inc., may include some further information concerning the size of the objects.

3.1.2 Kiernan Reentry Site (KREMS) Measurements

The KREMS at the Kwajalein Missile Range hosts ALCOR, ALTAIR, MMWR, and TRADEX and these were the only sites to

Figure 3-6 Number vs. inclination distribution: 39° cloud.

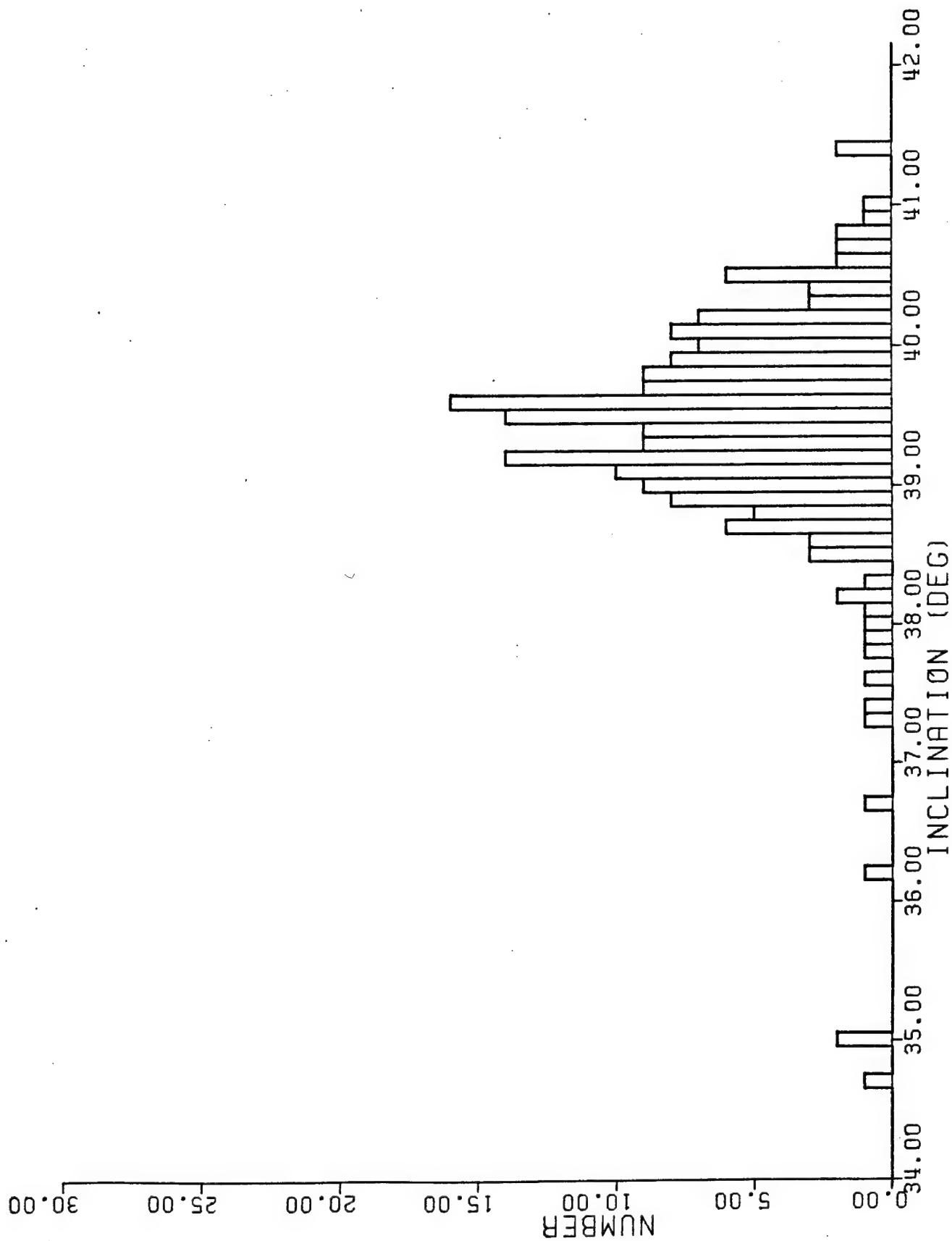
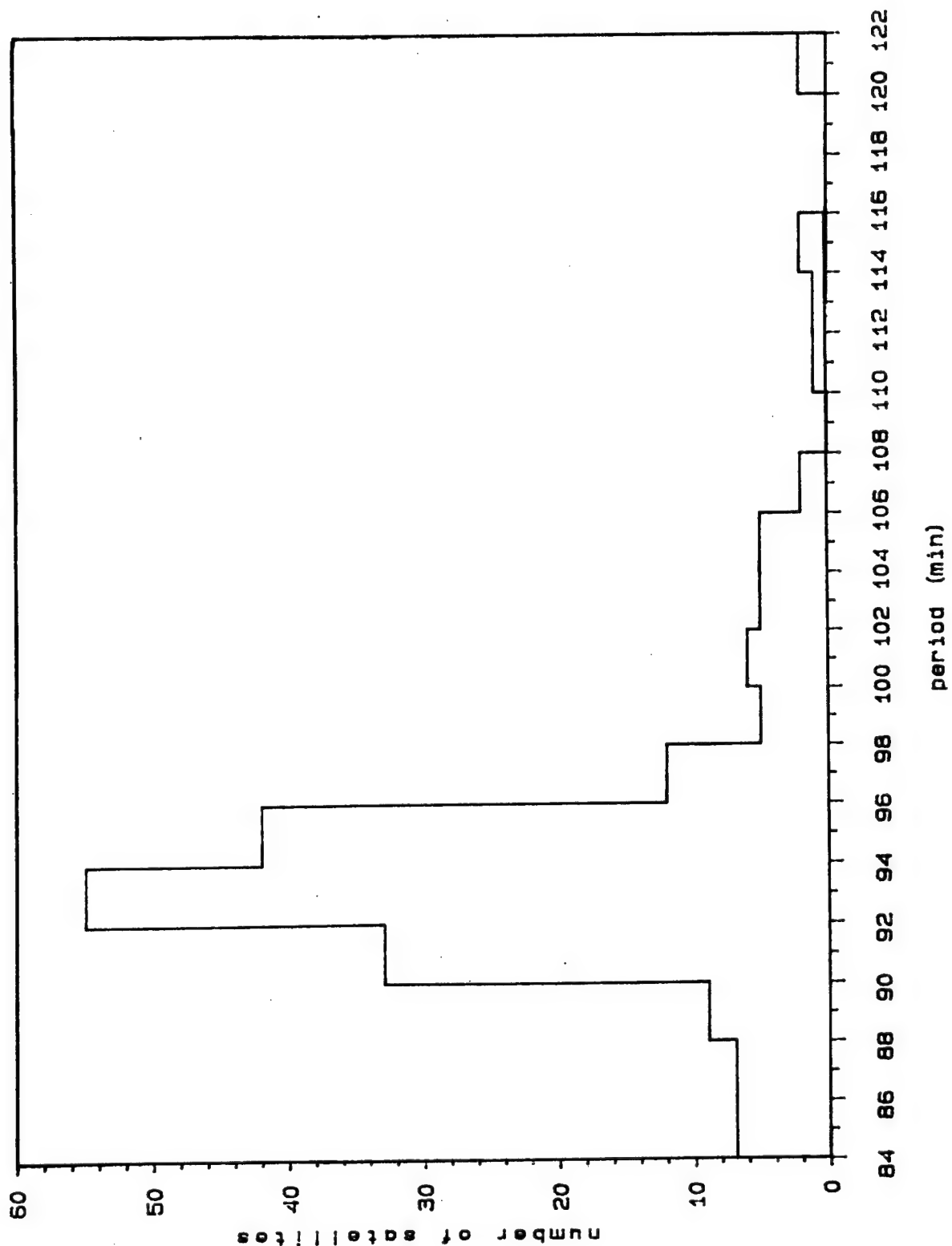


Figure 3-7 Number vs. period distribution: 23° cloud.

Debris Number vs Period Distribution

23° cloud



Debris Number vs Period Distribution

39° cloud

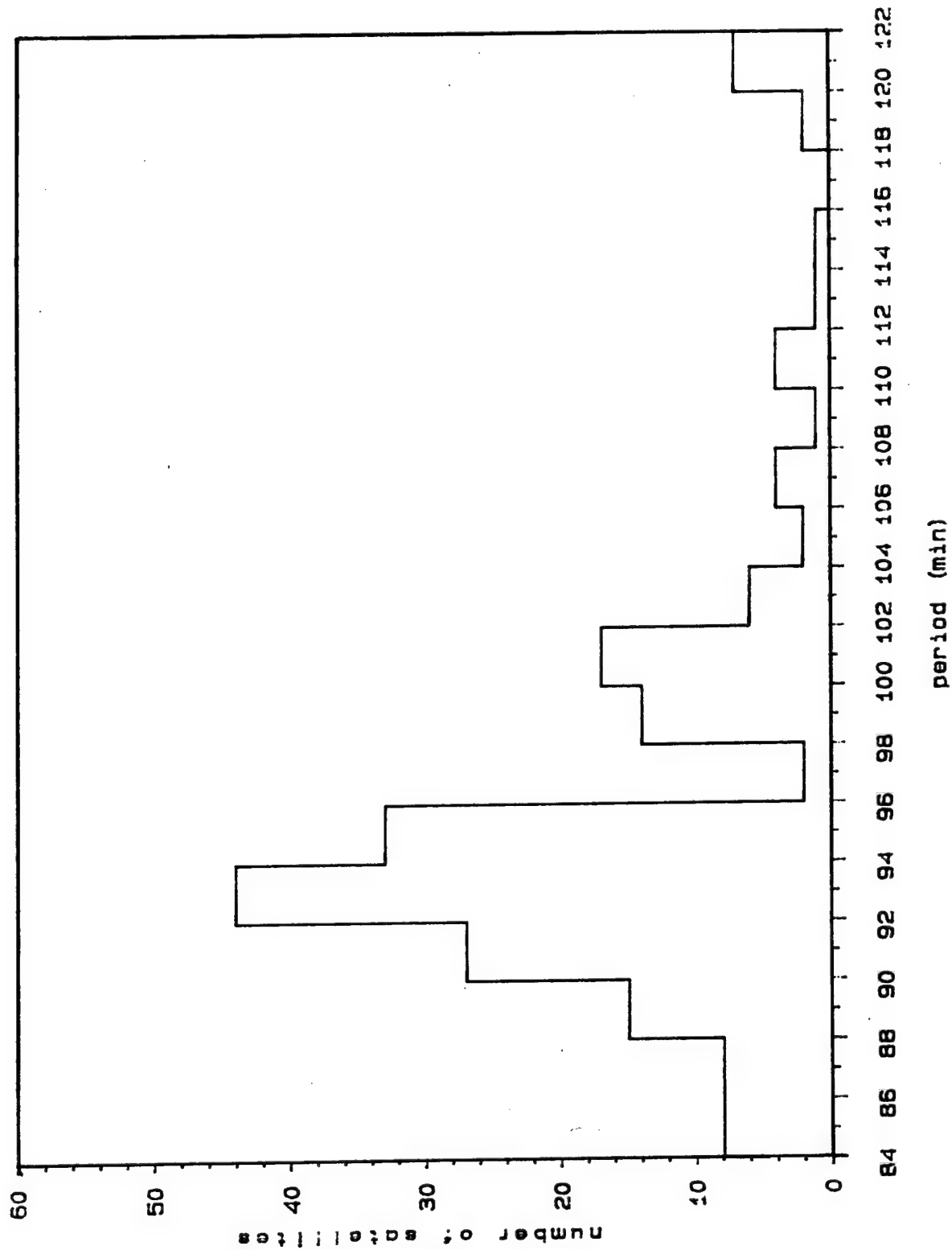
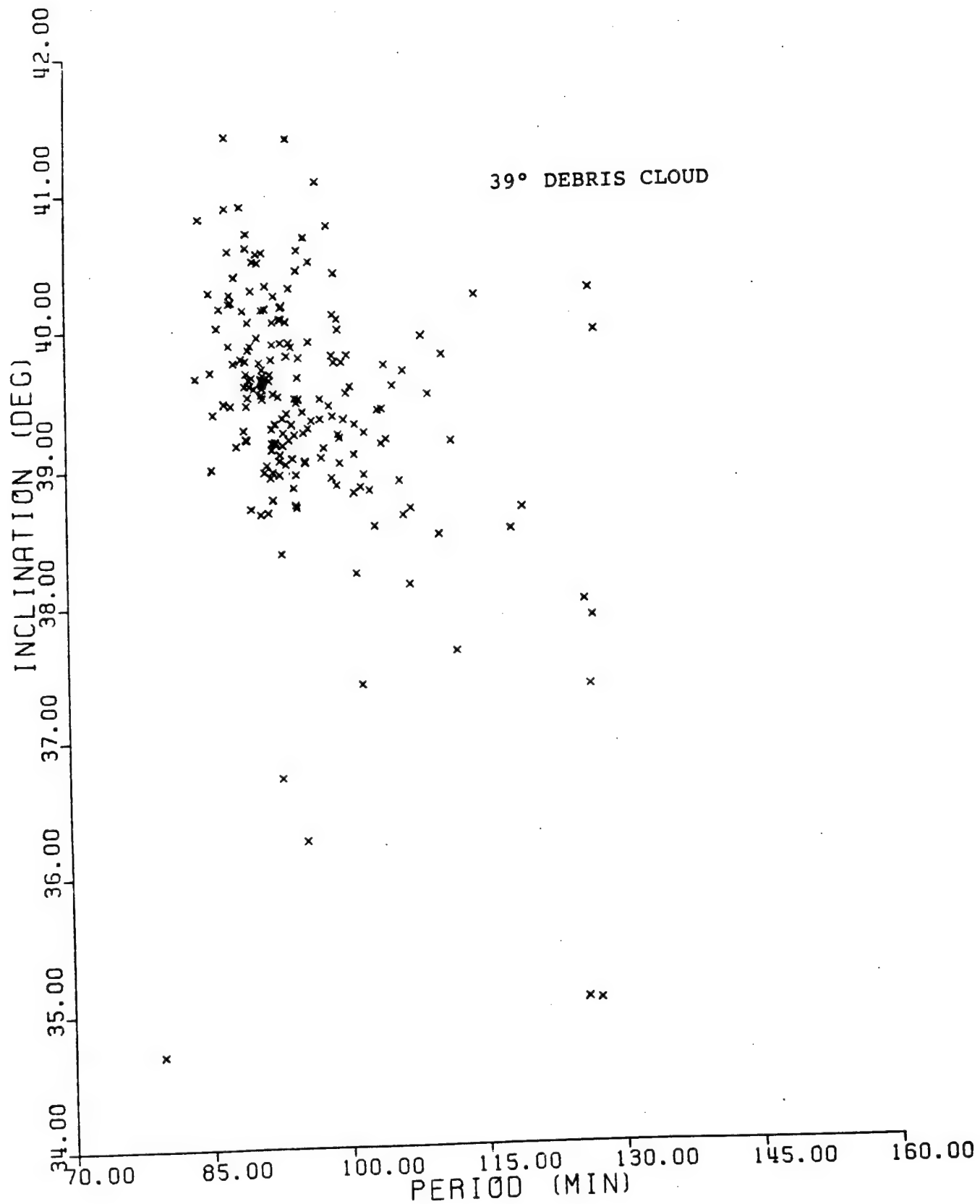


Figure 3-8 Number vs. period distribution: 39° cloud.

Figure 3-9 Inclination vs. period: 39° cloud.



collect EOM data. Each radar collected EOM data on the Delta-180 objects but only the post-EOM data are unclassified. A classified report on the EOM data will be published at a later date.

ALTAIR is a "contributing" sensor under contract to provide space surveillance data to the DoD. The mechanically-steered pencil-beam radar operates at both VHF and ultra high frequency (UHF) to provide range, azimuth, and elevation data, with additional capability for range rate in the coherent mode.

ALTAIR's normal mode of operation is to track a particular satellite for a period of time in order to determine the satellite's orbit. The amount of time necessary to acquire and track a debris object, however, would have severely limited the number of objects detected by ALTAIR. Therefore, a new procedure was developed in which the ALTAIR radar beam tracked the intersection of the two (23° and 39°) debris orbital planes and allowed the debris objects to pass through the beam.

Data were collected using this "beam park" operational mode for three passes during the period from approximately one to three days after the nominal end-of-mission. During this period, the debris from a breakup will remain in a toroidal shape with a focus or constriction of the torus near the latitude of the breakup. Although the intersection of the two toroids slowly drifts to the north of the interaction region due to slight differences in the nodal regressions of the two orbits, the drift is on the order of only a degree of latitude per day during the measurement period.

Therefore, by tracking the intersection of these two toroids, most of the measureable debris generated in the collision should pass through the radar beam. Rough orbits

may even be determined by knowing where the radar beam is pointed and by measuring the range and range rate of the object. Unfortunately, since the period of time that a debris object remains in the beam is short (10-40 secs.) coupled with uncertainties -- primarily in the range rate -- these orbits have large uncertainties.

Digital VHF (30-300 MHz) beam park data and paper Range-Time-Intensity plots (RTIs) were received at JSC in October, 1986. Film RTIs of the UHF (300 MHz - 3 GHz) observations were received in November, 1986. The digital data was processed using locally developed software implemented on a VAX 11/780 computer. The majority of the resulting element sets implied immediate reentry for the observed objects. Table 3-2 summarizes the number of those pieces (with perigees greater than -200km) and the number of those objects surviving one orbit (perigee greater than 100km). There could have been no objects with negative perigee altitude left in orbit after about an hour post-EOM, and objects with perigee altitude of less than 100km should have decayed within a couple of days. As the beam park data were collected on days 249, 250, and 251 (September 6, 7, and 8, respectively), the number of objects in these low perigee orbits more than a day after the breakup event reflects the large uncertainties associated with the measurements.

A sensitivity analysis of the data, including the propagation of the standard deviations from ALTAIR data to final element sets, demonstrated the sensitivity of the orbital elements to the range rate; in some cases, the standard deviation of this quantity was over a kilometer per second. As an example, one radar return, exhibiting one of the largest range rates, and a nominal standard deviation of 300 m/sec for that rate, was propagated through the transformation from topocentric coordinates to orbital elements. The resulting elements displayed only a 0.24° range

TABLE 3-2

SUMMARY OF SURVIVING OBJECTS

DOY	Objects	Surviving	Percentage
249	56	15	26.8 %
250	48	14	29.2 %
251	5	1	20.0 %

in inclination, but over a 30 minute difference in periods between a low range rate (mean rate minus one standard deviation unit) and a high range rate (mean rate plus one standard deviation unit). Other elements, such as mean motion, semimajor axis, and eccentricity, displayed exceptional variance.

A representative Gabbard plot of the data for day 249 is shown in Figure 3-10; the perigee height has been arbitrarily set at -200km, and no distinction has been made between the 23° and 39° clouds. For comparison, Figure 3-11 shows the same data, with all points plotted regardless of perigee. Note the points representing the highly elliptical data in the low-period area of the plot.

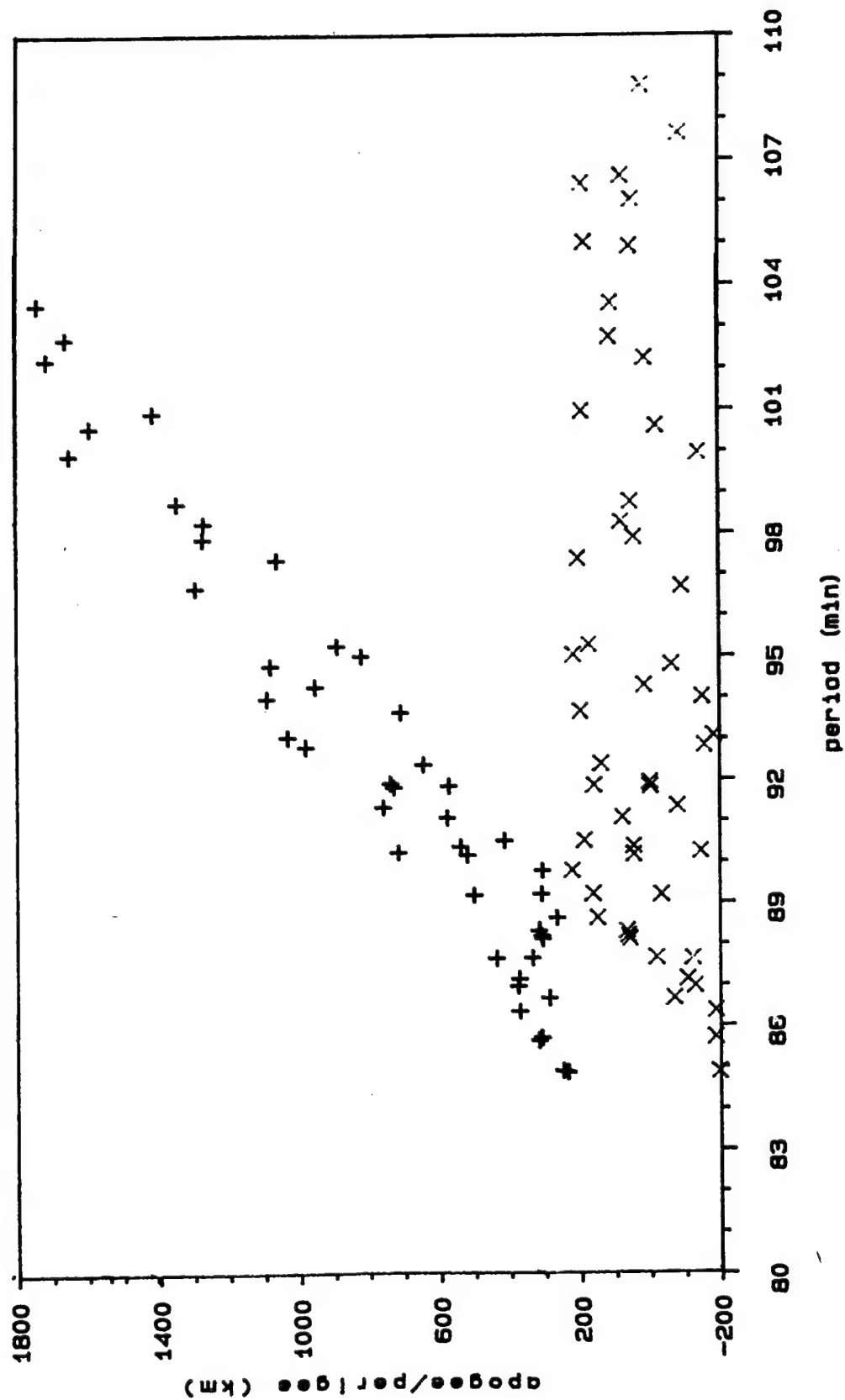
A further observation concerning the data is that there exists a discrepancy between the number of objects observed in the RTI format and the number of observations contained in the digital data. Table 3-3 records the number of objects observed as streaks in the paper RTIs, the number revealed by simply plotting the digital data, and the number of objects found by processing performed at JSC. Clearly, a great deal of useful debris data was lost between the RTI plots and the digital data.

A comparison of ALTAIR data with the Eglin data processed by Teledyne Brown is inconclusive beyond several specific observations. In particular, ALTAIR data is heavily biased toward the debris in the 23° cloud -- a fact for which there is no obvious operational reason since the radar was pointed at the intersection of the two orbits. In addition, a much greater percentage of the ALTAIR observations indicated debris objects about to deorbit than did the Eglin observations. This discrepancy is probably driven by uncertainties in the range rate data. If the suspect reentering objects are dropped, the ALTAIR and Eglin Gabbard plots are quite similar.

Hazard Analysis Project

ALTAIR data

Figure 3-10 Filtered ALTAIR data -- DOY 249.



Hazard Analysis Project

ALTAIR data

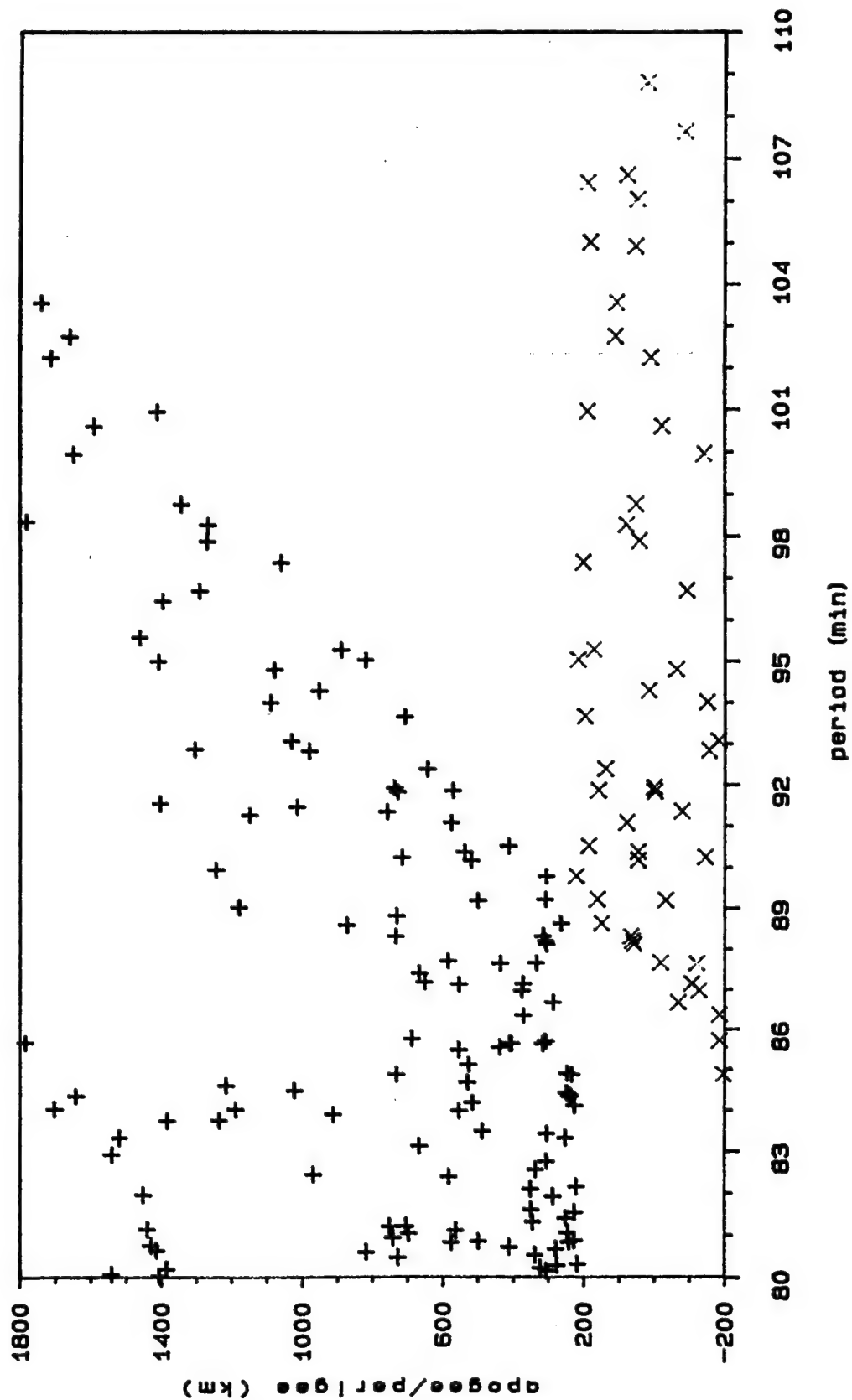


Figure 3-11 ALTAIR data -- DOY 249.

TABLE 3-3

Summary of ALTAIR Post-EOM Data

DOY	Number of Objects		
	RTI plots	Digital Tapes	JSC Processed
249	N/A	212	56
250	175	148	48
251	162	99	5

Unfortunately, the ALTAIR data was the only unclassified data containing size information available for processing. This data, converted to radar cross sections, and data from the then current NORAD SATellite CATalog (derived from Eglin data), is presented in Section 4.

UHF beam park RTIs for days 249, 250, and 251 were analyzed by hand, as no digital data were available for this time period and only a piece count was performed. The results of this count, plus the normalized number of counts per minute of observation time is shown in Table 3-4. In all three cases the number of objects observed in the UHF spectrum was larger than the corresponding VHF observation set. This is to be expected, since more particles may be observed by utilizing observational wavelengths on the order of the characteristic size of the particles.

3.1.3 Other DoD Radar Measurements

Post-EOM observations made by Antigua, Ascension, Beale, and San Miguel were automatically routed to NORAD and used for producing element sets on the Delta-180 objects. Antigua and Ascension are mechanically-steered C-band low-gain radars. Beale is an electronically-steered phased-array radar similar to Eglin. San Miguel is a mechanically-steered UHF radar with long pulse widths and low pulse-repetition frequencies. These data are automatically incorporated into the NORAD catalog.

Recent NORAD Satellite Catalogs report 18 objects (international designators 1986-069A through -069T) related to the Delta-180 mission. Data from this catalog appears in Table 3-5. Thirteen of these objects were in the 39° cloud. Using those values for which RCS was reported, objects in the 23° cloud have an average diameter of 85.5cm, while those in the 39° cloud have an average diameter of 56.5cm.

TABLE 3-4

Summary of ALTAIR UHF Data

DOY	Number of objects Observed	Elapsed Time (hh:mm:ss)	Frequency (min ⁻¹)
249	470	00:47:00	9.90
250	498	01:46:00	4.69
251	228	01:30:16	2.53

TABLE 3-5

NORAD's Delta-180 Related Objects

International Designator	Catalog Number	Inclination (degrees)	RCS (m ²)
1986-069A	16937	39.1	N/A
B	16938	22.8	1.55
C	16940	38.8	0.36
D	16941	39.2	0.60
E	16942	37.9	0.32
F	16943	39.5	0.08
G	16944	40.0	0.37
H	16945	39.4	0.22
J	16946	22.9	0.19
K	16947	22.7	1.03
L	16948	22.7	0.09
M	16949	23.0	0.01
N	16950	37.1	N/A
P	16951	39.0	0.04
Q	17019	39.5	0.22
R	17020	39.4	0.03
S	17021	39.4	0.26
T	17022	39.6	0.26

All values of RCS are supplied by Eglin.

Since most Delta-180 fragments remaining in orbit were expected to decay after a few weeks, it was important to learn as much about them as possible in a short time. The FPQ-14 radar at Kaena Point on Oahu, Hawaii was tasked to collect metric and Mission Payload Analysis data on the fragments.

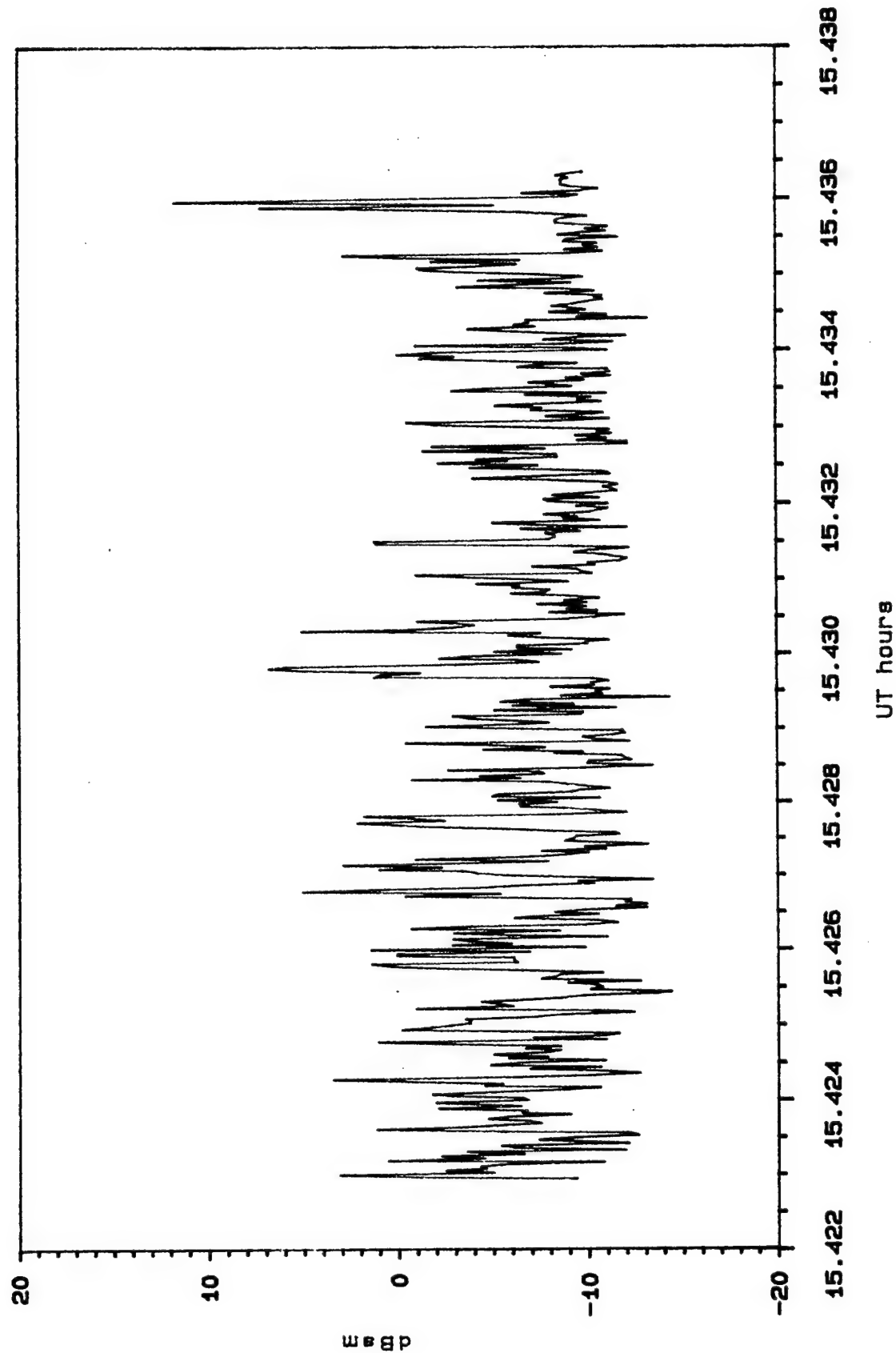
Six IBM-compatible, 1/2-inch, 9-track, 800-BPI tapes were produced on site with a Xerox Sigma 5 computer running OASYS software. Upon arrival at the Johnson Space Center, one of the six tapes was unreadable, presumably from damage in transit. The other five were read for time, position, velocity, and acceleration data on each object recorded. Additionally, Word 139 of the four hundred 32-bit words was of particular interest because it contained a digital-to-analog output signal for the function recorder in dBsm.

Of the many objects observed, one was assigned a provisional number of 85301. Another was identified as the fragment now associated with Catalog Number 16938. Values of dBsm too small for maintaining tracking signal strength accuracy to within 5 dBsm were rejected. The resulting data were plotted as dBsm versus time (see Figure 3-11a). These data were also converted to radar cross sections (RCSs) and time-averaged to derive a mean RCS; for Object 16938 a value of 0.29 m^2 was obtained. RCS values from radars operating at different frequencies, or from a given radar on a single pass, must be compared carefully. Because of the large apparent size variations associated with spacecraft attitude, the availability of Kaena Point data for 16938 on only one pass, and the variance of RCS with radar frequency, the Kaena Point value of 0.29 is not inconsistent with USSPACECOM's Eglin RCS of 1.55 last reported in the Space Surveillance Center Catalog for Object 16938 before its decay on 25 November 1986.

Additional work is currently being done on interpretation of the Kaena Point data as well as for other radars.

Kaena Point dBsm vs. time

object 16938 date: 10 SEP 86



3.1.4 NAVSPASUR

NAVSPASUR is not a radar in the typical sense. Transmitting at a VHF frequency of 217 MHz (1.38m), it combines the virtues of radar and radio interferometry into one system. A powerful transmitter in Texas produces a fan-shaped beam narrow in the north-south direction, but wide in the east-west direction. Receivers stationed across the southern United States detect any satellite with a large enough radar-cross section (RCS) passing less than 10,000 kilometers above latitude 33.5° North. This makes NAVSPASUR ideal for detecting objects from fragmentations, especially soon after the event, when orbits are poorly known.

NAVSPASUR was instrumental in monitoring the debris objects over a long period of time (September 30 - November 24), thus allowing an assessment of debris cloud evolution and the decay rate for debris objects. (Table 3-6 provides a summary of Space Surveillance Network (SSN) observations during this time period; note the short term rise in the number of objects in late October and early November.)

NAVSPASUR served to collect and analyze observations from several SSN sensors. Analysis allowed computation of provisional orbital elements for the objects so SSN sensors could be tasked to collect further observations. With the additional observations, objects could then be catalogued.

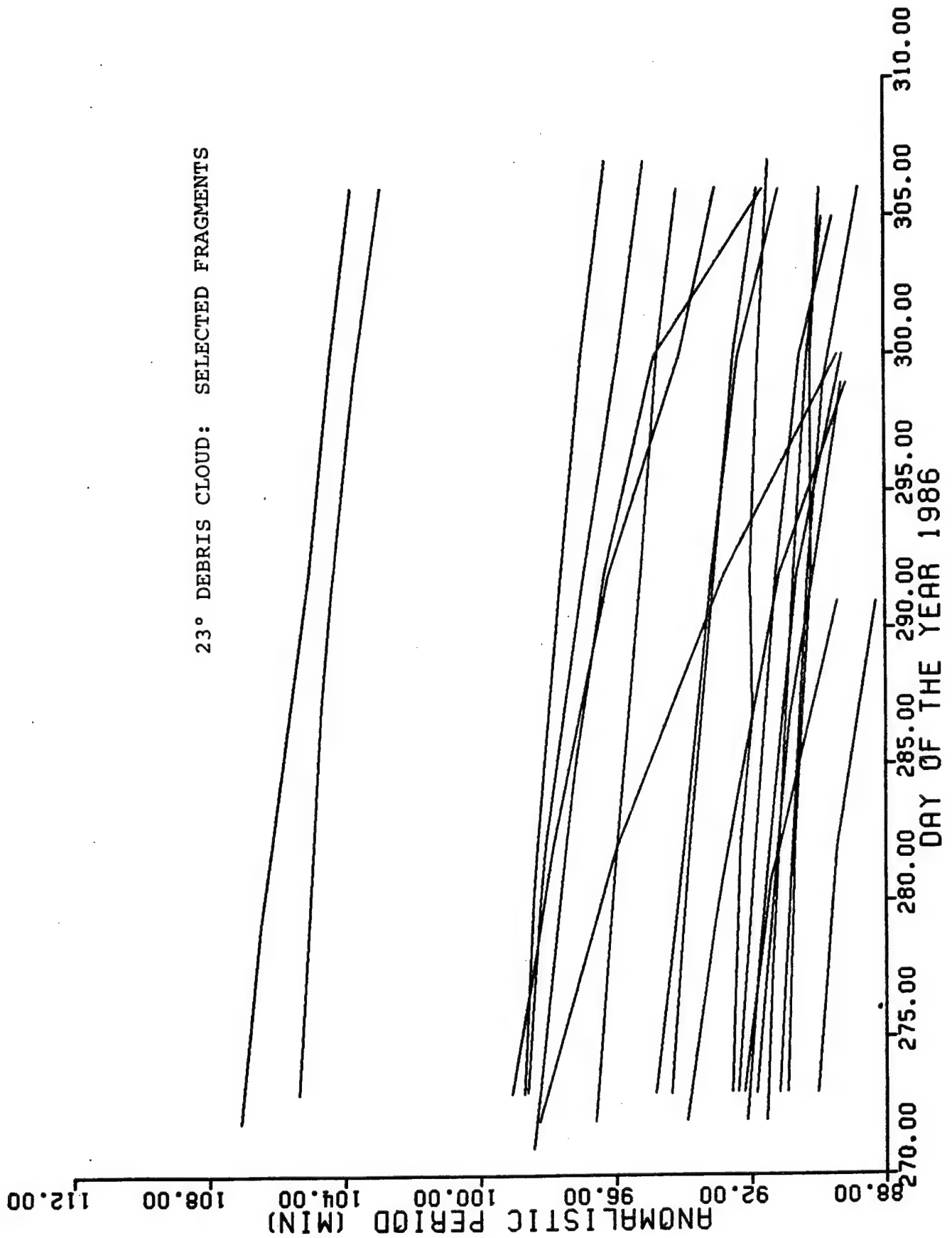
Twenty objects were analyzed for their decay characteristics. While necessarily incomplete, since not all objects have decayed to reentry, preliminary results of this study are shown in Figure 3-12. Differences in decay rates become more pronounced as pieces with higher apogee altitudes experience decay in apogee altitude. According to the predicted size vs. velocity relation, the smaller pieces should have received the larger delta-velocities and been in

TABLE 3-6

Summary of NAVSPASUR Observations

Date	DOY	Number of Objects Observed		
		23° Cloud	39° Cloud	Total
September 30	273	82	81	163
October 09	282	82	76	158
October 19	292	48	71	119
October 26	299	57	86	143
November 02	306	51	91	142
November 10	314	46	85	131
November 17	321	40	71	111
November 24	328	37	59	96

Figure 3-12 Debris decay -- 23° cloud.



the higher apogee initial orbits. Therefore, the differences in drag coefficients should become more apparent as time in orbit increases. Thus, at later times, when the orbits of the large and small pieces become similar, this decay data can be inverted to provide a distribution in the area to mass ratio in the debris.

Over 60 objects were assigned provisional catalog numbers by NAVSPASUR and transmitted to the Space Surveillance Center at Cheyenne Mountain Complex. The orbital elements were used for the preliminary findings of this report.

3.2 Meteor Radar Measurements

Ionospheric radars deployed on Kauai, Hawaii operated at two frequencies: 27.66 MHz (10.84m) and 49.92 Mhz (6.01m), referred to for convenience as 28 and 50 MHz (see Figure 3-13). The 28 MHz monostatic radar transmitted and received from a single antenna aligned on an east-west baseline. The five 50 MHz radar interferometer antennas were arranged to provide three azimuthal baselines and three elevation baselines for vector measurements. Beam centers were directed at an elevation of 30° , with half-power beam widths of 40° . Figure 3-14 illustrates the geometry of the ground track intercepts and the areas of sensitivity in the radar's cardioid beam pattern. Signals were transmitted with a pulse width of 10 microseconds and an interpulse period of 2 milliseconds. Peak radiated powers for the pulses were 10 kilowatts for the 50-MHz and 6 kilowatts for the 28 Mhz transmitter.

A preliminary analysis of the returns from first-pass ionization trails shows an order of magnitude increase in echoes for a 2-minute period post-EOM at the time appropriate for the down-range location of the instrument. A sample Range-Time-Intensity (RTI) plot of returns from the 50 MHz

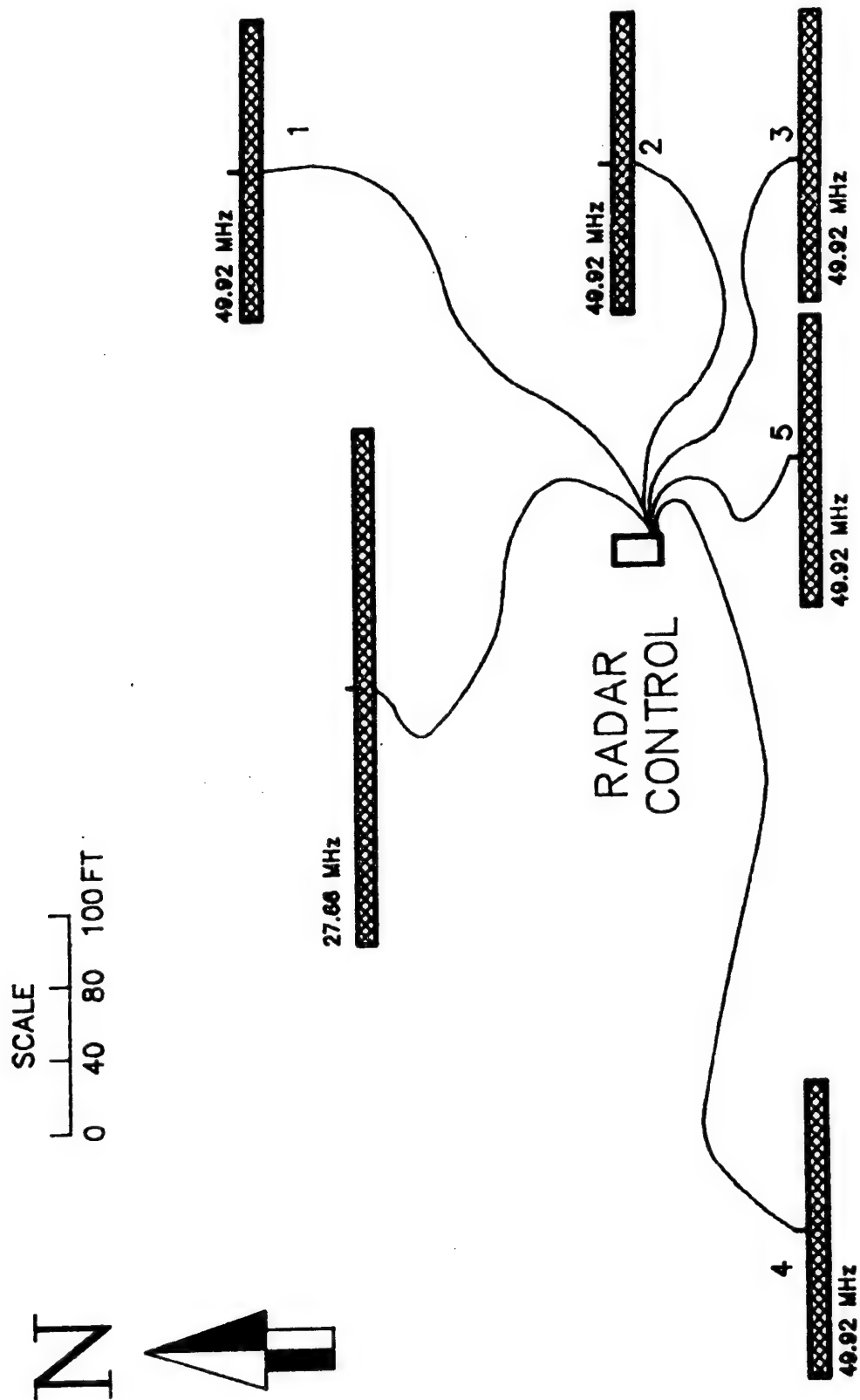
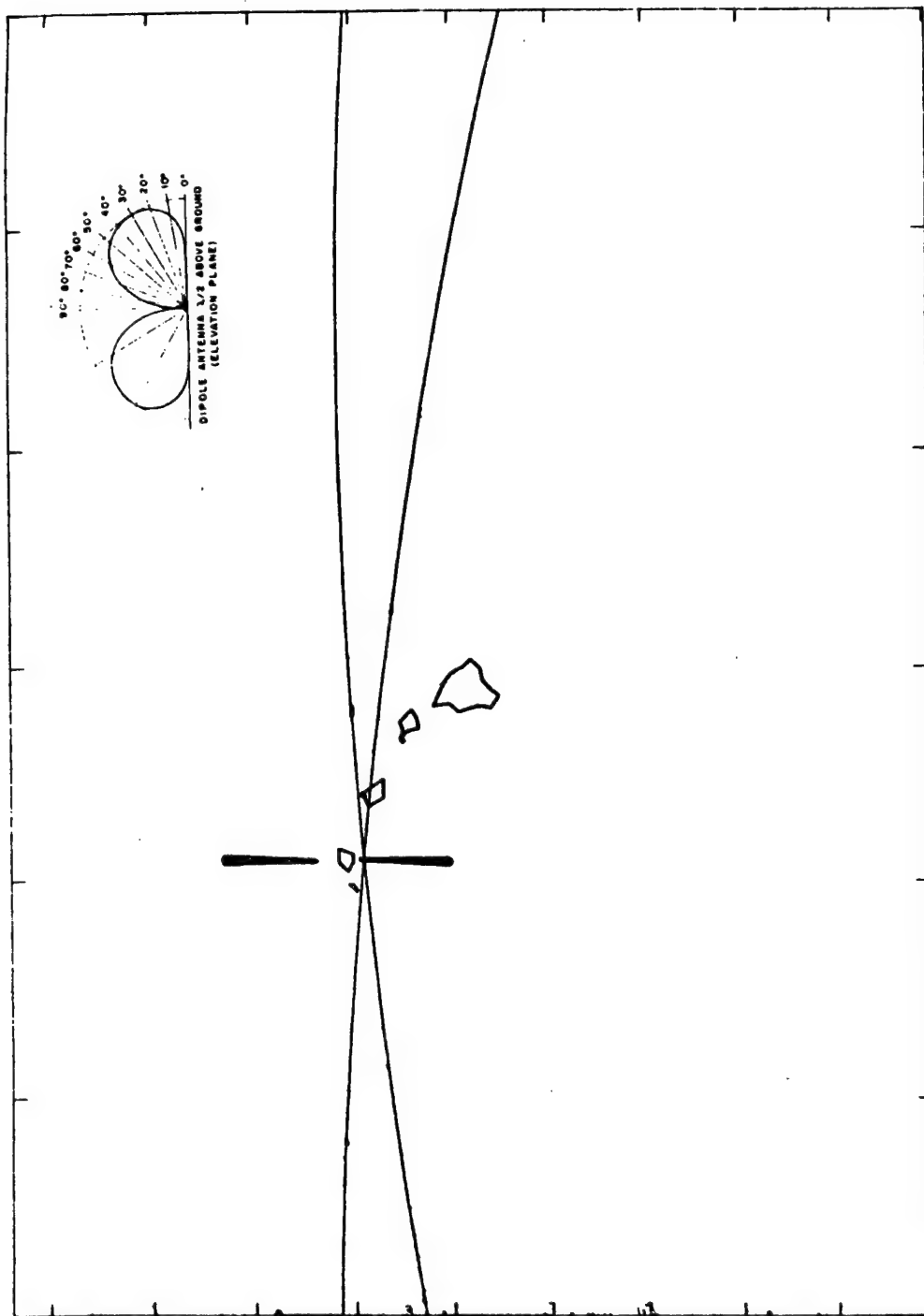


Figure 3-13 SRS Meteor radar array deployment.

Figure 3-14 Ground tracks superimposed on SRS Meteor Radar Radiation pattern.



radar is shown in Figure 3-15. Particle velocities of 7 kilometers per second distinguish the debris returns from meteor returns. Masses of between 5 and 1000 grams, with a strongly decreasing number distribution for increasing mass, have been calculated from the data (see Appendix C). Table 3-7 displays the data derived thus far from the calculations. A number vs. size distribution is shown in Figure 3-16. Work is underway to study data from the second pass and analyze the sensitivity of results to assumptions made.

3.3 Ground-based Optical/IR Measurements

3.3.1 AMOS/MOTIF/GEODSS

The AMOS, MOTIF, and GEODSS Electro-optical instruments are located on the island of Maui, Hawaii, just outside Haleakala Park at an altitude of 3.049km on the crest of Mount Haleakala. The latitude and longitude are 20.708472° N and 156.25797° W, respectively. The physical layout of the facilities is illustrated in Figure 1-2 -- the domes housing the various instruments are labeled. Each of these primary instruments will be briefly described and their specifications summarized in Table 3-8.

AMOS

AMOS is a telescope of 1.57m clear aperture with a focal length of 25m and an image scale of 8.25 arcseconds/mm at the Cassegrain focus. The telescope has instrument mounts at the rear of the telescope (classical Cassegrain focus) and on the side (folded Cassegrain focus). Focusing is achieved by driving the secondary mirror mount in and out; this function may be done automatically for non-infinite, changing target ranges. An AMOS Acquisition Telescope System (AATS) is mounted on the 1.6m telescope (Figure 3-17).

Figure 3-15 Typical meteor radar RTI.

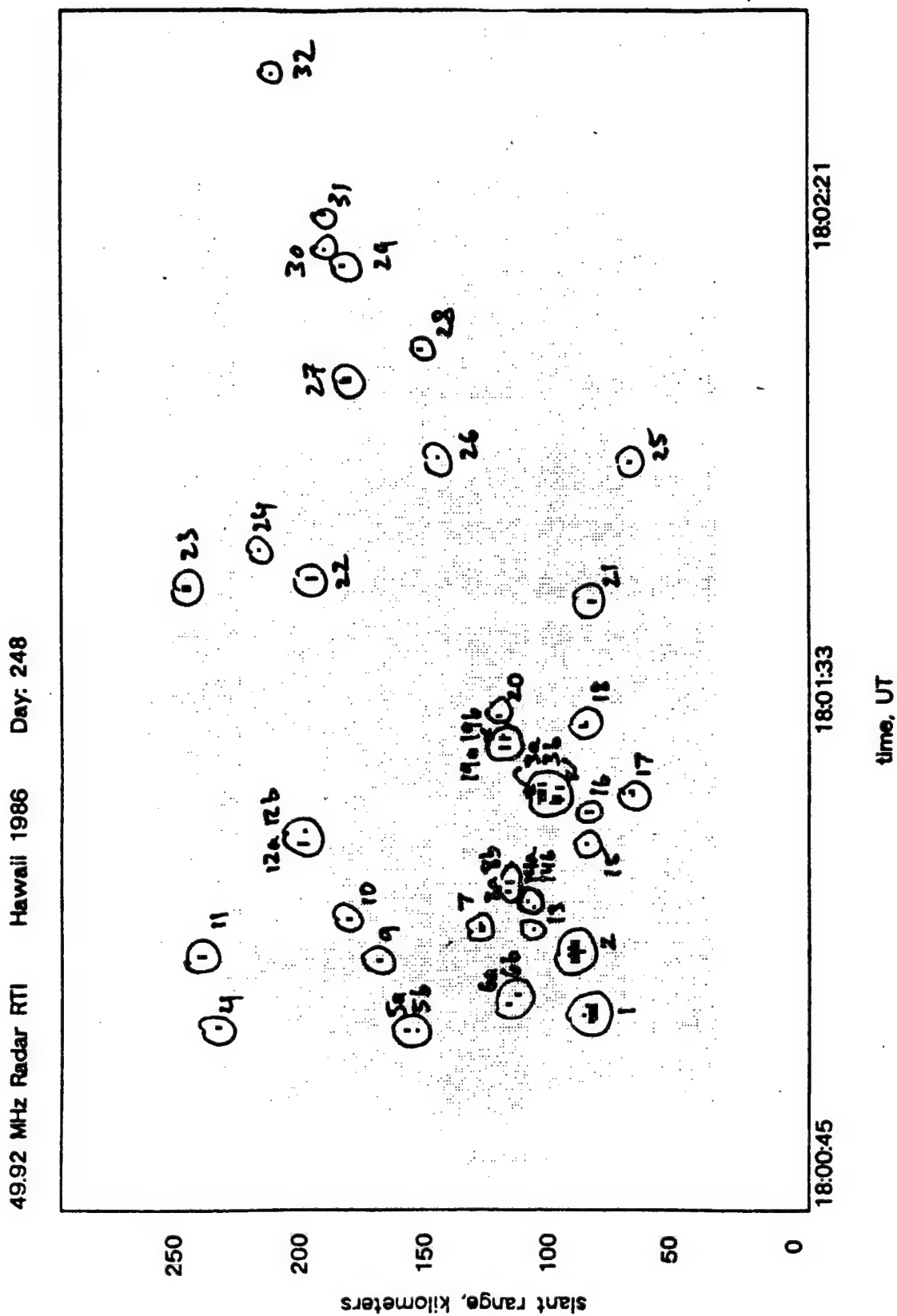


TABLE 3-7
Debris Particle Mass Estimates

EVENT	50 MHZ RADAR	28 MHZ RADAR
	Mass (grams)	Mass (grams)
1	82	63
2	164	24
3a	79	24
3b	63	15
4	51	
5a	35	
6a	18	
6b	24	
7	18	23
8a	14	
8b	29	
9	41	
10	35	
11	120	
12a	133	
12b	47	
13	10	
14a	20	
14b	12	
15	10	
16	12	
17	6	
18	12	
19a	35	
19b	98	31
20	21	
21	13	
22	133	
23	221	
24	76	88
25	142	44
26	35	
27	853	505
28	57	133
29	98	537
30	82	
31	126	379
32	158	
33		38

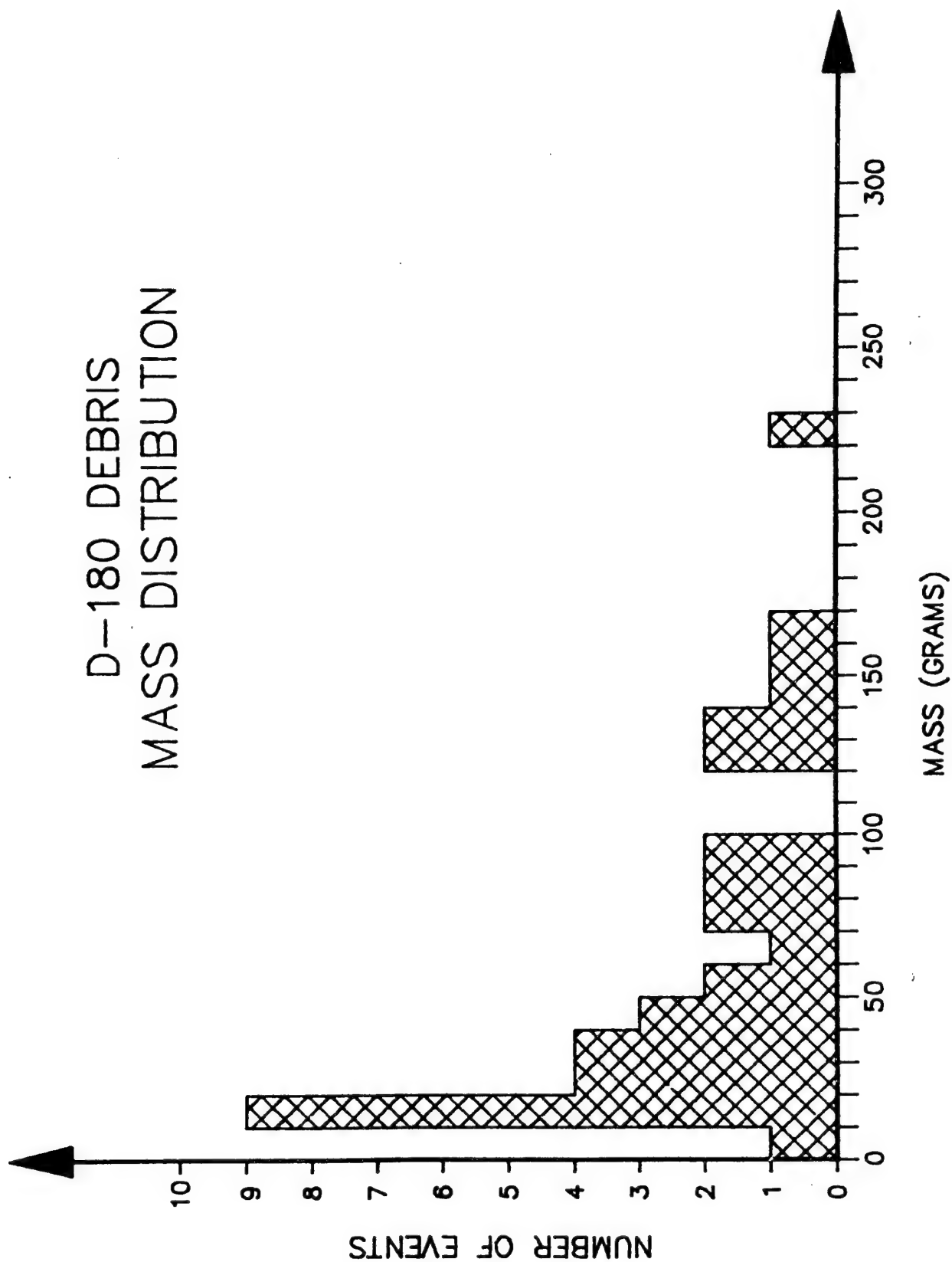


Figure 3-16 Mass distribution observed by meteor radar.

TABLE 3-8

AMOS/MOTIF/GEODSS Sensors

INSTRUMENT	PRIMARY APERTURE (CM)	DETECTOR FIELD OF VIEW
AMOS/AATS	20.3	3.0°
AMOS/ASR	159.6	*
AMOS/IRCCD	159.6	3.3'
MOTIF/AATS	15.2	3.0°
MOTIF/L ³ TV (B37)	121.9	260" X 130"
GEODSS-1	101.6	2.1°
GEODSS-2	101.6	2.1°
GEODSS-3	38.1	6.0°

* Not available in AMOS facilities manual.

The AATS is primarily used for the acquisition of visible targets. However, during the Delta-180 measurement campaign it also served as a principal detector. The AATS combines good sensitivity with multiple field-of-view options -- these are 3° , 0.5° , and 0.1° . Fields-of-view can be changed as the target is centered in each to provide more precise tracking (Figure 3-18). Within the AATS, two optical systems provide the three fields-of-view which are fed to a common Intensified Silicon Intensifier Target (ISIT) television sensor. The 1.6m AATS has a 0.56m Richey-Chretien mirror which provides the 0.5° and 0.1° fields. The 3° field is provided by a 0.20m catadioptric system. The television sensor itself is a Quantex QX-11 ISIT vidicon having a 40mm cathode.

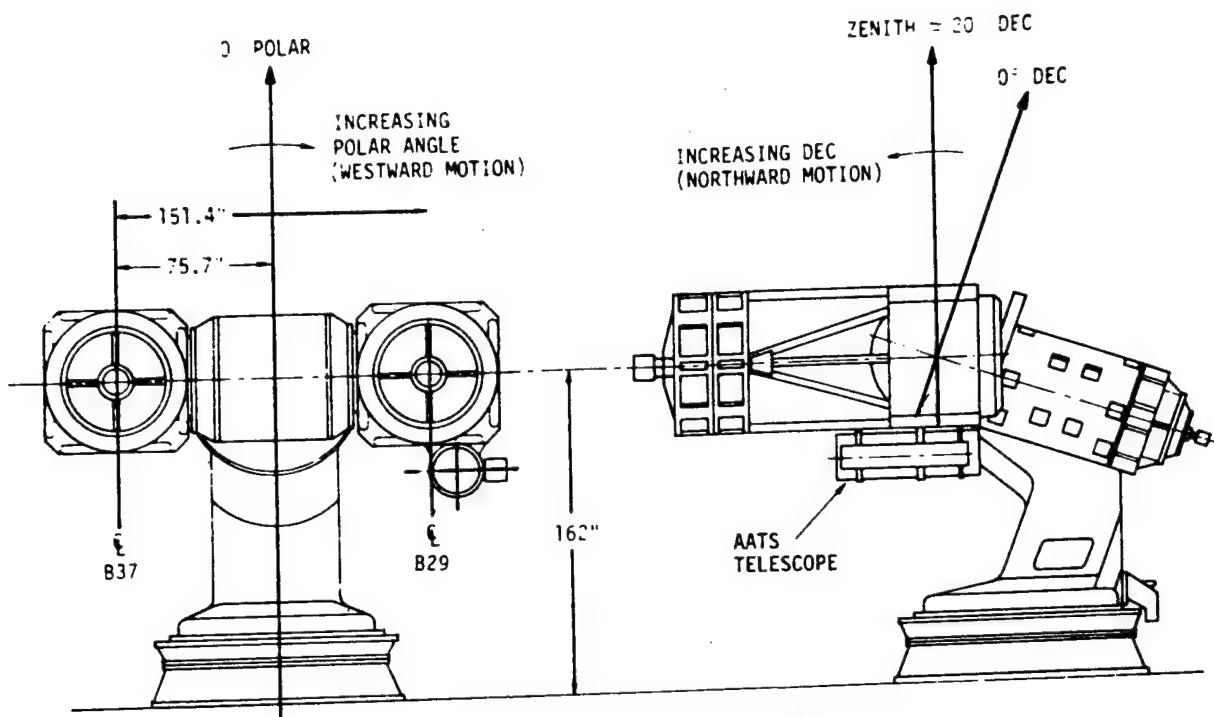
The AMOS telescope is mounted on a high performance three-axis mount. Each mount is a standard equatorial mount carried on an azimuth turntable. Tracking is done in the polar and declination axes with the azimuth turntable set to a fixed position optimized for the track. Mount capabilities include angular accelerations of 2 degrees/sec², angular tracking of 10 degrees/sec, and pointing to 2 to 3 arcseconds.

MOTIF

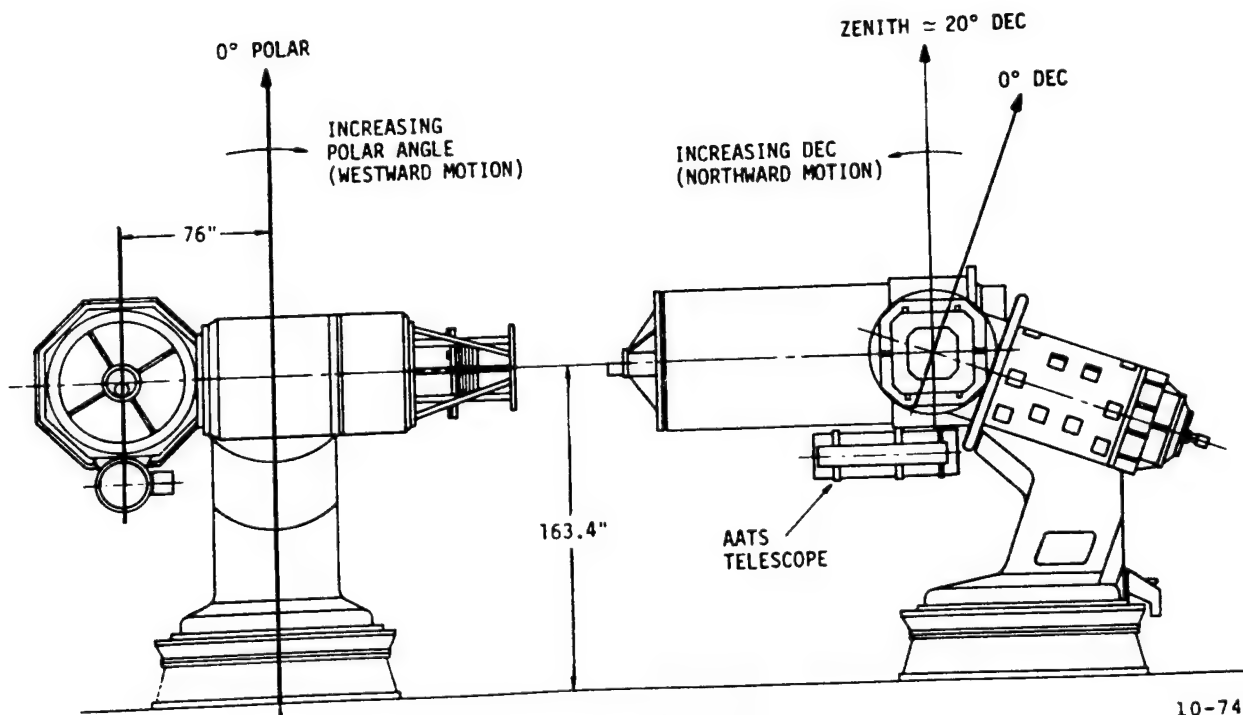
The MOTIF optical system consists of dual 1.2m telescopes mounted on opposite sides of a single polar axis; they are fixed to a common declination axis. The instrument is illustrated in Figure 3-17. Both telescopes are of classical Cassegrain design. One telescope, designated B29, has a 29-inch back focal distance; it has a focal length of 24.5m, a plate scale of 8.4 arcseconds/mm, and is used primarily for Long Wavelength Infrared (LWIR) and photometric data collection.

The other 1.2m telescope, designated B37, has a 37-inch back focal distance and two instrument mounting surfaces; it

Figure 3-17 AMOS and MOTIF instrument plan views.



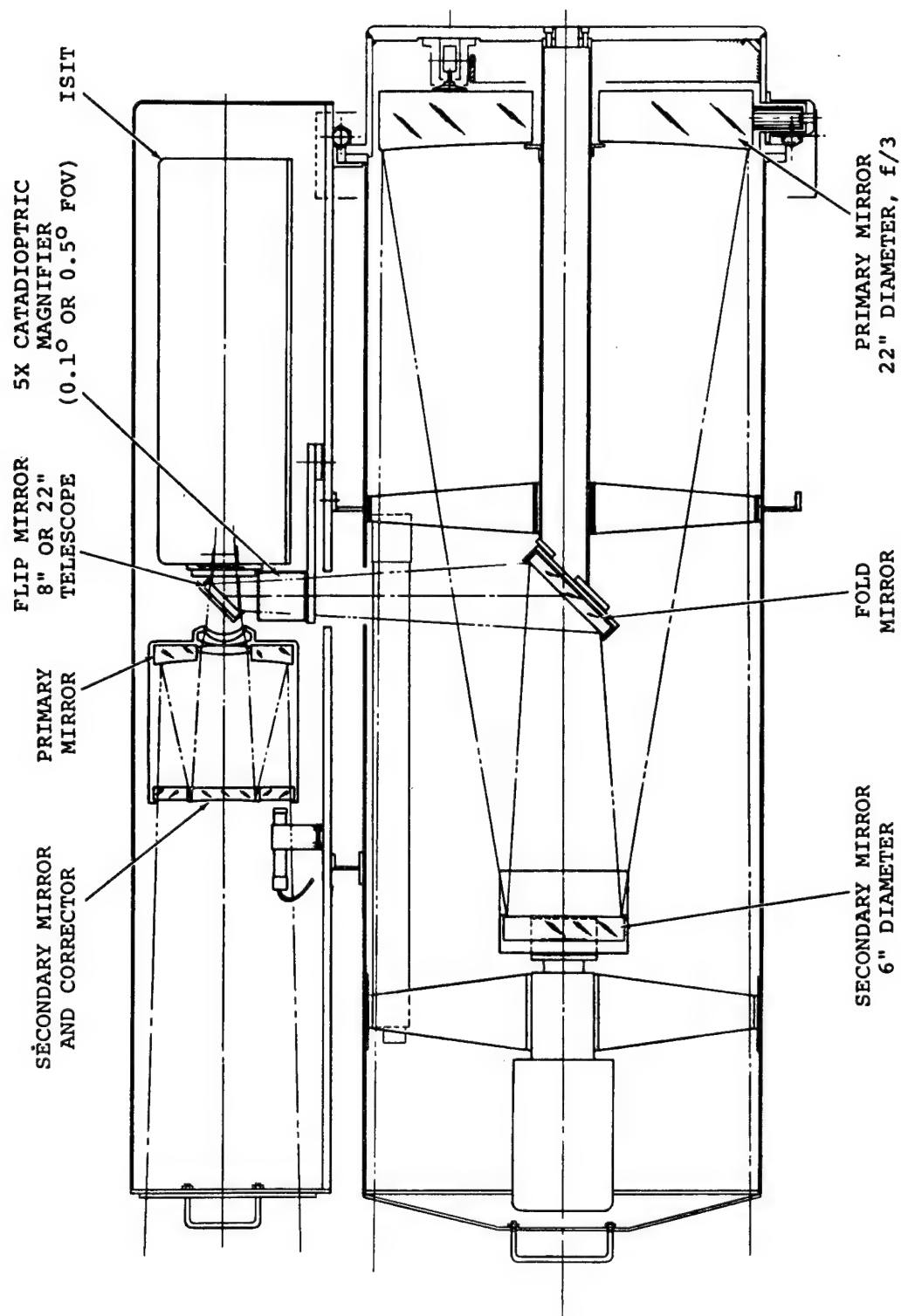
DUAL 1.2m TELESCOPE



1.6m TELESCOPE

10-741

Figure 3-18 AATS optical diagram.



has a focal length of 19.8m and an image scale of 10.4 arcseconds/mm at the Cassegrain focus. The B37 telescope is normally used for low light level signal detection and imagery as it was for the Delta-180 campaign.

As for the AMOS 1.6m telescope, the MOTIF system has an AATS dual aperture instrument mounted piggy-back on the B29 telescope. The AATS on B29 is virtually identical to the AATS mounted on the 1.6m AMOS instrument, with one exception; the 3° field is provided by a 0.15m lens. The television sensor is the same.

GEODSS

The final group of ground-based electro-optical detectors used during the Delta-180 observations were the three telescopes comprising the GEODSS facility on Maui; these are designated simply as GEODSS 1, GEODSS 2, and GEODSS 3. The three domes housing the GEODSS instruments are shown in Figure 1-2.

Each of these three telescopes is of standard Cassegrain design. The diameters and focal lengths of GEODSS 1, GEODSS 2, and GEODSS3 are: (D=1.02m, FL=2.18m), (D=1.02m, FL=2.18m) and, (D=0.38m, FL=0.76m), respectively. The fields of view associated with each are 2° for GEODSS 1 and 3, and 6° for GEODSS 2.

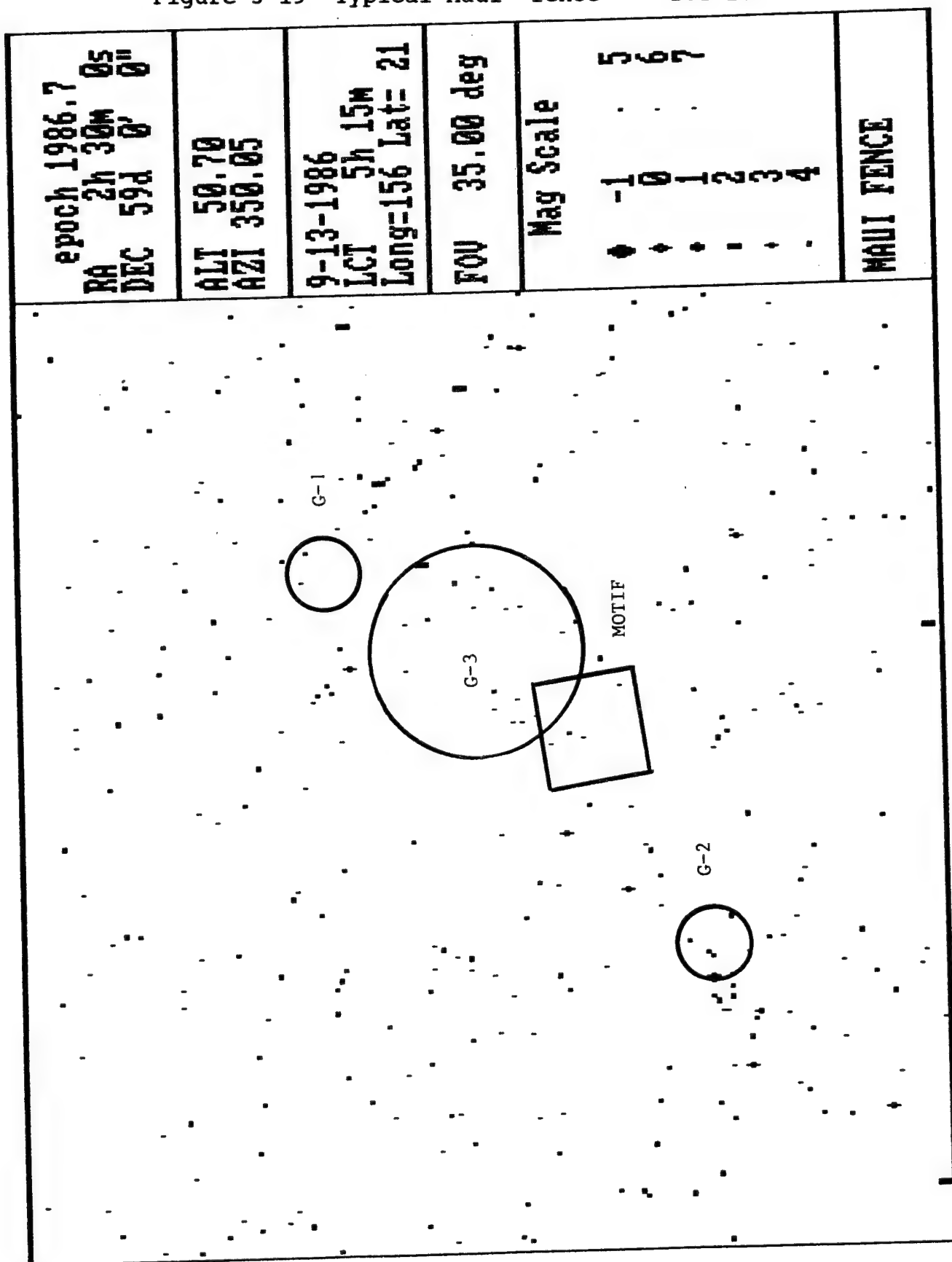
Because the GEODSS software was designed for "deep space" operations, new operational techniques had to be developed in order to observe objects in low earth orbit. The only procedure that would allow the telescopes to point to a particular spot in the sky, then follow that spot at the sidereal rate, was to input a satellite number whose orbital elements were in the GEODSS computer. When the satellite number was entered, the telescopes would move to the position

of the satellite at that time, and begin tracking the stars at the sidereal rate. However, the orbital period of the satellite had to be greater than 225 minutes in order to qualify as a "deep space" object, and computer software would only accept deep space objects. Since all of the Delta-180 objects had periods closer to 90 minutes, and because it was desired to detect objects whose exact orbital elements were not known, procedures to deceive the GEODSS computers programs had to be developed.

The procedure which was developed follows. Using known orbital elements, the AMOS/MOTIF computers were used to predict the path of objects across the sky as seen from Haleakala (i.e., azimuth and elevation as a function of time). This data was plotted in polar coordinates and used to approximately define the orbital plane of the fragments. Both theory and some experience had already suggested that the most sensitive position of the telescopes would be to point at the zenith to about thirty degrees away from the zenith in the direction away from the sun. However, in practice a given object, or its orbital plane may not be placed where lighting conditions are favorable. Therefore, these plots were used to determine when and where the most favorable conditions were approached.

Using the plots, azimuths and elevations were determined for each telescope such that each telescope became a picket in a "fence" which was perpendicular to the orbital plane (see Figure 3-19). The pointing information required to create this situation was given to Teledyne Brown Engineering, who then calculated "simulated" orbital element sets for each point in the sky that was to be observed with the telescopes. The chief characteristic of these fake orbital element sets is that the fake object would pass through the predetermined point in the sky at the time the observations with the telescopes were to begin. Typically, the fake objects had

Figure 3-19 Typical Maui "fence" -- DOY 256.



near circular orbits slightly greater than geosynchronous altitudes. Using orbits of higher fake altitudes tended to reduce telescope pointing errors caused by not pointing at the object at exactly the right time.

The fake orbital element sets used in the fence generation were entered into NORAD computers with numbers beginning with 89391; these were then transferred to GEODSS computers. Instructions were sent from NORAD to set up a fence using these objects at a particular GMT, and to record data for a given amount of time. After the observing was completed, the fake objects were deleted from the NORAD and GEODSS computers to prevent confusion for observations on the next day.

The data obtained with the GEODSS telescopes were different from the AMOS, MOTIF, and Kwajalein data in that it was preprocessed. Whereas in all of the other detectors a simple video image was recorded with a full gray scale of pixel values, the images recorded with the GEODSS detectors were of a threshold type. If the signal strength at a certain location was less than a specified value, no response was indicated; however, if the signal was greater than that minimum, the value was set to a constant. In essence the detection mode was binary -- either on or off.

Further, instead of a 1/30th of a second framing rate, the data provided to JSC was updated every 12/30ths of a second. The chief advantage to this mode of data recording was that every satellite appeared as a short streak on the detector field as opposed to a dot that might be mistaken for noise.

In addition, the tapes could also be processed to remove the background starfield. However, using the JSC Video Digital Analysis System (VDAS) facility, it was found that the starfields were useful for registration of each image against the celestial coordinate system. The registration procedure will be described in Section 3.5.

Ground-based optical observations were obtained on eight out of ten days. Two days were completely lost to clouds -- September 9th and 10th. Partial cloudiness and/or haze were reported for September 8th, 11th, and 14th. Clear sky conditions prevailed on the 12th, 13th, and 15th.

3.4 Airborne Optical Measurements

During the post-EOM phase of the Delta-180 experiment, image data were obtained of fragments of satellites 16937 and 16938 using two optical systems flown on board an Aeromet Learjet. The base of airborne operations was the Kwajalein Atoll. The Learjet Optical System (LOS) integration and support was provided by Aeromet, Inc. A description of the instrumentation and mission mode follows.

The LOS consists of three optical windows installed in the right side of the Aeromet Learjet as shown in Figure 3-20. The LOS had two optical platforms, each with a stabilized mirror for tracking of targets at the forward and aft positions -- windows #1 and #2, respectively. Further, an Aeromet-developed Airborne Pointing System (APS) utilized the predicted satellite files combined with data from the on-board navigation system to generate pointing information for the stabilized mirrors. Data were recorded on videotape. Timing information was provided by an on-board timing system, which was synchronized to the Kwajalein Missile Range (KMR) timing system.

During the Delta-180 mission, only the forward and aft windows were used by the two optical systems. A Lenzar Low Light Level Television (LLTV) was mounted on the forward platform while a dual wide field of view (WFOV)/narrow field of view (NFOV) video system was mounted on the aft platform. A diagram of the interior layout is shown in Figure 3-21. The pertinent characteristics of the optical systems are given in Table 3-9.

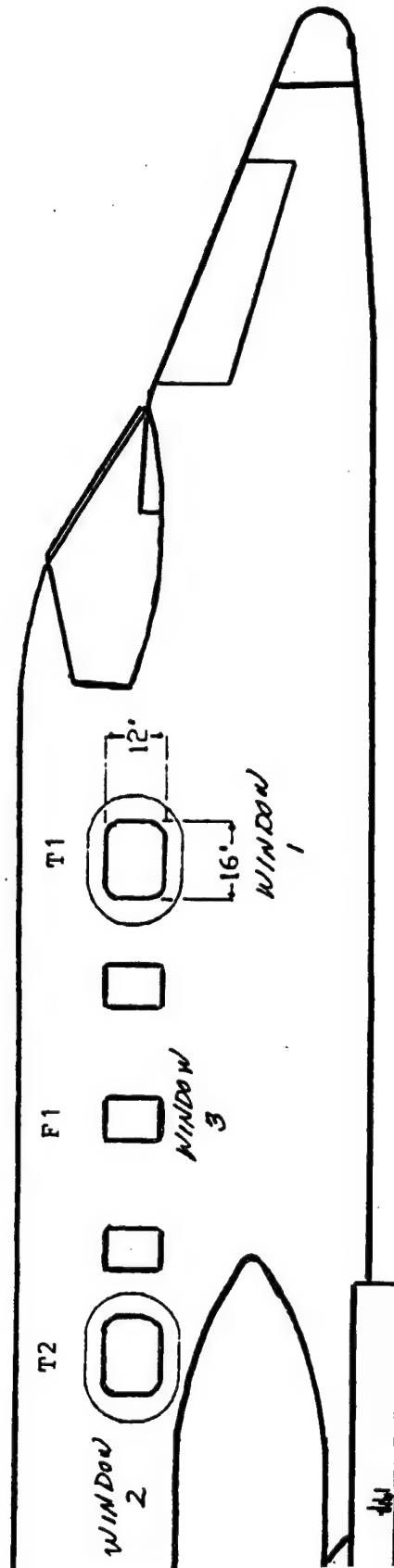


Figure 3-20 Optical window installation on Aeromet Learjet.

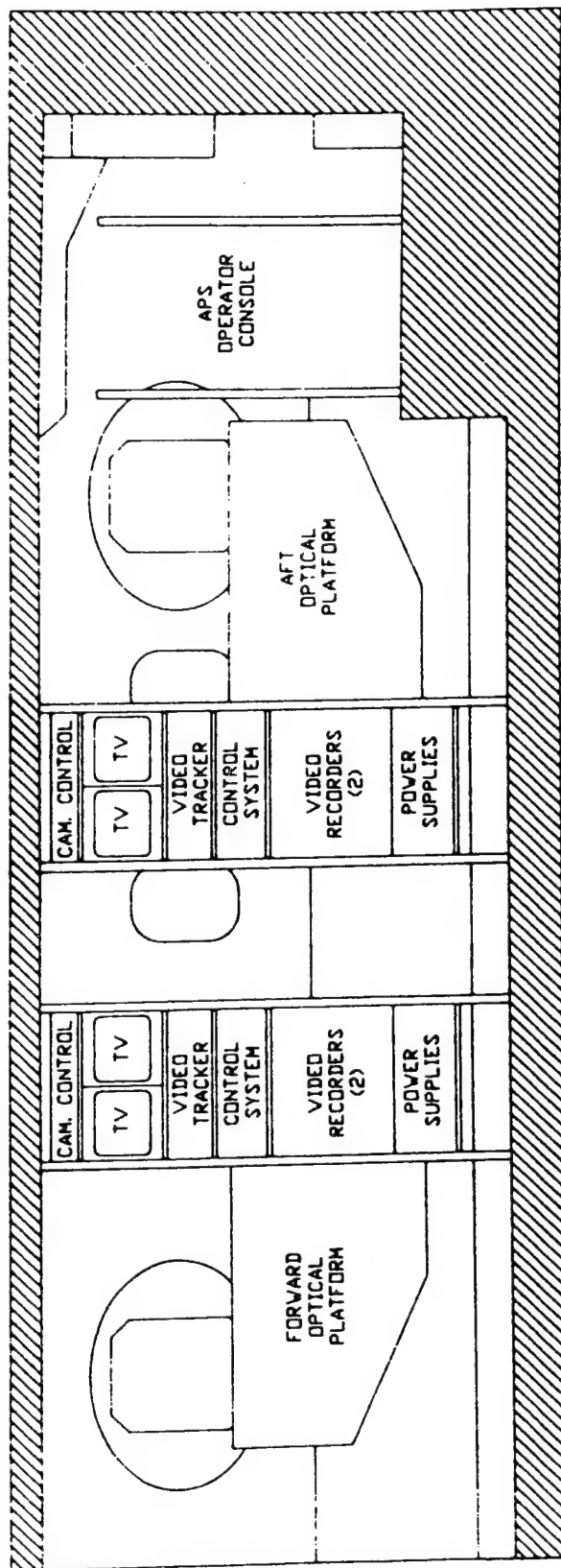


Figure 3-21 APS equipment layout on Aeromet Learjet.

TABLE 3-9

Learjet Optical Observing Site
Optical Systems Specifications

Instrument	Field-of-View		Focal Length (f/ ratio)	Camera Type	Frms./Sec.
	Horiz.	Vert.			
Lenzar	1.9°	X 1.9°	220mm (f/1.35)	Video (SIT)	30
WFOV	7.3°	X 5.5°	100mm (f/1.80)	Video (SIT)	30
NFOV	1.44°	X 1.08°	508mm (f/5.70)	Video (SIT)	30

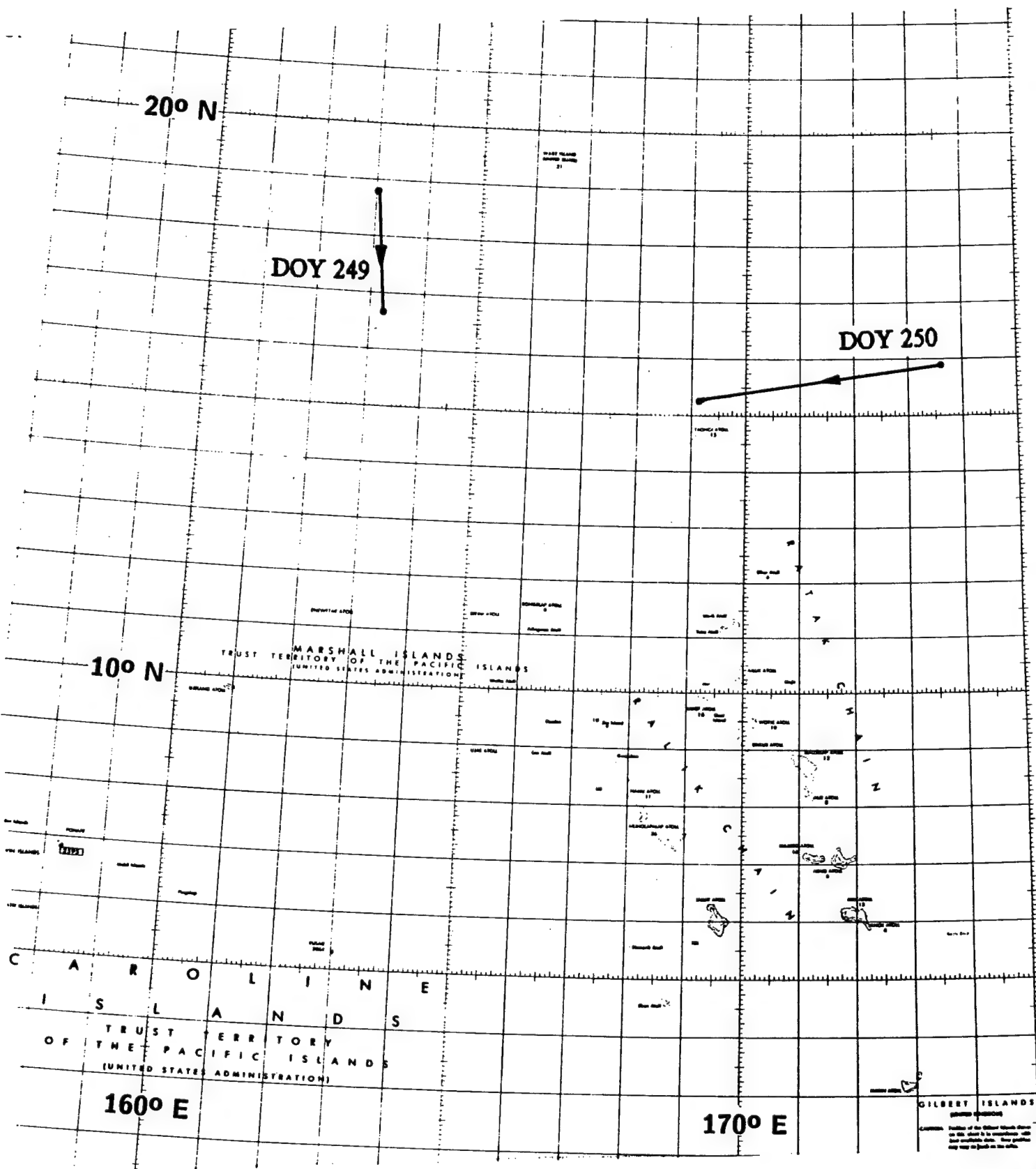
The mission plan called for two flights -- one on DOY 249 (September 6, 1986) and one on DOY 250 (September 7, 1986). During the first flight the Learjet arrived on station at 18:15:23 UT; its coordinates were Latitude: 18.7447° N, Longitude: 163.0124° E, and Altitude: 39,000 feet. The aircraft maintained a SSE heading, ending the data run at 18:34:09 UT; its coordinates were then Latitude: 16.6745° N, Longitude: 163.2432° E, and Altitude: 39,000 feet (Figure 3-22). The duration of the data gathering run was 00:18:24. No significant observations were obtained because the Learjet was located eastward (toward the sun) from the debris objects. Sunlight scattered by the atmosphere at the Learjet position was too intense to permit detection of debris objects west of the aircraft.

During the second flight a modified flight plan was used, such that the sensors looked northwards. This minimized the effects of scattered sunlight. The Learjet arrived on station at 17:05:00 UT; its coordinates were Latitude: 15.9349° N, Longitude: 173.6170° E, and Altitude: 43,000 feet. The aircraft maintained a WSW heading, ending the data run at 17:54:59 UT; its coordinates were then Latitude: 15.1082° N, Longitude: 167.8437° E, and Altitude: 43,000 feet (Figure 3-22). The duration of the data gathering run was 00:49:59. During that period of time a total of 18 "events" were recorded. The convention adopted here is that an "event" is any detection of any streak in any of the detectors.

3.5 Optical Data Reduction Procedures

Although the specific characteristics of each optical detector system were quite different from one another, the final form of the data delivered to JSC for reduction and analysis, was that of a video-tape record. The reduction and analysis procedures were similar for each data set regardless of source.

Figure 3-22 Learjet groundtracks DOY 249 and DOY 250.



A total of 98 video tapes were received at the JSC VDAS lab within several weeks of the end of mission. The tapes fell into two categories -- premission test tapes (25%) and post-EOM data tapes (75%). The tapes were logged in as they were received; each was assigned a serial number in the order of receipt.

The first task was to screen the data tapes for observable "events", which were defined as the appearance of an object passing through the field of view. To aid in this screening process, an optical data screening form was designed -- a sample is shown in Figure 3-23.

In depth screening of the tapes was restricted to those tapes designated as high priority. In coordination with the JSC Delta-180 field team, 23 tapes were identified as falling into this category. These tapes represented data from DOY 249, 250, 256, 257, and 258.

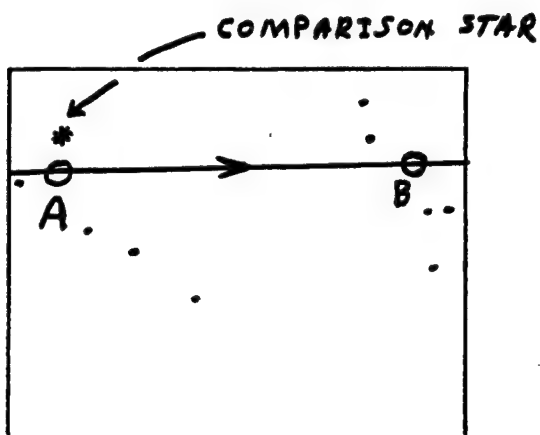
The screening was done using a video-tape replay unit and Inter-Range Instrumentation Group - B (IRIG-B) time decoder. Noted during the screening were time of the event, duration of the event, and apparent direction of travel. This information, was useful as a zeroth order discriminator in separating Delta-180 from non-Delta-180 events.

During the screening process a total of 80 casually identifiable events were recorded (Table 3-10). The phrase "casually identifiable" here means that the events were detected without any special enhancement. Of these, 21% were recorded using the airborne detectors, 29% with the AMOS/MOTIF instruments, and 50% with the three GEODSS telescopes.

Because some events were recorded simultaneously with more than one detector, the coincidence-corrected count is 64 unique events.

INDEX NO 11 OPTICAL DATA SCREENING FORM
 DAY 86250 TAPE NO 30 LOCATION LONG.: 188.6022 W
 DETECTORS/INSTRUMENT LENZAR / AIRBORNE FOV 2°
 FIELD COORDINATES: RA ~ 3h DEC ~ 75°
 AZI ~ 355° ELE ~ 30°
 T30: START 17:19 STOP 17:52

EVENT NO 11 IRIGB TIME 250:17:24:31 DUR 1.4 s FOV DEG 2°
 SAO FIELD: RA 3:03:29 DEC +76.9245 FOV 3° FNAME SAOSTARS
 PER 88.9 ALT 239 km INC 23.8 ☒ A RA 2:54:49
 DEC +76.2298



TIME 17:24:31.8
 FNAME LEN3A FR# 108
 xZM yZM
 xTR yTR ROT
 SATx SATy
☒ B RA 3:18:21
 DEC +76.7103
 TIME 17:24:33.2

STR+SKYxAREA 15546
 SKYxAREA 9369 STR MAG 9.2
 OBJ+SKYxAREA 11099
 SKYxAREA 9407 OBJ MAG 10.6

FNAME LEN3B FR# 149
 xZM yZM
 xTR yTR ROT
 SATx SATy

COMMENTS: GROUND TRACK ...

A: LONG: 188.34 W AZI.: 355.9
 LAT: 18.97 N ELE.: 28.8
 B: LONG: 188.44 W AZI.: 357.5
 LAT: 18.99 N ELE.: 28.6

= CROSS REFERENCE:

=
 = NID COINCIDENT
 = OBSERVATIONS.
 =
 =

Figure 3-23 Typical optical data screening form.

TABLE 3-10

Time-ordered Event List
Delta-180 Optical Observations

EVENT	DAY/TIME	DETECTOR	IDENTIFICATION /	COINCIDENT
				EVENTS
01	249:14:51:11	1.6-M/AATS	METEOR	
02	249:14:58:55	1.6-M/AATS	INTERLOPER SATELLITE	
03	249:15:01:49	1.6-M/AATS	INTERLOPER SATELLITE	
04	250:17:07:14	AIRBORNE/WFOV	METEOR	
05	250:17:15:07	AIRBORNE/WFOV	METEOR	
06	250:17:18:48	AIRBORNE/WFOV	INTERLOPER SAT./#7	
07	250:17:18:48	AIRBORNE/LENZAR	INTERLOPER SAT./#6	
08	250:17:20:22	AIRBORNE/WFOV	INTERLOPER SAT./#9,10	
09	250:17:20:30	AIRBORNE/LENZAR	INTERLOPER SAT./#8,10	
10	250:17:20:40	AIRBORNE/NFOV	INTERLOPER SAT./#8,9	
* 11	250:17:24:31	AIRBORNE/NFOV	***** DELTA-180 *****	
12	250:17:27:25	AIRBORNE/WFOV	INTERLOPER SAT./#13	
13	250:17:27:34	AIRBORNE/NFOV	INTERLOPER SAT./#12	
14	250:17:40:21	AIRBORNE/NFOV	INTERLOPER SAT./#16,17	
15	250:17:40:33	AIRBORNE/WFOV	INTERLOPER SAT./#18,19	
16	250:17:40:37	AIRBORNE/WFOV	INTERLOPER SAT./#14,17	
17	250:17:40:41	AIRBORNE/LENZAR	INTERLOPER SAT./#14,16	
18	250:17:40:46	AIRBORNE/LENZAR	INTERLOPER SAT./#15,#19	
19	250:17:40:56	AIRBORNE/NFOV	INTERLOPER SAT./#15,18	
20	250:17:43:33	AIRBORNE/WFOV	INTERLOPER SAT./#21	
21	250:17:43:38	AIRBORNE/NFOV	INTERLOPER SAT./#20	
22	256:14:50:17	GEODSS-3	INTERLOPER SATELLITE	
23	256:14:50:30	GEODSS-1	INTERLOPER SATELLITE	
24	256:14:51:00	GEODSS-1	INTERLOPER SATELLITE	
25	256:14:53:52	GEODSS-3	INTERLOPER SATELLITE	
26	256:14:55:00	GEODSS-3	INTERLOPER SATELLITE	
* 27	256:14:55:43	GEODSS-3	**** DELTA-180 ****	

28	256:15:04:20	GEODSS-1	METEOR
29	256:15:09:16	1.2-M/AATS	METEOR
30	256:15:09:17	1.2-M/AATS	INTERLOPER SATELLITE
31	256:15:10:17	GEODSS-1	INTERLOPER SATELLITE
* 32	256:15:12:22	1.2-M/AATS	**** DELTA-180 ****/#33
33	256:15:12:22	1.2-M/LLTV	**** DELTA-180 ****/#32
34	256:15:12:49	1.2-M/AATS	INTERLOPER SATELLITE
35	256:15:12:53	1.2-M/AATS	METEOR
36	256:15:13:25	GEODSS-2	INTERLOPER SATELLITE
* 37	256:15:18:10	GEODSS-2	**** DELTA-180 ****
38	256:15:18:43	GEODSS-1	INTERLOPER SATELLITE
39	256:15:18:49	GEODSS-3	INTERLOPER SAT./#40
40	256:15:19:11	1.2-M/AATS	INTERLOPER SAT./#39
* 41	256:15:19:53	GEODSS-2	**** DELTA-180 ****
42	256:15:19:55	1.2-M/AATS	INTERLOPER SATELLITE
* 43	256:15:20:53	GEODSS-2	**** DELTA-180 ****
* 44	256:15:23:30	1.6-M/AATS	**** DELTA-180 ****
* 45	256:15:24:44	GEODSS-1	**** DELTA-180 ****
46	257:14:57:51	GEODSS-1	METEOR
47	257:14:57:55	1.2-M/AATS	METEOR
48	257:14:58:07	GEODSS-2	INTERLOPER SATELLITE
49	257:14:58:33	GEODSS-3	METEOR
50	257:15:03:46	GEODSS-2	METEOR
51	257:15:04:30	GEODSS-2	INTERLOPER SATELLITE
52	257:15:04:35	GEODSS-3	METEOR
* 53	257:15:07:00	1.6-M/AATS	**** DELTA-180 ****
54	257:15:07:13	1.2-M/AATS	METEOR
55	257:15:08:51	1.2-M/AATS	METEOR
56	257:15:10:18	GEODSS-2	INTERLOPER SATELLITE
57	257:15:12:06	1.6-M/AATS	INTERLOPER SATELLITE
58	257:15:13:01	GEODSS-2	INTERLOPER SATELLITE
59	257:15:13:13	GEODSS-1	INTERLOPER SATELLITE
60	257:15:13:56	GEODSS-3	INTERLOPER SATELLITE
61	257:15:16:22	GEODSS-2	INTERLOPER SATELLITE
62	257:15:24:36	1.2-M/AATS	METEOR
63	257:15:27:28	1.2-M/AATS	INTERLOPER SAT./#64
64	257:15:27:36	GEODSS-3	INTERLOPER SAT./#63

65	258:15:03:03	GEODSS-2	METEOR
66	258:15:03:08	GEODSS-3	METEOR
67	258:15:05:50	GEODSS-2	INTERLOPER SATELLITE
68	258:15:07:30	GEODSS-3	INTERLOPER SATELLITE
69	258:15:08:00	1.2-M/AATS	METEOR
70	258:15:08:46	GEODSS-1	INTERLOPER SAT./#71
71	258:15:08:54	GEODSS-3	INTERLOPER SAT./#70
72	258:15:10:09	GEODSS-1	METEOR
73	258:15:18:54	1.2-M/AATS	INTERLOPER SAT./#74,75
74	258:15:18:54	GEODSS-2	INTERLOPER SAT./#73,75
75	258:15:19:13	GEODSS-3	INTERLOPER SAT./#73,74
76	258:15:25:15	1.2-M/AATS	INTERLOPER SAT./#77
77	258:15:25:18	GEODSS-2	INTERLOPER SAT./#76
* 78	258:15:28:25	GEODSS-3	**** DELTA-180 ****
79	258:15:33:16	GEODSS-1	INTERLOPER SATELLITE
80	258:15:33:20	GEODSS-3	INTERLOPER SATELLITE

<1> Asterisks in Column 1 identify principal observation of a Delta-180 fragment; redundant observations are noted in column 4.

<2> Total number of unique events : 64.

<3> Totals by category:

Delta-180 pieces:	10	(15.4%)
Interloper satellites:	37	(56.9%)
Meteors:	18	(27.7%)

Using the screening forms, individual events were identified as being worth more detailed investigation. Video frames for a given event were selected using the JSC VDAS Real Time Disk system. For any given event, the observation spanned a finite time ranging from a second to 45 seconds. The video frames for an event were selected with the maximum possible time base.

The two chosen frames were designated Event (X)/ Frame A, for the one near the beginning of the sequence, and Event (X)/ Frame B for the one at the end of the sequence. The IRIG-B time was noted for Frame A as well as the total number of frames between Frame A and Frame B. The framing rate provided the duration of the event.

A VDAS program, STARGEN, was used to overlay a Smithsonian Astrophysical Observatory (SAO) starfield on each frame. The program allowed correction for rotation and magnification of the SAO field to match the video frame field. Further, when distortions were a problem, the VDAS program TIE-POINT was used to allow for geometric distortion correction. Once the starfield had been registered, the R.A. and Dec. were measured for each of the frames in question. These values, along with the time (UT), were recorded. The procedure was repeated for the B frame.

With coordinates and time in hand an orbit was calculated for each event assuming eccentricity 0.0. This was satisfactory to determine inclination, which was used as the primary discriminant to cull Delta-180 objects from non-Delta-180 objects.

A total of 10 of these events were identified as Delta-180 debris fragments -- 2 tracked with AMOS (described in more detail below), 1 observed with the airborne platform, and 7 detected by the Maui fence. The Delta-180 fragment

observations are summarized in Table 3-11. Of all of the optical events 15% were Delta-180 related, 57% were unidentified satellite interlopers, and 28% were meteors. A more complete discussion of the information derived from these observations is presented in section 4.4.

With AMOS operating in the tracking mode two Delta-180 targets were acquired and tracked for extended periods of time. The first, acquired on DOY 256 at 15:23:30, was tracked for 80 seconds; the satellite object catalog number was 88290. From the NORAD data set of 01-OCT-86 this particular fragment had a period of 101.8 min, an eccentricity of 0.0867, perigee height of 216km, and inclination of 23.0495° . A magnitude could not be determined for the object in that it saturated the detector.

The second object, acquired on DOY 257 at 15:07:00, was tracked for 90 seconds; the object number was 16938 -- the Delta 2nd Stage. From the NORAD data set of 15-OCT-86 this particular fragment had a period of 91.8 min, an eccentricity of 0.0281, perigee of 217km, and inclination of 22.7915° . The RCS was 1.55m^2 . At the time of culmination, 15:08:28 UT the object was at $\text{AZI}=9^{\circ}$, $\text{EL}=68^{\circ}$, and $\text{Range}=290\text{km}$. An estimate of the visual magnitude was obtained and is discussed in Section 4.4.

Examination of the remaining AMOS data consisted of screening the tapes at the times target acquisition was attempted to see if the target object was present. In the aforementioned two cases, identification was trivial; for each of 10 other tracking intervals, approximately 780 frames were co-averaged using routines available at the JSC VDAS facility. The purpose of the procedure was to enhance signal-to-noise and bring up out of the background any faint, but localized, target object. However, no additional target acquisitions were identified. The AATS 3° field was used in all cases including the detection of objects 88920 and 16938.

TABLE 3-11

Delta-180 Fragments Identified from Optical Data

EVENT	PERIOD (MIN)	HT. AT OBS. (KM)	INCLINATION (°)	DOY/TIME (UT)
11	88.93	239	23.8	250:17:24:31
*27	108.00	1167	(42.1)	256:14:55:43
32	~ 80.00	reentry(?)	23.3	256:15:12:22
37	90.30	307	22.7	256:15:18:10
41	91.27	354	23.0	256:15:19:53
43	90.31	307	22.8	256:15:20:53
*45	98.55	707	(26.8)	256:15:24:44
78	133.30	2283	40.3	258:15:28:25

AMOS OBSERVATIONS . . .

SAT. #	PERIOD (MIN)	PERIGEE (KM)	INCLINATION (°)	DOY/TIME (UT)
88290	101.8	216	23.1	256:15:23:30
16938	91.8	217	22.8	257:15:08:28

NOTES: * Orbits were calculated for 37 out of the observed 64 to obtain the above list. Many objects on the original list were eliminated by virtue of observed trajectory.

* Satellite numbers 88290 and 16938 correspond to event numbers #44 and #53 of Table 3-10, respectively.

* Events #27 and #45 are marked with an asterisk to indicate that they may be slightly out of the range appropriate to their respective Delta-180 debris clouds. Typical range for the 23° cloud: 21.95-25.25° and for the 39° cloud: 34.7-41.4°.

* Event #32 was at the right inclination for Delta-180 debris. Apparent angular speed indicates that it is de-orbiting.

4.0 A Comparison of Pre- and Post-Mission Data

This section describes the comparison of pre-mission modeling with the analysis of the post-EOM data. Foremost areas of interest include the number and size distributions of the particles, the linear momentum transfer, the velocity distribution of the debris, the optical correlation of size to magnitude, and the orbital lifetimes of the debris.

A comparison of the radar (Kaena Point) and optical/IR (AMOS, MOTIF, Maui GEODSS) simultaneous observations made on days 256 and 257 (September 13 and 14) will be included in the Appendices of the final report. Reduction and analysis of the end-of-mission data will appear as a separate classified report.

4.1 Piece Counts and Size Distributions

The primary source of data used in this section was the ALTAIR data of days 249, 250 and 251. Only these data contained values of the radar cross section. Subsequent sources were the NORAD satellite catalogs for October 15, 1986 (day 288) and November 14, 1986 (day 318), as well as data supplied by SRS Corp. from the modified meteor radar. (Appendix C of this report).

In modeling the breakup of the Delta-180 satellites, masses of 873kg and 1455kg were input for the masses of the Delta second stage and satellite/PAS combination, respectively. Using these masses, the Delta second stage would produce 300 objects greater than 10cm in diameter, i.e., objects observable by radar, while the SDI satellite would produce 501 objects greater than 10cm in diameter. Thus, a total of 801 pieces would be produced in the breakup.

Alternate values for the satellite mass involved are those contained in Appendix B of this report. In The Collision of Satellites 16937 and 16938: A Preliminary Report, Teledyne Brown states a dry mass of 350kg for the Delta stage, and a dry mass of approximately 1380kg for the SDI satellite. These values produce 120 objects and 475 objects from the Delta stage and satellite. The piece count here totals 595 radar observable pieces.

Unknown at this time are the actual masses of the Delta stage and satellite. Among the unknowns are the mass of any sensor packages attached to the Delta stage, and the amount of liquid propellant on board both vehicles at the time of collision. However, the two alternate sets of mass data above effectively establish an envelope of reasonable values for the number of large objects created in the breakup event.

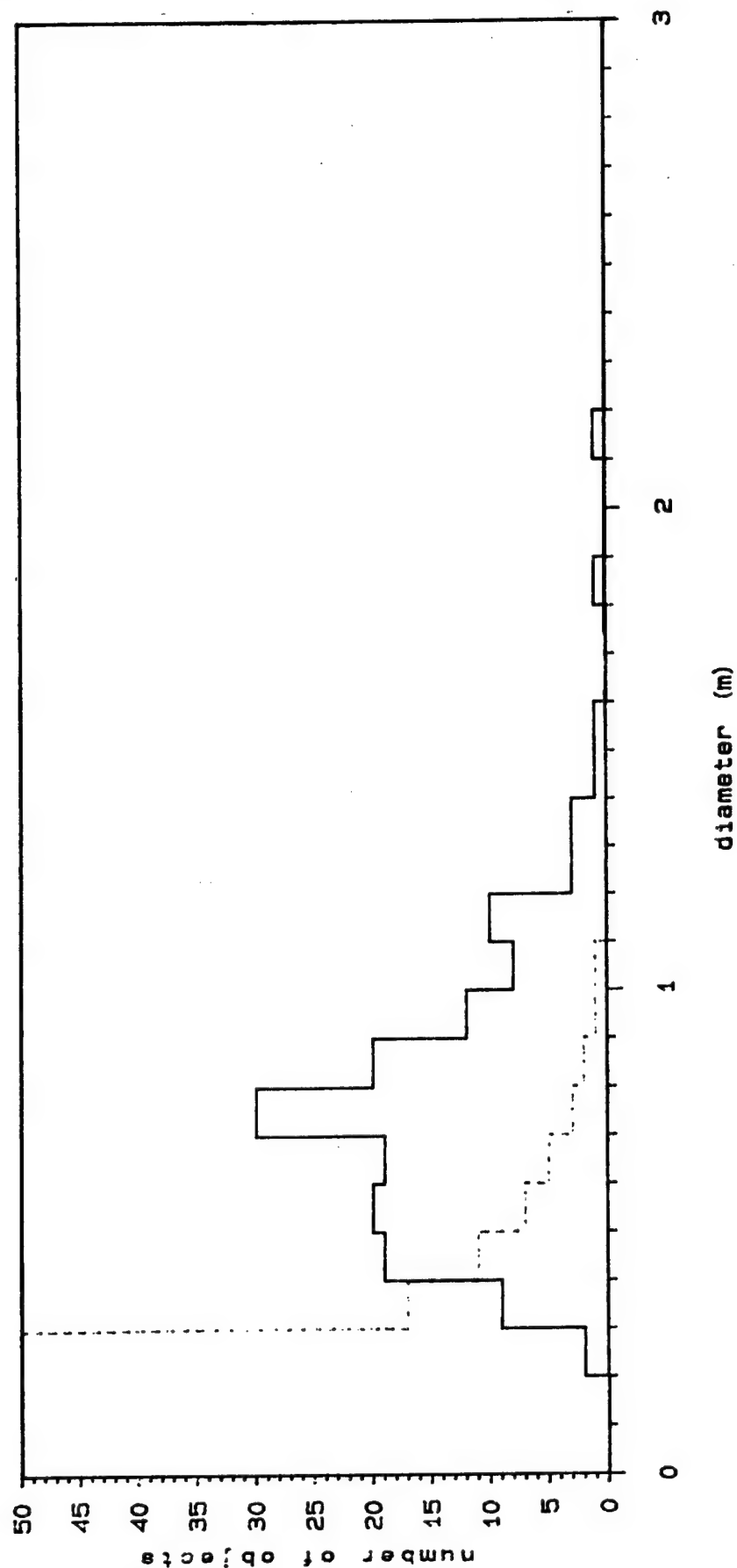
Figures 4-1 through 4-6 show the number of pieces vs. the piece diameter observed by ALTAIR on days 250 and 251. The dotted line in each graph represents the number of pieces predicted to exist at breakup by the computer model. Figure 4-7 depicts the number of objects as a function of diameter for those pieces cataloged by NORAD approximately five weeks after the event. The unusually low values plotted in Figure 4-7 may simply reflect the limited number of pieces catalogued by NORAD.

Perhaps the most striking feature of any of these graphics is the preponderance of fragments in the size range 0.4-1.4m observed in the 23° cloud on day 249, as well as very large fragments (diameter > 1.0m) in the 23° cloud on day 250. This same cloud exhibits a large number of objects in the 0.7-0.8m diameter bin also. Apart from this deviance, number distributions fit the predicted values well. Unfortunately, too few objects were observed in the 39° cloud to form a distribution. However, this cloud, observed on day 251, also

Hazard Analysis Project

ALTAIR data: day 249_23

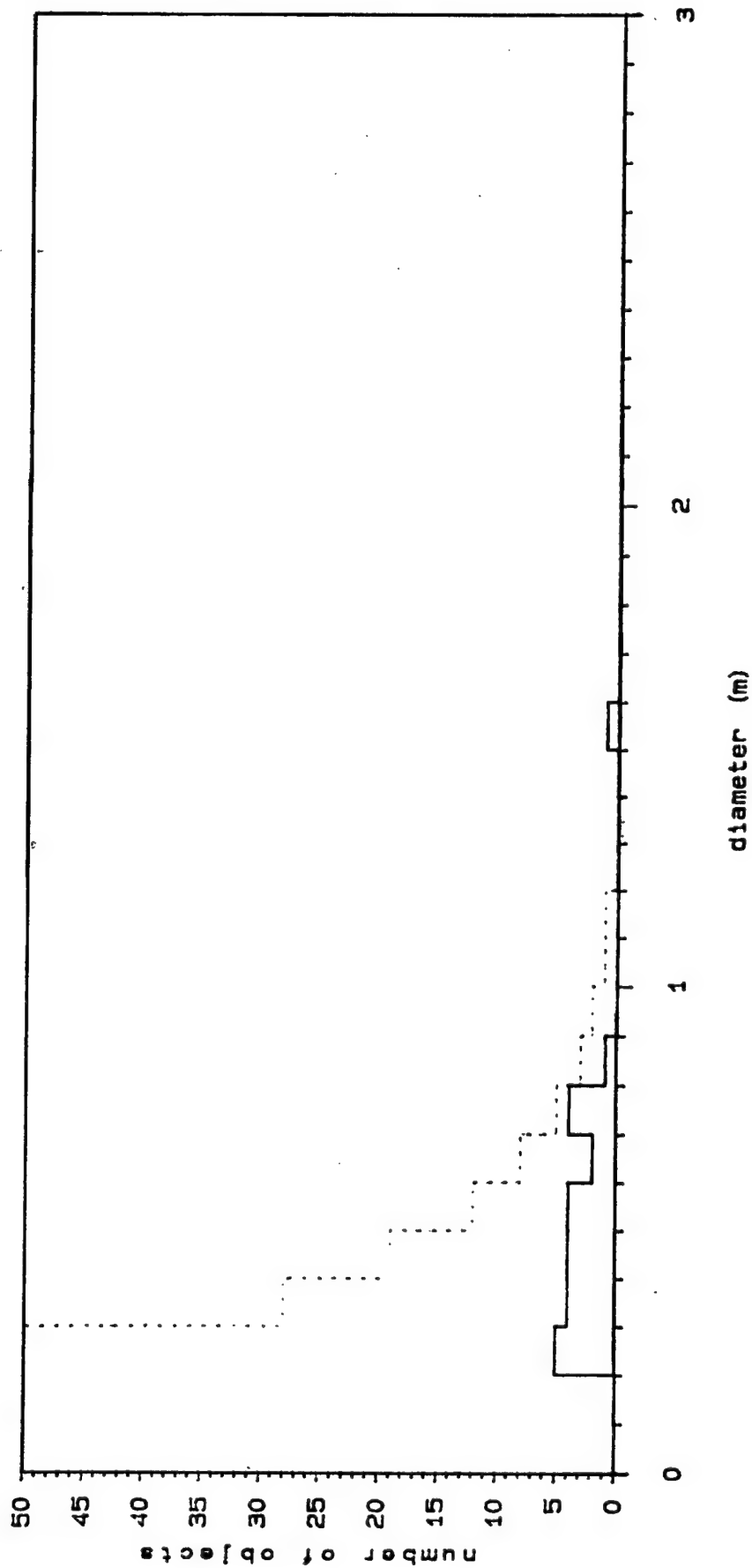
Figure 4-1 Number vs. diameter distribution -- DOY 249, 23^o cloud compared to theoretical distribution.



Hazard Analysis Project

ALTAIR data: day 249_39

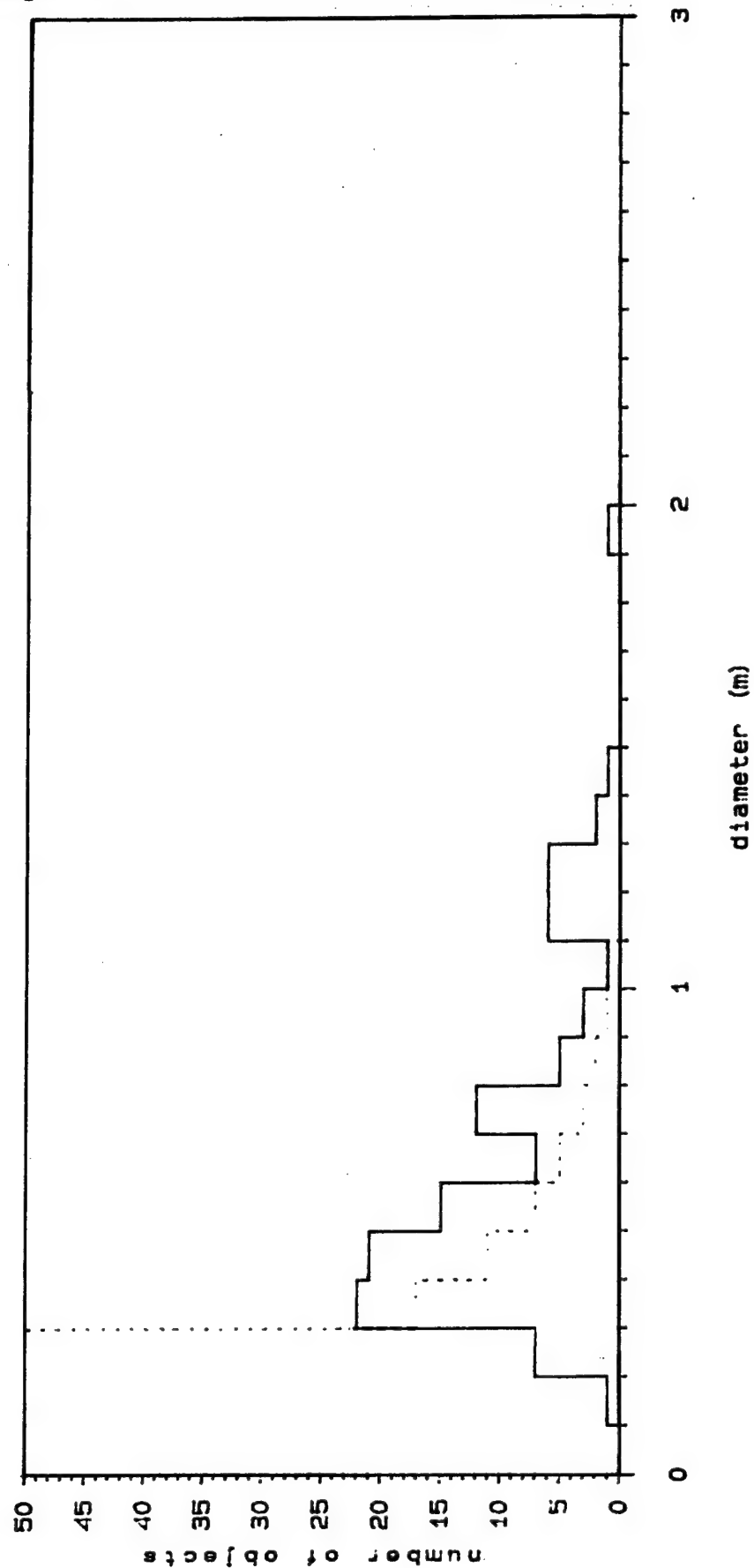
Figure 4-2 Number vs. diameter distribution -- DOY 249, 39° cloud compared to theoretical distribution.



Hazard Analysis Project

ALTAIR data: day 250_23

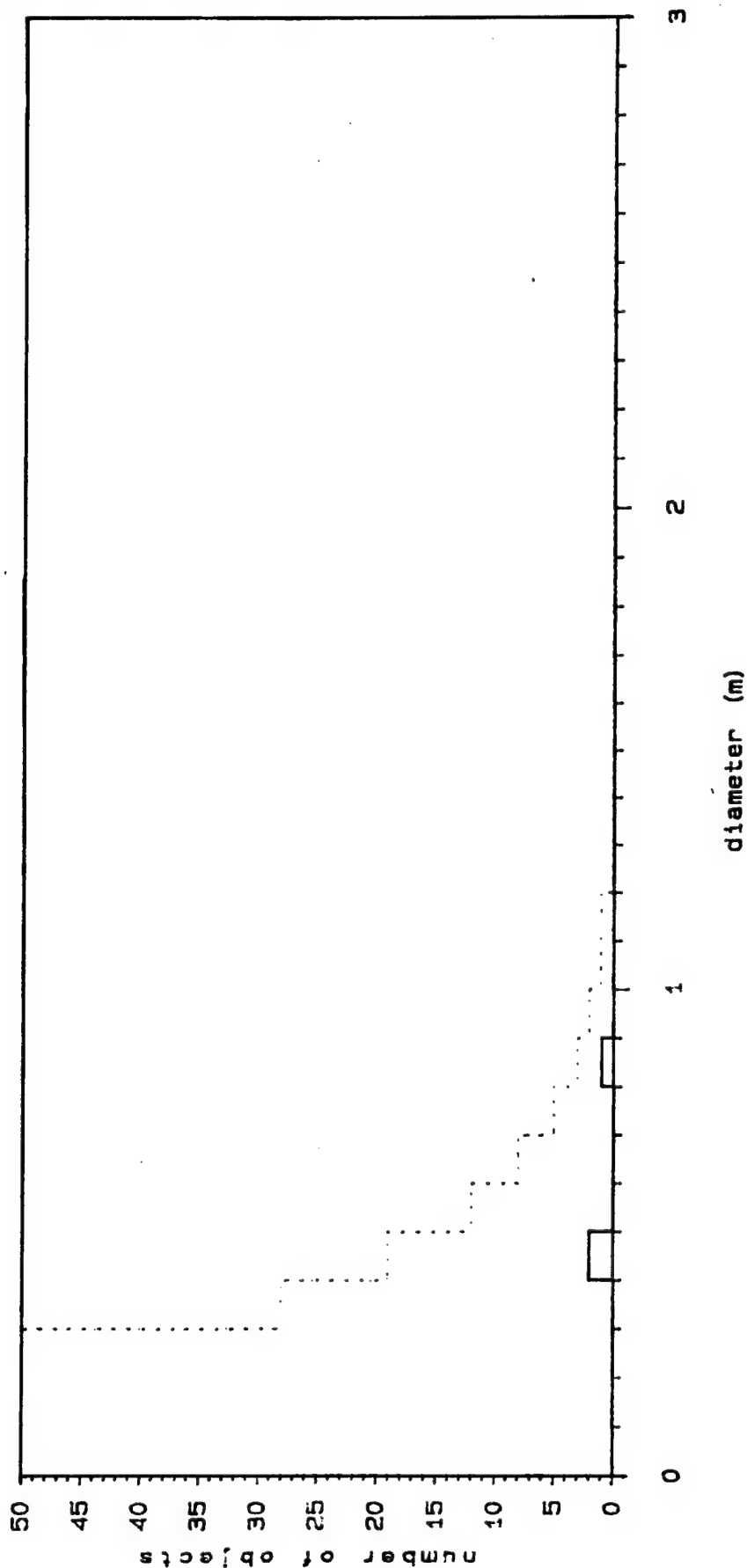
Figure 4-3 Number vs. diameter distribution -- DOY 250, 23° cloud compared to theoretical distribution.



Hazard Analysis Project

ALTAIR data: day 250_39

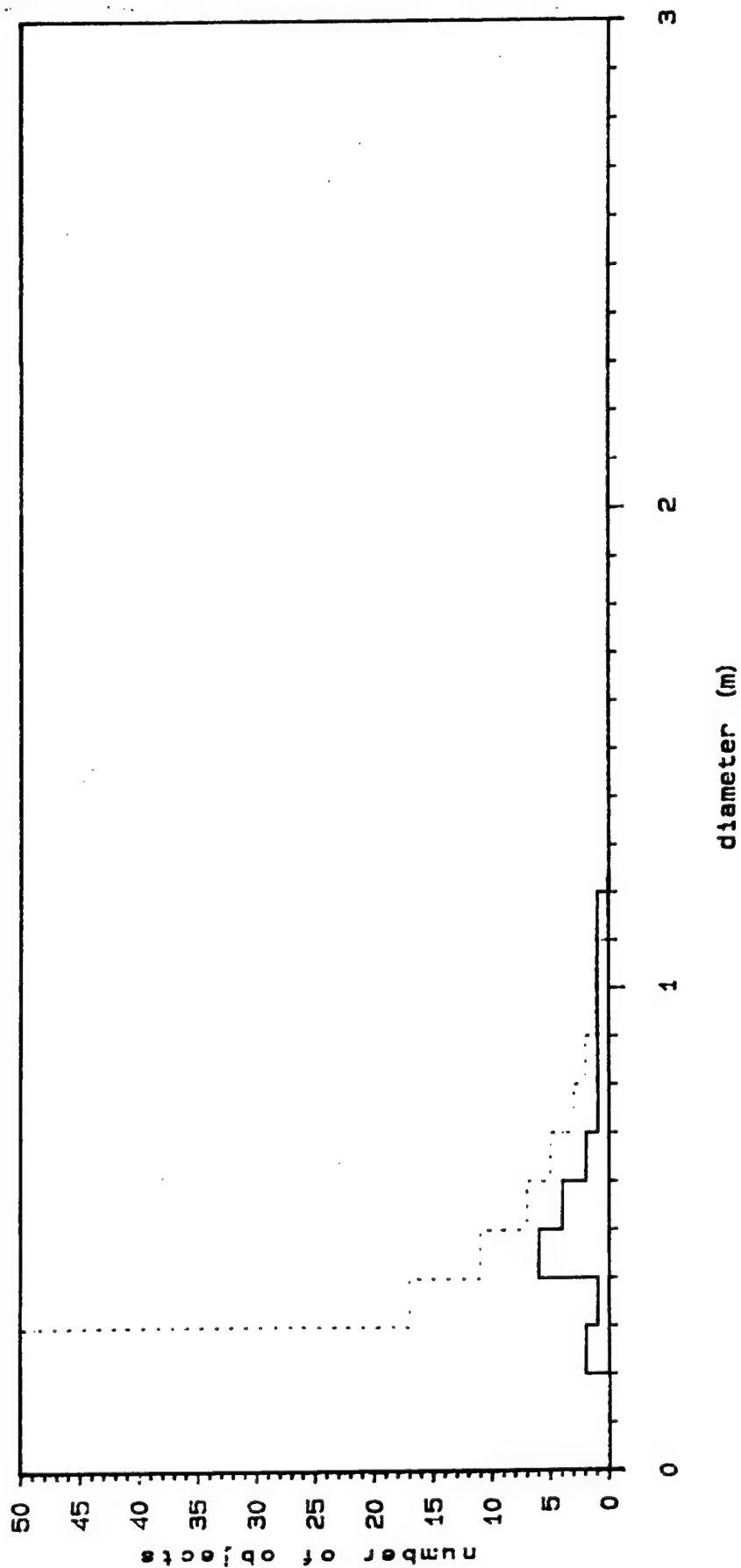
Figure 4-4 Number vs. diameter distribution -- DOY 250, 39° cloud compared to theoretical distribution.



Hazard Analysis Project

ALTAIR data: day 251_23

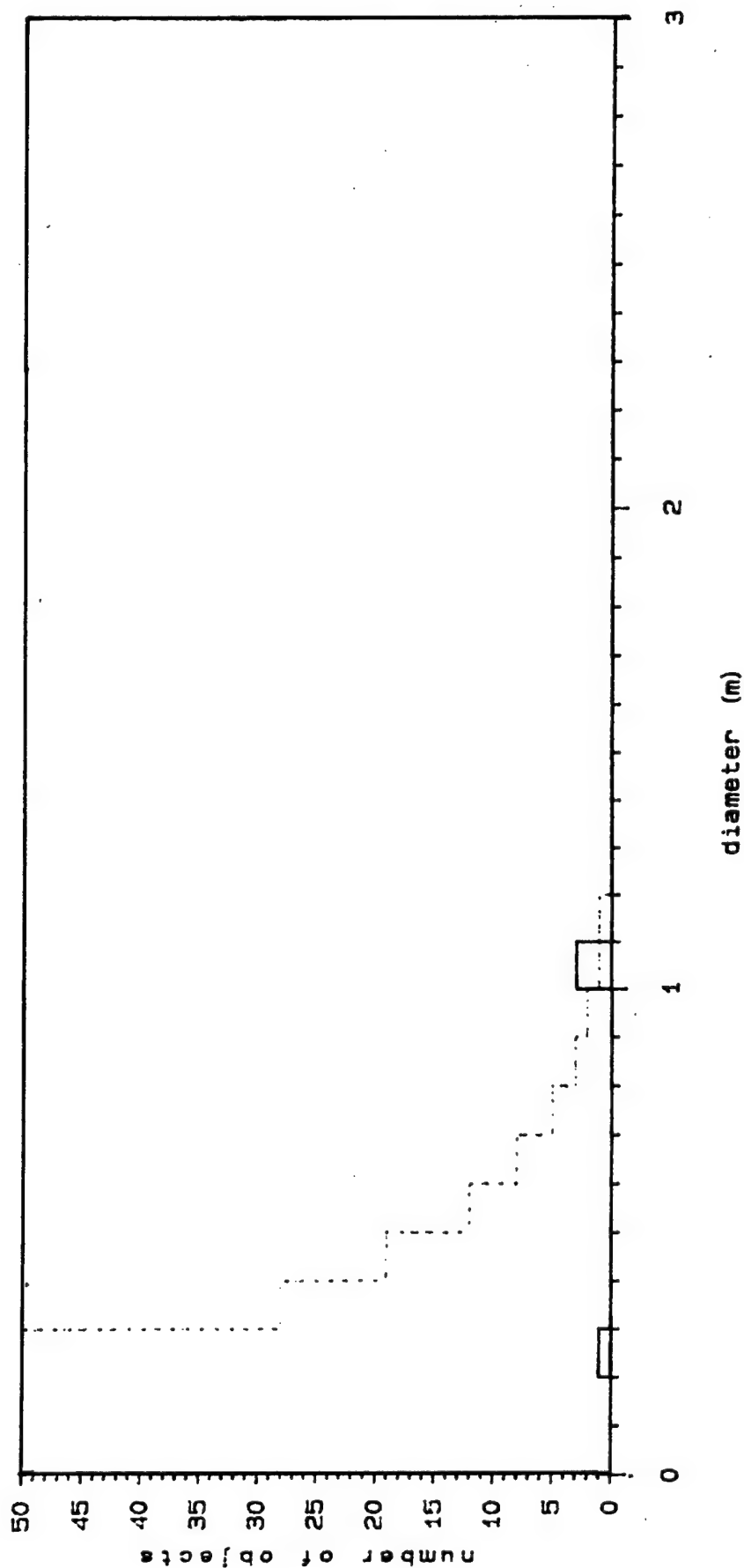
Figure 4-5 Number vs. diameter distribution -- DOY 251, 23° cloud compared to theoretical distribution.



Hazard Analysis Project

ALTAIR data: day 251_39

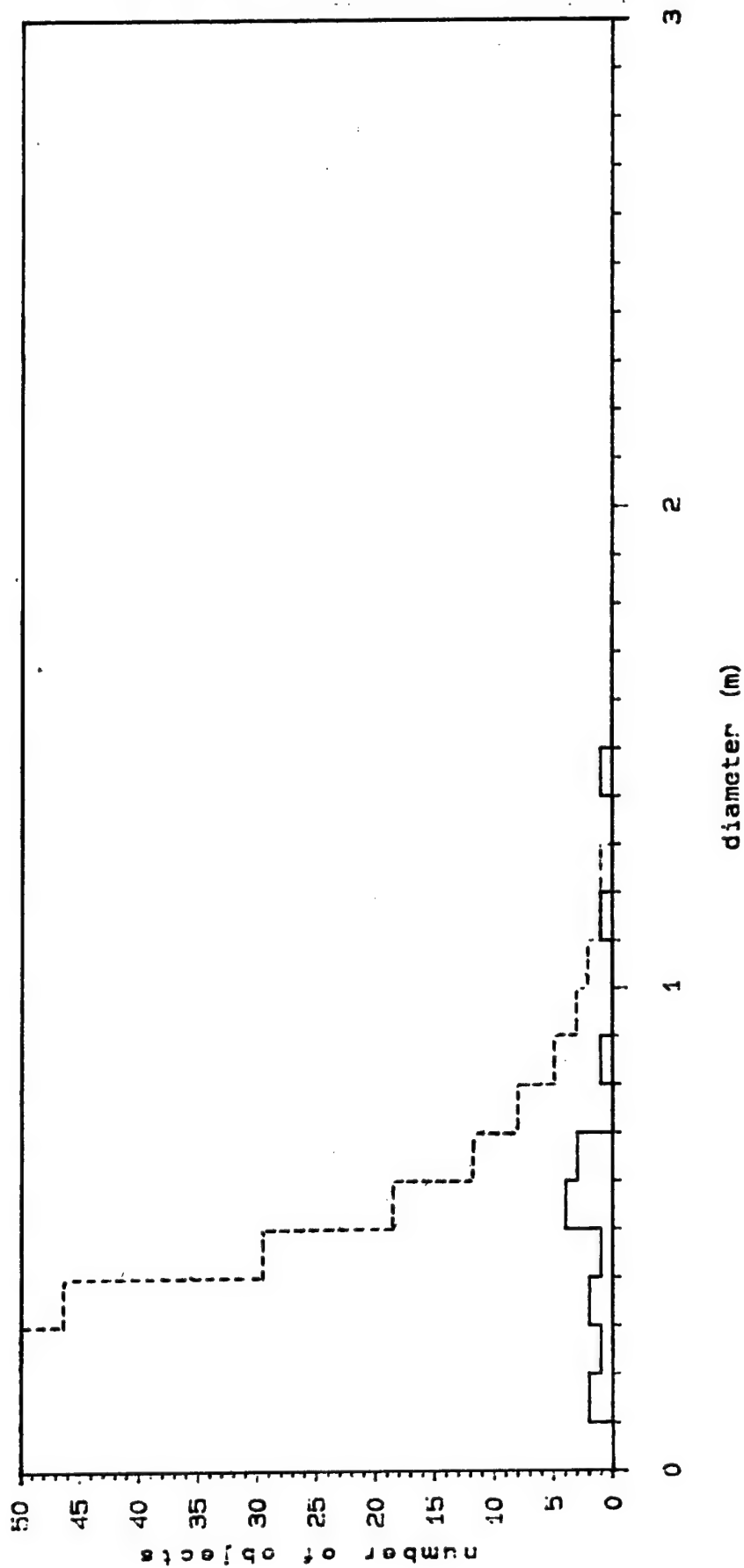
Figure 4-6 Number vs. diameter distribution -- DOY 251, 39° cloud compared to theoretical distribution.



Hazard Analysis Project

NSSC cataloged objects: day 318, 23 & 39 deg clouds

Figure 4-7 Number vs. diameter distribution -- DOY 318 NSSC cataloged objects compared to theoretical distribution.



possessed a large number (relatively) of objects in the 1.0-1.1m diameter bin.

The NORAD catalog set of pieces displayed too few observations to form a proper distribution. In the Delta stage cloud, there were 5 pieces; in the satellite cloud, there were 13 pieces, of which 11 had recorded radar cross sections. Once again, large pieces predominated in the 23° cloud, as two pieces accounted for about 93% of the cloud's total mass. The mass was concentrated in the diameter range 0.5-0.7m in the 39° cloud.

The total mass of each cloud on days 249 and 250 was calculated using the same formulae, relating diameter and mass, that were used in the computer model. These values are presented in Table 4-1. Pre-mission predictions yielded cloud (radar observable) masses of 740kg for the 23° cloud (or about 85% of modeled mass of 837kg) and 1296kg for the 39° cloud (about 89% of modeled mass). Derived from the measurement of the mass and the average cross section of various payloads, rocket motors, etc., the equations used by the computer model will not give accurate values for objects such as large flat plates. Such plates could have been produced (and considering the data, almost certainly were) in the fragmentation of the Delta second stage, which is basically a right circular cylinder composed of an outer skin and liquid fuel tanks.

Figure 4-8 demonstrates the results of the modified meteor radar established in Hawaii. The theoretical distribution here is based on that used in the computer model, and represents the summation of mass in the 23° cloud and the 39° cloud. This was done as there was no distinction between the two clouds in the reentry radar data. However, this should not make a great deal of difference in this case as the 39° cloud was not close to Hawaii on this pass. Approximately 10% of the mass theoretically produced in the mass range 10-170gm by

TABLE 4-1
Observed Cloud Mass

Diameter (m)	Bin Mass (kg) ^a					
	Day 249 ^b		Day 250 ^c		Day 251 ^d	
	23 ^o	39 ^o	23 ^o	39 ^o	23 ^o	39 ^o
0.1-0.2	0	0	1	0	0	0
0.2-0.3	4	10	14	0	4	2
0.3-0.4	40	18	97	0	4	0
0.4-0.5	148	31	163	16	47	0
0.5-0.6	244	49	183	0	49	0
0.6-0.7	339	36	125	0	36	0
0.7-0.8	739	99	296	0	25	0
0.8-0.9	653	33	163	33	33	0
0.9-1.0	504	0	126	0	42	0
1.0-1.1	422	0	53	0	53	158
1.1-1.2	647	0	388	0	65	0
1.2-1.3	234	0	469	0	0	0
1.3-1.4	279	0	186	0	0	0
1.4-1.5	109	0	109	0	0	0
1.5-1.6	127	127	0	0	0	0
1.6-1.7	0	0	0	0	0	0
1.7-1.8	0	0	0	0	0	0
1.8-1.9	190	0	0	0	0	0
1.9-2.0	0	0	213	48	0	0
2.0-2.1	0	0	0	0	0	0
2.1-2.2	266	0	0	0	0	0
2.2-2.3	0	0	0	0	0	0
total:	4945	403	2586	97	358	160

a assume mass given by $m = 47.2 d^{2.26}$ (m [kg], d [m])

b duration of observations = 1 hour, 45 minutes

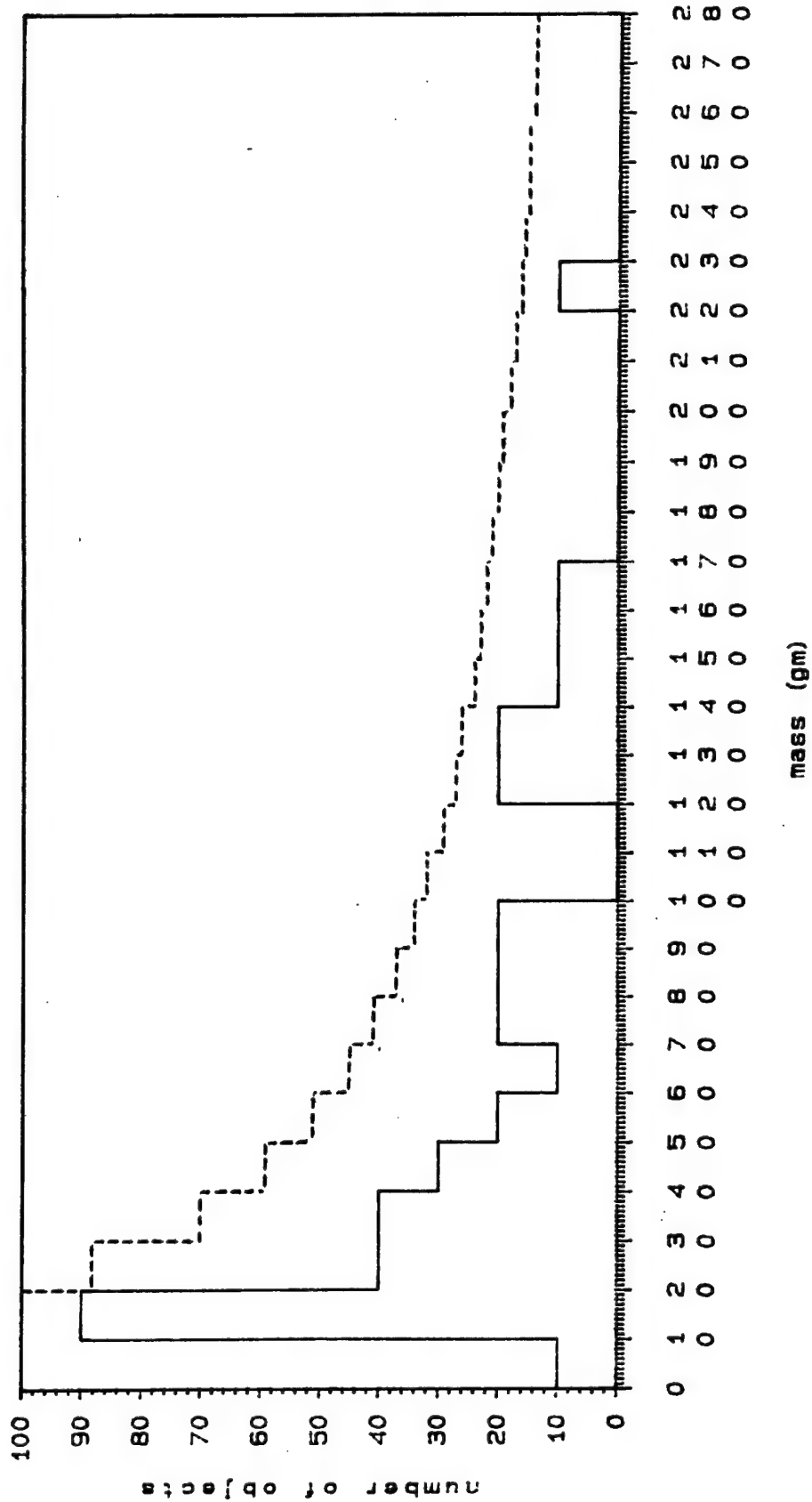
c duration of observations = 1 hour, 52 minutes

d duration of observations = 1 hour, 47 minutes

Hazard Analysis Project

VHF 50 MHz radar: day 249, 23 & 39 deg clouds

Figure 4-8 Number vs. mass distribution -- DOY 249 SRS meteor radar data compared to theoretical distribution.



radar data exaggerated by a factor of 10

the breakup event was observed to reenter shortly after EOM by radar. This is in agreement with model estimates performed post-EOM at JSC.

4.2 Momentum Transfer

The transfer of linear momentum between the satellites involved in the breakup, like the velocity distribution of the various-sized fragments discussed in Section 4.3, awaits the calculation of relative velocities for the fragments observed by radar. However, a qualitative analysis of the momentum transfer may be made by noting the distribution of debris inclinations around the mean inclination of the parent body (see Figures 3-5 and 3-6).

While there is some skewing of the distributions towards an intermediate value, there exists no detectable debris cloud between those clouds formed of the Delta stage and the satellite. Thus, the distribution of debris inclinations suggests little momentum transfer between the impacting bodies. In terms of pre-mission modeling, this is consistent with on-orbit explosions, in which no momentum is transferred.

Unknown at this time, however, are the detailed impact mechanics of large objects of similar mass, and the effects of any residual propellants on board the spacecraft at the time of impact. Both of these factors could have affected the net forces, and hence, the change in momentum with respect to time, acting on the debris objects produced in the event.

4.3 Velocity Distributions

At the time of writing, the computation of the velocity distribution for the Eglin data awaits the processing by Teledyne Brown Engineering of the classified end-of-mission state vectors. In conversations with Mr. Ronn Kling of

Teledyne Brown, a Meirovitch-derived analysis, similar to that performed following the breakup of the P-78 (Solwind) satellite, is planned for the data. Also, methods involving the rotation of the orbit (hence, the "adjustment" of the orbital elements) so as to propagate from point of impact through observed position will be implemented as a check.

Unfortunately, these data contain no information concerning object size; pending further analysis of the Eglin "Log S" data tapes by Xontech such information will not be forthcoming. One method of alleviating this difficulty would be the identification of provisional numbers with the NORAD catalog numbers. The provisional pieces contain velocity information, while the cataloged pieces (in most cases) have RCS values. Thus, the nineteen cataloged pieces could be used to calibrate the velocity distribution curve.

Until finalization of action on this matter, no quantitative comparisons may be drawn. However, some qualitative estimates of the velocity distribution may be gleaned from a comparison of the Eglin Gabbard diagrams of day 249 with Gabbard diagrams produced pre-mission by computer modeling. Figures 2-4 and 2-5 depict the case of a direct hit (100% mass overlap) utilizing the high velocity (100% kinetic energy transfer) curve and the medium velocity (50% kinetic energy transfer) curve, respectively.

As shown in Figures 2-4 and 2-5, the "arms" of the Gabbard diagram are indicators of the amount of kinetic energy transfer and the velocity distribution involved in the event. For the medium velocity curve, the arms of the Gabbard plot will not meet so as to form a complete cross. Those of the high velocity curve shown in Figure 2-5 will, however. This is indicative of the higher velocity given larger pieces of debris, such as those observable by radar, by a large energy transfer. Smaller pieces will tend to receive proportionately

smaller velocity increments in all energy transfer scenarios. Thus, the spread of large objects about the original apogee and perigee of the target or projectile provides an excellent clue as to the velocity distribution as a function of debris size.

Comparison of pre-mission plots and the Gabbard diagram produced on day 249 from Eglin data suggests that the high velocity distribution used in pre-mission modeling is the most reasonable. Even this distribution fails to scatter objects to the apogees observed. Also unexplained is the clumping visible in the 39° cloud (Eglin, day 249) between 98 minutes and 104 minutes of period.

4.4 Size vs. Optical Magnitude of Debris

To describe an object size from either magnitude or radar cross section requires some knowledge of the albedo, or reflectivity, of the object, the geometry of the object, and its physical nature. For a given recorded event, such as many of the video events recorded during the Delta-180 measurement campaign, a video brightness is the direct observable. If there exists adequate calibration, the video brightness may be converted to an apparent visual magnitude. This magnitude, by itself, is insufficient for the determination of size or albedo. One or the other of these latter two quantities must be known before the the remaining one can be determined.

With supporting radar data, it is possible to get an idea of the size of an object. However, values of radar cross section (RCS) cannot be considered a true measure of the physical dimensions of an object because the shape of the object as well as its size and physical character influence the returned signal from which the RCS value is determined.

Radar cross section is defined as the projected area of a perfectly conducting sphere which, if placed in the same position as the real target, would scatter the same amount of energy to the observer. Obviously, if an observed object is not a perfect conductor and/or not spherical, an unambiguous interpretation of RCS is not possible. Usually, an irregular or rough object will reflect more signal toward the illumination source, or in the "backscatter" direction, than a conducting sphere. This difference becomes significant when radar and optical data are compared because RCS values are based on measurements made from backscattered radiation (phase angle=0°); optical measurements are usually made at a phase angle of about 70° to 90°. For radar data, the difference arising from different phase functions alone, can be as much as a factor of five in the amount of backscattered radiation. The "typical" difference between a debris target object and a metallic calibration sphere would be on the order of 2.5.

If the reported RCS for an object is used to calculate the radius of an equivalent sphere there will usually be a tendency to overestimate this radius by virtue of not properly taking the phase function into account. In the following paragraphs the phrases "corrected radius" or "corrected cross section" refer to employing the above factor of 2.5.

Examination of Table 3-11 betrays several interesting features -- one of which is that only 10 Delta-180 objects were observed. For the moment, ignore the two AMOS observations since they were obtained as a direct result of an attempt to track a target; further, ignore the observation made from the Learjet. The remaining set of observations consists only of those targets observed from Maui on DOY 256, 257, 258 using the optical detectors comprising the optical fence. Since there were only 7 objects observed, it is important to back-track and calculate retroactive "predictions" of the passage of all Delta-180 fragments during the 40 minute observing intervals on each day.

To examine the problem, a window was defined having a width roughly equal to the linear extent of the fence of optical detectors. The program SATRAK was run for each of the nights and was constrained to give look angles only for illuminated passes within the window. The number of look angles "predicted" were 60, 36, and 8 for DOY 256, 257, and 258, respectively. Thus 104 Delta-180 targets passed through the fence.

If, in fact, 104 debris pieces passed through the detector fields and only 7 were observed, then 93% were too faint to be seen. The principal reasons for not seeing a debris piece are (1) low albedo, (2) small size, and (3) lack of detector sensitivity.

ALTAIR radar data on the 104 Delta-180 pieces that passed through the window reveals that their average radar cross section was $\langle \text{RCS} \rangle = 0.64 \pm 0.27 \text{m}^2$. Clearly objects as small as the average were not seen, otherwise the total number observed would be several times ten at least. If we assume that the objects observed were among the largest in the group, we may get some idea of the lower limit of detectability. An examination of the ALTAIR data shows that the seven largest objects had RCS values ranging between 1.14m^2 and 1.26m^2 . This may now be interpreted in terms of a threshold of optical detectability. Using the "corrected" RCS as the cross-sectional area of an object that was barely above the detection threshold of the Maui detectors, a radius of 0.30m is obtained.

In addition to look angles, SATRAK also calculated the range to the satellites. Averaging these values for all of the satellites predicted to pass through the window, a value of 400km was obtained; this value is used here as a typical detector-object distance.

In what follows, two approaches to the data are examined. In the first, the detector threshold is assumed and the albedo of the debris will be calculated. In the second, the albedo will be drawn from a separate discussion of another Delta-180 piece on the following page, and used to determine the threshold level for the detectors of the Maui fence.

Extrapolating from experience with the NASA JSC Lenzar, a 10th magnitude piece of debris should be very near the threshold of detectability. Thus using this value of magnitude, a distance of 400km, a corrected radius of 0.30m, and a phase of 90°, an albedo of 0.02 is obtained. If the distance has been underestimated by a factor of two, the value of the albedo increases to 0.07. Further if the threshold magnitude is 9.0 (and using 400km for the range), the albedo is 0.04; for a range of 800km, the albedo increases to 0.16. A fainter value of threshold magnitude, such as 11 or 12, only diminishes the value of albedo below 0.01.

The albedo derived for the nominal case, 0.02, seems impossibly low. The key assumption is the threshold magnitude. If we have a separate observation from which we may derive albedo, we can work the problem the other way and ask if the small number of objects detected might have been due to a relatively high threshold (especially for the GEODSS instruments).

From the discussion on the following page, we have at least one Delta-180 debris object with an albedo of about 0.13. If we assume that this value is characteristic of all of the Delta-180 debris pieces and apply it to the above problem to determine the detection threshold for the principle detectors in the Maui fence, we obtain 8th magnitude -- two magnitudes brighter than the assumed value of 10.

In that albedos of 0.01 - 0.04 are unphysically low, it appears that the low number of detected events with most of the elements of the Maui fence is due to a detectability threshold of about 8th magnitude. This may have been due to the optical characteristics of the system or (more likely) the methods by which the data were recorded and/or processed at the telescopes.

The Maui fence consisted of two types of detectors -- three GEODSS instruments, and the MOTIF/AATS. The GEODSS instruments have diameters of 1.0m, 1.0m, and 0.16m; their fields of view are 2°, 6°, and 2°, respectively. The MOTIF/AATS has a diameter of 0.15m and a field of view of 2°. Of the seven objects observed with the Maui fence, one was seen with the AATS while six were seen with the GEODSS instruments. This means that the GEODSS instruments observed 0.6 Delta-180 pieces per 1° field of view while the MOTIF/AATS recorded 0.33 Delta-180 pieces per 1° field of view.

Since one of the GEODSS telescopes has a diameter comparable to the AATS and the other two each have diameters almost seven times as great, it would seem reasonable to expect more sensitivity from the GEODSS instruments than the indicated factor of two. Clearly the suitability of the GEODSS telescopes for the detection of LEO targets, as currently instrumented, must be questioned.

Returning now to the AMOS observations listed in Table 3-11, Event #44 is presented in the interest of completeness. It was not possible to measure a magnitude for this object due to lack of suitable calibration of the video data and lack of supporting radar data. Further, this object was bright enough to saturate the detector throughout much of the 90 seconds it was tracked.

The second object tracked with AMOS was identified as the remnant of the Delta 2nd Stage -- object # 16938. It had an RCS of 1.55m², and culminated at 15:08:28 at a range of 290km. Due to a lack of calibration, it was not possible to make photometric measurements at a high confidence level. However, an image of this object at culmination, taken with the AMOS/AATS, was compared to an image of an identifiable starfield obtained previously with the MOTIF/AATS; both detectors use a Quantex QX-11 image system. Allowance was made for the slightly different apertures of these two telescopes. The comparison yielded an estimate of $m_v = 7 \pm 1$ for the magnitude of object #16938 at culmination.

Again using the model of a spherical reflector at phase=90°, and correcting the RCS to a more realistic value using the earlier assumptions, the albedo may be calculated using the range and magnitude values at the time of culmination. Using the nominal value of $m_v = 7$, the albedo is determined to be 0.13. For 8th magnitude, the corresponding albedo is 0.05. For 6th magnitude, the albedo is 0.32. Therefore, this observation is suggestive of generally moderate to low albedos for the Delta-180 debris.

Another individual observation that deserves some examination is the single 23° cloud object observed from the Learjet on DOY 250. Two questions arise when considering this observation: (1) what can be learned from this one observation about the debris piece that was observed, and (2) why was only one such piece observed?

Both questions can be examined by considering the ALTAIR radar data for DOY 250. During the flight of the Learjet the ALTAIR radar was on. During the overlapping period of observation, 17:00 to 18:00 UT, ALTAIR recorded 11 Delta-180 debris pieces in the 23° cloud, and 7 in the 39° cloud. None of the objects recorded by ALTAIR match the optical

observation. There are two reasons that the one optically detected object might not have been observed by the radar -- either it was not in the beam, or it was too small to give a detectable return.

By virtue of a negative detection, there is no way to know if the object was in the ALTAIR beam or not. However, since ALTAIR is a pencil-beam radar, there is a significant chance that it was not in the beam. On the other hand, if it was in the beam but not detected, an estimate of its size may be obtained. This line of reasoning will be explored bearing in mind that there is no more reason to believe that the object was in the beam undetected than outside of the beam.

Over 100 Delta-180 debris pieces were detected by ALTAIR in the 23° and 39° clouds -- the average range at the time of detection was 1300km and 1500km, respectively. The smallest RCS observed was 0.18m^2 for an object in the 23° cloud. If we assume that the observed object was not detected because it was too small, we may use 0.18m^2 as a means for estimating an upper limit to the radius of the object. This upper limit value would be $r=0.24\text{m}$.

The observed magnitude, $m_v=10.6$ does not include correction for the fact movement of the object relative to the background. In limited field tests at JSC, with the Lenzar optical system, it has been determined that a 2.5 correction in magnitude is appropriate for an object moving at the rate of 1° per second. Therefore, the corrected magnitude for this object is about $m_v=8.1$. At the time of observation the range was 465km. Again assuming the spherical reflector model, a phase angle of 90° , and radius of 0.24m, an albedo of 0.20 is determined.

This calculation assumes that the object is just below the threshold for detection by the ALTAIR radar. It is also

possible that the object is smaller and has a higher albedo. Of course, since the albedo cannot exceed 1, this allows for the calculation of a lower limit to the size of the object. This calculation yields a radius of 0.11m. Thus, within the assumptions, the radius of the object lies between 11 and 24cm with an albedo between 1.00 and 0.20. If the conjecture that the object was in the beam, yet undetected, is correct this one object, although small, had a high enough albedo to be recorded optically, and a small enough RCS not to be observed by the ALTAIR radar.

Regarding the second question as to why more Delta-180 debris objects weren't observed optically, it is first noted that a total of 18 debris pieces were observed by ALTAIR coincident with the optical observations. Of these 18 pieces only 5 had values of RCS greater than 0.70m^2 and none were greater than 1.15m^2 . Again, if the typical Delta-180 debris fragment has an albedo of 0.05 to 0.15 as suggested earlier, the lack of data from the Learjet is consistent with such relatively dark debris pieces.

In summary, the Delta-180 optical observations tend to support the suggestion that debris fragments created during a collision between two spacecraft are somehow darkened. The typical albedo implied by the Delta-180 data is on the order of 0.15 with some individual exceptions. Further, the actual optical piece count compared to the expected count, indicates that the GEODSS telescopes are not suitable for this type of LEO work with their present instrumentation.

4.5 Object Lifetimes

The full analysis of orbital lifetimes for the objects produced in the Delta-180 mission awaits further observations of the decay rate of cataloged pieces by Eglin and other radars. Nevertheless, estimates may be extracted from data

taken over the months following the breakup event. The sources of these data are Eglin and the NAVSPASUR network, as well as the contributing sensors of the NORAD system. Information concerning actual observations may be found in Appendix B, Section 5.

To summarize, approximately half of the original number of objects observed by Eglin and NAVSPASUR were still in orbit 58 days after the event. Observational selection effects and sensitivity effects (such as solar activity, which degraded the performance of NAVSPASUR during a portion of the observations) introduced some uncertainty into the data. For example, the number of objects in the 39° cloud actually increased during late-October and early-November. Unfortunately, several high-interest objects, such as the very high apogee objects, could not be correlated from observation to observation.

The NORAD cataloged objects exhibited an even more gradual decay rate. After 2 months in orbit, only 28% of the objects had decayed. While one should be wary of problems associated with the statistics of small sample sets, it is interesting to note that 4 out of the 5 decayed objects were fairly small (0.67m in diameter and less). This would, in general, tend to support the theory that the less massive, or smaller objects would decay at a faster rate than larger objects.

Pre-mission modeling indicates a decrease in the flux at breakup altitude and the number of particles by a factor of 2 after an elapsed time of 1 week, a further reduction by a factor of 2 after 1 month, and a reduction by a factor of 5 in the ensuing 2 months. Thus, after an elapsed time of 3 months, the spatial flux and the number of radar observable objects would be reduced by a factor of 20 below the levels present at breakup.

Such a rate would be faster than that observed by Eglin and the NAVSPASUR network, or by the associated NORAD sensors. The solar activity during this period cannot account for this discrepancy, since the solar minimum was modeled (average solar flux $F_{10.7}$ calculated was 81×10^4 Jy, a typical value during solar min.) in the decay routines. Any increase in the average solar flux would tend to shorten the lifetimes of objects in low earth orbit. While only those bodies surviving their first few hours in orbit will be detected by NORAD/NAVSPASUR sensors, those objects reentering immediately after breakup were not included in calculations of number in orbit, spatial density, or cumulative spatial flux. This negates a possible error by counting some debris as decayed (even though HAZARD does declare newly-created debris with perigees and/or apogees less than 100 km in altitude to be decayed, these were not included in the number of objects used in the calculation of the spatial densities or cumulative flux) before the sensors have an opportunity to observe them. At present, an investigation of the decay processes acting on the satellite objects, and the routines which model this decay, is continuing.

5.0 CONCLUSIONS

Pre-mission modelling of the collision produced three scenarios, differing by the amount of momentum transferred in the collision. Debris size distribution, orbital elements, momentum transfer, and energy transfer from these models were compared with data on the debris cloud gathered in the days and weeks following the event.

For this comparison, the most useful data were those obtained from the Eglin, NAVSPASUR, and ALTAIR radars. These radars followed the evolution of the debris cloud up to three weeks after the collision, and provided essential information on the number and size of debris particles and their decay and reentry.

The reentry radar located on Kauai provided a useful check on the early reentry of debris from the collision. Objects in the size range from 10 to 1000 grams were detected by the ionization trails produced upon reentry. The number and size distribution of particles reentering during the first pass of the debris cloud over Kauai was in approximate agreement with model predictions.

The optical data from the Kwajalein airborne effort and the Maui ground-based effort was less successful than the radar data. The total number of debris pieces detected by the optical system was 10 -- 8 associated with the 23° cloud and 2 associated with the 39° cloud. From an analysis of the optical image data, an estimate of the reflectivity of the debris pieces can be made. As a group, the Delta 180 debris fragments appear to be relatively dark, having albedos equal to or less than 0.15. The low albedo was the cause of difficulty in observing these fragments by optical techniques. Future efforts to observe debris by optical techniques should use more sensitive sensors. The GEODSS systems were found to

be sensitive to only 8th magnitude stars, although similar instrumentation at the MIT experimental site at Socorro, N.M. is sensitive to 16th magnitude stars at the angular velocities exhibited by the Delta-180 debris. The Lenzar camera system aboard the Learjet was sensitive to only 9th magnitude stars at the angular velocities of the debris. An increase of sensitivity of at least 3 magnitudes would be required for any future optical observations of debris.

The piece counts predicted pre-mission overestimate the number of detectable debris objects arising from the breakup event, even allowing for decay immediately after breakup. Subsequent modeling, using smaller masses for the Delta stage and satellite predicts a post-EOM environment similar to that actually observed during subsequent days. Size distributions based on the ALTAIR data suggest that many more large objects were observed than were predicted in the 23° inclination cloud (Delta rocket body). Estimates of the mass of these objects imply that many consisted of large (diameter > 0.5 m) plates, such as might be found in the fuel tanks and skin of a spacecraft. The number of objects observed in the 39° inclination cloud was consistently smaller than the predicted number-size distribution. This infers that while many pieces may have been produced, the number-size distribution is biased towards small pieces.

A great deal of information concerning the transfer of linear momentum between colliding bodies is conveyed in the Gabbard diagrams of the debris resulting from the breakup. The data examined reveals two distinct debris clouds spread about inclinations of 23° and 39° . Though the mean of the PAS/satellite's debris cloud is below that predicted by pre-mission modeling, conclusions drawn concerning the transfer of momentum during the collision are tenuous at best, since end-of-mission state vectors are at present classified. However, the gross structure of the clouds indicated very

little momentum exchange between the larger fragments since no cloud near the center-of-mass inclination of 33° has been detected.

The velocity distribution of the debris tends toward the 100% kinetic energy transfer curve used in pre-mission modeling performed at JSC. This indicates that the kinetic energy of the two parent satellites was transferred almost intact to the debris, i.e., little kinetic energy was spent in actually fragmenting the structure of the satellites. Unknown are the effects of chemical energies (the range safety packages and remaining fuels on board) liberated during the end-of-mission.

The orbital lifetimes of the debris appear to be in excess of that predicted by the model. This is arrived at by ratioing the number of objects observed and predicted at selected intervals of time. In general, the lighter pieces tend to decay more quickly than more massive pieces; this agrees with current theory.

Overall, the model performed adequately in predicting the number of pieces produced in the Delta 180 mission; the anomalous results in predicting the size distribution of the objects may be an artifact of processes occurring at EOM. Velocity distributions and linear momentum exchange scenarios also performed well in predicting the deposition of fragments post-EOM. However, the observed rates of decay appear to be slower than that predicted by the model. Thus, while fewer pieces appear to have been produced, the lifetimes experienced by these objects are longer by approximately a factor of two or three. Using the data derived from the Delta 180 mission, the model will be improved so as to be able to better predict hazards of on-orbit breakups.

For the longer term, dedicated space-based or more sophisticated ground-based instruments to monitor small orbital debris will be required to adequately support planning and safety activity.

Appendix A

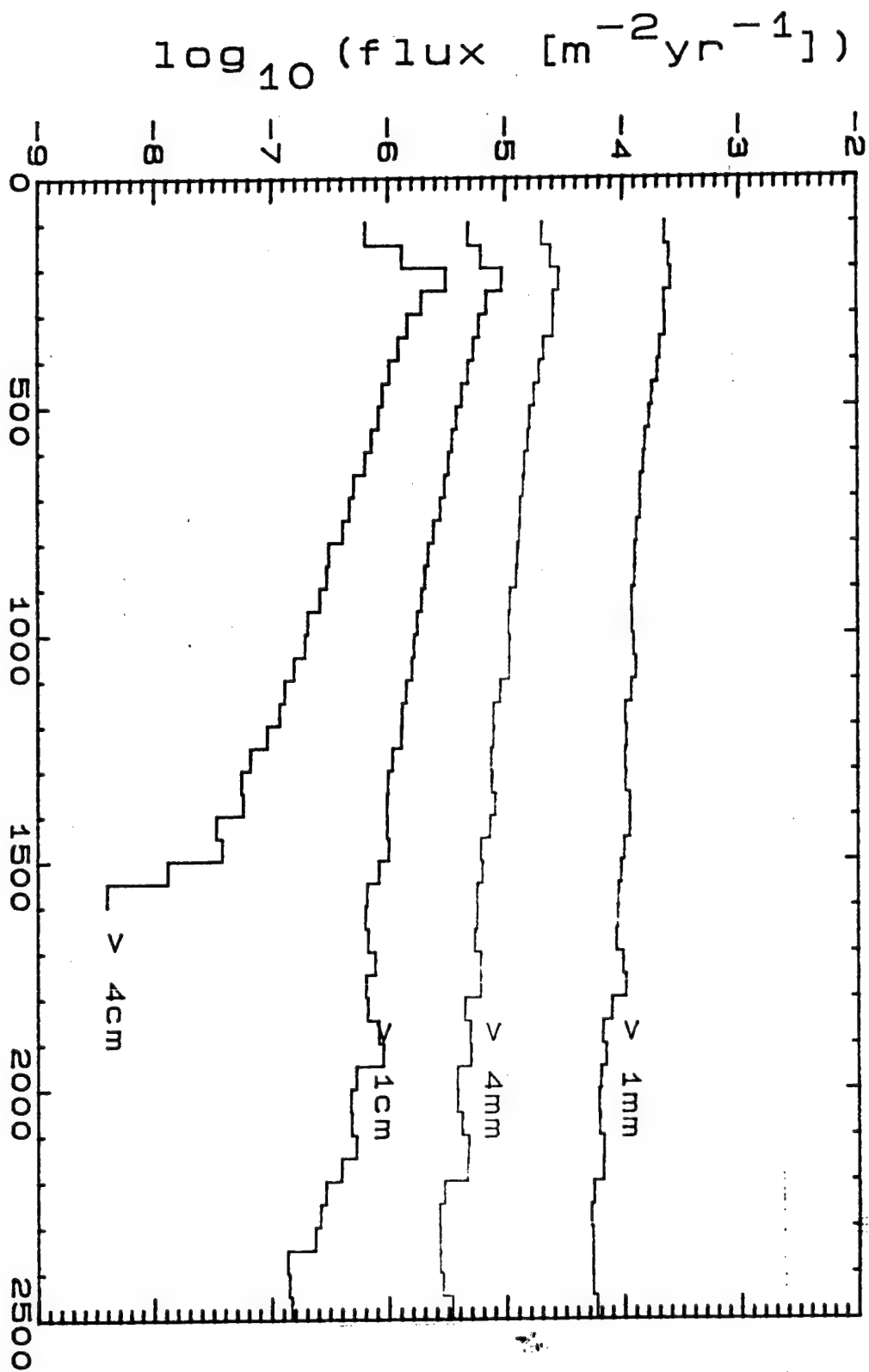
Pre-Mission Modeling

The contents of this appendix comprise plotted results of the pre-mission modeling performed during March and April, 1986, by NASA/JSC's Solar System Exploration Division. These graphics are in a format such that they describe the evolution of the cumulative flux arising from several scenarios over the elapsed time of 1 year. Several sets of data also include the natural meteoroid background flux, to serve as an indication of the relative magnitude of the debris flux.

As discussed previously, the three scenarios encompassed a head-on collision (or 100% collision), a grazing collision (or 10% collision), and proximity explosions of the two satellites. The other parameter of interest was the velocity distribution of the debris. High velocity (100% kinetic energy transfer), nominal velocity (50% kinetic energy transfer), and low velocity (10% kinetic energy transfer) distribution curves were utilized. In each case, the percentages refer to the amount of kinetic energy actually manifesting itself as a change in velocity of the debris objects (energy "sinks" potentially include material deformation, melting of material, light flash, etc.). For each case examined, the environment was sampled at elapsed times of 0 weeks (i.e., end-of-mission), 1 week, 1 month, 3 months, 6 months, and 1 year.

FIGURE A-1

10% impact
50% kinetic energy transfer
elapsed time = OWK



altitude [km]
meteoroids excluded

FIGURE A-2

10% impact
50% kinetic energy transfer
elapsed time = 1wk

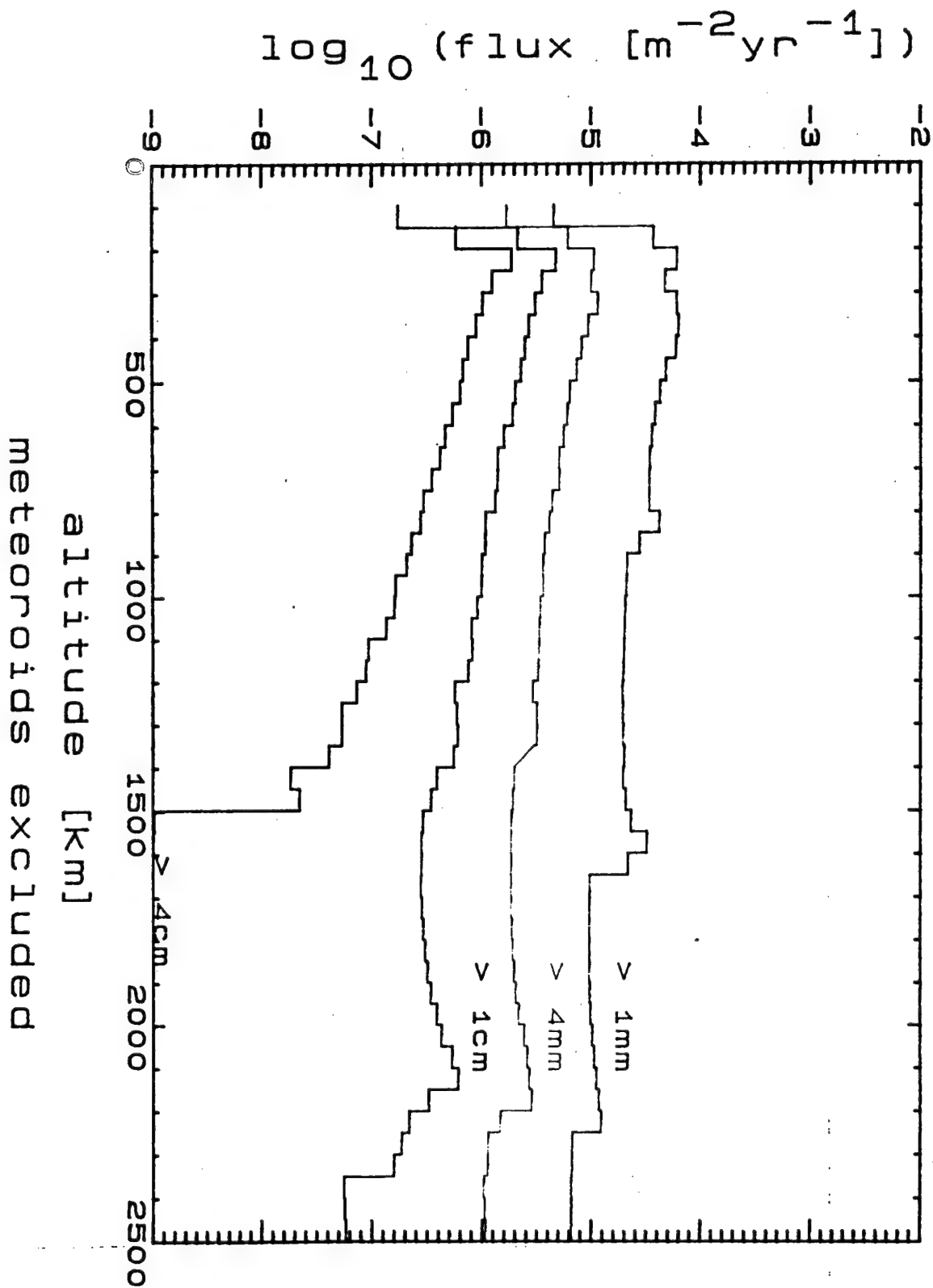


FIGURE A-3

10% impact transfer
50% kinetic energy transfer
elapsed time = 1mo

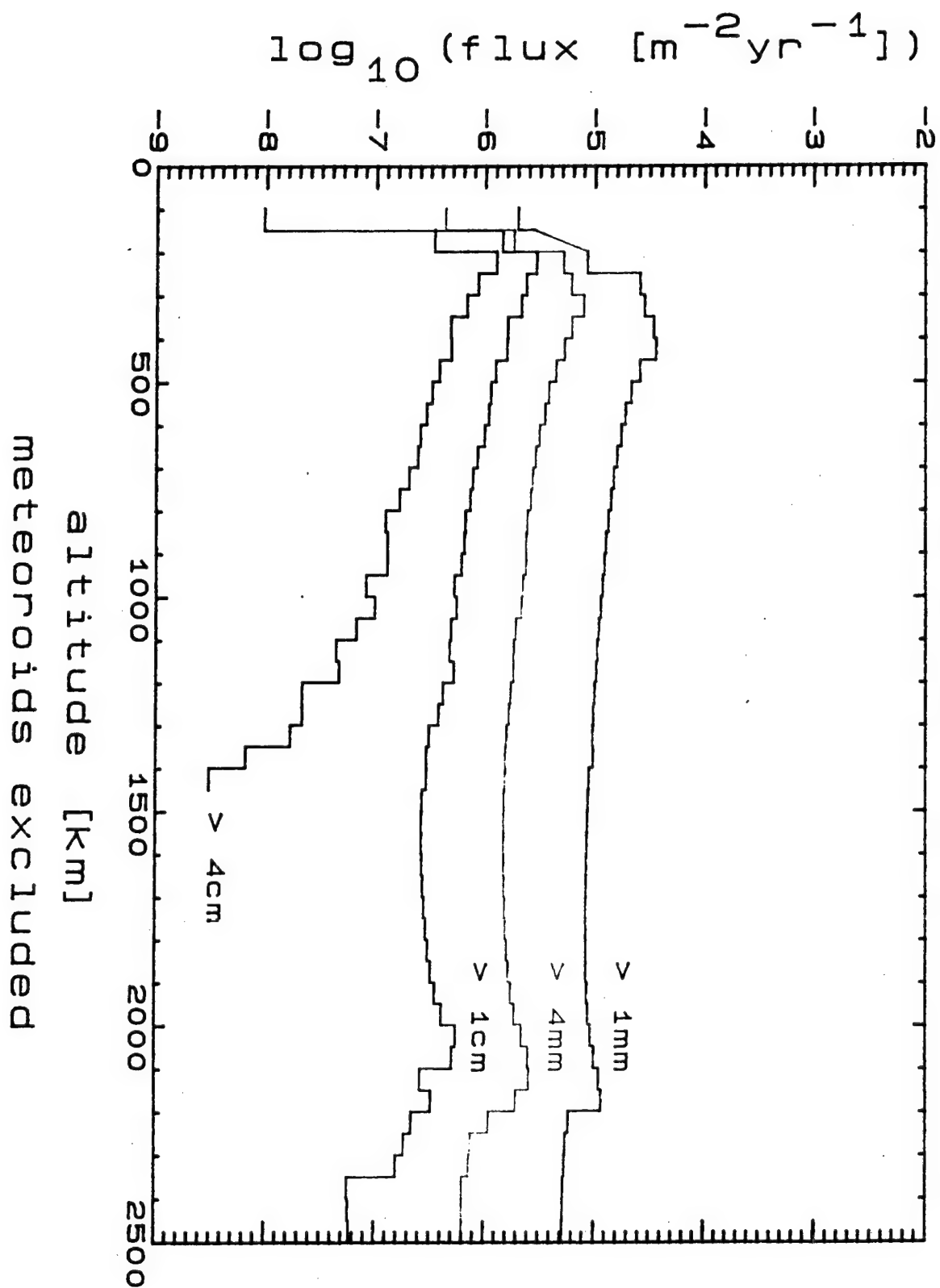
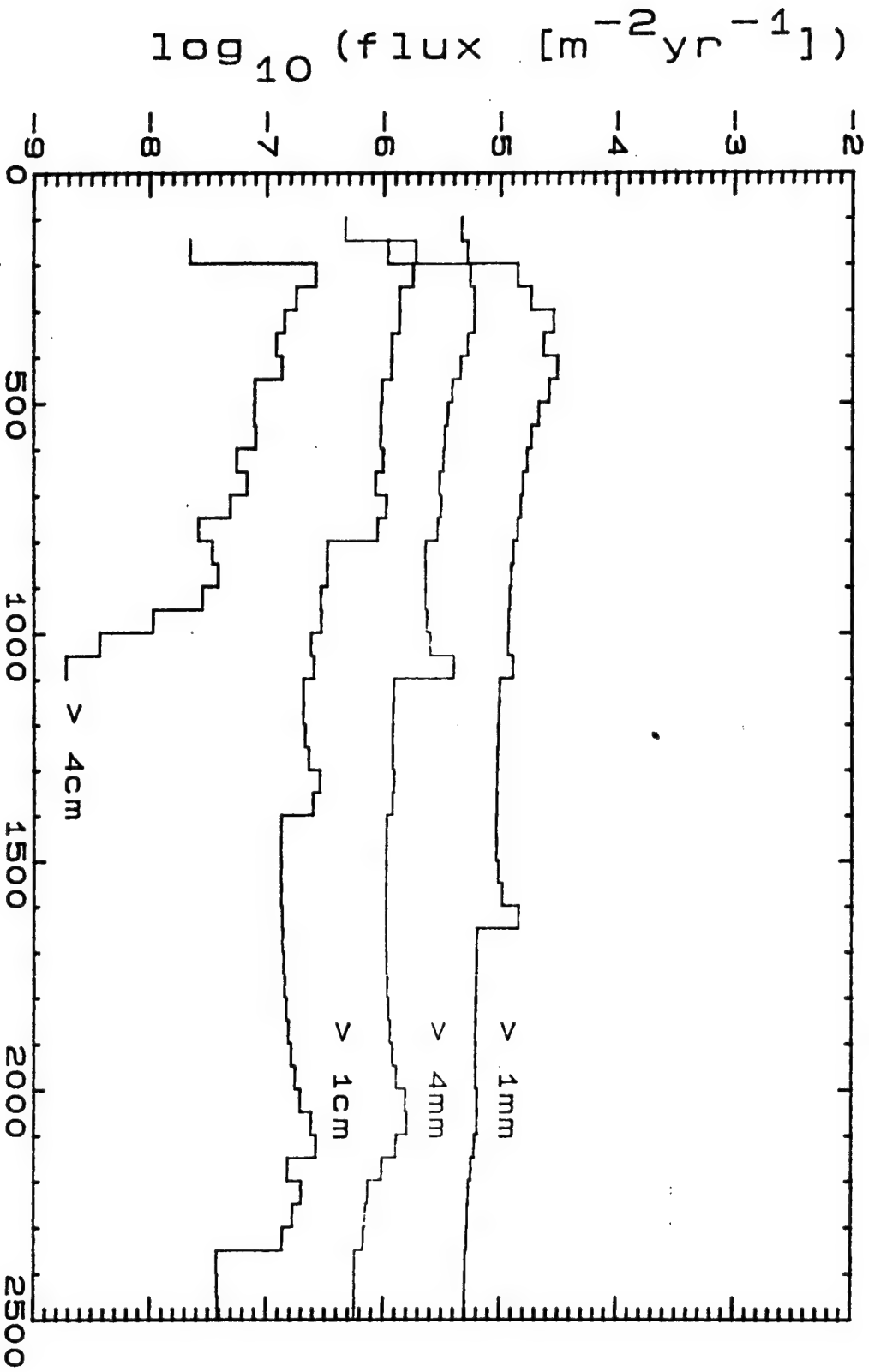


FIGURE A-4

10% impact
50% kinetic energy transfer
elapsed time = 3mo



altitude [km]
meteoroids excluded

FIGURE A-5

10% impact transfer
50% kinetic energy transfer
elapsed time = 6mo

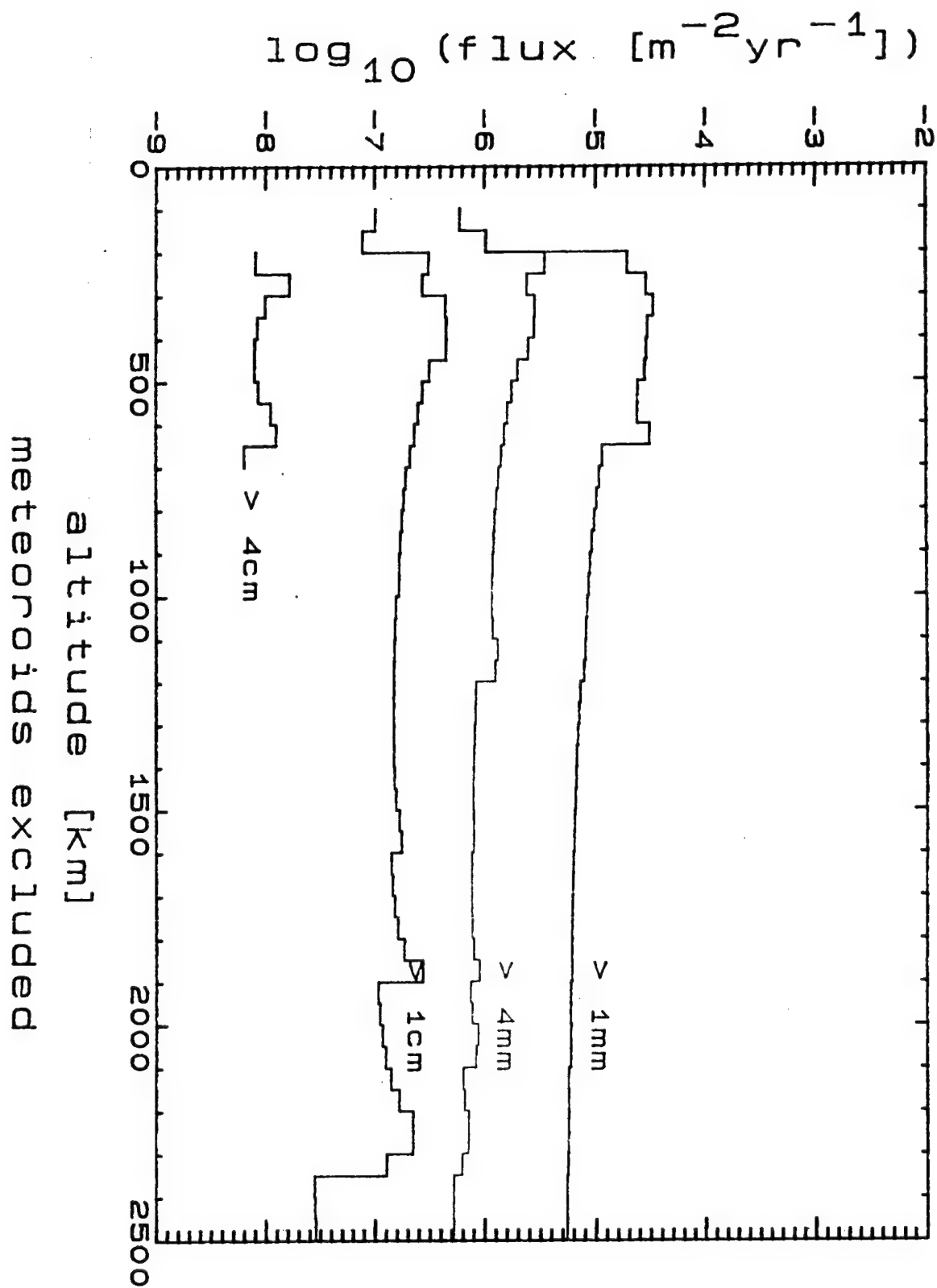


FIGURE A-6

10% impact
50% kinetic energy transfer
elapsed time = 1yr

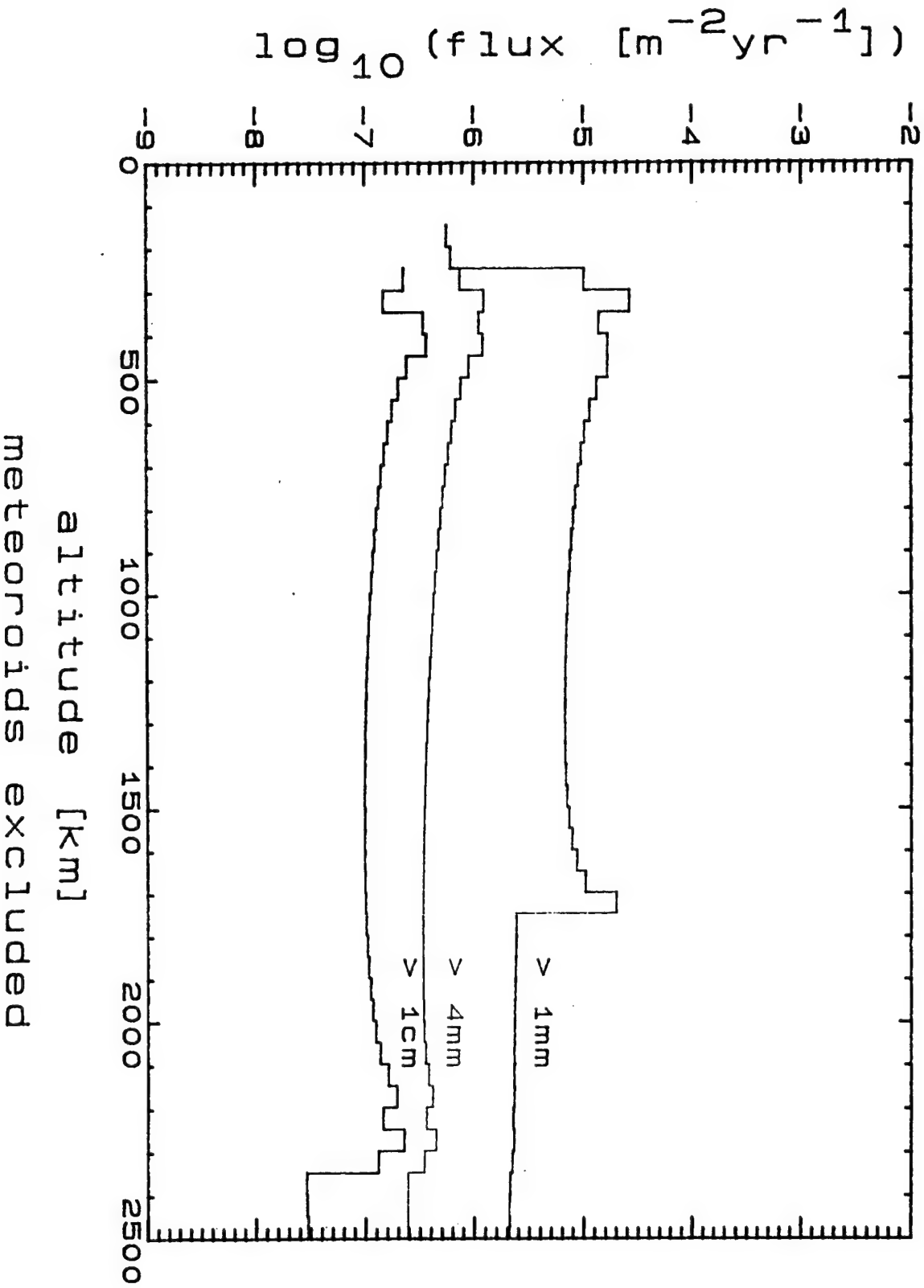


FIGURE A-7

10% impact transfer
10% kinetic energy transfer
elapsed time = 0wk

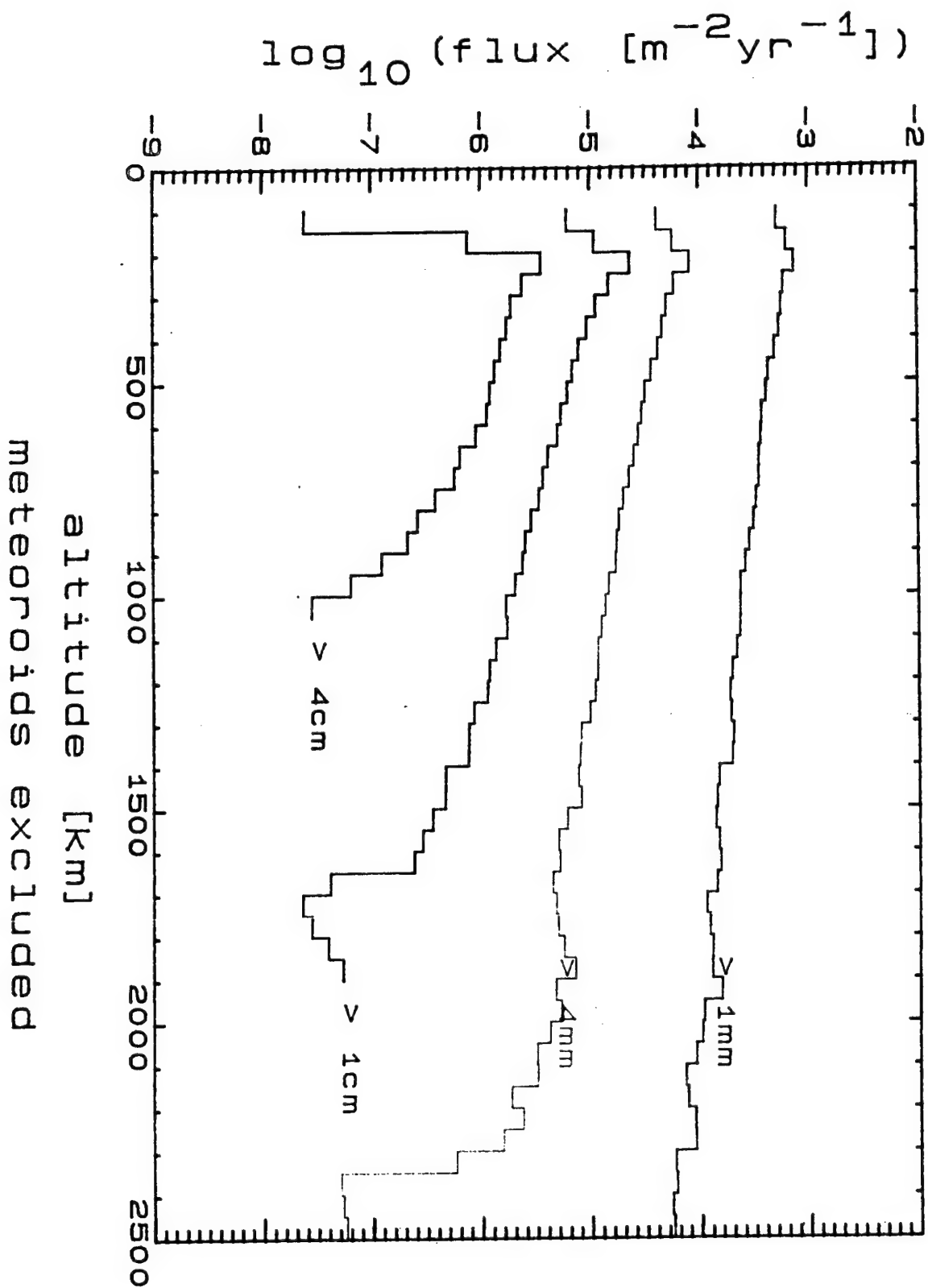


FIGURE A-8

10% impact kinetic energy transfer
elapsed time = 1wk

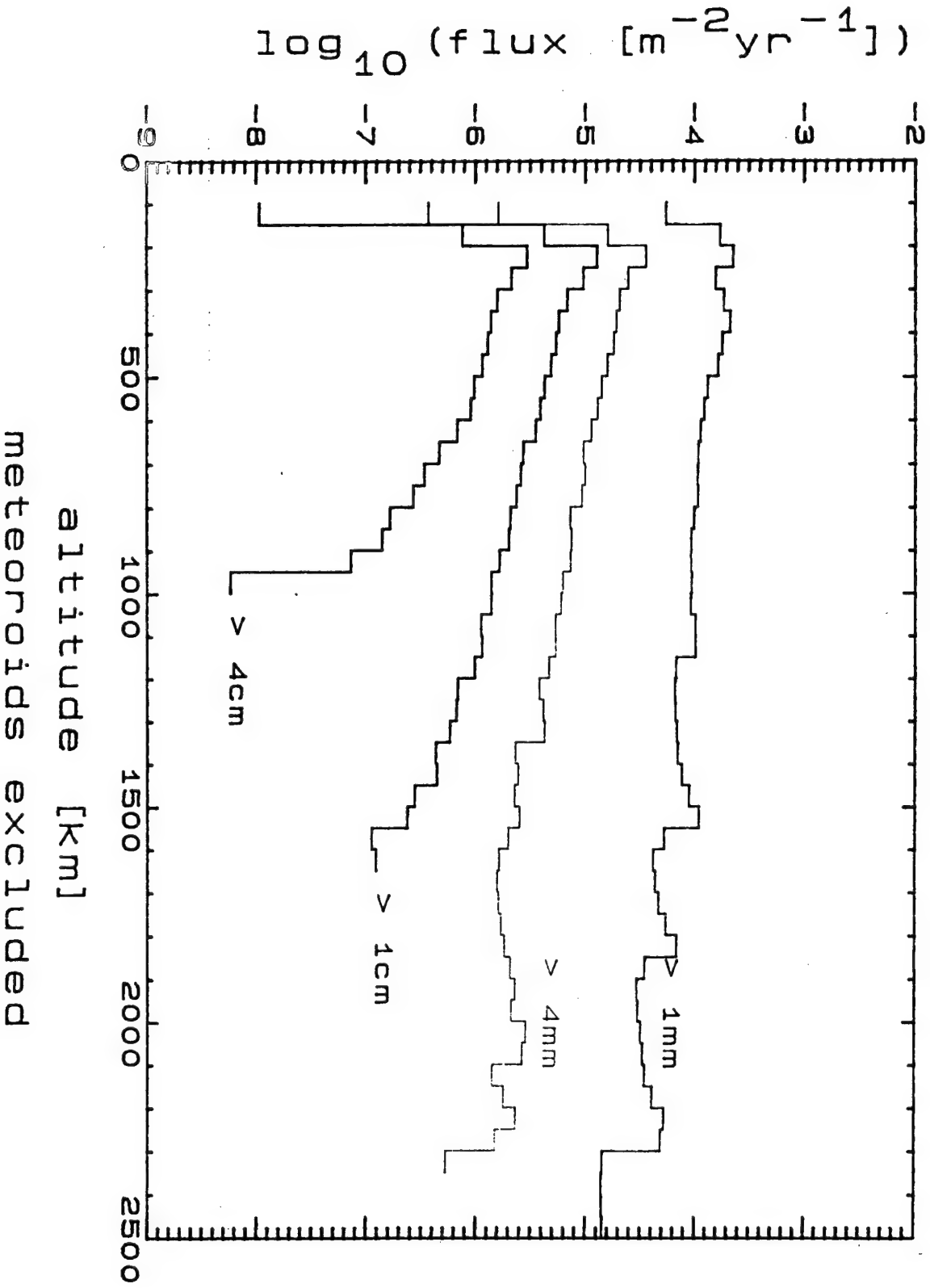


FIGURE A-9

10% impact
10% kinetic energy transfer
elapsed time = 1mo

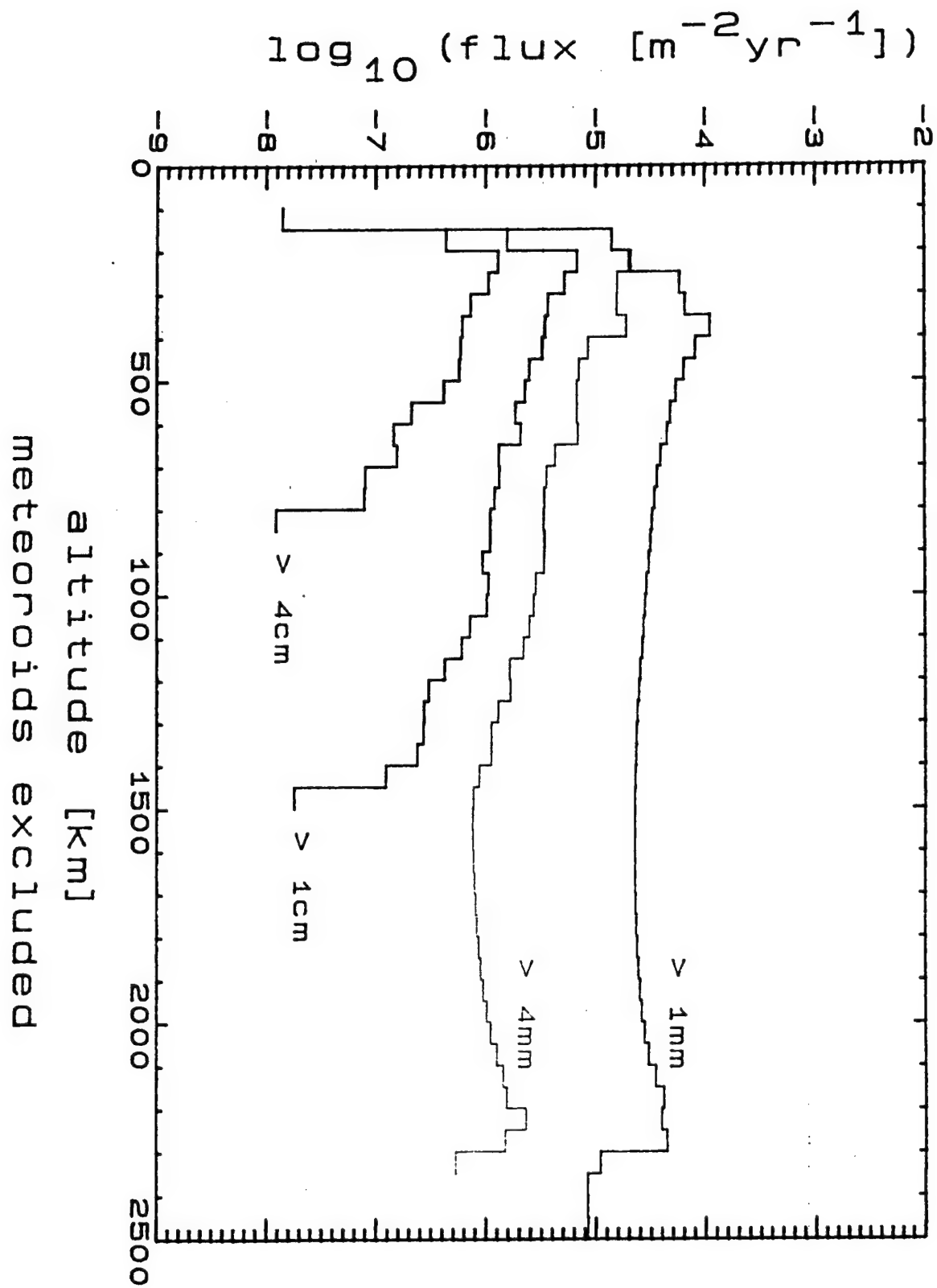


FIGURE A-10

10% impact transfer
10% kinetic energy transfer
elapsed time = 3mo

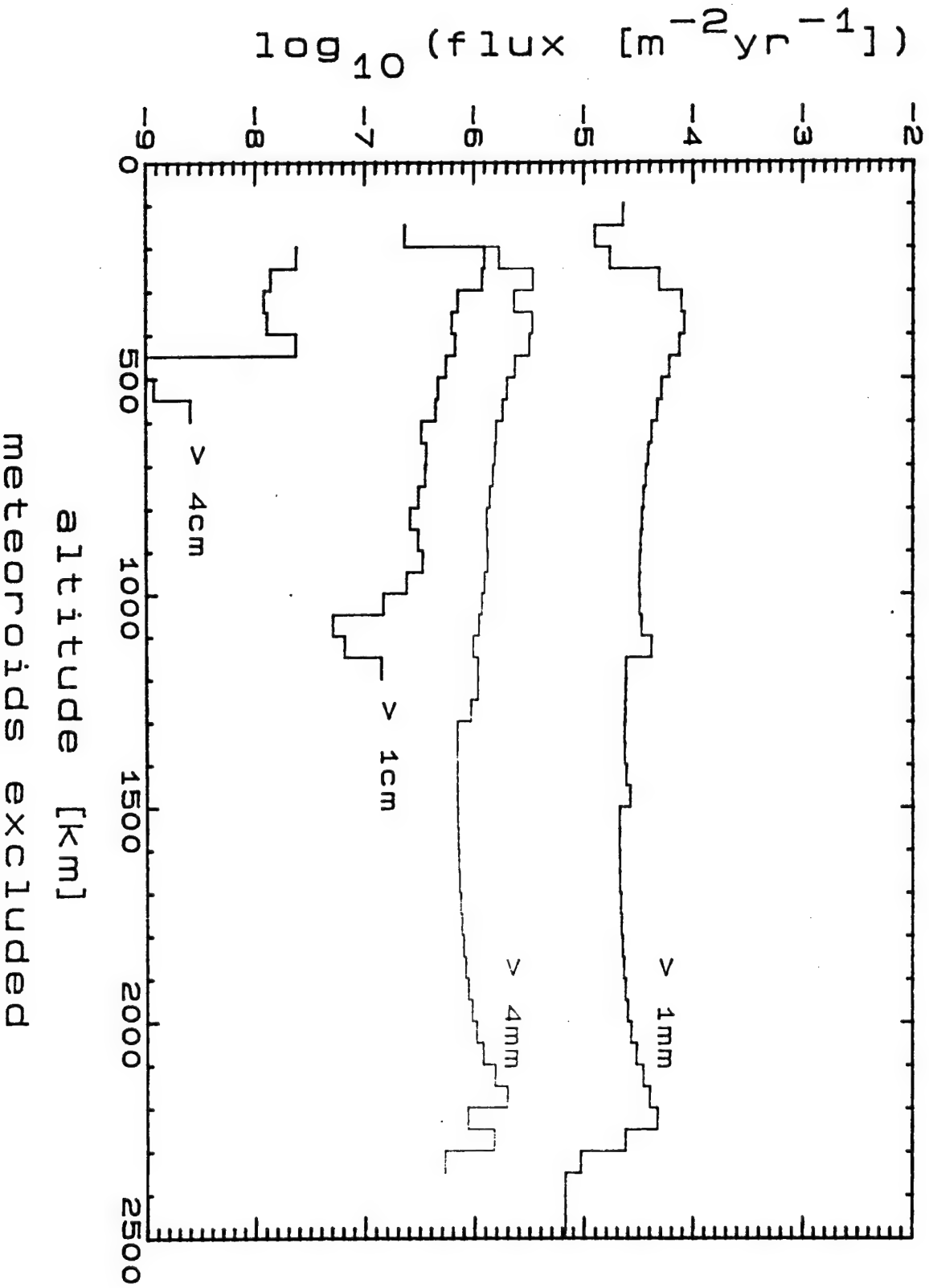


FIGURE A-11

10% impact
10% kinetic energy transfer
elapsed time = 6mo

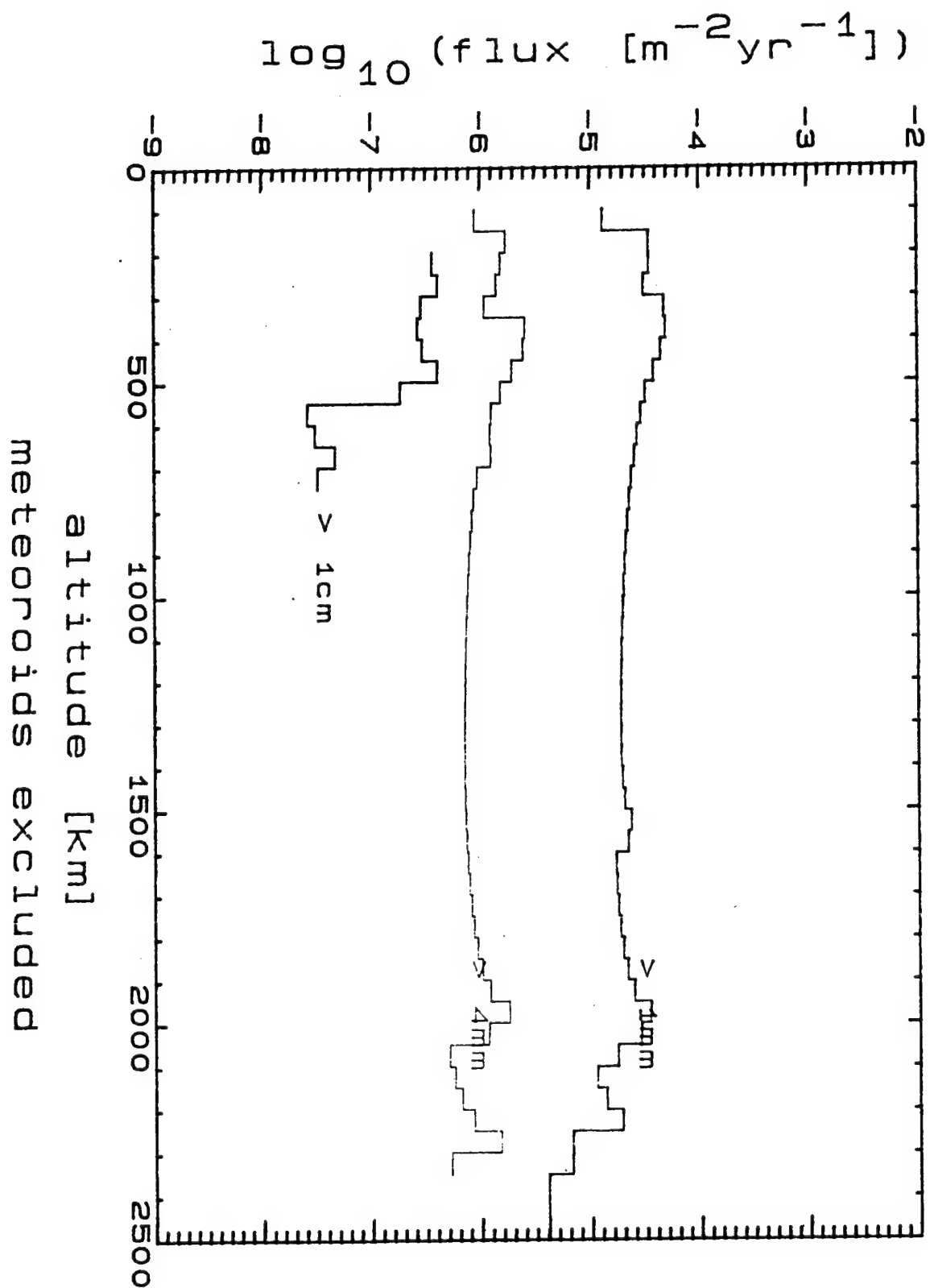


FIGURE A-12

10% impact kinetic energy transfer
elapsed time = 1yr

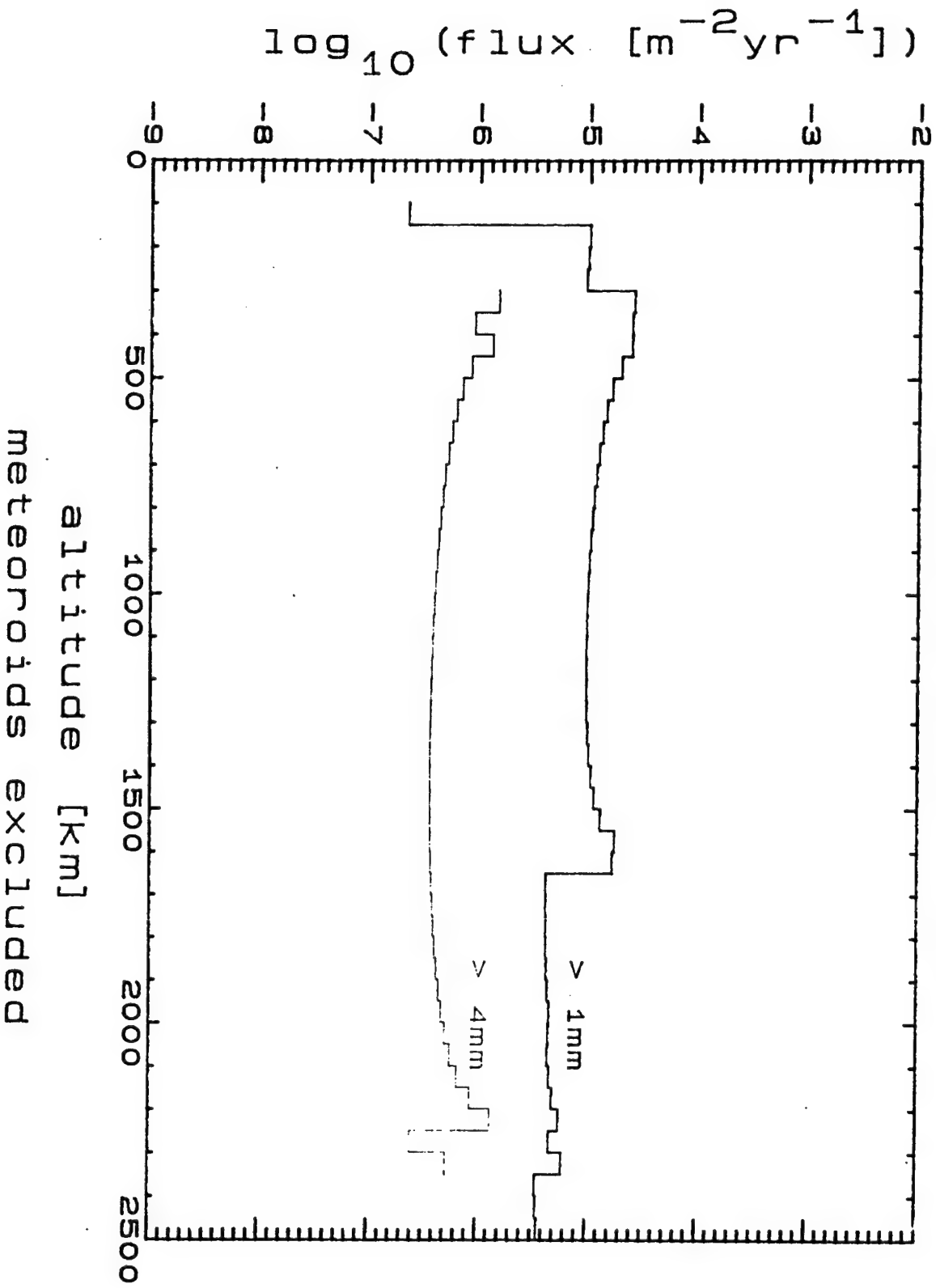


FIGURE A-13

10% impact
100% kinetic energy transfer
elapsed time = 0wk

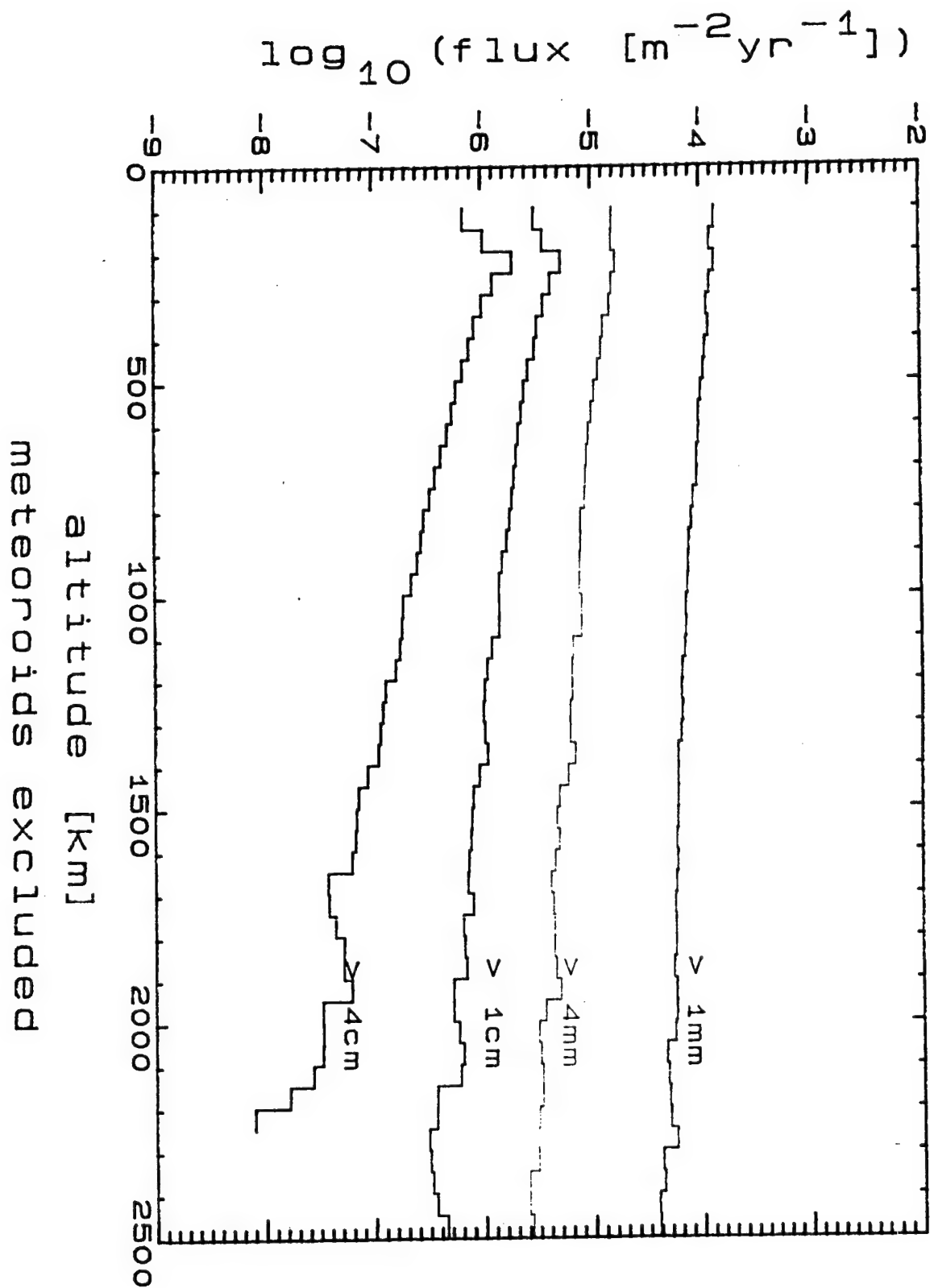


FIGURE A-14

10% impact
100% kinetic energy transfer
elapsed time = 1wk

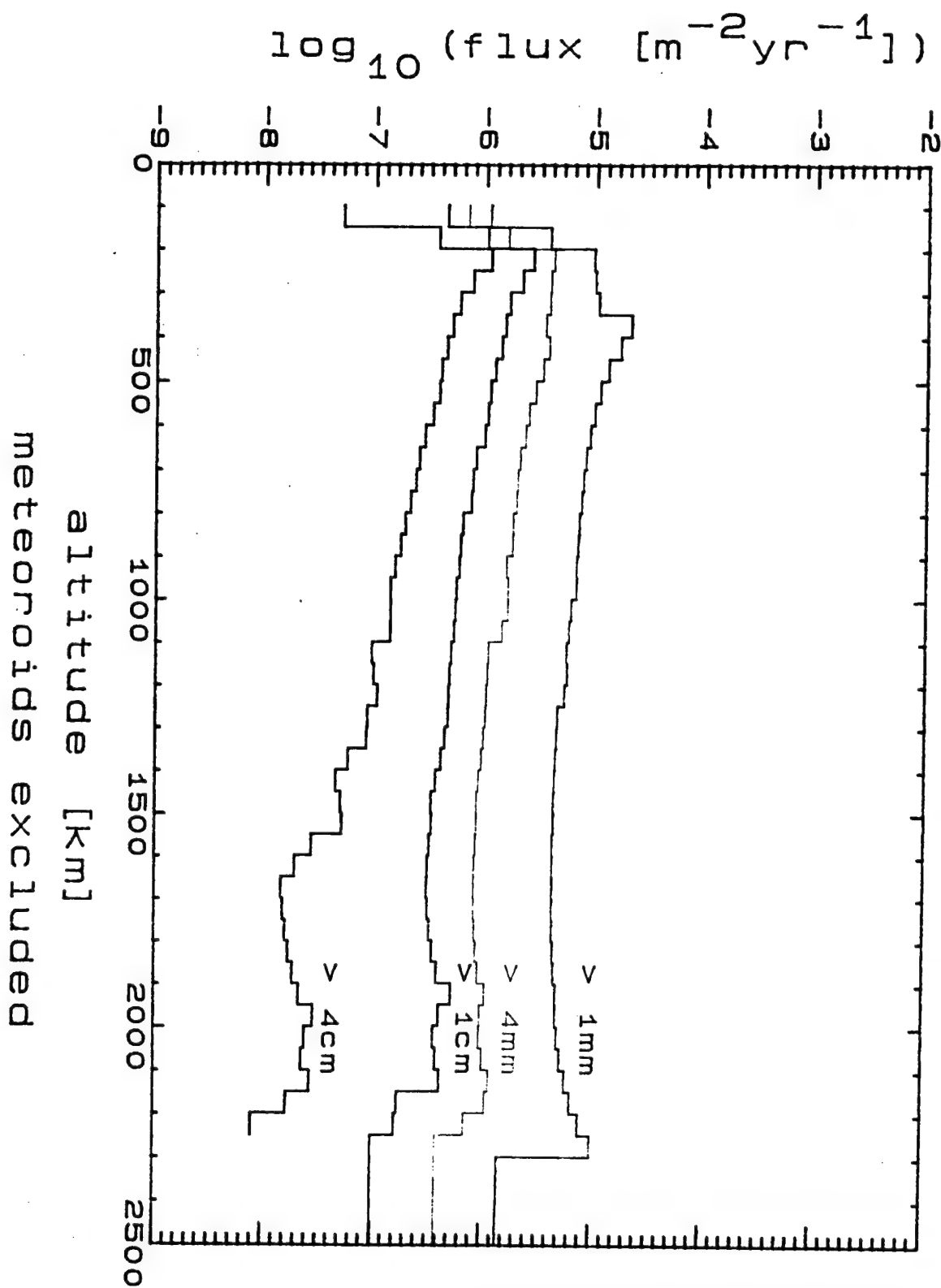


FIGURE A-15

10% impact
100% kinetic energy transfer
elapsed time = 1mo

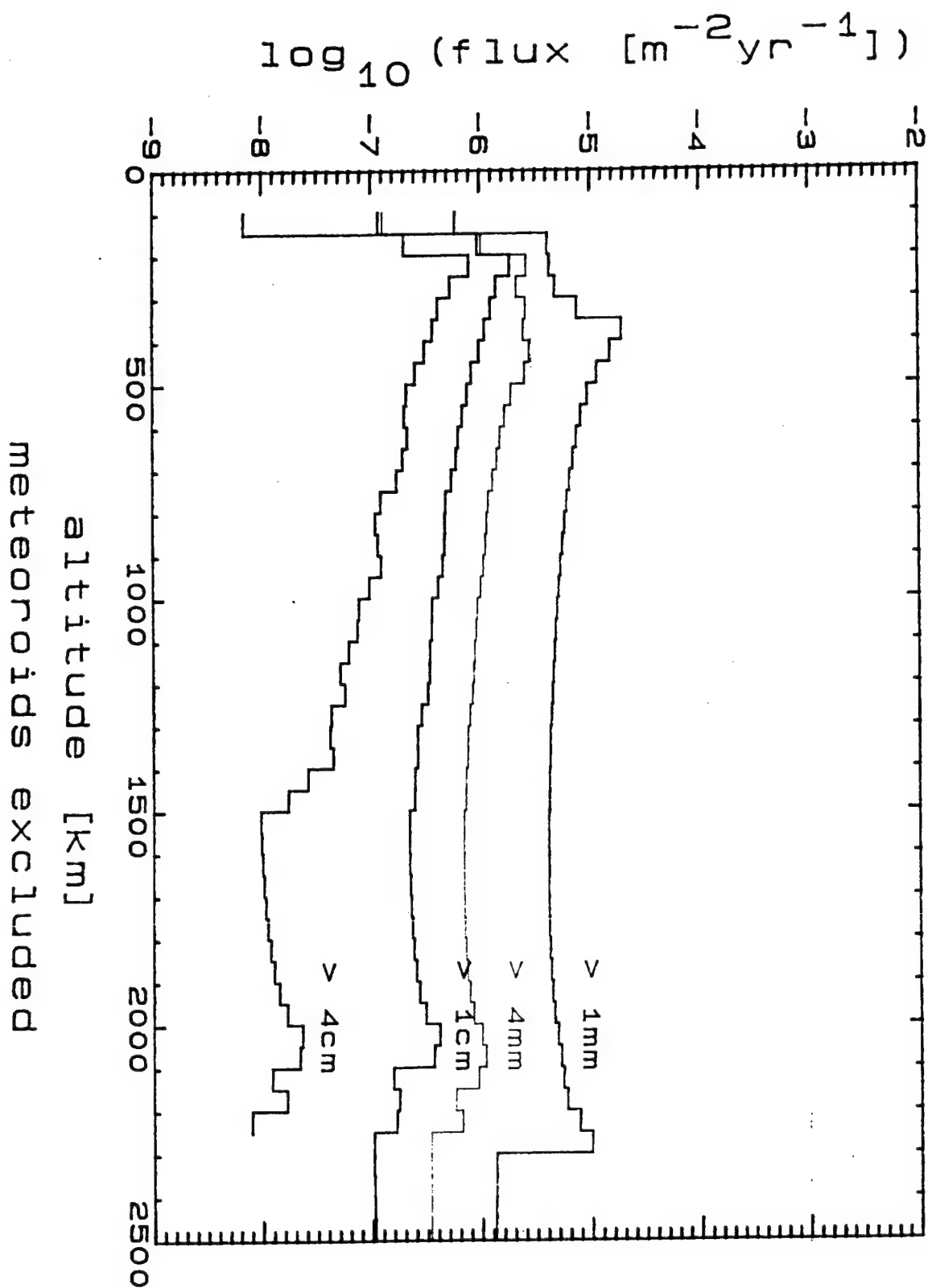


FIGURE A-16

10% impact
100% kinetic energy transfer
elapsed time = 3mo

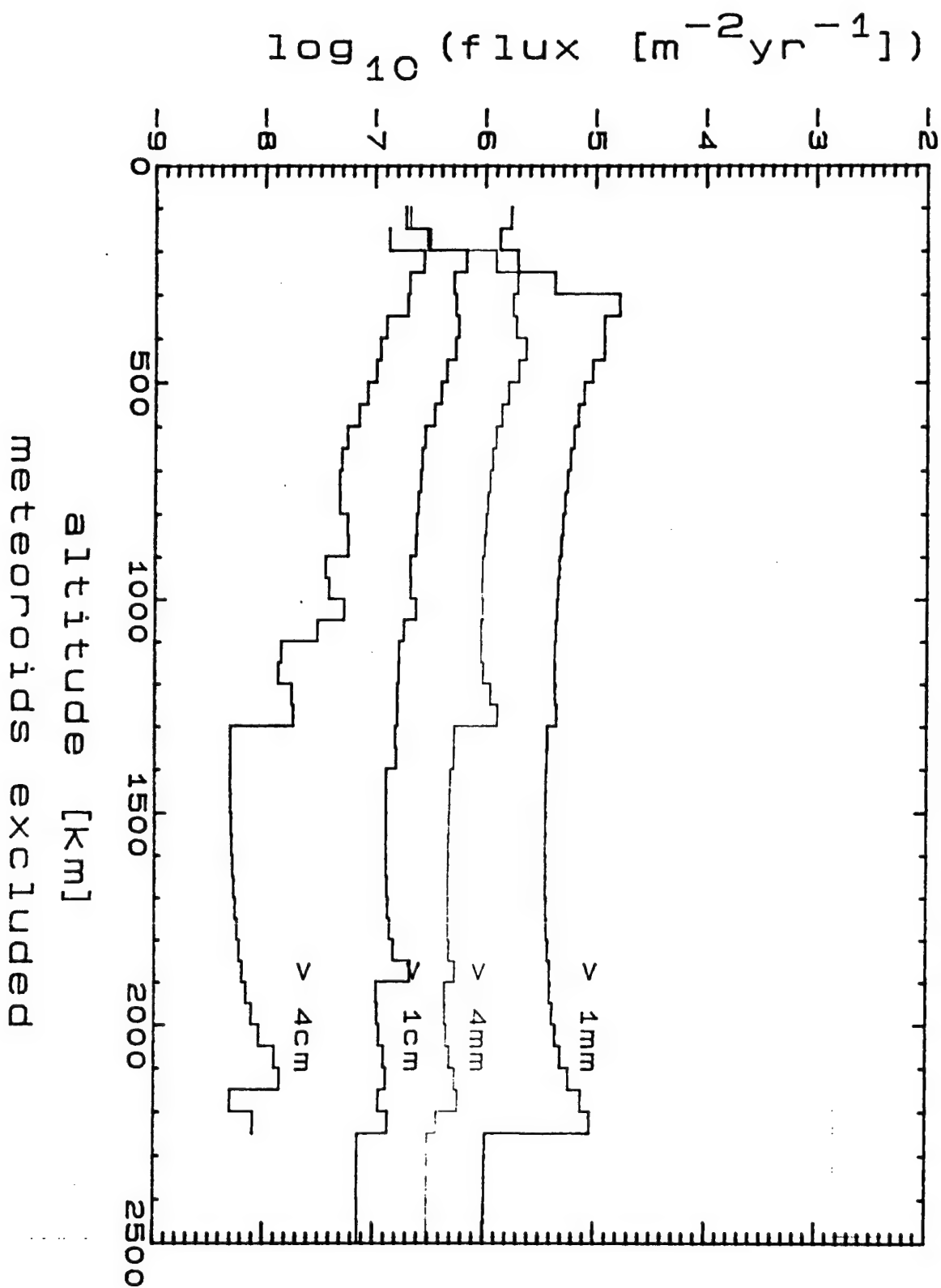


FIGURE A-17

10% impact
100% kinetic energy transfer
elapsed time = 6mo

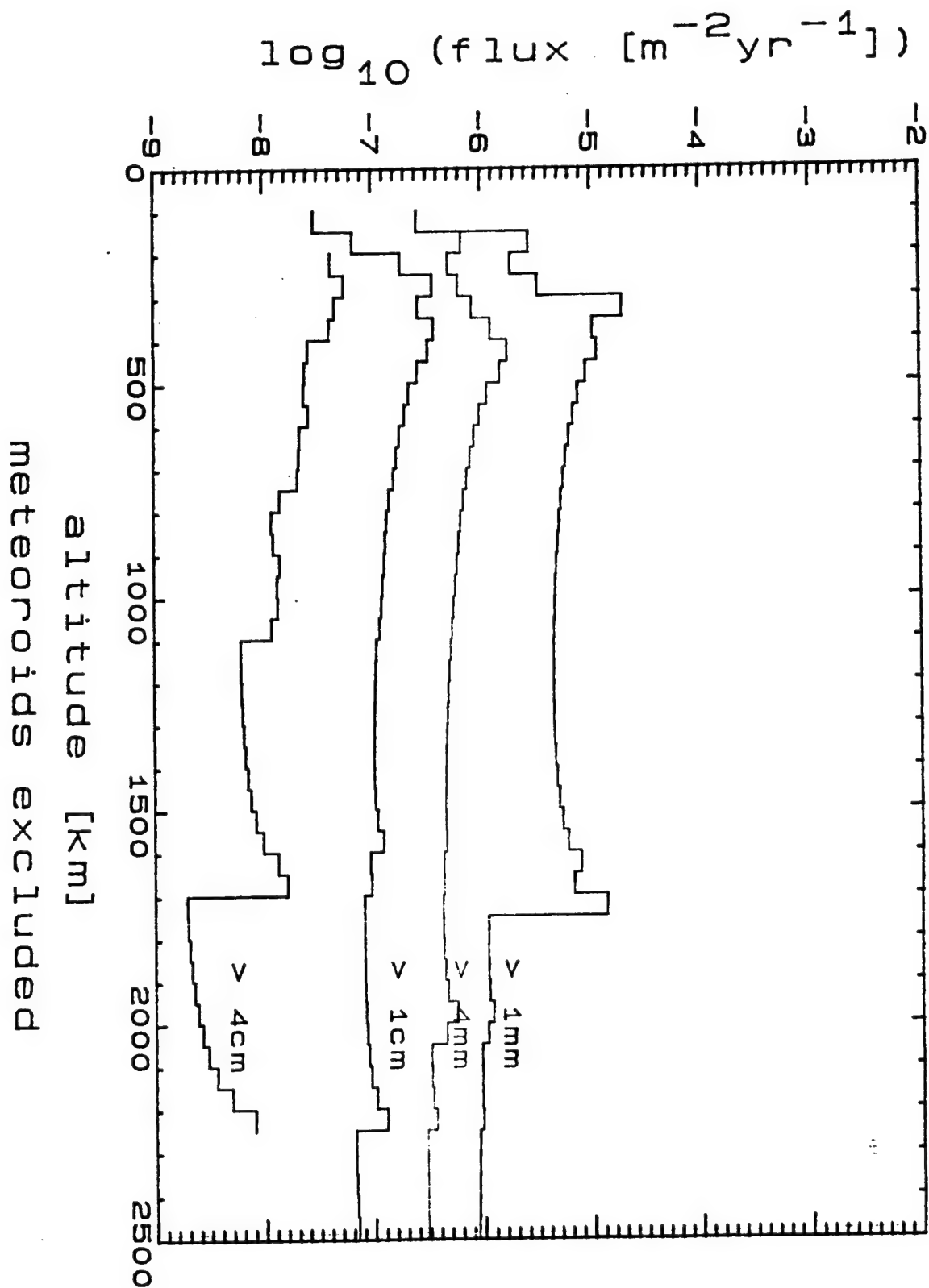


FIGURE A-18

10% impact
100% kinetic energy transfer
elapsed time = 1yr

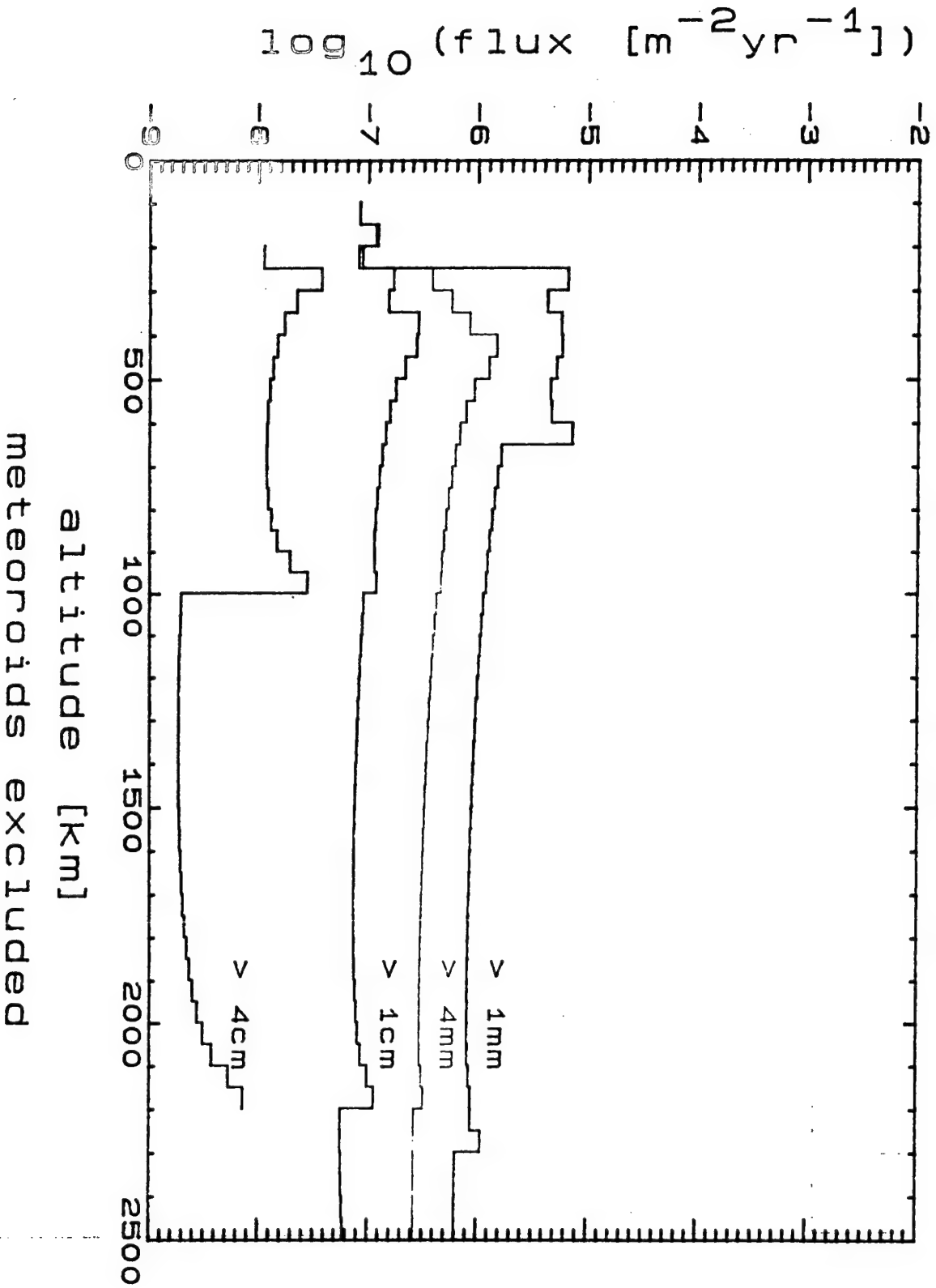


FIGURE A-19

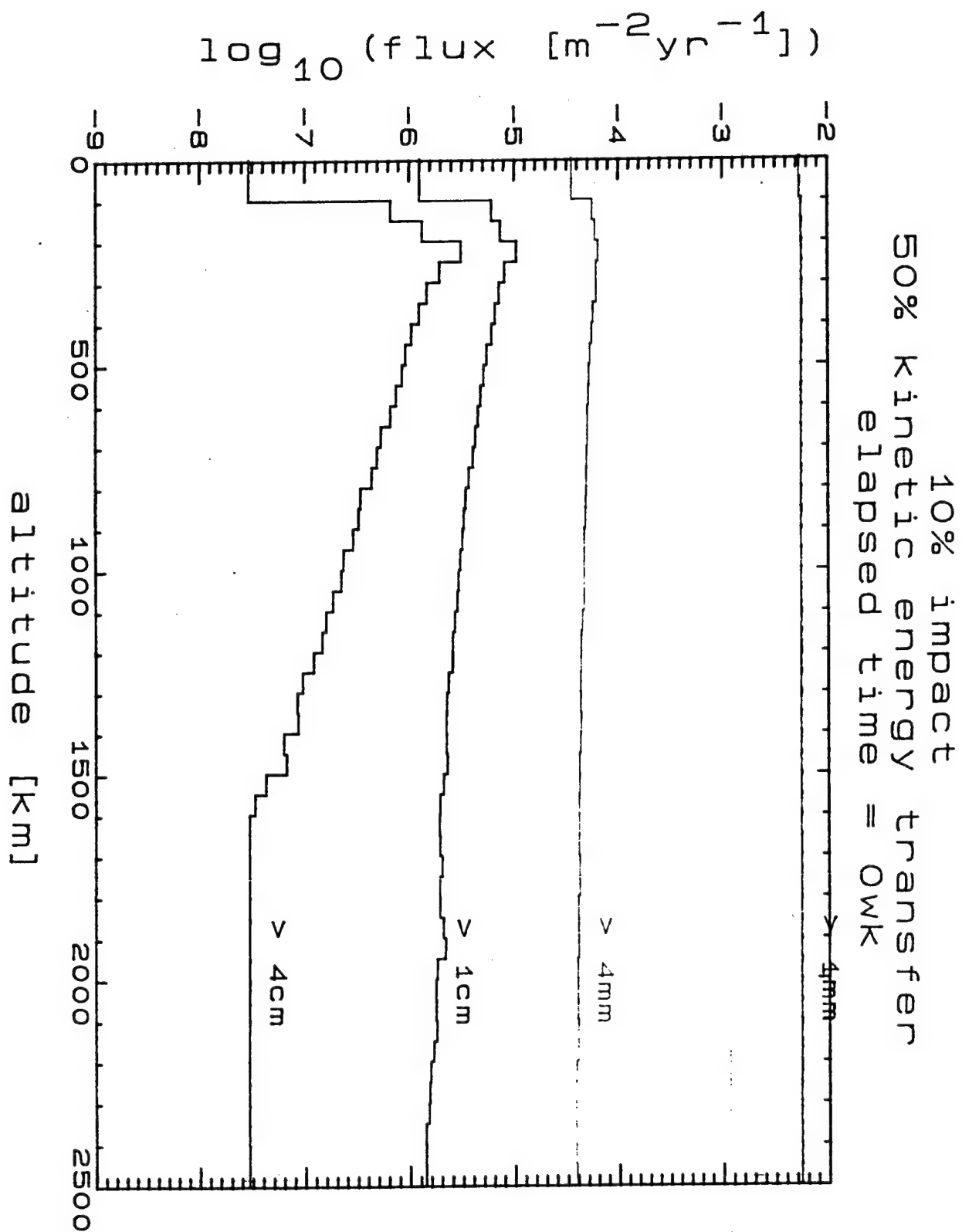


FIGURE A-20

10% impact
50% kinetic energy transfer
elapsed time = 1wk

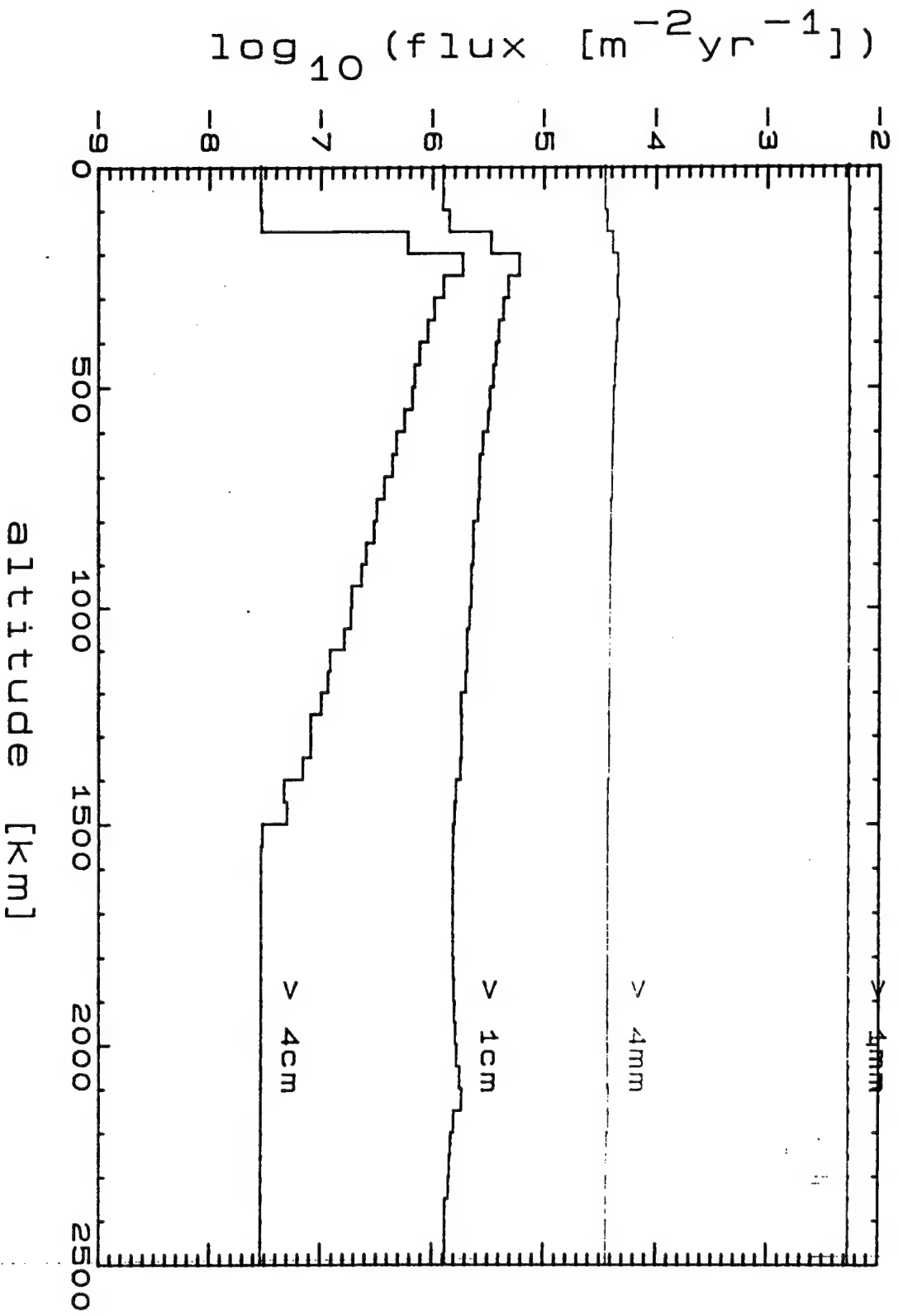


FIGURE A-21

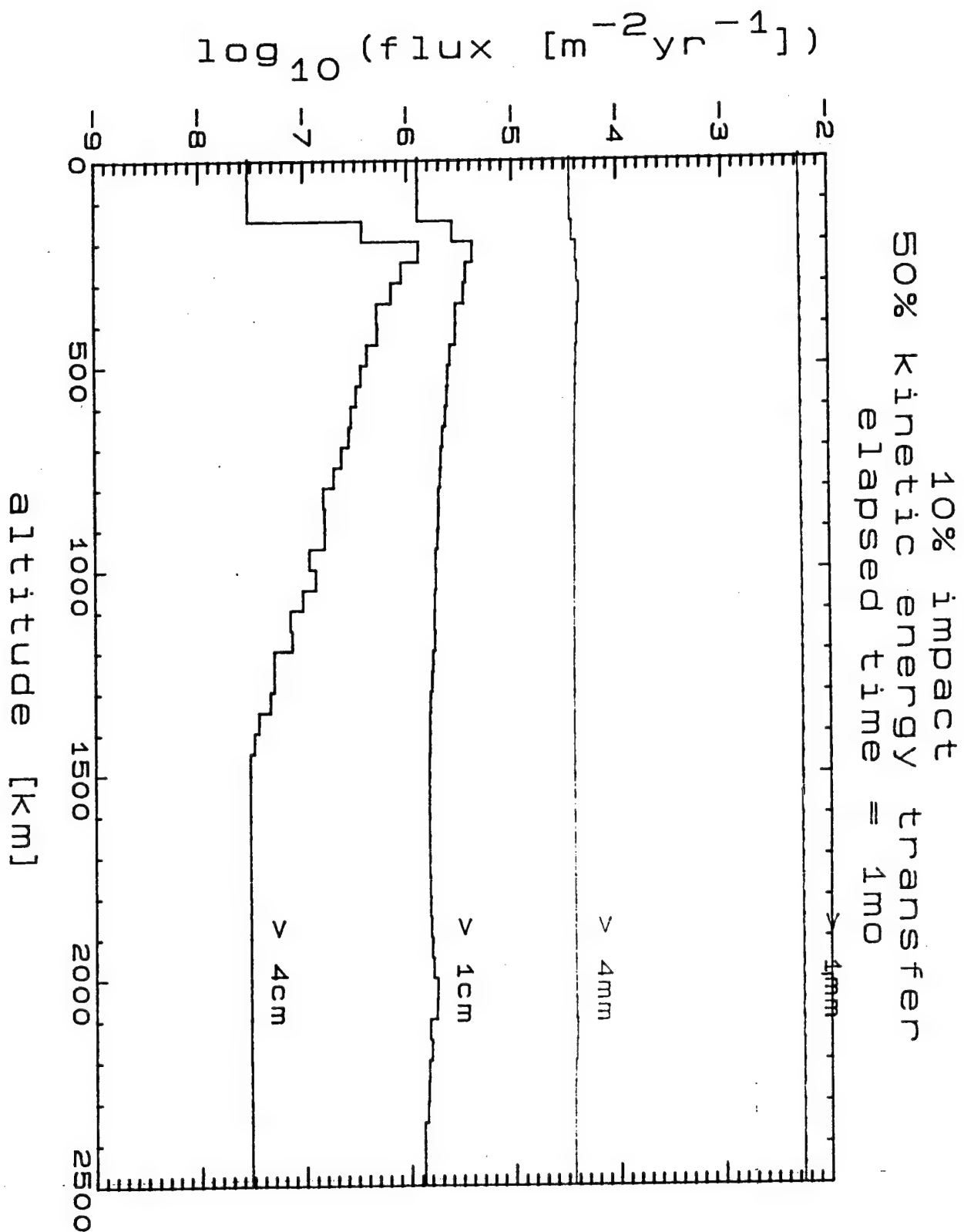


FIGURE A-22

10% impact
50% kinetic energy transfer
elapsed time = 3mo

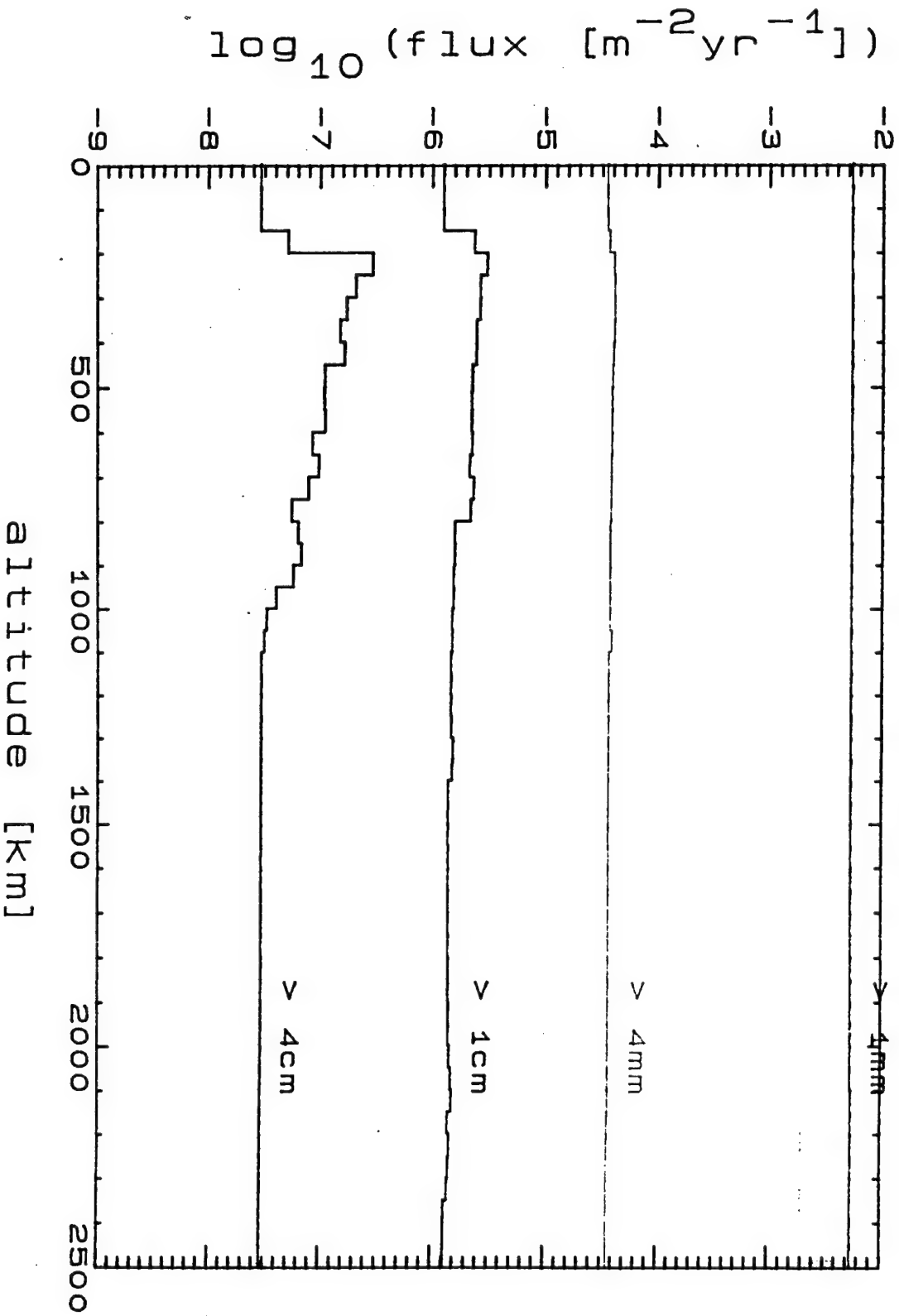


FIGURE A-23

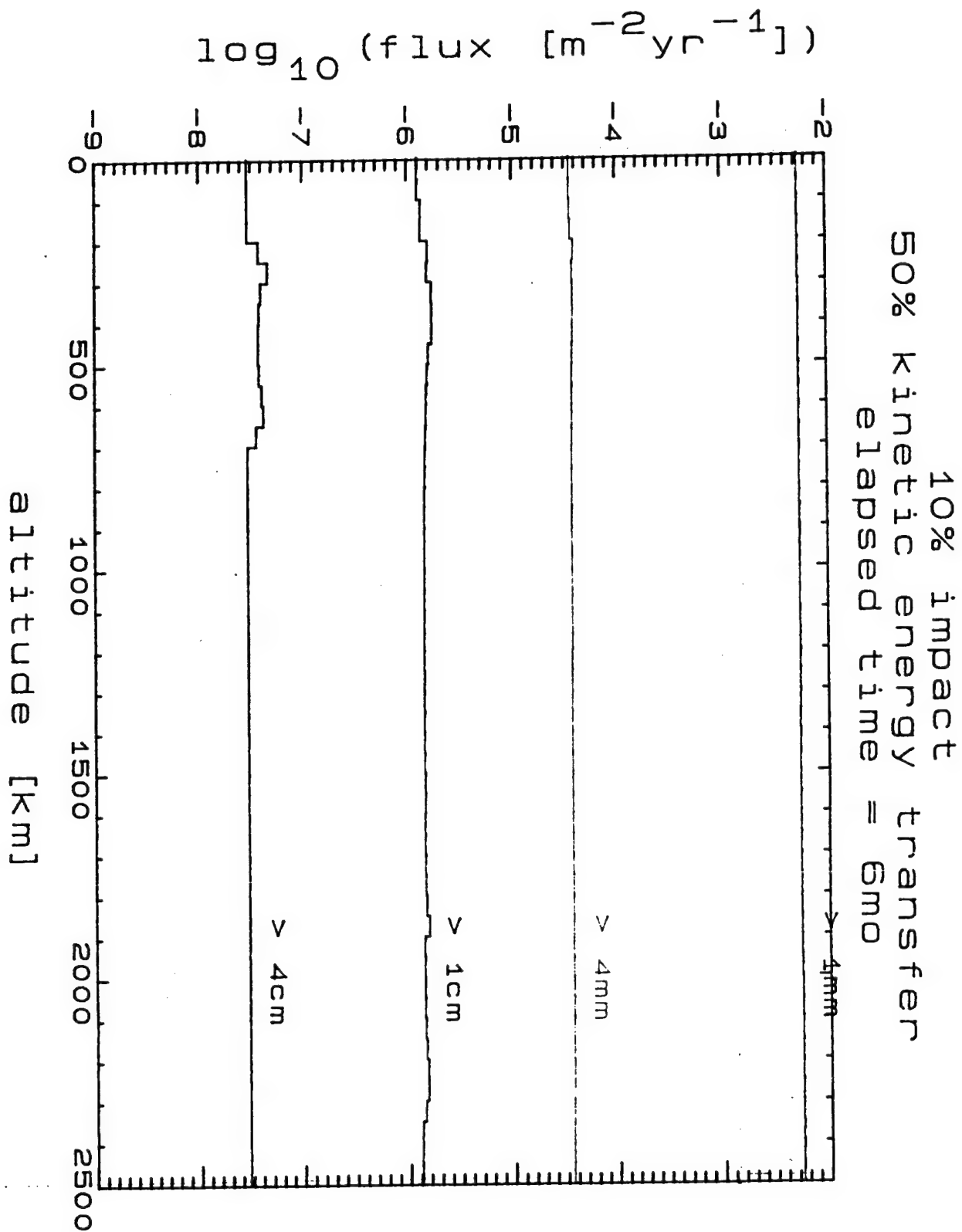


FIGURE A-24

10% impact
50% kinetic energy transfer
elapsed time = 1yr

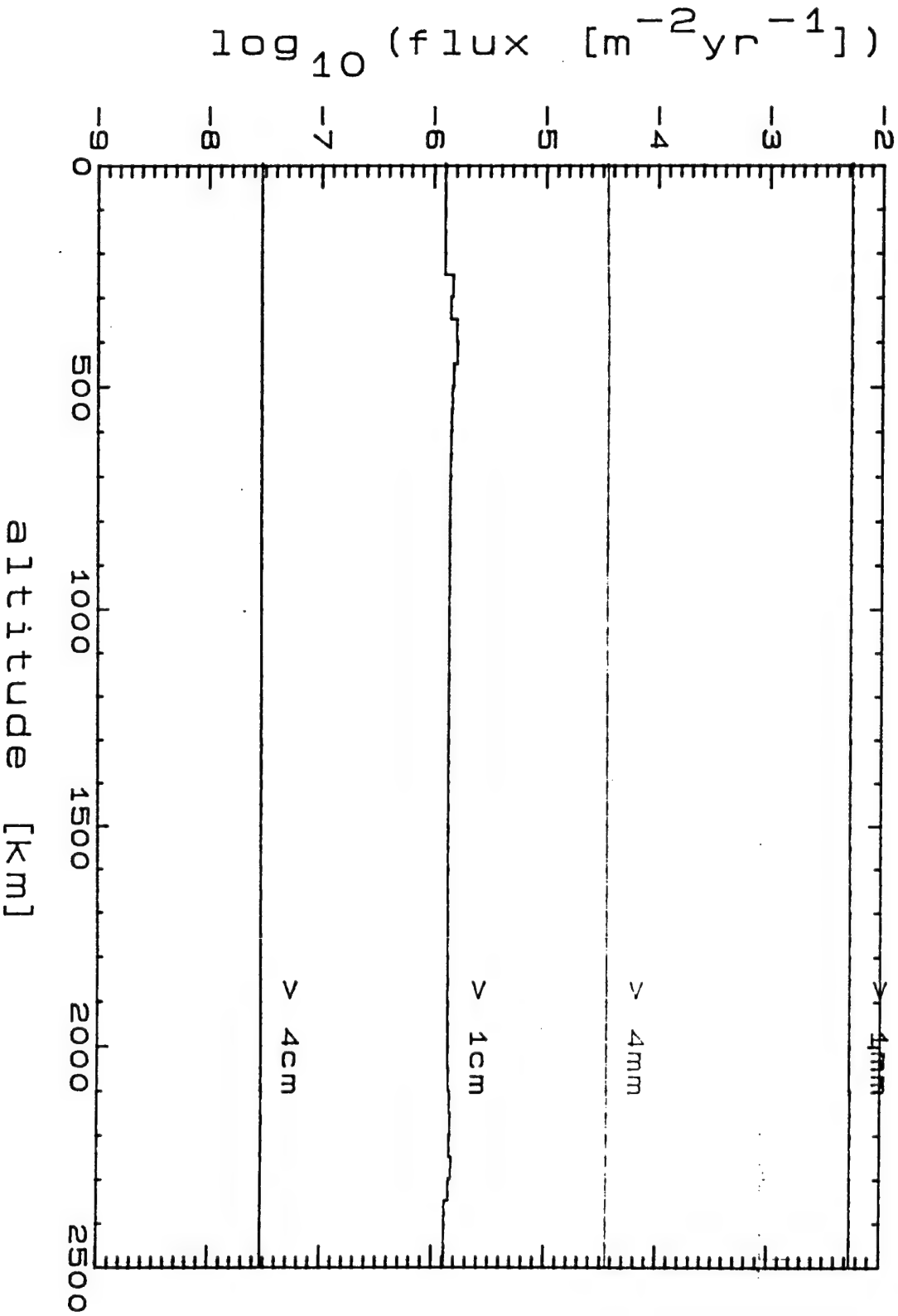


FIGURE A-25

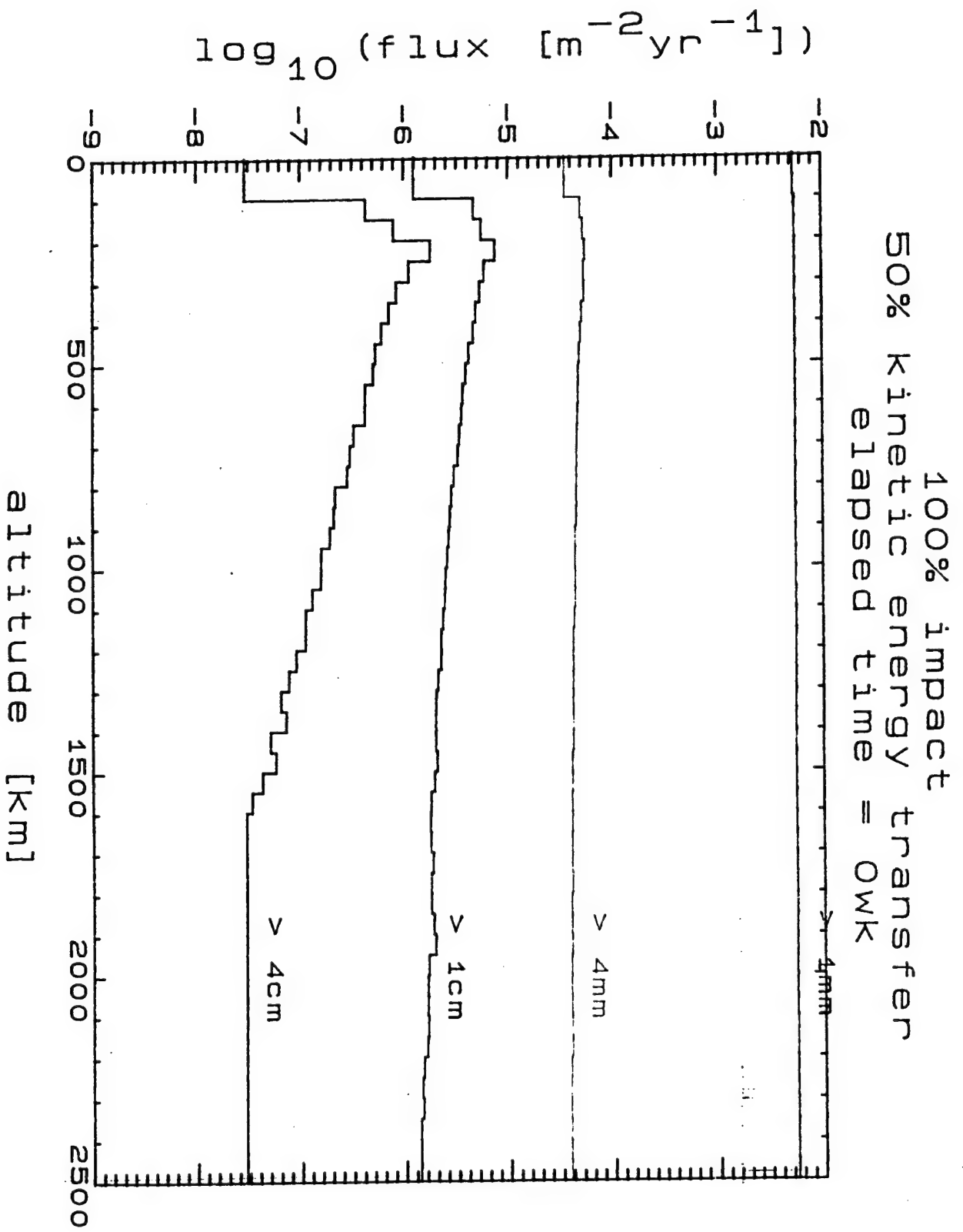


FIGURE A-26

100% impact
50% kinetic energy transfer
elapsed time = 1wk

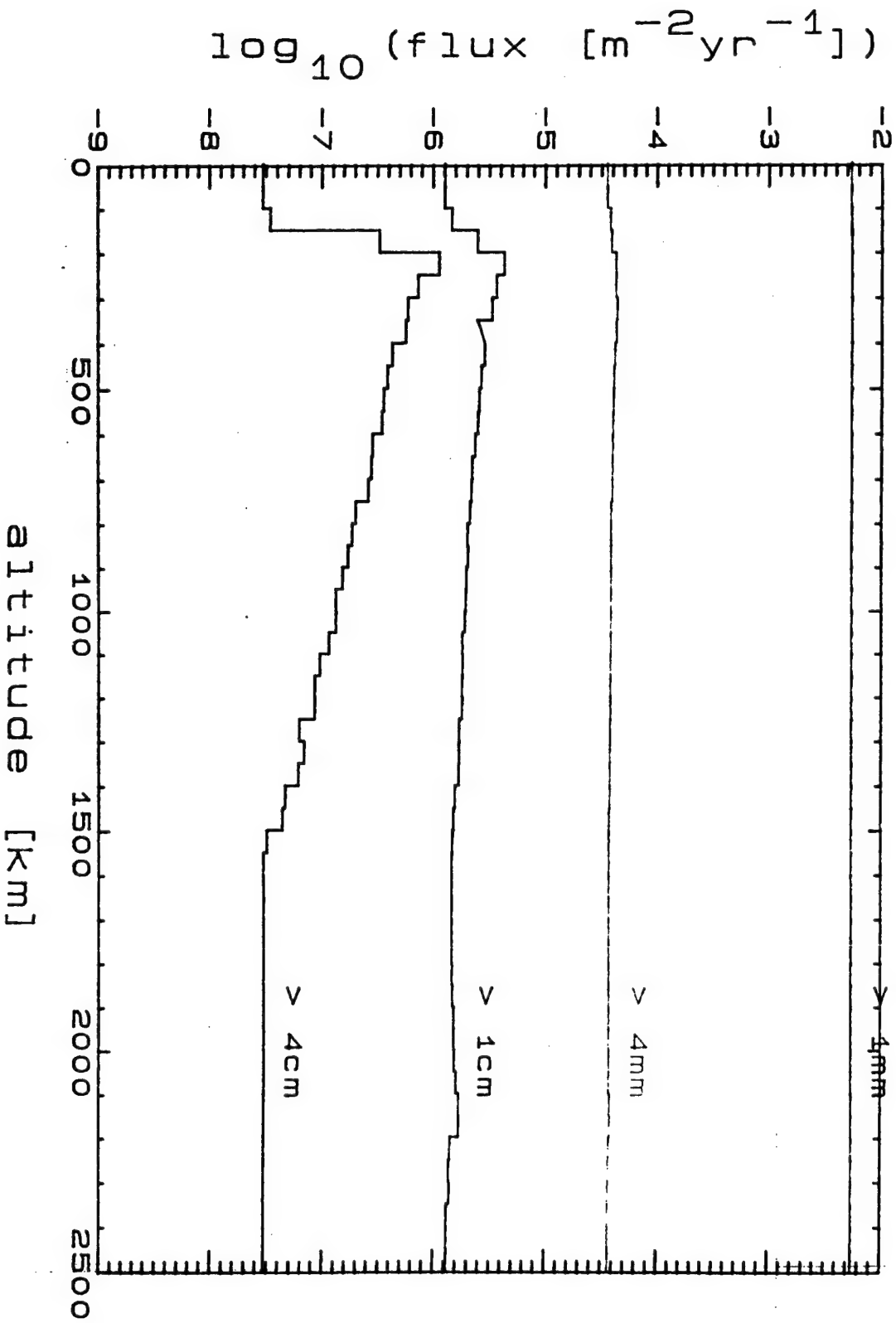


FIGURE A-27

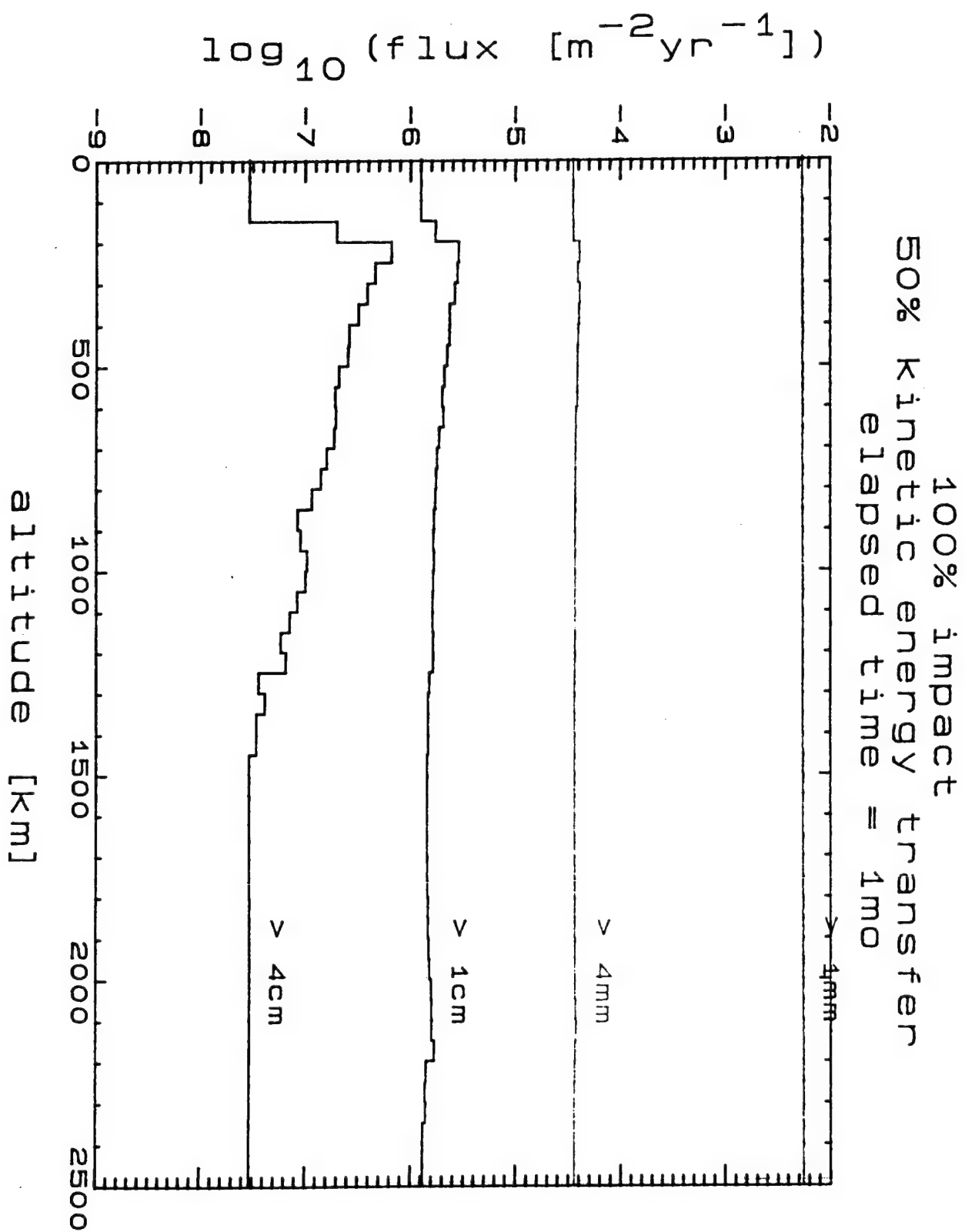


FIGURE A-28

100% impact
50% kinetic energy transfer
elapsed time = 3mo

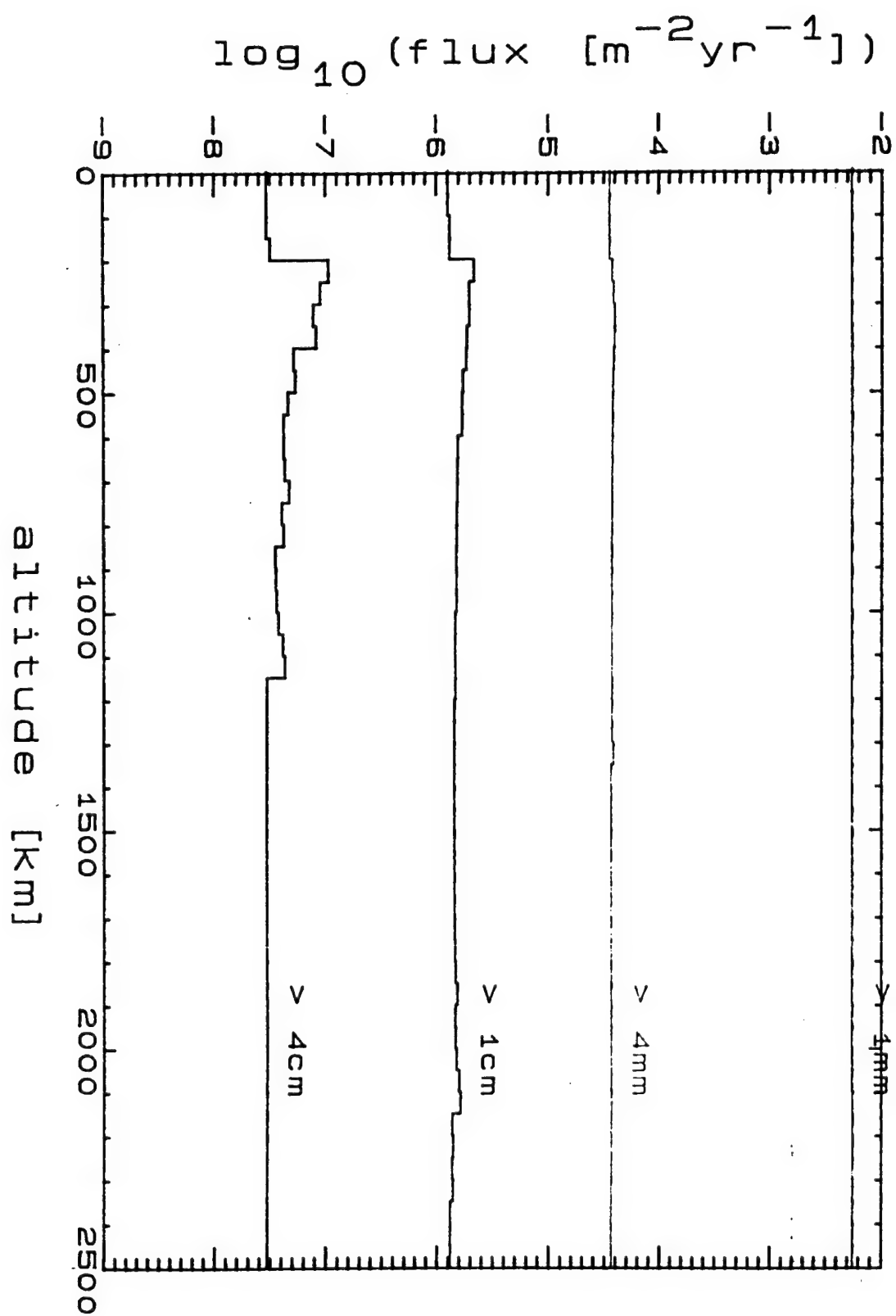


FIGURE A-29

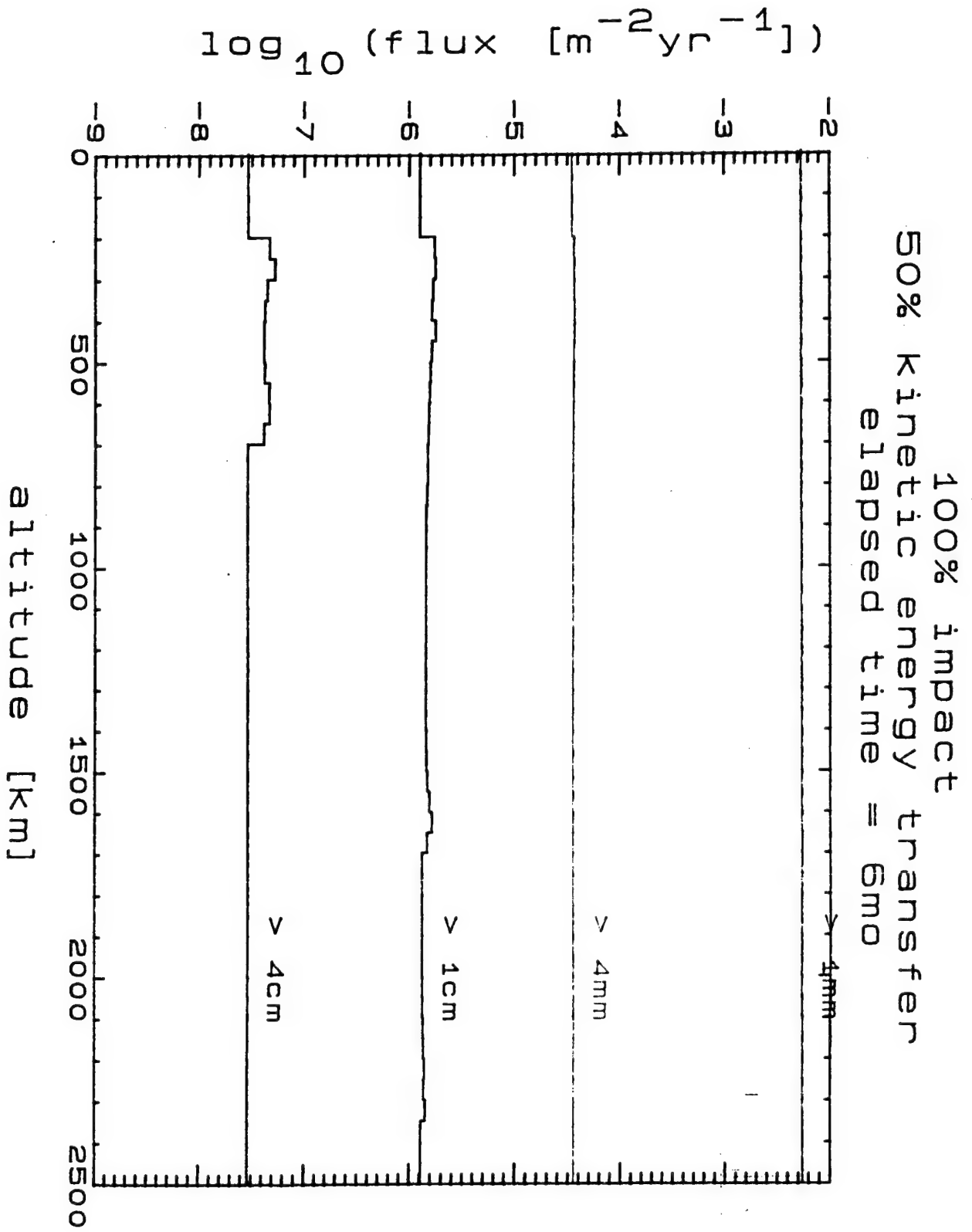


FIGURE A-30

100% impact
50% kinetic energy transfer
elapsed time = 1 yr

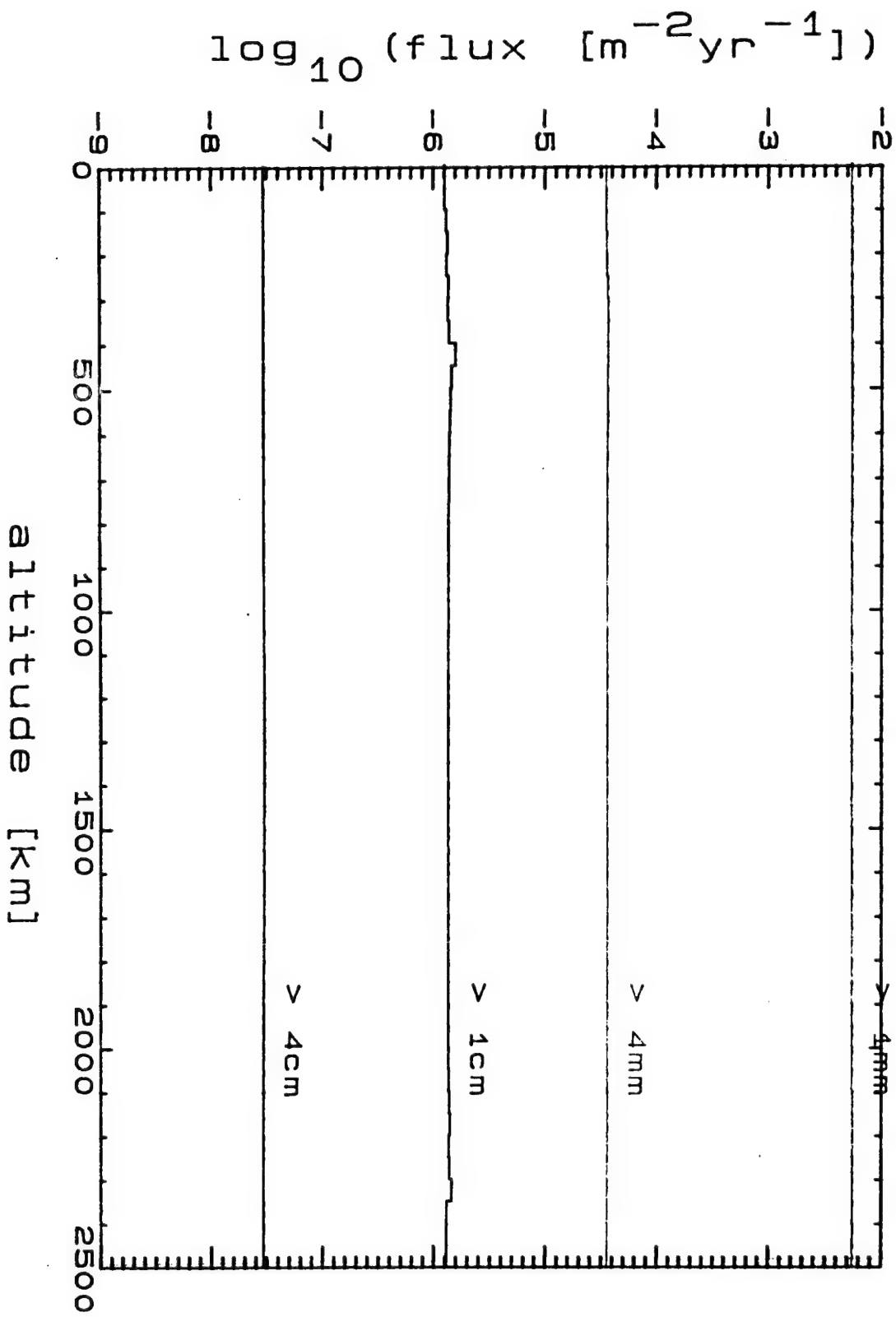


FIGURE A-31

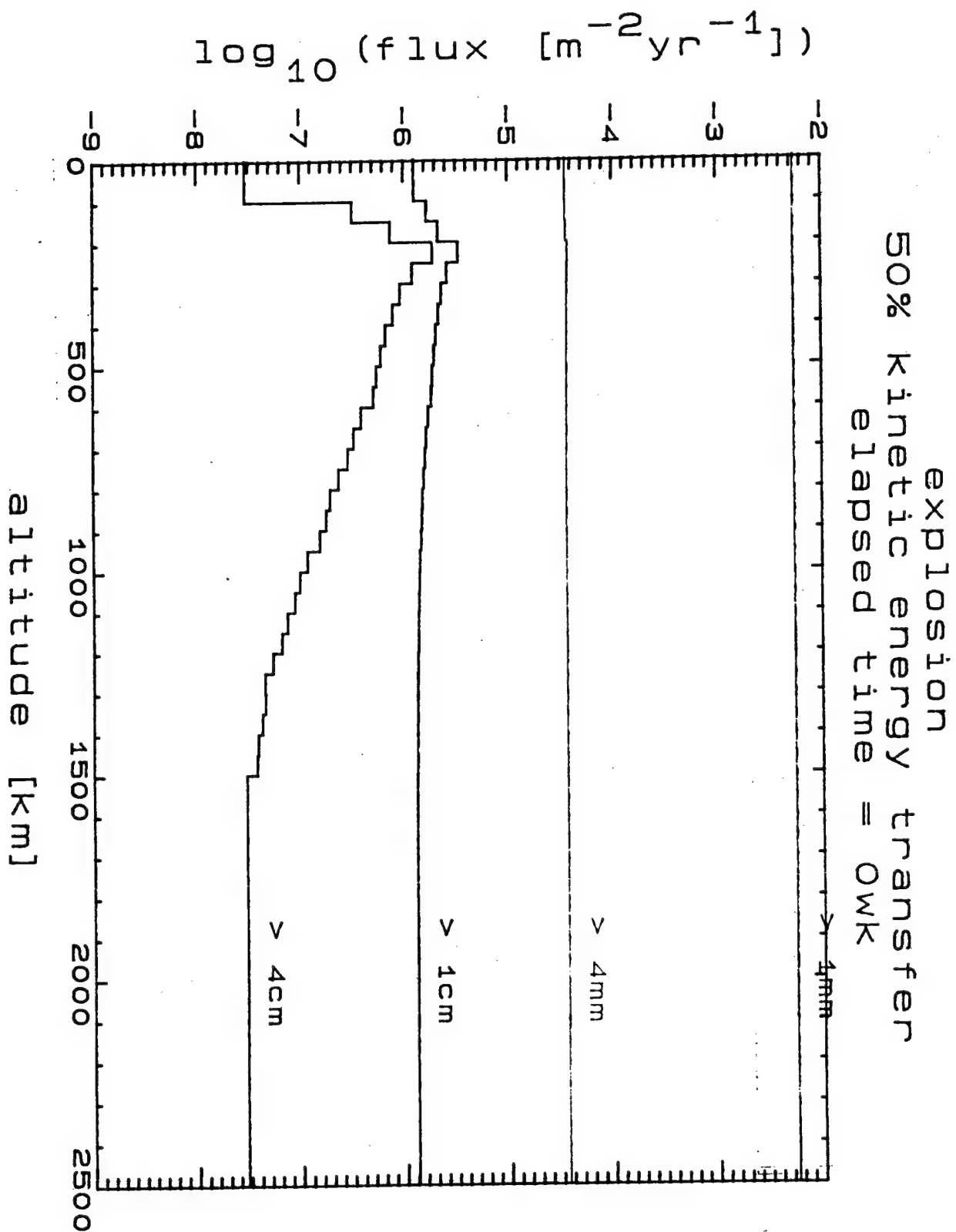


FIGURE A-32

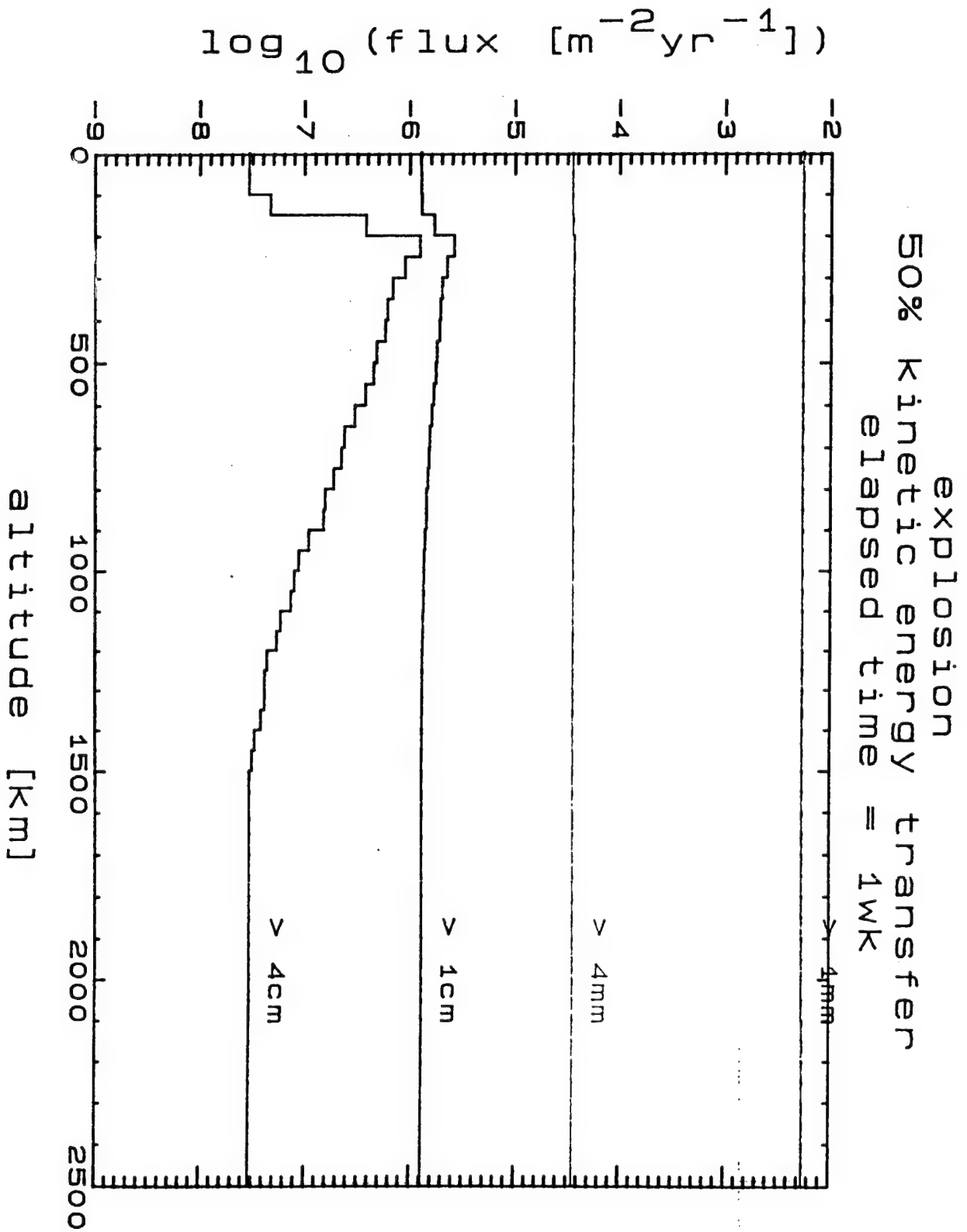


FIGURE A-33

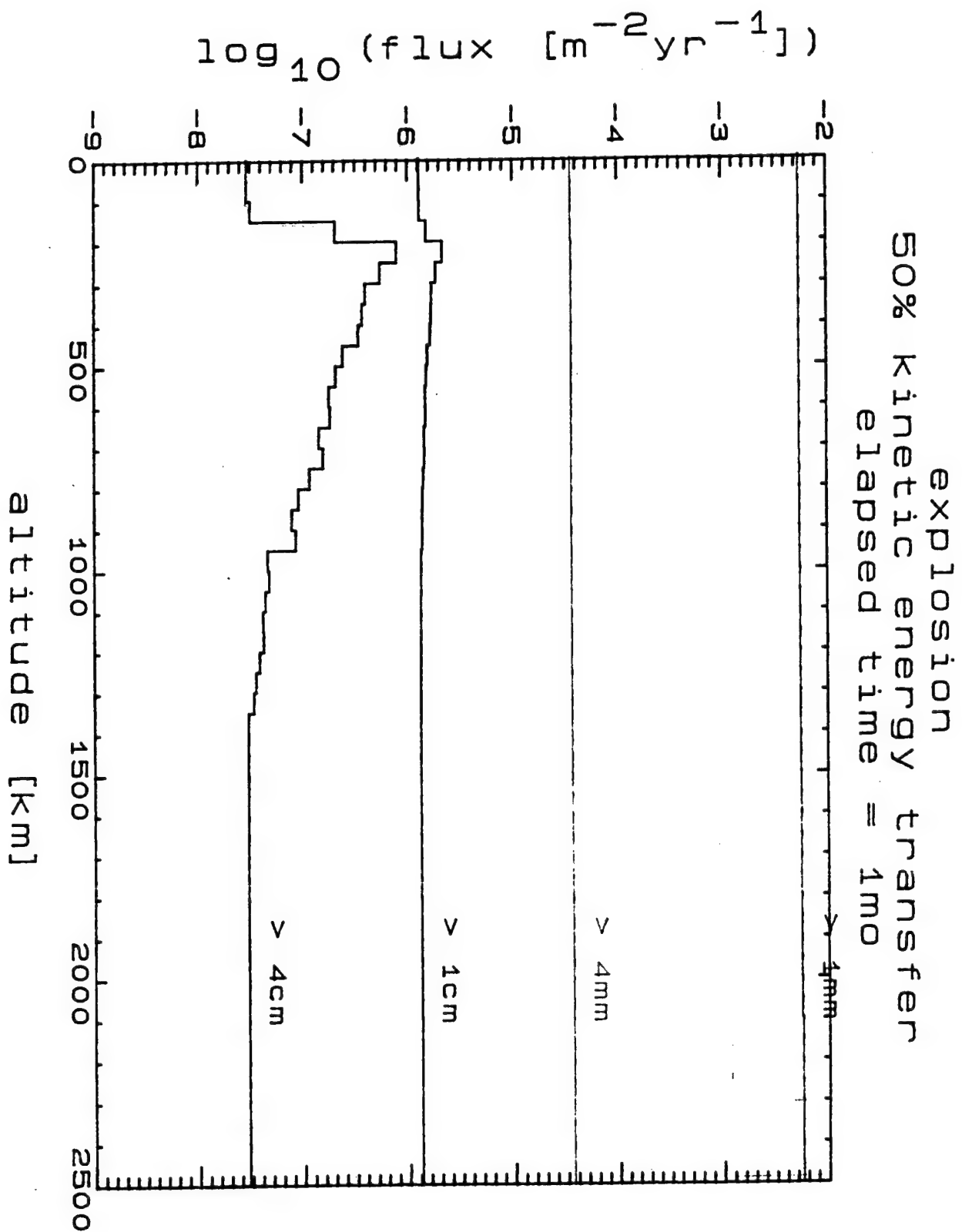


FIGURE A-34

explosion
50% kinetic energy transfer
elapsed time = 3mo

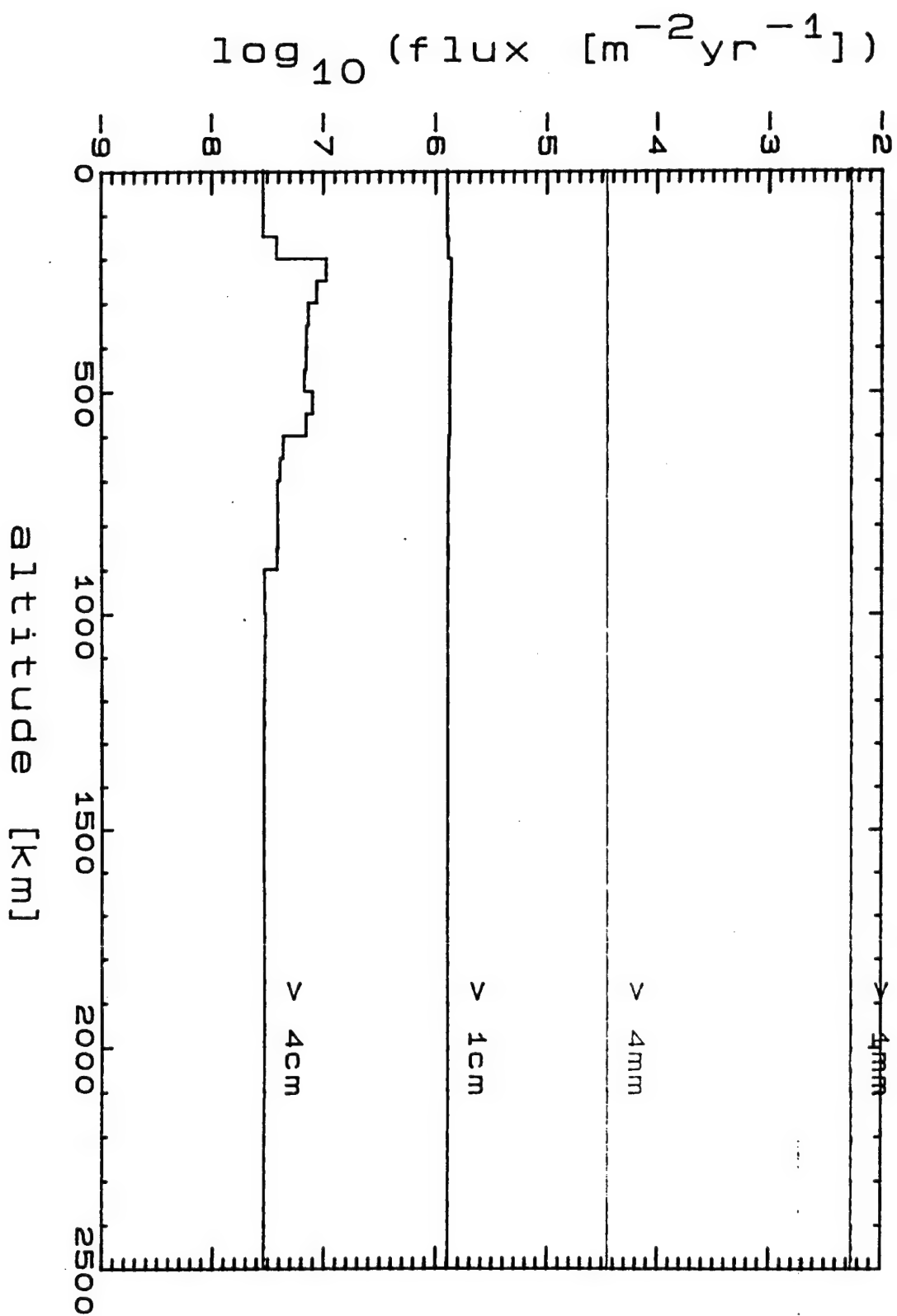


FIGURE A-35

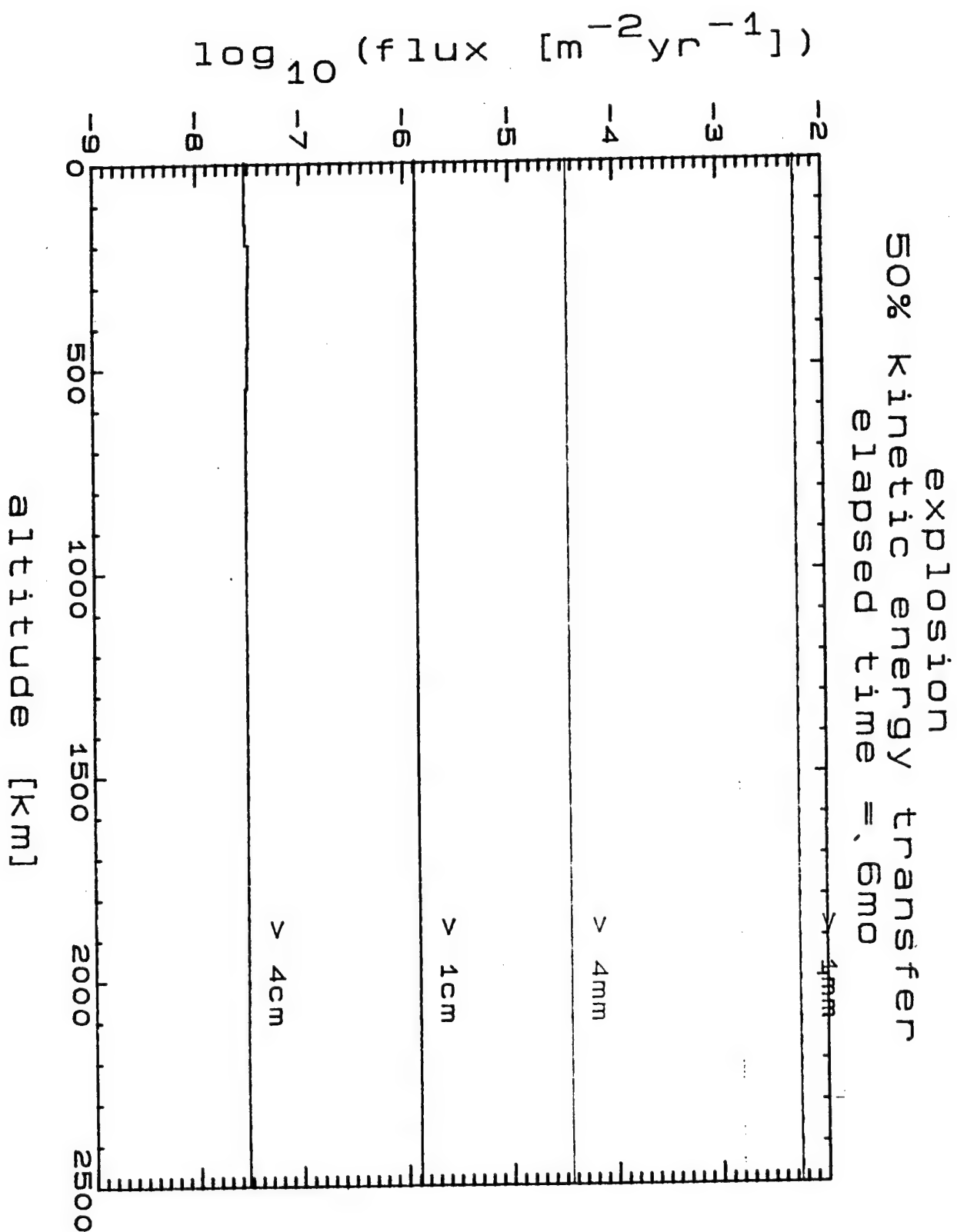


FIGURE A-36

explosion
50% kinetic energy transfer
elapsed time = 1yr

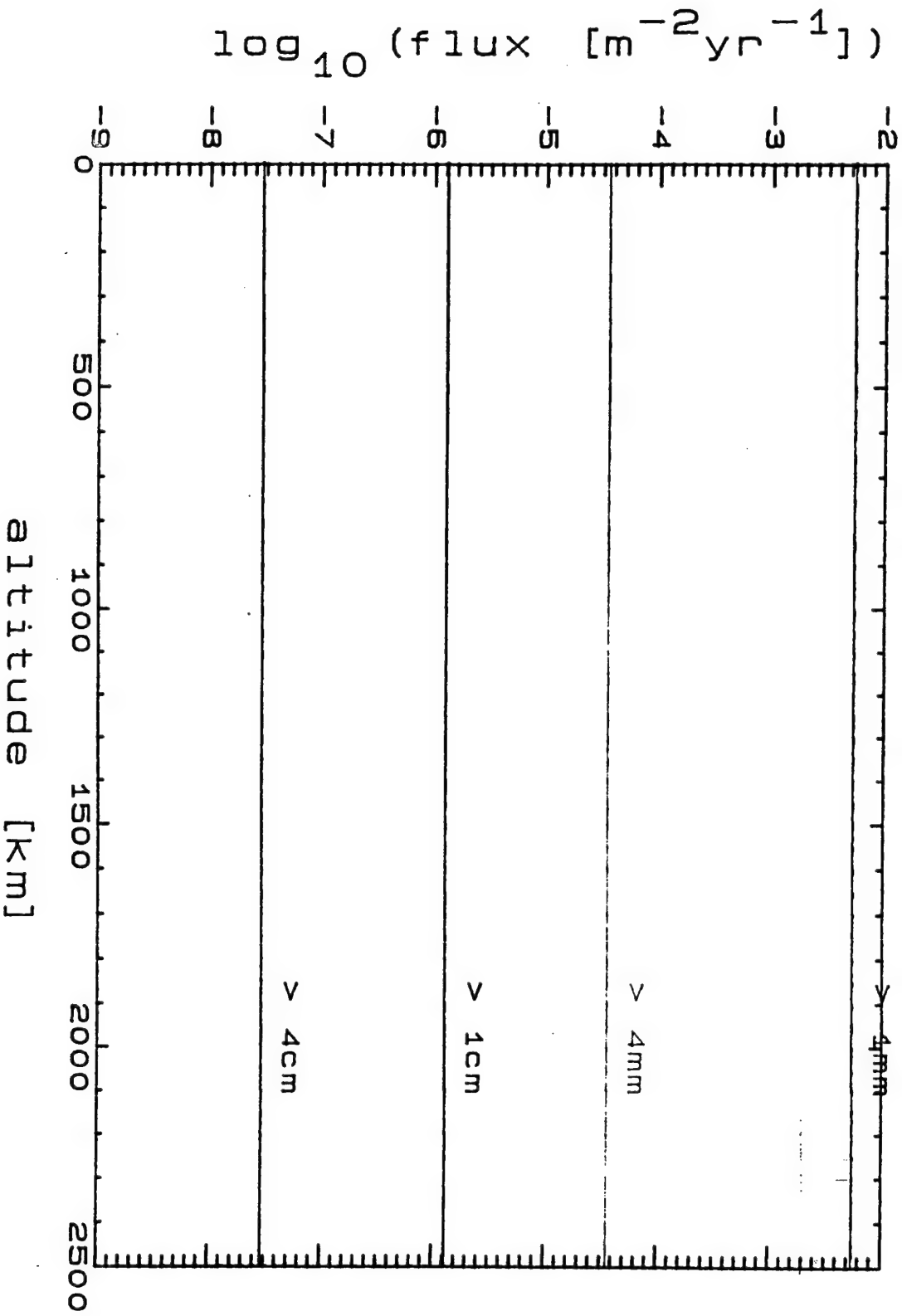


FIGURE A-37

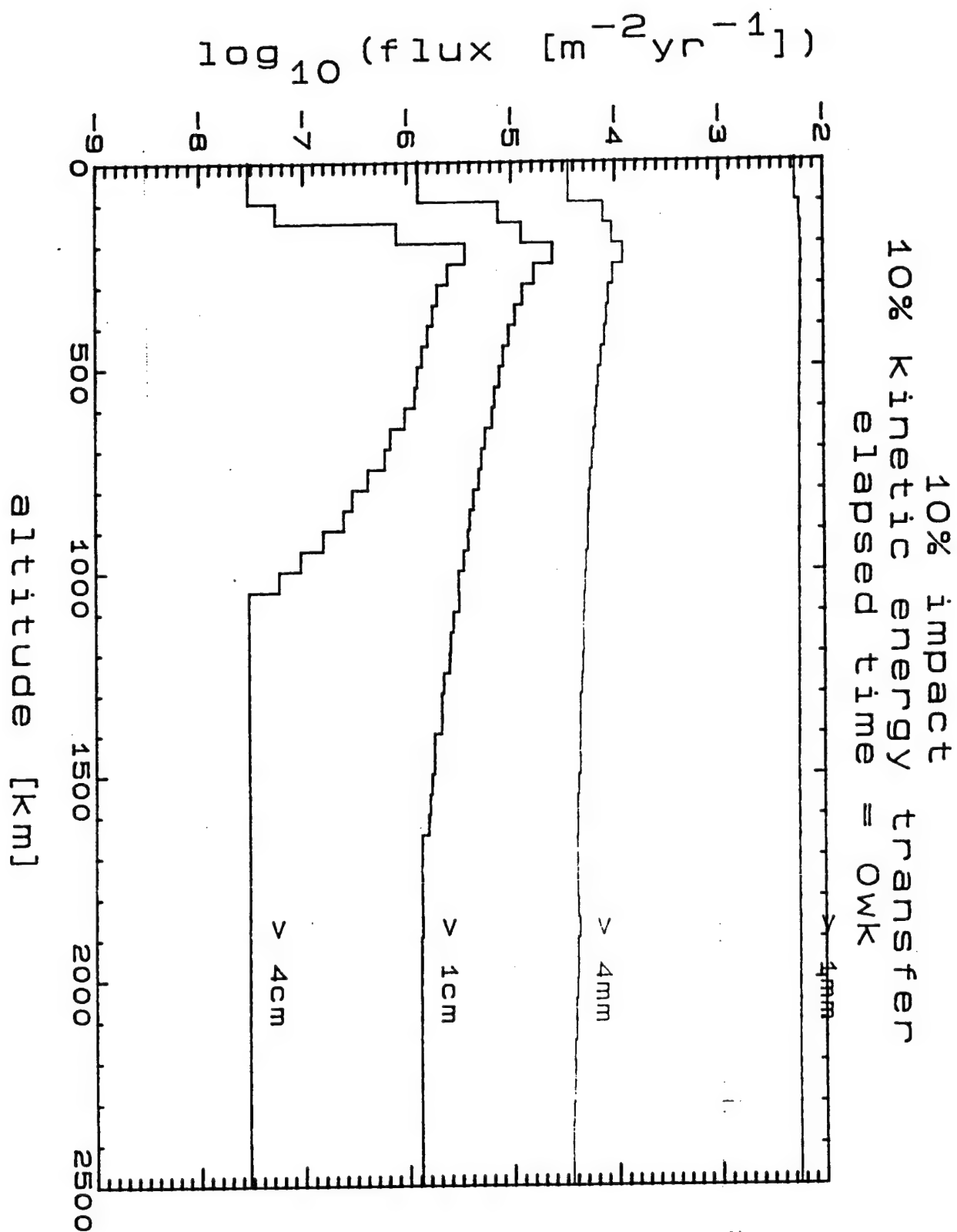


FIGURE A-38

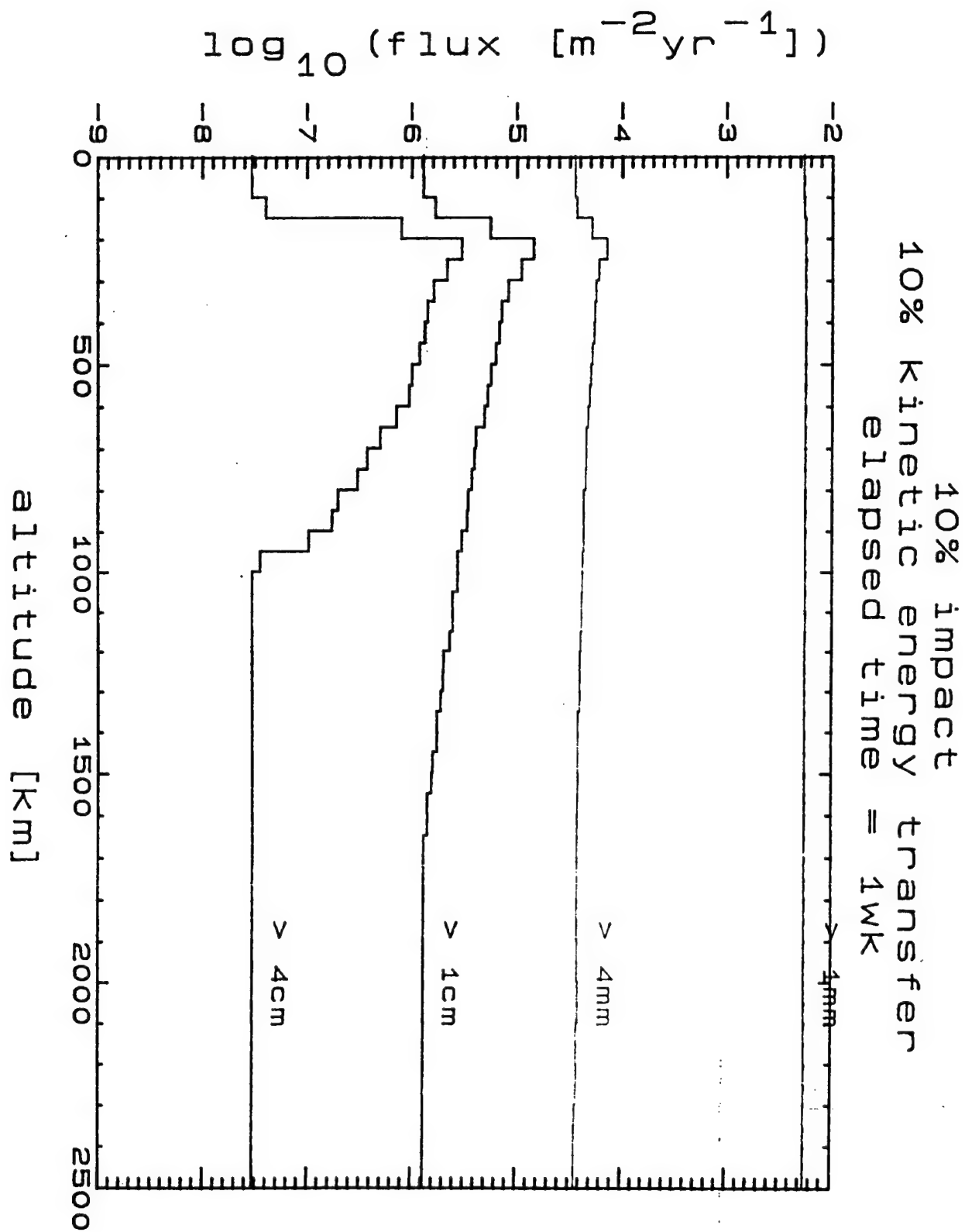


FIGURE A-39

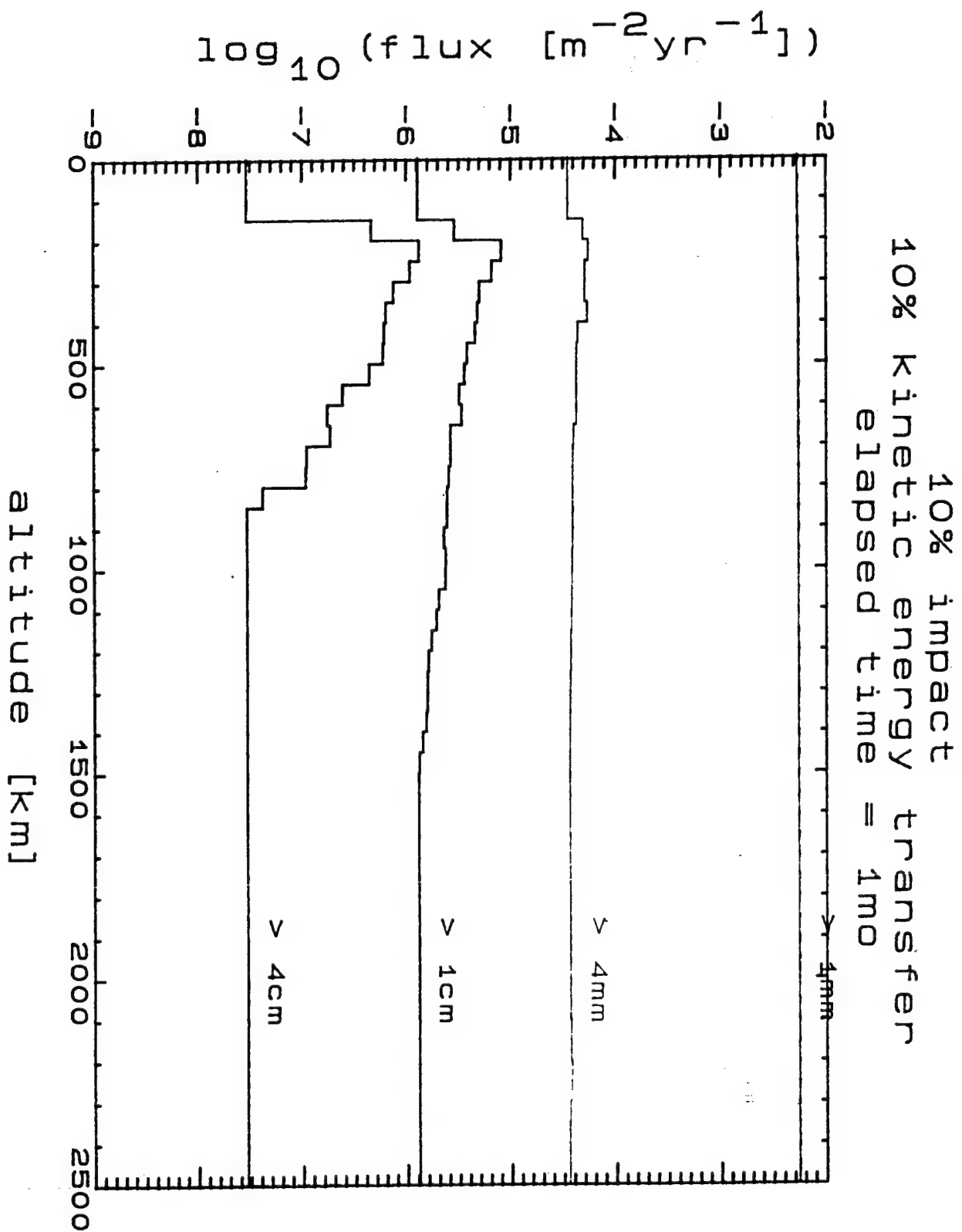


FIGURE A-40

10% impact kinetic energy transfer
elapsed time = 3mo

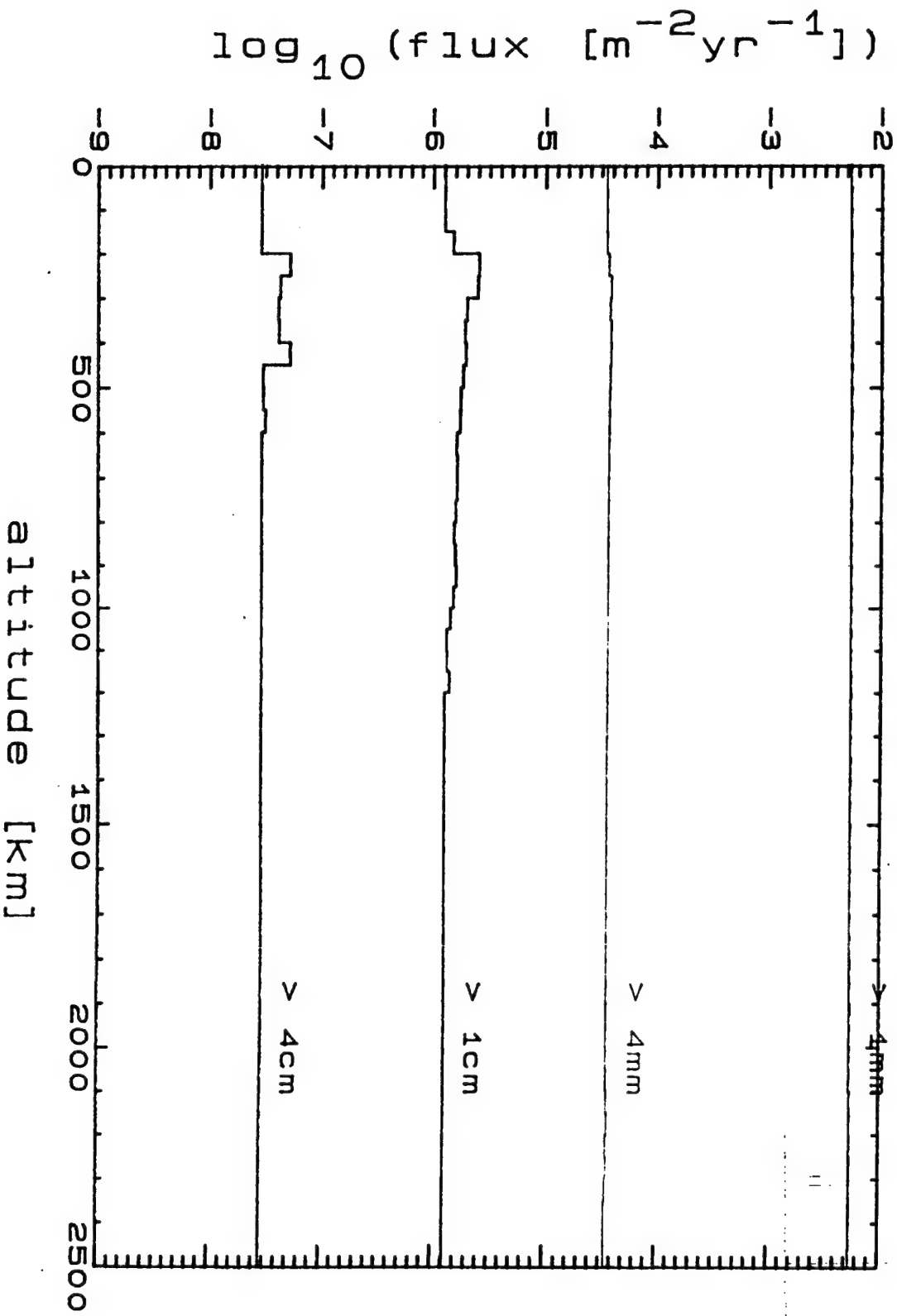


FIGURE A-41

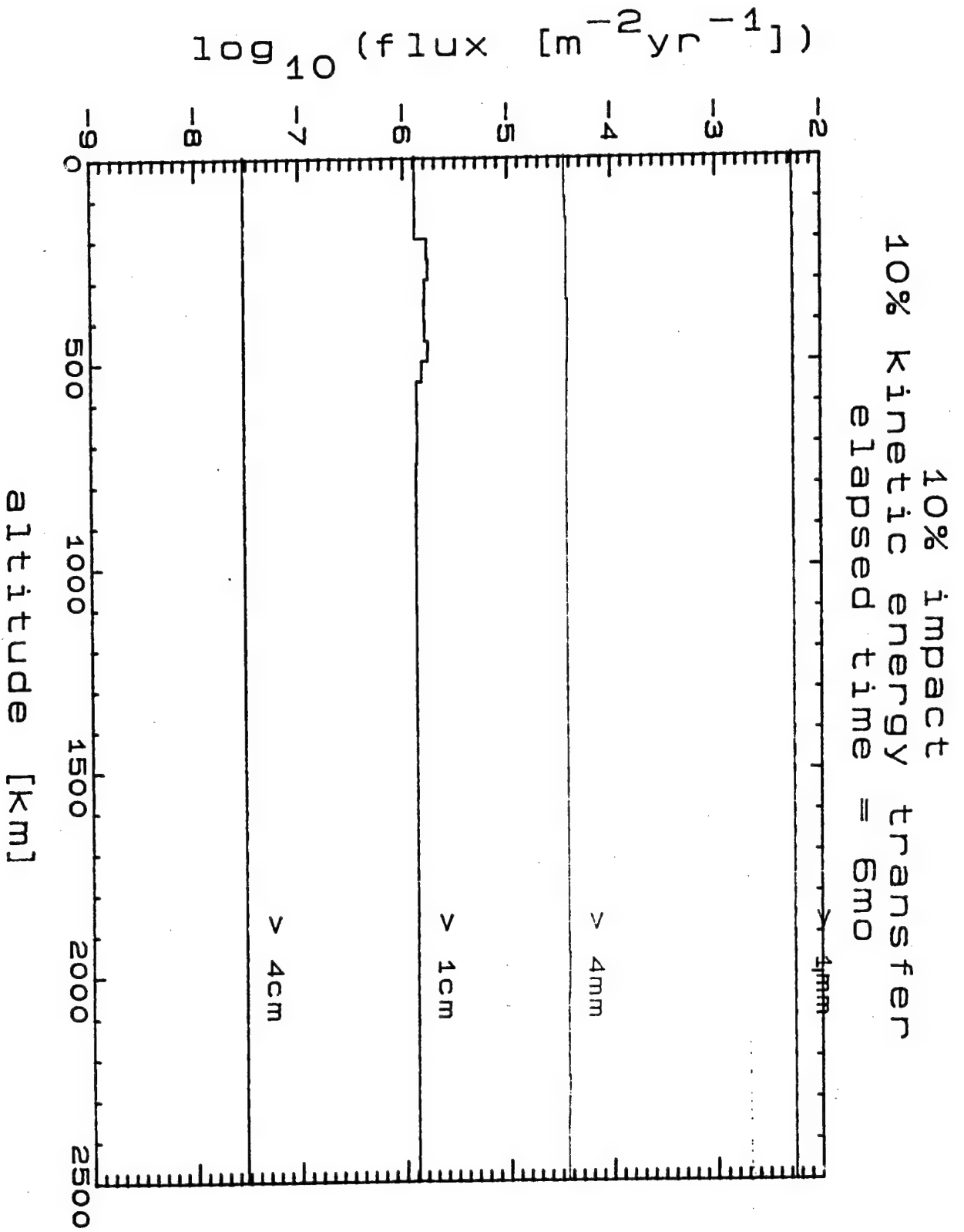


FIGURE A-42

10% impact kinetic energy transfer
elapsed time = 1 yr

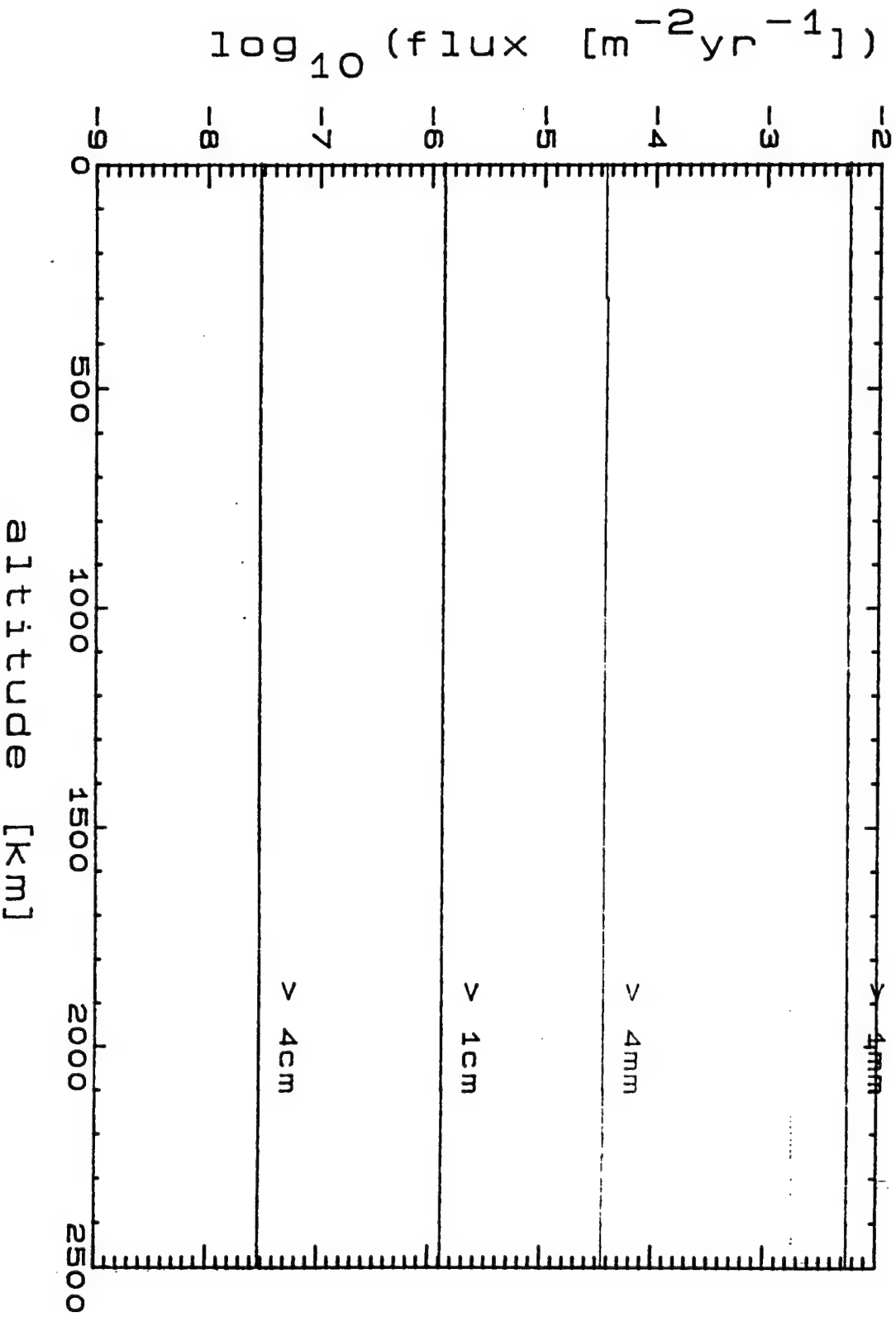


FIGURE A-43

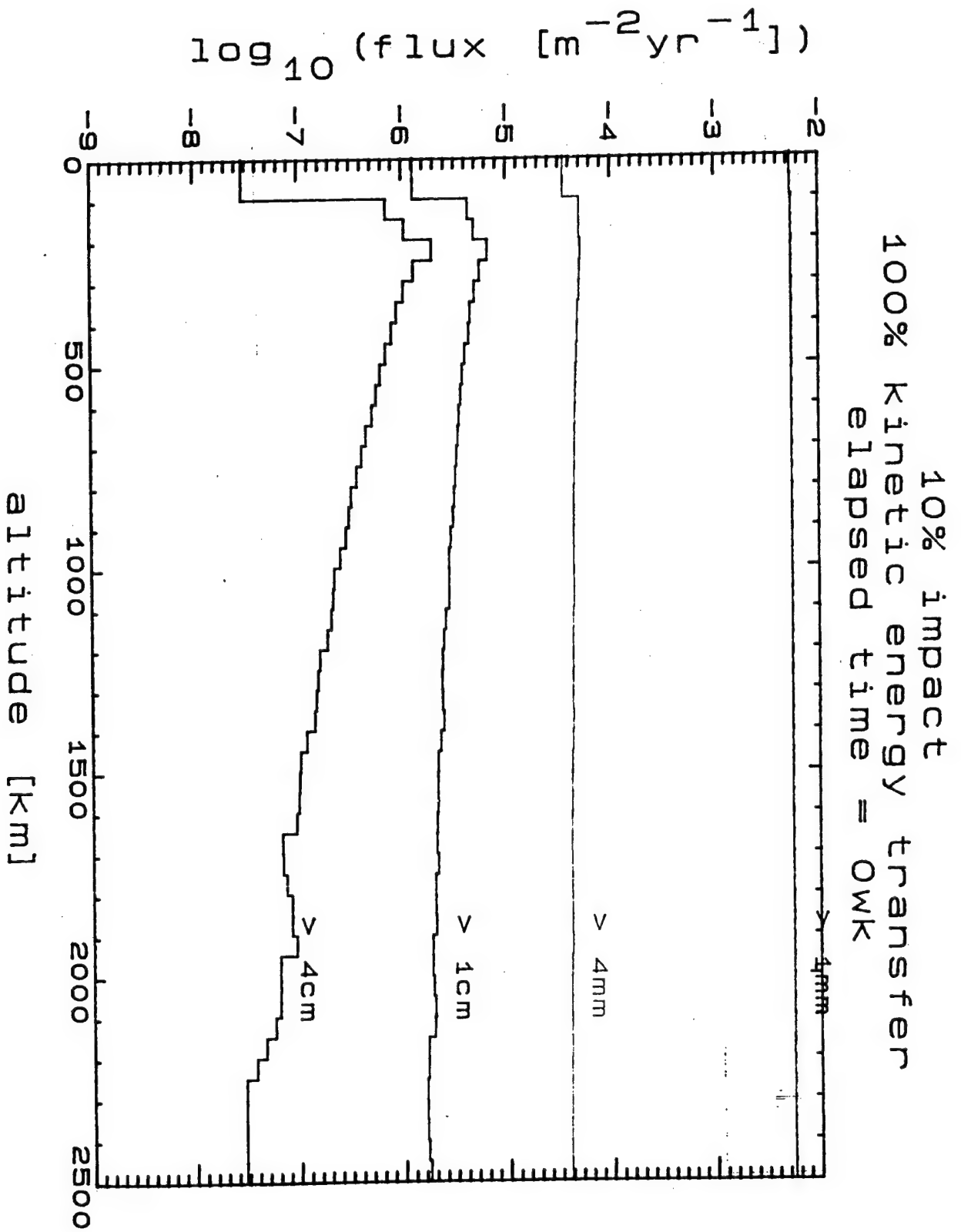


FIGURE A-44

10% impact
100% kinetic energy transfer
elapsed time = 1wk

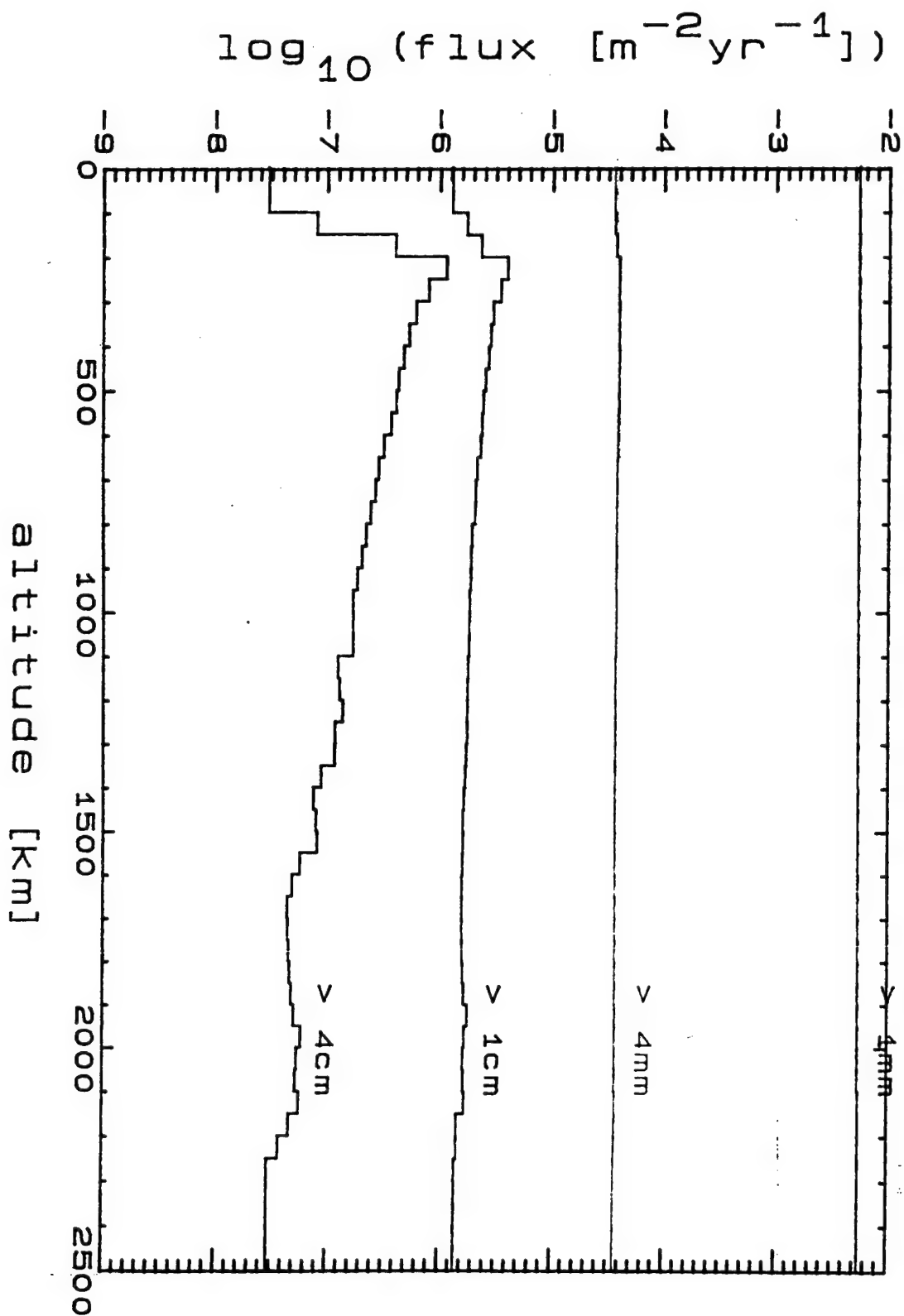


FIGURE A-45

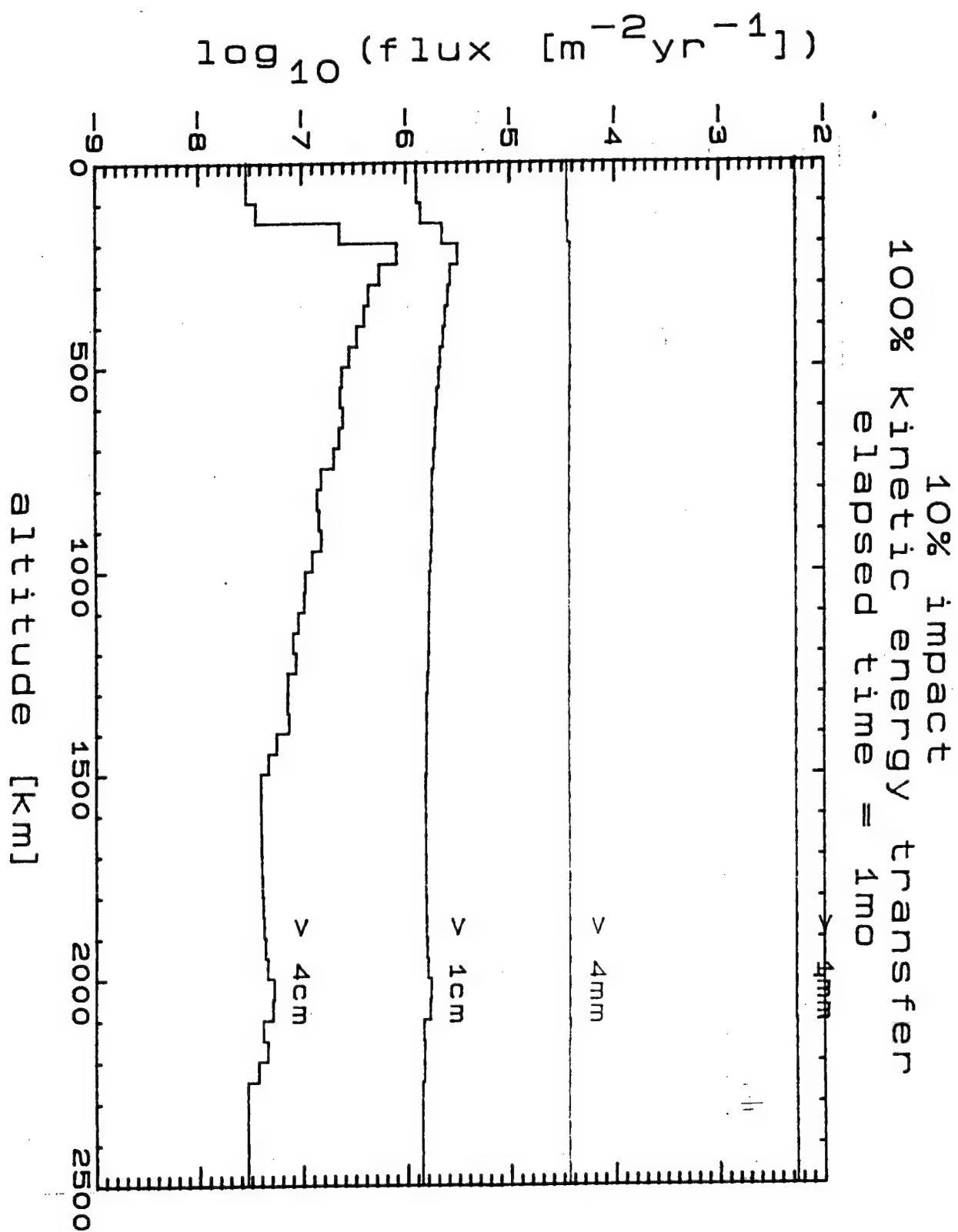


FIGURE A-46

10% impact
100% kinetic energy transfer
elapsed time = 3mo

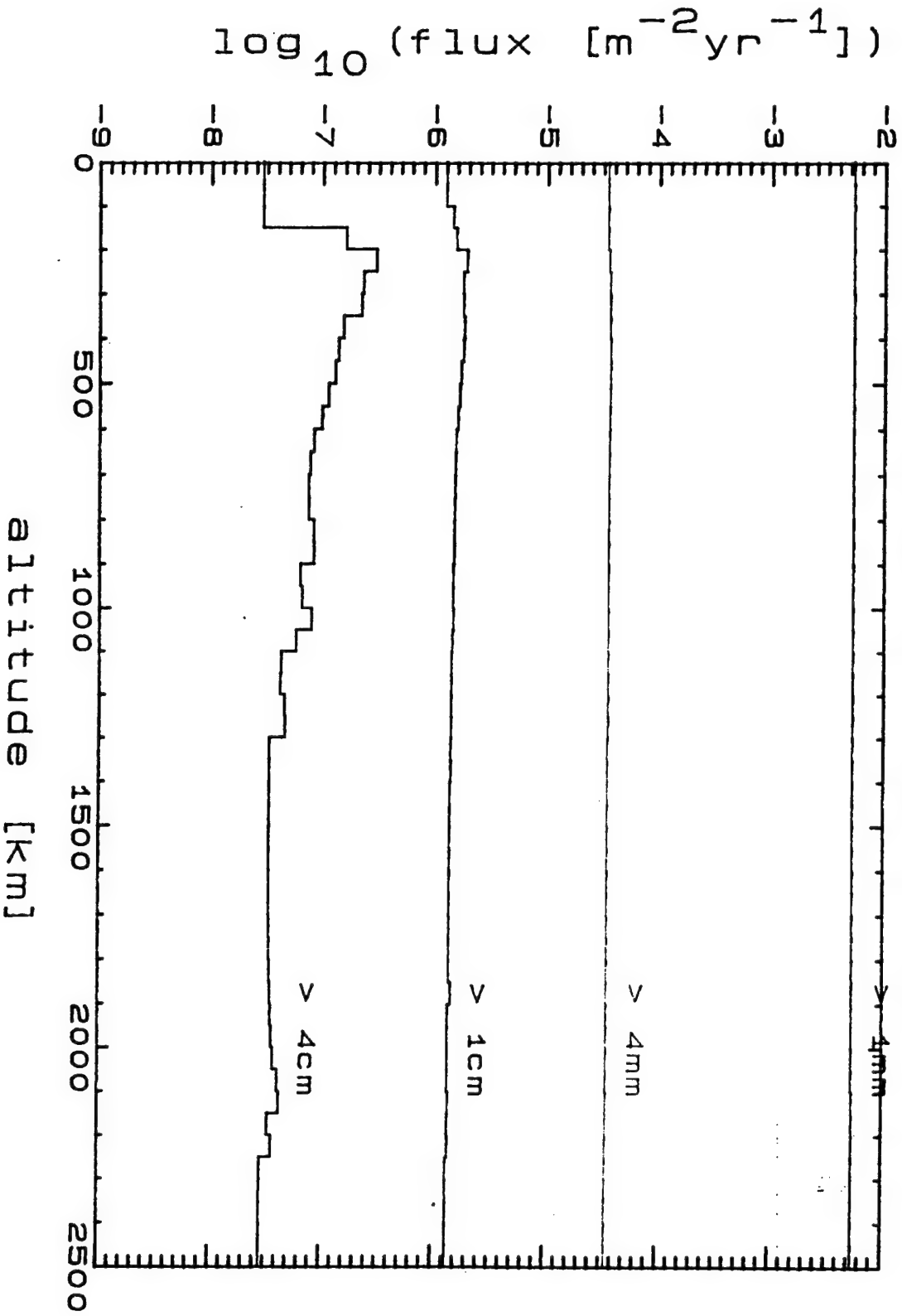


FIGURE A-47

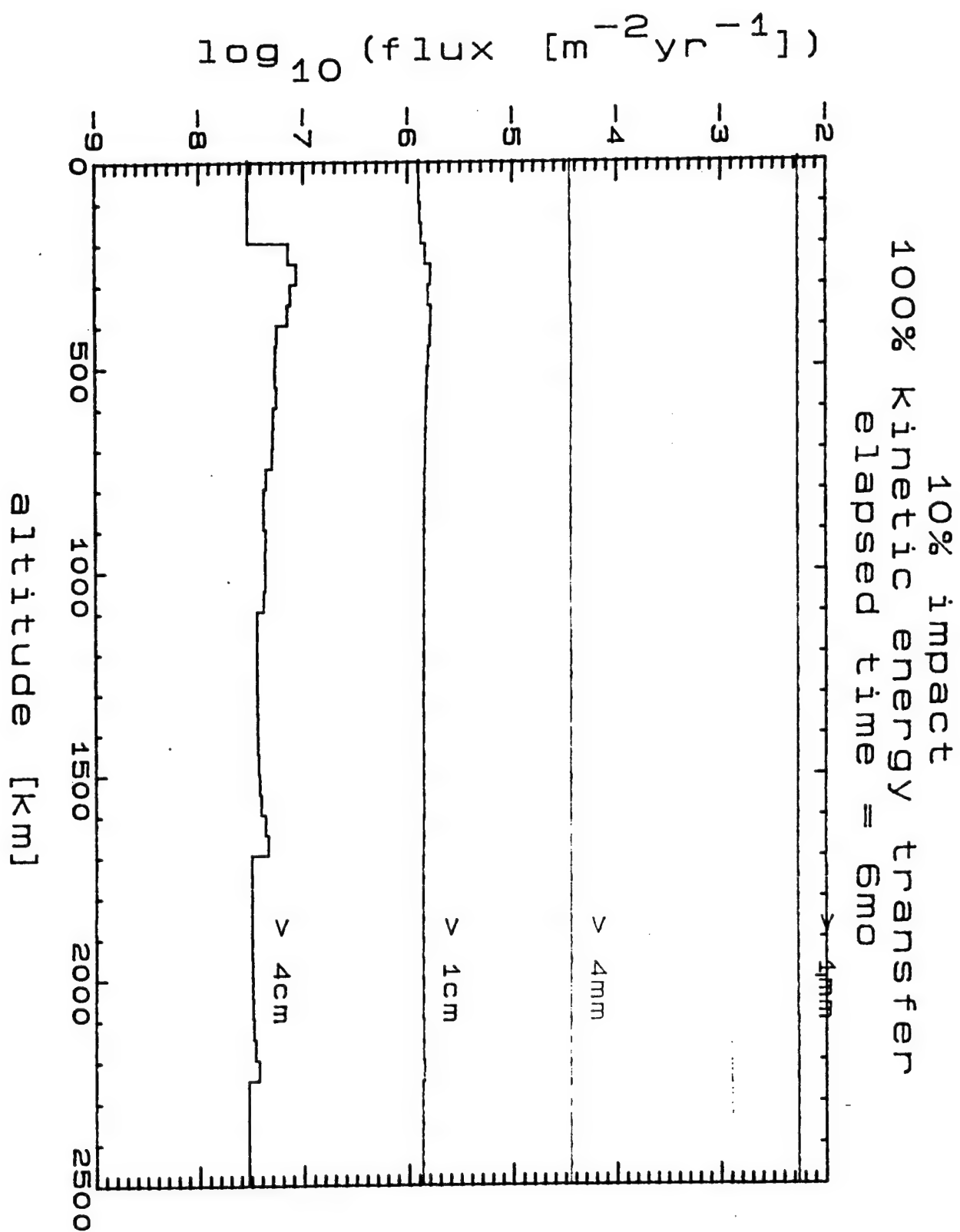
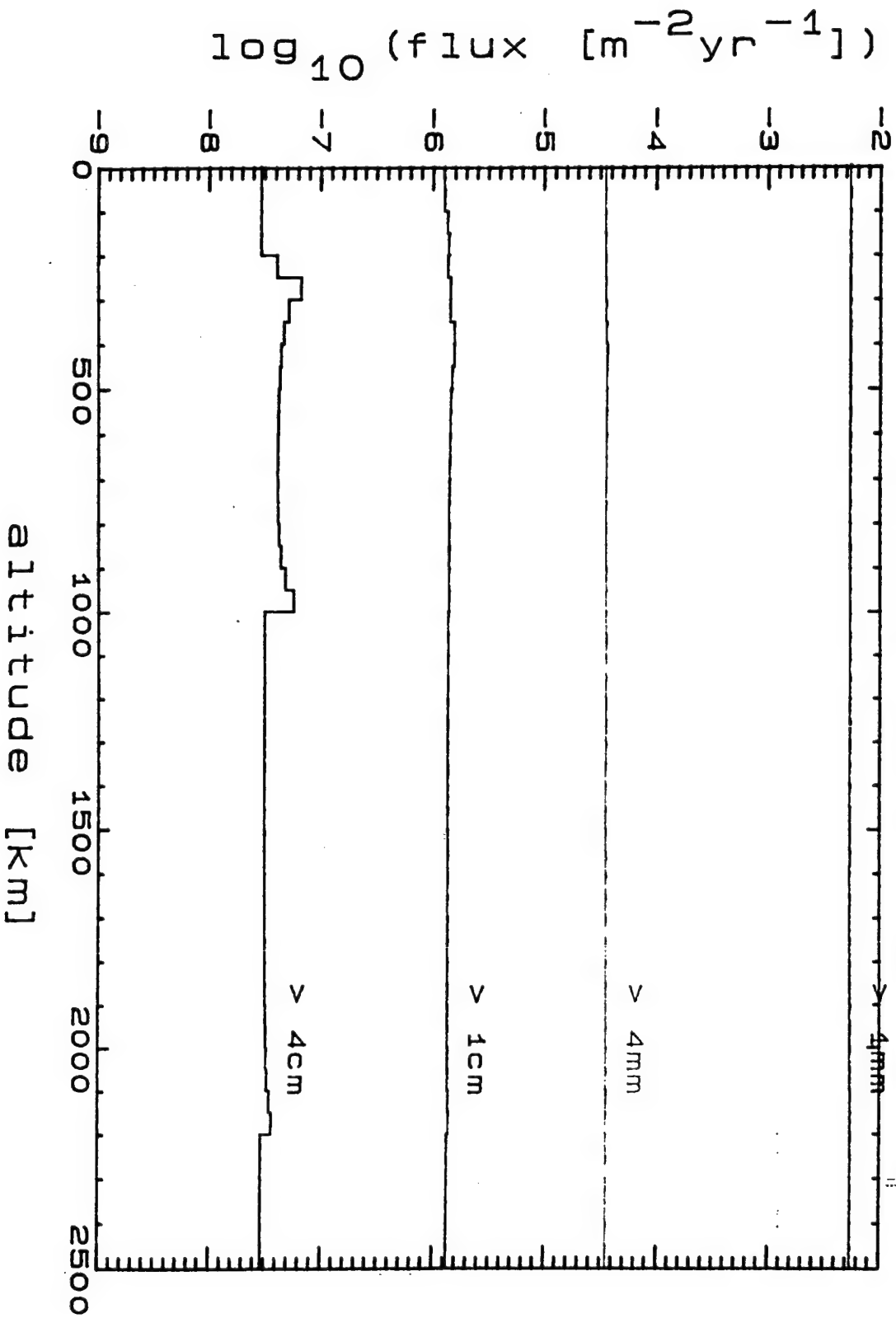


FIGURE A-48

10% impact
100% kinetic energy transfer
elapsed time = 1 yr



Appendix B

the Teledyne-Brown Report

This appendix contains the complete text, with figures and tables, of Teledyne-Brown Engineering's report on the Delta-180 mission. Topics include an analysis of the data derived from Elgin AFB observations of the debris clouds produced in the breakup event.

TECHNICAL REPORT CS87-LKD-001
THE COLLISION OF SATELLITES 16937 AND 16938:

A PRELIMINARY REPORT

NICHOLAS L. JOHNSON
ADVISORY SCIENTIST

15 NOVEMBER 1986

PREPARED FOR:

LOCKHEED EMSCO, INC.
HOUSTON, TEXAS 77258-8561

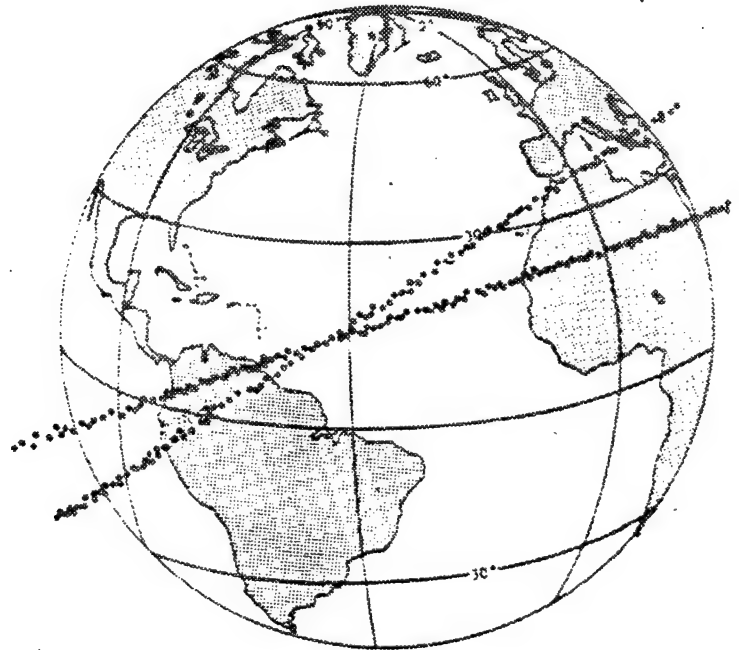
PURCHASE ORDER NUMBER 0200113094

PREPARED BY:

TELEDYNE BROWN ENGINEERING
1250 ACADEMY PARK LOOP, SUITE 240
COLORADO SPRINGS, COLORADO 80910-3799

THE COLLISION OF SATELLITES 16937 AND 16938: A PRELIMINARY REPORT

NOVEMBER 15, 1986



 **TELEDYNE
BROWN ENGINEERING**

1250 Academy Park Loop, Suite 240
Colorado Springs, Colorado 80910

TABLE OF CONTENTS

	PAGE
1.0 Executive Summary	1
2.0 Experiment Background	3
3.0 Data Collection	5
4.0 Characterization of the Initial Debris Clouds	7
4.1 23° Debris Cloud	7
4.2 39° Debris Cloud	10
5.0 Evolution of the Debris Clouds	13
5.1 23° Debris Cloud	13
5.1.1 Eglin Data	13
5.1.2 SSN Data	13
5.2 39° Debris Cloud	14
5.2.1 Eglin Data	14
5.2.2 SSN Data	14
References	15
Appendix A1 - Eglin 23° Debris Cloud, 6 September	45
Appendix A2 - Eglin 39° Debris Cloud, 5 September	61
Appendix A3 - Eglin 39° Debris Cloud, 6 September	67

1. Executive Summary

On 5 September 1986 two satellites of approximately the same order of mass collided at a relative velocity of about 3 km/s in a planned experiment. Instead of a single, diffuse cloud of debris spread between the orbital inclinations of the two parent satellites, two distinct debris clouds centered on the parents' orbits were found. Sixteen hours after the event more than 380 fragments had been detected by ground-based radars. An equal number of moderately sized objects are believed to have reentered the Earth's atmosphere within an hour of the event, while many times this number of very small debris were probably still in orbit.

Periodic assessments of the status of both debris clouds were made during the two months following the collision. Natural orbital decay removed approximately two-thirds of the known debris from near Earth space during this time. No long term space environment degradation nor hazard to artificial satellite operations will likely result from this experiment.

The nature of the initial debris clouds was not noticeably different than those originating from conventional explosions or higher velocity collisions and conformed to pre-experiment simulations. The number of particles detected soon after the event approximated the number expected for particles 5 cm in diameter or more. The two debris clouds were slightly asymmetric, with the greatest inclination deviations tending toward a regime between the two parent orbits. On-going analyses into the debris decay characteristics will prove useful in enhancing collision fragmentation models, particularly with respect to assessing the near- and far-term space debris hazards. Detailed analyses of component ejection velocities must await release by appropriate authorities of orbital parameters of the two parent satellites at the time of the impact.

TABLE 1-1. DEBRIS ASSESSMENT SUMMARY

DATE	DAYS AFTER THE EVENT	DATA SOURCE	NUMBER OF OBJECTS UNDER SURVEILLANCE		
			23° CLOUD	39° CLOUD	TOTAL
5 SEPT 86	0	EGLIN	0	21	21
6 SEPT 86	1	EGLIN	190	191	381
30 SEPT 86	25	SSN*	82	81	163
9 OCT 86	34	SSN	82	76	158
12 OCT 86	37	EGLIN	132	69	201
19 OCT 86	44	SSN	48	71	119
26 OCT 86	51	SSN	57	86	143
2 NOV 86	58	SSN	51	91	142

* SSN = Space Surveillance Network, from NAVSPASUR

2. Experiment Background

At 11:08 EDT on 5 September 1986, a Delta 3920 launch vehicle lifted-off a pad at Cape Canaveral, minutes later placing a mated second stage and special payload into an orbit of 220 km by 222 km with an inclination of 28.5° (References 1 and 2). Approximately 45 minutes after launch, the Delta second stage and payload separated. After another two hours and a series of maneuvers, the two vehicles collided at a relative velocity of about 3 km/s (References 3 and 4), creating two distinct clouds of space debris.

The payload, which was based on a Payload Assist System (PAS) framework, was designated USA-19 and received an international designator of 1986-69A and a Space Surveillance Center (SSC) catalog number of 16937. Following the collision, the fragment assigned the 16937 identity was found in an orbit of 213 km by 748 km at an inclination of 39.1° . The mass of the payload at launch was about 2300 kg, 60% of which was propellants (Reference 5).

The Delta second stage was designated USA-19 R/B (rocket body) and received an international designator of 1986-69B and SSC catalog number of 16938. Following the collision, the fragment identified as satellite 16398 was left in an orbit of 221 km by 561 km at an inclination of 22.8° . The Delta second stage approximates a right cylinder 2.4 m in diameter and 6 m in length with an empty mass on the order of 350 kg (References 2 and 6).

A collision velocity of only 3 km/s is below that usually associated with the natural collisions of objects in space. Consequently, the extent of hypervelocity impact phenomenology exhibited in the resulting debris was uncertain prior to the test and represented an area of investigation for post-flight analysis. The debris characterization objective was potentially complicated by the reported activation of an explosive device on one of the vehicles (the Delta second stage) at the time of the impact (Reference 7). Also unknown is the effect on the debris of the energy contribution of the residual propellants on board the vehicles at the moment of the collision.

If 5 cm diameter objects are considered the lower sensitivity threshold of the Space Surveillance Network (SSN) at the subsequent observation altitudes of only a few hundred kilometers, equations developed by Kessler and Cour-Palais (Reference 8) and Kessler and Su (Reference 9) can be applied to estimate the number of detectable objects created during the

collision of satellites 16937 and 16938. Assuming hypervelocity impact relationships are applicable in this case, the reported total dry mass of almost 1300 kg should have produced on the order of 850 pieces of debris visible to the SSN. However, due to the very low altitude of the collision and the assumed symmetric distribution of fragments, approximately half of these objects should have decayed within a few hours of the event. Therefore, only 400-500 observable pieces of debris might be expected in the first days following the experiment.

3. Data Collection

Prior to the experiment Teledyne Brown Engineering (TBE) assisted NASA Johnson Space Center (JSC) and the U.S. Air Force Space Command (AFSPACOM) in the definition of space surveillance data collection requirements for the purpose of assessing the consequent space debris environment. TBE furnished NASA JSC a set of preliminary recommendations for support from the SSN in December, 1985. A Fragment Working group meeting was held at NASA JSC on 7 March 1986 and attended by TBE representative Mr. Ronn Kling.

Due to the low inclinations of the colliding objects, the AN/FPS-85 phased-array radar at Eglin AFB, Florida, was chosen as the primary sensor for debris data collection. On 18 July 1986 Mr. David Nauer of TBE and Mr. John Stanley of NASA JSC met with Eglin radar personnel on site to discuss the operational impacts and needs of the forthcoming experiment. Among the items discussed were the lowering of the SLBM detection fence during the early passes of the expected debris cloud(s) through Eglin coverage and the special tasking of each identified piece of debris.

The ALTAIR and Kaena Point mechanical tracking radars were also selected to obtain specific data on the debris cloud(s) shortly after the test. These latter radars, however, are limited in the number of objects which can be tracked in a specified time interval and are unable to produce orbital data of the quality provided by Eglin. On 5 August 1986, Mr. Ronn Kling of TBE and Mr. Gene Stansbury of Lockheed (on behalf of NASA JSC) met with ALTAIR program personnel at Lincoln Laboratory. At that meeting three data collection modes were adopted: multiple object (short) tracking, single object (long) tracking, and beam park.

A meeting was then held at the TBE facility in Colorado Springs on 7 August 1986 to finalize data collection plans. Attendees included representatives from TBE, NASA JSC, USSPACECOM, AFSPACOM, PRC/Kentron, and AVCO/Textron. A recommendation of the attendees called for a "dry-run" exercise of the appropriate space surveillance sensors during the week of 18 August to verify the feasibility of non-standard data collection tasking and techniques. Also at this meeting, NASA JSC recommended the establishment of an optical fence using the AMOS, MOTIF, and Maui GEODSS sensors to obtain piece counts of very small debris (below the sensitivity threshold of ground-based radars). TBE was tasked to develop the software and procedures to erect said fence and to act as an interface between the SSC and NASA personnel at Maui. The subsequent exercises conducted in the second half of August confirmed the data collection procedures required to meet debris assessment objectives.

4. Characterization of the Initial Debris Clouds

Debris from the collision of satellites 16937 and 16938 was initially found in orbital inclinations ranging from 21° to 42° . However, the debris was distributed in two distinct "clouds", one centered near an inclination of 22.8° and one centered near an inclination of 39.6° . These inclinations correspond to the inclinations of the remnants of satellites 16938 and 16937, respectively. For the remainder of this preliminary report, the collision debris is denoted as part of the 23° debris cloud or as part of the 39° debris cloud, which are herewith discussed separately.

To characterize the 23° debris cloud and the 39° debris cloud, TBE reduced and analyzed data collected by the Eglin and ALTAIR radars on the day of the event and the following day. Data from ALTAIR were received by TBE in late October. Attempts to reduce the observations into orbital parameters of acceptable quality in time for inclusion into this report were unsuccessful. The inherent accuracy and utility of the ALTAIR data are currently under investigation. Further analysis of these data may be performed at a later date.

The Eglin radar observations, on the other hand, permitted a detailed assessment of the structure of the two clouds soon after the event. The following two subsections highlight the predominant initial characteristics of the two debris clouds as reconstructed from the Eglin data.

4.1 23° Debris Cloud

Selected data tapes recorded by Eglin on 5 September within hours of the event and examined by TBE revealed no debris associated with the 23° debris cloud. This lack of data was a consequence of pass geometry and the time interval available and not indicative of the nature of the cloud.

On 6 September, a 90-minute observation interval was selected during which the orbital plane of 16938 passed through Eglin coverage (Figure 1). Although the elevation angle of each fragment to Eglin was less than normally desired, the low inclination of the 23° debris cloud did not allow high elevation passes. Despite this limitation a total of 190 pieces of debris were positively identified with the 23° debris cloud. Figure 2 indicates the general time of first detection of each piece of debris and provides some insight into the dispersion of the cloud some 16 hours after the event.

Appendix A1 is a listing of all orbital element sets generated by TBE on this cloud. Even though the data span an interval greater than 90 minutes, those objects outside of the selected interval are not included in the piece count quoted above. Note that Eglin performed a pass-to-pass correlation for some objects. However, the consistency of this pass-to-pass correlation was uncertain and the 90-minute time window was selected to avoid duplicate counting. A deficiency of this technique is that an object with an orbital period greater than 90 minutes could be omitted. However, Figure 2 suggests that in this case the cloud was not yet uniformly distributed around the orbital plane and therefore the number of objects missed is likely to be very small. Finally, in a few cases an assigned 9X,XXX number appears to be cross-tagged during the track interval. No attempt has yet been made to examine exhaustively all element sets to determine the frequency with which this might have occurred. The total number of trackable objects in the 23° debris cloud less than one day after the experiment can be estimated to be on the order of 200.

The distribution of the debris in inclination was not fully symmetric. The range of inclinations was 21.95° to 25.25° with a higher deviation from the mean toward the higher inclinations (Figure 3). The potential significance of this characteristic is discussed further in Section 4.2.

The nominal variation in orbital periods for the 23° debris cloud was 79 minutes to 116 minutes. The Gabbard diagram of Figure 4 clearly demonstrates that several pieces appear to be on reentry trajectories. In fact, about 20% of the fragments were determined to be on their last orbit about the Earth. The horizontal arm of Figure 4 is at an altitude of 210-220 km, consistent with the initial orbit of satellites 16937 and 16938 and with their subsequent perigees. Unfortunately, the exact orbital parameters of 16937 and 16938 at the time of the impact were not yet available when this report was prepared. Reference 7 did report that both vehicles were accelerating at a rate of 5 g's (50 m/s²) when the collision occurred. Consequently, the proportion of fragments tracked on 6 September which were ejected in retrograde and posigrade directions is unknown. Certainly the majority of pieces are in higher energy orbits than the primary remnant of 16938 (orbital period about 92 minutes). However, if the distribution of ejecta was symmetric about the parent object as suggested by theory, a significant portion of the debris imparted with retrograde velocities would have reentered the atmosphere very shortly after the event before the Eglin pass that was analyzed.

The highest energy fragment (satellite 94998 in Appendix A1) associated with the 23° debris cloud had an apogee of about 5500 km and an orbital period of over 146 minutes. This represents an increase in velocity of about 1 km/s from the stated orbit of satellite 16938. This magnitude of ejection velocity is compatible in hypervelocity impact ground tests with a particle 1 mm in diameter or less. Although no radar cross-section (RCS) estimate on this object was available to TBE, the Eglin radar is incapable of detecting such a small object at the range of the observation. (In general the altitude of all fragments during this pass was between 200 and 300 km, i.e. near perigee.)

The fragment with the second highest ejection velocity (satellite 90100 in Appendix A1) also experienced one of the largest inclination changes of the 23° debris cloud. This suggests that the object might have been less massive than the majority of the debris cloud. Unfortunately, no subsequent data collected by Eglin or the SSN in general could be correlated with this particular object. Thus, no estimate of its ballistic coefficient or mass was possible.

A summary of the initial distribution of the 23° debris cloud by inclination and period is provided in Figure 5. Overall, the dispersion is moderately symmetric with the exception of the lower period pieces which had already fallen out of the environment and the trend noted earlier in which the low period, higher inclination fragments are more widely separated. An examination of eccentricity versus period for each fragment (Figure 6) reinforces the classic satellite breakup pattern seen in Figure 4.

Finally, the early Eglin data on the 23° debris cloud was analyzed to determine the relationship between inclination and right ascension. If the collision had taken place at a node (i.e. equator crossing), any cross-track (perpendicular to the orbit plane) velocity component would have been converted directly into a change of inclination and no alteration of the right ascension would have occurred. However, the collision actually took place at about 10° N latitude, resulting in a conversion of a portion of the cross-track velocity component into a torquing of the orbit plane. This relationship is well illustrated in Figure 7 and conforms to the expected trend. Moreover, this relationship was vital to differentiating debris associated with the event from other debris in these inclinations which are often used for missions originating from Cape Canaveral.

4.2 39° Debris Cloud

The Eglin observations of the 39° debris cloud collected on 5 September produced only marginal data. Shortly after the event the debris cloud penetrated Eglin's coverage volume, passing from north to south and hampering the acquisition of high quality track data. In fact only 21 identifiable fragments associated with this cloud were tracked and all these possessed orbital periods very close to that found for the parent, satellite 16937. Orbital element sets for these objects are provided in Appendix A2, but they are not referenced further in this report.

Like the 23° debris cloud, the 39° debris cloud experienced a very favorable pass through Eglin's coverage only 16 hours after the event (Figure 8). Somewhat remarkably, the total number of objects identified with the 39° debris cloud was 191, virtually the same as seen in the 23° debris cloud at the same time. Orbital element sets created by TBE from the Eglin observations for this period can be found in Appendix A3.

Several factors should have combined to make this "coincidence" highly unlikely. First and foremost, the mass of satellite 16937 (the 39° parent) is estimated to have been as much as 2.5 to 3 times that of satellite 16938 (the 23° parent). Presently unknown is the mass of the instrument packages added to the Delta second stage, which conceivably could have increased its mass to be comparable to that of satellite 16937. Therefore, a larger number of debris might be expected in the 39° debris orbital regime. Furthermore, the closer approach of the 39° debris cloud to Eglin (i.e. higher elevation angle) should have resulted in a greater probability of detection for the smaller fragments when compared to the 23° debris cloud.

On the other hand, the density of the 39° debris cloud was greater at the beginning of the observation period (Figure 2), possibly suggesting that the leading edge of the cloud was somehow missed. However, the 90-minute interval selected from the Eglin tapes was specifically tailored to prevent this potential problem. An examination of the element sets in Appendix A3 will reveal that the lower period pieces, the leading edge of the cloud, were in fact detected in the first 15 minute interval. Thus, the likelihood of Eglin "missing" a significant number of detectable fragments during the observation period is assessed to be quite low. At no time during the 90 minute interval did the combined densities of the both clouds reach a level which might have exceeded the hardware/software limitations of Eglin resulting in the loss of observations.

Other factors which might have influenced the number of detectable fragments created by the respective spacecraft are the relative densities of the vehicles and the location of the impact on the vehicles. The Delta second stage may have been not only less massive but also less dense than satellite 16937. Despite these unknowns, it is interesting to note that the total number of objects observed - 381 - is very close to that estimated in Section 2.

The spread of orbital inclinations for the 39° debris cloud was approximately twice that of the 23° debris cloud, i.e. 34.7° to 41.4°. Perhaps more importantly, a noticeably greater deviation is found at the lower inclinations of the 39° debris cloud (Figure 9). This appears to correspond to the trend toward greater inclinations in the 23° debris cloud. If the two colliding objects were of roughly the same mass and the collision were largely inelastic, the debris might be expected in inclinations centered around 31°. In reality, the collision apparently possessed features of both elastic and inelastic collisions, the latter being in part reflected in the debris migrating from both clouds towards a median inclination.

The Gabbard diagram of Figure 10 for the 39° debris cloud is virtually identical to that for the 23° debris cloud (Figure 4). One small difference is the larger number of fragments ejected into high orbits. In addition, a slightly smaller percentage, 15%, of the debris appear to be on reentry trajectories. As indicated in Figure 10, two fragments fell outside the confines of the graph: one with an orbital period of 242.5 minutes and the other with an extraordinary orbital period of more than 518 minutes. The latter object, satellite 94768, was subjected to a velocity increase in excess of 2.2 km/s or approximately three-fourths of the collision velocity. As with most of the Eglin observations reduced by TBE, no RCS data for this object was available.

Although the magnitudes are not comparable, it is curious that two objects in the 23° Debris cloud and two objects in the 39° debris cloud are clearly separated from the remainder of the clouds. A similar (and possibly related?) characteristic was noted in the only other known hyper-velocity collision in space (Reference 10).

The distribution of the 39° debris cloud in inclination and period is markedly different from that observed with the 23° debris cloud (Figure 11). The majority of pieces are in inclinations below that ascribed to the parent and exhibit a tendency of higher period/lower inclination pieces.

An examination of the relationship between eccentricity and orbital period (Figure 12) reveals a trend identical to that for the 23° debris cloud and in keeping with the Gabbard diagram of Figure 10.

An apparent structure did arise during the analysis of the inclination versus right ascension of the 39° debris cloud. Three distinct striations are apparent in Figure 13. No such pattern was visible in a similar plot for the 23° debris cloud (Figure 7). Since a time variation of up to 90 minutes exists in Figure 13, the values of right ascension appearing in Appendix A3 were propagated to a common epoch of 86249.48, just after the 90-minute observation interval. The resultant inclination versus right ascension data are presented in Figure 14. The striations have largely disappeared. The significance of the phantom structure which must be related to the time of detection and hence the orbital period has not yet been examined in depth. Also note that the scale factors for Figures 7 and 14 are the same, indicating that for an equal change in inclination the debris in the 39° debris cloud underwent a smaller change in right ascension as expected for a higher initial inclination parent.

5. Evolution of the Debris Clouds

At irregular intervals during the two months following the collision of satellites 16937 and 16938, TBE obtained orbital data on the two debris clouds from two primary sources. Magnetic tapes of Eglin observations were acquired for passes on 12 October, some 37 days after the event. On five occasions TBE received summaries of debris being tracked by the SSN as a whole either as a cataloged satellite or as a provisional 8X,XXX satellite. These summaries were compiled by the Naval Space Surveillance System (NAVSPASUR) in its role as the alternate SSC. NAVSPASUR personnel were instrumental throughout the period in converting observations on unknown objects from a variety of sensors into orbital elements which were then fed to the SSN via the SSC for tracking. The job was made more difficult by the small size of some of the debris and by solar activity during the period which temporarily degraded SSN capabilities.

5.1 23° Debris Cloud

5.1.1 Eglin data

Figure 15 is a Gabbard diagram of the fragments of satellite 16938 tracked during a 100-minute interval on 12 October 1986. In all, 132 objects were unambiguously associated with the 23° debris cloud. On this occasion the site was in its normal surveillance mode (SLBM fence erected). The quality of the element sets appears high with only three objects possessing questionable values of eccentricity. The diagram appears very similar to Figure 4 (note scale differences), particularly regarding the two high period fragments. Unfortunately, with Eglin data from only 6 September and 12 October, it was not possible to unequivocally correlate the two high period pieces in each figure.

5.1.2 SSN data

Table 1 and Figures 16-20 illustrate that portion of the 23° debris cloud being tracked by the SSN between 30 September and 2 November. The number of fragments varied considerably between 48 and 82, all substantially below the assessment of Eglin on 12 October. This discrepancy is the result of the exceptional ability of Eglin to detect objects on a single pass which are not large enough to be routinely tracked by either Eglin or the SSN as a whole. Of particular note is the high period fragment which appears for the first time in Figure 19. This may be one of the two high period pieces detected by Eglin alone two weeks earlier.

For the five-week period analyzed, 20 objects were selected for special study to ascertain their decay characteristics. The fact that all debris have virtually the same perigee heights should permit this technique to make assumptions regarding the relative nature of the respective ballistic coefficients. All fragments must be followed to their decays before any such assessments can be formulated. The preliminary results of this analysis are provided in Figure 21 where the decay rates of all debris in like orbits are clearly not uniform.

5.2 39° Debris Cloud

5.2.1 Eglin data

An attempt to define the status of the 39° debris cloud on 12 October using the Eglin radar met with mixed results. Only 69 fragments were detected during the same 100-minute interval examined for the 23° debris cloud (Section 5.1.1). Although some debris from the 39° debris cloud did pass through Eglin prior to this observation period, this does not fully explain the low piece count. The data obtained (Figure 22) is similar to the SSN database of 9 October but of slightly poorer quality.

5.2.2 SSN data

The apparent evolution of the 39° debris cloud based on SSN data is depicted in Figures 23-27. The total number of known fragments (Table 1) in orbit actually increased from mid-October to early November. The characterization of the 39° debris cloud was made easier by the contribution of the higher latitude sensors, particularly NAVSPASUR. Thus, almost two full months after the event approximately half of the 39° debris detected by Eglin during the first 24 hours was still in orbit. Like the experience with the 23° debris cloud, the SSN was better able to define fragments in high altitude orbits after several weeks had passed (see Figures 24 and 25).

An investigation into the decay characteristics of 20 selected objects from the 39° debris cloud was also undertaken. As noted with the 23° debris cloud (Figure 21) differences in decay rates at like altitudes are more prominent as the higher altitude pieces enter lower period orbits. In general this supports the theory that the "lighter" pieces are initially thrown into higher orbits. Once they reach lower altitudes they tend to decay faster than those fragments which began at that altitude. Again, further monitoring of the fragments is required before a more quantitative evaluation is possible.

REFERENCES

1. "Delta-Launched SDI Experiment Called 'Classic Textbook Success'", Aerospace Daily, 8 September 1986, pp. 379-380.
2. Craig Covault, "SDI Delta Space Experiment to Aid Kill-Vehicle Design", Aviation Week and Space Technology, 15 September 1986, pp. 18-19.
3. Trish Gilmartin, "SDI Experiment Yields Data Useful to Kinetic Kill Vehicle Design", Defense News, 15 September 1986, p. 30.
4. "Briefing on the Delta Strategic Defense Initiative Experiment", Defense Daily, 16 September 1986, pp. 75-78.
5. "Pentagon Conducts Star Wars Test in Space", Arms Control Today, October 1986, pp. 23-24.
6. The RAE Table of Earth Satellites 1983-1985, Royal Aircraft Establishment, 1 January 1986.
7. "SDIO flys 'milestone' ASAT", Military Space, 15 September 1986, p. 8.
8. D.J. Kessler and B. Cour-Palais, "Collision Frequency of Artificial Satellites: The Creation of a Debris Belt", Journal of Geophysical Research, Vol. 83, 1978, pp. 2637-2646.
9. S.-Y. Su and D. J. Kessler, "Contribution of Explosion and Future Collision Fragments to the Orbital Debris Environment", Advances in Space Research, Vol. 5, No. 2, 1985, pp. 25-34.
10. Ronn Kling, Postmortem of a Hypervelocity Impact, Teledyne Brown Engineering, Technical Report CS86-LKD-001, September 1986.

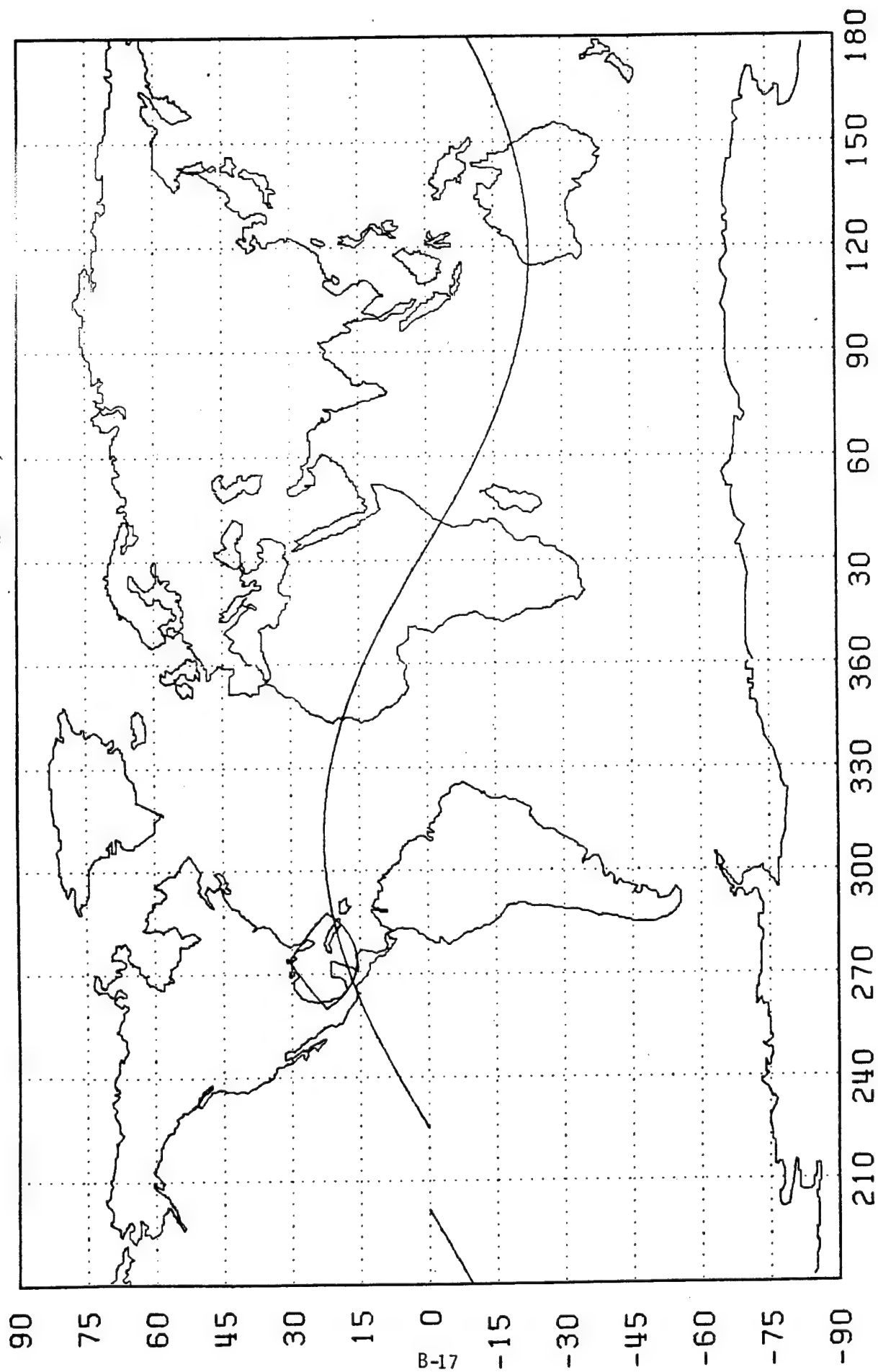


Figure 1. Sample geometry of 23° inclination debris cloud through Eglin coverage on 6 September 1986

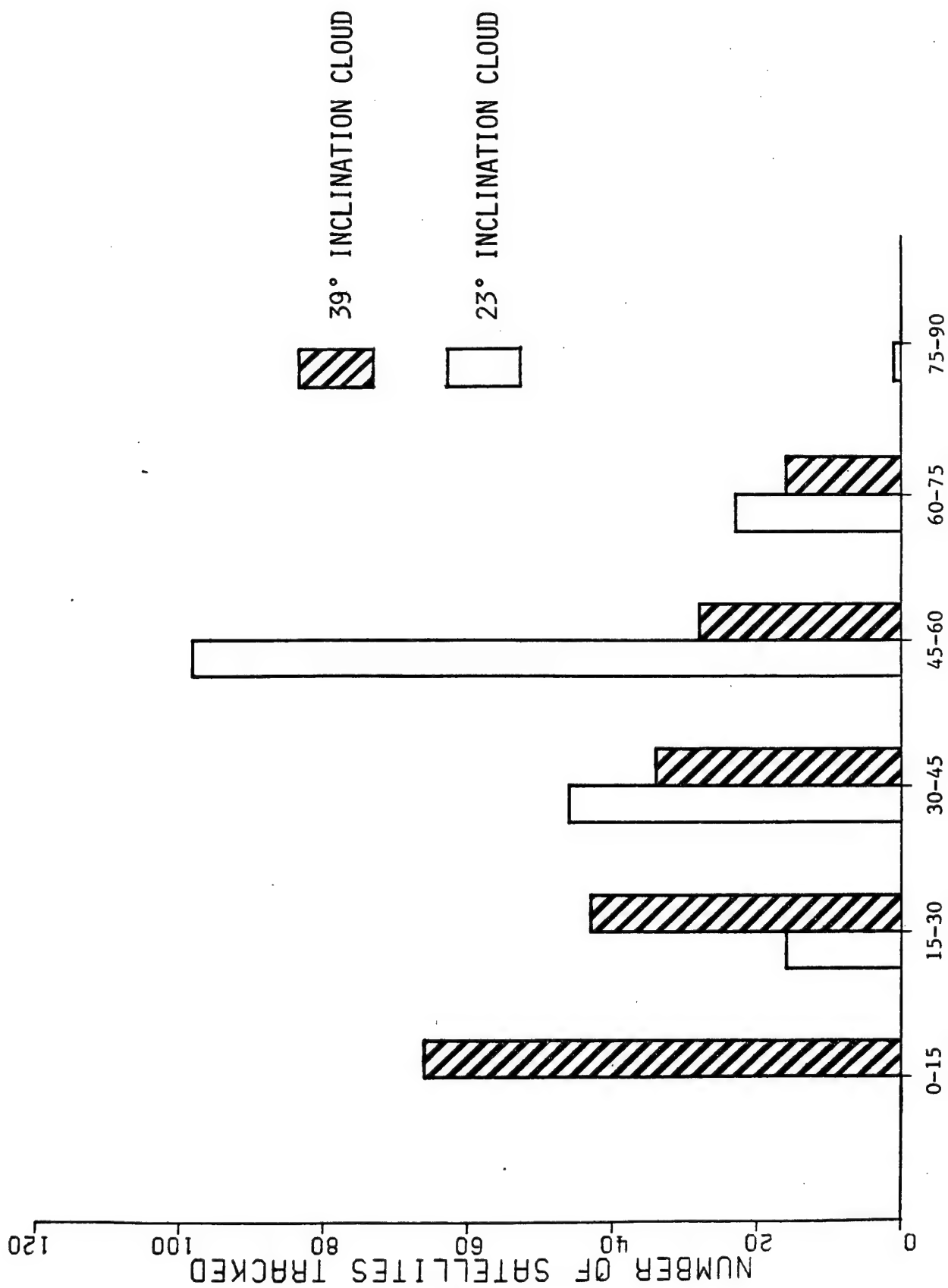


Figure 2:
TIME INTERVAL (minutes) IN WHICH FRAGMENT WAS FIRST DETECTED, 6 September 1986

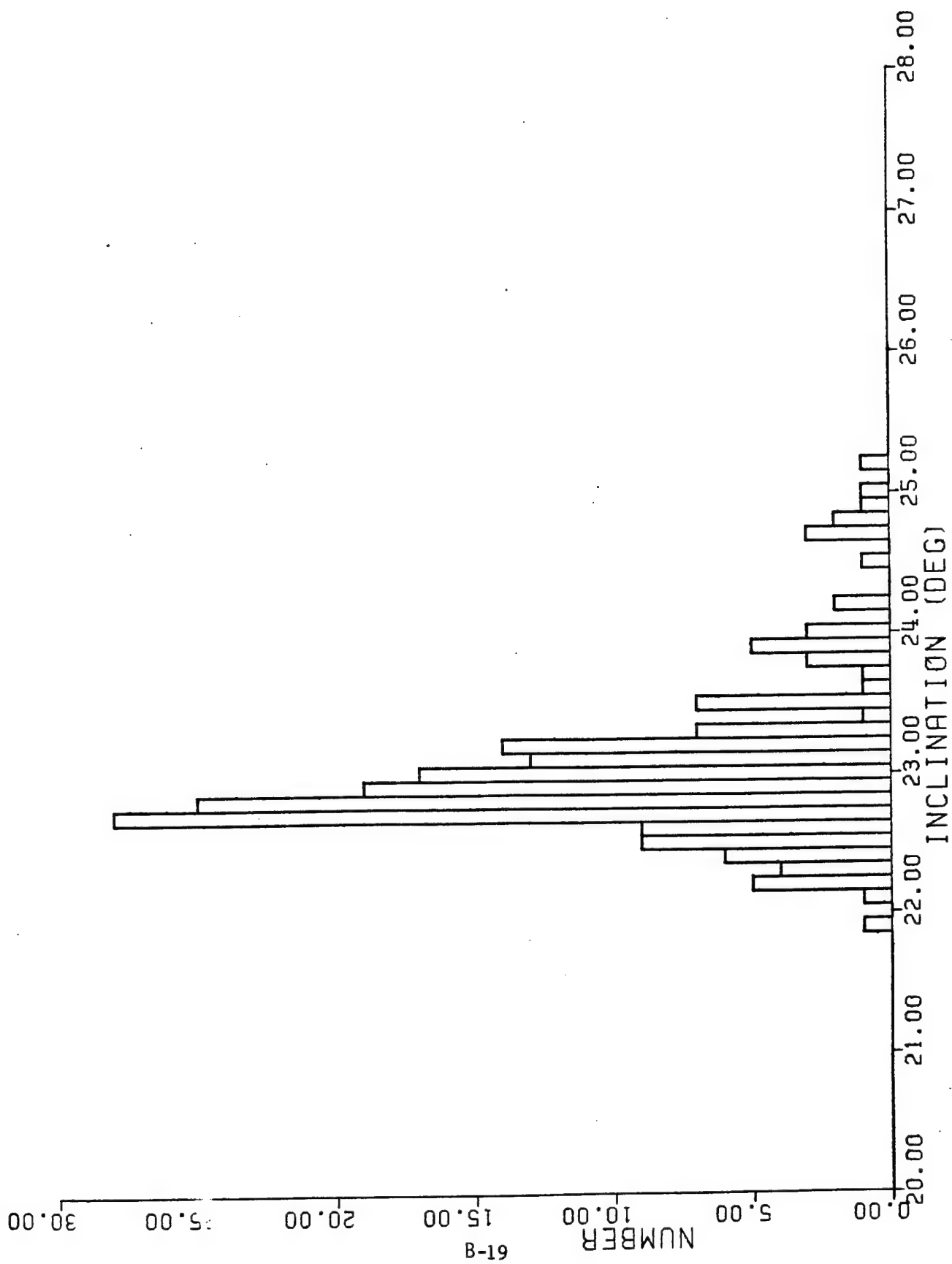


Figure 3

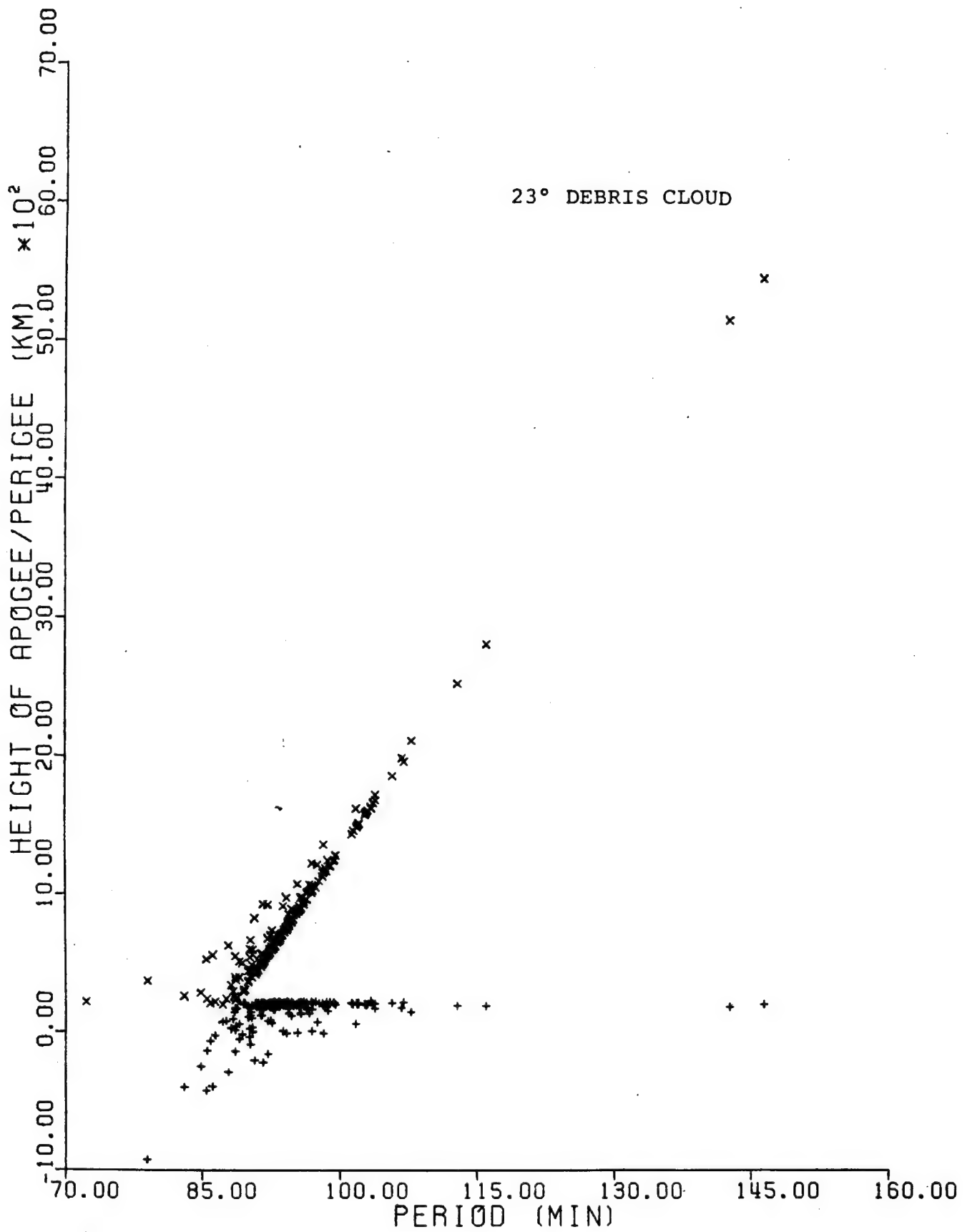


Figure 4

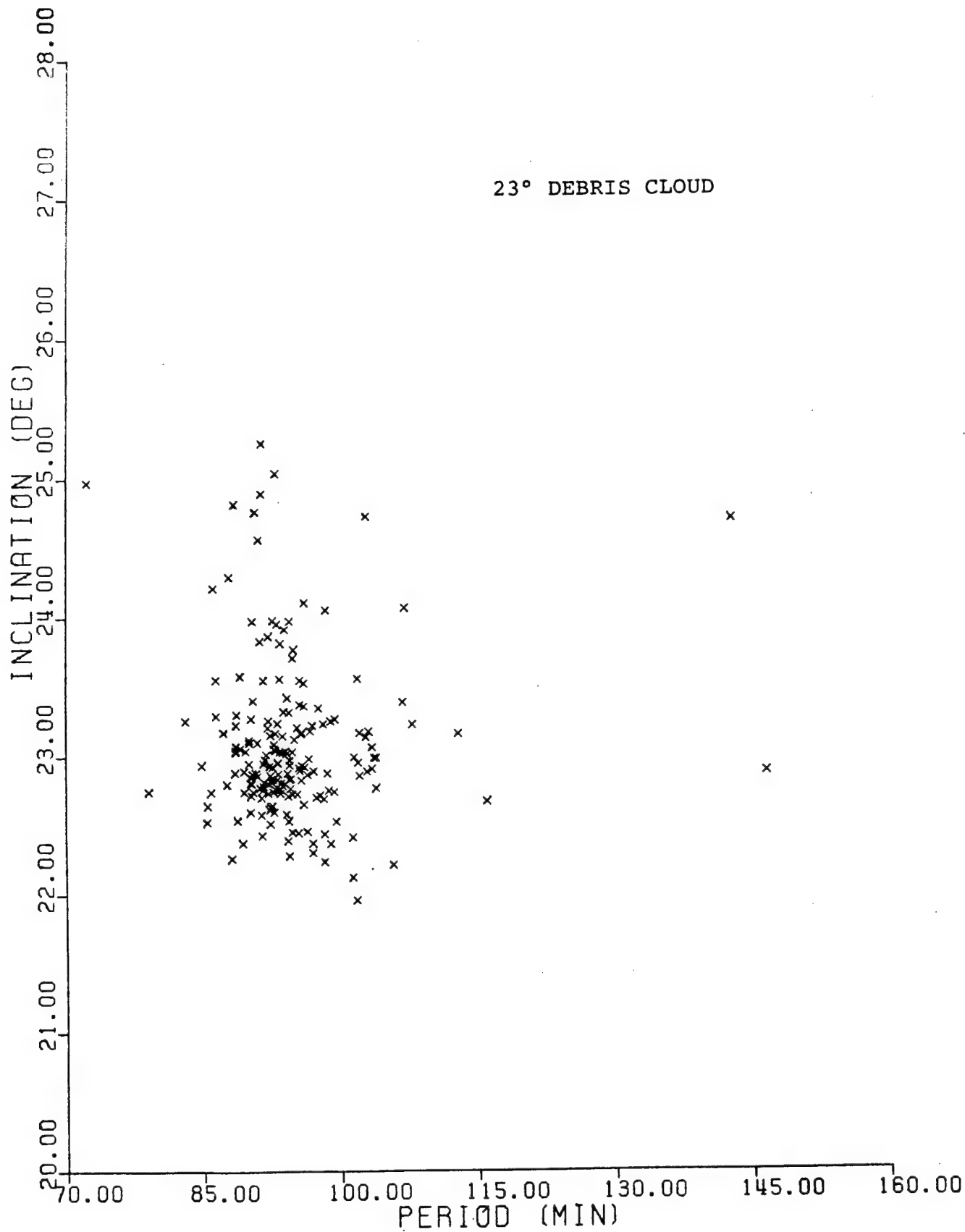


Figure 5

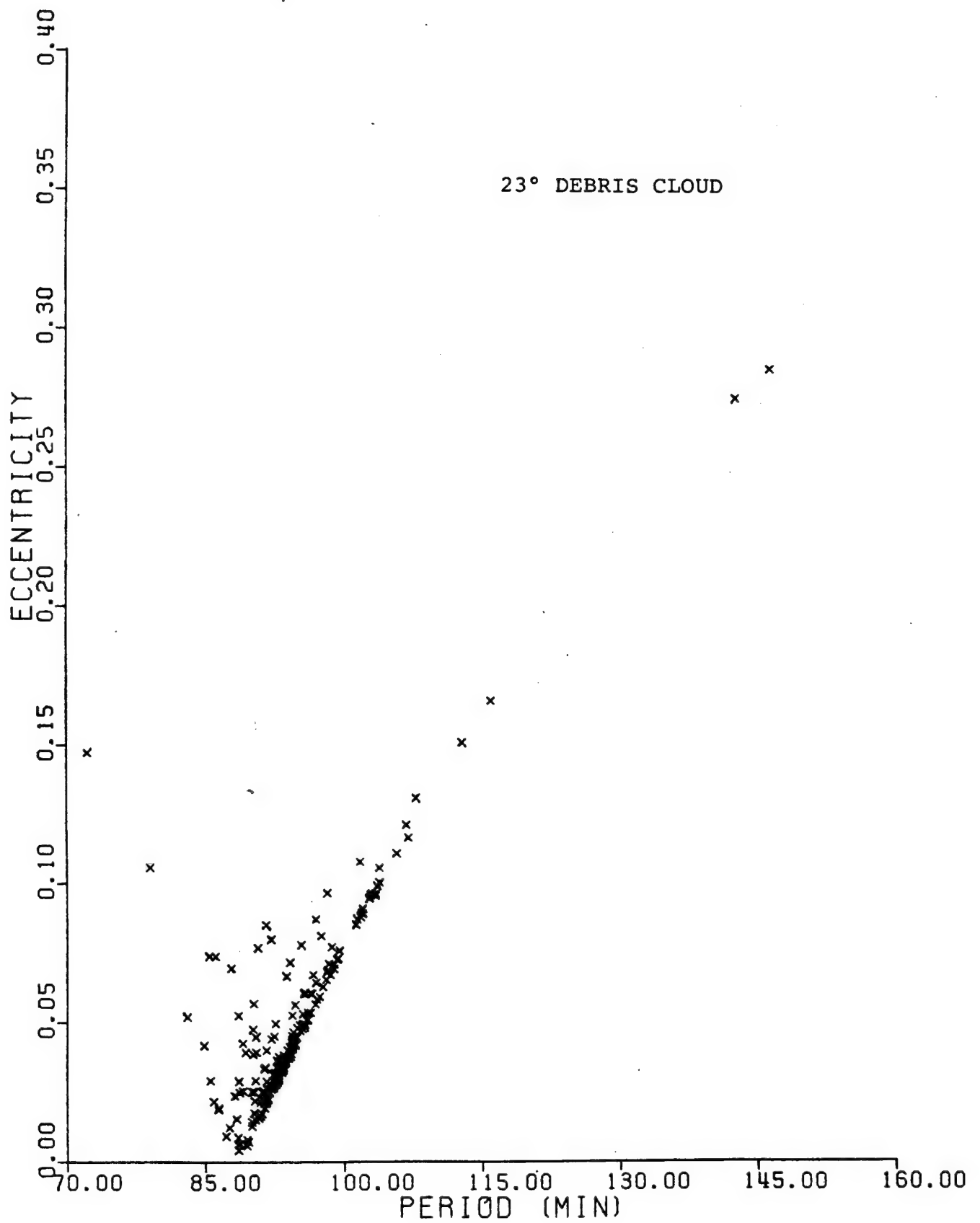


Figure 6

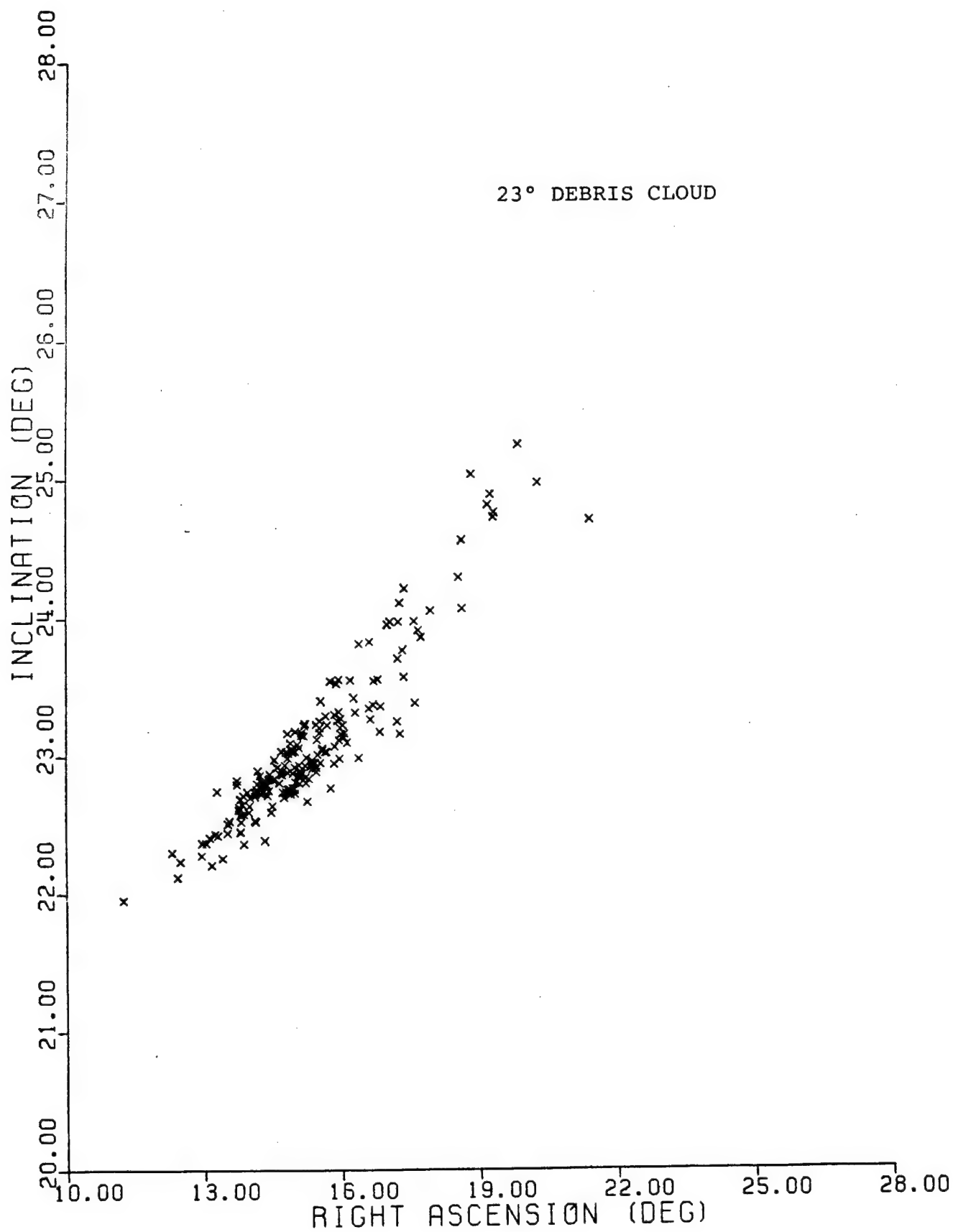


Figure 7

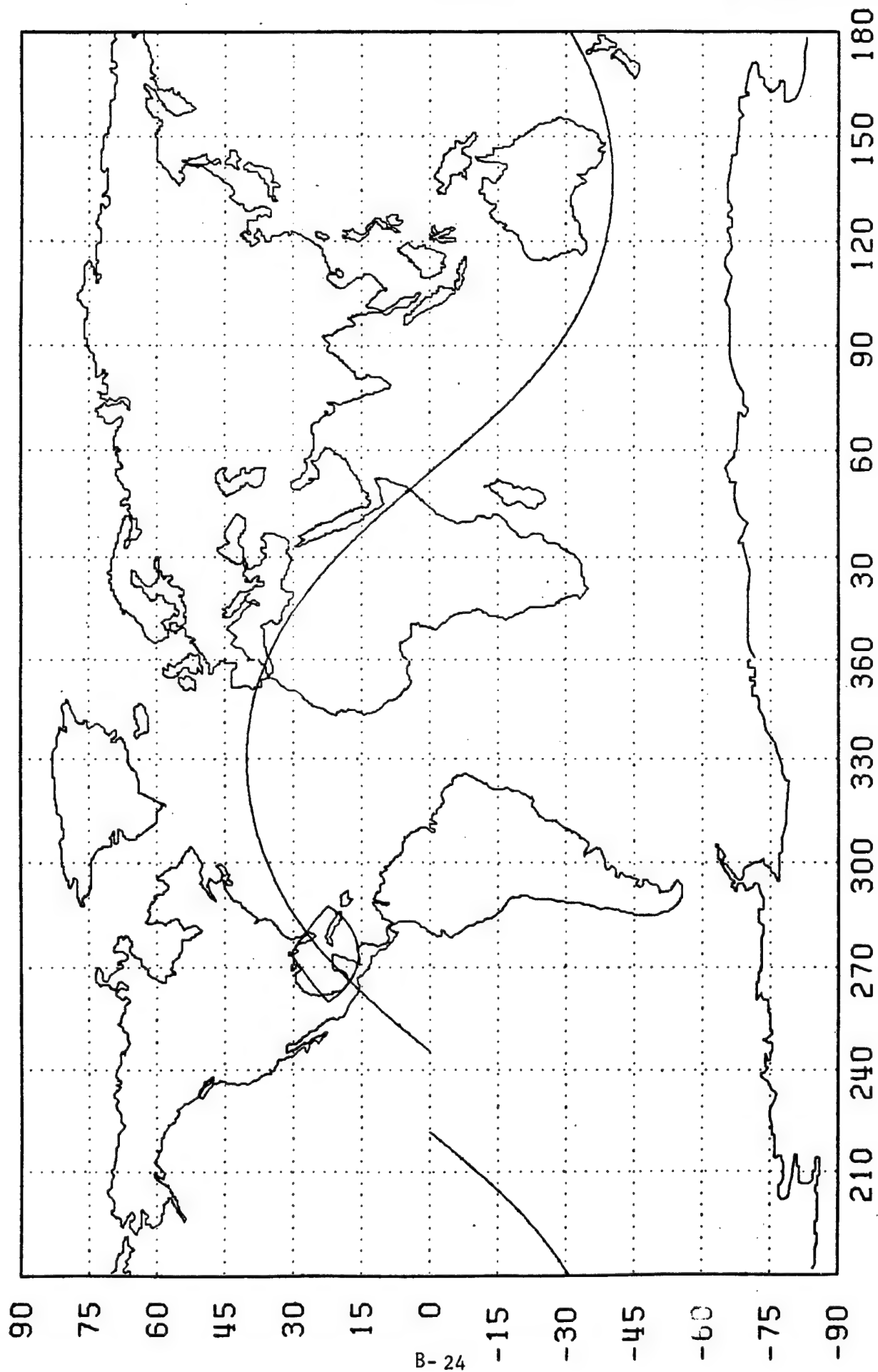


Figure 8. Sample geometry of 39° inclination debris cloud through Eglin coverage on 6 September 1986

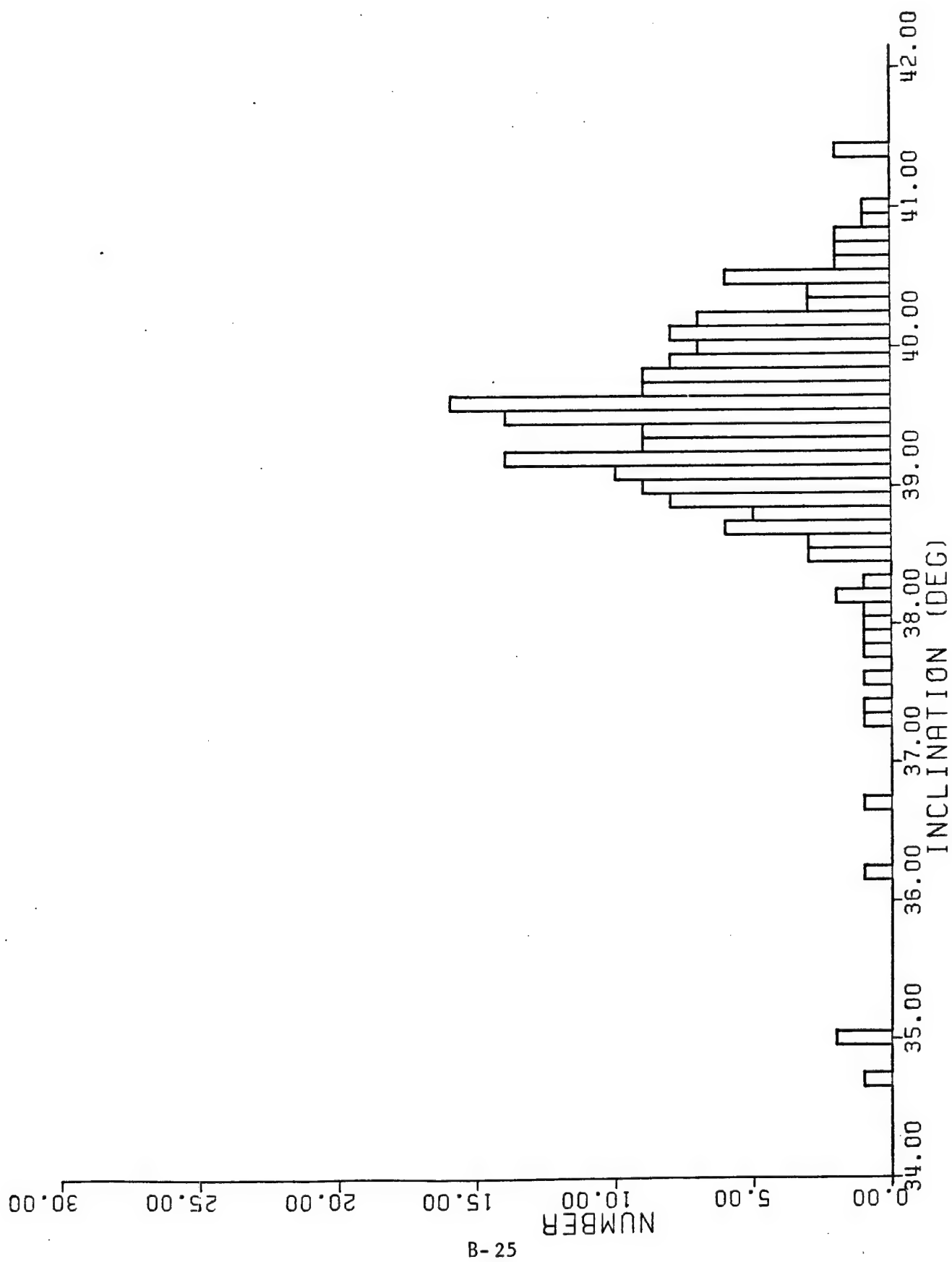


Figure 9

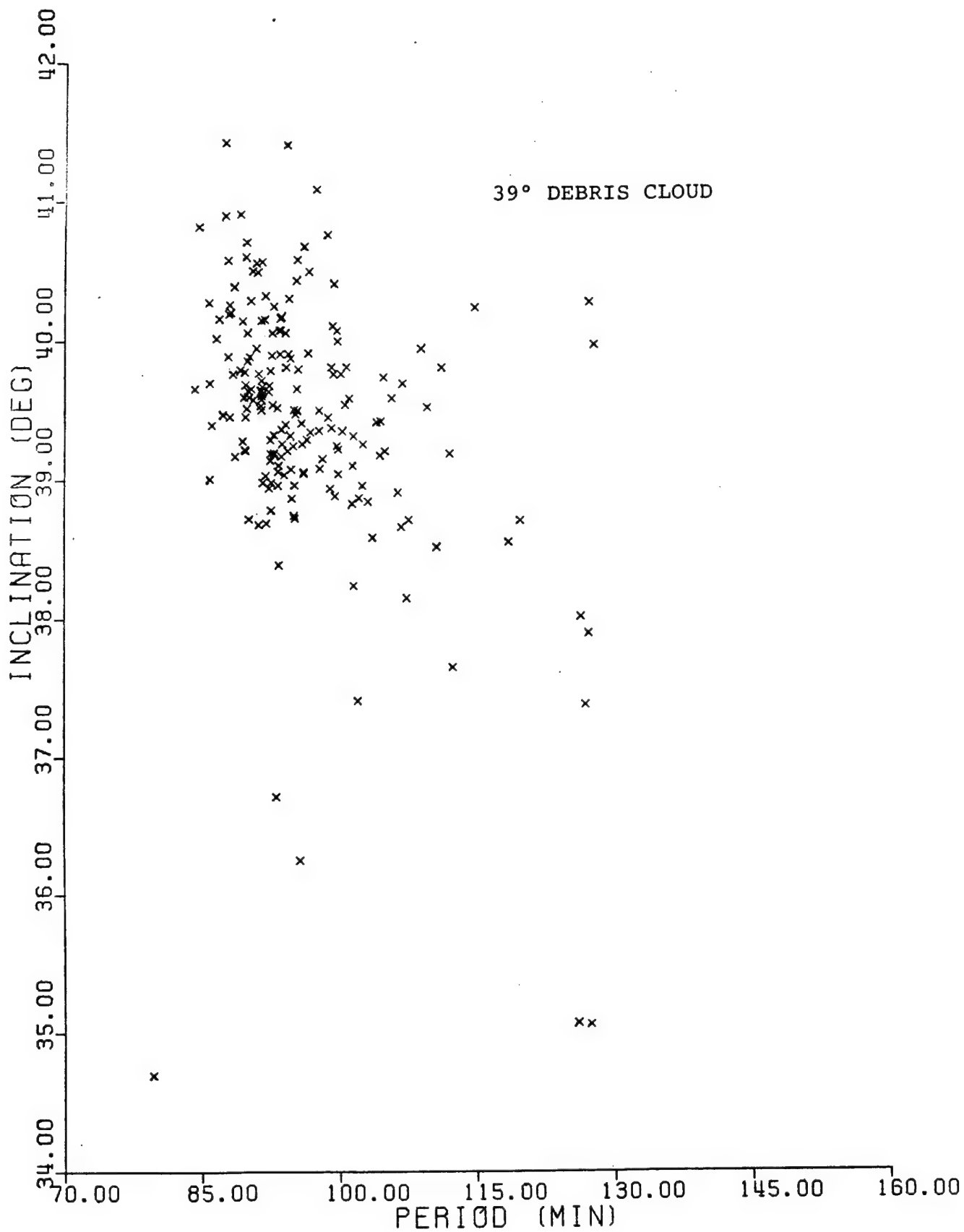


Figure 11

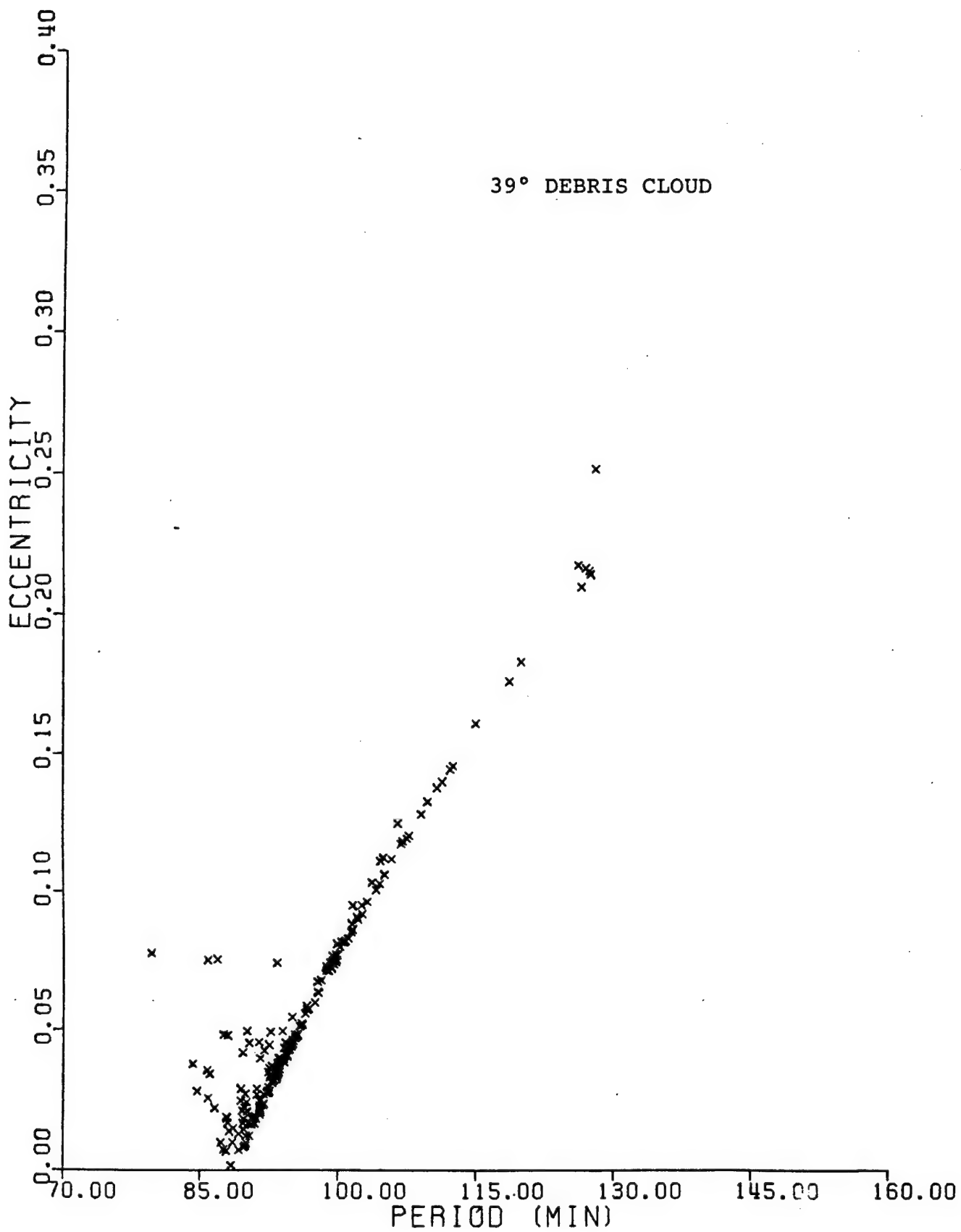


Figure 12

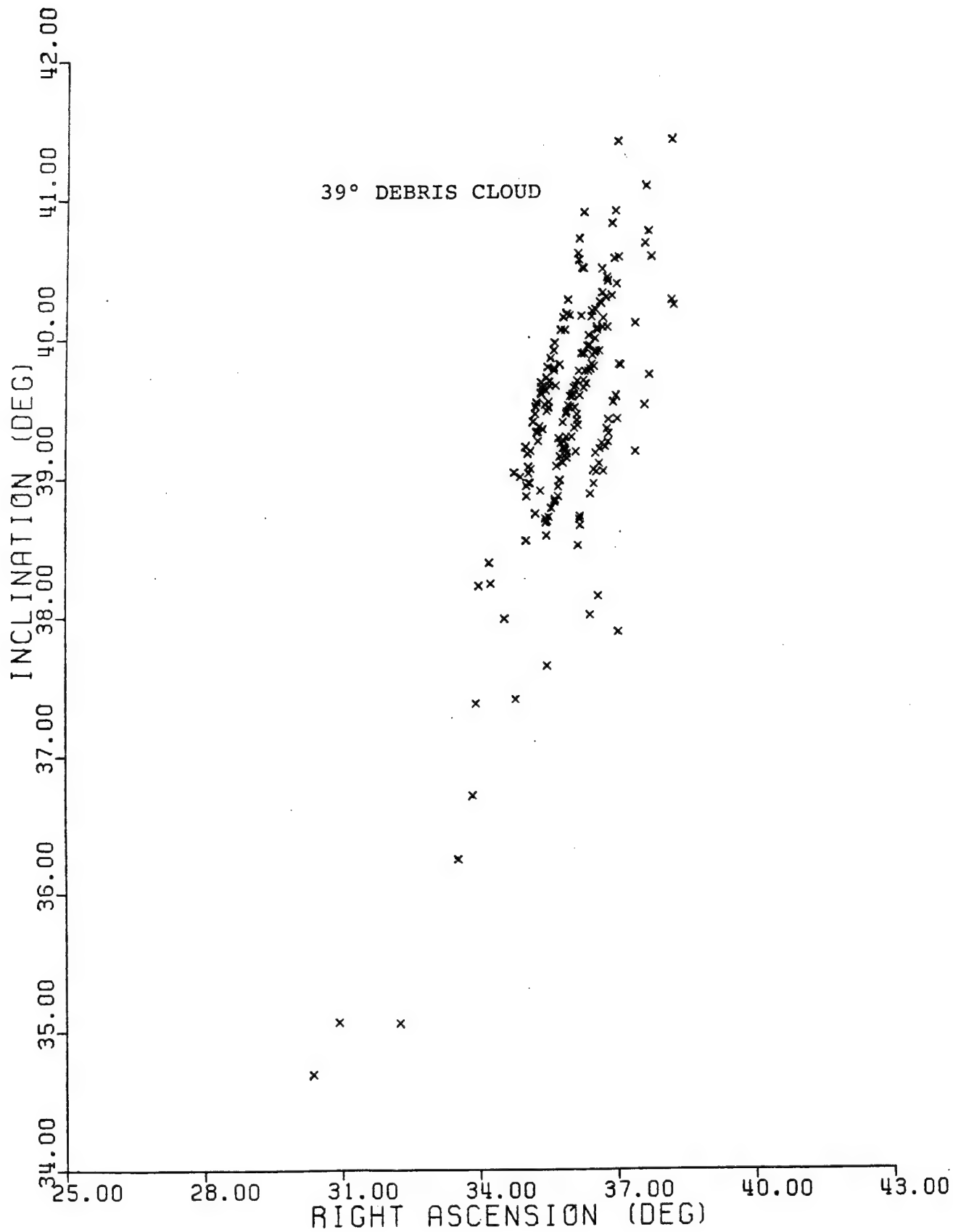


Figure 13

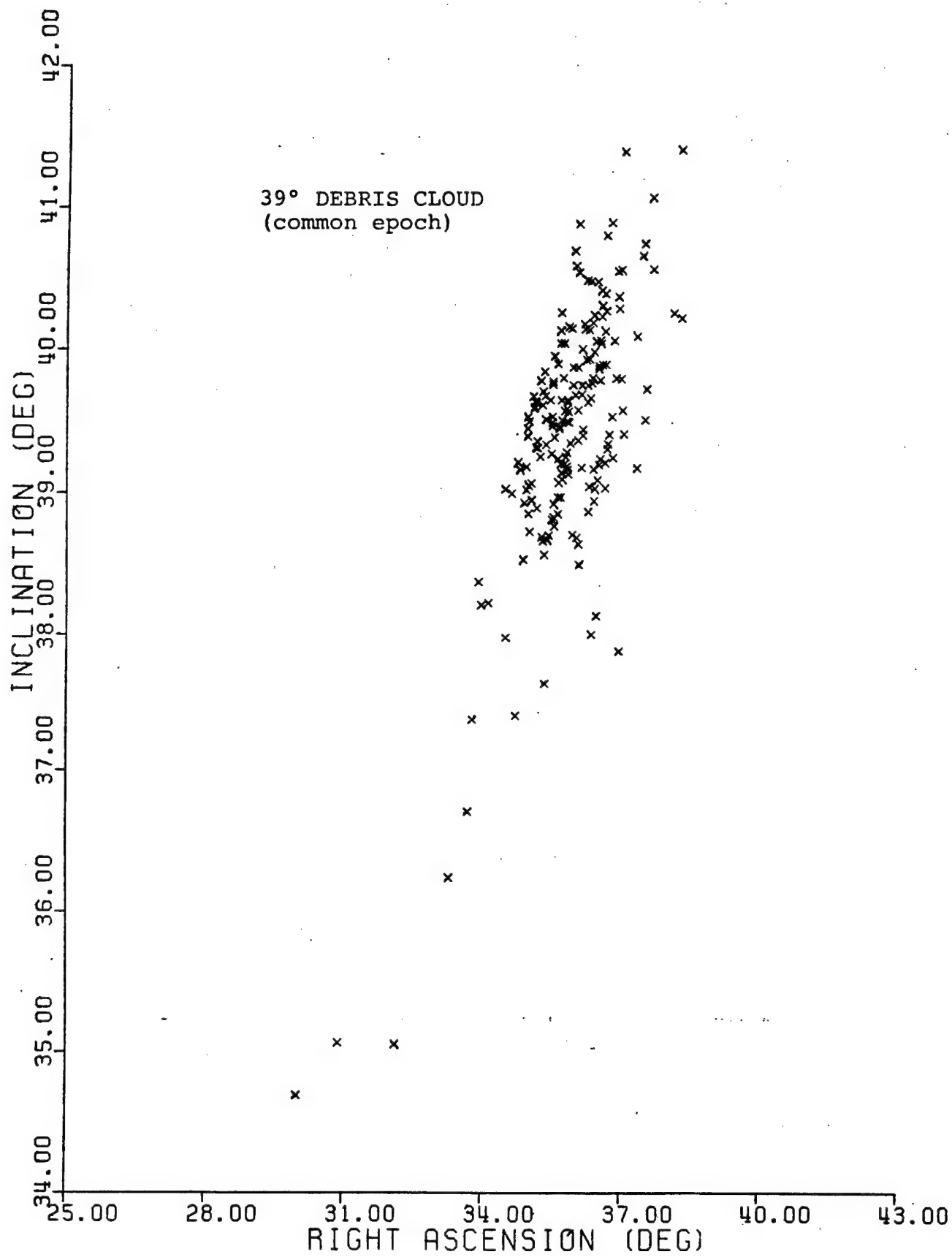


Figure 14

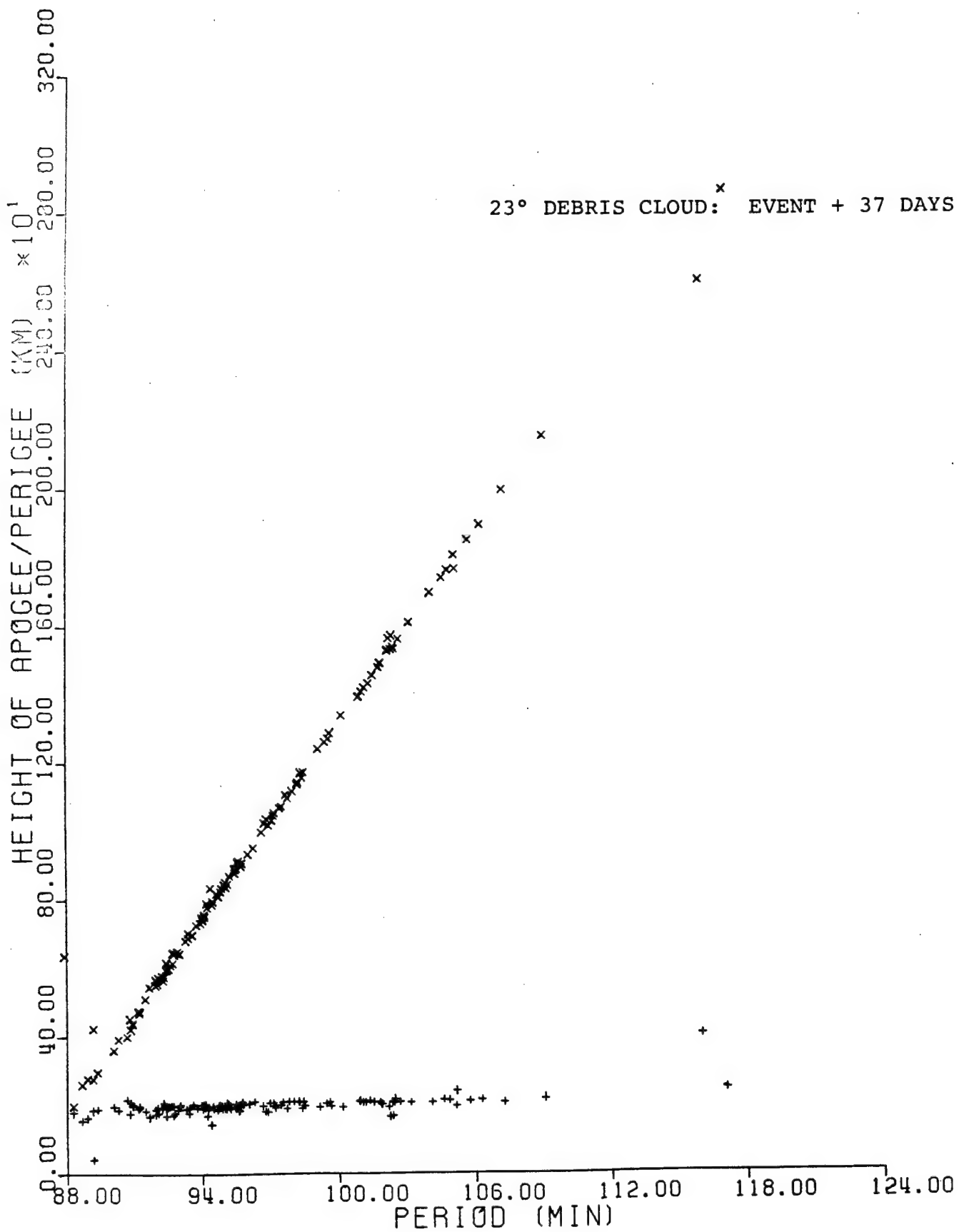


Figure 15

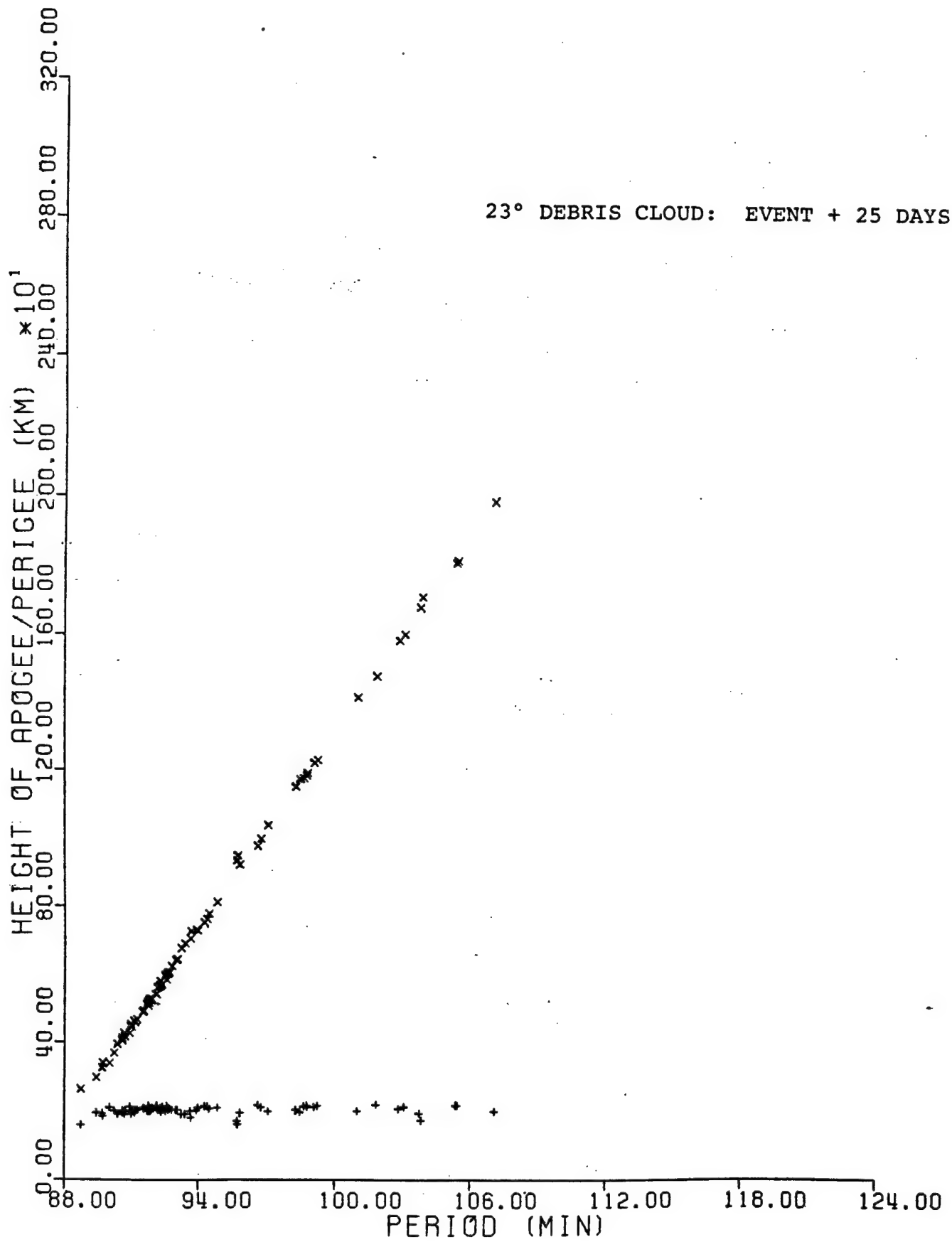


Figure 16

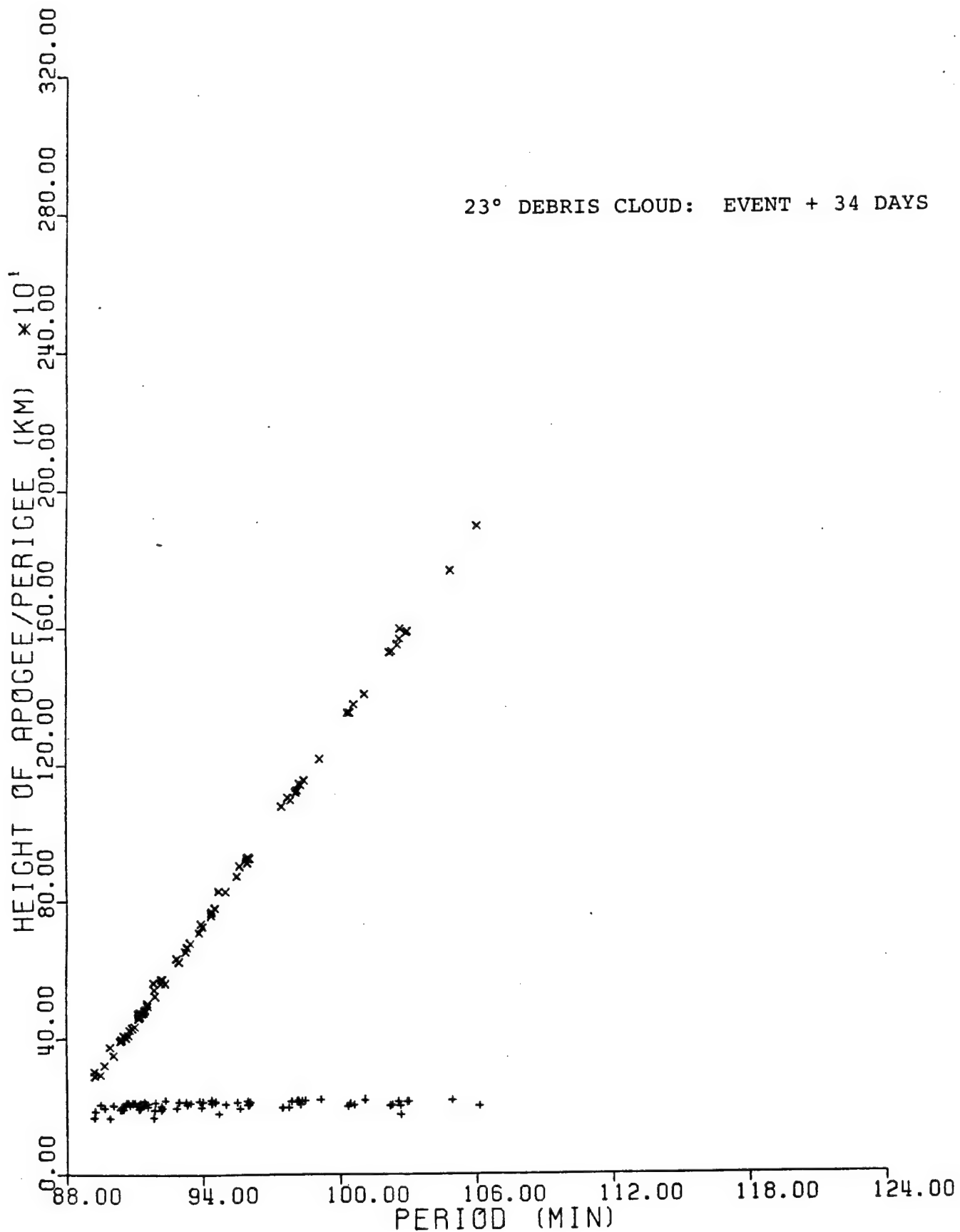


Figure 17

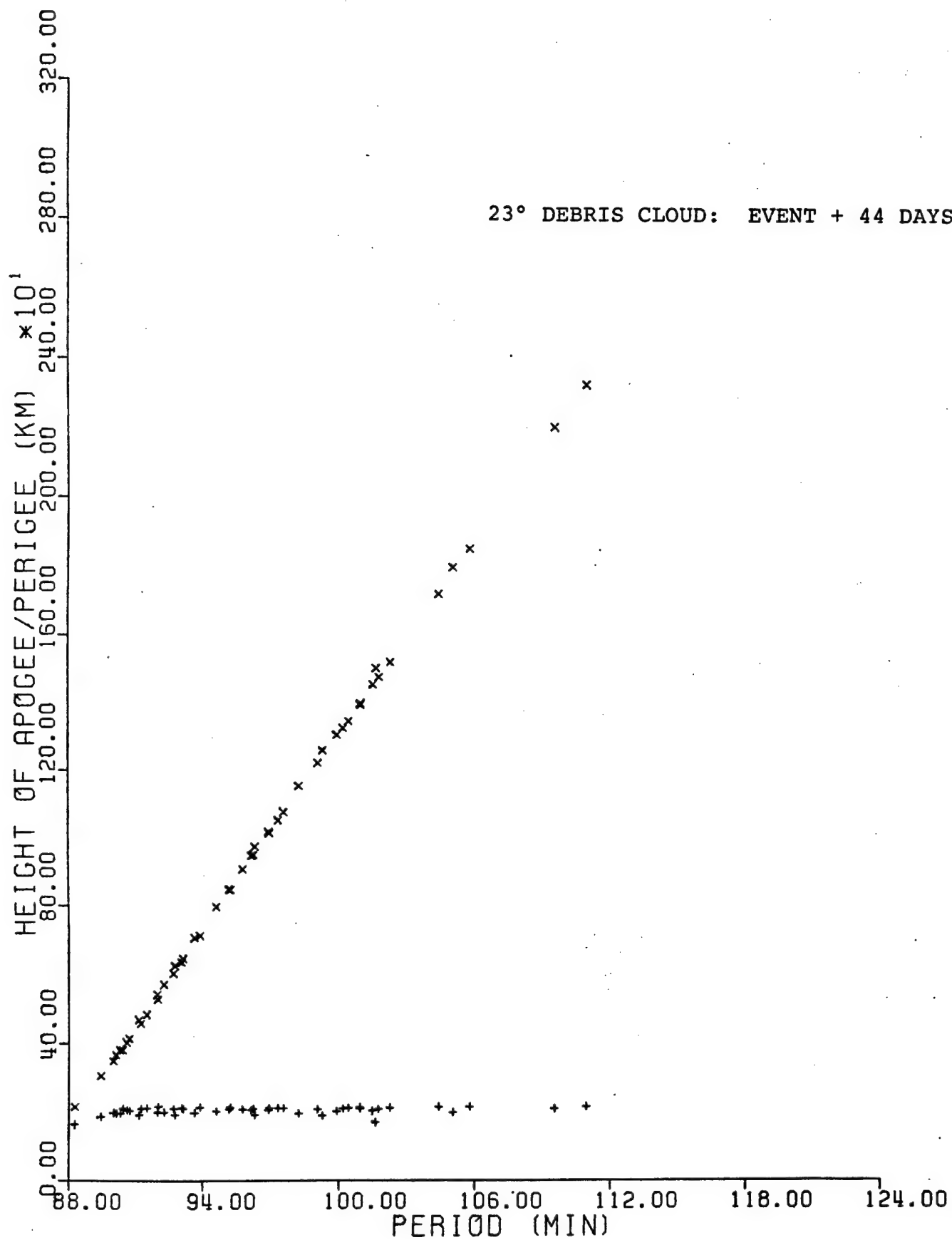


Figure 18

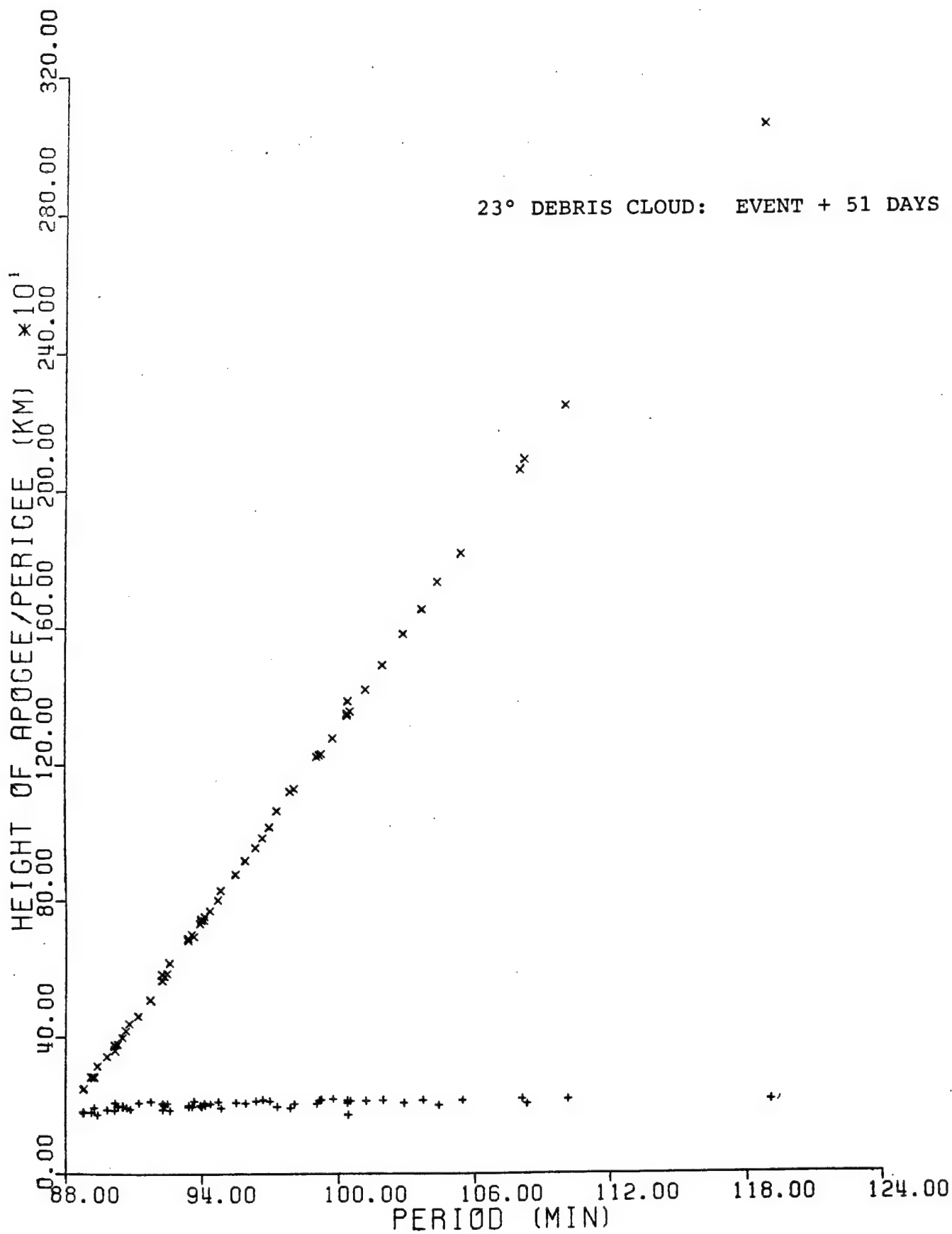


Figure 19

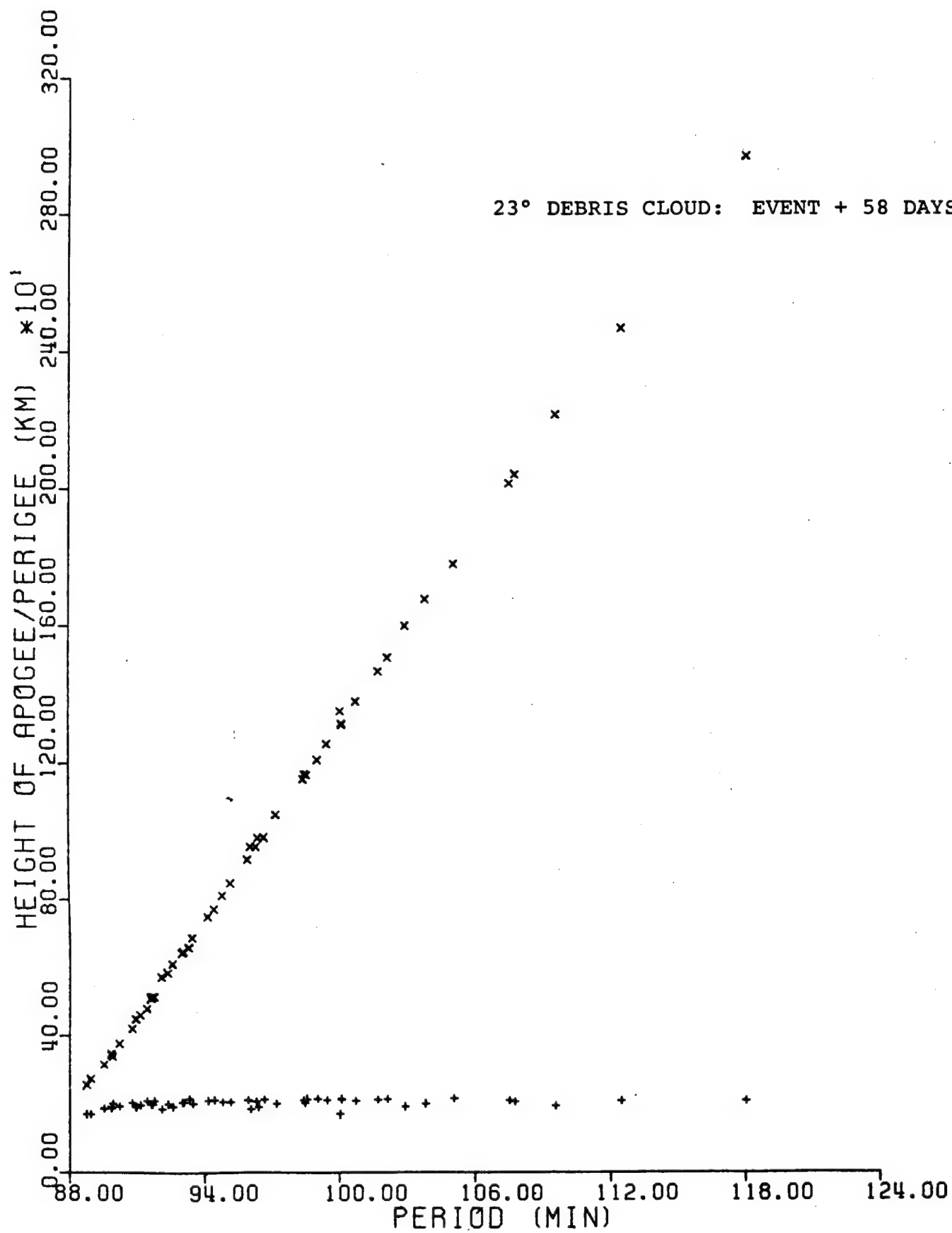
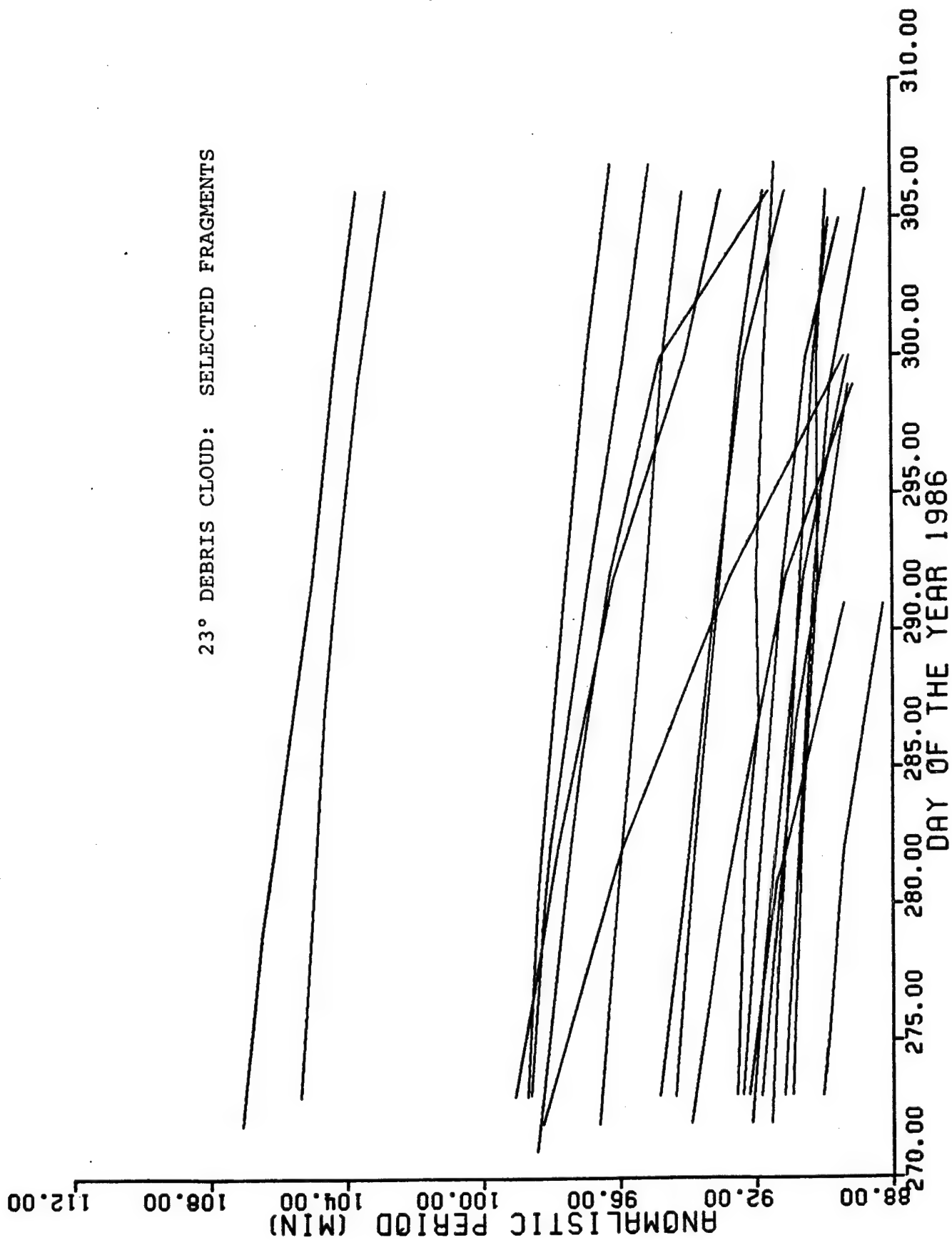


Figure 20



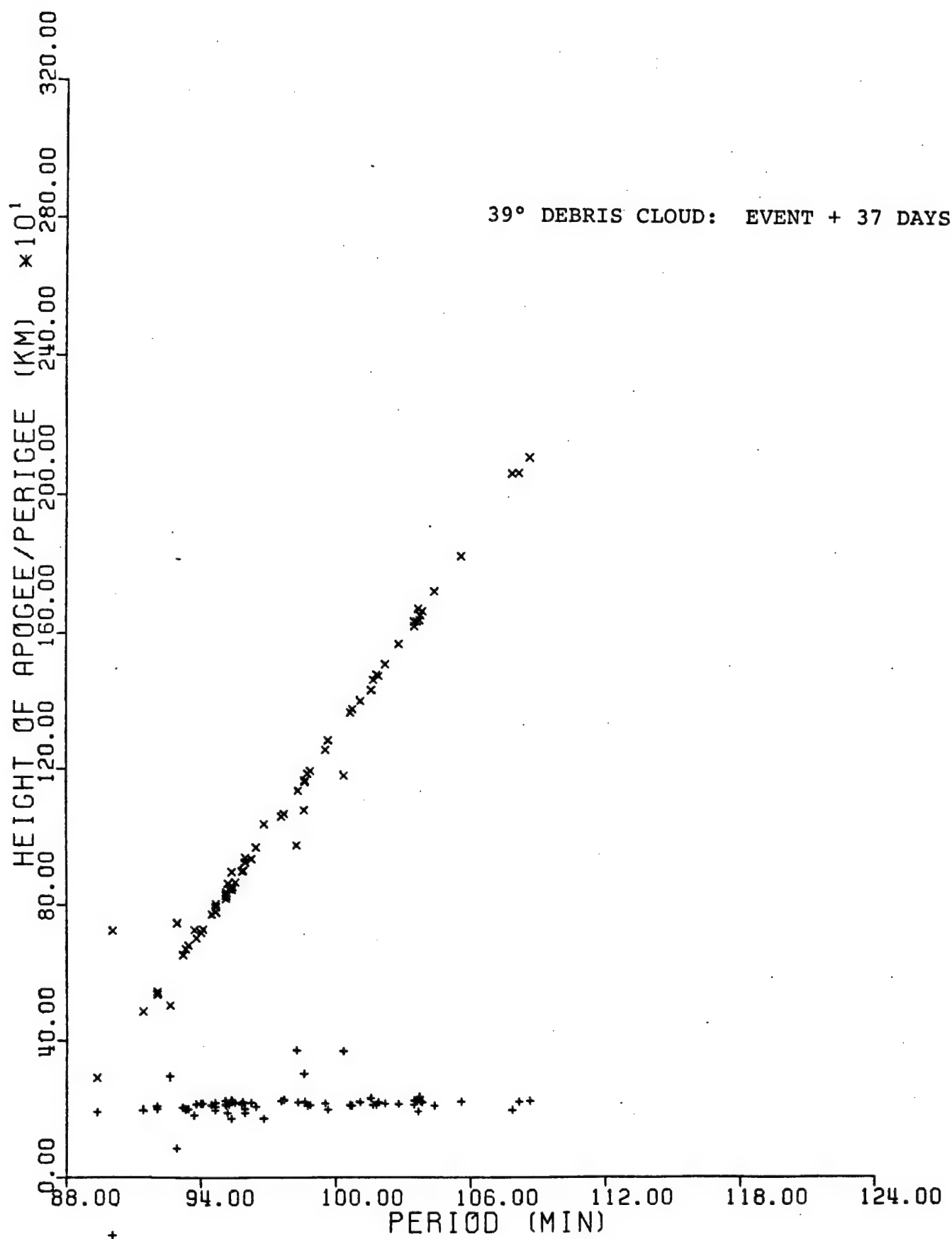


Figure 22

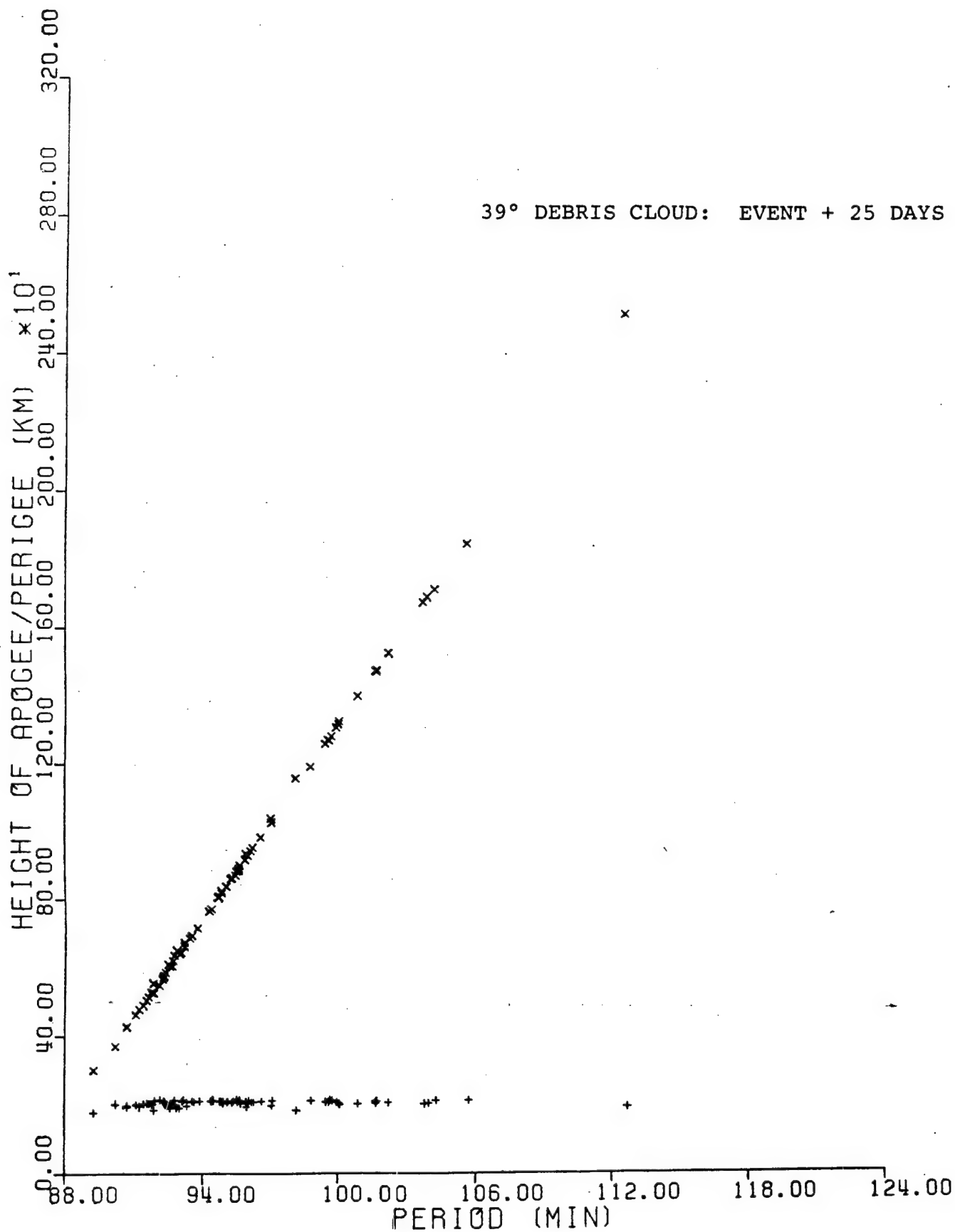


Figure 23

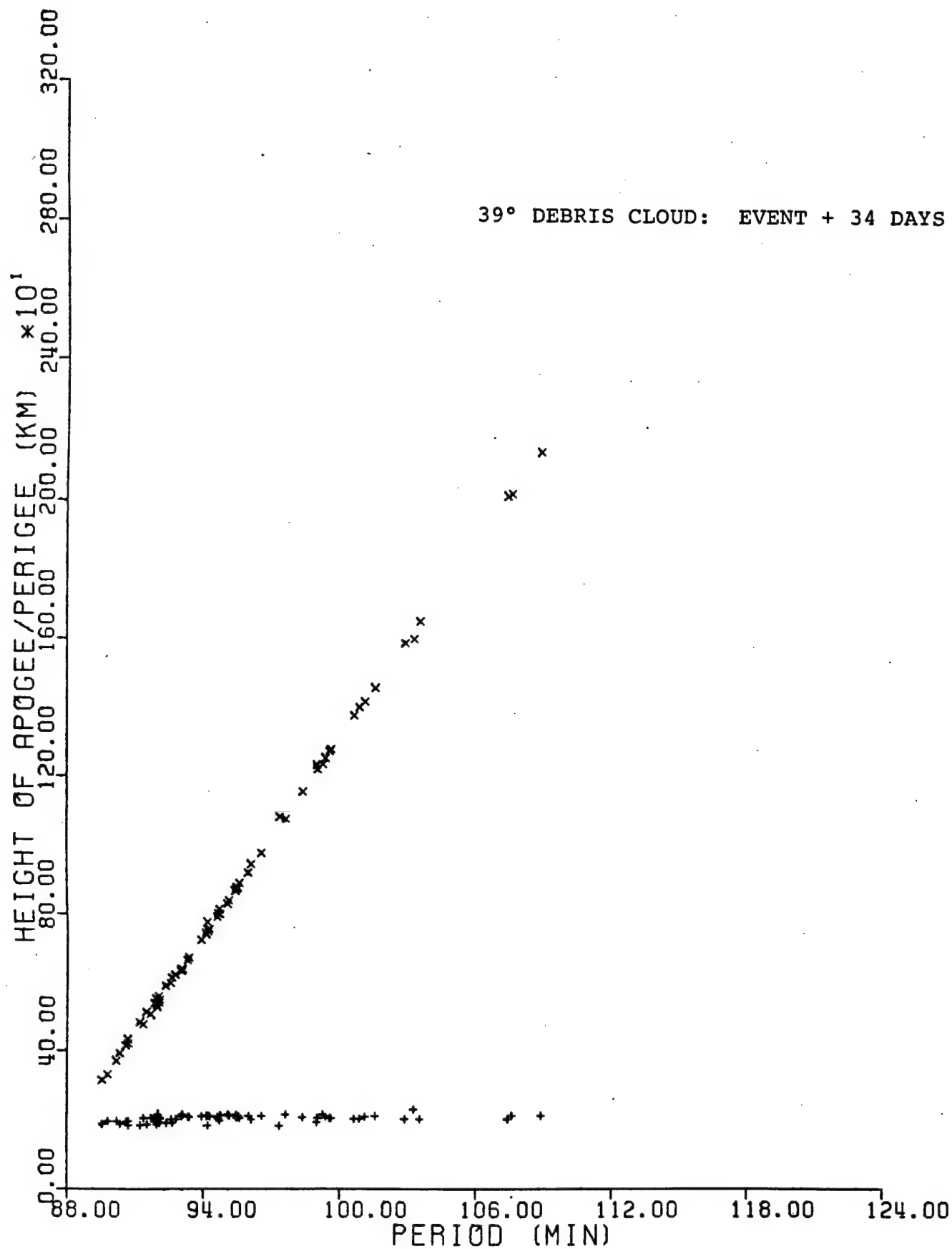


Figure 24

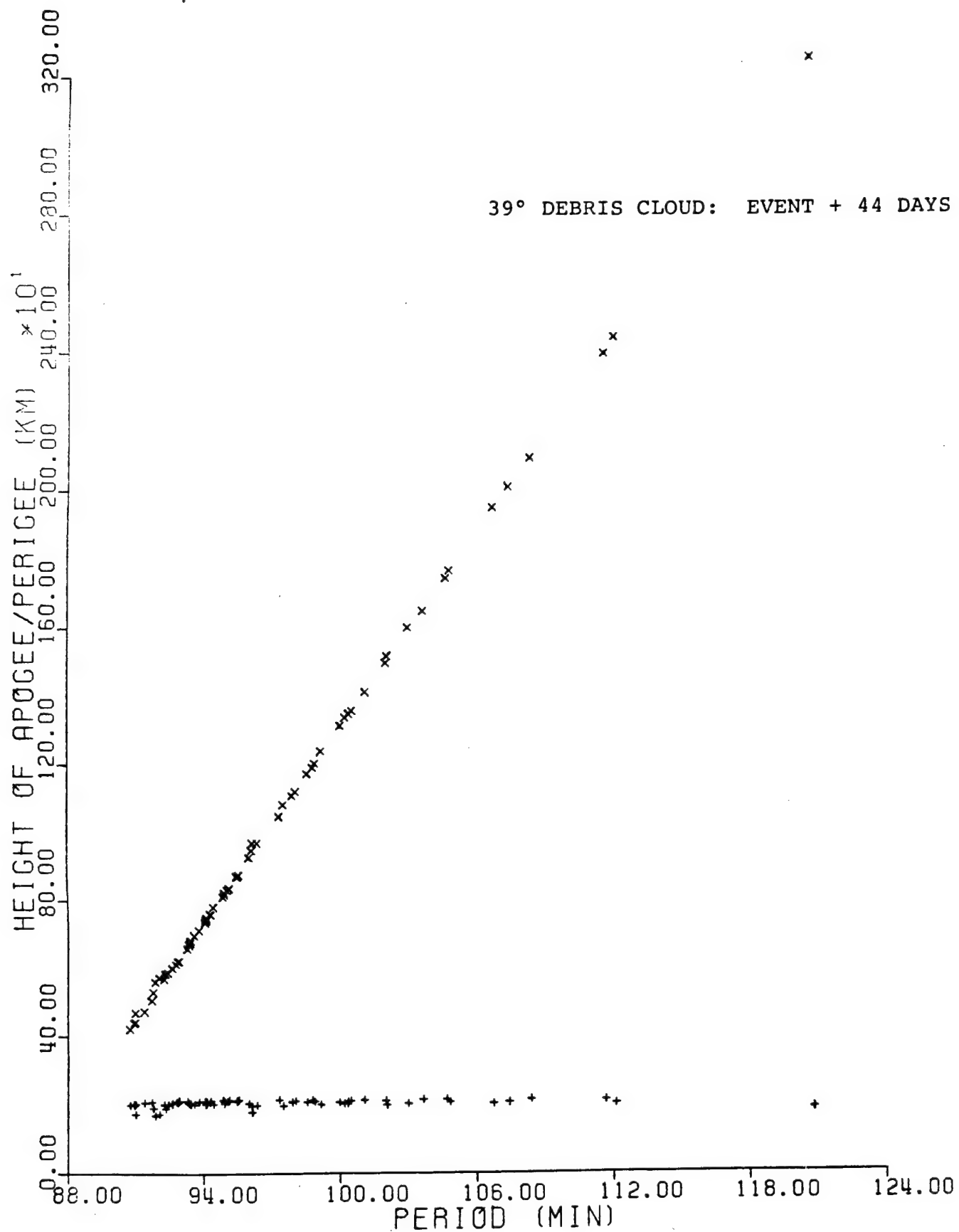


Figure 25

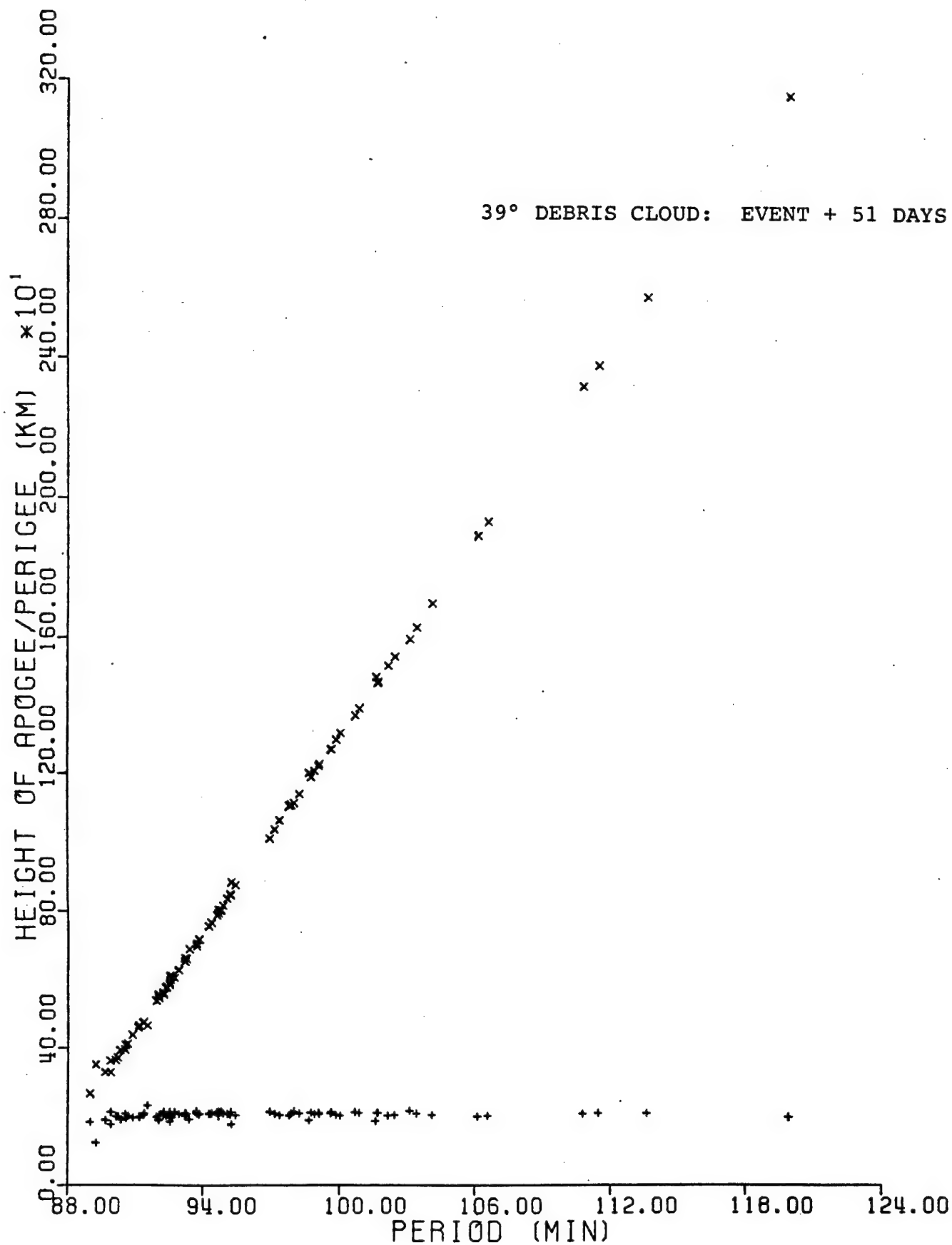


Figure 26

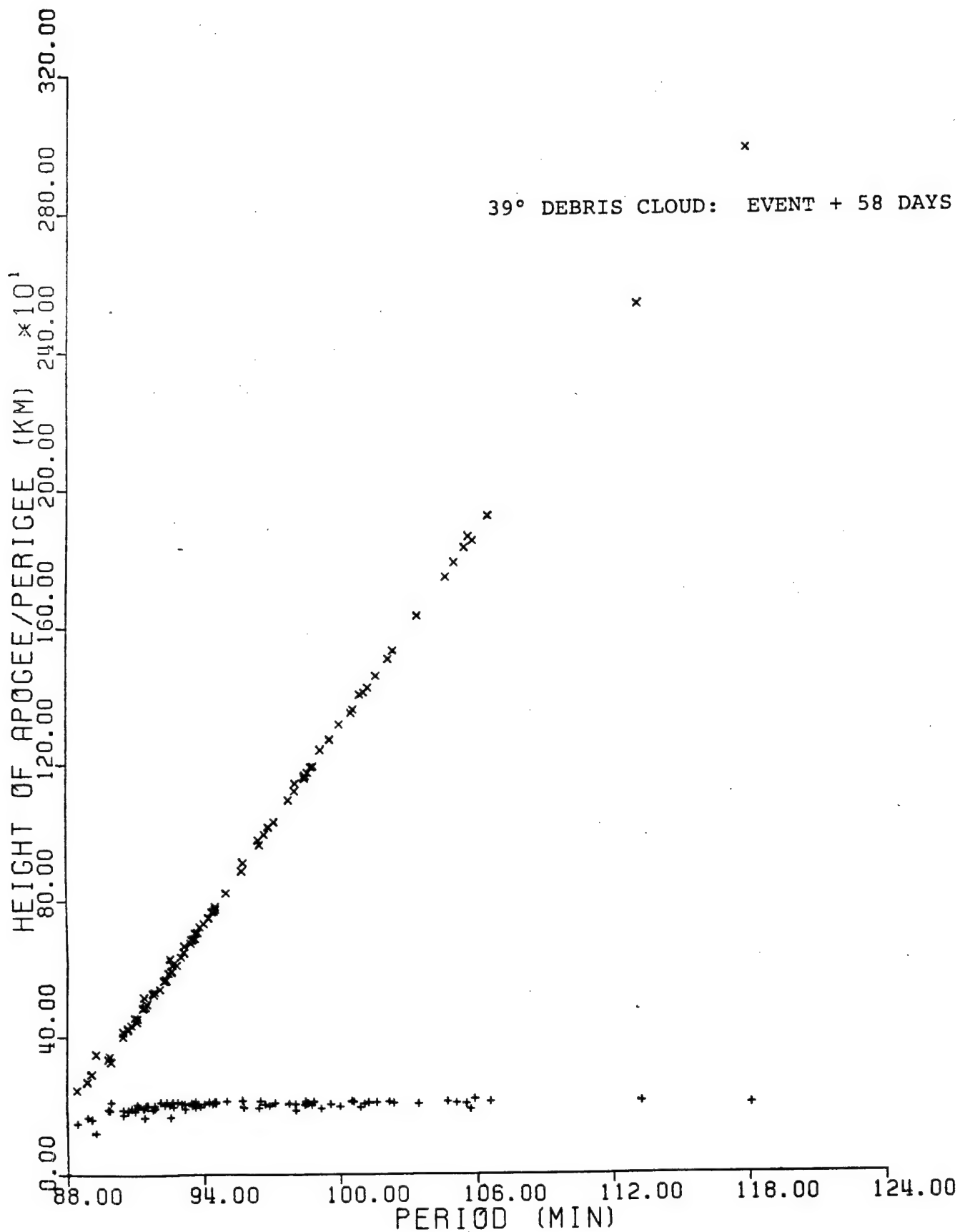


Figure 27

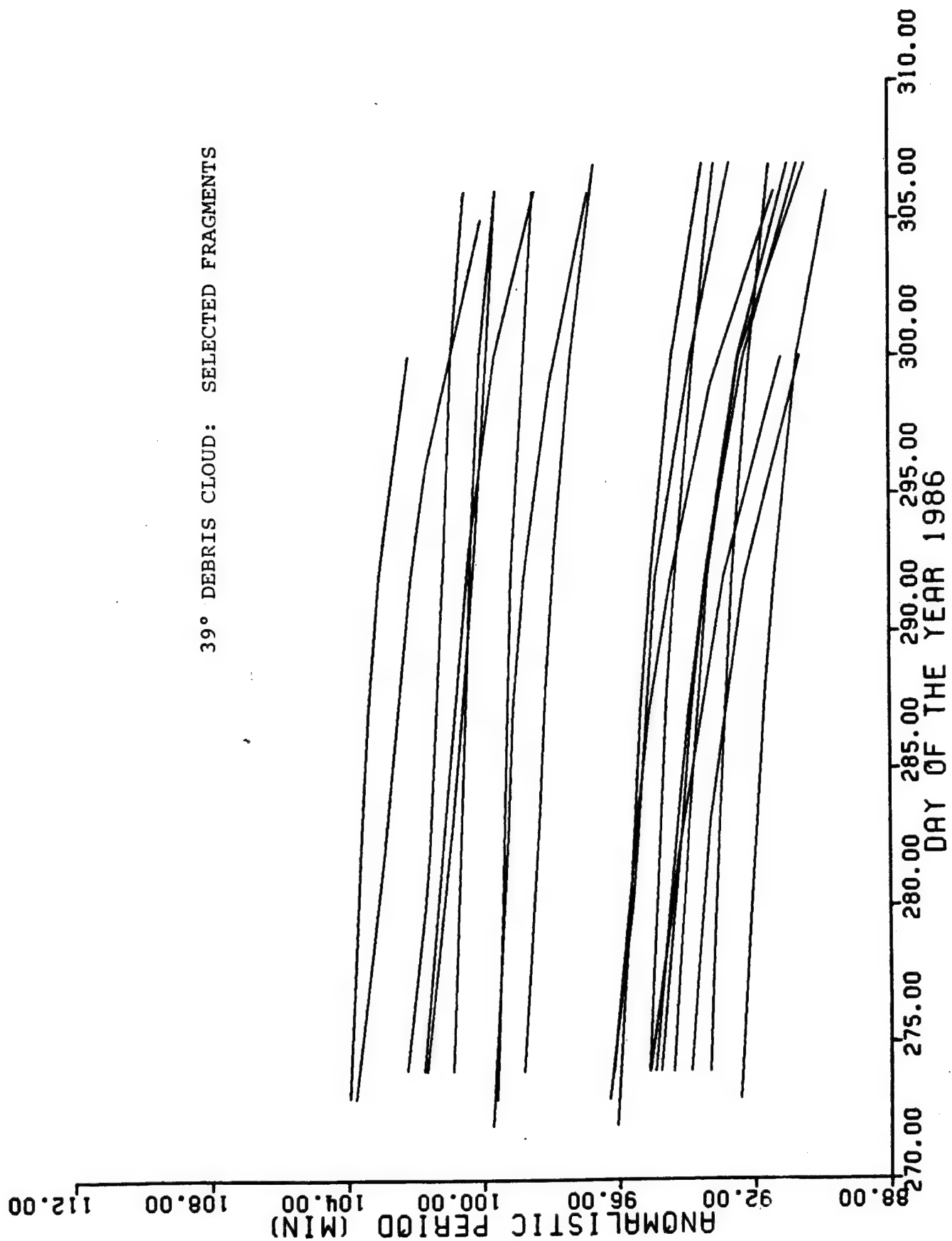


Figure 28

APPENDIX A1

EGLIN 23° DEBRIS CLOUD, 6 SEPTEMBER

1	94812U		86249.44318485	+	.00000000	+	.00000000	+	.00000000	-1.0	1145
2	94812	25.2482	19.8864	8218624	22.2888	26.8529	15.75578830	0000001			1146
1	94828U		86249.44588661	+	.00000000	+	.00000000	+	.00000000	-1.0	1279
2	94828	24.8892	19.2734	8193183	43.4576	7.3438	15.76342677	000001			1280
1	94833U		86249.44679555	+	.00000000	+	.00000000	+	.00000000	-1.0	1329
2	94833	24.5599	18.6353	8172292	42.9609	8.3296	15.81896568	000001			1330
1	94833U		86249.44788858	+	.00000000	+	.00000000	+	.00000000	-1.0	1339
2	94833	24.5588	18.6328	8233156	53.6060	359.6855	15.66291800	0000001			1340
1	94838U		86249.44591548	+	.00000000	+	.00000000	+	.00000000	-1.0	1367
2	94838	22.8889	14.3683	8218526	352.8196	59.8723	15.94495725	000001			1368
1	94838U		86249.44605793	+	.00000000	+	.00000000	+	.00000000	-1.0	1373
2	94838	22.7324	14.1399	8258794	34.6486	19.4692	15.62642828	000001			1374
1	94838U		86249.44615726	+	.00000000	+	.00000000	+	.00000000	-1.0	1377
2	94838	22.5498	13.4615	8196118	84.2383	333.1541	15.79784446	000001			1378
1	94838U		86249.57837652	+	.00000000	+	.00000000	+	.00000000	0.3	4785
2	94838	22.6794	12.9664	8284289	48.6451	46.1082	15.73875591	000001			4786
1	94848U		86249.44646492	+	.00000000	+	.00000000	+	.00000000	-1.0	1385
2	94848	22.7149	13.8661	8176241	102.3636	313.6116	15.94949962	000001			1386
1	94848U		86249.44663282	+	.00000000	+	.00000000	+	.00000000	-1.0	1391
2	94848	22.8784	14.3927	8163585	43.8462	11.5628	15.84854298	000001			1392
1	94848U		86249.44678714	+	.00000000	+	.00000000	+	.00000000	-1.0	1399
2	94848	22.9386	14.6893	8283717	48.4883	14.3888	15.56249147	000001			1400
1	94848U		86249.57927933	+	.00000000	+	.00000000	+	.00000000	0.1	4787
2	94848	22.8649	13.3888	8217866	48.1898	38.8378	15.78376256	000001			4788
1	94842U		86249.44673648	+	.00000000	+	.00000000	+	.00000000	-1.0	1395
2	94842	22.8716	14.4466	8158322	15.4814	37.4686	15.93191314	000001			1396
1	94842U		86249.44683879	+	.00000000	+	.00000000	+	.00000000	-1.0	1401
2	94842	22.8518	14.3775	8243845	42.7243	11.3922	15.64548259	000001			1402
1	94842U		86249.44781758	+	.00000000	+	.00000000	+	.00000000	-1.0	1409
2	94842	22.8228	14.2763	8199528	43.6944	11.6614	15.74698646	000001			1410
1	94842U		86249.57985422	+	.00000000	+	.00000000	+	.00000000	0.3	4791
2	94842	22.8232	13.2988	8229825	46.2926	48.8166	15.67867373	000001			4792
1	94846U		86249.44938964	+	.00000000	+	.00000000	+	.00000000	-1.0	1415
2	94846	22.8771	15.1381	8155263	41.6624	12.8388	15.86285698	000001			1416
1	94846U		86249.44946828	+	.00000000	+	.00000000	+	.00000000	-1.0	1431
2	94846	22.9125	15.2581	8262849	48.4285	6.9314	15.59768317	000001			1432
1	94847U		86249.44938884	+	.00000000	+	.00000000	+	.00000000	-1.0	1417
2	94847	22.8561	15.8929	8162761	47.3982	6.9182	15.83662898	000001			1418
1	94847U		86249.44945519	+	.00000000	+	.00000000	+	.00000000	-1.0	1425
2	94847	22.8592	15.1835	8288557	47.8854	7.3822	15.74552813	000001			1426
1	94847U		86249.44967584	+	.00000000	+	.00000000	+	.00000000	-1.0	1437
2	94847	22.8631	15.1178	8223387	47.6758	8.6275	15.69186559	000001			1438
1	94847U		86249.58211722	+	.00000000	+	.00000000	+	.00000000	0.2	4789
2	94847	22.8433	14.8625	8218461	51.7315	35.5878	15.69753112	000001			4790
1	94848U		86249.44938471	+	.00000000	+	.00000000	+	.00000000	-1.0	1419
2	94848	22.7311	14.9725	8264486	32.9188	28.5829	15.63726486	000001			1420
1	94848U		86249.44953886	+	.00000000	+	.00000000	+	.00000000	-1.0	1429
2	94848	22.5929	14.4935	8218398	69.8385	347.3974	15.73888894	000001			1438
1	94854U		86249.45029928	+	.00000000	+	.00000000	+	.00000000	-1.0	1459
2	94854	24.8134	19.2153	8151631	148.8784	261.8591	16.29337181	000001			1468
1	94854U		86249.45848575	+	.00000000	+	.00000000	+	.00000000	-1.0	1481
2	94854	24.6456	18.7987	8287648	91.9667	319.1723	15.72441986	000001			1482
1	94854U		86249.45869748	+	.00000000	+	.00000000	+	.00000000	-1.0	1501
2	94854	24.6814	18.8937	8288783	77.2597	334.2747	15.63873464	000001			1502
1	94854U		86249.45889389	+	.00000000	+	.00000000	+	.00000000	-1.0	1521
2	94854	24.6158	18.7111	8314422	98.5988	323.8653	15.65982882	000001			1522
1	94854U		86249.45116194	+	.00000000	+	.00000000	+	.00000000	-1.0	1541
2	94854	24.6963	18.9442	8329611	74.2398	339.9145	15.51933978	000001			1542
1	94854U		86249.58237168	+	.00000000	+	.00000000	+	.00000000	0.4	4783
2	94854	24.6446	17.1119	8289816	84.3779	2.6685	15.64966171	000001			4784
1	94858U		86249.45881693	+	.00000000	+	.00000000	+	.00000000	-1.0	1513
2	94858	22.7481	14.7229	8337674	83.8834	331.8626	15.54388373	000001			1514
1	94858U		86249.45893345	+	.00000000	+	.00000000	+	.00000000	-1.0	1523
2	94858	22.8842	15.1857	8263824	59.4829	354.1781	15.68875862	000001			1524
1	94858U		86249.45118823	+	.00000000	+	.00000000	+	.00000000	-1.0	1551
2	94858	22.8567	15.8928	8174139	66.7535	348.8479	15.83268482	000001			1552
1	94858U		86249.44948217	+	.00000000	+	.00000000	+	.00000000	-1.0	1577
2	94858	22.9248	14.6239	8358812	56.2895	359.3896	15.48845782	000001			1578
1	94858U		86249.58251881	+	.00000000	+	.00000000	+	.00000000	0.2	4793
2	94858	22.8687	13.4158	8246369	63.1557	25.2999	15.64944244	000001			4794
1	94861U		86249.45896776	+	.00000000	+	.00000000	+	.00000000	-1.0	1529
2	94861	22.7546	14.8447	8218146	39.5315	16.3816	15.73865771	000001			1530

1	94861U	86249.44929818	+.000000000	+000000+0	+000000+0	-1.0	1561	
2	94861	22.7658	14.1805	0218856	38.7228	18.6967	15.7122284500001	1562
1	94863U	86249.45107389	+.000000000	+000000+0	+000000+0	-1.0	1539	
2	94863	22.9442	15.3400	0215204	38.8656	14.0679	15.7167652000001	1540
1	94863U	86249.44927927	+.000000000	+000000+0	+000000+0	-1.0	1557	
2	94863	22.8925	14.4645	0253330	54.4780	0.1609	15.6125761400001	1558
1	94863U	86249.44945402	+.000000000	+000000+0	+000000+0	-1.0	1583	
2	94863	22.8986	14.4859	0327260	59.1384	356.7496	15.4379721700001	1584
1	94863U	86249.44965190	+.000000000	+000000+0	+000000+0	-1.0	1595	
2	94863	22.8320	14.2380	0189536	68.8440	348.6521	15.7790475300001	1596
1	94866U	86249.44939768	+.000000000	+000000+0	+000000+0	-1.0	1569	
2	94866	23.8107	16.3915	0381842	78.3167	334.8836	15.4148262700001	1570
1	94866U	86249.44960590	+.000000000	+000000+0	+000000+0	-1.0	1591	
2	94866	23.9079	16.6733	0279687	73.3182	340.0417	15.6100659000001	1592
1	94866U	86249.44985445	+.000000000	+000000+0	+000000+0	-1.0	1607	
2	94866	23.9107	16.6820	0255172	72.6216	342.0010	15.6625482200001	1608
1	94866U	86249.45006893	+.000000000	+000000+0	+000000+0	-1.0	1635	
2	94866	23.7996	16.3183	0565682	87.6581	331.0077	15.1003219300001	1636
1	94869U	86249.44983249	+.000000000	+000000+0	+000000+0	-1.0	1603	
2	94869	22.8934	14.1893	0490349	63.7670	352.7876	15.0809433300001	1604
1	94869U	86249.44998124	+.000000000	+000000+0	+000000+0	-1.0	1631	
2	94869	22.9165	14.2714	0228926	59.0556	357.6440	15.6937536200001	1632
1	94871U	86249.44997576	+.000000000	+000000+0	+000000+0	-1.0	1625	
2	94871	22.7983	14.1685	0372943	65.5112	351.0913	15.3428468600001	1626
1	94871U	86249.45015143	+.000000000	+000000+0	+000000+0	-1.0	1639	
2	94871	22.8249	14.2636	0268066	65.3965	351.9043	15.5898094900001	1640
1	94871U	86249.45035625	+.000000000	+000000+0	+000000+0	-1.0	1657	
2	94871	22.9475	14.7349	0232394	359.1957	56.1761	15.9128513200001	1658
1	94872U	86249.45015809	+.000000000	+000000+0	+000000+0	-1.0	1637	
2	94872	23.4202	16.2700	0715750	350.4624	55.0395	15.2888242200001	1638
1	94872U	86249.45026856	+.000000000	+000000+0	+000000+0	-1.0	1645	
2	94872	22.8056	14.2722	0254627	61.1284	354.2291	15.6180496000001	1646
1	94872U	86249.45054419	+.000000000	+000000+0	+000000+0	-1.0	1675	
2	94872	22.7962	14.2377	0285301	64.2942	352.8479	15.5497481800001	1676
1	94874U	86249.45070142	+.000000000	+000000+0	+000000+0	-1.0	1679	
2	94874	23.5455	15.7654	0288402	94.3923	318.6060	15.7198318600001	1680
1	94874U	86249.45088087	+.000000000	+000000+0	+000000+0	-1.0	1693	
2	94874	23.7508	16.3526	0222186	42.7636	8.1404	15.6867055900001	1694
1	94874U	86249.45108902	+.000000000	+000000+0	+000000+0	-1.0	1705	
2	94874	23.7501	16.3502	0298850	40.7101	11.1175	15.5076728100001	1706
1	94874U	86249.45324960	+.000000000	+000000+0	+000000+0	-1.0	1717	
2	94874	23.7782	17.1431	0259020	34.6296	18.0762	15.6165266300001	1718
1	94874U	86249.45348578	+.000000000	+000000+0	+000000+0	-1.0	1735	
2	94874	23.6864	16.8417	0275989	56.6468	358.7549	15.5477928900001	1736
1	94877U	86249.45079995	+.000000000	+000000+0	+000000+0	-1.0	1685	
2	94877	23.1347	16.0477	0945169	60.2758	354.3590	14.0262868800001	1686
1	94877U	86249.45094032	+.000000000	+000000+0	+000000+0	-1.0	1699	
2	94877	23.1579	16.1227	0926800	59.3177	355.7829	14.0645661900001	1700
1	94878U	86249.45324602	+.000000000	+000000+0	+000000+0	-1.0	1719	
2	94878	22.9280	15.2074	0491498	55.9482	356.8742	15.0447280100001	1720
1	94878U	86249.45348035	+.000000000	+000000+0	+000000+0	-1.0	1731	
2	94878	22.9707	15.3416	0275014	63.9109	350.3765	15.5735227200001	1732
1	94878U	86249.45366320	+.000000000	+000000+0	+000000+0	-1.0	1743	
2	94878	23.0242	15.5216	0226363	46.7986	7.5069	15.6814638500001	1744
1	94878U	86249.45396414	+.000000000	+000000+0	+000000+0	-1.0	1759	
2	94878	22.9793	15.3645	0276945	59.8927	356.8699	15.5595494600001	1760
1	94878U	86249.45425740	+.000000000	+000000+0	+000000+0	-1.0	1775	
2	94878	22.8691	14.9475	0292824	84.0860	336.0273	15.5978043400001	1776
1	94878U	86249.508771156	+.000000000	+000000+0	+000000+0	0.1	4945	
2	94878	22.9635	14.3286	0269655	62.5883	30.2546	15.5746087500001	4946
1	94881U	86249.45369506	+.000000000	+000000+0	+000000+0	-1.0	1755	
2	94881	23.1690	15.5219	0607505	88.9333	327.6294	15.0473139700001	1756
1	94881U	86249.45402129	+.000000000	+000000+0	+000000+0	-1.0	1767	
2	94881	23.5169	16.5718	0277208	69.1334	345.2340	15.5913092200001	1768
1	94881U	86249.45446891	+.000000000	+000000+0	+000000+0	-1.0	1783	
2	94881	23.5515	16.6844	0158971	43.4967	12.1690	15.8545826300001	1784
1	94881U	86249.50626135	+.000000000	+000000+0	+000000+0	0.0	4947	
2	94881	23.5079	14.8575	0280471	68.5336	20.1932	15.5718890700001	4948
1	94884U	86249.45389382	+.000000000	+000000+0	+000000+0	-1.0	1757	
2	94884	22.9523	15.5296	0343754	29.6707	24.8998	15.4724099900001	1758
1	94884U	86249.45398482	+.000000000	+000000+0	+000000+0	-1.0	1769	
2	94884	22.8651	15.2110	0201044	25.8135	30.1203	15.8018080500001	1770

1	94897U		86249.45354037	+.00000000	+00000+0	+00000+0	-1.0	1835
2	94897	25.0330	18.8479	0309490	62.9122	345.5558	15.50470660000001	1836
1	94897U		86249.45395331	+.00000000	+00000+0	+00000+0	-1.0	1859
2	94897	25.1174	19.0533	0287078	47.2096	2.4509	15.52828316000001	1860
1	94897U		86249.45455143	+.00000000	+00000+0	+00000+0	-1.0	1887
2	94897	25.1079	19.0285	0311158	47.2764	5.7291	15.47042710000001	1888
1	94897U		86249.45506219	+.00000000	+00000+0	+00000+0	-1.0	1905
2	94897	25.1271	19.0848	0417470	56.3751	0.0028	15.21808070000001	1906
1	94906U		86249.45736602	+.00000000	+00000+0	+00000+0	-1.0	1923
2	94906	22.8457	15.2027	0251086	349.9114	66.3926	15.96217929000001	1924
1	94908U		86249.45734201	+.00000000	+00000+0	+00000+0	-1.0	1921
2	94908	23.0278	15.6722	0062045	312.1299	99.5283	16.24718845000001	1922
1	94908U		86249.45768622	+.00000000	+00000+0	+00000+0	-1.0	1939
2	94908	22.9922	15.5601	0410502	38.4641	14.8113	15.25769124000001	1940
1	94909U		86249.45770340	+.00000000	+00000+0	+00000+0	-1.0	2129
2	94909	22.8824	14.8289	0087257	155.6561	264.7243	16.26004390000001	2130
1	94910U		86249.45789975	+.00000000	+00000+0	+00000+0	-1.0	2135
2	94910	22.9698	15.3510	0412256	64.2597	350.6042	15.25684865000001	2136
1	94912U		86249.45775555	+.00000000	+00000+0	+00000+0	-1.0	1943
2	94912	22.9483	15.3571	0091461	66.5766	352.4185	14.13970717000001	1944
1	94912U		86249.45809903	+.00000000	+00000+0	+00000+0	-1.0	1973
2	94912	22.9458	15.3471	0360284	64.6201	355.2335	15.37085191000001	1974
1	94913U		86249.45782337	+.00000000	+00000+0	+00000+0	-1.0	1949
2	94913	22.7594	14.8495	0328986	56.4005	3.2042	15.41839034000001	1950
1	94913U		86249.45792081	+.00000000	+00000+0	+00000+0	-1.0	1955
2	94913	22.7644	14.8703	0272300	53.2404	6.7570	15.55610433000001	1956
1	94913U		86249.45801806	+.00000000	+00000+0	+00000+0	-1.0	1963
2	94913	22.8348	15.1827	0365023	50.9203	9.0588	15.33946557000001	1964
1	94914U		86249.45783246	+.00000000	+00000+0	+00000+0	-1.0	1951
2	94914	22.7582	14.8718	0320936	52.3575	3.1174	15.44148034000001	1952
1	94914U		86249.45803396	+.00000000	+00000+0	+00000+0	-1.0	1961
2	94914	22.7921	14.9922	0314266	47.7163	8.4958	15.46133135000001	1962
1	94914U		86249.45829261	+.00000000	+00000+0	+00000+0	-1.0	1977
2	94914	22.8118	15.0670	0297872	40.0755	17.1092	15.51857293000001	1978
1	94914U		86249.45853756	+.00000000	+00000+0	+00000+0	-1.0	1993
2	94914	22.7554	14.8393	0267574	49.3611	9.9722	15.56711574000001	1994
1	94914U		86249.45871284	+.00000000	+00000+0	+00000+0	-1.0	2011
2	94914	22.7832	14.9501	0376928	55.5682	4.8666	15.29846608000001	2012
1	94915U		86249.45784993	+.00000000	+00000+0	+00000+0	-1.0	1953
2	94915	23.0113	15.4781	0247088	72.8557	341.4136	15.66609738000001	1954
1	94915U		86249.45806270	+.00000000	+00000+0	+00000+0	-1.0	1967
2	94915	23.0558	15.6221	0331494	56.1405	358.4450	15.42801180000001	1968
1	94915U		86249.45824382	+.00000000	+00000+0	+00000+0	-1.0	1979
2	94915	23.0252	15.5160	0111471	59.1260	356.5808	15.95804126000001	1980
1	94915U		86249.45854704	+.00000000	+00000+0	+00000+0	-1.0	1995
2	94915	23.0087	15.4560	0479097	64.5372	353.6254	15.09069894000001	1996
1	94915U		86249.45880552	+.00000000	+00000+0	+00000+0	-1.0	2007
2	94915	23.0658	15.6763	0316374	54.8191	3.7714	15.46924879000001	2008
1	94916U		86249.45799800	+.00000000	+00000+0	+00000+0	-1.0	2159
2	94916	23.5522	16.1897	0186570	232.9745	185.7220	16.66097662000001	2160
1	94917U		86249.45808884	+.00000000	+00000+0	+00000+0	-1.0	1965
2	94917	24.9759	20.3084	1472049	227.8555	179.4374	19.92855321000001	1966
1	94918U		86249.45821113	+.00000000	+00000+0	+00000+0	-1.0	1971
2	94918	22.9230	15.3222	0263232	67.3883	345.9874	15.61299068000001	1972
1	94918U		86249.45844195	+.00000000	+00000+0	+00000+0	-1.0	1987
2	94918	22.9284	15.3392	0336076	54.6947	359.3345	15.41565151000001	1988
1	94918U		86249.45870589	+.00000000	+00000+0	+00000+0	-1.0	2005
2	94918	22.9586	15.4420	0314946	50.0205	5.0981	15.46683944000001	2006
1	94918U		86249.45886271	+.00000000	+00000+0	+00000+0	-1.0	2021
2	94918	22.9193	15.3003	0412509	50.3715	358.2984	15.23345616000001	2022
1	94918U		86249.45718799	+.00000000	+00000+0	+00000+0	-1.0	2027
2	94918	22.8746	14.4325	0329884	66.5611	352.2851	15.44436158000001	2028
1	94919U		86249.45834235	+.00000000	+00000+0	+00000+0	-1.0	1983
2	94919	23.0540	15.5775	0251989	334.1544	83.9783	16.16661578000001	1984
1	94921U		86249.45863707	+.00000000	+00000+0	+00000+0	-1.0	2619
2	94921	22.9370	15.0737	0417612	192.2651	227.1085	16.96973592000001	2620
1	94922U		86249.45862675	+.00000000	+00000+0	+00000+0	-1.0	1999
2	94922	22.5365	14.1272	0065740	137.4478	283.8023	16.22264820000001	2000
1	94927U		86249.45715111	+.00000000	+00000+0	+00000+0	-1.0	2025
2	94927	22.6407	14.0021	0282832	60.4751	355.7072	15.56007377000001	2026
1	94927U		86249.45742284	+.00000000	+00000+0	+00000+0	-1.0	2059
2	94927	22.6012	13.8583	0333601	70.0218	348.4579	15.46195426000001	2060

1	94928U		86249.45721664	+	.00000000	+000000+0	+000000+0	-1.0	2033
2	94928	23.1472	15.1791 0356223		42.9071	15.3108	15.3851532900001		2034
1	94929U		86249.45716807	+	.00000000	+000000+0	+000000+0	-1.0	2029
2	94929	22.7267	14.2584 0489779		28.7219	22.3593	15.1278514400001		2030
1	94929U		86249.45754096	+	.00000000	+000000+0	+000000+0	-1.0	2063
2	94929	22.6449	13.9875 0282641		39.5633	15.3365	15.5526034100001		2064
1	94929U		86249.45775336	+	.00000000	+000000+0	+000000+0	-1.0	2081
2	94929	22.7380	14.3287 1424544		52.1127	3.5180	12.8766973300001		2082
1	94930U		86249.45725178	+	.00000000	+000000+0	+000000+0	-1.0	2035
2	94930	24.7254	19.3233 0947546		56.5559	353.5289	14.0089720700001		2036
1	94930U		86249.45752380	+	.00000000	+000000+0	+000000+0	-1.0	2057
2	94930	24.7196	19.3081 0894854		58.9631	352.8420	14.1436505300001		2058
1	94930U		86249.45770013	+	.00000000	+000000+0	+000000+0	-1.0	2079
2	94930	24.8353	19.6287 0729885		48.0114	2.6952	14.5052490000001		2080
1	94930U		86249.45817386	+	.00000000	+000000+0	+000000+0	-1.0	2117
2	94930	24.6211	19.0081 1045152		62.5569	353.6045	13.8119663200001		2118
1	94931U		86249.45733478	+	.00000000	+000000+0	+000000+0	-1.0	2039
2	94931	22.7086	14.1250 0387918		52.7772	2.4396	15.2860527100001		2040
1	94931U		86249.45751266	+	.00000000	+000000+0	+000000+0	-1.0	2055
2	94931	22.6755	14.0075 0389203		58.5209	358.2088	15.2055605900001		2056
1	94931U		86249.45771454	+	.00000000	+000000+0	+000000+0	-1.0	2075
2	94931	22.6825	14.0336 0325528		60.7877	357.1591	15.4395768900001		2076
1	94931U		86249.45793113	+	.00000000	+000000+0	+000000+0	-1.0	2093
2	94931	22.6595	13.9423 0278641		62.6827	356.6304	15.5533904800001		2094
1	94931U		86249.45815613	+	.00000000	+000000+0	+000000+0	-1.0	2111
2	94931	22.7548	14.3376 0359452		46.3882	12.7546	15.3738194900001		2112
1	94932U		86249.45730767	+	.00000000	+000000+0	+000000+0	-1.0	2041
2	94932	22.9748	14.5428 0222037		61.4160	359.2848	15.6902656100001		2042
1	94933U		86249.45746437	+	.00000000	+000000+0	+000000+0	-1.0	2047
2	94933	23.8244	16.6187 0244229		11.5270	44.6311	15.7877003500001		2048
1	94933U		86249.45760320	+	.00000000	+000000+0	+000000+0	-1.0	2071
2	94933	23.7338	16.2754 0242075		47.2062	11.5296	15.6351919600001		2072
1	94933U		86249.45774755	+	.00000000	+000000+0	+000000+0	-1.0	2087
2	94933	23.5818	15.6405 0571811		93.1471	330.9957	15.0427472000001		2088
1	94934U		86249.45744255	+	.00000000	+000000+0	+000000+0	-1.0	2049
2	94934	22.8375	14.4454 0278658		61.5944	352.4716	15.5565765100001		2050
1	94934U		86249.45762798	+	.00000000	+000000+0	+000000+0	-1.0	2065
2	94934	22.8316	14.4259 0296679		56.4866	358.3651	15.5065932700001		2066
1	94936U		86249.45745975	+	.00000000	+000000+0	+000000+0	-1.0	2053
2	94936	23.2887	15.6563 0191302		211.7527	200.9197	16.6643602800001		2054
1	94936U		86249.45775490	+	.00000000	+000000+0	+000000+0	-1.0	2077
2	94936	23.0281	14.8452 0340454		58.8609	355.8775	15.4077062500001		2078
1	94936U		86249.45802942	+	.00000000	+000000+0	+000000+0	-1.0	2103
2	94936	22.9833	14.6894 0421941		65.0034	351.9410	15.2279236900001		2104
1	94936U		86249.45830312	+	.00000000	+000000+0	+000000+0	-1.0	2125
2	94936	22.9460	14.5510 0314880		78.4505	340.7508	15.5270911400001		2126
1	94936U		86249.45856586	+	.00000000	+000000+0	+000000+0	-1.0	2145
2	94936	22.9434	14.5405 0257583		76.4946	343.8876	15.6492056300001		2146
1	94937U		86249.45767665	+	.00000000	+000000+0	+000000+0	-1.0	2069
2	94937	23.5564	16.7976 0876853		53.0535	6.0193	14.1416516800001		2070
1	94938U		86249.45771895	+	.00000000	+000000+0	+000000+0	-1.0	2073
2	94938	23.0362	14.6948 0071458		42.8885	15.7637	16.0576606900001		2074
1	94938U		86249.45787556	+	.00000000	+000000+0	+000000+0	-1.0	2091
2	94938	23.1322	15.0736 0338944		58.1108	1.2781	15.4080867700001		2092
1	94938U		86249.45800739	+	.00000000	+000000+0	+000000+0	-1.0	2113
2	94938	23.2680	15.6430 0833078		72.9108	348.9000	14.2926495100001		2114
1	94939U		86249.45781227	+	.00000000	+000000+0	+000000+0	-1.0	2085
2	94939	22.9198	14.6122 0280058		54.4471	3.2858	15.5556402800001		2086
1	94939U		86249.45795211	+	.00000000	+000000+0	+000000+0	-1.0	2095
2	94939	22.8790	14.4541 0314584		66.8044	352.5018	15.4838094600001		2096
1	94939U		86249.45824163	+	.00000000	+000000+0	+000000+0	-1.0	2121
2	94939	22.9090	14.5796 0355241		64.3550	356.4202	15.3833921800001		2122
1	94940U		86249.45789952	+	.00000000	+000000+0	+000000+0	-1.0	2089
2	94940	22.5291	13.5661 0451961		82.8208	335.1238	15.2735861800001		2090
1	94940U		86249.45818469	+	.00000000	+000000+0	+000000+0	-1.0	2115
2	94940	22.6506	13.9991 0302754		73.4769	344.4225	15.5486754600001		2116
1	94940U		86249.45857537	+	.00000000	+000000+0	+000000+0	-1.0	2143
2	94940	22.6311	13.9236 0283473		69.0072	350.8474	15.5796737600001		2144
1	94940U		86249.45892580	+	.00000000	+000000+0	+000000+0	-1.0	2171
2	94940	22.5595	13.6190 0546270		88.2086	336.1964	15.0934349800001		2172
1	94940U		86249.59440029	+	.00000000	+000000+0	+000000+0	0.0	4931
2	94940	22.6203	12.9107 0347875		75.0652	22.4107	15.4395181500001		4932

1	94941U		86249.45885765	+	.00000000	+	.00000000	+	.00000000	-1.0	2107
2	94941	23.5241	15.8882	0507089	47.9251	2.9709	15.0036640	4000001			2108
1	94941U		86249.45866507	+	.00000000	+	.00000000	+	.00000000	-1.0	2147
2	94941	23.5863	16.0705	0352825	52.0802	2.3897	15.3710781	4000001			2148
1	94942U		86249.45803088	+	.00000000	+	.00000000	+	.00000000	-1.0	2101
2	94942	22.5102	13.5341	0311196	87.7554	331.2048	15.5961237	5000001			2102
1	94942U		86249.45824054	+	.00000000	+	.00000000	+	.00000000	-1.0	2123
2	94942	22.5609	13.7266	0319442	75.7221	343.6044	15.5129138	8000001			2124
1	94943U		86249.45820266	+	.00000000	+	.00000000	+	.00000000	-1.0	2119
2	94943	23.3999	15.5541	0448614	125.8116	290.4108	15.9170506	0000001			2120
1	94943U		86249.45854886	+	.00000000	+	.00000000	+	.00000000	-1.0	2141
2	94943	23.5413	15.9705	0357713	71.8572	342.4401	15.4227180	6000001			2142
1	94943U		86249.45887175	+	.00000000	+	.00000000	+	.00000000	-1.0	2163
2	94943	23.5423	15.9735	0359354	70.9578	345.0746	15.4148017	7000001			2164
1	94943U		86249.46106899	+	.00000000	+	.00000000	+	.00000000	-1.0	2173
2	94943	23.6029	16.8862	0302549	59.2419	357.1198	15.5191102	2000001			2174
1	94943U		86249.46132546	+	.00000000	+	.00000000	+	.00000000	-1.0	2217
2	94943	23.5825	16.8164	0349008	64.5663	353.6707	15.4181930	7000001			2218
1	94944U		86249.45848702	+	.00000000	+	.00000000	+	.00000000	-1.0	2131
2	94944	22.6116	13.7827	0289607	81.2810	338.5295	15.6076873	6000001			2132
1	94944U		86249.45865678	+	.00000000	+	.00000000	+	.00000000	-1.0	2149
2	94944	22.6871	14.0825	0399940	70.2351	349.9088	15.3095792	9000001			2150
1	94944U		86249.45889691	+	.00000000	+	.00000000	+	.00000000	-1.0	2167
2	94944	22.6916	14.1017	0345138	70.2017	351.1443	15.4384979	2000001			2168
1	94945U		86249.45852072	+	.00000000	+	.00000000	+	.00000000	-1.0	2137
2	94945	22.9063	15.3518	0953810	54.6384	2.2767	13.9276495	8000001			2138
1	94945U		86249.45875865	+	.00000000	+	.00000000	+	.00000000	-1.0	2157
2	94945	23.0548	15.9057	0931985	43.4536	12.3180	14.0156812	9000001			2158
1	94945U		86249.46097482	+	.00000000	+	.00000000	+	.00000000	-1.0	2169
2	94945	23.0394	16.5489	0912916	43.6962	13.5428	14.0575253	6000001			2170
1	94945U		86249.46121640	+	.00000000	+	.00000000	+	.00000000	-1.0	2207
2	94945	23.0359	16.5341	0954877	47.2084	11.7469	13.9366338	9000001			2208
1	94945U		86249.46137429	+	.00000000	+	.00000000	+	.00000000	-1.0	2627
2	94945	22.8085	15.4802	1683407	85.1658	344.6658	12.4700891	4000001			2628
1	94946U		86249.45849898	+	.00000000	+	.00000000	+	.00000000	-1.0	2133
2	94946	22.7605	14.1574	0299829	62.3099	357.9824	15.5056370	2000001			2134
1	94946U		86249.45868372	+	.00000000	+	.00000000	+	.00000000	-1.0	2155
2	94946	22.8122	14.3751	0322817	54.5234	6.1292	15.4507785	3000001			2156
1	94947U		86249.45852358	+	.00000000	+	.00000000	+	.00000000	-1.0	2139
2	94947	23.0874	15.0364	0283793	46.9003	5.2678	15.5348549	9000001			2140
1	94947U		86249.46107381	+	.00000000	+	.00000000	+	.00000000	-1.0	2175
2	94947	23.0379	15.5853	0339367	49.4370	6.2865	15.4003667	7000001			2176
1	94947U		86249.46141768	+	.00000000	+	.00000000	+	.00000000	-1.0	2625
2	94947	23.1503	16.0078	0516691	37.6116	10.2588	15.0196340	4000001			2626
1	94950U		86249.45887969	+	.00000000	+	.00000000	+	.00000000	-1.0	2793
2	94950	22.3700	13.0535	0391879	139.4319	201.6261	16.1157305	5000001			2794
1	94951U		86249.45890395	+	.00000000	+	.00000000	+	.00000000	-1.0	2165
2	94951	22.8109	14.2784	0318670	84.4779	330.4596	15.5688591	6000001			2166
1	94951U		86249.46125012	+	.00000000	+	.00000000	+	.00000000	-1.0	2213
2	94951	22.8999	15.2702	0347119	56.1897	359.0300	15.3876050	3000001			2214
1	94951U		86249.46148215	+	.00000000	+	.00000000	+	.00000000	-1.0	2633
2	94951	22.9048	15.2074	0334120	55.4324	1.0076	15.4183963	9000001			2634
1	94951U		86249.46172880	+	.00000000	+	.00000000	+	.00000000	-1.0	2655
2	94951	22.8973	15.2590	0269069	51.8464	5.8231	15.5756038	6000001			2656
1	94951U		86249.46195704	+	.00000000	+	.00000000	+	.00000000	-1.0	2671
2	94951	22.8512	15.0754	0408957	65.6489	354.3643	15.2481147	5000001			2672
1	94952U		86249.46130579	+	.00000000	+	.00000000	+	.00000000	-1.0	2621
2	94952	22.7230	14.8936	0418707	50.4174	9.3458	15.2073820	0000001			2622
1	94952U		86249.46150828	+	.00000000	+	.00000000	+	.00000000	-1.0	2647
2	94952	22.6903	14.7475	0250451	30.0539	30.0454	15.6693663	5000001			2648
1	94953U		86249.46109173	+	.00000000	+	.00000000	+	.00000000	-1.0	2177
2	94953	23.7041	17.2310	0450740	29.4479	19.6108	15.1989878	6000001			2178
1	94953U		86249.46152486	+	.00000000	+	.00000000	+	.00000000	-1.0	2639
2	94953	23.4483	16.4779	0361762	69.9283	345.3183	15.4008433	6000001			2640
1	94953U		86249.46213243	+	.00000000	+	.00000000	+	.00000000	-1.0	2675
2	94953	23.4691	16.5448	0328725	66.4288	351.8225	15.4643078	1000001			2676
1	94953U		86249.46247035	+	.00000000	+	.00000000	+	.00000000	-1.0	2709
2	94953	23.4752	16.5672	0387867	64.4530	355.5972	15.3198704	5000001			2710
1	94955U		86249.46116208	+	.00000000	+	.00000000	+	.00000000	-1.0	2181
2	94955	23.3686	16.6943	0529279	30.5033	25.0063	15.0750709	5000001			2182
1	94955U		86249.46141362	+	.00000000	+	.00000000	+	.00000000	-1.0	2635
2	94955	23.1797	15.9580	0385689	57.9252	2.2932	15.3003836	2000001			2636

1	94957U		86249.46119620	+.00000000	+000000+0	+000000+0	-1.0	2203
2	94957	22.7516	14.4178	0768834	85.3143	335.9861	14.59274789000001	2204
1	94957U		86249.46158296	+.00000000	+000000+0	+000000+0	-1.0	2649
2	94957	23.1127	15.7488	0323282	54.1141	4.0308	15.444119600001	2650
1	94958U		86249.46140817	+.00000000	+000000+0	+000000+0	-1.0	2623
2	94958	22.0915	15.1023	0056798	41.9554	16.6544	16.00310362000001	2624
1	94958U		86249.46154706	+.00000000	+000000+0	+000000+0	-1.0	2651
2	94958	22.8877	15.0872	0312313	69.4940	350.7586	15.47847668000001	2652
1	94960U		86249.46181210	+.00000000	+000000+0	+000000+0	-1.0	2657
2	94960	23.1730	16.8407	0963004	61.7068	352.7633	13.98558897000001	2658
1	94960U		86249.46209481	+.00000000	+000000+0	+000000+0	-1.0	2677
2	94960	23.1944	16.9071	0959508	59.8809	355.6330	13.98374815000001	2678
1	94960U		86249.46226201	+.00000000	+000000+0	+000000+0	-1.0	2697
2	94960	23.1882	16.8859	1068596	60.2564	356.2774	13.73390135000001	2698
1	94962U		86249.46185581	+.00000000	+000000+0	+000000+0	-1.0	2659
2	94962	23.1664	16.0664	0907824	72.8173	350.5487	14.11194017000001	2660
1	94963U		86249.46201001	+.00000000	+000000+0	+000000+0	-1.0	2679
2	94963	22.9488	15.4089	0328952	66.7362	347.1090	15.45763458000001	2680
1	94963U		86249.46247584	+.00000000	+000000+0	+000000+0	-1.0	2711
2	94963	22.9817	15.5120	0334947	53.6884	1.8256	15.41640718000001	2712
1	94964U		86249.46202864	+.00000000	+000000+0	+000000+0	-1.0	2673
2	94964	22.5240	14.1353	0758058	69.8073	348.8806	14.47458362000001	2674
1	94964U		86249.46234570	+.00000000	+000000+0	+000000+0	-1.0	2699
2	94964	22.7891	15.1101	0277024	41.6806	15.2396	15.58149951000001	2700
1	94967U		86249.46243530	+.00000000	+000000+0	+000000+0	-1.0	2703
2	94967	22.8344	15.2789	0442344	33.1582	24.9448	15.22859384000001	2704
1	94967U		86249.46276734	+.00000000	+000000+0	+000000+0	-1.0	2729
2	94967	22.7419	14.8818	0339245	45.3965	16.1565	15.40080838000001	2730
1	94968U		86249.46243403	+.00000000	+000000+0	+000000+0	-1.0	2705
2	94968	22.6702	15.2571	1657973	63.3303	353.0607	12.41983873000001	2706
1	94968U		86249.46284481	+.00000000	+000000+0	+000000+0	-1.0	2727
2	94968	23.1689	16.8444	0924341	58.1797	356.9606	14.05002591000001	2728
1	94971U		86249.46260065	+.00000000	+000000+0	+000000+0	-1.0	2717
2	94971	22.4569	13.8082	0605897	87.2662	333.8511	14.95139041000001	2718
1	94972U		86249.46266133	+.00000000	+000000+0	+000000+0	-1.0	2721
2	94972	22.4493	13.8135	0563584	96.6693	321.8823	15.20623806000001	2722
1	94972U		86249.46104387	+.00000000	+000000+0	+000000+0	-1.0	2741
2	94972	22.8158	14.3358	0313560	60.4734	355.0338	15.47035340000001	2742
1	94973U		86249.46279384	+.00000000	+000000+0	+000000+0	-1.0	2725
2	94973	23.0297	15.6341	0423435	47.3332	10.1698	15.21050267000001	2726
1	94975U		86249.46113351	+.00000000	+000000+0	+000000+0	-1.0	2743
2	94975	23.1506	15.1320	0271572	41.9848	18.0495	15.59891495000001	2744
1	94975U		86249.46129561	+.00000000	+000000+0	+000000+0	-1.0	2775
2	94975	23.1335	15.0578	0324138	58.7402	3.1084	15.44438716000001	2776
1	94976U		86249.46121201	+.00000000	+000000+0	+000000+0	-1.0	2749
2	94976	22.6522	13.8586	0512713	65.5309	351.1480	15.01273834000001	2750
1	94976U		86249.46163504	+.00000000	+000000+0	+000000+0	-1.0	2791
2	94976	22.7869	14.3365	0322500	53.0040	4.4649	15.44417133000001	2792
1	94976U		86249.46210676	+.00000000	+000000+0	+000000+0	-1.0	2831
2	94976	22.7776	14.2996	0320810	49.7608	10.1401	15.43307550000001	2832
1	94978U		86249.46127245	+.00000000	+000000+0	+000000+0	-1.0	2759
2	94978	22.8233	13.7300	0602861	99.6676	327.0790	15.04997711000001	2760
1	94978U		86249.46144601	+.00000000	+000000+0	+000000+0	-1.0	2779
2	94978	23.1108	15.0352	0344943	53.4980	8.4546	15.38881699000001	2780
1	94979U		86249.46138400	+.00000000	+000000+0	+000000+0	-1.0	2765
2	94979	22.2810	12.9584	0525695	93.8004	325.4253	15.25380963000001	2766
1	94979U		86249.46164861	+.00000000	+000000+0	+000000+0	-1.0	2795
2	94979	22.4280	13.4861	0424646	80.0400	338.5439	15.32887026000001	2796
1	94979U		86249.46186249	+.00000000	+000000+0	+000000+0	-1.0	2813
2	94979	22.4091	13.4131	0359345	91.5013	328.7660	15.55390402000001	2814
1	94980U		86249.46136803	+.00000000	+000000+0	+000000+0	-1.0	2767
2	94980	23.2226	15.6840	0523882	323.2664	90.8379	16.25899237000001	2768
1	94981U		86249.46141444	+.00000000	+000000+0	+000000+0	-1.0	2771
2	94981	23.0481	14.9146	0293934	65.0431	348.4510	15.53098433000001	2772
1	94981U		86249.46183636	+.00000000	+000000+0	+000000+0	-1.0	2807
2	94981	23.0500	14.9206	0399538	51.4909	3.5218	15.25919603000001	2808
1	94981U		86249.46227743	+.00000000	+000000+0	+000000+0	-1.0	2843
2	94981	23.0640	14.9685	0345591	51.7635	5.7028	15.38771257000001	2844
1	94982U		86249.46140188	+.00000000	+000000+0	+000000+0	-1.0	2763
2	94982	24.7579	19.3412	0768375	326.5854	75.9075	15.87006804000001	2764
1	94983U		86249.46145711	+.00000000	+000000+0	+000000+0	-1.0	2773
2	94983	22.7377	14.2877	0214580	241.3732	175.8886	16.76163435000001	2774

1	94984U		86249.46147924	+.00000000	+000000+0	+000000+0	-1.0	2777
2	94984	22.7293	14.1429	0337478	50.1755	10.8581	15.41414200000001	2778
1	94985U		86249.46159119	+.00000000	+000000+0	+000000+0	-1.0	2787
2	94985	23.0306	14.8057	0343358	70.0273	344.3999	15.42966536000001	2788
1	94985U		86249.46200852	+.00000000	+000000+0	+000000+0	-1.0	2823
2	94985	23.0867	14.9869	0393134	54.8932	0.6942	15.27344157000001	2824
1	94985U		86249.46242989	+.00000000	+000000+0	+000000+0	-1.0	2851
2	94985	23.1379	15.1634	0342739	46.7279	10.5014	15.39885740000001	2852
1	94985U		86249.46286076	+.00000000	+000000+0	+000000+0	-1.0	2879
2	94985	23.1029	15.0306	0360642	52.0575	7.9993	15.34798376000001	2880
1	94985U		86249.46522542	+.00000000	+000000+0	+000000+0	-1.0	2913
2	94985	23.1496	15.9304	0404940	48.0595	13.7128	15.25166693000001	2914
1	94986U		86249.46162840	+.00000000	+000000+0	+000000+0	-1.0	3019
2	94986	23.5554	15.9392	0320586	57.3789	356.7539	15.42751784000001	3020
1	94987U		86249.46173436	+.00000000	+000000+0	+000000+0	-1.0	2803
2	94987	22.8312	14.5202	0323800	41.5516	14.1372	15.46619015000001	2804
1	94987U		86249.46200528	+.00000000	+000000+0	+000000+0	-1.0	2825
2	94987	22.7681	14.2859	0359058	57.2235	1.1527	15.36233271000001	2826
1	94987U		86249.46223915	+.00000000	+000000+0	+000000+0	-1.0	2839
2	94987	22.7983	14.4082	0373627	52.7651	6.4707	15.33022581000001	2840
1	94987U		86249.46246110	+.00000000	+000000+0	+000000+0	-1.0	2853
2	94987	22.8020	14.4238	0318036	44.1116	15.8910	15.48192829000001	2854
1	94988U		86249.46190246	+.00000000	+000000+0	+000000+0	-1.0	2817
2	94988	23.2986	15.8564	0247686	320.7005	91.9252	16.23613216000001	2818
1	94988U		86249.46214718	+.00000000	+000000+0	+000000+0	-1.0	2833
2	94988	23.0043	14.8266	0353182	51.7661	5.7089	15.37060778000001	2834
1	94989U		86249.46195758	+.00000000	+000000+0	+000000+0	-1.0	3047
2	94989	23.1692	15.1328	0093596	185.4013	233.8869	16.50398501000001	3048
1	94990U		86249.46202196	+.00000000	+000000+0	+000000+0	-1.0	2827
2	94990	22.6907	13.8045	0680795	72.7021	345.5052	14.67002189000001	2828
1	94990U		86249.46235634	+.00000000	+000000+0	+000000+0	-1.0	2849
2	94990	23.0580	15.0995	0322907	32.8420	22.5256	15.49453222000001	2850
1	94990U		86249.46269225	+.00000000	+000000+0	+000000+0	-1.0	2871
2	94990	22.8585	14.3628	0463829	69.2358	351.1697	15.13381026000001	2872
1	94990U		86249.46509838	+.00000000	+000000+0	+000000+0	-1.0	2903
2	94990	22.9567	15.4620	0397905	55.9997	5.4156	15.27010456000001	2904
1	94990U		86249.46550908	+.00000000	+000000+0	+000000+0	-1.0	2939
2	94990	22.9335	15.3588	0353394	57.1616	6.7396	15.37523820000001	2940
1	94991U		86249.46229423	+.00000000	+000000+0	+000000+0	-1.0	2847
2	94991	23.0349	14.9836	0372848	42.3385	9.9329	15.33540707000001	2848
1	94991U		86249.46276446	+.00000000	+000000+0	+000000+0	-1.0	2875
2	94991	22.9605	14.7431	0385737	51.8479	3.9001	15.29407644000001	2876
1	94991U		86249.46517705	+.00000000	+000000+0	+000000+0	-1.0	2907
2	94991	22.9805	15.5187	0384754	48.9731	9.0306	15.29897359000001	2908
1	94991U		86249.46566553	+.00000000	+000000+0	+000000+0	-1.0	2961
2	94991	22.9908	15.5586	0390140	48.6937	11.9326	15.28661297000001	2962
1	94991U		86249.46602417	+.00000000	+000000+0	+000000+0	-1.0	2983
2	94991	22.6844	14.1761	0275400	102.6183	324.2511	15.70500823000001	2984
1	94992U		86249.46228863	+.00000000	+000000+0	+000000+0	-1.0	2845
2	94992	22.7416	14.1435	0392955	124.8523	292.8069	15.91376863000001	2846
1	94992U		86249.46265463	+.00000000	+000000+0	+000000+0	-1.0	2863
2	94992	22.8805	14.5964	0375146	60.0972	355.4684	15.33159569000001	2864
1	94992U		86249.46508350	+.00000000	+000000+0	+000000+0	-1.0	2901
2	94992	22.8462	15.1828	0376509	64.9244	353.7205	15.33926931000001	2902
1	94992U		86249.46547459	+.00000000	+000000+0	+000000+0	-1.0	2933
2	94992	22.8295	15.1182	0371555	66.7717	354.2149	15.35523107000001	2934
1	94992U		86249.46580636	+.00000000	+000000+0	+000000+0	-1.0	2973
2	94992	22.8547	15.2146	0388713	62.5713	0.3080	15.30561815000001	2974
1	94993U		86249.46249335	+.00000000	+000000+0	+000000+0	-1.0	3091
2	94993	23.9682	17.0606	0418876	38.7235	17.4065	15.26258467000001	3092
1	94994U		86249.46248075	+.00000000	+000000+0	+000000+0	-1.0	2855
2	94994	23.2339	15.2092	0351579	80.0793	338.9049	15.46270372000001	2856
1	94994U		86249.46267879	+.00000000	+000000+0	+000000+0	-1.0	2867
2	94994	23.3448	15.6142	0387938	59.9947	358.4207	15.30748050000001	2868
1	94994U		86249.46486689	+.00000000	+000000+0	+000000+0	-1.0	2885
2	94994	23.3098	16.1800	0270522	60.7293	359.1208	15.50806407000001	2886
1	94994U		86249.46503343	+.00000000	+000000+0	+000000+0	-1.0	2905
2	94994	23.4559	16.7835	0775350	65.8472	355.2480	14.40454561000001	2906
1	94994U		86249.46538991	+.00000000	+000000+0	+000000+0	-1.0	2943
2	94994	23.3369	16.2936	0518732	72.9667	350.8842	15.02972341000001	2944
1	94995U		86249.46252200	+.00000000	+000000+0	+000000+0	-1.0	2857
2	94995	22.5746	13.8148	0216909	66.7259	354.2325	15.75682577000001	2858

1	94996U		86249.46268272	+	00000000	+000000+0	+000000+0	-1.0	2869
2	94996	22.4368	13.2482	0687781	73.3816	345.3818	14.65984992000001		2870
1	94996U		86249.46288702	+	00000000	+000000+0	+000000+0	-1.0	2883
2	94996	22.6224	13.9319	0367244	69.0485	348.9523	15.37397824000001		2884
1	94996U		86249.46505591	+	00000000	+000000+0	+000000+0	-1.0	2897
2	94996	22.6681	14.8135	0405460	59.4789	358.8974	15.26390415000001		2898
1	94996U		86249.46527623	+	00000000	+000000+0	+000000+0	-1.0	2917
2	94996	22.6811	14.8660	0293207	52.5613	6.5746	15.53418817000001		2918
1	94996U		86249.46561205	+	00000000	+000000+0	+000000+0	-1.0	2955
2	94996	22.6066	14.5469	0346720	67.7711	354.4588	15.41147901000001		2956
1	94998U		86249.46268214	+	00000000	+000000+0	+000000+0	-1.0	2865
2	94998	22.8866	15.1010	2846934	55.7015	1.3685	9.83337166000001		2866
1	94999U		86249.46289017	+	00000000	+000000+0	+000000+0	-1.0	3115
2	94999	23.9694	17.2432	0290733	342.9852	66.9103	15.93145674000001		3116
1	90001U		86249.46284052	+	00000000	+000000+0	+000000+0	-1.0	2877
2	90001	22.4261	13.3173	0336642	109.3084	310.5382	15.74507621000001		2878
1	90002U		86249.46284781	+	00000000	+000000+0	+000000+0	-1.0	2881
2	90002	23.2679	15.9814	0568010	337.1506	77.3853	15.95026050000001		2882
1	90004U		86249.46494170	+	00000000	+000000+0	+000000+0	-1.0	2891
2	90004	22.8103	15.0018	0245607	84.0811	333.8859	15.70515440000001		2892
1	90005U		86249.46525149	+	00000000	+000000+0	+000000+0	-1.0	2915
2	90005	22.7637	15.7621	1003528	61.6751	353.4250	13.86702990000001		2916
1	90005U		86249.46565308	+	00000000	+000000+0	+000000+0	-1.0	2959
2	90005	23.0244	16.5944	0972070	44.3048	8.9950	13.92182957000001		2960
1	90005U		86249.46605526	+	00000000	+000000+0	+000000+0	-1.0	2993
2	90005	22.9720	16.4139	1009363	47.9155	8.1230	13.82193462000001		2994
1	90005U		86249.46644764	+	00000000	+000000+0	+000000+0	-1.0	3029
2	90005	22.9965	16.5061	0941185	44.9996	12.5519	13.99276761000001		3030
1	90005U		86249.46489338	+	00000000	+000000+0	+000000+0	-1.0	3067
2	90005	23.0104	15.8579	0918654	38.9081	19.6747	14.09624152000001		3068
1	90006U		86249.46518674	+	00000000	+000000+0	+000000+0	-1.0	2909
2	90006	22.6982	14.7596	0592521	53.1357	0.6504	14.80489833000001		2910
1	90006U		86249.46561899	+	00000000	+000000+0	+000000+0	-1.0	2953
2	90006	22.8216	15.1690	0380784	56.3666	359.7043	15.30987339000001		2954
1	90006U		86249.46595291	+	00000000	+000000+0	+000000+0	-1.0	2977
2	90006	22.7854	15.0397	0414452	61.1029	357.2935	15.23542735000001		2978
1	90006U		86249.46637672	+	00000000	+000000+0	+000000+0	-1.0	3027
2	90006	22.7766	15.0055	0344332	61.8811	358.9006	15.40319520000001		3028
1	90006U		86249.46676657	+	00000000	+000000+0	+000000+0	-1.0	3059
2	90006	22.7978	15.0951	0407724	59.4927	3.1829	15.25062744000001		3060
1	90007U		86249.46521142	+	00000000	+000000+0	+000000+0	-1.0	2911
2	90007	23.7637	17.3311	0443759	47.4825	7.2974	15.18281761000001		2912
1	90007U		86249.46538011	+	00000000	+000000+0	+000000+0	-1.0	2935
2	90007	23.6049	16.7843	0440145	74.1102	344.3013	15.24188856000001		2936
1	90007U		86249.46567694	+	00000000	+000000+0	+000000+0	-1.0	2967
2	90007	23.6475	16.9414	0334450	65.8600	353.2019	15.45834137000001		2968
1	90008U		86249.46527184	+	00000000	+000000+0	+000000+0	-1.0	2919
2	90008	22.8741	15.0984	0669209	57.6844	358.9523	14.62228991000001		2920
1	90008U		86249.46551973	+	00000000	+000000+0	+000000+0	-1.0	2945
2	90008	22.9824	15.4907	0412199	52.5819	4.5987	15.22936524000001		2946
1	90011U		86249.46561170	+	00000000	+000000+0	+000000+0	-1.0	2949
2	90011	23.1147	15.9377	0126742	93.4652	320.1996	15.99606442000001		2950
1	90012U		86249.46587063	+	00000000	+000000+0	+000000+0	-1.0	3239
2	90012	22.7689	14.9291	0253047	93.2940	324.0716	15.78106862000001		3240
1	90014U		86249.46606206	+	00000000	+000000+0	+000000+0	-1.0	2995
2	90014	22.9173	15.4429	0476513	58.0537	4.4668	15.00595739000001		2996
1	90015U		86249.46610693	+	00000000	+000000+0	+000000+0	-1.0	3001
2	90015	22.9916	15.2422	0071180	67.6829	351.1491	14.19725369000001		3002
1	90017U		86249.46625878	+	00000000	+000000+0	+000000+0	-1.0	3017
2	90017	22.7983	15.0915	0265322	40.3141	19.7573	15.62757294000001		3018
1	90018U		86249.46632641	+	00000000	+000000+0	+000000+0	-1.0	3021
2	90018	22.8533	15.0622	00809264	50.5025	4.1344	14.11124430000001		3022
1	90019U		86249.46651418	+	00000000	+000000+0	+000000+0	-1.0	3333
2	90019	22.9814	15.9590	0603680	31.4941	25.0563	14.92251917000001		3334
1	90020U		86249.46650608	+	00000000	+000000+0	+000000+0	-1.0	3033
2	90020	24.0489	17.9466	0710942	28.1212	20.5283	14.63713380000001		3034
1	90020U		86249.46495514	+	00000000	+000000+0	+000000+0	-1.0	3075
2	90020	23.9018	16.8046	0406404	53.6390	0.8305	15.25232463000001		3076
1	90021U		86249.46654620	+	00000000	+000000+0	+000000+0	-1.0	3043
2	90021	22.8062	15.2182	0384296	343.4548	75.3491	15.96911334000001		3044
1	90022U		86249.46653576	+	00000000	+000000+0	+000000+0	-1.0	3037
2	90022	22.8727	14.9375	0376860	64.8981	359.2679	15.29084441000001		3038

1	90024U		86249.46491942	+	00000000	+000000+0	+000000+0	-1.0	3375
2	90024	23.8589	17.7439	0798518	341.8341	69.4374	15.63229588000001		3376
1	90025U		86249.46673344	+	00000000	+000000+0	+000000+0	-1.0	3057
2	90025	23.2658	16.6267	0729802	58.0138	3.9641	14.49396906000001		3058
1	90027U		86249.46489223	+	00000000	+000000+0	+000000+0	-1.0	3065
2	90027	23.2278	15.4389	0653170	63.7647	357.2877	14.68109612000001		3066
1	90029U		86249.46508687	+	00000000	+000000+0	+000000+0	-1.0	3085
2	90029	22.6275	13.7777	0450722	109.2687	309.5536	15.58321420000001		3086
1	90030U		86249.46518797	+	00000000	+000000+0	+000000+0	-1.0	3093
2	90030	22.9832	14.8321	0989630	71.6577	352.3177	13.89472186000001		3094
1	90031U		86249.46531377	+	00000000	+000000+0	+000000+0	-1.0	3421
2	90031	23.2063	15.5263	0259718	28.1679	24.0847	15.64303328000001		3422
1	90033U		86249.46541248	+	00000000	+000000+0	+000000+0	-1.0	3099
2	90033	22.3704	12.9721	0643680	85.8838	336.0026	14.86221027000001		3100
1	90034U		86249.46544840	+	00000000	+000000+0	+000000+0	-1.0	3105
2	90034	23.2197	15.1944	0565891	57.7209	359.0657	14.86525744000001		3106
1	90034U		86249.46577821	+	00000000	+000000+0	+000000+0	-1.0	3133
2	90034	23.4380	15.9738	0409327	32.8885	23.0833	15.29807984000001		3134
1	90038U		86249.46578386	+	00000000	+000000+0	+000000+0	-1.0	3137
2	90038	23.9518	17.0104	0335958	35.3537	22.3984	15.48019265000001		3138
1	90038U		86249.46600998	+	00000000	+000000+0	+000000+0	-1.0	3155
2	90038	23.9557	17.0251	0378031	42.8248	16.5013	15.35146175000001		3156
1	90039U		86249.46571208	+	00000000	+000000+0	+000000+0	-1.0	3129
2	90039	22.8100	14.3205	0262831	73.7682	346.0114	15.70464242000001		3130
1	90040U		86249.46574902	+	00000000	+000000+0	+000000+0	-1.0	3131
2	90040	22.9354	14.7725	0405198	57.8390	356.1019	15.25711638000001		3132
1	90040U		86249.46610345	+	00000000	+000000+0	+000000+0	-1.0	3159
2	90040	22.8006	14.3246	0311915	101.8000	316.8182	15.72356463000001		3160
1	90040U		86249.46651514	+	00000000	+000000+0	+000000+0	-1.0	3211
2	90040	22.9335	14.7940	0572544	46.4145	10.4752	14.88011669000001		3212
1	90040U		86249.46886466	+	00000000	+000000+0	+000000+0	-1.0	3269
2	90040	22.8350	15.1181	0449873	70.8052	350.9357	15.18375823000001		3270
1	90040U		86249.46925693	+	00000000	+000000+0	+000000+0	-1.0	3339
2	90040	22.9126	15.4467	0429193	58.5443	4.0107	15.21189891000001		3340
1	90042U		86249.46589725	+	00000000	+000000+0	+000000+0	-1.0	3145
2	90042	22.8878	14.7077	0583255	49.2821	8.3549	14.84702672000001		3146
1	90042U		86249.46618923	+	00000000	+000000+0	+000000+0	-1.0	3173
2	90042	22.8175	14.4263	0427060	62.2987	358.5101	15.20973665000001		3174
1	90042U		86249.46644303	+	00000000	+000000+0	+000000+0	-1.0	3203
2	90042	22.8580	14.6041	0405468	54.1771	7.2295	15.26423280000001		3204
1	90042U		86249.46666787	+	00000000	+000000+0	+000000+0	-1.0	3237
2	90042	22.8102	14.3804	0333114	57.0892	6.0517	15.43265853000001		3238
1	90042U		86249.46885315	+	00000000	+000000+0	+000000+0	-1.0	3281
2	90042	22.7959	15.0135	0532265	76.4910	349.7029	14.98757207000001		3282
1	90043U		86249.46591567	+	00000000	+000000+0	+000000+0	-1.0	3149
2	90043	22.5821	13.8786	0412915	75.6453	341.1500	15.30550847000001		3150
1	90043U		86249.46625912	+	00000000	+000000+0	+000000+0	-1.0	3183
2	90043	22.5230	13.6685	0467752	78.7544	340.5695	15.20346152000001		3184
1	90043U		86249.46664150	+	00000000	+000000+0	+000000+0	-1.0	3219
2	90043	22.6269	14.0590	0406309	64.0890	355.6384	15.27784071000001		3220
1	90043U		86249.46894330	+	00000000	+000000+0	+000000+0	-1.0	3285
2	90043	22.6032	14.6675	0382722	67.2412	354.7033	15.34031030000001		3286
1	90043U		86249.46932064	+	00000000	+000000+0	+000000+0	-1.0	3351
2	90043	22.6133	14.7119	0459505	67.0943	356.9471	15.15809877000001		3352
1	90044U		86249.46594096	+	00000000	+000000+0	+000000+0	-1.0	3147
2	90044	22.8598	14.2349	0265223	57.0500	7.4046	15.59075650000001		3148
1	90045U		86249.46613892	+	00000000	+000000+0	+000000+0	-1.0	3165
2	90045	24.2896	18.5709	0695417	312.8680	92.9102	16.39286771000001		3166
1	90047U		86249.46624437	+	00000000	+000000+0	+000000+0	-1.0	3461
2	90047	22.7130	14.3897	0627200	60.1760	1.8790	14.74420733000001		3462
1	90048U		86249.46626328	+	00000000	+000000+0	+000000+0	-1.0	3185
2	90048	23.0414	14.9139	0377142	90.1225	325.5353	15.50019857000001		3186
1	90048U		86249.46659998	+	00000000	+000000+0	+000000+0	-1.0	3221
2	90048	23.1792	15.3526	0329027	61.6941	353.4636	15.44359229000001		3222
1	90049U		86249.46629025	+	00000000	+000000+0	+000000+0	-1.0	3187
2	90049	22.8867	15.4446	0958468	64.5304	352.8185	13.99904679000001		3188
1	90051U		86249.46663736	+	00000000	+000000+0	+000000+0	-1.0	3223
2	90051	23.1673	14.8290	0293014	68.7484	355.5815	15.50839420000001		3224
1	90051U		86249.46670704	+	00000000	+000000+0	+000000+0	-1.0	3265
2	90051	23.5262	16.5121	0579671	44.7619	16.2002	14.87114784000001		3266
1	90052U		86249.46665363	+	00000000	+000000+0	+000000+0	-1.0	3227
2	90052	23.2255	16.0268	1307791	73.8689	344.5581	13.35681196000001		3228

1	90053U		86249.46667965	+.000000000	+000000+0	+000000+0	-1.0	3235
2	90053	22.8282	14.4158 0421609	70.5720	345.1933	15.25819805000001		3236
1	90053U		86249.46901671	+.000000000	+000000+0	+000000+0	-1.0	3303
2	90053	22.8304	15.1282 0426164	68.8324	348.9070	15.23952606000001		3304
1	90053U		86249.46947505	+.000000000	+000000+0	+000000+0	-1.0	3371
2	90053	22.9493	15.5581 0315177	49.5411	8.9359	15.47927594000001		3372
1	90053U		86249.46986415	+.000000000	+000000+0	+000000+0	-1.0	3413
2	90053	22.8201	15.0394 0532323	68.2732	354.2717	14.97528622000001		3414
1	90053U		86249.47020184	+.000000000	+000000+0	+000000+0	-1.0	3443
2	90053	22.8651	15.2210 0539995	68.2689	355.9535	14.95787603000001		3444
1	90054U		86249.46679656	+.000000000	+000000+0	+000000+0	-1.0	3521
2	90054	23.1624	17.2707 1506562	36.4204	12.1680	12.76688309000001		3522
1	90055U		86249.46895958	+.000000000	+000000+0	+000000+0	-1.0	3289
2	90055	22.6418	14.5056 0289828	206.7113	214.9345	16.83300404000001		3290
1	90055U		86249.46913982	+.000000000	+000000+0	+000000+0	-1.0	3315
2	90055	22.7733	15.0511 0428845	58.7784	1.5081	15.20088803000001		3316
1	90055U		86249.46941355	+.000000000	+000000+0	+000000+0	-1.0	3357
2	90055	22.7518	14.9562 0413735	63.3811	358.8606	15.23880761000001		3358
1	90056U		86249.46916000	+.000000000	+000000+0	+000000+0	-1.0	3321
2	90056	23.2558	15.5126 0520978	272.1217	148.3896	17.33228541000001		3322
1	90057U		86249.46932013	+.000000000	+000000+0	+000000+0	-1.0	3353
2	90057	23.0414	15.5798 0042360	157.5496	262.6375	16.25915617000001		3354
1	90057U		86249.46954667	+.000000000	+000000+0	+000000+0	-1.0	3383
2	90057	23.0537	15.6304 0420860	68.1901	353.4358	15.24242581000001		3384
1	90057U		86249.46976692	+.000000000	+000000+0	+000000+0	-1.0	3407
2	90057	23.1125	15.8900 0487887	61.5560	0.5181	15.07409701000001		3408
1	90057U		86249.47005704	+.000000000	+000000+0	+000000+0	-1.0	3431
2	90057	23.1822	16.2101 0477038	57.1022	5.8727	15.10211042000001		3432
1	90058U		86249.46953975	+.000000000	+000000+0	+000000+0	-1.0	3581
2	90058	22.3649	13.8825 0707428	65.2919	353.1648	14.56906662000001		3582
1	90059U		86249.46971021	+.000000000	+000000+0	+000000+0	-1.0	3593
2	90059	22.2366	12.4898 0965613	113.9403	318.4925	14.66649529000001		3594
1	90060U		86249.46977139	+.000000000	+000000+0	+000000+0	-1.0	3397
2	90060	22.7408	14.7967 0724629	60.3880	356.7645	14.50873752000001		3398
1	90061U		86249.46976876	+.000000000	+000000+0	+000000+0	-1.0	3399
2	90061	23.0975	16.1259 0211561	12.3259	40.7187	15.83373665000001		3400
1	90062U		86249.47000952	+.000000000	+000000+0	+000000+0	-1.0	3425
2	90062	23.2054	15.9668 0469932	66.9294	349.3723	15.13065004000001		3426
1	90063U		86249.47010581	+.000000000	+000000+0	+000000+0	-1.0	3433
2	90063	24.0660	18.6463 1165081	51.3875	2.1371	13.45963832000001		3434
1	90063U		86249.47045658	+.000000000	+000000+0	+000000+0	-1.0	3447
2	90063	24.2397	19.1938 0990729	43.4855	10.0039	13.88009657000001		3448
1	90063U		86249.46885734	+.000000000	+000000+0	+000000+0	-1.0	3459
2	90063	24.1984	18.3512 1066232	46.7815	9.0419	13.69144099400001		3460
1	90063U		86249.46923960	+.000000000	+000000+0	+000000+0	-1.0	3487
2	90063	24.1848	18.3017 0982193	46.4683	11.4014	13.88503333000001		3488
1	90063U		86249.46966036	+.000000000	+000000+0	+000000+0	-1.0	3531
2	90063	24.2161	18.4252 1023509	45.2735	14.2762	13.79897520000001		3532
1	90064U		86249.47002565	+.000000000	+000000+0	+000000+0	-1.0	3427
2	90064	23.2491	17.2207 0691289	45.0236	6.7257	14.56037577000001		3428
1	90065U		86249.47015273	+.000000000	+000000+0	+000000+0	-1.0	3435
2	90065	22.4443	13.5288 0776721	113.5420	312.4000	15.10610158000001		3436
1	90066U		86249.47017953	+.000000000	+000000+0	+000000+0	-1.0	3439
2	90066	22.2090	13.1805 1107854	59.8885	357.0518	13.61947666000001		3440
1	90067U		86249.47022060	+.000000000	+000000+0	+000000+0	-1.0	3445
2	90067	23.3192	15.9436 0665080	112.5234	307.9072	15.36038271000001		3446
1	90067U		86249.47058609	+.000000000	+000000+0	+000000+0	-1.0	3449
2	90067	23.6610	17.0422 0371960	83.0399	334.1679	15.46564695000001		3450
1	90068U		86249.47057761	+.000000000	+000000+0	+000000+0	-1.0	3451
2	90068	23.5729	17.3714 0424949	330.3237	84.2034	16.16444836000001		3452
1	90069U		86249.47060839	+.000000000	+000000+0	+000000+0	-1.0	3453
2	90069	23.0704	15.8525 0280393	146.1032	270.5120	16.25156077000001		3454
1	90070U		86249.46881881	+.000000000	+000000+0	+000000+0	-1.0	3457
2	90070	22.7403	13.9614 0080951	97.3887	325.8164	16.08412609000001		3458
1	90070U		86249.46896200	+.000000000	+000000+0	+000000+0	-1.0	3465
2	90070	22.8859	14.6335 0418750	60.2480	2.4749	15.23392054000001		3466
1	90070U		86249.46911447	+.000000000	+000000+0	+000000+0	-1.0	3485
2	90070	23.1060	15.6948 0801241	60.9763	1.6320	14.33025236000001		3486
1	90071U		86249.46916010	+.000000000	+000000+0	+000000+0	-1.0	3689
2	90071	23.3596	16.0517 0513307	62.5122	351.9524	15.00747435000001		3690
1	90073U		86249.46916593	+.000000000	+000000+0	+000000+0	-1.0	3467
2	90073	22.7465	13.2993 1057833	280.4665	138.4898	18.23553356000001		3468

1	90074U		86249.46916767	+.00000000	+000000+0	+000000+0	-1.0	3469
2	90074	23.3449	16.5938	0811108	15.3312	37.2696	14.76919679000001	3470
1	90075U		86249.46917667	+.00000000	+000000+0	+000000+0	-1.0	3471
2	90075	23.0612	15.0667	0963376	65.6659	356.9523	13.93027362000001	3472
1	90075U		86249.46937794	+.00000000	+000000+0	+000000+0	-1.0	3513
2	90075	23.0471	15.0030	0499507	56.9614	5.6197	15.00986712000001	3514
1	90075U		86249.46957104	+.00000000	+000000+0	+000000+0	-1.0	3533
2	90075	22.9022	14.2710	0191413	15.8309	47.5037	15.88570805000001	3534
1	90076U		86249.46932703	+.00000000	+000000+0	+000000+0	-1.0	3499
2	90076	22.7933	13.7368	0121830	199.3939	224.9833	16.42901411000001	3500
1	90076U		86249.46959844	+.00000000	+000000+0	+000000+0	-1.0	3535
2	90076	23.0412	14.9001	0369044	50.6668	12.3608	15.33524956000001	3536
1	90077U		86249.46937171	+.00000000	+000000+0	+000000+0	-1.0	3501
2	90077	22.3004	12.3078	0868999	108.1005	315.9144	14.85808553000001	3502
1	90078U		86249.46940379	+.00000000	+000000+0	+000000+0	-1.0	3505
2	90078	23.9764	17.5959	0495107	1.8891	52.1907	15.55442099000001	3506
1	90078U		86249.46955874	+.00000000	+000000+0	+000000+0	-1.0	3527
2	90078	23.6473	16.3029	0440110	69.0550	352.4994	15.23080195000001	3528
1	90078U		86249.46977656	+.00000000	+000000+0	+000000+0	-1.0	3545
2	90078	23.6677	16.3925	0530203	70.8706	352.1097	15.02432515000001	3546
1	90079U		86249.46945055	+.00000000	+000000+0	+000000+0	-1.0	3517
2	90079	22.1176	12.4353	0849546	56.2376	0.8575	14.21811684000001	3518
1	90079U		86249.47010616	+.00000000	+000000+0	+000000+0	-1.0	3565
2	90079	22.3793	13.4286	0432033	59.4099	0.7441	15.20328990000001	3566
1	90085U		86249.46996212	+.00000000	+000000+0	+000000+0	-1.0	3551
2	90085	22.5268	13.8265	0737416	167.4320	255.7571	16.84504223000001	3552
1	90087U		86249.47010013	+.00000000	+000000+0	+000000+0	-1.0	3567
2	90087	22.5972	13.9955	0361294	86.4266	335.8689	15.53523564000001	3568
1	90087U		86249.47034460	+.00000000	+000000+0	+000000+0	-1.0	3583
2	90087	22.5527	13.8016	0484234	87.9959	336.5299	15.28040685000001	3584
1	90087U		86249.47043736	+.00000000	+000000+0	+000000+0	-1.0	3601
2	90087	22.7148	14.5748	0480861	54.5023	6.8331	15.18644799000001	3602
1	90087U		86249.47270745	+.00000000	+000000+0	+000000+0	-1.0	3617
2	90087	22.5588	14.5183	0536432	88.4389	338.5991	15.16380233000001	3618
1	90088U		86249.47019512	+.00000000	+000000+0	+000000+0	-1.0	3573
2	90088	23.1175	15.4587	0401047	34.4986	26.8276	15.17230075000001	3574
1	90088U		86249.47041670	+.00000000	+000000+0	+000000+0	-1.0	3591
2	90088	22.9846	14.8013	0387820	53.1944	11.7301	15.28536348000001	3592
1	90089U		86249.47025794	+.00000000	+000000+0	+000000+0	-1.0	3579
2	90089	22.8688	14.6612	0342007	73.2472	343.0664	15.45454404000001	3580
1	90089U		86249.47279866	+.00000000	+000000+0	+000000+0	-1.0	3621
2	90089	22.0283	15.2242	0450053	62.8048	356.3205	15.16223983000001	3622
1	90089U		86249.47320212	+.00000000	+000000+0	+000000+0	-1.0	3641
2	90089	22.8363	15.2554	0444131	61.6973	359.5043	15.17636194000001	3642
1	90089U		86249.47456790	+.00000000	+000000+0	+000000+0	-1.0	3711
2	90089	22.8182	15.1737	0445738	63.7401	5.1684	15.17431353000001	3712
1	90091U		86249.47037018	+.00000000	+000000+0	+000000+0	-1.0	3585
2	90091	22.7836	14.2518	0360653	61.1370	4.1856	15.38360907000001	3586
1	90092U		86249.47036957	+.00000000	+000000+0	+000000+0	-1.0	3587
2	90092	23.0208	14.8499	0392848	70.7855	345.2117	15.31249622000001	3588
1	90092U		86249.47204989	+.00000000	+000000+0	+000000+0	-1.0	3623
2	90092	23.1258	15.9111	0425701	49.1798	7.7337	15.19556233000001	3624
1	90092U		86249.47322559	+.00000000	+000000+0	+000000+0	-1.0	3649
2	90092	23.0202	15.5141	0609881	60.1243	0.1091	14.75668153000001	3650
1	90092U		86249.47455749	+.00000000	+000000+0	+000000+0	-1.0	3709
2	90092	23.1201	15.9199	0341370	43.8623	22.3265	15.41598773000001	3710
1	90097U		86249.47317018	+.00000000	+000000+0	+000000+0	-1.0	3639
2	90097	22.2585	13.4158	0235529	325.7310	99.0846	16.32964459000001	3640
1	90097U		86249.47332672	+.00000000	+000000+0	+000000+0	-1.0	3663
2	90097	22.3618	14.0167	0371865	62.2797	5.1922	15.34486714000001	3664
1	90100U		86249.47335605	+.00000000	+000000+0	+000000+0	-1.0	3659
2	90100	24.7064	21.4494	2742611	66.1941	356.8567	10.09246998000001	3660
1	90102U		86249.47365097	+.00000000	+000000+0	+000000+0	-1.0	3685
2	90102	22.3079	14.3325	0405919	61.3893	357.3064	15.28065355000001	3686
1	90102U		86249.47459105	+.00000000	+000000+0	+000000+0	-1.0	3713
2	90102	22.3856	14.3217	0399297	61.5911	2.3025	15.29651667000001	3714
1	90103U		86249.47365256	+.00000000	+000000+0	+000000+0	-1.0	3687
2	90103	23.5435	16.7009	0493999	67.7763	346.9880	15.07974010000001	3688
1	90103U		86249.47299538	+.00000000	+000000+0	+000000+0	-1.0	3721
2	90103	23.6466	16.3198	0462603	55.2134	5.1332	15.11519099000001	3722
1	90103U		86249.47336412	+.00000000	+000000+0	+000000+0	-1.0	3737
2	90103	23.6421	16.3010	0444335	56.0005	6.4581	15.15774348000001	3738

1 90103U		86249.47373648	+.00000000	+000000+0	+000000+0	-1.0	3743
2 90103	23.6393	16.2883 0432573	53.0242	11.2479	15.19121524000001		3744
1 90103U		86249.47411821	+.00000000	+000000+0	+000000+0	-1.0	3761
2 90103	23.6746	16.4624 0487831	53.9014	12.2543	15.05832073000001		3762
1 90105U		86249.47279910	+.00000000	+000000+0	+000000+0	-1.0	3715
2 90105	23.0253	14.9343 0369690	40.2830	23.6035	15.37868025000001		3716
1 90106U		86249.47284427	+.00000000	+000000+0	+000000+0	-1.0	3717
2 90106	22.7775	14.3543 0848953	343.2395	76.6569	15.71846002000001		3718
1 90106U		86249.47298727	+.00000000	+000000+0	+000000+0	-1.0	3727
2 90106	23.1072	16.3166 1153089	53.9015	11.7052	13.43327923000001		3728
1 90107U		86249.47285582	+.00000000	+000000+0	+000000+0	-1.0	3719
2 90107	23.3827	17.6034 1210403	54.7612	3.9059	13.48997245000001		3720
1 90107U		86249.47298168	+.00000000	+000000+0	+000000+0	-1.0	3723
2 90107	23.3253	17.3731 1623376	61.1580	359.7656	12.55190053000001		3724
1 90107U		86249.47326333	+.00000000	+000000+0	+000000+0	-1.0	3733
2 90107	23.2876	17.2050 1769174	66.0964	357.7215	12.23834127000001		3734
1 90107U		86249.55657277	+.00000000	+000000+0	+000000+0	0.1	4433
2 90107	23.2910	16.8584 1664585	63.9219	13.9032	12.46414675000001		4434
1 90108U		86249.47305074	+.00000000	+000000+0	+000000+0	-1.0	3725
2 90108	22.8034	14.6492 0349175	50.2722	8.2370	15.41024987000001		3726
1 90108U		86249.47331339	+.00000000	+000000+0	+000000+0	-1.0	3731
2 90108	22.6785	14.1366 0464669	66.9337	354.7457	15.14047252000001		3732
1 90108U		86249.47353194	+.00000000	+000000+0	+000000+0	-1.0	3739
2 90108	22.6686	14.0913 0464942	68.5125	354.5375	15.14333780000001		3740
1 90108U		86249.47374277	+.00000000	+000000+0	+000000+0	-1.0	3745
2 90108	22.7350	14.4074 0473505	57.2032	5.7065	15.11815174000001		3746
1 90108U		86249.47392806	+.00000000	+000000+0	+000000+0	-1.0	3755
2 90108	22.9179	15.2990 0605525	36.9138	23.8503	14.91838158000001		3756
1 90109U		86249.47327927	+.00000000	+000000+0	+000000+0	-1.0	3729
2 90109	22.4118	13.1305 0851610	62.4843	356.3328	14.21972441000001		3730
1 90109U		86249.47362363	+.00000000	+000000+0	+000000+0	-1.0	3741
2 90109	22.7338	14.3712 0388246	56.5864	2.2220	15.30398492000001		3742
1 90109U		86249.47397896	+.00000000	+000000+0	+000000+0	-1.0	3757
2 90109	22.6901	14.1961 0471338	59.0293	2.0495	15.10639843000001		3758
1 90109U		86249.47434784	+.00000000	+000000+0	+000000+0	-1.0	3771
2 90109	22.7140	14.2997 0442696	57.3134	5.5549	15.17500473000001		3772
1 90109U		86249.47667874	+.00000000	+000000+0	+000000+0	-1.0	3789
2 90109	22.6899	14.8898 0425791	60.9731	4.3796	15.21277374000001		3790
1 90112U		86249.47373062	+.00000000	+000000+0	+000000+0	-1.0	3747
2 90112	22.9197	14.9730 0534964	44.5869	17.6582	14.99507382000001		3748
1 90112U		86249.47388236	+.00000000	+000000+0	+000000+0	-1.0	3753
2 90112	22.8215	14.4794 0468241	60.6668	4.4779	15.09800124000001		3754
1 90112U		86249.47411470	+.00000000	+000000+0	+000000+0	-1.0	3763
2 90112	22.9100	14.9668 0567285	57.1833	8.3393	14.87055281000001		3764
1 90113U		86249.47382845	+.00000000	+000000+0	+000000+0	-1.0	3749
2 90113	22.6985	14.0206 0333610	105.7349	314.2296	15.75584362000001		3750
1 90113U		86249.47418387	+.00000000	+000000+0	+000000+0	-1.0	3765
2 90113	22.7507	14.2142 0355003	68.4802	351.2636	15.44885794000001		3766
1 90113U		86249.47672356	+.00000000	+000000+0	+000000+0	-1.0	3793
2 90113	22.8064	15.1404 0331929	56.3822	5.6161	15.48862596000001		3794
1 90113U		86249.47715032	+.00000000	+000000+0	+000000+0	-1.0	3817
2 90113	22.7772	15.0069 0340907	62.4504	2.4313	15.46554170000001		3818
1 90115U		86249.47401335	+.00000000	+000000+0	+000000+0	-1.0	3759
2 90115	22.8656	14.7041 0534482	54.1098	10.6748	14.94991110000001		3760
1 90115U		86249.47419905	+.00000000	+000000+0	+000000+0	-1.0	3769
2 90115	22.8407	14.5720 0476044	56.9112	9.3700	15.07964172000001		3770
1 90117U		86249.47417138	+.00000000	+000000+0	+000000+0	-1.0	3767
2 90117	23.1815	14.9898 0669381	89.0801	330.4243	14.90652480000001		3768
1 90117U		86249.47665778	+.00000000	+000000+0	+000000+0	-1.0	3787
2 90117	23.4514	16.5134 0493724	72.5382	346.6247	15.12720583000001		3788
1 90117U		86249.47705877	+.00000000	+000000+0	+000000+0	-1.0	3807
2 90117	23.4520	16.6153 0507422	70.1578	350.9918	15.00346181000001		3808
1 90117U		86249.47743698	+.00000000	+000000+0	+000000+0	-1.0	3875
2 90117	23.4529	16.6188 0535636	71.1609	352.1061	15.02179920000001		3876
1 90117U		86249.47782152	+.00000000	+000000+0	+000000+0	-1.0	3917
2 90117	23.4769	16.7245 0457370	66.4608	358.3542	15.19393810000001		3918
1 90119U		86249.47430466	+.00000000	+000000+0	+000000+0	-1.0	3785
2 90119	24.2099	17.3790 0736345	162.1969	261.7497	16.72687233000001		3786
1 90120U		86249.47695971	+.00000000	+000000+0	+000000+0	-1.0	3803
2 90120	23.1597	15.9789 0484122	50.0985	7.4140	15.05832000000001		3804
1 90120U		86249.47740893	+.00000000	+000000+0	+000000+0	-1.0	3867
2 90120	23.1887	16.0923 0441848	46.6181	13.7502	15.16827202000001		3868

1	90121U		86249.47445929	+	.00000000	+	.00000000	+	.00000000	-	1.0	3775
2	90121	21.9529	11.2495	1078205	96.0139	332.4236	14.16035713	0000001				3776
1	90121U		86249.47663782	+	.00000000	+	.00000000	+	.00000000	-	1.0	3781
2	90121	22.5352	14.5310	0298221	70.4272	351.0039	15.63595829	0000001				3782
1	90121U		86249.47687746	+	.00000000	+	.00000000	+	.00000000	-	1.0	3795
2	90121	22.5207	14.4654	0362775	70.3061	352.6280	15.48202269	0000001				3796
1	90121U		86249.47707421	+	.00000000	+	.00000000	+	.00000000	-	1.0	3811
2	90121	22.5237	14.4801	0332290	73.1945	350.9668	15.56154653	0000001				3812
1	90121U		86249.47750133	+	.00000000	+	.00000000	+	.00000000	-	1.0	3885
2	90121	22.5334	14.5258	0329447	70.6906	355.6591	15.56238190	0000001				3886
1	90123U		86249.47657261	+	.00000000	+	.00000000	+	.00000000	-	1.0	3779
2	90123	22.7672	14.9715	0465975	83.9256	334.5116	15.24390261	0000001				3780
1	90123U		86249.47708982	+	.00000000	+	.00000000	+	.00000000	-	1.0	3809
2	90123	22.8218	15.1601	0563023	59.7129	359.3164	14.88541809	0000001				3810
1	90123U		86249.47765251	+	.00000000	+	.00000000	+	.00000000	-	1.0	3905
2	90123	22.8527	15.2852	0495413	63.1354	359.1503	15.05340356	0000001				3906
1	90123U		86249.47850866	+	.00000000	+	.00000000	+	.00000000	-	1.0	3973
2	90123	22.8685	15.3524	0488373	58.9184	7.5503	15.06712736	0000001				3974
1	90123U		86249.47710710	+	.00000000	+	.00000000	+	.00000000	-	1.0	4047
2	90123	22.8768	14.6907	0510019	58.2717	11.0458	15.01676522	0000001				4048
1	90126U		86249.47692572	+	.00000000	+	.00000000	+	.00000000	-	1.0	3799
2	90126	22.9434	15.8404	0250117	2.5254	56.1254	15.99690841	0000001				3800
1	90126U		86249.47717478	+	.00000000	+	.00000000	+	.00000000	-	1.0	3815
2	90126	22.7894	15.1584	0380721	66.4554	356.9971	15.42101871	0000001				3816
1	90130U		86249.47657151	+	.00000000	+	.00000000	+	.00000000	-	1.0	3975
2	90130	24.1037	17.2821	0509642	52.7642	5.6382	15.00071198	0000001				3976
1	90130U		86249.47708103	+	.00000000	+	.00000000	+	.00000000	-	1.0	4041
2	90130	24.1109	17.3078	0516433	52.3733	8.7078	14.98481017	0000001				4042
1	90130U		86249.47760144	+	.00000000	+	.00000000	+	.00000000	-	1.0	4085
2	90130	24.0929	17.2339	0496916	54.8742	9.3501	15.02620315	0000001				4086
1	90130U		86249.47816289	+	.00000000	+	.00000000	+	.00000000	-	1.0	4099
2	90130	24.0918	17.2284	0476535	50.0255	16.8488	15.08877065	0000001				4100
1	90133U		86249.47777043	+	.00000000	+	.00000000	+	.00000000	-	1.0	3913
2	90133	23.2534	15.9105	0441164	113.5049	306.4132	15.63223060	0000001				3914
1	90133U		86249.47833525	+	.00000000	+	.00000000	+	.00000000	-	1.0	3955
2	90133	23.5049	16.7744	0480409	43.9587	13.0312	15.06952467	0000001				3956
1	90133U		86249.47677950	+	.00000000	+	.00000000	+	.00000000	-	1.0	4007
2	90133	23.5162	16.1120	0477368	41.3635	17.5242	15.08737564	0000001				4008
1	90135U		86249.47795197	+	.00000000	+	.00000000	+	.00000000	-	1.0	3931
2	90135	22.5940	14.4636	0475444	136.5032	287.9264	15.96779599	0000001				3932
1	90135U		86249.47831294	+	.00000000	+	.00000000	+	.00000000	-	1.0	3953
2	90135	22.7320	15.0222	0431572	69.5216	352.0234	15.22462910	0000001				3954
1	90135U		86249.47669606	+	.00000000	+	.00000000	+	.00000000	-	1.0	3993
2	90135	22.7210	14.2700	0563716	64.2969	358.7519	14.89957049	0000001				3994
1	90135U		86249.47703167	+	.00000000	+	.00000000	+	.00000000	-	1.0	4035
2	90135	22.7435	14.3741	0491248	62.7433	1.8663	15.06997003	0000001				4036
1	90135U		86249.47737206	+	.00000000	+	.00000000	+	.00000000	-	1.0	4075
2	90135	22.7274	14.2925	0507787	65.6084	1.1857	15.03181956	0000001				4076
1	90136U		86249.47798035	+	.00000000	+	.00000000	+	.00000000	-	1.0	3933
2	90136	22.9849	16.3675	1055485	73.4888	345.4821	13.86592580	0000001				3934
1	90136U		86249.47849286	+	.00000000	+	.00000000	+	.00000000	-	1.0	3971
2	90136	23.1234	16.8484	1153573	58.1160	0.0920	13.53224309	0000001				3972
1	90136U		86249.47704842	+	.00000000	+	.00000000	+	.00000000	-	1.0	4033
2	90136	23.1474	16.2307	1106399	58.6929	2.0601	13.64167012	0000001				4034
1	90136U		86249.47756195	+	.00000000	+	.00000000	+	.00000000	-	1.0	4083
2	90136	23.1202	16.1186	1109093	60.6305	3.1181	13.63505120	0000001				4084
1	90136U		86249.47807969	+	.00000000	+	.00000000	+	.00000000	-	1.0	4097
2	90136	23.1349	16.1866	1104400	59.2800	6.6800	13.64859264	0000001				4098
1	90137U		86249.47803437	+	.00000000	+	.00000000	+	.00000000	-	1.0	3935
2	90137	23.3130	16.3062	0436394	79.0152	340.8836	15.27455310	0000001				3936
1	90137U		86249.47837335	+	.00000000	+	.00000000	+	.00000000	-	1.0	3961
2	90137	23.3340	16.3066	0547347	63.2893	357.1865	14.94647717	0000001				3962
1	90137U		86249.47676372	+	.00000000	+	.00000000	+	.00000000	-	1.0	4005
2	90137	23.3354	15.6868	0499427	65.8245	356.7203	15.06513844	0000001				4006
1	90137U		86249.47710404	+	.00000000	+	.00000000	+	.00000000	-	1.0	4049
2	90137	23.3200	15.6186	0497992	66.9252	357.6260	15.07055585	0000001				4050
1	90137U		86249.47745665	+	.00000000	+	.00000000	+	.00000000	-	1.0	4079
2	90137	23.3320	15.6750	0530042	67.3998	359.0735	14.99540364	0000001				4080
1	90138U		86249.47825855	+	.00000000	+	.00000000	+	.00000000	-	1.0	3951
2	90138	23.9115	17.6868	0400705	49.4496	13.5185	15.34005843	0000001				3952
1	90138U		86249.47838321	+	.00000000	+	.00000000	+	.00000000	-	1.0	3963
2	90138	23.8069	17.5716	0404524	65.2210	359.7637	15.12051581	0000001				3964

1	90138U		86249.47657386	+.00000000	+00000+0	+00000+0	-1.0	3987
2	90138	23.8439	16.6417	0386910	57.9938	7.4272	15.3596599900001	3988
1	90138U		86249.47673629	+.00000000	+00000+0	+00000+0	-1.0	4009
2	90138	23.8933	16.9096	0610571	76.2173	351.6452	14.8423507800001	4010
1	90142U		86249.48863274	+.00000000	+00000+0	+00000+0	-1.0	4255
2	90142	23.0936	14.8963	0143112	60.9608	5.2328	16.0005465000001	4256

APPENDIX A2

EGLIN 39° DEBRIS CLOUD, 5 SEPTEMBER

1	51186U		86248.88354855	+.00000000	+000000+0	+000000+0	1.0	1135
2	51186	41.8157	33.7663	0417922	32.6060	121.3060	15.21576099000001	1136
1	09406U		86248.83348068	+.00000000	+000000+0	+000000+0	-1.0	1467
2	09406	39.1186	39.6847	0173468	21.5162	133.6059	15.63367817000001	1468
1	09406U		86248.83375709	+.00000000	+000000+0	+000000+0	-1.0	1481
2	09406	39.1266	39.6779	0213961	12.6656	143.9766	15.74901072000001	1482
1	09406U		86248.83208082	+.00000000	+000000+0	+000000+0	-1.0	1493
2	09406	39.1696	38.9389	0207658	9.7816	148.6010	15.75344504000001	1494
1	09406U		86248.83235522	+.00000000	+000000+0	+000000+0	-1.0	1515
2	09406	39.1016	38.9931	0178149	12.6993	147.2846	15.68573881000001	1516
1	09406U		86248.83297595	+.00000000	+000000+0	+000000+0	-1.0	1527
2	09406	39.1021	38.9928	0179593	12.1258	151.3736	15.69080367000001	1528
1	09406U		86248.83615403	+.00000000	+000000+0	+000000+0	-1.0	1701
2	09406	39.3692	40.7637	0433200	10.6104	143.6295	15.38415849000001	1702
1	94593U		86248.82889651	+.00000000	+000000+0	+000000+0	-1.0	1359
2	94593	40.1495	39.1701	0222629	314.8878	186.9752	15.86391025000001	1360
1	94593U		86248.82965843	+.00000000	+000000+0	+000000+0	-1.0	1379
2	94593	39.8977	39.5035	0187874	352.8293	151.6433	15.71106128000001	1380
1	94593U		86248.83231803	+.00000000	+000000+0	+000000+0	-1.0	1403
2	94593	39.8963	40.2125	0191905	356.0357	152.2899	15.70440770000001	1404
1	94593U		86248.83302591	+.00000000	+000000+0	+000000+0	-1.0	1439
2	94593	39.8683	40.2447	0143658	5.2731	147.0263	15.57693795000001	1440
1	94593U		86248.83373820	+.00000000	+000000+0	+000000+0	-1.0	1479
2	94593	39.9020	40.2157	0182219	355.3764	161.0351	15.68618077000001	1480
1	94594U		86248.82901045	+.00000000	+000000+0	+000000+0	-1.0	1361
2	94594	39.7942	39.6512	0218736	2.9338	136.5435	15.61860363000001	1362
1	94594U		86248.82974055	+.00000000	+000000+0	+000000+0	-1.0	1383
2	94594	39.8980	39.5151	0169902	352.7844	151.5480	15.58318706000001	1384
1	94594U		86248.83239376	+.00000000	+000000+0	+000000+0	-1.0	1407
2	94594	39.8986	40.2216	0202190	341.8784	166.6276	15.68559720000001	1408
1	94594U		86248.83309722	+.00000000	+000000+0	+000000+0	-1.0	1443
2	94594	39.8997	40.2226	0206638	341.2420	171.2440	15.69639033000001	1444
1	94594U		86248.83380755	+.00000000	+000000+0	+000000+0	-1.0	1483
2	94594	39.9063	40.2105	0213809	342.2901	174.1501	15.70990574000001	1484
1	94595U		86248.82910759	+.00000000	+000000+0	+000000+0	-1.0	1363
2	94595	40.0520	38.6801	0128285	301.9633	200.5147	15.55074032000001	1364
1	94595U		86248.82987755	+.00000000	+000000+0	+000000+0	-1.0	1387
2	94595	39.6573	39.1975	0155660	358.5598	146.2305	15.54793187000001	1388
1	94595U		86248.83255843	+.00000000	+000000+0	+000000+0	-1.0	1415
2	94595	39.5738	40.0074	0209336	355.2483	153.3217	15.66119907000001	1416
1	94595U		86248.83331705	+.00000000	+000000+0	+000000+0	-1.0	1453
2	94595	39.5657	40.0183	0176216	358.6588	154.2176	15.58183578000001	1454
1	94596U		86248.82920037	+.00000000	+000000+0	+000000+0	-1.0	1365
2	94596	39.7696	39.5567	0182729	34.7254	104.7610	15.29858140000001	1366
1	94596U		86248.82998419	+.00000000	+000000+0	+000000+0	-1.0	1391
2	94596	39.8917	39.3983	0146662	349.7364	155.4393	15.48665691000001	1392
1	94596U		86248.83264310	+.00000000	+000000+0	+000000+0	-1.0	1421
2	94596	39.8474	40.1594	0242425	335.8405	173.4551	15.72903147000001	1422
1	94596U		86248.83335715	+.00000000	+000000+0	+000000+0	-1.0	1457
2	94596	39.8234	40.1870	0223730	340.2093	172.9182	15.67742272000001	1458
1	94596U		86248.83212255	+.00000000	+000000+0	+000000+0	-1.0	1497
2	94596	39.8571	39.4532	0232524	338.3738	178.9022	15.69976659000001	1498
1	94597U		86248.82919489	+.00000000	+000000+0	+000000+0	-1.0	1367
2	94597	39.3301	39.8047	0407048	357.8275	140.3083	16.03463716000001	1368
1	94597U		86248.82996200	+.00000000	+000000+0	+000000+0	-1.0	1389
2	94597	39.6611	39.3627	0201990	33.1553	110.2546	15.43544531000001	1390
1	94597U		86248.83261835	+.00000000	+000000+0	+000000+0	-1.0	1417
2	94597	39.6514	40.0820	0203259	18.2404	129.3604	15.54666557000001	1418
1	94597U		86248.83332206	+.00000000	+000000+0	+000000+0	-1.0	1455
2	94597	39.6663	40.0681	0198684	14.9642	136.7097	15.56081674000001	1456
1	94597U		86248.83207722	+.00000000	+000000+0	+000000+0	-1.0	1495
2	94597	39.6919	39.3414	0198019	11.7366	144.0208	15.57754800000001	1496
1	94598U		86248.82925161	+.00000000	+000000+0	+000000+0	-1.0	1369
2	94598	39.6626	39.4570	03000545	57.1101	80.7884	15.30513726000001	1370
1	94598U		86248.83003628	+.00000000	+000000+0	+000000+0	-1.0	1393
2	94598	39.7138	39.3914	0238034	23.3170	120.0144	15.65046772000001	1394
1	94598U		86248.83269047	+.00000000	+000000+0	+000000+0	-1.0	1423
2	94598	39.7410	40.0652	0227113	44.4599	102.5770	15.45179775000001	1424
1	94598U		86248.83340059	+.00000000	+000000+0	+000000+0	-1.0	1459
2	94598	39.6891	40.1227	0243940	40.0013	110.0000	15.49182565000001	1460
1	94598U		86248.83215151	+.00000000	+000000+0	+000000+0	-1.0	1499
2	94598	39.7048	39.4053	0243835	38.4777	116.3021	15.51288630000001	1500

1	94599U	86248.82932834	+.00000000	+000000+0	+000000+0	-1.0	1371	
2	94599	39.7996	39.6820	0222058	29.9290	109.3206	15.3433274800001	1372
1	94599U	86248.83204014	+.00000000	+000000+0	+000000+0	-1.0	1395	
2	94599	39.9595	40.1774	0197418	347.4003	157.6345	15.5807341700001	1396
1	94599U	86248.83275007	+.00000000	+000000+0	+000000+0	-1.0	1429	
2	94599	39.9033	40.2478	0222100	347.8597	160.9750	15.6289265000001	1430
1	94599U	86248.83345665	+.00000000	+000000+0	+000000+0	-1.0	1465	
2	94599	39.9240	40.2280	0225084	345.3700	167.5487	15.6430166200001	1466
1	94599U	86248.83223196	+.00000000	+000000+0	+000000+0	-1.0	1505	
2	94599	39.8968	39.5498	0212600	347.0041	169.9435	15.6107543800001	1506
1	94600U	86248.82941953	+.00000000	+000000+0	+000000+0	-1.0	1373	
2	94600	39.4810	39.7552	0398479	1.5423	136.4125	16.0170769100001	1374
1	94600U	86248.83213543	+.00000000	+000000+0	+000000+0	-1.0	1397	
2	94600	39.7558	40.0942	0244135	40.8974	101.8640	15.4209852400001	1398
1	94600U	86248.83284019	+.00000000	+000000+0	+000000+0	-1.0	1431	
2	94600	39.7396	40.1163	0244944	38.1007	108.5793	15.4475347800001	1432
1	94600U	86248.83354012	+.00000000	+000000+0	+000000+0	-1.0	1469	
2	94600	39.6900	40.1719	0255134	39.6638	110.7184	15.4367258600001	1470
1	94600U	86248.83229229	+.00000000	+000000+0	+000000+0	-1.0	1511	
2	94600	39.7457	39.4171	0235535	35.7399	118.8839	15.4582411200001	1512
1	94601U	86248.82955132	+.00000000	+000000+0	+000000+0	-1.0	1375	
2	94601	38.7974	39.0748	0441377	343.2556	156.1922	16.2271052000001	1376
1	94601U	86248.83222913	+.00000000	+000000+0	+000000+0	-1.0	1399	
2	94601	38.9548	39.5702	0257548	34.0101	108.7633	15.4440349200001	1400
1	94601U	86248.83293134	+.00000000	+000000+0	+000000+0	-1.0	1435	
2	94601	38.9246	39.6103	0264230	42.0751	104.3561	15.3629296100001	1436
1	94601U	86248.83363214	+.00000000	+000000+0	+000000+0	-1.0	1471	
2	94601	39.0351	39.4921	0264840	22.3649	128.5178	15.5584064800001	1472
1	94601U	86248.83238385	+.00000000	+000000+0	+000000+0	-1.0	1517	
2	94601	38.9420	38.8765	0257104	36.7040	117.6897	15.4160061600001	1518
1	94602U	86248.83241395	+.00000000	+000000+0	+000000+0	-1.0	1521	
2	94602	39.7165	39.4471	0262246	35.3266	118.9940	15.4515589000001	1522
1	94602U	86248.83307144	+.00000000	+000000+0	+000000+0	-1.0	1587	
2	94602	39.7055	39.4550	0282333	28.8441	129.1509	15.5355713000001	1588
1	94603U	86248.82969847	+.00000000	+000000+0	+000000+0	-1.0	1385	
2	94603	39.1772	39.0494	0282833	13.7109	125.9989	15.6572061500001	1386
1	94603U	86248.83243359	+.00000000	+000000+0	+000000+0	-1.0	1411	
2	94603	39.1816	39.7511	0257981	32.2076	111.5459	15.4498520900001	1412
1	94603U	86248.83313814	+.00000000	+000000+0	+000000+0	-1.0	1447	
2	94603	39.2081	39.7215	0254037	30.1021	117.7573	15.4676842900001	1448
1	94603U	86248.83384955	+.00000000	+000000+0	+000000+0	-1.0	1487	
2	94603	39.2013	39.7306	0254513	31.5885	120.1735	15.4533766300001	1488
1	94603U	86248.83300952	+.00000000	+000000+0	+000000+0	-1.0	1529	
2	94603	39.1453	39.0753	0272091	28.7653	129.0720	15.4988484900001	1530
1	94604U	86248.83229358	+.00000000	+000000+0	+000000+0	-1.0	1401	
2	94604	39.7323	40.0808	0266696	54.1606	88.3695	15.2512588000001	1402
1	94604U	86248.83299797	+.00000000	+000000+0	+000000+0	-1.0	1437	
2	94604	39.7468	40.0651	0244712	32.2670	114.6357	15.4678809000001	1438
1	94604U	86248.83370014	+.00000000	+000000+0	+000000+0	-1.0	1475	
2	94604	39.6491	40.1719	0263440	42.0615	108.2626	15.3818649100001	1476
1	94604U	86248.83245467	+.00000000	+000000+0	+000000+0	-1.0	1523	
2	94604	39.7320	39.3922	0248981	34.3422	120.2777	15.4462833700001	1524
1	94604U	86248.83302167	+.00000000	+000000+0	+000000+0	-1.0	1535	
2	94604	39.7204	39.4004	0269645	27.6088	130.1800	15.5304154600001	1536
1	94605U	86248.82966491	+.00000000	+000000+0	+000000+0	-1.0	1381	
2	94605	39.4388	39.8794	0379145	37.1957	99.5088	15.3023067800001	1382
1	94605U	86248.83232413	+.00000000	+000000+0	+000000+0	-1.0	1405	
2	94605	39.6694	40.2758	0277397	19.6928	122.6736	15.4540547700001	1406
1	94605U	86248.83303315	+.00000000	+000000+0	+000000+0	-1.0	1441	
2	94605	39.8035	40.1101	0221730	12.9484	134.2040	15.4426036300001	1442
1	94605U	86248.83373495	+.00000000	+000000+0	+000000+0	-1.0	1477	
2	94605	39.7627	40.1565	0264934	8.5740	142.2710	15.5395971600001	1478
1	94605U	86248.83249208	+.00000000	+000000+0	+000000+0	-1.0	1525	
2	94605	39.8172	39.4021	0230851	8.8993	146.1652	15.4789060800001	1526
1	94605U	86248.83302572	+.00000000	+000000+0	+000000+0	-1.0	1541	
2	94605	39.8058	39.4104	0261187	4.4184	153.6388	15.5607008800001	1542
1	94606U	86248.83241799	+.00000000	+000000+0	+000000+0	-1.0	1409	
2	94606	39.2814	39.7676	0283757	44.7811	97.2878	15.2816446900001	1410
1	94606U	86248.83312243	+.00000000	+000000+0	+000000+0	-1.0	1445	
2	94606	39.2530	39.8056	0281442	35.4947	110.5829	15.3835790100001	1446
1	94606U	86248.83383295	+.00000000	+000000+0	+000000+0	-1.0	1485	
2	94606	39.2595	39.8006	0285989	32.7424	117.2876	15.4157615300001	1486

1	94606U		86248.83304074	+.000000000	+000000+0	+000000+0	-1.0	1543
2	94606	39.3036	39.0534 0278424	27.2308	129.5374	15.46397253000001		1544
1	94607U		86248.83246412	+.000000000	+000000+0	+000000+0	-1.0	1413
2	94607	39.8229	40.2570 0316864	29.0117	112.9208	15.44768542000001		1414
1	94607U		86248.83317058	+.000000000	+000000+0	+000000+0	-1.0	1449
2	94607	39.8643	40.2077 0288588	39.9552	105.9963	15.30369137000001		1450
1	94607U		86248.83387692	+.000000000	+000000+0	+000000+0	-1.0	1489
2	94607	39.8448	40.2309 0309975	30.1115	119.7308	15.42919291000001		1490
1	94607U		86248.83304479	+.000000000	+000000+0	+000000+0	-1.0	1545
2	94607	39.8593	39.5117 0298870	27.5269	128.7584	15.44550193000001		1546
1	94608U		86248.83260911	+.000000000	+000000+0	+000000+0	-1.0	1419
2	94608	38.9436	39.5713 0280138	25.9931	117.5433	15.45967520000001		1420
1	94608U		86248.83331203	+.000000000	+000000+0	+000000+0	-1.0	1451
2	94608	38.9208	39.5914 0269575	39.9536	107.2690	15.30534298000001		1452
1	94608U		86248.83205899	+.000000000	+000000+0	+000000+0	-1.0	1491
2	94608	38.9978	38.0156 0270866	25.1730	126.3238	15.45454668000001		1492
1	94608U		86248.83305403	+.000000000	+000000+0	+000000+0	-1.0	1551
2	94608	38.8768	38.9254 0293024	28.7037	127.9081	15.44599477000001		1552
1	94609U		86248.83268358	+.000000000	+000000+0	+000000+0	-1.0	1425
2	94609	40.5333	40.6258 0337608	328.7141	177.0170	15.73285487000001		1426
1	94609U		86248.83340124	+.000000000	+000000+0	+000000+0	-1.0	1461
2	94609	40.5038	40.6631 0302212	334.3271	175.0900	15.64053800000001		1462
1	94609U		86248.83216326	+.000000000	+000000+0	+000000+0	-1.0	1503
2	94609	40.5106	39.9530 0282980	333.6028	179.8909	15.59796003000001		1504
1	94609U		86248.83306386	+.000000000	+000000+0	+000000+0	-1.0	1553
2	94609	40.5397	39.9263 0314093	329.9896	188.8364	15.67015972000001		1554
1	94610U		86248.83272260	+.000000000	+000000+0	+000000+0	-1.0	1427
2	94610	40.1827	40.4207 0279558	358.6748	145.6120	15.54727583000001		1428
1	94610U		86248.83342982	+.000000000	+000000+0	+000000+0	-1.0	1463
2	94610	40.1661	40.4427 0273306	5.3362	142.6163	15.48711114300001		1464
1	94610U		86248.83217737	+.000000000	+000000+0	+000000+0	-1.0	1501
2	94610	40.2626	39.6394 0245126	0.7750	151.5349	15.46643005000001		1502
1	94610U		86248.83309159	+.000000000	+000000+0	+000000+0	-1.0	1555
2	94610	40.1270	39.7607 0265868	3.7496	153.3099	15.48803487000001		1556
1	94611U		86248.83284815	+.000000000	+000000+0	+000000+0	-1.0	1433
2	94611	39.7114	40.0437 0264412	23.6178	120.7774	15.41729057000001		1434
1	94611U		86248.83362610	+.000000000	+000000+0	+000000+0	-1.0	1473
2	94611	39.6740	40.0899 0282566	24.5317	123.9322	15.42559769000001		1474
1	94611U		86248.83239528	+.000000000	+000000+0	+000000+0	-1.0	1519
2	94611	39.7102	39.3426 0261690	24.2573	128.4458	15.40372075000001		1520
1	94611U		86248.83313490	+.000000000	+000000+0	+000000+0	-1.0	1583
2	94611	39.6892	39.3740 0258426	26.1521	130.5841	15.38183563000001		1584

APPENDIX A3

EGLIN 39° DEBRIS CLOUD, 6 SEPTEMBER

1	94732U		86249.43016504	+.00000000	+000000+0	+000000+0	-1.0	335
2	94732	39.7352	37.7556	1122931	5.9631	23.2153	13.7305136700001	336
1	94732U		86249.43032122	+.00000000	+000000+0	+000000+0	-1.0	369
2	94732	39.6775	37.6960	1406607	18.2554	13.3061	12.9392717600001	370
1	94732U		86249.43049205	+.00000000	+000000+0	+000000+0	-1.0	379
2	94732	39.6139	37.6245	1534510	27.6857	6.8608	12.5694452500001	380
1	94732U		86249.50861722	+.00000000	+000000+0	+000000+0	0.1	1129
2	94732	39.6449	37.3281	1322853	16.7435	25.8880	13.1465098000001	1130
1	94733U		86249.43055762	+.00000000	+000000+0	+000000+0	-1.0	391
2	94733	38.7212	36.2199	0466150	11.7085	21.8491	15.1437958500001	392
1	94733U		86249.43071119	+.00000000	+000000+0	+000000+0	-1.0	413
2	94733	38.8389	36.3467	0734870	17.7461	16.1862	14.4944787100001	414
1	94733U		86249.43090806	+.00000000	+000000+0	+000000+0	-1.0	433
2	94733	38.7990	36.3002	0708009	20.4277	15.0060	14.5354011100001	434
1	94734U		86249.43091413	+.00000000	+000000+0	+000000+0	-1.0	427
2	94734	40.7619	37.7507	0729684	5.6768	25.5021	14.5871231100001	428
1	94734U		86249.43109466	+.00000000	+000000+0	+000000+0	-1.0	447
2	94734	40.8463	37.8360	0849820	10.8516	21.3501	14.2644504600001	448
1	94735U		86249.43119743	+.00000000	+000000+0	+000000+0	-1.0	449
2	94735	40.1894	36.5124	0106407	290.9201	101.3995	16.3574247300001	450
1	94735U		86249.43133794	+.00000000	+000000+0	+000000+0	-1.0	467
2	94735	40.0705	36.3928	0113105	286.2696	107.8270	16.3478102700001	468
1	94736U		86249.43136345	+.00000000	+000000+0	+000000+0	-1.0	465
2	94736	39.8874	36.2632	0168585	359.8007	34.0702	15.9499960200001	466
1	94737U		86249.42984648	+.00000000	+000000+0	+000000+0	-1.0	479
2	94737	39.5005	36.1202	0674662	6.1015	23.6053	14.7160179200001	480
1	94737U		86249.43000037	+.00000000	+000000+0	+000000+0	-1.0	487
2	94737	39.6403	36.2542	0723529	356.7446	32.7600	14.7303865700001	488
1	94737U		86249.43030958	+.00000000	+000000+0	+000000+0	-1.0	491
2	94737	39.6222	36.2353	0718514	354.9745	35.5972	14.7689453800001	492
1	94737U		86249.43056633	+.00000000	+000000+0	+000000+0	-1.0	499
2	94737	39.5649	36.1720	0830569	11.2782	22.0999	14.3023059200001	500
1	94738U		86249.43063550	+.00000000	+000000+0	+000000+0	-1.0	503
2	94738	39.0352	34.7859	0497297	72.2484	325.9809	15.3206231100001	504
1	94738U		86249.43081018	+.00000000	+000000+0	+000000+0	-1.0	509
2	94738	39.5452	35.3107	0071977	313.9598	00.6833	16.2433726600001	510
1	94738U		86249.43094679	+.00000000	+000000+0	+000000+0	-1.0	519
2	94738	39.4345	35.1803	0060315	52.4232	344.1234	16.1313493600001	520
1	94739U		86249.43091018	+.00000000	+000000+0	+000000+0	-1.0	511
2	94739	39.6020	35.3834	0278694	30.3592	2.7944	15.5961129500001	512
1	94739U		86249.43108933	+.00000000	+000000+0	+000000+0	-1.0	521
2	94739	39.7435	35.4428	0063289	31.8770	2.3980	16.1171394200001	522
1	94739U		86249.43147665	+.00000000	+000000+0	+000000+0	-1.0	529
2	94739	39.7827	35.4831	0124393	27.2552	9.0761	15.9702860900001	530
1	94740U		86249.43141053	+.00000000	+000000+0	+000000+0	-1.0	639
2	94740	38.6982	36.2024	1830779	18.9420	10.4912	12.0124155400001	640
1	94741U		86249.43144899	+.00000000	+000000+0	+000000+0	-1.0	643
2	94741	39.5371	35.2681	0223166	54.2667	338.9885	15.7487838000001	644
1	94742U		86249.43152885	+.00000000	+000000+0	+000000+0	-1.0	651
2	94742	40.4286	36.8329	0485305	9.4693	20.2701	15.1067738300001	652
1	94743U		86249.43367763	+.00000000	+000000+0	+000000+0	-1.0	557
2	94743	40.6727	37.6765	0520529	19.9214	9.9350	14.9737633600001	558
1	94743U		86249.43412106	+.00000000	+000000+0	+000000+0	-1.0	565
2	94743	40.7815	37.7684	0718913	7.0953	22.9672	14.5975631100001	566
1	94744U		86249.43368996	+.00000000	+000000+0	+000000+0	-1.0	661
2	94744	39.2789	35.7549	0209968	108.9601	286.8093	16.0938649700001	662
1	94745U		86249.43362249	+.00000000	+000000+0	+000000+0	-1.0	541
2	94745	40.8169	36.9570	0283546	222.9973	170.2158	17.0031382800001	542
1	94745U		86249.43392110	+.00000000	+000000+0	+000000+0	-1.0	561
2	94745	40.8083	36.9486	0115761	342.0386	52.4401	16.1343586700001	562
1	94745U		86249.43427407	+.00000000	+000000+0	+000000+0	-1.0	577
2	94745	40.7364	36.8710	0052479	325.0933	72.0041	16.2618837100001	578
1	94746U		86249.43163746	+.00000000	+000000+0	+000000+0	-1.0	537
2	94746	38.3840	34.2208	0741392	96.7496	302.9494	15.4204355400001	538
1	94747U		86249.43367514	+.00000000	+000000+0	+000000+0	-1.0	545
2	94747	40.0145	36.4265	0221516	256.9455	132.7362	16.6160579900001	546
1	94747U		86249.43411898	+.00000000	+000000+0	+000000+0	-1.0	567
2	94747	39.6701	36.1147	0054224	354.0476	39.1263	16.1446856100001	568
1	94749U		86249.43383283	+.00000000	+000000+0	+000000+0	-1.0	553
2	94749	40.9052	37.0323	0129806	316.8813	72.7639	16.1350137600001	554
1	94749U		86249.43436699	+.00000000	+000000+0	+000000+0	-1.0	575
2	94749	40.8238	36.9616	0115569	340.6230	52.5753	16.0466055200001	576

1	94750U		86249.43432186	+.000000000	+000000+0	+000000+0	-1.0	695
2	94750	39.6897	36.1705	1182638	41.1772	357.0140	13.46285667000001	696
1	94751U		86249.43424393	+.000000000	+000000+0	+000000+0	-1.0	571
2	94751	39.3938	35.8384	0344362	158.2800	238.1215	16.72348814000001	572
1	94751U		86249.43459491	+.000000000	+000000+0	+000000+0	-1.0	587
2	94751	39.6232	36.0593	01111417	38.3460	356.7703	15.97022322000001	588
1	94752U		86249.43439553	+.000000000	+000000+0	+000000+0	-1.0	581
2	94752	39.5786	36.0143	0210384	31.7442	1.1212	15.73451224000001	582
1	94752U		86249.43474183	+.000000000	+000000+0	+000000+0	-1.0	591
2	94752	39.6878	36.1182	0071301	23.3565	11.3365	16.07260007000001	592
1	94753U		86249.43453518	+.000000000	+000000+0	+000000+0	-1.0	585
2	94753	38.7386	35.2450	0548392	67.4161	329.1154	15.14956937000001	586
1	94754U		86249.43476816	+.000000000	+000000+0	+000000+0	-1.0	589
2	94754	39.6552	36.1320	0380033	240.8921	153.5001	17.08871111000001	590
1	94754U		86249.43496837	+.000000000	+000000+0	+000000+0	-1.0	599
2	94754	39.7638	36.2495	0473438	266.4125	126.7105	16.94153011000001	600
1	94755U		86249.43482581	+.000000000	+000000+0	+000000+0	-1.0	593
2	94755	37.9826	34.5491	4932031	18.3655	4.4224	5.93845285000001	594
1	94756U		86249.43490347	+.000000000	+000000+0	+000000+0	-1.0	595
2	94756	39.6418	36.0945	0243205	326.2500	62.9895	15.97994418000001	596
1	94756U		86249.43534627	+.000000000	+000000+0	+000000+0	-1.0	607
2	94756	39.7348	36.1790	0089692	356.2355	37.4236	16.06930924000001	608
1	94756U		86249.43359419	+.000000000	+000000+0	+000000+0	-1.0	615
2	94756	39.6416	35.3777	0120452	35.3695	0.1744	15.95146668000001	616
1	94757U		86249.43499164	+.000000000	+000000+0	+000000+0	-1.0	597
2	94757	37.3733	33.9193	2166250	45.1894	352.6952	11.34467470000001	598
1	94758U		86249.43518775	+.000000000	+000000+0	+000000+0	-1.0	601
2	94758	40.2697	38.2484	2147176	30.7059	3.2505	11.29958599000001	602
1	94759U		86249.43526775	+.000000000	+000000+0	+000000+0	-1.0	603
2	94759	39.4555	35.9136	0144809	86.0429	307.4637	16.03488603000001	604
1	94759U		86249.43368152	+.000000000	+000000+0	+000000+0	-1.0	617
2	94759	39.6555	35.3937	0089220	38.7810	355.4870	16.02340420000001	618
1	94760U		86249.43528850	+.000000000	+000000+0	+000000+0	-1.0	605
2	94760	40.2527	36.6757	0482060	292.1813	94.6113	16.35474142000001	606
1	94760U		86249.43367811	+.000000000	+000000+0	+000000+0	-1.0	619
2	94760	39.8136	35.5625	0208433	270.4673	122.1019	16.48691404000001	620
1	94761U		86249.43545640	+.000000000	+000000+0	+000000+0	-1.0	609
2	94761	39.4716	35.9331	0100312	211.8718	186.1966	16.49466896000001	610
1	94762U		86249.43551089	+.000000000	+000000+0	+000000+0	-1.0	611
2	94762	38.9073	35.3466	1248052	60.3570	341.3709	13.52506965000001	612
1	94763U		86249.43553253	+.000000000	+000000+0	+000000+0	-1.0	613
2	94763	38.5433	35.0375	1760269	32.5901	0.2390	12.13830236000001	614
1	94764U		86249.43379774	+.000000000	+000000+0	+000000+0	-1.0	621
2	94764	40.2688	35.9820	0357065	261.3626	127.2084	16.77823154000001	622
1	94764U		86249.43423544	+.000000000	+000000+0	+000000+0	-1.0	653
2	94764	39.5684	35.3400	0155415	47.7290	347.5089	15.08726650000001	654
1	94765U		86249.43386693	+.000000000	+000000+0	+000000+0	-1.0	625
2	94765	34.6952	30.3742	0774939	233.3819	158.1291	18.07163706000001	626
1	94766U		86249.43386363	+.000000000	+000000+0	+000000+0	-1.0	623
2	94766	35.0508	32.2672	2144773	36.2427	358.0576	11.29821945000001	624
1	94767U		86249.43395171	+.000000000	+000000+0	+000000+0	-1.0	627
2	94767	39.4574	35.2461	0170643	134.6046	259.8357	16.35038579000001	628
1	94768U		86249.43397007	+.000000000	+000000+0	+000000+0	-1.0	631
2	94768	38.2179	33.9943	6960977	17.3319	2.2167	2.77838789000001	632
1	94769U		86249.43396685	+.000000000	+000000+0	+000000+0	-1.0	633
2	94769	39.5029	35.2553	0244824	58.6611	334.5255	15.72870094000001	634
1	94769U		86249.43430046	+.000000000	+000000+0	+000000+0	-1.0	655
2	94769	39.7777	35.5068	0141481	16.6294	16.6096	15.92026436000001	656
1	94769U		86249.43450494	+.000000000	+000000+0	+000000+0	-1.0	669
2	94769	39.5902	35.3171	0116905	108.8150	287.5183	16.17815147000001	670
1	94769U		86249.43486378	+.000000000	+000000+0	+000000+0	-1.0	685
2	94769	39.8370	35.5780	0148478	3.6087	32.4303	15.94359845000001	686
1	94770U		86249.43401881	+.000000000	+000000+0	+000000+0	-1.0	635
2	94770	36.2441	33.5347	0484530	23.9078	9.3427	15.05597932000001	636
1	94771U		86249.43395766	+.000000000	+000000+0	+000000+0	-1.0	629
2	94771	39.9670	35.6807	2516689	351.4041	24.3080	11.25383714000001	630
1	94772U		86249.43403199	+.000000000	+000000+0	+000000+0	-1.0	637
2	94772	40.8931	36.3358	0076131	248.1159	142.2141	16.43515972000001	638
1	94772U		86249.43430994	+.000000000	+000000+0	+000000+0	-1.0	659
2	94772	40.7964	36.2525	00803755	341.7560	50.0693	16.15182194000001	660
1	94772U		86249.43450365	+.000000000	+000000+0	+000000+0	-1.0	667
2	94772	40.8769	36.3283	0209170	334.4632	57.1469	16.00047950000001	668

1	94772U		86249.43477164	+.0000000000	+000000+0	+000000+0	-1.0	681
2	94772	40.8427	36.2946	0197638	1.9098	32.1232	15.8609602000001	682
1	94772U		86249.43494488	+.0000000000	+000000+0	+000000+0	-1.0	691
2	94772	40.8412	36.2931	0161004	1.5521	33.6907	15.9380062700001	692
1	94773U		86249.43414645	+.0000000000	+000000+0	+000000+0	-1.0	645
2	94773	39.2909	36.0369	0560425	17.8340	15.6510	14.9221701100001	646
1	94773U		86249.43430079	+.0000000000	+000000+0	+000000+0	-1.0	663
2	94773	39.0439	35.7746	0980970	45.8527	352.3685	13.9336861700001	664
1	94773U		86249.43471538	+.0000000000	+000000+0	+000000+0	-1.0	677
2	94773	39.3030	36.0723	0513749	6.3055	29.3915	15.1454828700001	678
1	94774U		86249.43416392	+.0000000000	+000000+0	+000000+0	-1.0	647
2	94774	39.7887	35.5305	0072927	336.8223	55.6956	16.1359474300001	648
1	94774U		86249.43451375	+.0000000000	+000000+0	+000000+0	-1.0	675
2	94774	39.6993	35.4441	0117907	26.4618	8.6728	15.9537856500001	676
1	94774U		86249.43501144	+.0000000000	+000000+0	+000000+0	-1.0	697
2	94774	39.5845	35.3181	0270746	70.9583	329.0681	15.7000636100001	698
1	94775U		86249.43415745	+.0000000000	+000000+0	+000000+0	-1.0	649
2	94775	38.7044	35.4518	1201356	28.4017	3.2178	13.3747638500001	650
1	94775U		86249.43460167	+.0000000000	+000000+0	+000000+0	-1.0	673
2	94775	39.3625	36.0706	0828666	4.4060	25.7401	14.3982649000001	674
1	94775U		86249.43492280	+.0000000000	+000000+0	+000000+0	-1.0	689
2	94775	39.3068	36.0118	0770718	7.7411	24.8545	14.4790174600001	690
1	94776U		86249.43429877	+.0000000000	+000000+0	+000000+0	-1.0	657
2	94776	39.6363	35.4068	0274631	10.9270	19.9410	15.6073895000001	658
1	94776U		86249.43453250	+.0000000000	+000000+0	+000000+0	-1.0	665
2	94776	39.5669	35.3438	0131949	38.4326	355.0885	15.9203162100001	666
1	94776U		86249.43482490	+.0000000000	+000000+0	+000000+0	-1.0	683
2	94776	39.7522	35.5279	0107683	294.8243	98.9071	16.2704403600001	684
1	94776U		86249.43510521	+.0000000000	+000000+0	+000000+0	-1.0	699
2	94776	39.6429	35.4122	0180005	24.3847	11.8789	15.8009527600001	700
1	94776U		86249.43550585	+.0000000000	+000000+0	+000000+0	-1.0	711
2	94776	39.5966	35.3598	0093053	21.2772	17.4836	16.0099764300001	712
1	94778U		86249.43450642	+.0000000000	+000000+0	+000000+0	-1.0	671
2	94778	39.2199	35.0333	0419866	110.7768	205.9571	16.0454109300001	672
1	94778U		86249.43477541	+.0000000000	+000000+0	+000000+0	-1.0	679
2	94778	39.6801	35.4500	0104132	54.6548	338.6210	16.0219027900001	680
1	94778U		86249.43490875	+.0000000000	+000000+0	+000000+0	-1.0	693
2	94778	39.7055	35.4747	0120632	40.0522	354.1467	15.9655213600001	694
1	94778U		86249.43520958	+.0000000000	+000000+0	+000000+0	-1.0	701
2	94778	39.7133	35.4827	0093018	39.9777	355.4718	16.0319866500001	702
1	94778U		86249.43547212	+.0000000000	+000000+0	+000000+0	-1.0	709
2	94778	39.7028	35.4714	00082051	39.0254	357.9242	16.0581873600001	710
1	94779U		86249.43513775	+.0000000000	+000000+0	+000000+0	-1.0	707
2	94779	39.9401	36.3993	1278868	31.5042	0.1942	13.2065228900001	708
1	94779U		86249.43757107	+.0000000000	+000000+0	+000000+0	-1.0	719
2	94779	40.6090	37.6883	0750643	17.3358	14.4619	14.4557109400001	720
1	94779U		86249.43795773	+.0000000000	+000000+0	+000000+0	-1.0	729
2	94779	40.5772	37.6556	0913299	27.7823	7.2650	14.0256719500001	730
1	94782U		86249.43535531	+.0000000000	+000000+0	+000000+0	-1.0	703
2	94782	39.1687	35.0821	0149185	300.1852	90.5458	16.2379743200001	704
1	94782U		86249.43553284	+.0000000000	+000000+0	+000000+0	-1.0	713
2	94782	39.0524	34.9715	0153004	331.4191	60.6110	16.0461408800001	714
1	94782U		86249.43779111	+.0000000000	+000000+0	+000000+0	-1.0	723
2	94782	39.0529	35.6770	0201978	340.3869	53.1006	15.9233777300001	724
1	94782U		86249.43807264	+.0000000000	+000000+0	+000000+0	-1.0	731
2	94782	39.0098	35.6300	0157239	339.3969	56.1418	15.9948509600001	732
1	94782U		86249.43833311	+.0000000000	+000000+0	+000000+0	-1.0	737
2	94782	39.0752	35.7057	0212996	316.4545	79.6447	16.1043916400001	738
1	94783U		86249.43543355	+.0000000000	+000000+0	+000000+0	-1.0	705
2	94783	39.6471	35.3861	0217670	51.6969	343.6624	15.7354564400001	706
1	94783U		86249.43756414	+.0000000000	+000000+0	+000000+0	-1.0	717
2	94783	39.7412	36.1869	0141739	37.2202	358.4301	15.8932987000001	718
1	94783U		86249.43776502	+.0000000000	+000000+0	+000000+0	-1.0	725
2	94783	39.9345	36.3990	0184274	298.5298	95.9913	16.2797442100001	726
1	94783U		86249.43806081	+.0000000000	+000000+0	+000000+0	-1.0	735
2	94783	39.7091	36.1403	0104002	272.4832	125.1197	16.3606224100001	736
1	94784U		86249.43775727	+.0000000000	+000000+0	+000000+0	-1.0	721
2	94784	39.7601	36.2122	0017606	266.6004	128.6066	16.2756239800001	722
1	94784U		86249.43789634	+.0000000000	+000000+0	+000000+0	-1.0	727
2	94784	39.7414	36.1928	00087652	26.4123	9.6252	16.0302098000001	728
1	94784U		86249.43806059	+.0000000000	+000000+0	+000000+0	-1.0	733
2	94784	39.8485	36.3131	0181278	6.5440	29.5426	15.8624227900001	734

1	94784U		86249.43834171	+.000000000	+000000+0	+000000+0	-1.0	741
2	94784	39.7155	36.1577	0220060	56.4710	343.1459	15.74101790000001	742
1	94784U		86249.43844560	+.000000000	+000000+0	+000000+0	-1.0	745
2	94784	40.7234	37.3768	0721218	328.2311	62.6827	15.52526416000001	746
1	94785U		86249.43785419	+.000000000	+000000+0	+000000+0	-1.0	739
2	94785	39.5142	35.9658	0271412	102.7204	293.5209	16.01061253000001	740
1	94787U		86249.43839070	+.000000000	+000000+0	+000000+0	-1.0	743
2	94787	39.8852	36.3302	0069148	176.8217	216.0509	16.38264224000001	744
1	94787U		86249.43861235	+.000000000	+000000+0	+000000+0	-1.0	747
2	94787	39.7568	36.2118	0109182	31.2519	2.5124	15.97725653000001	748
1	94787U		86249.43884320	+.000000000	+000000+0	+000000+0	-1.0	755
2	94787	39.8121	36.2677	0187194	14.7865	19.6183	15.80997100000001	756
1	94787U		86249.43918190	+.000000000	+000000+0	+000000+0	-1.0	763
2	94787	39.7583	36.2105	0103171	31.1142	5.9339	15.98867421000001	764
1	94787U		86249.43944191	+.000000000	+000000+0	+000000+0	-1.0	779
2	94787	39.8332	36.2961	0117807	323.1256	74.1946	16.15171787000001	780
1	94788U		86249.43867889	+.000000000	+000000+0	+000000+0	-1.0	749
2	94788	39.8095	37.0949	0741900	10.8545	18.0322	14.51501624000001	750
1	94788U		86249.43884644	+.000000000	+000000+0	+000000+0	-1.0	753
2	94788	39.9891	37.2572	0764474	359.8614	28.2641	14.58788193000001	754
1	94788U		86249.43914136	+.000000000	+000000+0	+000000+0	-1.0	761
2	94788	39.9136	37.1845	0823644	4.9588	25.1132	14.39298692000001	762
1	94788U		86249.43935702	+.000000000	+000000+0	+000000+0	-1.0	773
2	94788	40.0189	37.2930	0808292	358.3793	31.9567	14.52377116000001	774
1	94788U		86249.43765393	+.000000000	+000000+0	+000000+0	-1.0	785
2	94788	39.9700	36.5375	0770425	358.6785	33.2782	14.59633138000001	786
1	94789U		86249.43877649	+.000000000	+000000+0	+000000+0	-1.0	751
2	94789	39.0540	36.5205	0525019	18.8896	11.2176	14.98792078000001	752
1	94789U		86249.43901580	+.000000000	+000000+0	+000000+0	-1.0	757
2	94789	39.2780	36.7227	0803212	358.7572	29.0108	14.54238498000001	758
1	94789U		86249.43928711	+.000000000	+000000+0	+000000+0	-1.0	769
2	94789	39.2859	36.7304	0824879	359.5040	29.6489	14.48569497000001	770
1	94789U		86249.43758917	+.000000000	+000000+0	+000000+0	-1.0	783
2	94789	39.2726	36.0115	0809917	0.6624	30.0709	14.49820833000001	784
1	94789U		86249.43792718	+.000000000	+000000+0	+000000+0	-1.0	799
2	94789	39.3026	36.0445	0761729	353.5093	38.4422	14.71677391000001	800
1	94790U		86249.43893448	+.000000000	+000000+0	+000000+0	-1.0	759
2	94790	39.1740	36.5690	1026903	26.0143	5.4276	13.77792124000001	760
1	94790U		86249.43924761	+.000000000	+000000+0	+000000+0	-1.0	767
2	94790	39.6177	36.9807	0762108	9.9600	20.8008	14.48189659000001	768
1	94790U		86249.43754400	+.000000000	+000000+0	+000000+0	-1.0	781
2	94790	39.5566	36.2126	0829832	15.0006	17.6251	14.28195150000001	782
1	94790U		86249.43792256	+.000000000	+000000+0	+000000+0	-1.0	793
2	94790	39.6236	36.2857	0739554	7.6074	26.3186	14.56037130000001	794
1	94790U		86249.43819462	+.000000000	+000000+0	+000000+0	-1.0	859
2	94790	39.6118	36.2717	0760789	8.2147	27.1078	14.50763644000001	860
1	94791U		86249.43915900	+.000000000	+000000+0	+000000+0	-1.0	765
2	94791	40.4891	36.7293	0181554	28.7391	2.9891	15.79897104000001	766
1	94791U		86249.43935919	+.000000000	+000000+0	+000000+0	-1.0	775
2	94791	40.7309	36.9454	0190130	336.5388	54.5075	15.95922550000001	776
1	94791U		86249.43771051	+.000000000	+000000+0	+000000+0	-1.0	787
2	94791	40.6939	36.2049	0189693	344.6858	48.3256	15.91028413000001	788
1	94791U		86249.43809616	+.000000000	+000000+0	+000000+0	-1.0	849
2	94791	40.6872	36.1980	0167516	338.1800	57.1141	15.98215446000001	850
1	94791U		86249.43841115	+.000000000	+000000+0	+000000+0	-1.0	881
2	94791	40.7471	36.2646	0219441	339.0200	57.5480	15.90508522000001	882
1	94792U		86249.43936613	+.000000000	+000000+0	+000000+0	-1.0	777
2	94792	39.5955	36.0769	0210965	88.2621	305.0353	15.96638400000001	778
1	94792U		86249.43776117	+.000000000	+000000+0	+000000+0	-1.0	791
2	94792	39.8992	35.6421	0066769	13.1929	19.6642	16.08573306000001	792
1	94792U		86249.43821904	+.000000000	+000000+0	+000000+0	-1.0	863
2	94792	39.8116	35.5594	0162625	22.4586	12.9992	15.85010477000001	864
1	94792U		86249.43864588	+.000000000	+000000+0	+000000+0	-1.0	905
2	94792	39.7673	35.5128	0166219	40.0971	358.3944	15.83594358000001	906
1	94792U		86249.43905753	+.000000000	+000000+0	+000000+0	-1.0	947
2	94792	39.8240	35.5783	0106869	6.4535	33.6543	16.01264886000001	948
1	94794U		86249.43772017	+.000000000	+000000+0	+000000+0	-1.0	789
2	94794	39.0045	34.9181	0256809	180.7518	216.3822	16.76081606000001	790
1	94794U		86249.43792055	+.000000000	+000000+0	+000000+0	-1.0	797
2	94794	39.1347	35.0566	0147318	26.4784	9.7623	15.88450825000001	798
1	94794U		86249.43823476	+.000000000	+000000+0	+000000+0	-1.0	865
2	94794	39.1209	35.0409	0082329	11.3243	26.6330	16.05489701000001	866

1	94794U		86249.43850527	+.000000000	+000000+0	+000000+0	-1.0	893
2	94794	39.2001	35.1369	0235379	29.3326	10.0963	15.6703644700001	894
1	94794U		86249.43866935	+.000000000	+000000+0	+000000+0	-1.0	911
2	94794	39.0835	34.9954	0135415	38.2614	2.6450	15.9062062700001	912
1	94795U		86249.43793422	+.000000000	+000000+0	+000000+0	-1.0	889
2	94795	39.7592	36.3449	0767530	50.4087	345.2692	14.4877411500001	890
1	94796U		86249.43794450	+.000000000	+000000+0	+000000+0	-1.0	887
2	94796	40.7055	36.2289	0086907	23.9285	7.3166	16.0126891000001	888
1	94796U		86249.43862923	+.000000000	+000000+0	+000000+0	-1.0	907
2	94796	40.6713	36.1990	0147683	9.3666	25.3217	15.8857065000001	908
1	94796U		86249.43883965	+.000000000	+000000+0	+000000+0	-1.0	929
2	94796	40.6967	36.2257	0196653	11.9529	23.7629	15.7696232500001	930
1	94796U		86249.43904407	+.000000000	+000000+0	+000000+0	-1.0	949
2	94796	40.6764	36.2033	0109167	326.6039	70.0642	16.1096958800001	950
1	94796U		86249.43930189	+.000000000	+000000+0	+000000+0	-1.0	975
2	94796	40.6558	36.1795	0174595	20.7235	18.0333	15.7951928000001	976
1	94797U		86249.43798601	+.000000000	+000000+0	+000000+0	-1.0	801
2	94797	38.9365	35.7340	0712381	40.5547	352.1961	14.5414765900001	802
1	94797U		86249.43817264	+.000000000	+000000+0	+000000+0	-1.0	857
2	94797	39.2046	35.9779	0755884	21.4434	9.4644	14.4306802200001	858
1	94797U		86249.43841165	+.000000000	+000000+0	+000000+0	-1.0	879
2	94797	39.1832	35.9571	0741702	22.6468	9.7130	14.4583448200001	880
1	94797U		86249.43862796	+.000000000	+000000+0	+000000+0	-1.0	909
2	94797	39.1892	35.9633	0742950	21.5584	11.7703	14.46080996400001	910
1	94797U		86249.43890575	+.000000000	+000000+0	+000000+0	-1.0	935
2	94797	39.1894	35.9635	0713599	19.5810	15.0114	14.5401602900001	936
1	94798U		86249.43831978	+.000000000	+000000+0	+000000+0	-1.0	869
2	94798	40.4026	36.8445	0750935	14.2386	13.4485	14.4718174500001	870
1	94798U		86249.43865777	+.000000000	+000000+0	+000000+0	-1.0	903
2	94798	40.5054	36.9297	0846427	6.4819	21.4571	14.3226319800001	904
1	94798U		86249.43899910	+.000000000	+000000+0	+000000+0	-1.0	941
2	94798	40.4607	36.8902	0805354	9.3955	20.9254	14.3823336100001	942
1	94798U		86249.43941893	+.000000000	+000000+0	+000000+0	-1.0	985
2	94798	40.5078	36.9355	0807912	7.5975	24.6054	14.3964511600001	986
1	94798U		86249.44179496	+.000000000	+000000+0	+000000+0	-1.0	1031
2	94798	40.4890	37.6200	0801327	8.6213	25.9575	14.3978446700001	1032
1	94799U		86249.43837870	+.000000000	+000000+0	+000000+0	-1.0	873
2	94799	39.5969	35.3757	0211403	101.2606	292.2172	16.0584598500001	874
1	94799U		86249.43872211	+.000000000	+000000+0	+000000+0	-1.0	915
2	94799	39.7010	35.4686	0219414	34.0709	359.1476	15.7005959700001	916
1	94799U		86249.43913199	+.000000000	+000000+0	+000000+0	-1.0	959
2	94799	39.8458	35.6056	0137382	18.3729	16.6439	15.9057944900001	960
1	94799U		86249.44145051	+.000000000	+000000+0	+000000+0	-1.0	999
2	94799	39.7925	36.2555	0172165	32.3608	5.1322	15.0105518000001	1000
1	94799U		86249.44189415	+.000000000	+000000+0	+000000+0	-1.0	1039
2	94799	39.8035	36.2668	0131972	21.2764	18.4971	15.9145614400001	1040
1	94800U		86249.43893465	+.000000000	+000000+0	+000000+0	-1.0	945
2	94800	39.3559	36.1000	0636919	40.3761	352.6885	14.7214172400001	946
1	94800U		86249.43920111	+.000000000	+000000+0	+000000+0	-1.0	963
2	94800	39.2997	36.0486	0752325	34.3748	359.4403	14.4332537600001	964
1	94800U		86249.43943863	+.000000000	+000000+0	+000000+0	-1.0	987
2	94800	39.2930	36.0418	0749186	33.6985	1.2594	14.4401897900001	988
1	94800U		86249.44169701	+.000000000	+000000+0	+000000+0	-1.0	1017
2	94800	39.3411	36.7983	0755919	30.8197	5.2764	14.4269587600001	1018
1	94800U		86249.44194999	+.000000000	+000000+0	+000000+0	-1.0	1049
2	94800	39.3133	36.7664	0866187	35.2960	2.7207	14.1635558500001	1050
1	94801U		86249.43891649	+.000000000	+000000+0	+000000+0	-1.0	933
2	94801	39.8547	35.5894	0098614	33.6312	357.3081	15.9962946900001	934
1	94801U		86249.43925815	+.000000000	+000000+0	+000000+0	-1.0	969
2	94801	39.8404	35.5770	0208766	9.6574	22.3276	15.7576215300001	970
1	94801U		86249.44160358	+.000000000	+000000+0	+000000+0	-1.0	1011
2	94801	39.9556	36.3897	0203135	353.8420	39.7761	15.8333914600001	1012
1	94801U		86249.44195199	+.000000000	+000000+0	+000000+0	-1.0	1047
2	94801	39.9592	36.3935	0185591	352.8420	42.8638	15.8715679100001	1048
1	94801U		86249.44238121	+.000000000	+000000+0	+000000+0	-1.0	1089
2	94801	39.9522	36.3863	0176495	347.9234	50.1947	15.9127793000001	1090
1	94802U		86249.43919566	+.000000000	+000000+0	+000000+0	-1.0	971
2	94802	39.3981	35.2028	0397277	42.1640	350.4145	15.2941911800001	972
1	94802U		86249.43942932	+.000000000	+000000+0	+000000+0	-1.0	991
2	94802	39.7898	35.5526	0137052	39.6515	353.3947	15.9038990000001	992
1	94802U		86249.44172863	+.000000000	+000000+0	+000000+0	-1.0	1023
2	94802	39.7993	36.2668	0151937	29.5529	5.1809	15.8652831100001	1024

1	94802U		86249.44197577	+.00000000	+000000+0	+000000+0	-1.0	1053
2	94802	39.8026	36.2703	0169652	31.5772	4.6115	15.82176617000001	1054
1	94802U		86249.44224228	+.00000000	+000000+0	+000000+0	-1.0	1069
2	94802	39.8195	36.2880	0158327	26.2884	11.2528	15.85205553000001	1070
1	94803U		86249.43942388	+.00000000	+000000+0	+000000+0	-1.0	983
2	94803	39.6038	35.3673	0229066	37.5081	358.1709	15.73693245000001	984
1	94803U		86249.44157361	+.00000000	+000000+0	+000000+0	-1.0	1015
2	94803	39.8859	36.3691	0211773	339.7129	54.7888	15.98293616000001	1016
1	94803U		86249.44183979	+.00000000	+000000+0	+000000+0	-1.0	1033
2	94803	39.8371	36.3145	0163418	327.2037	69.1509	16.12743088000001	1034
1	94803U		86249.44208411	+.00000000	+000000+0	+000000+0	-1.0	1055
2	94803	39.8289	36.3048	0174026	340.0038	57.8510	16.03470822000001	1056
1	94804U		86249.44166314	+.00000000	+000000+0	+000000+0	-1.0	1021
2	94804	39.5055	36.0048	0449581	31.1837	1.3535	15.14636790000001	1022
1	94804U		86249.44192287	+.00000000	+000000+0	+000000+0	-1.0	1043
2	94804	39.8587	36.3310	0137055	18.5674	14.9330	15.90271189000001	1044
1	94804U		86249.44224132	+.00000000	+000000+0	+000000+0	-1.0	1071
2	94804	39.7554	36.2261	0172119	40.5286	355.4998	15.81123836000001	1072
1	94804U		86249.44247660	+.00000000	+000000+0	+000000+0	-1.0	1099
2	94804	39.8242	36.3010	0131678	19.0037	17.7228	15.91885758000001	1100
1	94804U		86249.44269446	+.00000000	+000000+0	+000000+0	-1.0	1125
2	94804	39.8261	36.3031	0144371	18.9927	18.9349	15.88927400000001	1126
1	94805U		86249.44170717	+.00000000	+000000+0	+000000+0	-1.0	1019
2	94805	40.1514	36.4874	0233642	36.1125	356.0770	15.66417566000001	1020
1	94805U		86249.44188675	+.00000000	+000000+0	+000000+0	-1.0	1041
2	94805	40.3941	36.7072	0213927	359.1655	32.3782	15.78019813000001	1042
1	94805U		86249.44215326	+.00000000	+000000+0	+000000+0	-1.0	1061
2	94805	40.4967	36.8057	0206728	341.2909	51.2068	15.89458925000001	1062
1	94805U		86249.44234245	+.00000000	+000000+0	+000000+0	-1.0	1077
2	94805	40.3917	36.6986	0241397	8.6160	25.7250	15.67648744000001	1078
1	94805U		86249.44256680	+.00000000	+000000+0	+000000+0	-1.0	1117
2	94805	40.4268	36.7345	0191026	353.5137	41.8567	15.85014848000001	1118
1	94806U		86249.44182278	+.00000000	+000000+0	+000000+0	-1.0	1045
2	94806	39.2439	36.6955	0772917	14.1461	14.8199	14.42895617000001	1046
1	94806U		86249.44207737	+.00000000	+000000+0	+000000+0	-1.0	1057
2	94806	39.3544	36.7937	0828382	6.7209	22.2368	14.37150646000001	1058
1	94806U		86249.44233152	+.00000000	+000000+0	+000000+0	-1.0	1075
2	94806	39.4212	36.8593	0818461	3.9420	25.9485	14.42822170000001	1076
1	94806U		86249.44252411	+.00000000	+000000+0	+000000+0	-1.0	1111
2	94806	39.4954	36.9365	0788396	357.9290	32.3068	14.58174252000001	1112
1	94806U		86249.44281295	+.00000000	+000000+0	+000000+0	-1.0	1133
2	94806	39.4076	36.8451	0803488	3.7255	28.7298	14.46303358000001	1134
1	94807U		86249.44210116	+.00000000	+000000+0	+000000+0	-1.0	1067
2	94807	39.5189	37.6446	1325331	19.9064	10.3372	13.12897970000001	1068
1	94807U		86249.44238912	+.00000000	+000000+0	+000000+0	-1.0	1091
2	94807	39.5132	37.6390	1474651	21.8169	9.9303	12.78039323000001	1092
1	94807U		86249.44263113	+.00000000	+000000+0	+000000+0	-1.0	1121
2	94807	39.4910	37.6151	1413981	21.7525	11.2476	12.91566105000001	1122
1	94807U		86249.44292040	+.00000000	+000000+0	+000000+0	-1.0	1139
2	94807	39.5169	37.6428	1421394	21.1027	13.0449	12.90509573000001	1140
1	94808U		86249.44181155	+.00000000	+000000+0	+000000+0	-1.0	1037
2	94808	39.2467	35.8018	0443225	33.4412	357.2853	15.16665817000001	1038
1	94808U		86249.44216426	+.00000000	+000000+0	+000000+0	-1.0	1063
2	94808	39.8894	36.3538	0254809	349.3603	40.7893	15.74545998000001	1064
1	94808U		86249.44251693	+.00000000	+000000+0	+000000+0	-1.0	1109
2	94808	39.8740	36.3399	0228006	353.1440	39.3498	15.77363412000001	1110
1	94808U		86249.44286859	+.00000000	+000000+0	+000000+0	-1.0	1135
2	94808	39.8404	36.3069	0203166	1.2376	33.7214	15.78272548000001	1136
1	94808U		86249.44324745	+.00000000	+000000+0	+000000+0	-1.0	1147
2	94808	39.8798	36.3489	0188629	343.9554	52.7590	15.90071044000001	1148
1	94809U		86249.44219995	+.00000000	+000000+0	+000000+0	-1.0	1065
2	94809	39.5755	36.0526	0185083	68.0287	326.1581	15.89253245000001	1066
1	94809U		86249.44236830	+.00000000	+000000+0	+000000+0	-1.0	1083
2	94809	39.8646	36.3278	0177324	351.5893	40.8202	15.92144633000001	1084
1	94809U		86249.44256810	+.00000000	+000000+0	+000000+0	-1.0	1115
2	94809	39.9317	36.3953	0274451	349.3133	43.3631	15.75711922000001	1116
1	94809U		86249.44279663	+.00000000	+000000+0	+000000+0	-1.0	1131
2	94809	39.8826	36.3437	0166353	344.4346	50.3465	15.97323050000001	1132
1	94809U		86249.44305330	+.00000000	+000000+0	+000000+0	-1.0	1141
2	94809	39.9258	36.3914	0212071	342.2096	53.5452	15.91601586000001	1142
1	94810U		86249.44239433	+.00000000	+000000+0	+000000+0	-1.0	1085
2	94810	38.1475	36.6046	1191340	26.9924	5.3793	13.40072900000001	1086

1	94813U		86249.44154469	+.00000000	+000000+0	+000000+0	-1.0	1151
2	94813	39.9925	36.5673	0751633	31.1993	359.4145	14.42539517000001	1152
1	94813U		86249.44188897	+.00000000	+000000+0	+000000+0	-1.0	1161
2	94813	40.0295	36.5992	0797019	24.8003	6.6140	14.32210756000001	1162
1	94813U		86249.44239469	+.00000000	+000000+0	+000000+0	-1.0	1179
2	94813	40.1115	36.6745	0781677	20.6871	12.7129	14.37269215000001	1180
1	94813U		86249.44277491	+.00000000	+000000+0	+000000+0	-1.0	1203
2	94813	40.0944	36.6569	0797303	21.0267	14.3559	14.33480359000001	1204
1	94813U		86249.44321141	+.00000000	+000000+0	+000000+0	-1.0	1229
2	94813	40.0673	36.6288	0772630	21.3511	16.4255	14.38950472000001	1230
1	94814U		86249.44174527	+.00000000	+000000+0	+000000+0	-1.0	1157
2	94814	38.8228	35.6597	0853522	21.3460	10.0884	14.19528877000001	1158
1	94814U		86249.44193403	+.00000000	+000000+0	+000000+0	-1.0	1165
2	94814	39.0033	35.8368	0818624	13.4880	17.7000	14.32947676000001	1166
1	94814U		86249.44228248	+.00000000	+000000+0	+000000+0	-1.0	1175
2	94814	39.0236	35.8581	0802996	12.6985	20.2216	14.37184893000001	1176
1	94814U		86249.44253407	+.00000000	+000000+0	+000000+0	-1.0	1185
2	94814	38.9840	35.8132	0767279	13.2436	21.2353	14.44510478000001	1186
1	94814U		86249.44276946	+.00000000	+000000+0	+000000+0	-1.0	1205
2	94814	38.9756	35.8035	0798683	15.3249	20.5367	14.35481116000001	1206
1	94815U		86249.44187326	+.00000000	+000000+0	+000000+0	-1.0	1159
2	94815	40.5992	36.2073	0221927	321.4114	66.6147	16.02039091000001	1160
1	94815U		86249.44221309	+.00000000	+000000+0	+000000+0	-1.0	1169
2	94815	40.3844	36.0248	0276766	344.5288	45.6812	15.74972473000001	1170
1	94815U		86249.44254891	+.00000000	+000000+0	+000000+0	-1.0	1191
2	94815	40.4486	36.0833	0272995	336.6312	55.2084	15.82284510000001	1192
1	94815U		86249.44289277	+.00000000	+000000+0	+000000+0	-1.0	1211
2	94815	40.3389	35.9753	0247028	350.6675	43.8901	15.75452739000001	1212
1	94815U		86249.44328490	+.00000000	+000000+0	+000000+0	-1.0	1231
2	94815	40.3721	36.0107	0265400	349.5212	47.0415	15.72994994000001	1232
1	94816U		86249.44225645	+.00000000	+000000+0	+000000+0	-1.0	1173
2	94816	40.0770	36.7284	0343717	20.2608	11.8641	15.39927774000001	1174
1	94816U		86249.44250495	+.00000000	+000000+0	+000000+0	-1.0	1183
2	94816	39.6820	36.3562	0791449	24.6841	8.6145	14.33865666000001	1184
1	94816U		86249.44272247	+.00000000	+000000+0	+000000+0	-1.0	1199
2	94816	39.7274	36.4039	0777173	21.7614	12.2354	14.38610783000001	1200
1	94816U		86249.44294028	+.00000000	+000000+0	+000000+0	-1.0	1213
2	94816	39.6832	36.3551	0871654	26.1381	9.4676	14.14516326000001	1214
1	94816U		86249.44320332	+.00000000	+000000+0	+000000+0	-1.0	1227
2	94816	39.5834	36.2392	0674770	26.7136	10.8131	14.59711204000001	1228
1	94817U		86249.44223425	+.00000000	+000000+0	+000000+0	-1.0	1171
2	94817	39.7135	35.4968	0205429	30.2705	1.3865	15.72998754000001	1172
1	94817U		86249.44258522	+.00000000	+000000+0	+000000+0	-1.0	1193
2	94817	39.8873	35.6543	0254310	0.0879	31.9901	15.69015513000001	1194
1	94817U		86249.44296669	+.00000000	+000000+0	+000000+0	-1.0	1217
2	94817	39.9430	35.7080	0199772	351.3344	42.9345	15.84517491000001	1218
1	94817U		86249.44550843	+.00000000	+000000+0	+000000+0	-1.0	1241
2	94817	39.8515	36.3170	0209386	7.9754	30.1857	15.74836462000001	1242
1	94817U		86249.44594374	+.00000000	+000000+0	+000000+0	-1.0	1267
2	94817	39.9621	36.4488	0256428	357.8790	41.9605	15.70682806000001	1268
1	94818U		86249.44241024	+.00000000	+000000+0	+000000+0	-1.0	1181
2	94818	40.0706	36.6124	0745920	30.5101	0.7385	14.43365875000001	1182
1	94818U		86249.44275254	+.00000000	+000000+0	+000000+0	-1.0	1197
2	94818	40.2419	36.7640	0805058	18.9627	12.2042	14.32307365000001	1198
1	94818U		86249.44310054	+.00000000	+000000+0	+000000+0	-1.0	1221
2	94818	40.2308	36.7537	0875778	19.1424	13.6600	14.15993996000001	1222
1	94818U		86249.44550697	+.00000000	+000000+0	+000000+0	-1.0	1243
2	94818	40.2156	37.4432	0775274	21.0389	14.6689	14.37684960000001	1244
1	94818U		86249.44589655	+.00000000	+000000+0	+000000+0	-1.0	1261
2	94818	40.2625	37.4964	0795023	17.2157	19.8640	14.36265432000001	1262
1	94819U		86249.44256707	+.00000000	+000000+0	+000000+0	-1.0	1187
2	94819	39.1883	35.1385	0275969	27.9833	4.3900	15.56701451000001	1188
1	94819U		86249.44291772	+.00000000	+000000+0	+000000+0	-1.0	1215
2	94819	39.2177	35.1666	0203782	38.2374	356.5719	15.74424256000001	1216
1	94819U		86249.44534086	+.00000000	+000000+0	+000000+0	-1.0	1239
2	94819	39.1641	35.8171	0206492	49.9757	348.0111	15.75685532000001	1240
1	94819U		86249.44576957	+.00000000	+000000+0	+000000+0	-1.0	1255
2	94819	39.1414	35.7914	0243282	53.6216	347.0634	15.68059672000001	1256
1	94820U		86249.44273380	+.00000000	+000000+0	+000000+0	-1.0	1201
2	94820	38.8406	35.6868	0963239	18.7500	11.9549	13.96245016000001	1202
1	94821U		86249.44303588	+.00000000	+000000+0	+000000+0	-1.0	1219
2	94821	37.6451	35.4842	1455154	26.8783	3.4838	12.80852985000001	1220

1	94821U		86249.44532943	+.0000000000	+000000+0	+000000+0	-1.0	1237
2	94821	37.8862	36.4153	1453497	19.9272	10.0700	12.84459964000001	1238
1	94821U		86249.44568546	+.0000000000	+000000+0	+000000+0	-1.0	1251
2	94821	37.8486	36.3779	1498113	20.7342	11.0354	12.73881254000001	1252
1	94821U		86249.44608441	+.0000000000	+000000+0	+000000+0	-1.0	1275
2	94821	37.8954	36.4288	1392990	19.9031	13.7433	12.97931865000001	1276
1	94821U		86249.44647342	+.0000000000	+000000+0	+000000+0	-1.0	1305
2	94821	37.8709	36.3996	1431561	20.1847	15.2422	12.89130586000001	1306
1	94821U		86249.52410426	+.0000000000	+000000+0	+000000+0	0.2	3111
2	94821	37.8636	35.3630	1427620	20.5617	25.0377	12.90051437000001	3112
1	94822U		86249.44572593	+.0000000000	+000000+0	+000000+0	-1.0	1265
2	94822	39.5399	36.9576	0815864	38.5734	356.4658	14.30208993000001	1266
1	94822U		86249.44635807	+.0000000000	+000000+0	+000000+0	-1.0	1295
2	94822	39.5413	36.9588	0826846	38.0231	0.1863	14.27471488000001	1296
1	94822U		86249.44675484	+.0000000000	+000000+0	+000000+0	-1.0	1323
2	94822	39.5742	36.9968	0734348	33.5560	6.0721	14.49187433000001	1324
1	94823U		86249.44325187	+.0000000000	+000000+0	+000000+0	-1.0	1259
2	94823	39.8026	37.1217	1397515	31.6315	359.1991	12.94031797000001	1260
1	94823U		86249.44607710	+.0000000000	+000000+0	+000000+0	-1.0	1277
2	94823	40.1002	38.0763	1428761	20.1878	11.6137	12.89036983000001	1278
1	94823U		86249.44624602	+.0000000000	+000000+0	+000000+0	-1.0	1289
2	94823	40.0673	38.0407	1470246	21.6484	11.2250	12.78401451000001	1290
1	94823U		86249.44645644	+.0000000000	+000000+0	+000000+0	-1.0	1303
2	94823	40.1281	38.1089	1388690	18.4311	14.8018	12.99997658000001	1304
1	94823U		86249.44669028	+.0000000000	+000000+0	+000000+0	-1.0	1319
2	94823	40.1438	38.1273	1437843	18.4635	15.6975	12.89205466000001	1320
1	94824U		86249.44545413	+.0000000000	+000000+0	+000000+0	-1.0	1271
2	94824	40.1977	36.5796	0140564	127.6145	266.2259	16.32308577000001	1272
1	94825U		86249.44553438	+.0000000000	+000000+0	+000000+0	-1.0	1247
2	94825	39.2110	35.8940	0082487	13.3575	17.2724	16.03800662000001	1248
1	94825U		86249.44590841	+.0000000000	+000000+0	+000000+0	-1.0	1263
2	94825	39.0582	35.7576	0213087	7.3470	24.8342	15.75096511000001	1264
1	94825U		86249.44631472	+.0000000000	+000000+0	+000000+0	-1.0	1293
2	94825	39.0423	35.7423	0206601	9.2868	25.3131	15.75896724000001	1294
1	94825U		86249.44670407	+.0000000000	+000000+0	+000000+0	-1.0	1315
2	94825	39.0024	35.7002	0217599	15.3866	21.6345	15.71516836000001	1316
1	94825U		86249.44711740	+.0000000000	+000000+0	+000000+0	-1.0	1335
2	94825	39.0375	35.7407	0204509	6.6134	32.4607	15.77530648000001	1336
1	94826U		86249.44568804	+.0000000000	+000000+0	+000000+0	-1.0	1249
2	94826	39.0393	36.5846	0770247	17.8361	12.0030	14.41311795000001	1250
1	94826U		86249.44606481	+.0000000000	+000000+0	+000000+0	-1.0	1273
2	94826	39.0984	36.6394	0862530	11.7634	18.7998	14.24892162000001	1274
1	94826U		86249.44640837	+.0000000000	+000000+0	+000000+0	-1.0	1297
2	94826	39.0382	36.5795	0842056	15.4751	17.5267	14.26049727000001	1298
1	94826U		86249.44676060	+.0000000000	+000000+0	+000000+0	-1.0	1321
2	94826	39.0377	36.5790	0811411	16.2225	18.8123	14.32239237000001	1322
1	94826U		86249.44716688	+.0000000000	+000000+0	+000000+0	-1.0	1341
2	94826	39.0580	36.6027	0808468	14.2185	22.6236	14.34902612000001	1342
1	94827U		86249.44578494	+.0000000000	+000000+0	+000000+0	-1.0	1257
2	94827	38.8800	36.4449	0736904	28.7544	2.0056	14.46253829000001	1258
1	94827U		86249.44617617	+.0000000000	+000000+0	+000000+0	-1.0	1283
2	94827	39.0240	36.5724	0855623	14.0051	16.3741	14.24296865000001	1284
1	94827U		86249.44655327	+.0000000000	+000000+0	+000000+0	-1.0	1309
2	94827	39.1163	36.6620	0803759	11.4415	20.6337	14.38227405000001	1310
1	94827U		86249.44701585	+.0000000000	+000000+0	+000000+0	-1.0	1333
2	94827	39.0525	36.5946	0513243	0.5556	34.3593	15.12429564000001	1334
1	94827U		86249.44558175	+.0000000000	+000000+0	+000000+0	-1.0	1353
2	94827	39.0461	35.8820	1142825	20.3685	16.8837	13.53599283000001	1354
1	94829U		86249.44608748	+.0000000000	+000000+0	+000000+0	-1.0	1281
2	94829	39.3137	36.8518	0949313	2.1240	25.1010	14.17568730000001	1282
1	94829U		86249.44644583	+.0000000000	+000000+0	+000000+0	-1.0	1299
2	94829	39.0598	36.6157	0826327	12.3797	18.9461	14.32391370000001	1300
1	94829U		86249.44681278	+.0000000000	+000000+0	+000000+0	-1.0	1325
2	94829	38.9408	36.4940	0845833	18.2869	15.8205	14.22949793000001	1326
1	94829U		86249.44719144	+.0000000000	+000000+0	+000000+0	-1.0	1343
2	94829	39.0298	36.5931	0808076	13.4421	21.9786	14.35862823000001	1344
1	94829U		86249.44569890	+.0000000000	+000000+0	+000000+0	-1.0	1361
2	94829	38.9822	35.8304	0800417	14.7732	23.2855	14.36104130000001	1362
1	94830U		86249.44620480	+.0000000000	+000000+0	+000000+0	-1.0	1287
2	94830	39.1009	36.6346	0882621	13.2930	15.9573	14.18781800000001	1288
1	94830U		86249.44655513	+.0000000000	+000000+0	+000000+0	-1.0	1307
2	94830	39.1202	36.6529	0836125	13.4903	17.7307	14.29066470000001	1308

1	94830U		86249.44692925	+.000000000	+000000+0	+000000+0	-1.0	1327
2	94830	39.0995	36.6321 0837408	14.9327	18.4352	14.27472970000001		1328
1	94830U		86249.44539302	+.000000000	+000000+0	+000000+0	-1.0	1349
2	94830	39.1269	35.9571 0829800	13.5213	21.7939	14.30558054000001		1350
1	94830U		86249.44583068	+.000000000	+000000+0	+000000+0	-1.0	1365
2	94830	39.0888	35.9112 0784892	11.7049	25.8639	14.42495119000001		1366
1	94831U		86249.44624182	+.000000000	+000000+0	+000000+0	-1.0	1291
2	94831	38.6555	36.2198 1173488	19.5388	9.8428	13.47914899000001		1292
1	94831U		86249.44663342	+.000000000	+000000+0	+000000+0	-1.0	1313
2	94831	39.1074	36.6400 0803385	15.2172	16.0447	14.34869395000001		1314
1	94831U		86249.44712914	+.000000000	+000000+0	+000000+0	-1.0	1337
2	94831	39.1133	36.6459 0832084	13.8169	19.6892	14.29584841000001		1338
1	94831U		86249.44571114	+.000000000	+000000+0	+000000+0	-1.0	1359
2	94831	39.1186	35.9468 0816642	12.9715	23.2317	14.33873295000001		1360
1	94831U		86249.44610646	+.000000000	+000000+0	+000000+0	-1.0	1375
2	94831	39.0896	35.9105 0840525	16.3962	22.2455	14.24728343000001		1376
1	94835U		86249.44722736	+.000000000	+000000+0	+000000+0	-1.0	1347
2	94835	39.2036	36.6587 1058944	30.8714	0.3686	13.71307334000001		1348
1	94835U		86249.44561471	+.000000000	+000000+0	+000000+0	-1.0	1305
2	94835	39.6691	36.3691 0843521	23.5742	7.9864	14.21967002000001		1356
1	94835U		86249.44602747	+.000000000	+000000+0	+000000+0	-1.0	1369
2	94835	39.7149	36.4124 0813749	23.3189	10.3446	14.28934596000001		1370
1	94835U		86249.44637254	+.000000000	+000000+0	+000000+0	-1.0	1381
2	94835	39.6037	36.2968 0837233	27.9255	8.2470	14.21721194000001		1382
1	94835U		86249.44672397	+.000000000	+000000+0	+000000+0	-1.0	1393
2	94835	39.6398	36.3344 0807414	25.6253	12.0309	14.29384320000001		1394
1	94836U		86249.44538782	+.000000000	+000000+0	+000000+0	-1.0	1351
2	94836	38.5819	35.4887 1031816	48.8895	345.8864	13.89044253000001		1352
1	94836U		86249.44573417	+.000000000	+000000+0	+000000+0	-1.0	1357
2	94836	38.8343	35.7198 0917974	46.8428	348.8571	14.12662313000001		1358
1	94836U		86249.44608648	+.000000000	+000000+0	+000000+0	-1.0	1371
2	94836	38.9657	35.8473 0836103	47.1192	350.1554	14.31558466000001		1372
1	94836U		86249.44643009	+.000000000	+000000+0	+000000+0	-1.0	1383
2	94836	38.9245	35.8040 0840080	47.5350	351.6102	14.30909872000001		1384
1	94836U		86249.44679087	+.000000000	+000000+0	+000000+0	-1.0	1397
2	94836	38.9289	35.8090 0896241	46.6111	354.3201	14.17424558000001		1398
1	94839U		86249.44617579	+.000000000	+000000+0	+000000+0	-1.0	1379
2	94839	39.5861	36.2218 0828923	36.2452	356.7595	14.23876612000001		1380
1	94841U		86249.44658054	+.000000000	+000000+0	+000000+0	-1.0	1389
2	94841	39.7595	36.4212 0800725	44.4032	348.7359	14.37062814000001		1390
1	94841U		86249.44695379	+.000000000	+000000+0	+000000+0	-1.0	1403
2	94841	39.8773	36.5254 0839714	33.3824	359.9698	14.23011702000001		1404
1	94841U		86249.44929140	+.000000000	+000000+0	+000000+0	-1.0	1413
2	94841	39.7981	37.1552 0873800	35.7964	359.9610	14.15467805000001		1414
1	94841U		86249.44962945	+.000000000	+000000+0	+000000+0	-1.0	1433
2	94841	39.8060	37.2467 0800738	33.7068	3.4113	14.32382448000001		1434
1	94841U		86249.45006895	+.000000000	+000000+0	+000000+0	-1.0	1449
2	94841	39.0573	37.2168 0849314	35.1569	4.4326	14.21096632000001		1450
1	94843U		86249.44703757	+.000000000	+000000+0	+000000+0	-1.0	1405
2	94843	39.6202	35.4841 0206804	39.0250	353.3166	15.72219995000001		1406
1	94843U		86249.44937337	+.000000000	+000000+0	+000000+0	-1.0	1421
2	94843	39.7437	36.3030 0226111	8.8945	24.2391	15.70665331000001		1422
1	94843U		86249.44983420	+.000000000	+000000+0	+000000+0	-1.0	1441
2	94843	39.6944	36.2542 0224020	12.1217	23.7923	15.70051407000001		1442
1	94843U		86249.45018966	+.000000000	+000000+0	+000000+0	-1.0	1453
2	94843	39.6619	36.2186 0208000	16.4283	21.4623	15.55690465000001		1454
1	94843U		86249.45059172	+.000000000	+000000+0	+000000+0	-1.0	1495
2	94843	39.6793	36.2377 0261517	14.2008	25.9068	15.60866164000001		1496
1	94844U		86249.44702941	+.000000000	+000000+0	+000000+0	-1.0	1407
2	94844	39.6870	35.5552 0181286	94.2320	298.0441	16.03496953000001		1408
1	94844U		86249.44936743	+.000000000	+000000+0	+000000+0	-1.0	1423
2	94844	39.7842	36.3441 0239852	3.8236	27.5100	15.69633335000001		1424
1	94844U		86249.44977073	+.000000000	+000000+0	+000000+0	-1.0	1439
2	94844	39.6550	36.2240 0274699	12.0310	21.8737	15.58624377000001		1440
1	94844U		86249.45011196	+.000000000	+000000+0	+000000+0	-1.0	1451
2	94844	39.6664	36.2357 0226748	16.0847	20.1109	15.68222801000001		1452
1	94844U		86249.45045421	+.000000000	+000000+0	+000000+0	-1.0	1479
2	94844	39.6625	36.2316 0264923	16.8463	21.1646	15.59178817000001		1480
1	94845U		86249.44717273	+.000000000	+000000+0	+000000+0	-1.0	1411
2	94845	40.1464	35.8707 0198565	26.5310	4.8805	15.73972827000001		1412
1	94845U		86249.44951186	+.000000000	+000000+0	+000000+0	-1.0	1427
2	94845	40.3159	36.7273 0252223	358.7516	33.3853	15.69329282000001		1428

1	94845U		86249.44987565	+.000000000	+000000+0	+000000+0	-1.0	1445
2	94845	40.2854	36.6981 0247618	359.7525	34.5304	15.6973932900001		1446
1	94845U		86249.45024263	+.000000000	+000000+0	+000000+0	-1.0	1455
2	94845	40.2995	36.7129 0287073	358.3137	37.7004	15.6267749900001		1456
1	94845U		86249.45064869	+.000000000	+000000+0	+000000+0	-1.0	1499
2	94845	40.2993	36.7127 0264205	355.0715	43.2677	15.6930309400001		1500
1	94849U		86249.44944472	+.000000000	+000000+0	+000000+0	-1.0	1435
2	94849	38.6765	35.4646 0288859	82.6269	311.6415	15.7864495200001		1436
1	94849U		86249.45001563	+.000000000	+000000+0	+000000+0	-1.0	1447
2	94849	38.8411	35.6146 0238430	37.4346	357.6747	15.6497152100001		1448
1	94849U		86249.45059433	+.000000000	+000000+0	+000000+0	-1.0	1493
2	94849	38.8015	35.5735 0268169	39.1656	359.3258	15.5799776800001		1494
1	94849U		86249.45100352	+.000000000	+000000+0	+000000+0	-1.0	1535
2	94849	38.8041	35.5767 0212311	41.5266	359.3623	15.7154543100001		1536
1	94849U		86249.44949414	+.000000000	+000000+0	+000000+0	-1.0	1581
2	94849	38.7888	34.8533 0195254	36.1869	7.0199	15.7545706400001		1582
1	94851U		86249.44986306	+.000000000	+000000+0	+000000+0	-1.0	1443
2	94851	40.1073	37.4512 0725000	33.2807	358.3082	14.4982926700001		1444
1	94851U		86249.45024169	+.000000000	+000000+0	+000000+0	-1.0	1457
2	94851	39.8081	37.1843 0853918	35.3574	358.7239	14.2017622100001		1458
1	94851U		86249.45070636	+.000000000	+000000+0	+000000+0	-1.0	1505
2	94851	39.7626	37.1402 0851173	37.7737	359.0978	14.2137873800001		1506
1	94851U		86249.45113034	+.000000000	+000000+0	+000000+0	-1.0	1543
2	94851	39.7899	37.1697 0838562	36.4325	2.3777	14.2414678100001		1544
1	94853U		86249.45077178	+.000000000	+000000+0	+000000+0	-1.0	1507
2	94853	39.1836	37.4303 1441640	29.8289	3.5158	12.8411969800001		1508
1	94853U		86249.45113511	+.000000000	+000000+0	+000000+0	-1.0	1545
2	94853	39.1975	37.4445 1497772	27.8659	6.5681	12.7204926100001		1546
1	94853U		86249.44987861	+.000000000	+000000+0	+000000+0	-1.0	1611
2	94853	39.1861	36.7268 1441744	28.1059	9.6944	12.8445122300001		1612
1	94857U		86249.45076429	+.000000000	+000000+0	+000000+0	-1.0	1647
2	94857	40.3210	36.7275 0236710	22.0734	9.1399	15.6512361500001		1648
1	94857U		86249.45046103	+.000000000	+000000+0	+000000+0	-1.0	1665
2	94857	40.3546	36.0500 0263289	7.2690	32.4280	15.6291444600001		1666
1	94860U		86249.45089147	+.000000000	+000000+0	+000000+0	-1.0	1519
2	94860	40.5807	37.8064 0474252	16.9905	11.9467	15.0915841000001		1520
1	94862U		86249.45106711	+.000000000	+000000+0	+000000+0	-1.0	1537
2	94862	39.3494	36.8267 0816459	46.4208	347.2375	14.3457433200001		1538
1	94862U		86249.44956335	+.000000000	+000000+0	+000000+0	-1.0	1589
2	94862	39.5874	36.3351 0847387	28.0011	4.9896	14.2060714100001		1590
1	94862U		86249.44997380	+.000000000	+000000+0	+000000+0	-1.0	1621
2	94862	39.4990	36.2485 0892674	30.2508	5.2027	14.0975967500001		1622
1	94862U		86249.45041350	+.000000000	+000000+0	+000000+0	-1.0	1653
2	94862	39.5318	36.2839 0833927	30.7718	7.0508	14.2327674400001		1654
1	94862U		86249.45085534	+.000000000	+000000+0	+000000+0	-1.0	1609
2	94862	39.5644	36.3227 0950542	31.3624	8.6051	13.9611149500001		1690
1	94864U		86249.44935045	+.000000000	+000000+0	+000000+0	-1.0	1695
2	94864	39.3755	36.1788 0727765	42.2159	350.5921	14.5215670200001		1696
1	94865U		86249.44939287	+.000000000	+000000+0	+000000+0	-1.0	1567
2	94865	39.8094	36.4923 0821226	36.1062	357.0327	14.2785106400001		1568
1	94865U		86249.44978460	+.000000000	+000000+0	+000000+0	-1.0	1599
2	94865	39.7370	36.4243 0891567	34.9422	0.0829	14.1122410100001		1600
1	94865U		86249.45020428	+.000000000	+000000+0	+000000+0	-1.0	1641
2	94865	39.7613	36.4491 0857952	35.7724	1.5116	14.1913428400001		1642
1	94865U		86249.45060490	+.000000000	+000000+0	+000000+0	-1.0	1671
2	94865	39.7941	36.4857 0833783	33.5628	5.4109	14.2405454100001		1672
1	94865U		86249.45106633	+.000000000	+000000+0	+000000+0	-1.0	1703
2	94865	39.7598	36.4438 0849872	35.0363	6.5412	14.2083390100001		1704
1	94867U		86249.44953563	+.000000000	+000000+0	+000000+0	-1.0	1585
2	94867	38.8653	35.7376 0897734	21.2016	8.6725	14.0978076600001		1586
1	94867U		86249.44988478	+.000000000	+000000+0	+000000+0	-1.0	1609
2	94867	39.1807	36.0257 0920824	8.9512	20.4326	14.1403739000001		1610
1	94867U		86249.45035566	+.000000000	+000000+0	+000000+0	-1.0	1651
2	94867	39.1852	36.0301 0891678	9.8834	22.1684	14.1935844100001		1652
1	94867U		86249.45071681	+.000000000	+000000+0	+000000+0	-1.0	1681
2	94867	39.2446	36.0944 0905511	6.7482	26.5639	14.2054587000001		1682
1	94867U		86249.45111432	+.000000000	+000000+0	+000000+0	-1.0	1709
2	94867	39.1605	36.0034 0888361	10.0468	25.9385	14.1987523800001		1710
1	94868U		86249.44963452	+.000000000	+000000+0	+000000+0	-1.0	1593
2	94868	38.5114	36.1806 1375820	20.1561	8.6417	13.0009668500001		1594
1	94868U		86249.44999151	+.000000000	+000000+0	+000000+0	-1.0	1627
2	94868	38.7661	36.4153 1481525	10.4770	17.1414	12.8687387700001		1628

1	94868U		86249.45048322	+.000000000	+000000+0	+000000+0	-1.0	1661
2	94868	38.7283	36.3782	1543627	10.3070	19.3174	12.73742179000001	1662
1	94868U		86249.45098680	+.000000000	+000000+0	+000000+0	-1.0	1701
2	94868	38.7507	36.4030	1519626	9.9577	21.9815	12.79450998000001	1702
1	94868U		86249.45347909	+.000000000	+000000+0	+000000+0	-1.0	1729
2	94868	38.7170	37.0662	1518384	10.9671	23.7310	12.77682087000001	1730
1	94870U		86249.44997160	+.000000000	+000000+0	+000000+0	-1.0	1623
2	94870	40.5544	36.2152	0165357	33.7326	357.2584	15.82057108000001	1624
1	94870U		86249.45036103	+.000000000	+000000+0	+000000+0	-1.0	1649
2	94870	40.5037	36.1714	0261614	7.8610	24.1122	15.62927676000001	1650
1	94870U		86249.45095904	+.000000000	+000000+0	+000000+0	-1.0	1697
2	94870	40.5202	36.1869	0288010	2.9302	32.0160	15.59502283000001	1698
1	94870U		86249.45328016	+.000000000	+000000+0	+000000+0	-1.0	1721
2	94870	40.4579	36.8253	0265168	8.8637	28.6057	15.61214284000001	1722
1	94870U		86249.45370664	+.000000000	+000000+0	+000000+0	-1.0	1745
2	94870	40.4713	36.8395	0286559	9.6602	30.1113	15.56141978000001	1746
1	94873U		86249.45049224	+.000000000	+000000+0	+000000+0	-1.0	1663
2	94873	40.0570	35.9039	0121447	69.6240	322.6756	15.99397280000001	1664
1	94873U		86249.45083281	+.000000000	+000000+0	+000000+0	-1.0	1687
2	94873	39.7220	35.6024	0262081	38.7995	355.1656	15.59540680000001	1688
1	94873U		86249.45313661	+.000000000	+000000+0	+000000+0	-1.0	1711
2	94873	39.7423	36.3271	0285071	29.6068	5.8163	15.53608807000001	1712
1	94873U		86249.45348092	+.000000000	+000000+0	+000000+0	-1.0	1733
2	94873	39.7121	36.2955	0259512	39.2668	358.6311	15.59829337000001	1734
1	94873U		86249.45382485	+.000000000	+000000+0	+000000+0	-1.0	1753
2	94873	39.7215	36.3062	0259891	35.3595	4.2616	15.59630641000001	1754
1	94875U		86249.45077197	+.000000000	+000000+0	+000000+0	-1.0	1683
2	94875	40.0543	35.8200	0438110	4.5948	25.0528	15.29559025000001	1684
1	94875U		86249.45113233	+.000000000	+000000+0	+000000+0	-1.0	1707
2	94875	40.4046	36.1304	0276885	346.8518	44.6176	15.75870038000001	1708
1	94875U		86249.45345017	+.000000000	+000000+0	+000000+0	-1.0	1727
2	94875	40.2702	36.7065	0353013	356.3325	37.1540	15.53832933000001	1728
1	94875U		86249.45380642	+.000000000	+000000+0	+000000+0	-1.0	1751
2	94875	40.4088	36.8510	0295243	342.0422	53.1811	15.76981764000001	1752
1	94875U		86249.45417524	+.000000000	+000000+0	+000000+0	-1.0	1771
2	94875	40.3210	36.7522	0316711	353.3185	44.3161	15.63079080000001	1772
1	94876U		86249.45420396	+.000000000	+000000+0	+000000+0	-1.0	1773
2	94876	37.8897	37.0376	2157969	17.2990	14.8586	11.30977528000001	1774
1	94879U		86249.45394828	+.000000000	+000000+0	+000000+0	-1.0	1761
2	94879	40.2441	36.7022	0317700	8.9868	22.6220	15.50099777000001	1762
1	94879U		86249.45432470	+.000000000	+000000+0	+000000+0	-1.0	1777
2	94879	40.3382	36.7899	0245501	6.9515	26.9450	15.67038121000001	1778
1	94879U		86249.45470544	+.000000000	+000000+0	+000000+0	-1.0	1791
2	94879	40.2825	36.7335	0289979	7.3869	28.4765	15.57147842000001	1792
1	94879U		86249.45333001	+.000000000	+000000+0	+000000+0	-1.0	1813
2	94879	40.2702	36.0148	0290620	8.5757	30.5890	15.56366199000001	1814
1	94880U		86249.45361400	+.000000000	+000000+0	+000000+0	-1.0	1741
2	94880	39.2217	36.7688	0810850	51.1193	343.2557	14.40626588000001	1742
1	94880U		86249.45402245	+.000000000	+000000+0	+000000+0	-1.0	1763
2	94880	39.2844	36.8246	0873465	35.1833	358.8993	14.15415540000001	1764
1	94880U		86249.45464945	+.000000000	+000000+0	+000000+0	-1.0	1787
2	94880	39.2595	36.8002	0887955	34.9650	2.2871	14.11997392000001	1788
1	94880U		86249.45501953	+.000000000	+000000+0	+000000+0	-1.0	1801
2	94880	39.2023	36.7351	0899025	38.3469	1.3892	14.09584356000001	1802
1	94880U		86249.45356313	+.000000000	+000000+0	+000000+0	-1.0	1837
2	94880	39.2323	36.0640	0864465	35.7222	6.1036	14.17429364000001	1838
1	94882U		86249.45369555	+.000000000	+000000+0	+000000+0	-1.0	1747
2	94882	40.2860	36.8038	0123571	28.1763	2.5373	15.92745014000001	1748
1	94882U		86249.45407978	+.000000000	+000000+0	+000000+0	-1.0	1765
2	94882	39.7670	36.3568	0295163	26.6742	6.3494	15.51469116000001	1766
1	94882U		86249.45443200	+.000000000	+000000+0	+000000+0	-1.0	1781
2	94882	39.7439	36.3347	0287113	32.8418	2.5222	15.53179270000001	1782
1	94882U		86249.45476892	+.000000000	+000000+0	+000000+0	-1.0	1795
2	94882	39.7121	36.3018	0319872	33.3987	3.8835	15.45317511000001	1796
1	94882U		86249.45315866	+.000000000	+000000+0	+000000+0	-1.0	1809
2	94882	39.7761	35.6683	0259319	31.5728	7.5315	15.59921749000001	1810
1	94885U		86249.45420575	+.000000000	+000000+0	+000000+0	-1.0	1819
2	94885	38.9545	36.5199	0950636	46.8687	348.2396	14.04441864000001	1820
1	94885U		86249.45343045	+.000000000	+000000+0	+000000+0	-1.0	1833
2	94885	38.8500	35.7158	1025817	51.6768	350.4737	13.92684744000001	1834
1	94886U		86249.45431844	+.000000000	+000000+0	+000000+0	-1.0	1779
2	94886	39.9461	36.4394	0191910	58.6208	334.2416	15.82176370000001	1780

1	94886U		86249.45467922	+.00000000	+000000+0	+000000+0	-1.0	1789
2	94886	40.2159	36.6796	0350449	350.7625	40.3872	15.5615753800001	1790
1	94886U		86249.45505750	+.00000000	+000000+0	+000000+0	-1.0	1805
2	94886	40.2675	36.7294	0346564	347.8328	45.2869	15.5957273000001	1806
1	94886U		86249.45345860	+.00000000	+000000+0	+000000+0	-1.0	1823
2	94886	40.2527	36.0088	0378959	349.3322	45.5901	15.5231763400001	1824
1	94886U		86249.45381372	+.00000000	+000000+0	+000000+0	-1.0	1847
2	94886	40.2901	36.0512	0355389	344.2572	52.5951	15.6180301000001	1848
1	94887U		86249.45351045	+.00000000	+000000+0	+000000+0	-1.0	1831
2	94887	39.7847	35.6603	0283342	28.9455	8.9431	15.5722632300001	1832
1	94887U		86249.45372391	+.00000000	+000000+0	+000000+0	-1.0	1841
2	94887	39.7297	35.5943	0285758	33.7819	5.6148	15.5607046500001	1842
1	94887U		86249.45391544	+.00000000	+000000+0	+000000+0	-1.0	1857
2	94887	39.6979	35.5542	0291584	39.7363	1.0941	15.5442948300001	1858
1	94887U		86249.45417857	+.00000000	+000000+0	+000000+0	-1.0	1871
2	94887	39.7806	35.6624	0323719	30.5053	11.1269	15.4768942700001	1872
1	94888U		86249.45444627	+.00000000	+000000+0	+000000+0	-1.0	1867
2	94888	39.6942	36.3097	0753161	140.6422	259.0876	16.7616828200001	1868
1	94889U		86249.45464280	+.00000000	+000000+0	+000000+0	-1.0	1785
2	94889	38.9798	35.7705	0250602	61.5501	330.9868	15.7038200200001	1786
1	94889U		86249.45499851	+.00000000	+000000+0	+000000+0	-1.0	1799
2	94889	38.9055	35.7036	0314334	28.2906	4.6764	15.4635863000001	1800
1	94889U		86249.45341023	+.00000000	+000000+0	+000000+0	-1.0	1821
2	94889	38.9425	35.0344	0285888	31.8598	3.3440	15.5307320600001	1822
1	94889U		86249.45377723	+.00000000	+000000+0	+000000+0	-1.0	1845
2	94889	38.9259	35.0171	0243488	37.9404	359.6565	15.6339116700001	1846
1	94889U		86249.45418990	+.00000000	+000000+0	+000000+0	-1.0	1869
2	94889	38.9535	35.0485	0311020	24.7558	14.3319	15.4838548800001	1870
1	94890U		86249.45470676	+.00000000	+000000+0	+000000+0	-1.0	1793
2	94890	39.4134	36.8498	1005543	25.0741	5.3606	13.8322914300001	1794
1	94890U		86249.45506408	+.00000000	+000000+0	+000000+0	-1.0	1807
2	94890	39.7951	37.1943	0893933	17.9969	12.9812	14.1197939300001	1808
1	94890U		86249.45350290	+.00000000	+000000+0	+000000+0	-1.0	1829
2	94890	39.8297	36.5225	0909295	16.3867	16.2523	14.0968419300001	1830
1	94890U		86249.45387764	+.00000000	+000000+0	+000000+0	-1.0	1851
2	94890	39.8423	36.5357	0900903	16.1349	18.3864	14.1178164000001	1852
1	94890U		86249.45421873	+.00000000	+000000+0	+000000+0	-1.0	1873
2	94890	39.8509	36.5456	0894153	15.1945	20.9333	14.1426777800001	1874
1	94892U		86249.45493910	+.00000000	+000000+0	+000000+0	-1.0	1797
2	94892	39.1051	35.8474	0332642	36.8421	355.0740	15.4229946800001	1798
1	94892U		86249.45335917	+.00000000	+000000+0	+000000+0	-1.0	1815
2	94892	39.2261	35.2530	0293124	28.3447	5.0441	15.5125106200001	1816
1	94892U		86249.45370227	+.00000000	+000000+0	+000000+0	-1.0	1843
2	94892	39.1789	35.2068	0324191	28.5290	6.7819	15.4380373600001	1844
1	94892U		86249.45403915	+.00000000	+000000+0	+000000+0	-1.0	1863
2	94892	39.1900	35.2271	0283266	33.5091	3.9983	15.5329286500001	1864
1	94892U		86249.45439881	+.00000000	+000000+0	+000000+0	-1.0	1881
2	94892	39.2501	35.2864	0263206	26.3390	12.7895	15.5805323500001	1882
1	94893U		86249.45505245	+.00000000	+000000+0	+000000+0	-1.0	1803
2	94893	36.7118	33.8525	0322369	45.0217	348.7507	15.4687774900001	1804
1	94893U		86249.45346222	+.00000000	+000000+0	+000000+0	-1.0	1825
2	94893	37.1435	33.5841	0320937	1.9095	30.9471	15.5438928200001	1826
1	94893U		86249.45387060	+.00000000	+000000+0	+000000+0	-1.0	1853
2	94893	37.1436	33.5843	0365811	0.0503	34.7022	15.4638076400001	1854
1	94893U		86249.45425811	+.00000000	+000000+0	+000000+0	-1.0	1877
2	94893	37.1176	33.5538	0317416	4.0518	33.4148	15.5334680200001	1878
1	94893U		86249.45463273	+.00000000	+000000+0	+000000+0	-1.0	1891
2	94893	37.1261	33.5646	0320026	2.0515	37.3828	15.5423673900001	1892
1	94894U		86249.45325009	+.00000000	+000000+0	+000000+0	-1.0	1811
2	94894	39.0579	35.1377	0330877	22.3142	8.3143	15.4283597100001	1812
1	94894U		86249.45358904	+.00000000	+000000+0	+000000+0	-1.0	1839
2	94894	38.8752	34.9721	0321605	37.6296	355.9782	15.4512736600001	1840
1	94894U		86249.45398733	+.00000000	+000000+0	+000000+0	-1.0	1861
2	94894	39.0456	35.1372	0293665	25.0800	9.8856	15.5176837400001	1862
1	94894U		86249.45434351	+.00000000	+000000+0	+000000+0	-1.0	1879
2	94894	38.9900	35.0785	0278934	32.4656	4.9648	15.5457306300001	1880
1	94894U		86249.45468208	+.00000000	+000000+0	+000000+0	-1.0	1893
2	94894	38.9871	35.0753	0282102	31.9202	7.3774	15.5381980900001	1894
1	94895U		86249.45337345	+.00000000	+000000+0	+000000+0	-1.0	1817
2	94895	39.3648	35.3337	0376174	54.9642	337.5354	15.3725890600001	1818
1	94895U		86249.45392162	+.00000000	+000000+0	+000000+0	-1.0	1855
2	94895	39.8356	35.7444	0256040	35.3419	358.4287	15.5802941600001	1856

1	94895U		86249.45447840	+.00000000	+000000+0	+000000+0	-1.0	1883
2	94895	39.6719	35.5923	0320852	34.4042	2.5349	15.42436576000001	1884
1	94895U		86249.45498923	+.00000000	+000000+0	+000000+0	-1.0	1901
2	94895	39.7568	35.6826	0292848	30.5776	8.9336	15.49233101000001	1902
1	94895U		86249.45746573	+.00000000	+000000+0	+000000+0	-1.0	1927
2	94895	39.7351	36.3647	0286419	31.6333	10.8820	15.50679299000001	1928
1	94896U		86249.45349507	+.00000000	+000000+0	+000000+0	-1.0	1827
2	94896	39.0324	35.0917	0269671	61.1221	332.2874	15.65908986000001	1828
1	94896U		86249.45387291	+.00000000	+000000+0	+000000+0	-1.0	1849
2	94896	39.1975	35.2422	0278172	20.6390	12.6855	15.55776126000001	1850
1	94896U		86249.45426542	+.00000000	+000000+0	+000000+0	-1.0	1875
2	94896	39.0832	35.1285	0290857	29.6564	6.4192	15.51532185000001	1876
1	94896U		86249.45464346	+.00000000	+000000+0	+000000+0	-1.0	1889
2	94896	39.1548	35.2064	0298706	19.7750	17.7782	15.51608390000001	1890
1	94896U		86249.45499203	+.00000000	+000000+0	+000000+0	-1.0	1903
2	94896	39.1673	35.2212	0294854	19.2194	20.2533	15.52676113000001	1904
1	94898U		86249.45382360	+.00000000	+000000+0	+000000+0	-1.0	1985
2	94898	39.3250	35.3059	0311859	48.5601	344.8666	15.50171331000001	1986
1	94899U		86249.45409106	+.00000000	+000000+0	+000000+0	-1.0	1865
2	94899	38.0118	36.4268	2100512	32.3111	359.9544	11.38635678000001	1866
1	94899U		86249.45449264	+.00000000	+000000+0	+000000+0	-1.0	1885
2	94899	38.2003	36.6033	2139561	26.4051	5.2394	11.30545132000001	1886
1	94899U		86249.45485271	+.00000000	+000000+0	+000000+0	-1.0	1899
2	94899	38.1380	36.5389	2189102	26.7237	6.4650	11.19749921000001	1900
1	94899U		86249.45719195	+.00000000	+000000+0	+000000+0	-1.0	1911
2	94899	38.1800	37.2923	2150012	26.4142	8.2616	11.28317031000001	1912
1	94899U		86249.45761306	+.00000000	+000000+0	+000000+0	-1.0	1931
2	94899	38.1387	37.2403	2210440	27.7932	8.9993	11.14162542000001	1932
1	94900U		86249.45422852	+.00000000	+000000+0	+000000+0	-1.0	2013
2	94900	39.7648	35.6721	0269846	78.4732	315.2534	15.78557015000001	2014
1	94901U		86249.45465114	+.00000000	+000000+0	+000000+0	-1.0	1897
2	94901	38.2326	34.2614	0860833	31.5980	0.9566	14.17157749000001	1898
1	94901U		86249.45703400	+.00000000	+000000+0	+000000+0	-1.0	1909
2	94901	39.5040	36.1477	0312339	43.3278	351.5347	15.48560288000001	1910
1	94902U		86249.45477479	+.00000000	+000000+0	+000000+0	-1.0	1895
2	94902	38.9402	35.0457	0281680	53.7575	338.9240	15.59657191000001	1896
1	94902U		86249.45723826	+.00000000	+000000+0	+000000+0	-1.0	1913
2	94902	38.9939	35.8004	0316682	28.2873	5.8008	15.45813110000001	1914
1	94902U		86249.45776157	+.00000000	+000000+0	+000000+0	-1.0	1941
2	94902	38.9706	35.7780	0324621	29.0507	7.9988	15.43843707000001	1942
1	94902U		86249.45826991	+.00000000	+000000+0	+000000+0	-1.0	1975
2	94902	38.9629	35.7700	0299546	31.8423	8.2458	15.49562645000001	1976
1	94902U		86249.45879131	+.00000000	+000000+0	+000000+0	-1.0	2009
2	94902	38.9767	35.7872	0336259	27.4511	15.1748	15.41585173000001	2010
1	94903U		86249.45703262	+.00000000	+000000+0	+000000+0	-1.0	1907
2	94903	39.2888	35.9162	03350960	71.7896	323.3328	15.57140878000001	1908
1	94903U		86249.45742461	+.00000000	+000000+0	+000000+0	-1.0	1925
2	94903	39.0542	36.4381	0291435	13.5069	19.8668	15.54672771000001	1926
1	94903U		86249.45777325	+.00000000	+000000+0	+000000+0	-1.0	1945
2	94903	39.9271	36.5108	0310464	4.0978	30.5810	15.54946231000001	1946
1	94903U		86249.45820234	+.00000000	+000000+0	+000000+0	-1.0	1969
2	94903	39.0943	36.4755	0317801	6.2319	30.9409	15.52090889000001	1970
1	94904U		86249.45727069	+.00000000	+000000+0	+000000+0	-1.0	1915
2	94904	39.7733	36.4547	0166382	94.5978	298.3055	16.04309502000001	1916
1	94904U		86249.45768743	+.00000000	+000000+0	+000000+0	-1.0	1937
2	94904	39.2130	35.9493	0317648	38.5974	355.7695	15.46090586000001	1938
1	94905U		86249.45732809	+.00000000	+000000+0	+000000+0	-1.0	1917
2	94905	39.1477	35.7779	0678950	29.0497	3.2760	14.66119251000001	1918
1	94905U		86249.45767489	+.00000000	+000000+0	+000000+0	-1.0	1933
2	94905	39.0383	36.4298	0341229	32.7600	1.4845	15.46454946000001	1934
1	94905U		86249.45801814	+.00000000	+000000+0	+000000+0	-1.0	1959
2	94905	39.9235	36.5140	0346382	24.2399	11.2801	15.45978846000001	1960
1	94905U		86249.45835982	+.00000000	+000000+0	+000000+0	-1.0	1981
2	94905	39.8517	36.4375	0313149	35.7334	2.5229	15.52766525000001	1982
1	94905U		86249.45871106	+.00000000	+000000+0	+000000+0	-1.0	2003
2	94905	39.8858	36.4767	0395123	27.2140	12.2692	15.34213412000001	2004
1	94907U		86249.45733692	+.00000000	+000000+0	+000000+0	-1.0	1919
2	94907	38.7132	35.5290	0498009	111.2745	206.2574	15.97251490000001	1920
1	94907U		86249.45769128	+.00000000	+000000+0	+000000+0	-1.0	1935
2	94907	38.9507	35.7506	0320257	34.9166	359.0566	15.45192395000001	1936
1	94911U		86249.45782571	+.00000000	+000000+0	+000000+0	-1.0	1947
2	94911	39.2102	35.8520	0434374	55.3917	338.2446	15.25325156000001	1948

1	94911U		86249.45846237	+.00000000	+000000+0	+000000+0	-1.0	1989
2	94911	39.7544	36.3365	0297491	33.8632	1.1433	15.48770658000001	1990
1	94911U		86249.45882174	+.00000000	+000000+0	+000000+0	-1.0	2015
2	94911	39.7663	36.3487	0336184	26.3071	10.1826	15.40031885000001	2016
1	94911U		86249.45721767	+.00000000	+000000+0	+000000+0	-1.0	2031
2	94911	39.7785	35.6571	0286978	29.7757	8.9429	15.51178032000001	2032
1	94911U		86249.45760246	+.00000000	+000000+0	+000000+0	-1.0	2061
2	94911	39.7745	35.6524	0330876	27.6502	12.9951	15.41159480000001	2062
1	94920U		86249.45851396	+.00000000	+000000+0	+000000+0	-1.0	1991
2	94920	38.6839	35.4946	0428331	89.7501	307.2373	15.64631922000001	1992
1	94920U		86249.45888771	+.00000000	+000000+0	+000000+0	-1.0	2019
2	94920	39.1515	35.9457	0300447	29.7869	4.7370	15.49573822000001	2020
1	94920U		86249.45727907	+.00000000	+000000+0	+000000+0	-1.0	2037
2	94920	39.0418	35.1281	0336187	31.8179	4.7995	15.40927953000001	2038
1	94920U		86249.45764045	+.00000000	+000000+0	+000000+0	-1.0	2067
2	94920	39.0770	35.1673	0320411	30.9520	7.6056	15.44756388000001	2068
1	94920U		86249.45799846	+.00000000	+000000+0	+000000+0	-1.0	2097
2	94920	39.0569	35.1432	0336739	32.7029	7.9476	15.40653267000001	2098
1	94923U		86249.45863851	+.00000000	+000000+0	+000000+0	-1.0	2001
2	94923	39.0469	36.7259	0524639	15.3031	14.5589	14.99015450000001	2002
1	94924U		86249.45884351	+.00000000	+000000+0	+000000+0	-1.0	2017
2	94924	40.5657	37.0018	0208535	27.7034	4.5516	15.71484611000001	2018
1	94924U		86249.45740985	+.00000000	+000000+0	+000000+0	-1.0	2045
2	94924	40.5409	36.2740	0338025	5.1249	28.5019	15.47876640000001	2046
1	94924U		86249.45778948	+.00000000	+000000+0	+000000+0	-1.0	2083
2	94924	40.3922	36.1215	0366118	15.1871	21.1474	15.36204887000001	2084
1	94924U		86249.45815957	+.00000000	+000000+0	+000000+0	-1.0	2109
2	94924	40.5659	36.3152	0223634	352.6644	45.3958	15.78986635000001	2110
1	94924U		86249.45874201	+.00000000	+000000+0	+000000+0	-1.0	2151
2	94924	40.4086	36.1255	0411478	20.4197	21.3180	15.23045292000001	2152
1	94926U		86249.45895212	+.00000000	+000000+0	+000000+0	-1.0	2023
2	94926	40.5743	37.0927	0189388	140.2335	252.6765	16.37709410000001	2024
1	94935U		86249.45747352	+.00000000	+000000+0	+000000+0	-1.0	2051
2	94935	39.6535	35.5555	0456135	107.0724	289.3313	15.92702294000001	2052
1	94935U		86249.45800000	+.00000000	+000000+0	+000000+0	-1.0	2099
2	94935	39.9767	35.8437	0333793	17.9089	15.3342	15.42891909000001	2100
1	94935U		86249.45847208	+.00000000	+000000+0	+000000+0	-1.0	2127
2	94935	40.0209	35.8872	0301325	15.7476	20.0738	15.51112859000001	2128
1	94935U		86249.45888235	+.00000000	+000000+0	+000000+0	-1.0	2161
2	94935	39.9474	35.8068	0376102	17.0306	20.9098	15.33537733000001	2162
1	94935U		86249.46117700	+.00000000	+000000+0	+000000+0	-1.0	2187
2	94935	39.9524	36.5171	03350648	16.9309	22.9929	15.39384855000001	2188
1	94948U		86249.45885587	+.00000000	+000000+0	+000000+0	-1.0	2781
2	94948	39.5100	35.4555	0354841	56.0263	337.8587	15.44344629000001	2782
1	94949U		86249.45892389	+.00000000	+000000+0	+000000+0	-1.0	2785
2	94949	39.3186	35.2731	0435438	47.0359	347.5917	15.21043443000001	2786
1	94954U		86249.46106278	+.00000000	+000000+0	+000000+0	-1.0	2179
2	94954	40.1400	36.7434	0248742	109.0096	205.2059	16.08987595000001	2180
1	94954U		86249.46145176	+.00000000	+000000+0	+000000+0	-1.0	2629
2	94954	39.7518	36.3941	0409249	11.6454	20.6633	15.27954186000001	2630
1	94954U		86249.46186723	+.00000000	+000000+0	+000000+0	-1.0	2661
2	94954	39.8163	36.4572	0299002	21.0094	14.5443	15.49845239000001	2662
1	94954U		86249.46227839	+.00000000	+000000+0	+000000+0	-1.0	2693
2	94954	39.7656	36.4028	0359014	16.6237	20.7803	15.37506152000001	2694
1	94956U		86249.46114236	+.00000000	+000000+0	+000000+0	-1.0	2183
2	94956	40.3863	37.0379	0099968	129.0188	264.1551	16.25486092000001	2184
1	94956U		86249.46162357	+.00000000	+000000+0	+000000+0	-1.0	2643
2	94956	39.4741	36.1904	0360196	27.2812	7.7108	15.35436848000001	2644
1	94956U		86249.46195938	+.00000000	+000000+0	+000000+0	-1.0	2667
2	94956	39.4957	36.2130	0315588	30.9977	6.1399	15.45681928000001	2668
1	94956U		86249.46229639	+.00000000	+000000+0	+000000+0	-1.0	2691
2	94956	39.4279	36.1367	0380954	29.7157	9.1626	15.30278397000001	2692
1	94956U		86249.46263284	+.00000000	+000000+0	+000000+0	-1.0	2719
2	94956	39.4484	36.1616	0356147	31.8011	9.1058	15.35796192000001	2720
1	94959U		86249.46148375	+.00000000	+000000+0	+000000+0	-1.0	2837
2	94959	39.1681	35.9309	0359452	38.3367	354.3688	15.36269970000001	2838
1	94961U		86249.46187793	+.00000000	+000000+0	+000000+0	-1.0	2663
2	94961	39.0796	35.7167	0636246	34.0060	359.1909	14.71075830000001	2664
1	94961U		86249.46221735	+.00000000	+000000+0	+000000+0	-1.0	2687
2	94961	40.0732	36.6586	0375836	19.5106	13.7713	15.34331945000001	2688
1	94961U		86249.46255127	+.00000000	+000000+0	+000000+0	-1.0	2713
2	94961	40.0126	36.5989	0338796	30.2008	5.7732	15.41139674000001	2714

1	94961U		86249.46288528	+.00000000	+000000+0	+000000+0	-1.0	2731
2	94961	39.9854	36.5699	0395283	24.5566	12.7853	15.2872767800001	2732
1	94961U		86249.46127137	+.00000000	+000000+0	+000000+0	-1.0	2757
2	94961	40.0090	35.8920	0329877	29.0000	10.6516	15.4309595400001	2758
1	94965U		86249.46214764	+.00000000	+000000+0	+000000+0	-1.0	2681
2	94965	39.2597	35.8764	0513848	41.9952	351.9383	15.0131426100001	2682
1	94966U		86249.46238351	+.00000000	+000000+0	+000000+0	-1.0	2893
2	94966	38.9787	35.7806	0364151	73.2678	322.6334	15.5534348800001	2894
1	94969U		86249.46248049	+.00000000	+000000+0	+000000+0	-1.0	2707
2	94969	39.1405	35.9399	0294468	55.5807	337.9591	15.5711331400001	2708
1	94970U		86249.46259293	+.00000000	+000000+0	+000000+0	-1.0	2715
2	94970	39.1958	35.9070	0371261	69.7814	325.1059	15.5089088500001	2716
1	94970U		86249.46118043	+.00000000	+000000+0	+000000+0	-1.0	2745
2	94970	39.4581	35.4478	0293891	42.2897	353.4764	15.5225144700001	2746
1	94974U		86249.46106387	+.00000000	+000000+0	+000000+0	-1.0	2739
2	94974	37.4060	34.7950	0908596	17.0769	13.7510	14.1129164300001	2740
1	94974U		86249.46142697	+.00000000	+000000+0	+000000+0	-1.0	2769
2	94974	36.9708	34.3422	1030330	21.4801	11.9275	13.8068538700001	2770
1	94974U		86249.46180541	+.00000000	+000000+0	+000000+0	-1.0	2805
2	94974	37.0177	34.3951	0925164	25.3134	10.8780	14.0232471800001	2806
1	94974U		86249.46221917	+.00000000	+000000+0	+000000+0	-1.0	2835
2	94974	37.0106	34.3864	0945019	23.7545	14.2125	13.9880309700001	2836
1	94974U		86249.46256122	+.00000000	+000000+0	+000000+0	-1.0	2859
2	94974	36.9623	34.3214	0958339	24.7436	15.1159	13.9502705800001	2860
1	94977U		86249.46123922	+.00000000	+000000+0	+000000+0	-1.0	2753
2	94977	40.1608	36.0126	0350636	25.7240	6.3204	15.3798676500001	2754
1	94977U		86249.46187470	+.00000000	+000000+0	+000000+0	-1.0	2811
2	94977	40.1372	35.9909	0368135	22.0129	13.2710	15.3446030400001	2812
1	94997U		86249.46269330	+.00000000	+000000+0	+000000+0	-1.0	2873
2	94997	40.1701	35.9558	0402605	59.6909	334.5132	15.3623760100001	2874
1	94997U		86249.46505467	+.00000000	+000000+0	+000000+0	-1.0	2895
2	94997	40.5898	37.0411	0390102	20.8376	12.4164	15.2909686600001	2896
1	94997U		86249.46541677	+.00000000	+000000+0	+000000+0	-1.0	2931
2	94997	40.6325	37.0826	0375833	20.2850	14.9320	15.3258921900001	2932
1	94997U		86249.46576110	+.00000000	+000000+0	+000000+0	-1.0	2965
2	94997	40.5783	37.0256	0367637	24.4643	13.0080	15.3325531600001	2966
1	94997U		86249.46611925	+.00000000	+000000+0	+000000+0	-1.0	2999
2	94997	40.6109	37.0627	0353263	21.6183	17.6559	15.3751403600001	3000
1	90003U		86249.46486460	+.00000000	+000000+0	+000000+0	-1.0	2887
2	90003	39.8975	36.5474	0332116	66.2391	327.6985	15.5416951700001	2888
1	90003U		86249.46536908	+.00000000	+000000+0	+000000+0	-1.0	2925
2	90003	39.7476	36.4112	0374232	41.4438	353.9649	15.3136968300001	2926
1	90009U		86249.46560551	+.00000000	+000000+0	+000000+0	-1.0	2947
2	90009	39.2568	36.8396	0918246	35.9144	357.6974	14.0352629600001	2948
1	90009U		86249.46598619	+.00000000	+000000+0	+000000+0	-1.0	2985
2	90009	39.4484	37.0213	0905486	21.8394	11.0258	13.8969724800001	2986
1	90009U		86249.46633354	+.00000000	+000000+0	+000000+0	-1.0	3023
2	90009	39.4611	37.0344	0971718	21.7935	12.8271	13.9284920300001	3024
1	90009U		86249.46667457	+.00000000	+000000+0	+000000+0	-1.0	3051
2	90009	39.4345	37.0048	0973199	22.2249	14.1952	13.9219858300001	3052
1	90009U		86249.46505714	+.00000000	+000000+0	+000000+0	-1.0	3081
2	90009	39.3577	36.2067	1001163	24.4064	14.0577	13.8418107300001	3082
1	90010U		86249.46553648	+.00000000	+000000+0	+000000+0	-1.0	2941
2	90010	38.7814	35.5955	0447603	85.0530	311.6736	15.5509146000001	2942
1	90010U		86249.46604214	+.00000000	+000000+0	+000000+0	-1.0	2987
2	90010	39.4051	36.1890	0411344	13.6191	19.9884	15.2684936800001	2988
1	90013U		86249.46600663	+.00000000	+000000+0	+000000+0	-1.0	2981
2	90013	40.0554	36.6039	0341244	67.4361	327.5337	15.5351119900001	2982
1	90016U		86249.46625019	+.00000000	+000000+0	+000000+0	-1.0	3013
2	90016	39.6396	36.3163	0456897	97.8362	299.5090	15.7432858300001	3014
1	90023U		86249.46657962	+.00000000	+000000+0	+000000+0	-1.0	3045
2	90023	39.6709	36.3691	0398943	91.9409	304.5070	15.7229236500001	3046
1	90023U		86249.46515148	+.00000000	+000000+0	+000000+0	-1.0	3089
2	90023	39.7107	35.7020	0436419	24.2246	10.4996	15.1770630900001	3090
1	90023U		86249.46566074	+.00000000	+000000+0	+000000+0	-1.0	3125
2	90023	39.7865	35.7784	0378895	31.4022	6.7113	15.3037201600001	3126
1	90026U		86249.46487364	+.00000000	+000000+0	+000000+0	-1.0	3069
2	90026	41.0867	37.7060	0601213	29.8319	1.8419	14.7696349900001	3070
1	90028U		86249.46491171	+.00000000	+000000+0	+000000+0	-1.0	3071
2	90028	39.0754	35.0989	0432535	28.7891	4.2305	15.1926749900001	3072
1	90032U		86249.46530287	+.00000000	+000000+0	+000000+0	-1.0	3095
2	90032	35.0689	30.9446	2176962	13.7602	14.1673	11.4169579500001	3096

1	90035U		86249.46552847	+.00000000	+000000+0	+000000+0	-1.0	3109
2	90035	40.4989	36.2937	0163022	60.1524	333.7597	15.89349983000001	3110
1	90035U		86249.46563588	+.00000000	+000000+0	+000000+0	-1.0	3127
2	90035	40.5774	36.3676	0441440	350.9465	39.3695	15.41240376000001	3128
1	90035U		86249.46582650	+.00000000	+000000+0	+000000+0	-1.0	3141
2	90035	40.5904	36.3807	0476987	349.8950	41.1305	15.35931009000001	3142
1	90035U		86249.46596874	+.00000000	+000000+0	+000000+0	-1.0	3153
2	90035	40.5502	36.3384	0394805	354.2676	38.4664	15.46214663000001	3154
1	90035U		86249.46607493	+.00000000	+000000+0	+000000+0	-1.0	3157
2	90035	40.6331	36.4254	0432147	350.0469	42.6817	15.43811646000001	3158
1	90035U		86249.46615802	+.00000000	+000000+0	+000000+0	-1.0	3167
2	90035	40.6210	36.4121	0331680	349.6505	44.3336	15.61887947000001	3168
1	90035U		86249.46625136	+.00000000	+000000+0	+000000+0	-1.0	3177
2	90035	40.7312	36.5338	0385232	345.0028	48.7500	15.57749536000001	3178
1	90035U		86249.46633306	+.00000000	+000000+0	+000000+0	-1.0	3189
2	90035	40.6414	36.4346	0429991	349.5754	44.5711	15.44755898000001	3190
1	90035U		86249.46641493	+.00000000	+000000+0	+000000+0	-1.0	3199
2	90035	40.7522	36.5639	0378142	341.5739	52.9883	15.62960301000001	3200
1	90035U		86249.46651565	+.00000000	+000000+0	+000000+0	-1.0	3215
2	90035	40.6799	36.4796	0403064	347.1573	48.0693	15.52229135000001	3216
1	90035U		86249.46660088	+.00000000	+000000+0	+000000+0	-1.0	3225
2	90035	40.6376	36.4302	0396340	348.4833	47.3802	15.51794297000001	3226
1	90035U		86249.46670285	+.00000000	+000000+0	+000000+0	-1.0	3241
2	90035	40.5886	36.3693	0395229	349.9412	46.6193	15.50289860000001	3242
1	90035U		86249.46678093	+.00000000	+000000+0	+000000+0	-1.0	3253
2	90035	40.5910	36.3723	0435169	352.4618	44.3398	15.40413943000001	3254
1	90035U		86249.46882687	+.00000000	+000000+0	+000000+0	-1.0	3261
2	90035	40.5977	37.0856	0433400	351.8375	45.4512	15.41487583000001	3262
1	90035U		86249.46890039	+.00000000	+000000+0	+000000+0	-1.0	3277
2	90035	40.6257	37.1224	0336411	337.2055	60.7276	15.74002191000001	3278
1	90035U		86249.46897960	+.00000000	+000000+0	+000000+0	-1.0	3293
2	90035	40.6369	37.1370	0413575	346.2506	51.7302	15.51914658000001	3294
1	90035U		86249.46905559	+.00000000	+000000+0	+000000+0	-1.0	3305
2	90035	40.5975	37.0853	0421908	351.9918	46.6717	15.43228849000001	3306
1	90035U		86249.46915034	+.00000000	+000000+0	+000000+0	-1.0	3319
2	90035	40.6083	37.0994	0421002	350.4311	48.6730	15.45329259000001	3320
1	90035U		86249.46922873	+.00000000	+000000+0	+000000+0	-1.0	3331
2	90035	40.6234	37.1206	0436510	350.2416	49.1373	15.43101592000001	3332
1	90035U		86249.46933376	+.00000000	+000000+0	+000000+0	-1.0	3349
2	90035	40.6424	37.1473	0442887	349.7559	50.1050	15.42732846000001	3350
1	90036U		86249.46561795	+.00000000	+000000+0	+000000+0	-1.0	3123
2	90036	41.4047	37.0946	0458283	359.2799	30.5308	15.27236995000001	3124
1	90036U		86249.46579146	+.00000000	+000000+0	+000000+0	-1.0	3143
2	90036	40.4358	36.1924	0434536	36.0725	358.4109	15.18156161000001	3144
1	90036U		86249.46605739	+.00000000	+000000+0	+000000+0	-1.0	3161
2	90036	40.5703	36.3314	0378102	40.8867	355.2990	15.32179182000001	3162
1	90036U		86249.46622268	+.00000000	+000000+0	+000000+0	-1.0	3181
2	90036	40.5522	36.3116	0436940	32.0034	4.4057	15.17933104000001	3182
1	90036U		86249.46638456	+.00000000	+000000+0	+000000+0	-1.0	3205
2	90036	40.5257	36.2826	0439958	34.8249	2.7260	15.17052382000001	3206
1	90036U		86249.46656630	+.00000000	+000000+0	+000000+0	-1.0	3217
2	90036	40.7042	36.4915	0302538	36.6541	1.9445	15.49784632000001	3218
1	90036U		86249.46668930	+.00000000	+000000+0	+000000+0	-1.0	3243
2	90036	40.6156	36.3800	0391886	35.0316	4.1639	15.28479686000001	3244
1	90036U		86249.46877091	+.00000000	+000000+0	+000000+0	-1.0	3263
2	90036	40.6241	37.1036	0311015	39.1007	1.1548	15.47594451000001	3264
1	90036U		86249.46894176	+.00000000	+000000+0	+000000+0	-1.0	3295
2	90036	40.5924	37.0640	0382916	36.8200	4.1854	15.30468729000001	3296
1	90036U		86249.46908032	+.00000000	+000000+0	+000000+0	-1.0	3317
2	90036	40.5915	37.0628	0389103	35.5557	6.1130	15.29151983000001	3318
1	90036U		86249.46928326	+.00000000	+000000+0	+000000+0	-1.0	3345
2	90036	40.5454	37.0013	0406656	39.7006	3.3566	15.24606907000001	3346
1	90036U		86249.46945890	+.00000000	+000000+0	+000000+0	-1.0	3379
2	90036	40.6951	37.2151	0448037	32.9223	10.4073	15.16070916000001	3380
1	90036U		86249.46962312	+.00000000	+000000+0	+000000+0	-1.0	3391
2	90036	40.5515	37.0099	0334250	32.7501	11.8623	15.42950900000001	3392
1	90037U		86249.46557392	+.00000000	+000000+0	+000000+0	-1.0	3121
2	90037	38.9615	35.0909	0451279	25.7098	7.0596	15.13632022000001	3122
1	90037U		86249.46573252	+.00000000	+000000+0	+000000+0	-1.0	3135
2	90037	39.1093	35.2364	0434461	16.3290	16.4551	15.20479874000001	3136
1	90037U		86249.46595690	+.00000000	+000000+0	+000000+0	-1.0	3151
2	90037	39.0847	35.2103	0421311	19.9517	14.4091	15.21935227000001	3152

1	98037U		86249.46618142	+.88888888	+888888+8	+888888+8	-1.8	3171
2	98037	39.2418	35.3848 8381743	15.8685	19.4305	15.3279267888881		3172
1	98037U		86249.46632555	+.88888888	+888888+8	+888888+8	-1.8	3193
2	98037	38.9608	35.8556 8427711	28.8789	9.8521	15.1758974388881		3194
1	98037U		86249.46658688	+.88888888	+888888+8	+888888+8	-1.8	3209
2	98037	39.8756	35.1909 8481309	23.5278	14.1938	15.2586952388881		3218
1	98037U		86249.46664888	+.88888888	+888888+8	+888888+8	-1.8	3231
2	98037	39.2847	35.3528 8372888	16.4325	21.4996	15.3479857388881		3232
1	98037U		86249.46675747	+.88888888	+888888+8	+888888+8	-1.8	3247
2	98037	39.1998	35.3448 8386725	15.6467	22.8254	15.3214638888881		3248
1	98037U		86249.46883391	+.88888888	+888888+8	+888888+8	-1.8	3271
2	98037	39.1428	35.9798 8411175	19.3881	19.9881	15.2464591888881		3272
1	98037U		86249.46894833	+.88888888	+888888+8	+888888+8	-1.8	3291
2	98037	39.8782	35.8925 8414975	26.5353	14.8565	15.2848344788881		3292
1	98037U		86249.46986885	+.88888888	+888888+8	+888888+8	-1.8	3307
2	98037	39.1985	36.8441 8481771	16.5249	23.8766	15.2841525288881		3308
1	98037U		86249.46917913	+.88888888	+888888+8	+888888+8	-1.8	3327
2	98037	39.1638	36.8881 8399177	18.5555	22.6791	15.2778879788881		3328
1	98037U		86249.46938114	+.88888888	+888888+8	+888888+8	-1.8	3343
2	98037	39.1458	35.9888 8348883	16.1282	25.8867	15.4832814388881		3344
1	98037U		86249.46942821	+.88888888	+888888+8	+888888+8	-1.8	3363
2	98037	39.1567	35.9977 8415991	21.2485	21.4484	15.2244871988881		3364
1	98037U		86249.46955882	+.88888888	+888888+8	+888888+8	-1.8	3381
2	98037	39.1482	35.9853 8378588	16.8747	27.2367	15.3562288288881		3382
1	98037U		86249.46971217	+.88888888	+888888+8	+888888+8	-1.8	3401
2	98037	39.1727	36.8237 8461347	24.6851	19.6685	15.1886368888881		3402
1	98041U		86249.46588115	+.88888888	+888888+8	+888888+8	-1.8	3163
2	98041	39.2583	35.2995 8397828	56.7743	338.5684	15.3517725188881		3164
1	98041U		86249.46622184	+.88888888	+888888+8	+888888+8	-1.8	3175
2	98041	39.5571	35.5874 8432118	19.8173	14.3844	15.2838362388881		3176
1	98041U		86249.46632734	+.88888888	+888888+8	+888888+8	-1.8	3191
2	98041	39.4264	35.4432 8436854	28.6671	6.8541	15.1656295588881		3192
1	98041U		86249.46646949	+.88888888	+888888+8	+888888+8	-1.8	3207
2	98041	39.6542	35.6998 8329887	28.6837	7.6663	15.4188275488881		3208
1	98041U		86249.46659885	+.88888888	+888888+8	+888888+8	-1.8	3233
2	98041	39.3649	35.3632 8527675	24.5755	11.8793	14.9664678488881		3234
1	98041U		86249.46674289	+.88888888	+888888+8	+888888+8	-1.8	3251
2	98041	39.5651	35.6828 8398238	25.8191	11.7846	15.2629843788881		3252
1	98041U		86249.46888183	+.88888888	+888888+8	+888888+8	-1.8	3259
2	98041	39.7618	36.5485 8381459	18.7658	19.8838	15.5115891588881		3268
1	98041U		86249.46889189	+.88888888	+888888+8	+888888+8	-1.8	3279
2	98041	39.6264	36.3831 8354917	25.1128	13.4994	15.3662832288881		3288
1	98041U		86249.46899888	+.88888888	+888888+8	+888888+8	-1.8	3299
2	98041	39.5635	36.3826 8393193	26.5211	12.6898	15.2725462288881		3308
1	98041U		86249.46989266	+.88888888	+888888+8	+888888+8	-1.8	3311
2	98041	39.6889	36.3584 8484492	23.8887	16.4436	15.2597248788881		3312
1	98041U		86249.46917322	+.88888888	+888888+8	+888888+8	-1.8	3325
2	98041	39.4225	36.1118 8427154	35.9768	5.8564	15.1681214388881		3326
1	98041U		86249.46929258	+.88888888	+888888+8	+888888+8	-1.8	3337
2	98041	39.5293	36.2547 8442322	29.1781	11.8129	15.1477343388881		3338
1	98041U		86249.46938583	+.88888888	+888888+8	+888888+8	-1.8	3365
2	98041	39.5499	36.2835 8312481	26.6816	15.8424	15.4582863388881		3366
1	98041U		86249.46958561	+.88888888	+888888+8	+888888+8	-1.8	3385
2	98041	39.5734	36.3162 8349235	23.4973	18.4793	15.3858884288881		3386
1	98041U		86249.46975415	+.88888888	+888888+8	+888888+8	-1.8	3405
2	98041	39.5513	36.2839 8392495	26.8636	16.5889	15.2715954688881		3406
1	98041U		86249.46989525	+.88888888	+888888+8	+888888+8	-1.8	3419
2	98041	39.5511	36.2836 8317543	18.1898	33.4468	15.5344392388881		3428
1	98046U		86249.46628885	+.88888888	+888888+8	+888888+8	-1.8	3169
2	98046	39.9117	35.6657 8586479	51.8814	344.2788	14.9867925588881		3178
1	98046U		86249.46629818	+.88888888	+888888+8	+888888+8	-1.8	3179
2	98046	48.7665	36.5888 8388789	38.2623	356.8973	15.3126148988881		3188
1	98046U		86249.46638418	+.88888888	+888888+8	+888888+8	-1.8	3195
2	98046	48.6148	36.3448 8396845	52.8776	343.2282	15.3388586288881		3196
1	98046U		86249.46658582	+.88888888	+888888+8	+888888+8	-1.8	3213
2	98046	48.9684	36.7848 8346938	33.9778	1.1876	15.4125268588881		3214
1	98046U		86249.46668897	+.88888888	+888888+8	+888888+8	-1.8	3229
2	98046	48.6865	36.4121 8354741	55.5623	341.7253	15.4444175188881		3238
1	98046U		86249.46671438	+.88888888	+888888+8	+888888+8	-1.8	3245
2	98046	48.6715	36.3957 8442818	35.7823	8.8668	15.1879875788881		3246
1	98046U		86249.46877738	+.88888888	+888888+8	+888888+8	-1.8	3257
2	98046	48.6911	37.1227 8416489	42.8286	354.9138	15.2549828488881		3258

1 90046U		86249.46885871	+.00000000	+00000+0	+00000+0	-1.0	3267
2 90046	40.7065	37.1404 0382793	44.2077	354.0307	15.3374423900001		3268
1 90046U		86249.46893288	+.00000000	+00000+0	+00000+0	-1.0	3283
2 90046	40.6737	37.1021 0454614	37.9410	0.2671	15.1599921800001		3284
1 90046U		86249.46901350	+.00000000	+00000+0	+00000+0	-1.0	3297
2 90046	40.7579	37.2021 0353773	46.2631	352.8970	15.4095718100001		3298
1 90046U		86249.46910047	+.00000000	+00000+0	+00000+0	-1.0	3309
2 90046	40.8185	37.2750 0310104	42.7340	356.5830	15.5087339900001		3310
1 90046U		86249.46917490	+.00000000	+00000+0	+00000+0	-1.0	3323
2 90046	40.7349	37.1724 0423242	38.4267	1.0967	15.2362095400001		3324
1 90046U		86249.46925589	+.00000000	+00000+0	+00000+0	-1.0	3335
2 90046	40.7400	37.1788 0376715	41.2326	358.9489	15.3478128600001		3336
1 90046U		86249.46933419	+.00000000	+00000+0	+00000+0	-1.0	3347
2 90046	40.7190	37.1521 0383844	42.7311	358.0148	15.3316413300001		3348
1 90046U		86249.46940974	+.00000000	+00000+0	+00000+0	-1.0	3367
2 90046	40.7571	37.2013 0469135	36.7639	3.8549	15.1290395400001		3368
1 90046U		86249.46950541	+.00000000	+00000+0	+00000+0	-1.0	3373
2 90046	40.6846	37.1060 0320381	50.9305	351.2090	15.4938531400001		3374
1 90046U		86249.46960234	+.00000000	+00000+0	+00000+0	-1.0	3389
2 90046	40.7288	37.1653 0417276	41.6473	0.4866	15.2516551100001		3390
1 90046U		86249.46971038	+.00000000	+00000+0	+00000+0	-1.0	3395
2 90046	40.7484	37.1921 0386455	39.4804	3.0706	15.3259572200001		3396
1 90046U		86249.46982154	+.00000000	+00000+0	+00000+0	-1.0	3409
2 90046	40.6640	37.0738 0415463	49.4955	354.5368	15.2623916400001		3410
1 90046U		86249.46991907	+.00000000	+00000+0	+00000+0	-1.0	3417
2 90046	40.7677	37.2225 0444469	42.0364	1.8182	15.1877144500001		3418
1 90050U		86249.46673681	+.00000000	+00000+0	+00000+0	-1.0	3249
2 90050	38.9622	35.1184 0338699	49.7414	345.5077	15.4284955200001		3250
1 90050U		86249.46877289	+.00000000	+00000+0	+00000+0	-1.0	3255
2 90050	39.0922	35.9554 0415698	17.5976	15.6801	15.2422531900001		3256
1 90050U		86249.46886403	+.00000000	+00000+0	+00000+0	-1.0	3273
2 90050	39.1451	36.0124 0406644	15.2753	18.3161	15.2739274600001		3274
1 90050U		86249.46894479	+.00000000	+00000+0	+00000+0	-1.0	3287
2 90050	39.3174	36.2006 0293933	20.9662	13.6682	15.5106089400001		3288
1 90050U		86249.46902865	+.00000000	+00000+0	+00000+0	-1.0	3301
2 90050	38.7738	35.5899 0452155	30.0439	5.8353	15.1178973700001		3302
1 90050U		86249.46912807	+.00000000	+00000+0	+00000+0	-1.0	3313
2 90050	39.1430	36.0143 0484125	10.0354	24.2527	15.1400033200001		3314
1 90050U		86249.46920803	+.00000000	+00000+0	+00000+0	-1.0	3329
2 90050	38.9228	35.7566 0473299	22.7260	13.3242	15.0869820500001		3330
1 90050U		86249.46928978	+.00000000	+00000+0	+00000+0	-1.0	3341
2 90050	39.2985	36.2020 0280967	13.9742	22.2737	15.5629525400001		3342
1 90050U		86249.46937003	+.00000000	+00000+0	+00000+0	-1.0	3355
2 90050	39.0519	35.9056 0407332	17.2381	19.0495	15.0842412900001		3356
1 90050U		86249.46944624	+.00000000	+00000+0	+00000+0	-1.0	3369
2 90050	39.1461	36.0212 0290639	20.8749	16.7108	15.5136116900001		3370
1 90050U		86249.46952385	+.00000000	+00000+0	+00000+0	-1.0	3377
2 90050	38.9546	35.7815 0548451	18.8275	18.2954	14.9382626700001		3378
1 90050U		86249.46960009	+.00000000	+00000+0	+00000+0	-1.0	3387
2 90050	39.1666	36.0512 0409379	13.9219	23.5817	15.2797910300001		3388
1 90050U		86249.46969444	+.00000000	+00000+0	+00000+0	-1.0	3393
2 90050	39.0901	35.9526 0378059	20.5007	18.1835	15.3127997000001		3394
1 90050U		86249.46976854	+.00000000	+00000+0	+00000+0	-1.0	3403
2 90050	38.9512	35.7690 0493081	22.6791	16.3243	15.0387571300001		3404
1 90050U		86249.46985133	+.00000000	+00000+0	+00000+0	-1.0	3411
2 90050	39.0761	35.9368 0371355	21.8714	17.8179	15.3213078500001		3412
1 90050U		86249.46992338	+.00000000	+00000+0	+00000+0	-1.0	3415
2 90050	39.2078	36.1154 0379124	8.2142	30.8053	15.3892752000001		3416
1 90050U		86249.47000508	+.00000000	+00000+0	+00000+0	-1.0	3423
2 90050	39.0000	35.8298 0313162	21.2529	19.5424	15.4548830000001		3424
1 90050U		86249.47008043	+.00000000	+00000+0	+00000+0	-1.0	3429
2 90050	39.1313	36.0134 0499381	18.6251	21.4997	15.0529037900001		3430
1 90050U		86249.47015431	+.00000000	+00000+0	+00000+0	-1.0	3437
2 90050	39.1642	36.0601 0381059	8.0886	32.2334	15.3888419400001		3438
1 90050U		86249.47022947	+.00000000	+00000+0	+00000+0	-1.0	3441
2 90050	39.0682	35.9213 0409340	18.4992	22.8885	15.2523494200001		3442
1 90080U		86249.46958483	+.00000000	+00000+0	+00000+0	-1.0	3525
2 90080	39.8122	35.7817 0385582	33.7712	359.6487	15.2783539100001		3526
1 90080U		86249.47011306	+.00000000	+00000+0	+00000+0	-1.0	3563
2 90080	39.9812	35.9453 0516876	7.3528	26.2787	15.0642732300001		3564
1 90080U		86249.47063627	+.00000000	+00000+0	+00000+0	-1.0	3603
2 90080	39.9156	35.8782 0478177	13.0791	24.1218	15.1075485300001		3604

1	900080U		86249.47309612	+.00000000	+000000+0	+000000+0	-1.0	3637
2	900080	39.9847	36.6634	0454392	11.4795	28.4137	15.1707414600001	3638
1	900080U		86249.47360213	+.00000000	+000000+0	+000000+0	-1.0	3683
2	900080	39.9221	36.5831	0473792	13.8355	28.9489	15.1102977100001	3684
1	900081U		86249.46974908	+.00000000	+000000+0	+000000+0	-1.0	3537
2	900081	39.3472	35.4055	0577695	17.8980	14.7278	14.8694266800001	3538
1	900081U		86249.47024357	+.00000000	+000000+0	+000000+0	-1.0	3575
2	900081	39.5651	35.6228	0462641	19.9491	15.7318	15.1259001300001	3576
1	900081U		86249.47059601	+.00000000	+000000+0	+000000+0	-1.0	3597
2	900081	39.5700	35.6282	0425108	24.4071	13.6704	15.1960484400001	3598
1	900081U		86249.47288315	+.00000000	+000000+0	+000000+0	-1.0	3625
2	900081	39.5601	36.3215	0451777	22.8775	16.8270	15.1401865900001	3626
1	900081U		86249.47323734	+.00000000	+000000+0	+000000+0	-1.0	3647
2	900081	39.5623	36.3243	0444659	22.7234	18.9219	15.1571713000001	3648
1	900083U		86249.46986927	+.00000000	+000000+0	+000000+0	-1.0	3547
2	900083	39.5425	35.5524	0495416	89.0290	309.1320	15.5341572200001	3548
1	900083U		86249.47042475	+.00000000	+000000+0	+000000+0	-1.0	3589
2	900083	39.8187	35.8223	0448562	34.3913	2.1089	15.1479235700001	3590
1	900083U		86249.47300235	+.00000000	+000000+0	+000000+0	-1.0	3631
2	900083	39.8076	36.5162	0453004	33.9377	5.9284	15.1369982400001	3632
1	900083U		86249.47351497	+.00000000	+000000+0	+000000+0	-1.0	3669
2	900083	39.8263	36.5388	0444783	33.8962	8.7532	15.1563191900001	3670
1	900083U		86249.47439661	+.00000000	+000000+0	+000000+0	-1.0	3697
2	900083	39.8104	36.5170	0422057	33.7771	13.7463	15.2106985900001	3698
1	900084U		86249.46998395	+.00000000	+000000+0	+000000+0	-1.0	3553
2	900084	38.8668	35.0428	0445606	49.0827	347.3435	15.1857222300001	3554
1	900084U		86249.47059102	+.00000000	+000000+0	+000000+0	-1.0	3595
2	900084	39.0354	35.2210	0453977	32.1995	5.9567	15.1309911100001	3596
1	900084U		86249.47289462	+.00000000	+000000+0	+000000+0	-1.0	3627
2	900084	39.1017	36.0045	0439018	31.2905	8.6629	15.1676347800001	3628
1	900084U		86249.47323041	+.00000000	+000000+0	+000000+0	-1.0	3645
2	900084	39.0623	35.9544	0441734	33.3513	8.6392	15.1573252400001	3646
1	900084U		86249.47357425	+.00000000	+000000+0	+000000+0	-1.0	3677
2	900084	39.0585	35.9491	0441645	33.0223	10.8198	15.1582159000001	3678
1	900086U		86249.47005884	+.00000000	+000000+0	+000000+0	-1.0	3561
2	900086	39.4996	35.5473	0473813	37.2524	356.8750	15.0854243600001	3562
1	900086U		86249.47062661	+.00000000	+000000+0	+000000+0	-1.0	3605
2	900086	39.6970	35.7426	0473993	26.4402	9.6348	15.0858090000001	3606
1	900086U		86249.47309256	+.00000000	+000000+0	+000000+0	-1.0	3635
2	900086	39.6787	36.4206	0435550	33.8146	5.7680	15.1679805200001	3636
1	900086U		86249.47360144	+.00000000	+000000+0	+000000+0	-1.0	3681
2	900086	39.7175	36.4749	0450279	27.8979	13.8975	15.1436617000001	3682
1	900086U		86249.47438330	+.00000000	+000000+0	+000000+0	-1.0	3695
2	900086	39.6175	36.3413	0440196	32.0239	14.5052	15.1552262200001	3696
1	900089U		86249.47021846	+.00000000	+000000+0	+000000+0	-1.0	3577
2	900089	40.1560	36.2674	0755127	136.1936	265.4452	16.5603363700001	3578
1	900089U		86249.47201398	+.00000000	+000000+0	+000000+0	-1.0	3619
2	900089	39.2059	36.1254	0425693	32.9760	4.2717	15.2024902800001	3620
1	900089U		86249.47335405	+.00000000	+000000+0	+000000+0	-1.0	3655
2	900089	39.2956	36.1363	0433537	31.0076	9.0107	15.1850457200001	3656
1	900089U		86249.47454649	+.00000000	+000000+0	+000000+0	-1.0	3707
2	900089	39.2609	36.0919	0416726	31.9753	14.7183	15.2230799000001	3708
1	900095U		86249.47296578	+.00000000	+000000+0	+000000+0	-1.0	3629
2	900095	39.1058	36.1232	0369554	70.4098	326.8111	15.5088551900001	3630
1	900095U		86249.47354155	+.00000000	+000000+0	+000000+0	-1.0	3673
2	900095	38.8976	35.8220	0465014	39.7235	358.8839	15.1190866600001	3674
1	900095U		86249.47444638	+.00000000	+000000+0	+000000+0	-1.0	3699
2	900095	38.9483	35.8008	0420007	42.6176	1.1308	15.2279584000001	3700
1	900096U		86249.47304097	+.00000000	+000000+0	+000000+0	-1.0	3633
2	900096	40.2354	38.2914	1607865	13.5915	13.5800	12.5313593300001	3634
1	900096U		86249.47354447	+.00000000	+000000+0	+000000+0	-1.0	3671
2	900096	40.2310	38.2878	1790877	8.6105	18.7221	12.1996311100001	3672
1	900096U		86249.47436536	+.00000000	+000000+0	+000000+0	-1.0	3693
2	900096	40.2296	38.2787	1642881	11.1704	21.1943	12.4801750100001	3694
1	900098U		86249.47319696	+.00000000	+000000+0	+000000+0	-1.0	3643
2	900098	39.4504	36.1548	0714756	15.3339	16.1027	14.5742644400001	3644
1	900098U		86249.47381578	+.00000000	+000000+0	+000000+0	-1.0	3691
2	900098	39.9507	36.6551	0449595	29.2053	7.2334	15.1375277800001	3692
1	900098U		86249.47449962	+.00000000	+000000+0	+000000+0	-1.0	3703
2	900098	39.9507	36.6457	0425094	28.9651	11.3102	15.1960433200001	3704
1	900099U		86249.47335398	+.00000000	+000000+0	+000000+0	-1.0	3657
2	900099	39.8726	36.5023	0430002	47.6799	347.2079	15.2103897700001	3658

1	900990		86249.47451466	+.00000000	+00000+0	+00000+0	-1.0	3705
2	90099	40.1618	36.7829	0441620	22.0903	16.7956	15.16430880000001	3706
1	901010		86249.47353795	+.00000000	+00000+0	+00000+0	-1.0	3675
2	90101	40.3014	36.9392	0406959	25.8890	6.8887	15.23846592000001	3676
1	901010		86249.47445795	+.00000000	+00000+0	+00000+0	-1.0	3701
2	90101	40.2296	36.8697	0443812	16.0925	20.8895	15.18227581000001	3702
1	901110		86249.47333913	+.00000000	+00000+0	+00000+0	-1.0	3735
2	90111	39.4746	35.4966	0462477	44.9008	350.6124	15.12582093000001	3736
1	901110		86249.47386574	+.00000000	+00000+0	+00000+0	-1.0	3751
2	90111	39.7113	35.7377	0505839	24.6874	11.6251	15.01216686000001	3752
1	901110		86249.47444508	+.00000000	+00000+0	+00000+0	-1.0	3773
2	90111	39.7860	35.8184	0485572	25.9646	13.5914	15.05544608000001	3774
1	901110		86249.47694107	+.00000000	+00000+0	+00000+0	-1.0	3801
2	90111	39.8354	36.5837	0467564	24.7390	17.6630	15.10165745000001	3802
1	901110		86249.47744934	+.00000000	+00000+0	+00000+0	-1.0	3883
2	90111	39.8035	36.5448	0477580	25.8247	19.4229	15.07393659000001	3884
1	901140		86249.47691289	+.00000000	+00000+0	+00000+0	-1.0	3797
2	90114	39.7964	36.5351	0478679	22.9996	15.6177	15.07989196000001	3798
1	901140		86249.47724517	+.00000000	+00000+0	+00000+0	-1.0	3855
2	90114	39.7731	36.5064	0517246	21.7690	18.4253	14.99766495000001	3856
1	901140		86249.47757908	+.00000000	+00000+0	+00000+0	-1.0	3899
2	90114	39.8022	36.5448	0455296	24.7752	17.6880	15.12293386000001	3900
1	901140		86249.47791705	+.00000000	+00000+0	+00000+0	-1.0	3927
2	90114	39.8119	36.5586	0496049	23.6899	20.3523	15.03612292000001	3928
1	901220		86249.47456478	+.00000000	+00000+0	+00000+0	-1.0	3777
2	90122	39.6547	35.6915	0471608	42.8127	352.8821	15.10233271000001	3778
1	901220		86249.47706397	+.00000000	+00000+0	+00000+0	-1.0	3805
2	90122	39.7434	36.4885	0525435	27.7256	9.4044	14.96609712000001	3806
1	901220		86249.47757816	+.00000000	+00000+0	+00000+0	-1.0	3897
2	90122	39.8540	36.6104	0471623	31.5053	8.7678	15.08600984000001	3898
1	901220		86249.47812318	+.00000000	+00000+0	+00000+0	-1.0	3937
2	90122	39.7750	36.5137	0495377	31.9058	11.3785	15.02901634000001	3938
1	901220		86249.47667841	+.00000000	+00000+0	+00000+0	-1.0	3991
2	90122	39.8084	35.8549	0482148	30.4652	15.4385	15.06432894000001	3992
1	901240		86249.47661861	+.00000000	+00000+0	+00000+0	-1.0	3783
2	90124	40.0775	36.8357	0383928	58.2857	338.3218	15.37599798000001	3784
1	901240		86249.47713602	+.00000000	+00000+0	+00000+0	-1.0	3813
2	90124	39.6873	36.4337	0534784	28.1676	9.1165	14.94293562000001	3814
1	901240		86249.47765709	+.00000000	+00000+0	+00000+0	-1.0	3903
2	90124	39.8520	36.6159	0473679	31.7563	8.6591	15.08054578000001	3904
1	901240		86249.47816508	+.00000000	+00000+0	+00000+0	-1.0	3939
2	90124	39.7967	36.5480	0486302	30.9979	12.1234	15.05229521000001	3940
1	901240		86249.47672001	+.00000000	+00000+0	+00000+0	-1.0	3997
2	90124	39.7722	35.8094	0487933	31.6200	14.3192	15.04630148000001	3998
1	901250		86249.47670483	+.00000000	+00000+0	+00000+0	-1.0	3791
2	90125	39.9060	36.5795	0414236	49.7274	345.5479	15.25062661000001	3792
1	901250		86249.47724024	+.00000000	+00000+0	+00000+0	-1.0	3853
2	90125	40.1161	36.7871	0507891	17.8712	17.3486	15.02129156000001	3854
1	901250		86249.47775672	+.00000000	+00000+0	+00000+0	-1.0	3909
2	90125	40.1593	36.8327	0492385	18.3100	19.7664	15.05415712000001	3910
1	901250		86249.47826629	+.00000000	+00000+0	+00000+0	-1.0	3947
2	90125	40.0795	36.7392	0493318	20.1467	20.9128	15.04169580000001	3948
1	901250		86249.47681895	+.00000000	+00000+0	+00000+0	-1.0	4015
2	90125	40.1209	36.0887	0518262	18.4053	25.0812	14.99710713000001	4016
1	901280		86249.47833782	+.00000000	+00000+0	+00000+0	-1.0	3957
2	90128	39.4180	37.0381	1109513	5.3664	20.9639	13.77329989000001	3958
1	901280		86249.47671723	+.00000000	+00000+0	+00000+0	-1.0	3999
2	90128	39.3536	36.2488	1118806	6.6470	29.5516	13.72967572000001	4000
1	901280		86249.47704941	+.00000000	+00000+0	+00000+0	-1.0	4037
2	90128	39.4302	36.3551	1078969	5.0908	32.6643	13.84044272000001	4038
1	901280		86249.47738291	+.00000000	+00000+0	+00000+0	-1.0	4077
2	90128	39.3775	36.2768	1101825	6.3131	33.2078	13.76983111000001	4078
1	901320		86249.47770790	+.00000000	+00000+0	+00000+0	-1.0	3907
2	90132	41.4215	38.2781	0485293	135.8968	263.1820	16.43504469000001	3908
1	901320		86249.47821717	+.00000000	+00000+0	+00000+0	-1.0	3941
2	90132	38.9826	35.8255	0376315	46.7349	352.4012	15.32141360000001	3942
1	901320		86249.47677310	+.00000000	+00000+0	+00000+0	-1.0	4001
2	90132	39.1595	35.3207	0686101	8.2857	29.0454	14.72758477000001	4002
1	901320		86249.47727023	+.00000000	+00000+0	+00000+0	-1.0	4067
2	90132	39.2625	35.4500	0501140	18.9206	23.0321	15.03212983000001	4068
1	901320		86249.47778394	+.00000000	+00000+0	+00000+0	-1.0	4091
2	90132	39.2473	35.4291	0517973	19.5725	25.1055	14.98986868000001	4092

1 90134U		86249.47781517	+.00000000	+000000+0	+000000+0	-1.0	3919
2 90134	39.4094	36.1505	0514809	48.2903	347.8992	15.02084886000001	3920
1 90134U		86249.47847848	+.00000000	+000000+0	+000000+0	-1.0	3969
2 90134	39.8121	36.5713	0498406	32.5438	5.3978	15.02193523000001	3970
1 90134U		86249.47703469	+.00000000	+000000+0	+000000+0	-1.0	4031
2 90134	39.8624	35.9225	0489215	31.2520	9.2937	15.04490781000001	4032
1 90134U		86249.47754167	+.00000000	+000000+0	+000000+0	-1.0	4081
2 90134	39.8170	35.8664	0507448	30.5542	12.6661	15.00358357000001	4082
1 90134U		86249.47805213	+.00000000	+000000+0	+000000+0	-1.0	4095
2 90134	39.7948	35.8358	0497846	32.3136	13.8742	15.02004662000001	4096
1 90139U		86249.47820375	+.00000000	+000000+0	+000000+0	-1.0	3943
2 90139	39.9039	36.6579	0400001	65.5620	331.7760	15.39405842000001	3944
1 90139U		86249.47677034	+.00000000	+000000+0	+000000+0	-1.0	4003
2 90139	39.8087	35.8549	0511046	30.5495	6.9579	14.99614423000001	4004
1 90139U		86249.47727773	+.00000000	+000000+0	+000000+0	-1.0	4069
2 90139	39.7777	35.8210	0538208	29.6080	10.5156	14.93348379000001	4070
1 90139U		86249.47778303	+.00000000	+000000+0	+000000+0	-1.0	4089
2 90139	39.8723	35.9377	0475695	33.0762	10.1469	15.07233569000001	4090
1 90139U		86249.47828867	+.00000000	+000000+0	+000000+0	-1.0	4101
2 90139	39.8144	35.8587	0497862	31.3332	14.4695	15.02526682000001	4102
1 90140U		86249.47822219	+.00000000	+000000+0	+000000+0	-1.0	3945
2 90140	39.5845	37.0139	1118134	43.1247	353.8455	13.61467043000001	3946
1 90140U		86249.47662294	+.00000000	+000000+0	+000000+0	-1.0	3985
2 90140	40.0009	36.8228	1110010	32.2719	3.8875	13.60618146000001	3986
1 90140U		86249.47695870	+.00000000	+000000+0	+000000+0	-1.0	4023
2 90140	40.1925	36.9444	1066396	33.0297	4.8932	13.70503393000001	4024
1 90140U		86249.47729188	+.00000000	+000000+0	+000000+0	-1.0	4073
2 90140	40.0079	36.7271	1122503	34.1333	5.7225	13.57418636000001	4074
1 90140U		86249.47762896	+.00000000	+000000+0	+000000+0	-1.0	4087
2 90140	40.1279	36.8795	1075094	34.0363	7.4211	13.68261985000001	4088
1 90141U		86249.47680227	+.00000000	+000000+0	+000000+0	-1.0	4011
2 90141	40.4970	36.3190	0574270	14.0238	20.9233	14.88996953000001	4012
1 90141U		86249.47731590	+.00000000	+000000+0	+000000+0	-1.0	4071
2 90141	40.6527	36.4831	0507141	17.0936	21.0731	15.02080448000001	4072
1 90141U		86249.47782122	+.00000000	+000000+0	+000000+0	-1.0	4093
2 90141	40.6309	36.4578	0515976	16.8804	23.9739	15.00224277000001	4094
1 90141U		86249.47833017	+.00000000	+000000+0	+000000+0	-1.0	4103
2 90141	40.6135	36.4354	0519917	17.9765	25.7178	14.98507244000001	4104

Appendix C

the SRS Report

Appendix C contains the text, with figures and tables, of the Systems Planning Corp./Remote Sensing report on their observations of the reentering debris following the breakup of satellites 16937 and 16938. Included as SPC/RS appendices are field notes taken during the observations, and a theoretical study of the velocity of the reentering debris.



SPC REMOTE SENSING CORPORATION

4418 Illinois Street

• Dickinson, Texas 77539 •

(713) 534-2882

A SUBSIDIARY OF SYSTEM PLANNING CORPORATION

VHF RADAR BACKSCATTER OBSERVATIONS DURING DELTA 180

Prepared For

LOCKHEED ENGINEERING AND MANagements SERVICE COMPANY, INC.

And

**NATIONAL AERONAUTICS AND SPACE ADMINISTRATION
LYNDON B. JOHNSON SPACE CENTER
HOUSTON, TEXAS**

Under Contract NAS9-15800

February 1987

VHF RADAR BACKSCATTER OBSERVATIONS DURING DELTA 180

TABLE OF CONTENTS

	<u>Page</u>
1. OVERVIEW	1
2. EXPERIMENTAL SETUP AND ACTIVITY	3
2.1 Radar Configuration	3
2.2 Summary of Field Activity	9
3. OBSERVATIONAL RESULTS AND DISCUSSION	13
3.1 Range-Time-Intensity of Debris Events	13
3.2 Debris Particle Velocity (Indirect Measurement)	53
3.3 Debris Particle Velocity (Direct Measurement)	56
3.4 Entry Mass	61
3.5 Mass Calculation Sensitivity	70
4. SUMMARY AND RECOMMENDATIONS	74
4.1 Summary	74
4.2 Recommendations	74
APPENDIX A	76
APPENDIX B	106

VHF RADAR BACKSCATTER OBSERVATIONS DURING DELTA 180

1. OVERVIEW

Limited statistical evidence, from recent VHF radar studies of meteor fluxes, indicate that orbital debris decay processes can lead to the production of meteor-like ionization trails in the upper atmosphere. Unpublished works by Jost and Potter (NASA/JSC, 1983-1986) show, in several cases (e.g., Shuttle, ASAT, and other orbiting vehicles), that an increase in the observed radar meteor flux occurs at times when the vehicle orbital plane intersects the radar radiation patterns.

With this basis, SPC Remote Sensing Corporation (SRS) installed and operated a complex VHF, backscatter radar system to measure ionization trails produced by entering debris from an SDI DELTA 180 (D-180) experiment. A dual-frequency radar "farm" was located at a remote site in Kauai, Hawaii to optimize the backscatter geometry for detecting entering debris ionization trails in the upper atmosphere. The system was activated several days prior to the space-based experiment to establish the background meteor flux. Data were collected throughout a period extending from 24 hours pre-mission to four days post-mission.

Operation during a critical phase of the mission indicated an order of magnitude increase in meteor-like echoes over the background flux for a 2 minute period. This flux increase, com-

bined with its corresponding, measured particle velocities in the range of 6.5 to 7.5 km/s, provides unequivocal evidence for the detection of entering orbital debris. The mass range for the debris particles was determined to range from a few grams to nearly a kilogram with a strongly decreasing number distribution for increasing mass.

2. EXPERIMENTAL SETUP AND ACTIVITY

2.1 Radar Configuration

The VHF backscatter system was deployed on the northern shore of the island of Kauai just east of Hanalei in the Princeville Development Community. This region is delineated in Figure 1 with the radar icon. An expanded view of the specific remote site is shown in Figure 2; Block 25 is the field site where the entering debris radars were located.

Two long-wavelength radars were deployed with slightly different operational objectives. Standard meteor-radar frequencies of 27.66 MHz and 49.92 MHz were selected to enable wavelength dependent studies of the return echo signatures. Also, the frequency span provided a high probability for ionization detection as well as providing system redundancy. The 27.66 MHz radar was operated as a fixed fan-beam, monostatic system. An interferometric detection concept was incorporated into the 49.92 MHz radar configuration to allow vector measurements of velocity and location of the entering debris particles.

The radar interferometer antenna layout consisted of two orthogonal sets of linear dipole arrays. A total of five fan-beam sub-arrays were arranged, as shown in Figure 3, to provide three azimuthal baselines and three elevation baselines for the vector measurements. The elevation (vertical) plane was covered by antennas 1, 2, and 3, while the azimuthal (horizontal) plane consisted of antennas 3, 4, and 5. Antenna 3 served as the pri-

mary transmit (and receive) antenna with the other four sub-arrays operating as passive receive-only antennas. All sub-arrays were constructed from 24 half-wave dipole sections. As a result, the 49.92 MHz antenna arrays were each 47.4 meters in length. The monostatic 27.66 MHz antenna was designed to view the same volume of space as the interferometer, and therefore, also consisted of 24 half-wave dipoles with a total length of 85.5 meters.

The radiation patterns were controlled by the array orientation (i.e., horizontal azimuth) and height above the ground. All antennas were placed $1/2$ wavelength above the ground plane and aligned on an east-west baseline. This provided twin, mirror-image fan beams (opposed at the zenith) directed along a true north-south plane with an elevation angle of 30° for the beam centers. The half-power beam widths were approximately 40° . Figure 4 shows the radiation pattern geometry in the elevation and azimuth planes relative to the D-180 ground tracks for both the immediate post-event phase groundtrack and the ground track for one orbit later.

The radar systems were operated in a standard single pulse mode with a pulse width of $10 \mu\text{s}$ and an interpulse period of approximately 2 ms. A system synchronizer controlled both radars so that their transmitted pulses occurred simultaneously. The peak-pulse (radiated) power of the 50 MHz system was about 10 kW; 6 kW of radiated power was produced by the 28 MHz radar.



Figure 2. VHF radar field site near Princeville Development Community (Block 25).

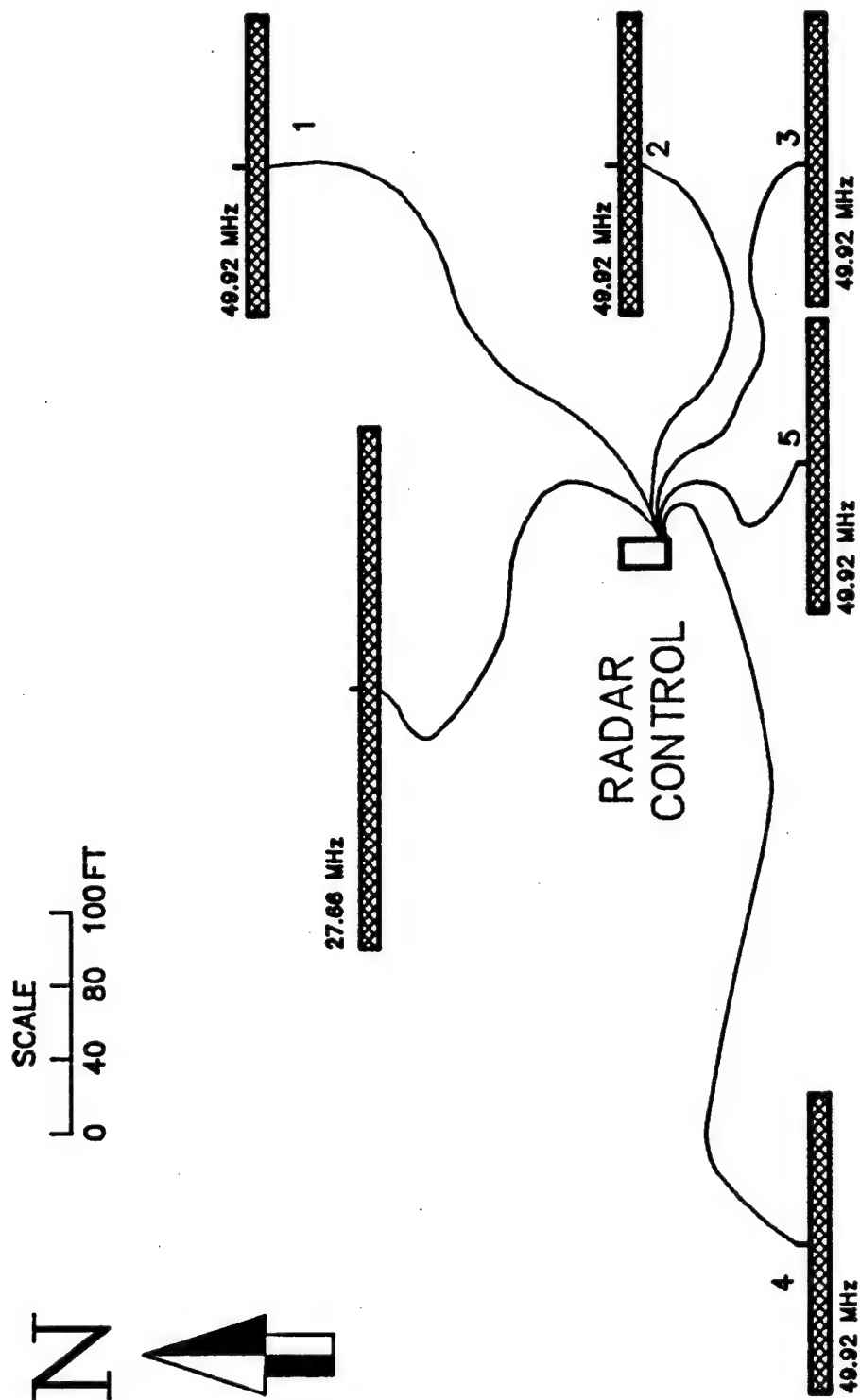


Figure 3. Physical layout of antenna arrays for the 50 MHz interferometer and 28 MHz monostatic radars.

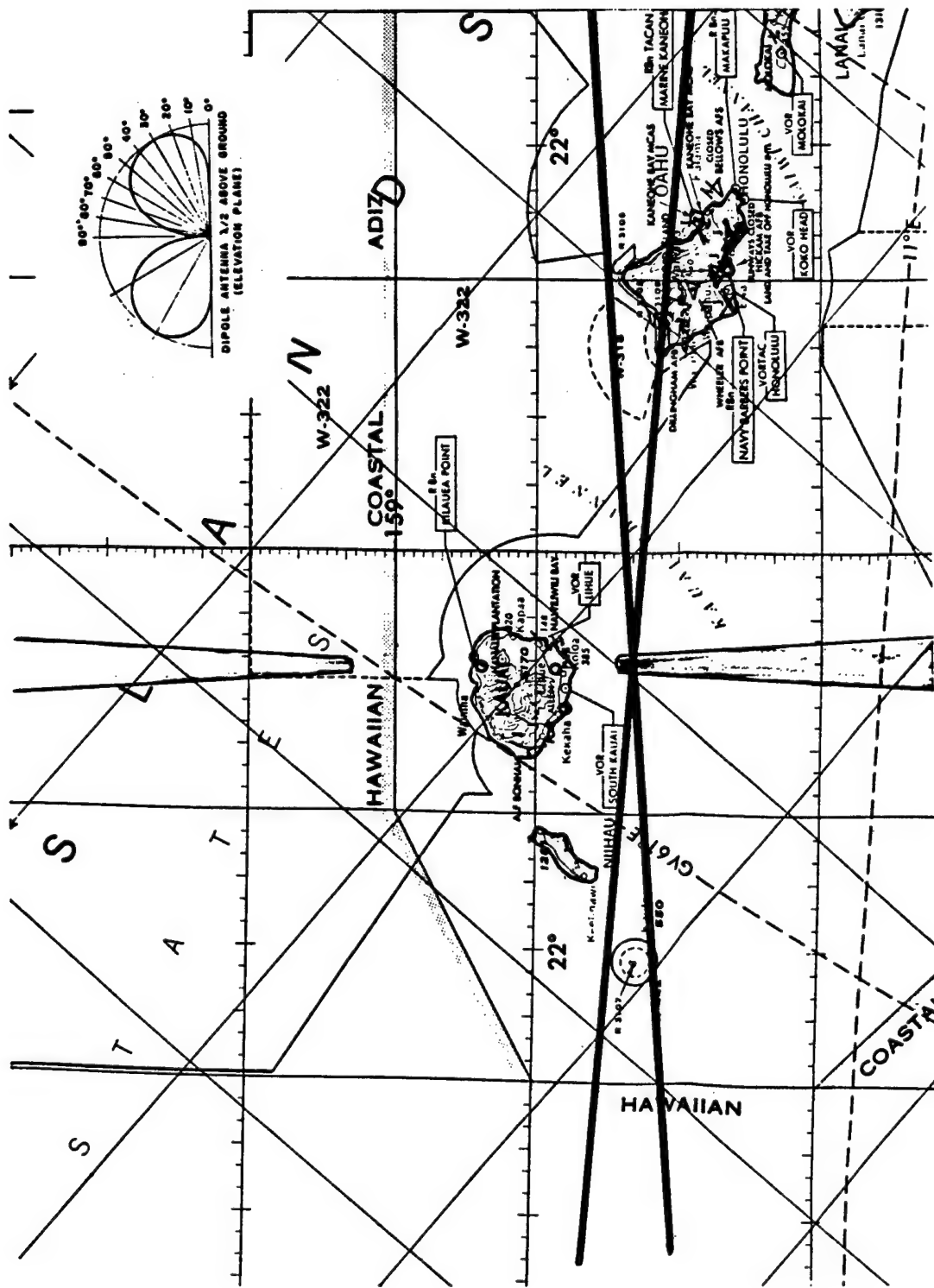


Figure 4. General geometry for ground track intercepts and areas of sensitivity for radars.

2.2 Summary of Field Activity

The field-site design calculations, radar testing, equipment inventory, and the acquisition of materials were carried out during a period of several weeks prior to field-team arrival at Kauai. With the exception of the site selection, these activities were conducted at SRS facilities and at NASA/JCS.

The site selected on the north coast of Kauai was located at geographic coordinates 22.2° N and 159.5° W. This region was given first priority for radar location based on geometrical requirements for observing the entering debris ionization trails. Radar echoes are highly aspect sensitive to the long meteor-like ionization tails, which required in this case, that the radiation patterns be directed as near perpendicular to the groundtracks as possible (i.e., a north-south azimuth).

Astronomical observations were made on the night of August 30, 1986. Antenna deployment began on the following day. The azimuthal orientation for both radars was determined independently by these observations and by compass readings. Azimuth and elevation angles of 0 and 30 degrees, respectively, were selected to provide optimum coverage and to maximize the line-of-sight doppler anticipated from the relatively low altitude events.

A 12-passenger van (without rear seats) was used to house the radar hardware and data recording system. Power was derived from a portable generator. A 14-track Honeywell Model 101 tape recorder was used to record the radar signals, time code, and

synch pulses. General site photographs are shown in Figure 5. The radar operations log is provided in Appendix A -- Hawaii Meteor Campaign Field Notes.

Standard radar calibration procedures were implemented. These included feedline/receiver phase angle and transmitter power measurements. The power at the antenna feed point was 6.0 kW for the 27.66 MHz system and 10.2 kW for the 49.92 MHz radar. Power measured at the respective transmitters was approximately 3 dB greater than the power measured at the end of the feedline (3 dB feedline loss).

Forty-two tapes of data were collected which comprise over 35 hours of total radar observations. Background ionospheric and meteoric measurements were made for periods both before and after the mission. Observations of subsequent orbital crossings were made for four days following the prime D-180 event.

All equipment was secured and readied for shipment on September 9-10, 1986 and shipped back to JSC on September 10. The shipment was available for pickup at JSC on September 19 at which time items relevant to the data reduction process were re-routed to Cornell University, Ithaca, New York.

Data processing had been pre-arranged to be conducted at Cornell University and began on September 22, 1986. The requirements established for the Hawaii data processing greatly exceeded those normally conducted with the Cornell data reduction system.

Consequently, a number of software changes were necessary which introduced delays in processing these data.

Analysis was focussed on the period immediately surrounding the initial influx of debris particles that occurred approximately eight minutes after the event at closest approach. This effort has been directed toward determining the range-time-intensity (RTI), line-of-sight doppler spectra, cross-spectra between interferometer baselines, free-space velocities, entry-process velocities, and preliminary mass estimates of the debris particles. Prior to initiating the bulk processing, several areas of system software upgrades were identified and implemented (improvements are still being implemented). Staff members at Cornell (SRS consultants) are currently involved in these targeted upgrades.



Figure 5a. Radar van at the Kauai field site; 28 MHz antenna in background.

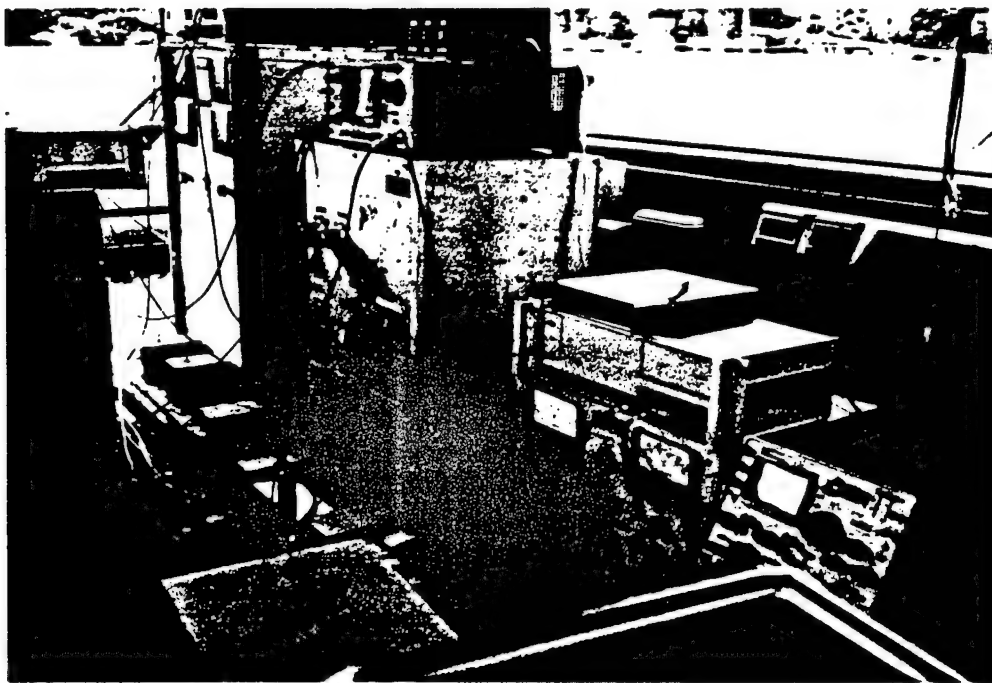


Figure 5b. VhF radar electronic equipment in van.

3. OBSERVATIONAL RESULTS AND DISCUSSION

3.1 Range-Time-Intensity of Debris Events

RTI displays are shown, for the time period surrounding the initial debris observations, in Figure 6 (49.92 MHz) and Figure 7 (27.66 MHz). As illustrated, both radars observed a large increase in echo activity at approximately 18:01 UT (on day 248). This increased activity is attributed to debris entering the upper atmosphere following the event at closest approach for the D-180 payload. For future reference, the debris events have been cataloged according to the numeric designators shown in Figures 8 and 9 for the two sets of data.

The extent in slant range of detectable debris varied from 70 to 250 km. To first order, this corresponds to an altitude extent of 35 to 125 km based on the limits of the radiation patterns. Natural meteors seldom penetrate to altitudes below about 100 km due to the velocity dependent energy loss mechanisms involved in meteoric evaporation. The altitude of maximum ionization generally scales with velocity. Extraterrestrial meteor velocities are higher than orbital escape velocity and range from about 20 km/s to greater than 80 km/s. Entering debris particles should not exceed 10 km/s and as a result should "burn up" at comparatively lower altitudes (≤ 70 km).

Although most of the debris echoes last no more than a fraction of a second in duration, a few echoes persisted for

longer than a second. The duration of the debris echo is theoretically proportional to the square of the wavelength, and the power returned is proportional to the wavelength cubed.

At VHF, however, the cosmic noise level increases as wavelength to the 2.4 power. Consequently, with the relatively lower transmitter power at 27.66 MHz and the increase in background noise, a $S/N > 1$ is more difficult to achieve at 27.66 MHz than at 49.92 MHz. For this reason, relatively fewer echoes were observed at 27.66 MHz and the echoes were, in general, shorter lived than those at 49.92 MHz. RTI displays for "Rev 2" (i.e., an hour time period centered on the time 92 minutes past initial debris contact) are shown in Figures 10-38).

Two display formats are provided to give insight into the debris identification process. Figure 39 shows the range of each event during the one-hour period of time studied and Figure 40 depicts the instantaneous frequency of particle detection for the same period. These displays provide a powerful method for obtaining a first-order determination of debris related activity.

In general, debris particles with their inherently lower velocities decay at altitudes significantly lower than meteor particles. Furthermore, an increase in the frequency of detection should occur as the time of orbital crossing is approached. As is apparent from Figures 39-40, these signatures are not readily evident and therefore indicate that no sizeable collection of debris particles were detected during Rev 2. There is, however, the

possibility that up to 4 of the events shown in Figure 39 are D-180 debris. These events contain signatures (range, time, intensity) which are consistent with those expected for entering debris.

49.92 MHz Radar RTI Hawaii 1986 Day: 248

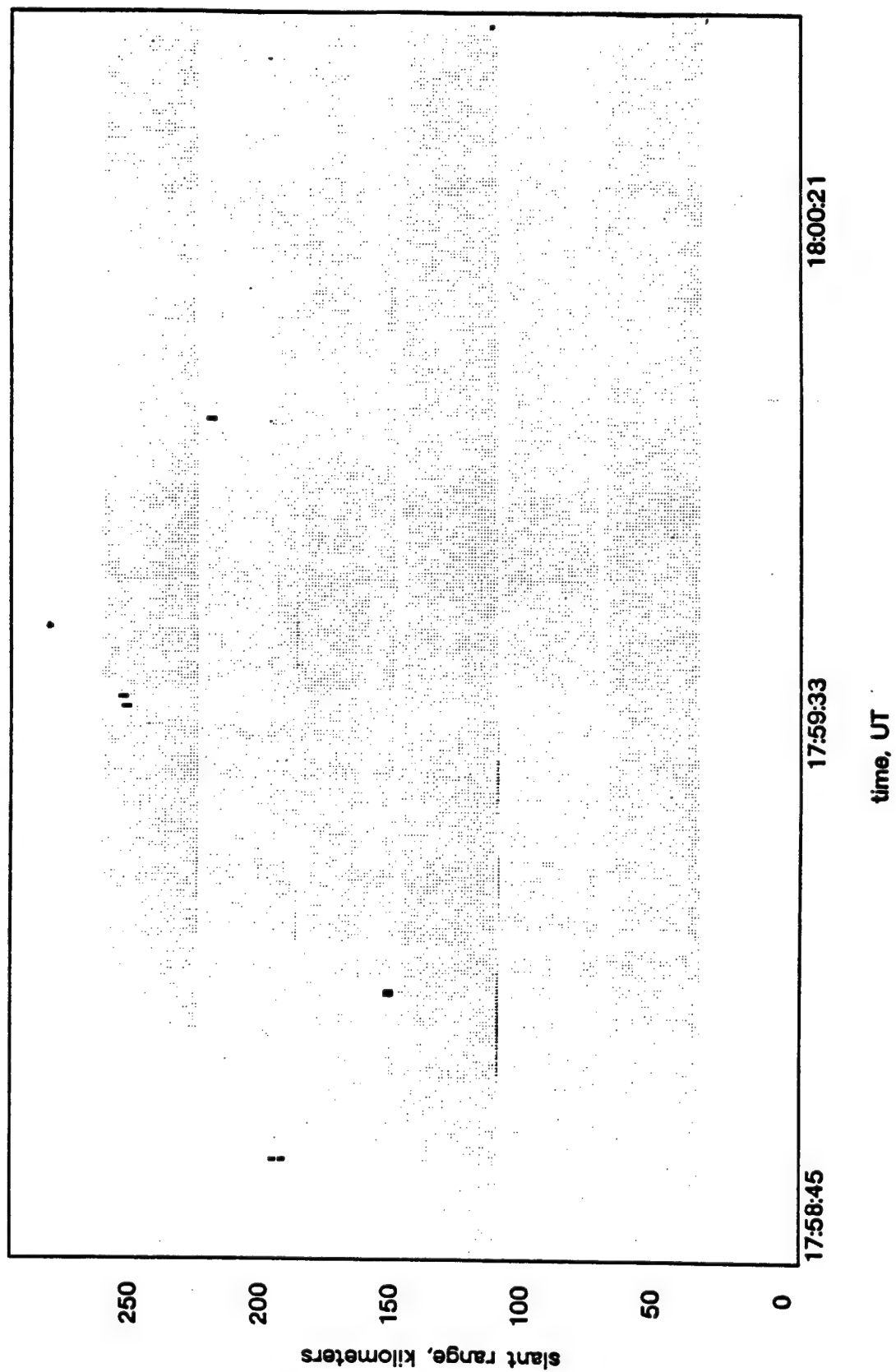


Figure 6a. RTI for 50 MHz radar; 2 minute period preceding primary activity.

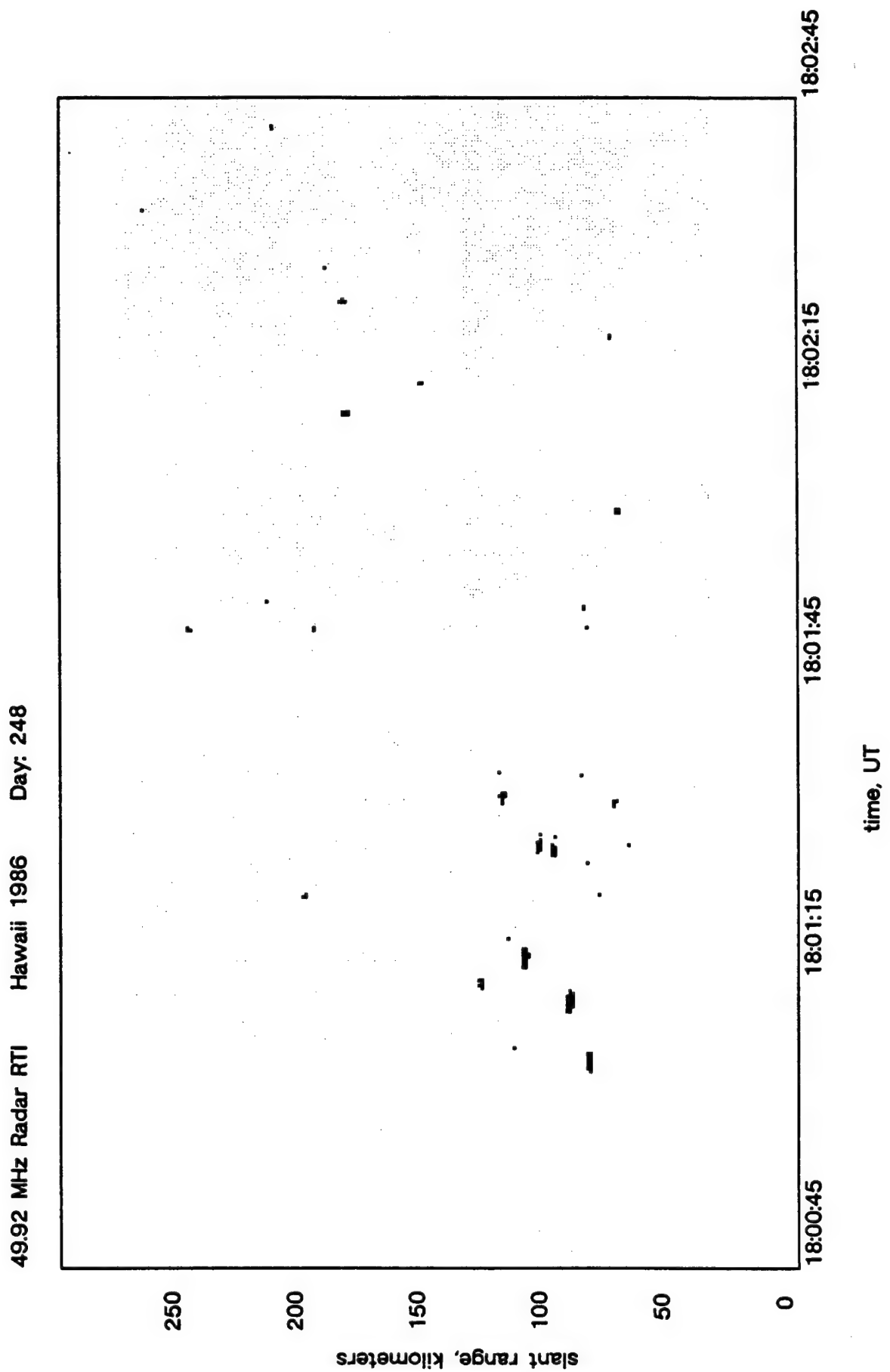


Figure 6b. RTI for 50 MHz radar; 2 minute period of primary activity.

27.66 MHz Radar RTI Hawaii 1986 Day: 248

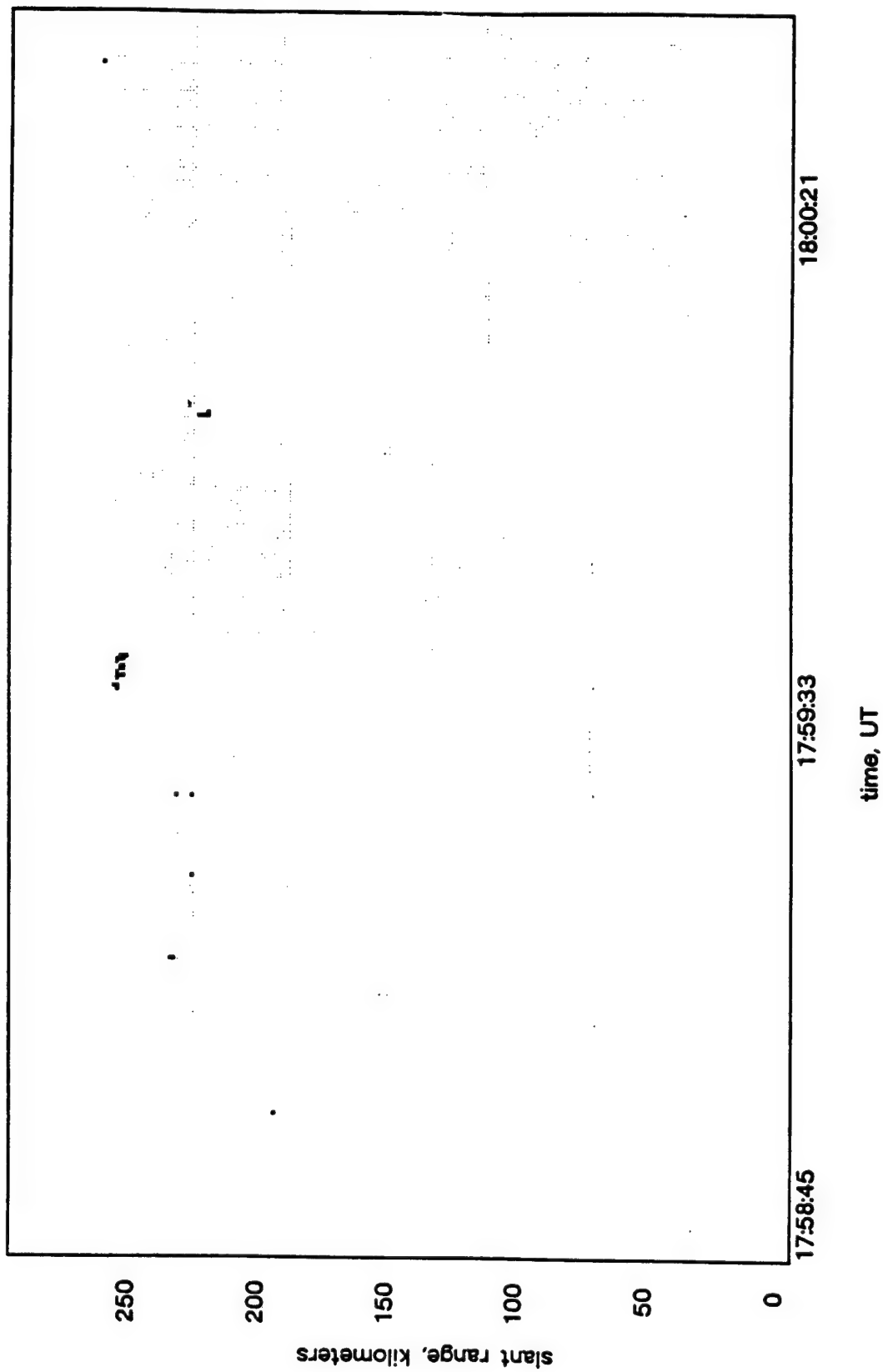


Figure 7a. RTI for 28 MHz radar; 2 minute period preceding primary activity.



C-19

4992 MHz Radar RTI Hawaii 1986 Day: 248

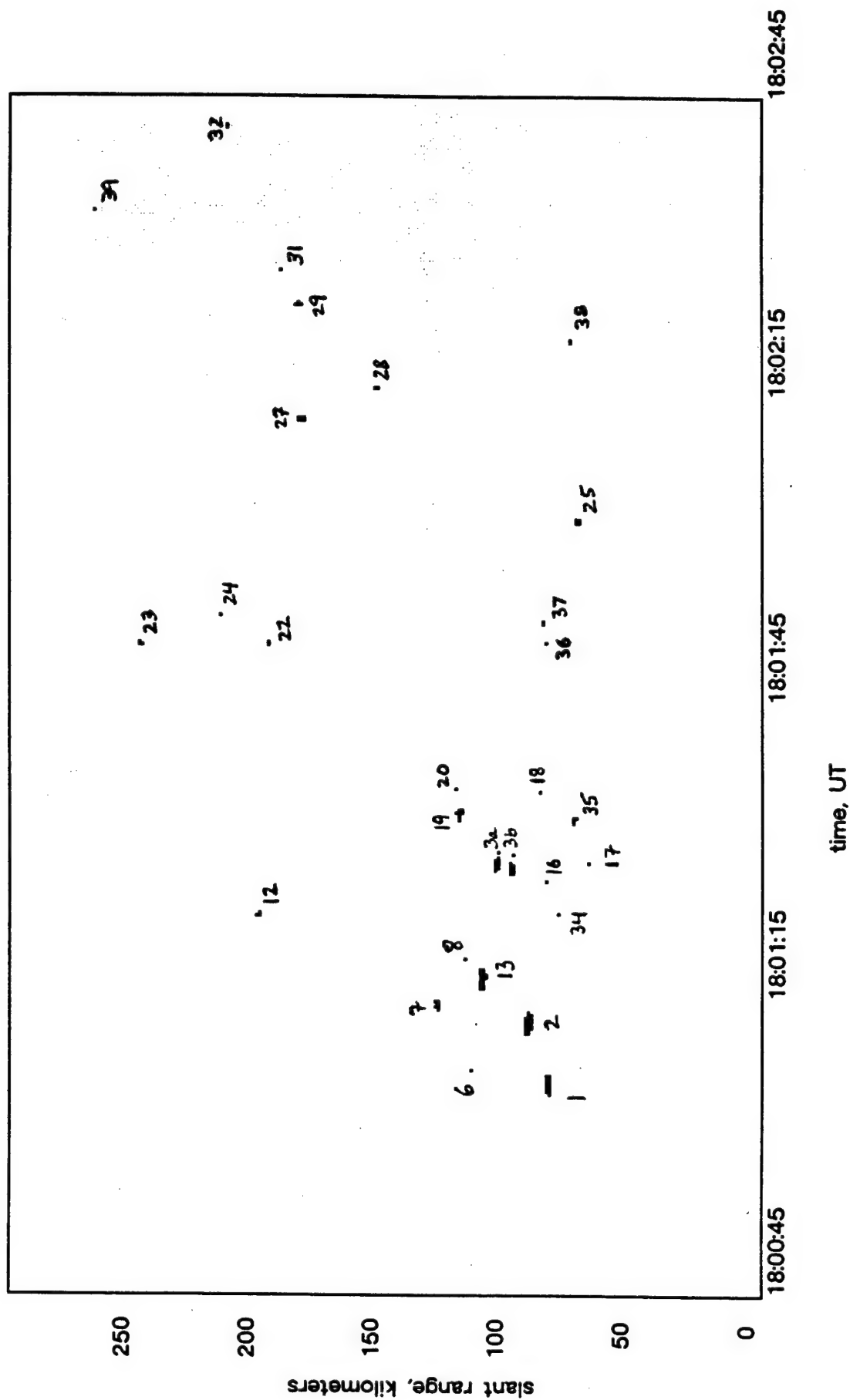


Figure 8. Labeled debris events for 50 MHz radar.

27.66 MHz Radar RTI Hawaii 1986 Day: 248

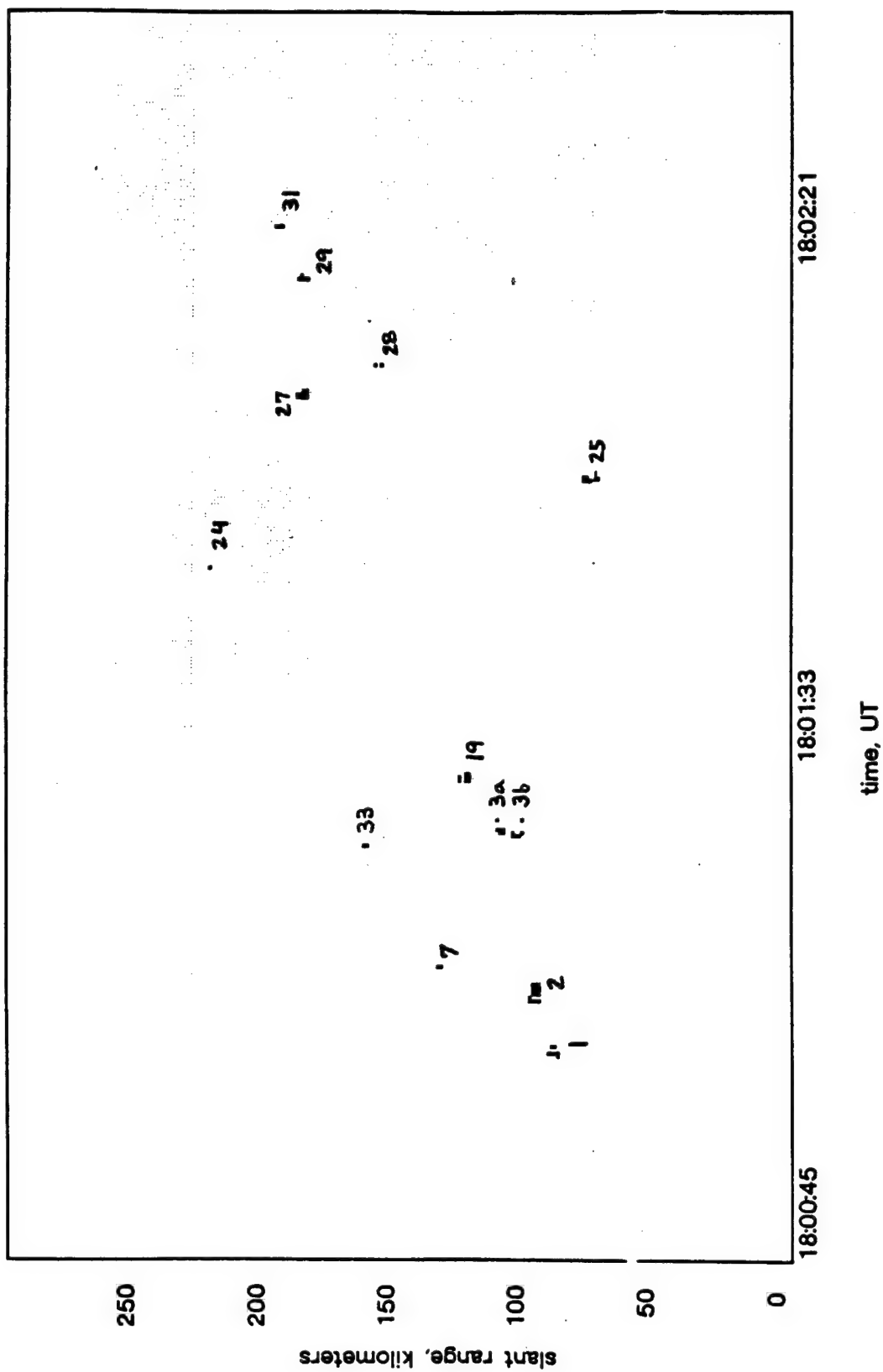


Figure 9. Labeled debris events for the 28 MHz radar.

49.92 MHz Radar RTI Hawaii 1986 Day: 248

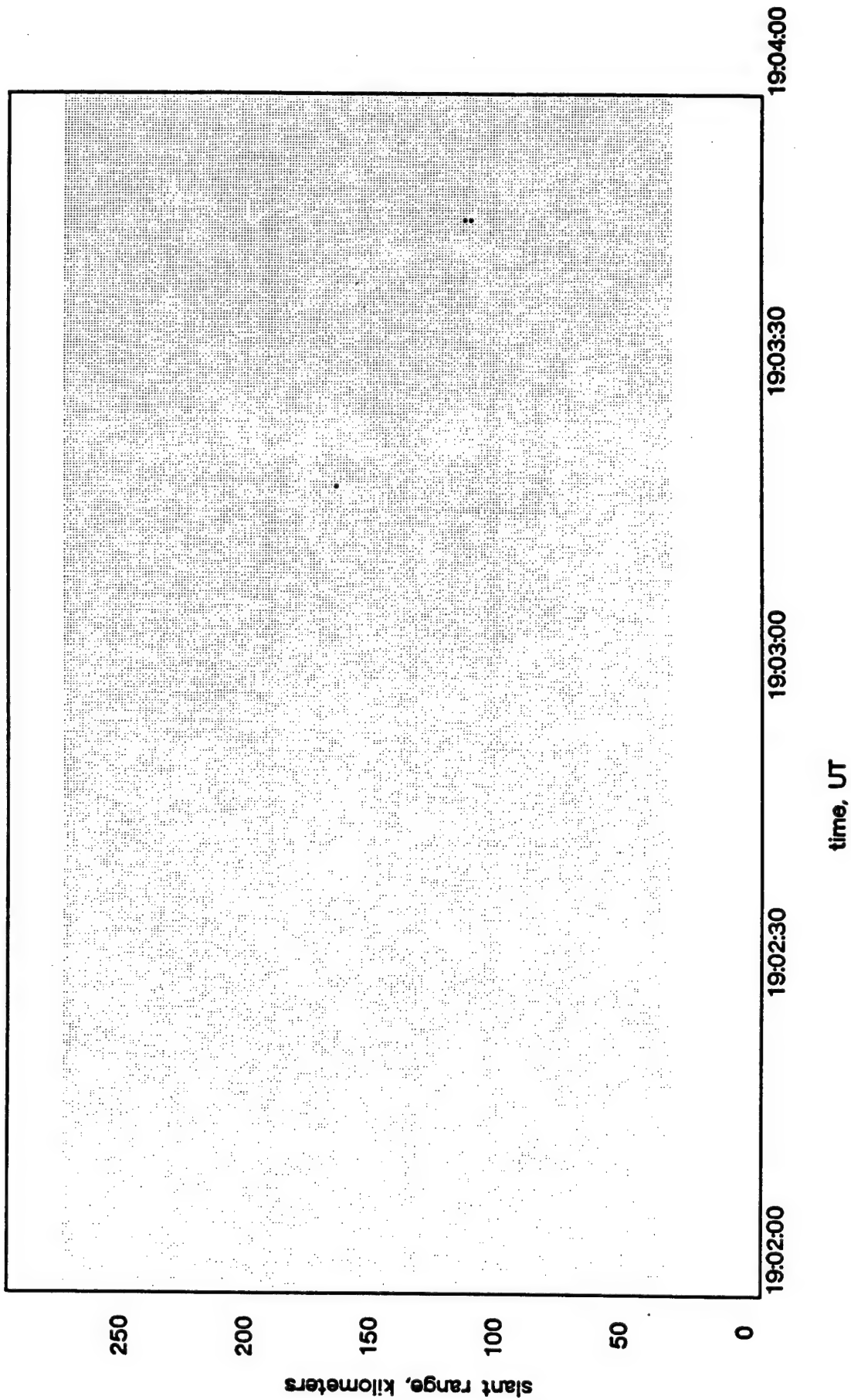


Figure 10. Rev 2 RTI.

49.92 MHz Radar RTI Hawaii 1986 Day: 248

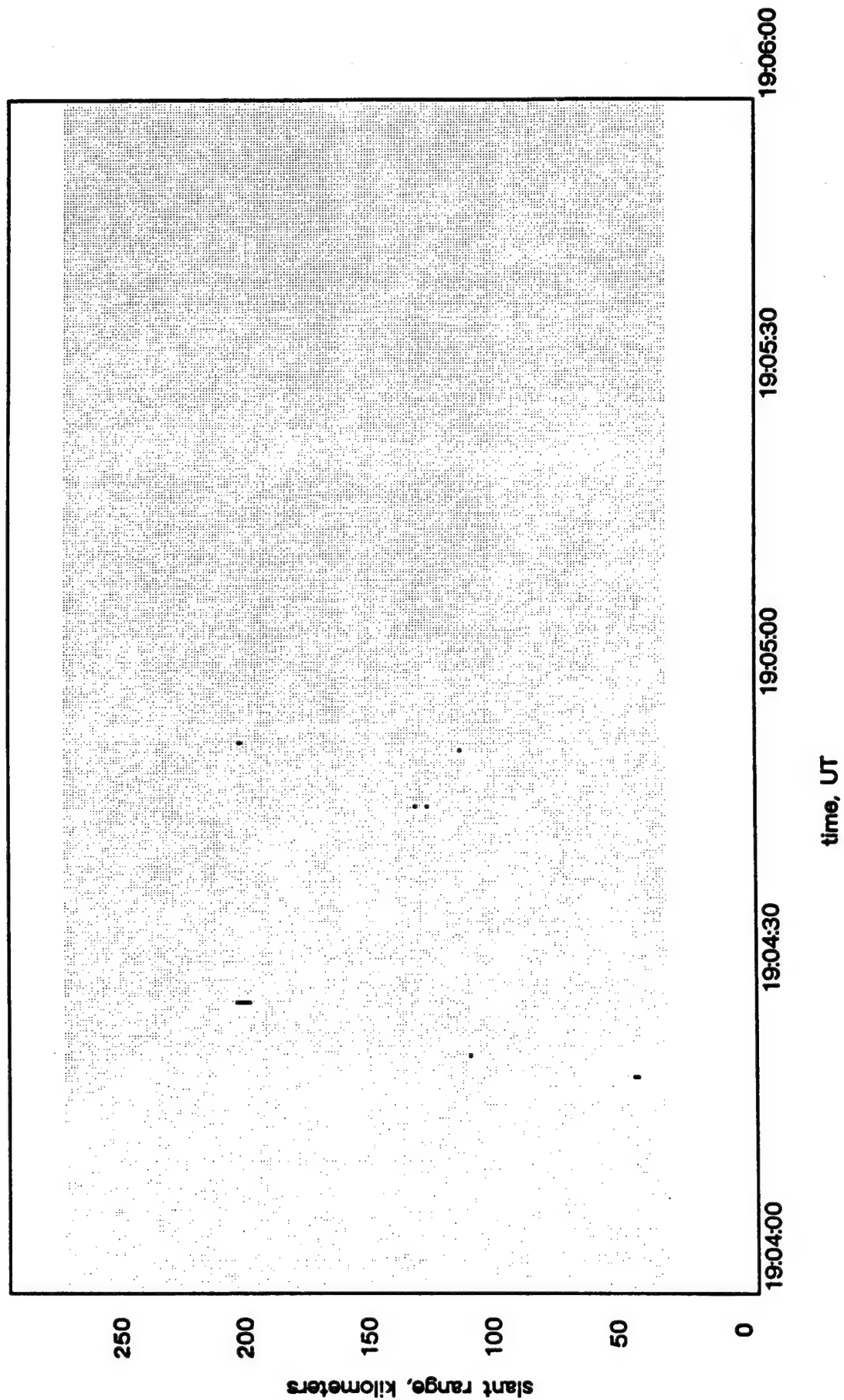


Figure 11. Rev 2 RTI.

49.92 MHz Radar RTI Hawaii 1986 Day: 248

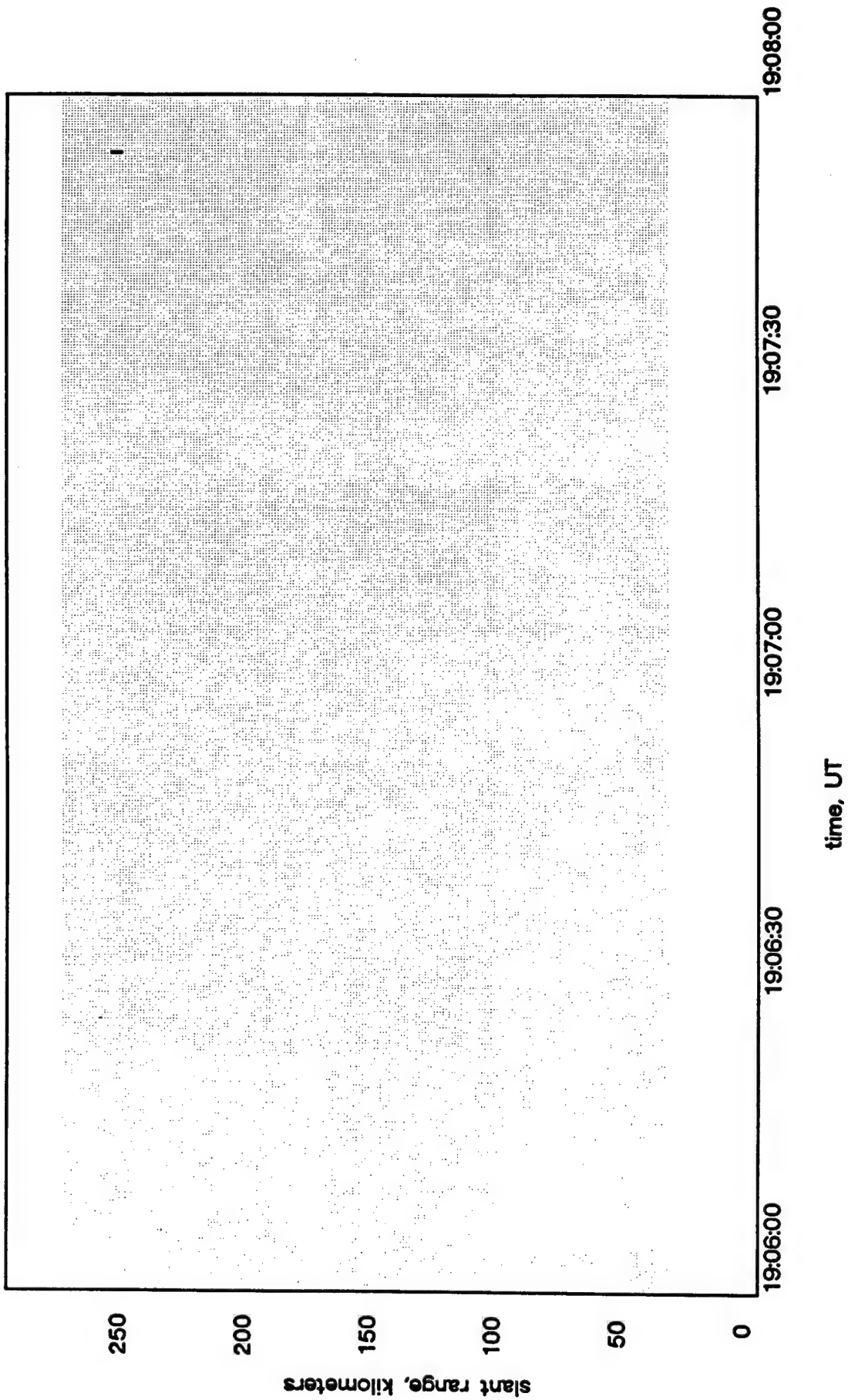


Figure 12. Rev 2 RTI.

49.92 MHz Radar RTI Hawaii 1986 Day: 248

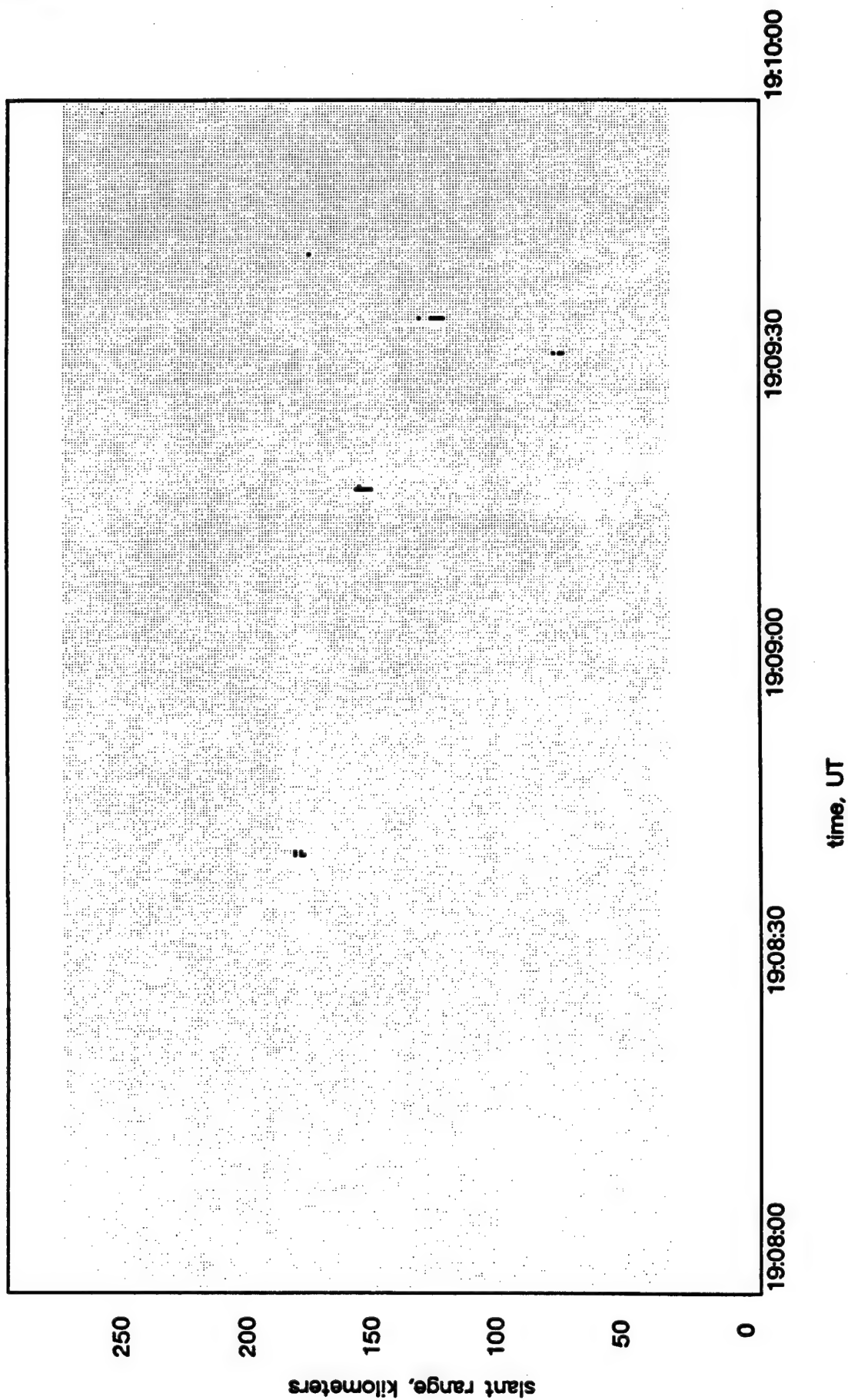


Figure 13. Rev 2 RTI.

49.92 MHz Radar RTI Hawaii 1986 Day: 248

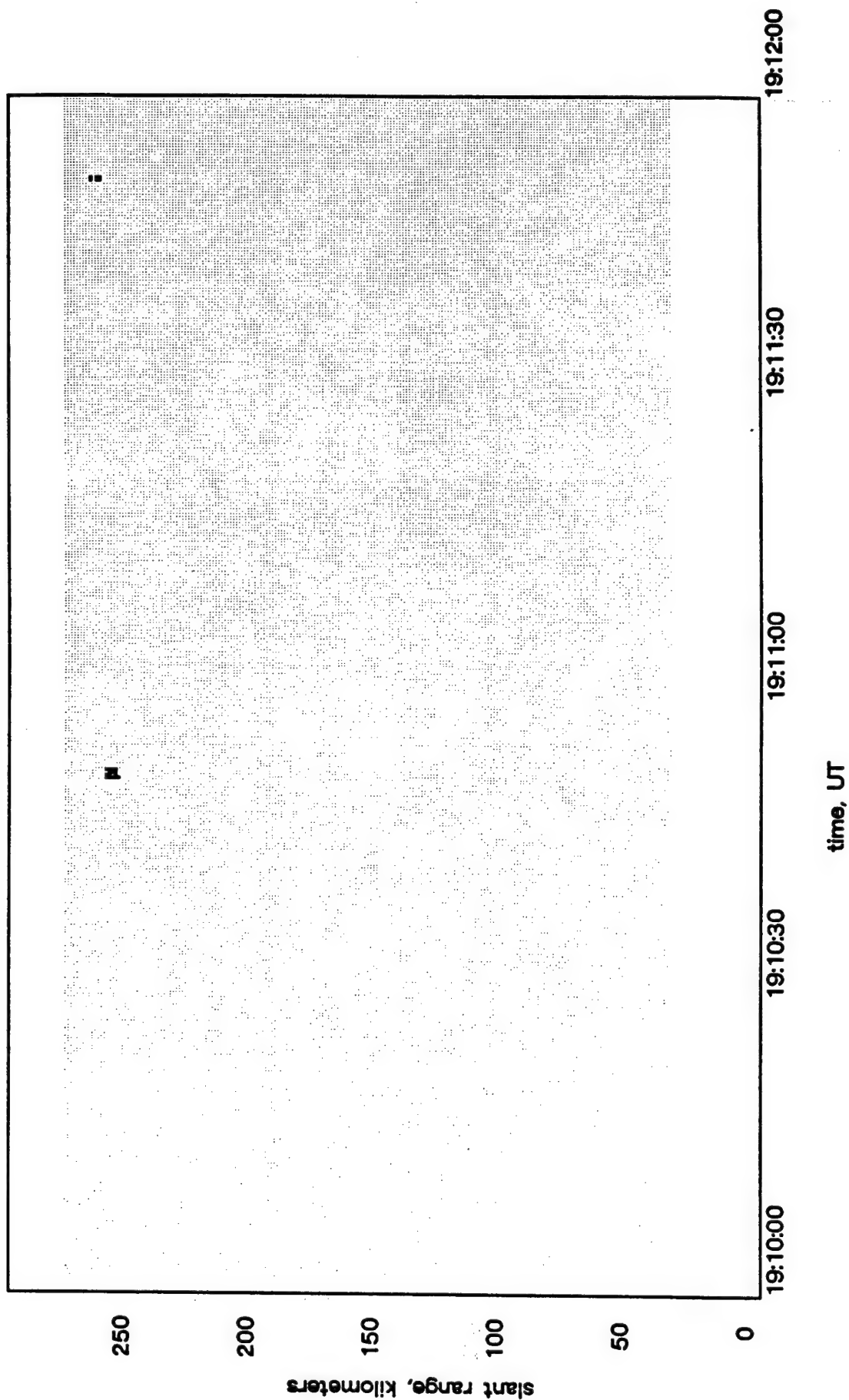


Figure 14. Rev 2 RTI.

49.92 MHz Radar RTI Hawaii 1986 Day: 248

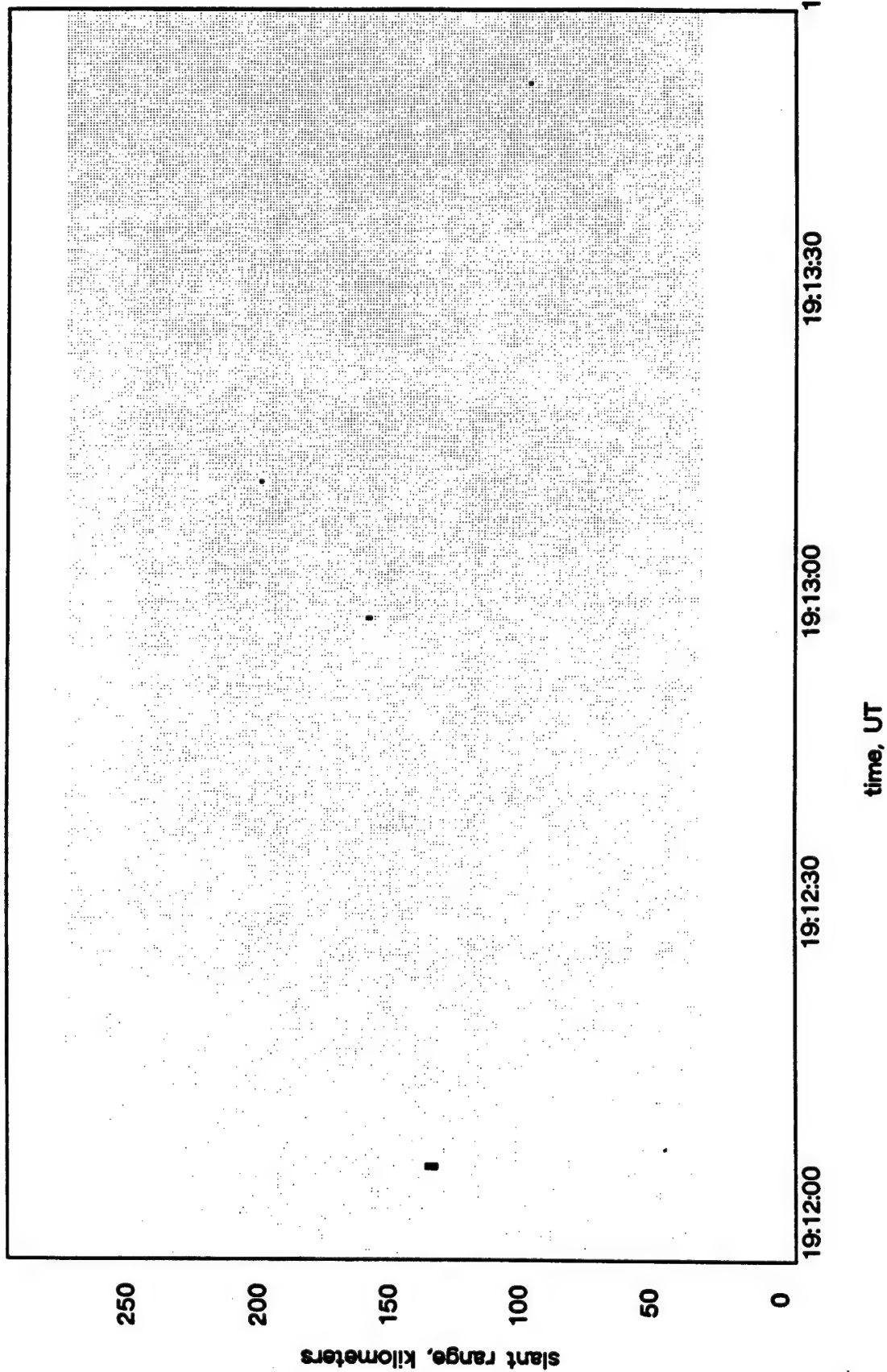


Figure 15. Rev 2 RTI.

49.92 MHz Radar RTI Hawaii 1986 Day: 248

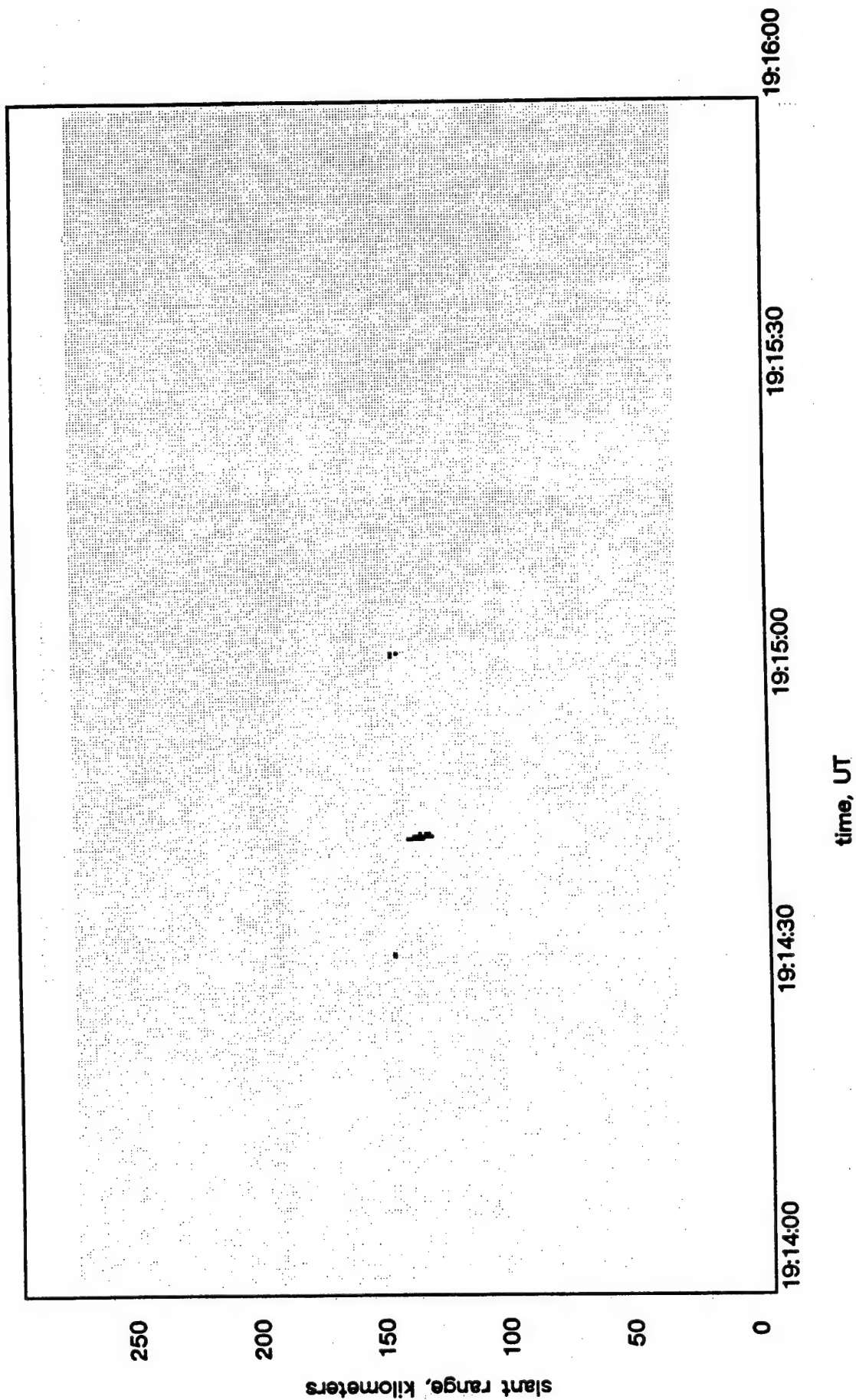


Figure 16. Rev 2 RTI.

49.92 MHz Radar RTI Hawaii 1986 Day: 248

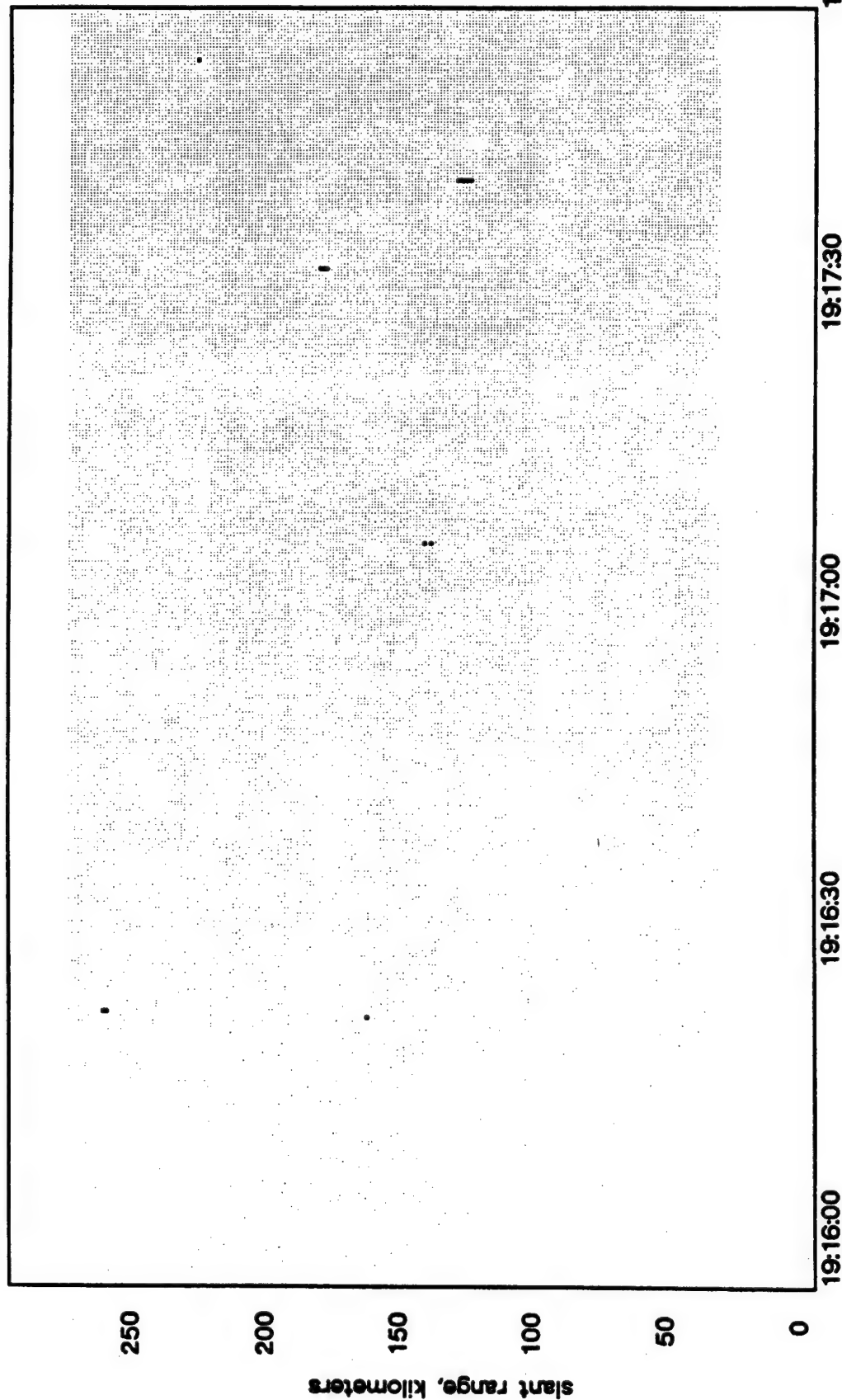


Figure 17. Rev 2 RTI.

49.92 MHz Radar RTI Hawaii 1986 Day: 248

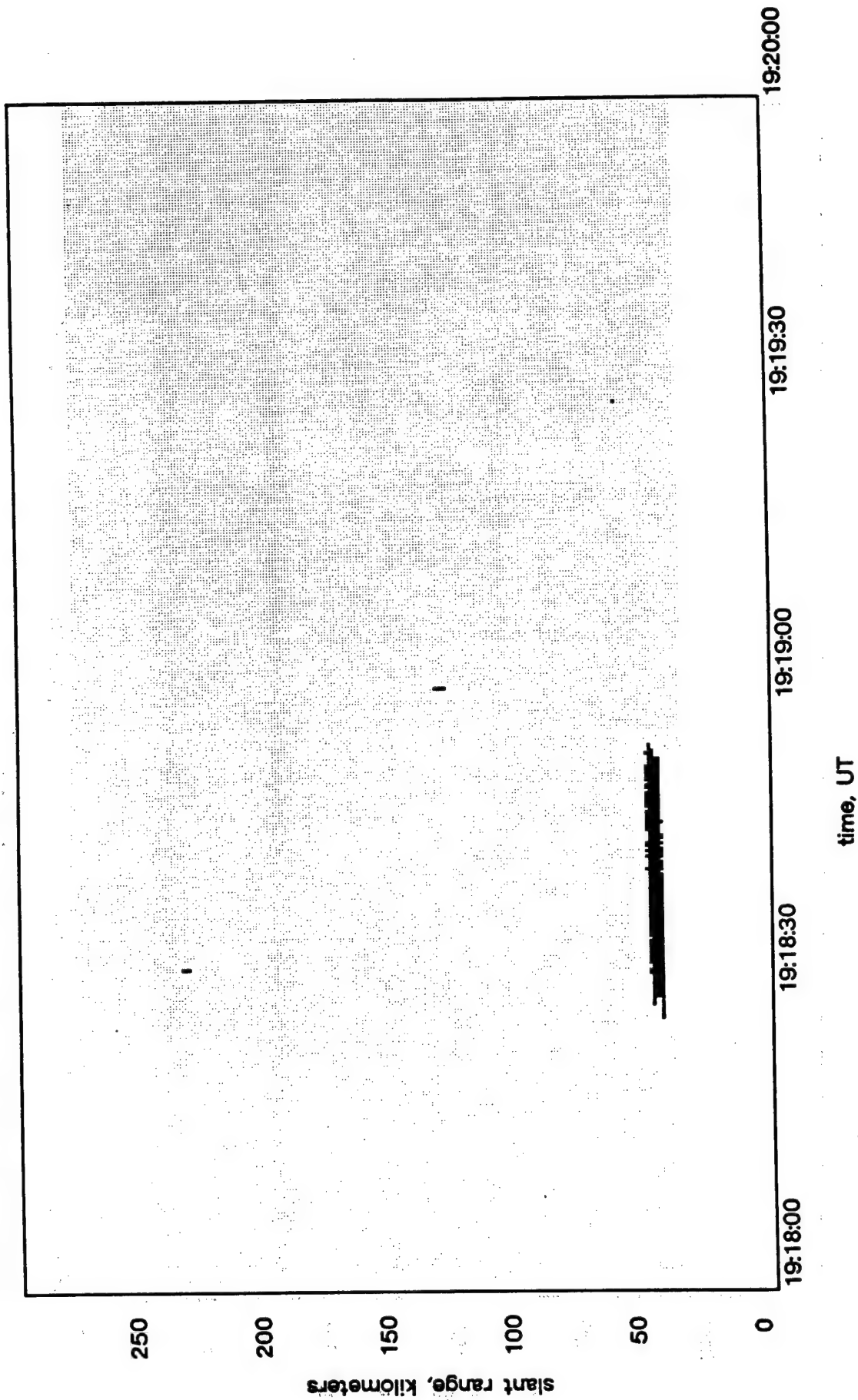


Figure 18. Rev 2 RTI.

49.92 MHz Radar RTI Hawaii 1986 Day: 248

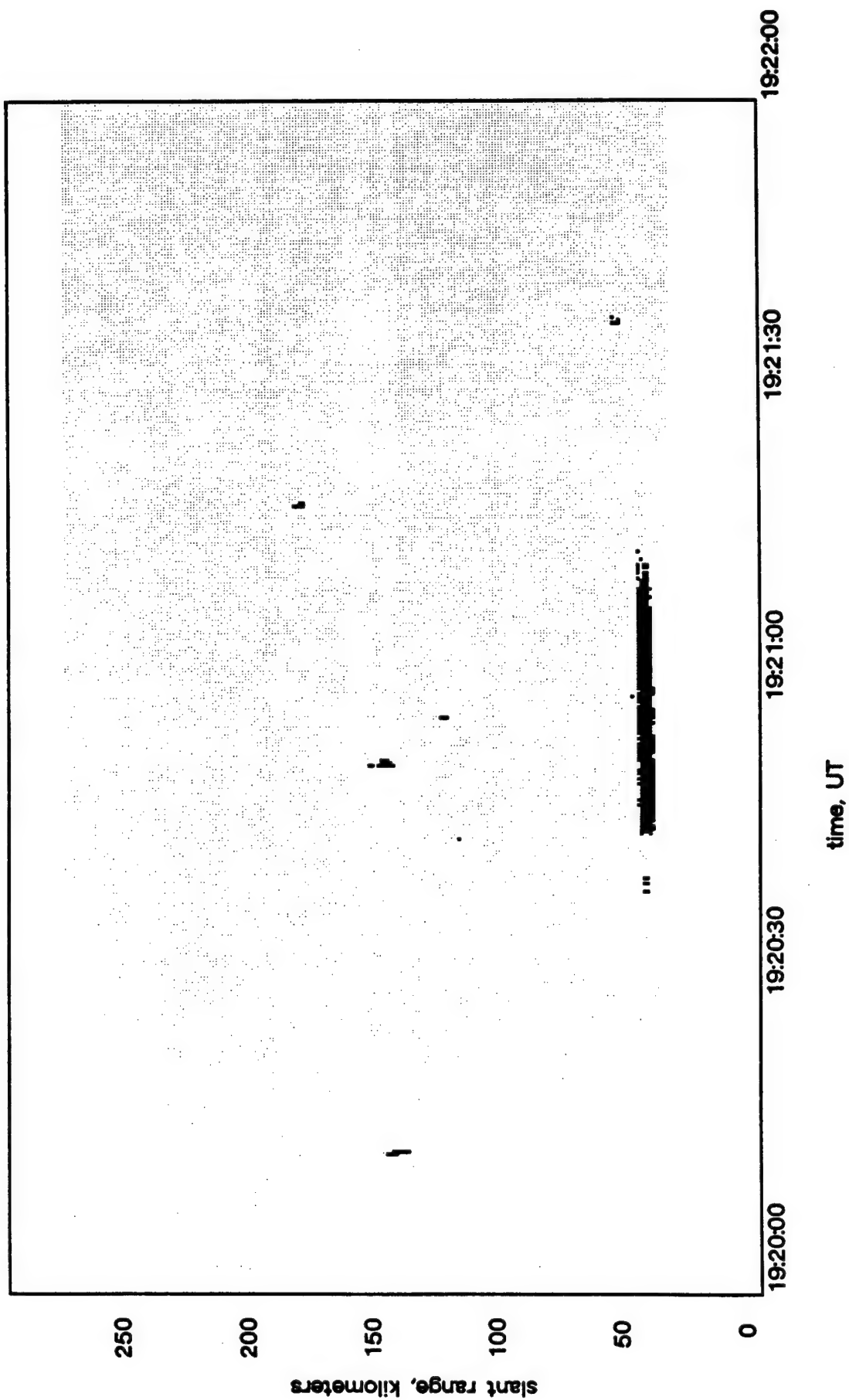


Figure 19. Rev 2 RTI.

49.92 MHz Radar RTI Hawaii 1986 Day: 248

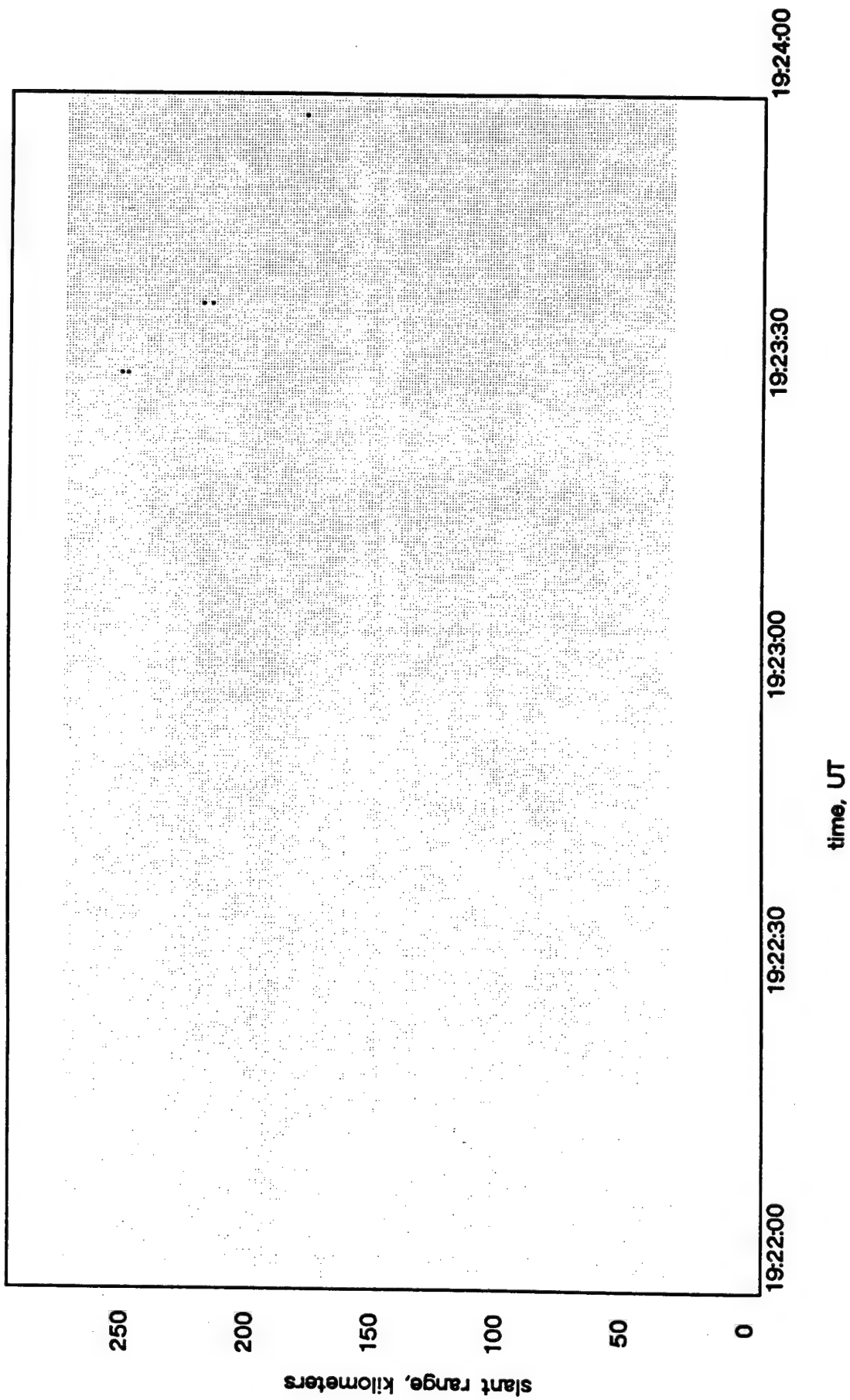


Figure 20. Rev 2 RTI.

49.92 MHz Radar RTI Hawaii 1986 Day: 248

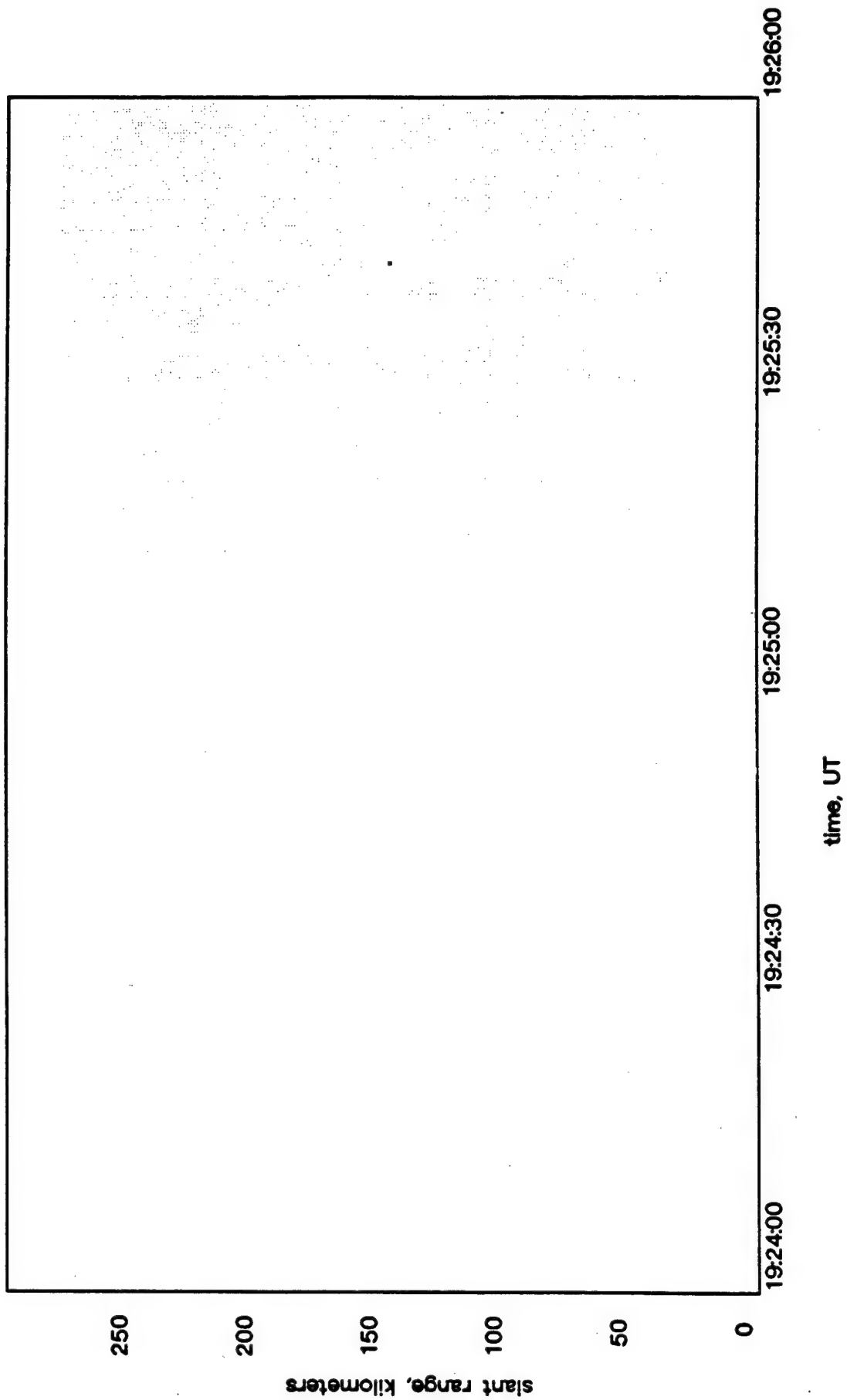


Figure 21. Rev 2 RTI.

49.92 MHz Radar RTI Hawaii 1986 Day: 248

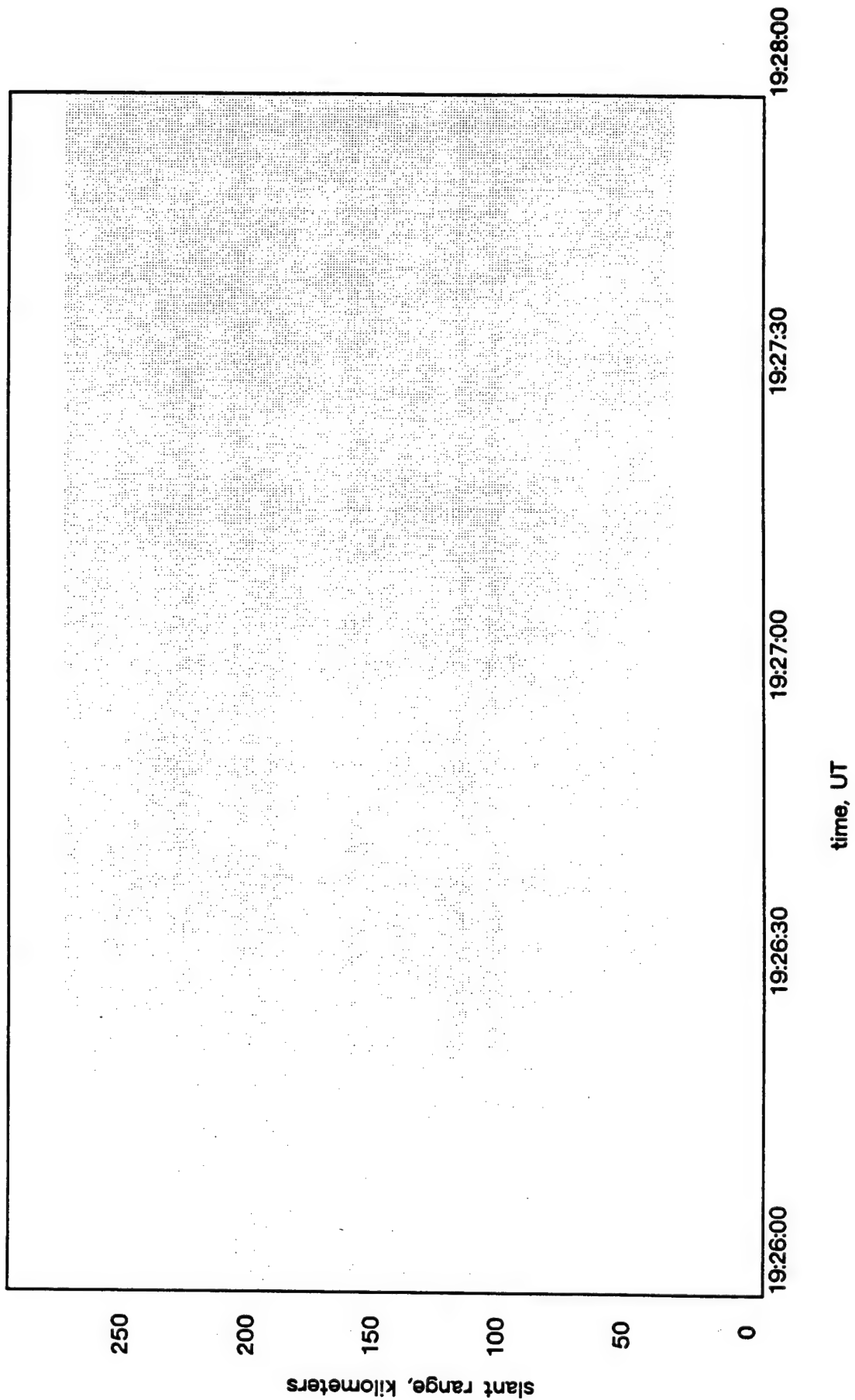


Figure 22. Rev 2 RTI.

49.92 MHz Radar RTI Hawaii 1986 Day: 248

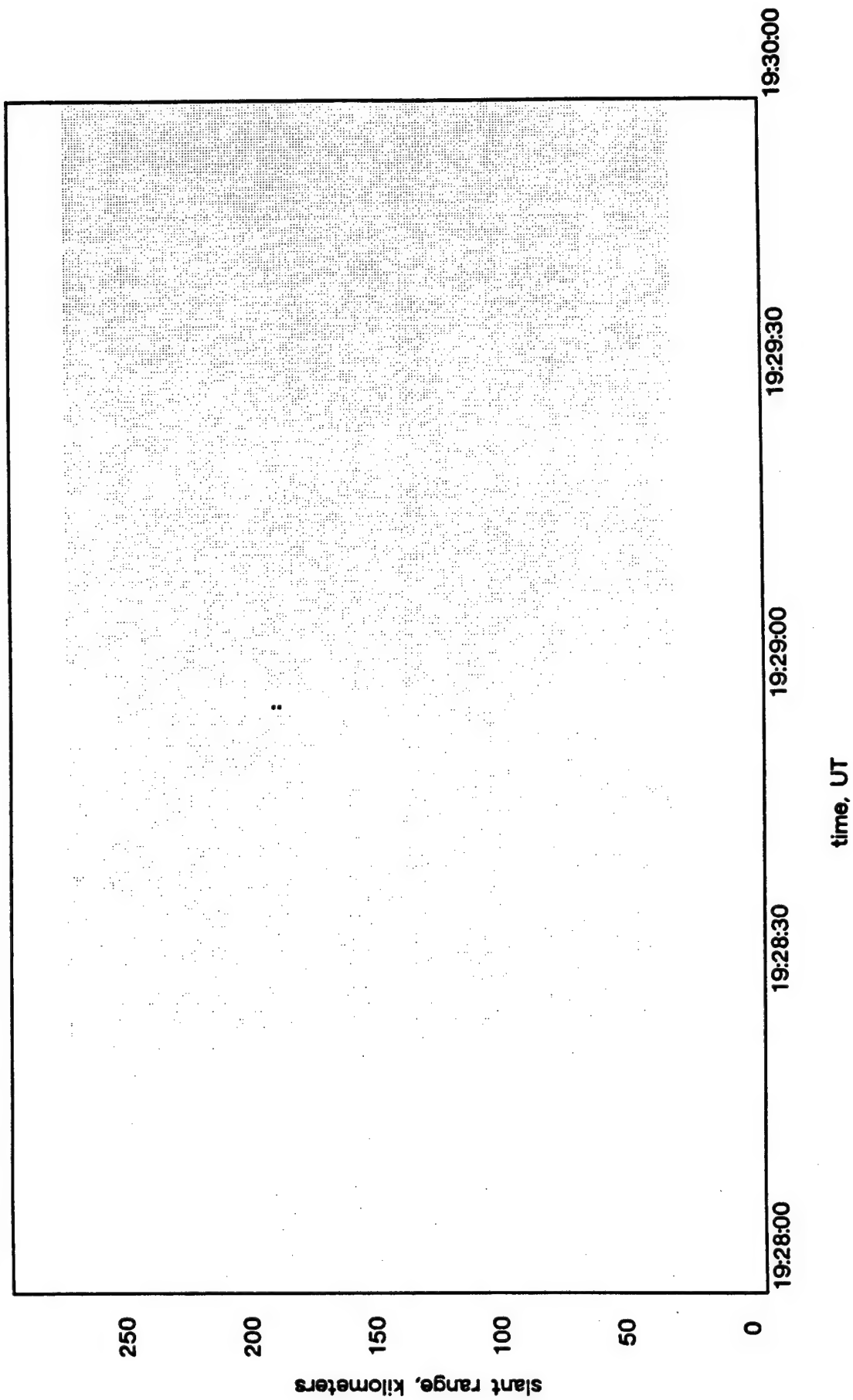


Figure 23. Rev 2 RTI.

49.92 MHz Radar RTI Hawaii 1986 Day: 248

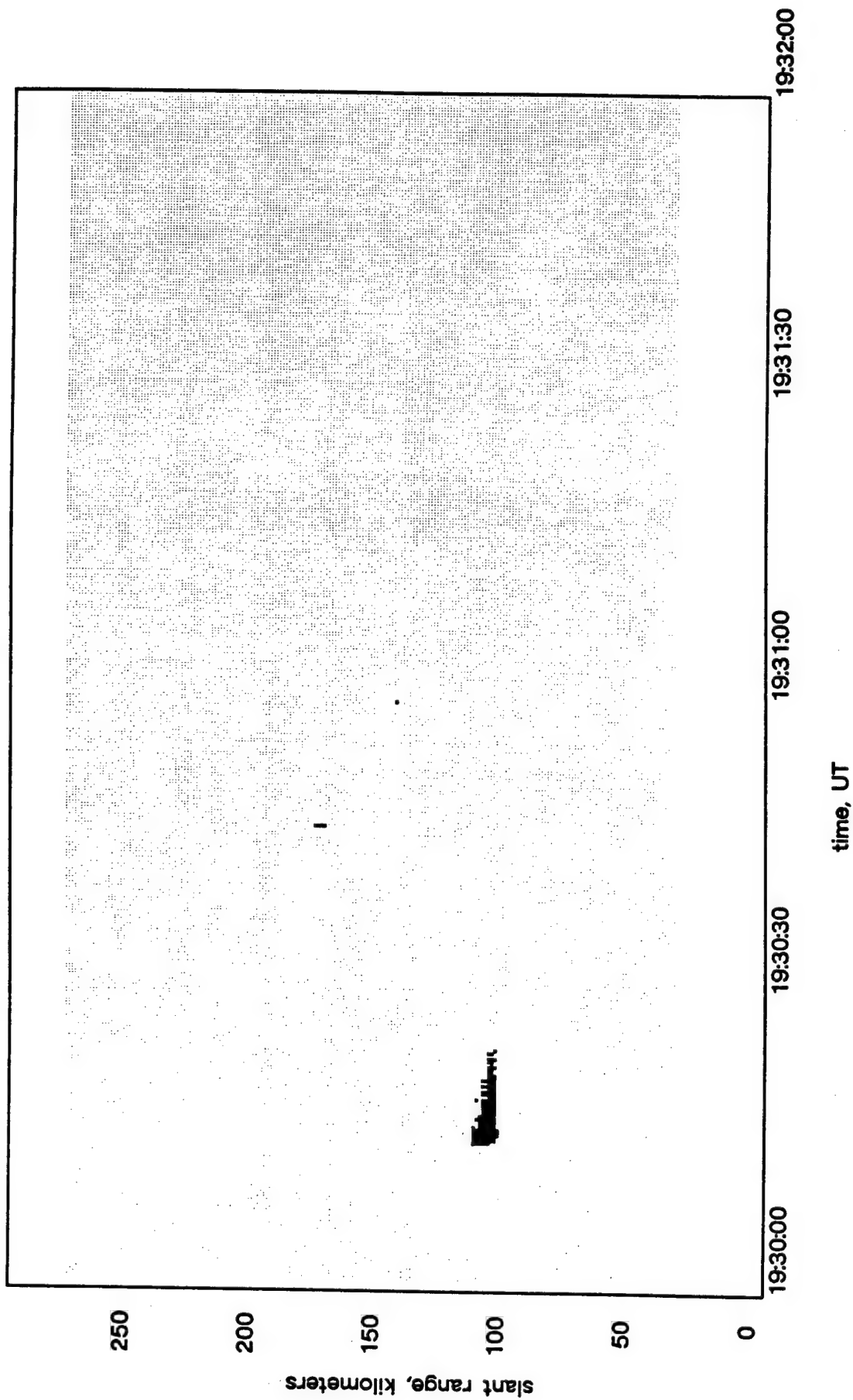


Figure 24. Rev 2 RTI.

49.92 MHz Radar RTI Hawaii 1986 Day: 248

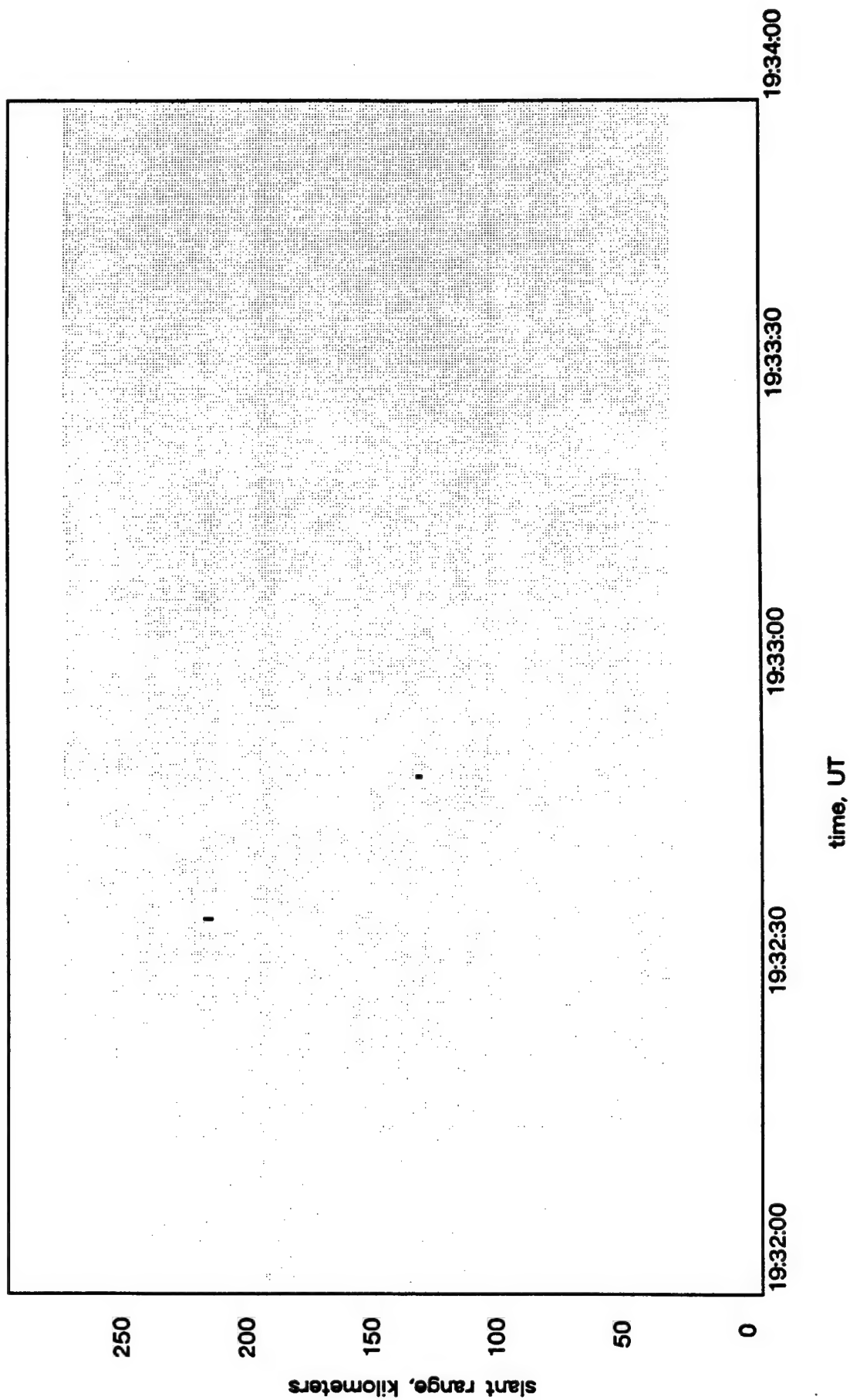


Figure 25. Rev 2 RTI.

49.92 MHz Radar RTI Hawaii 1986 Day: 248

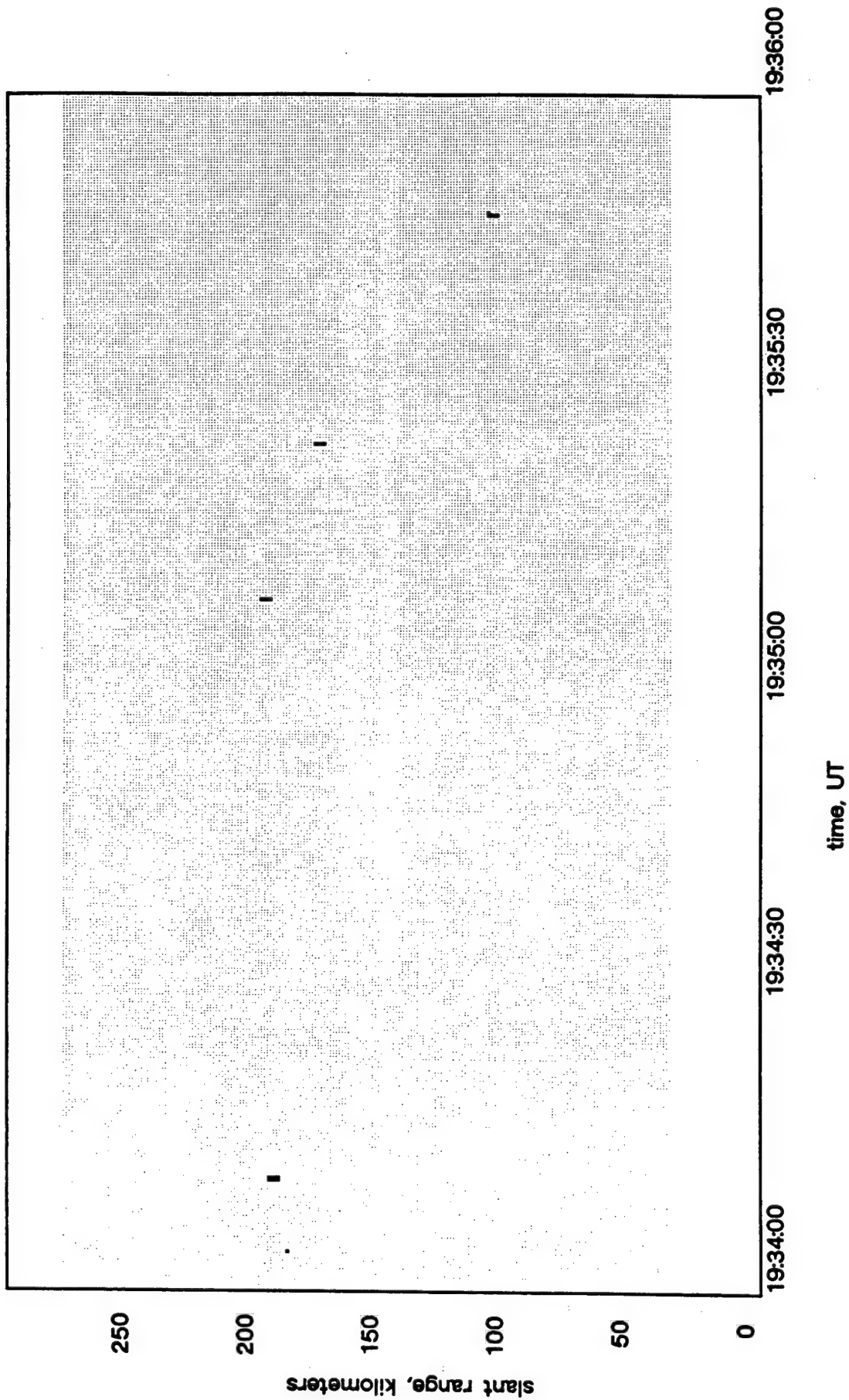


Figure 26. Rev 2 RTI.

49.92 MHz Radar RTI Hawaii 1986 Day: 248

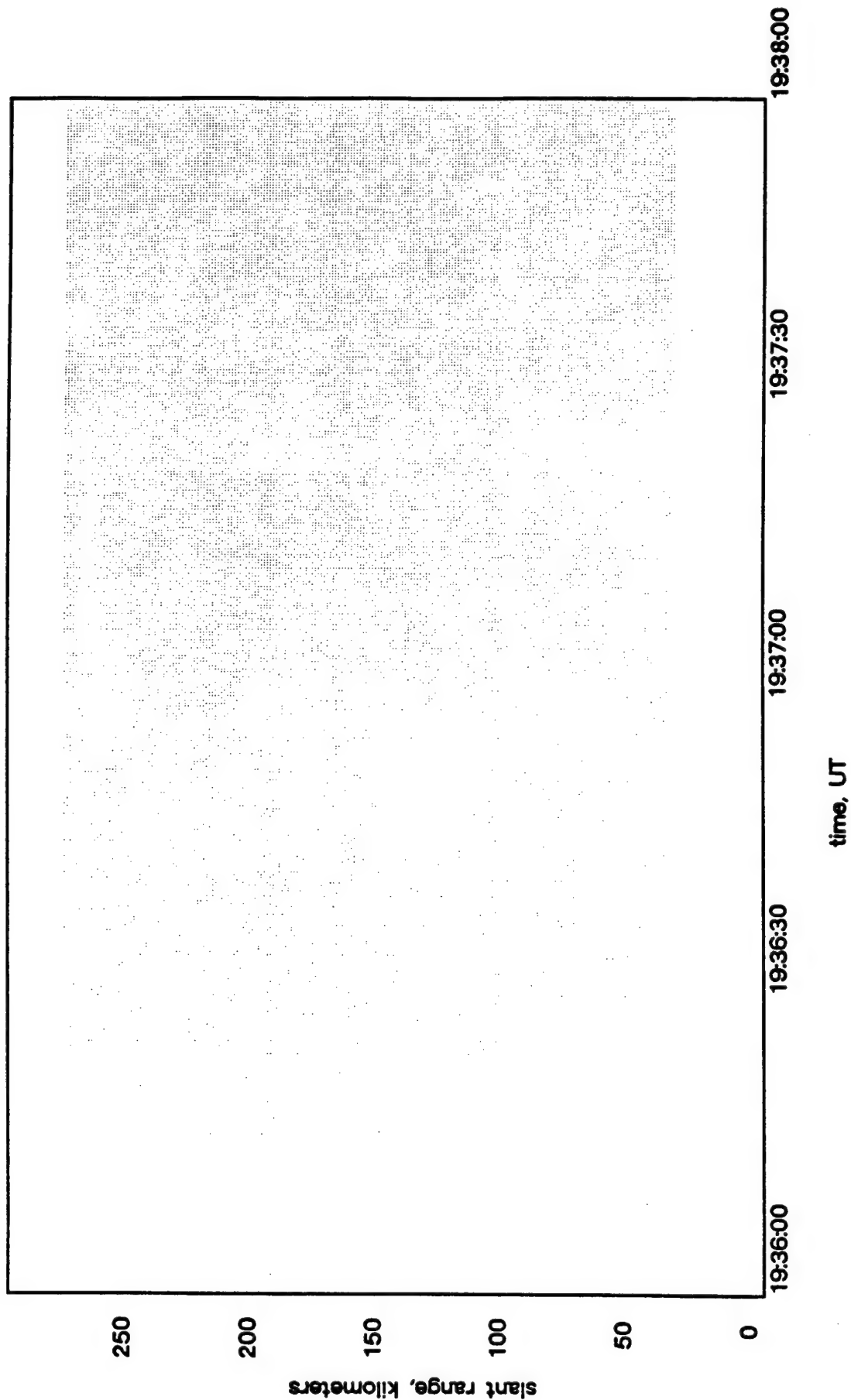


Figure 27. Rev 2 RTI.

49.92 MHz Radar RTI Hawaii 1986 Day: 248

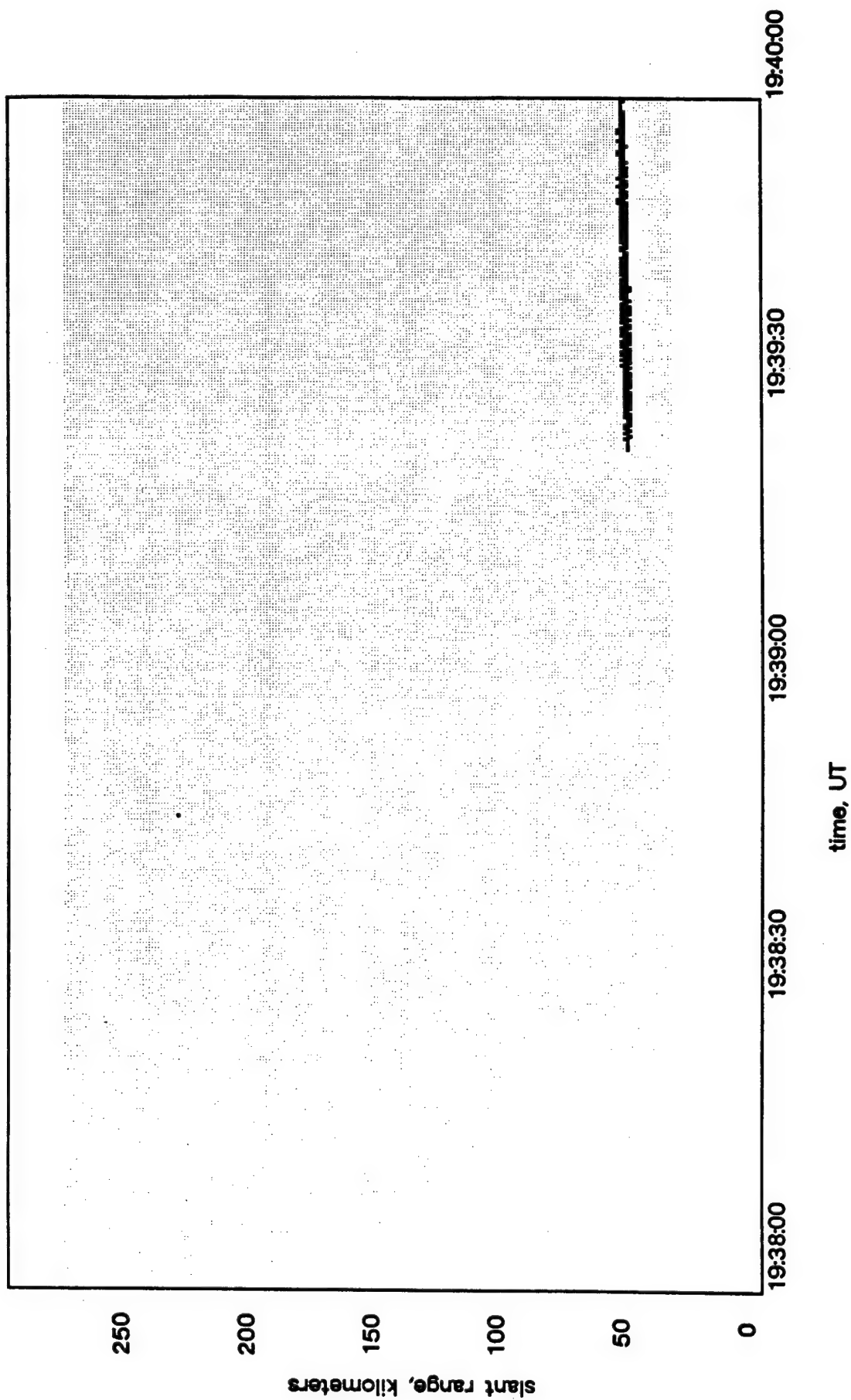


Figure 28. Rev 2 RTI.

49.92 MHz Radar RTI Hawaii 1986 Day: 248

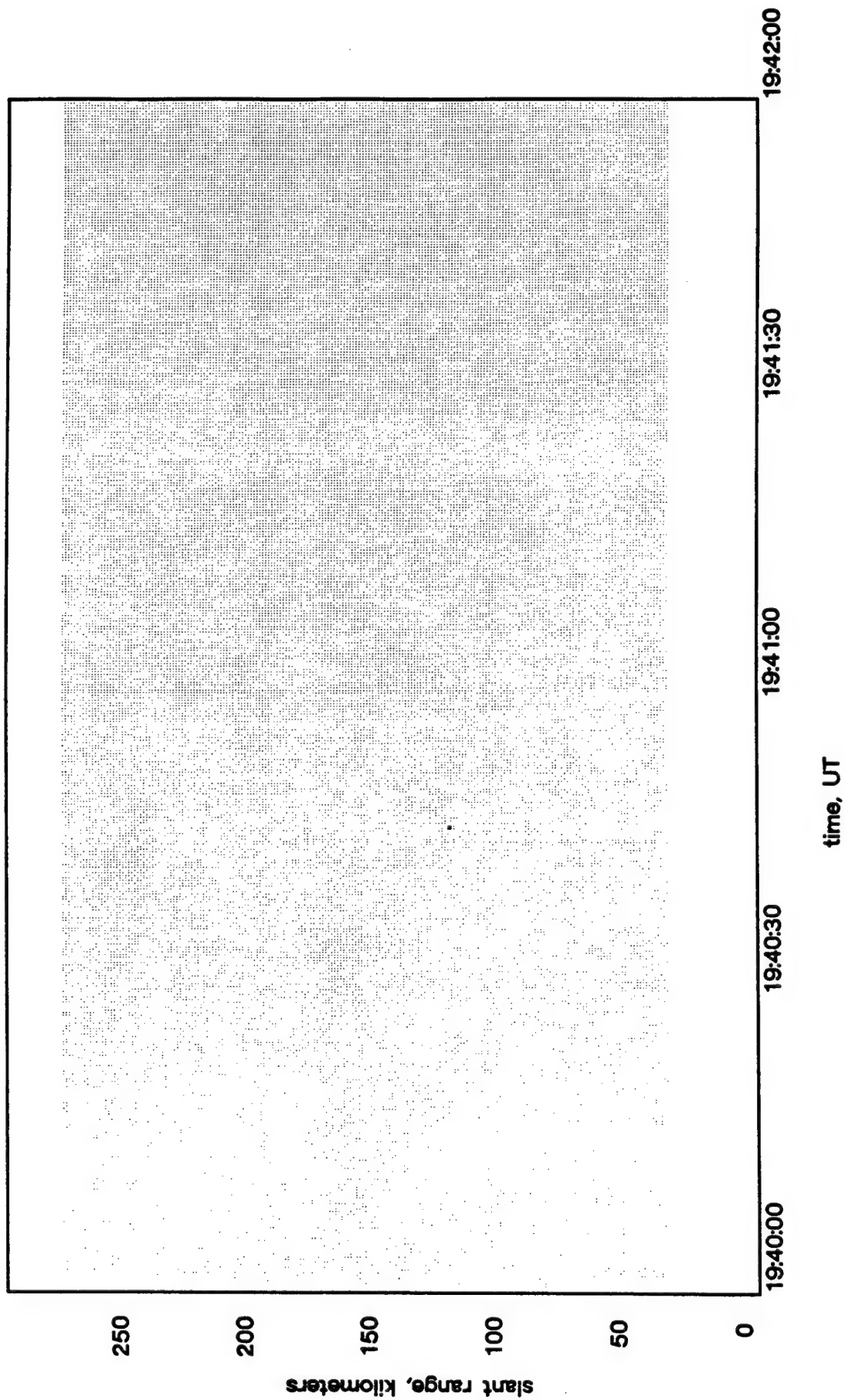


Figure 29. Rev 2 RTI.

49.92 MHz Radar RTI Hawaii 1986 Day: 248

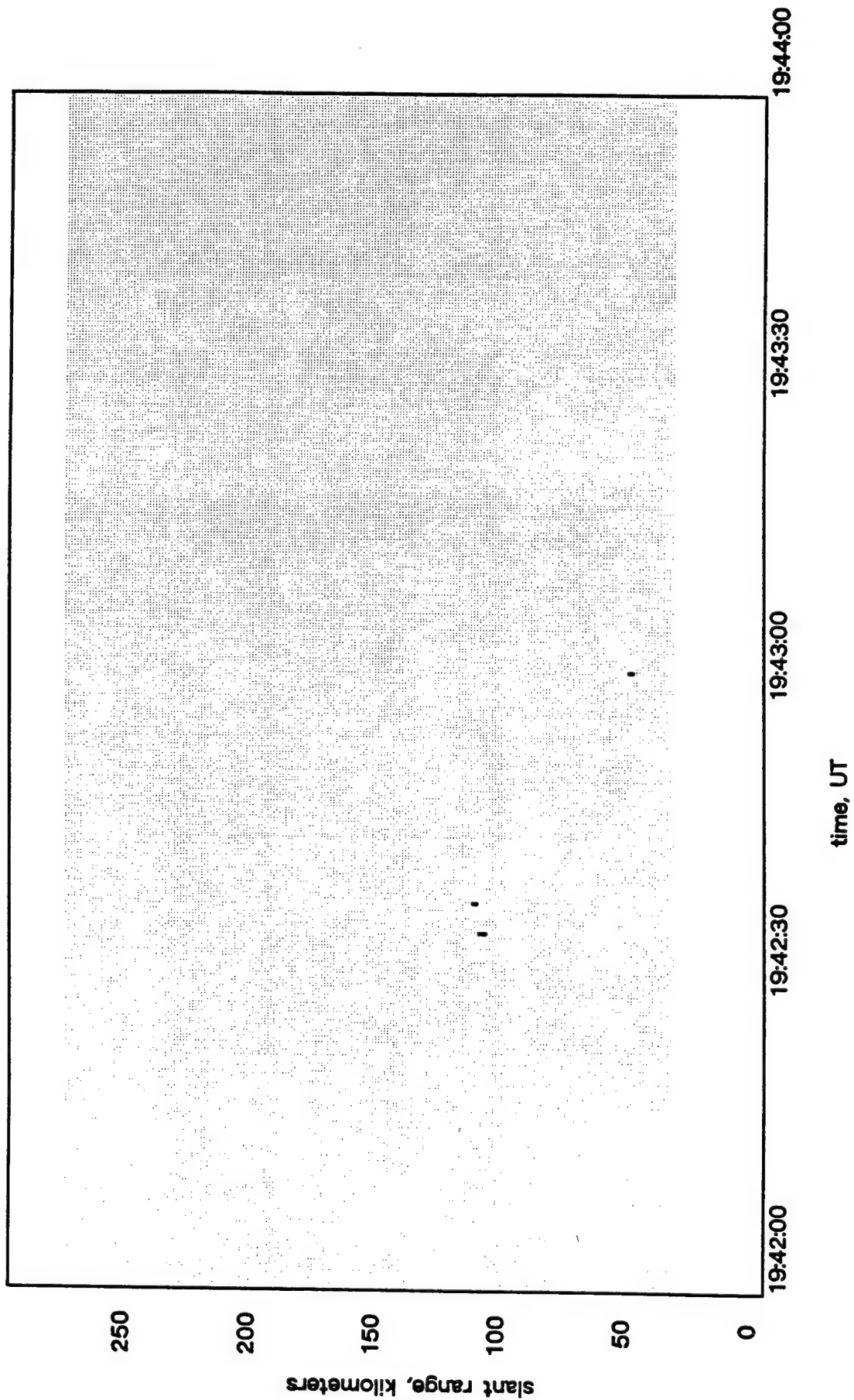


Figure 30. Rev 2 RTI.

49.92 MHz Radar RTI Hawaii 1986 Day: 248

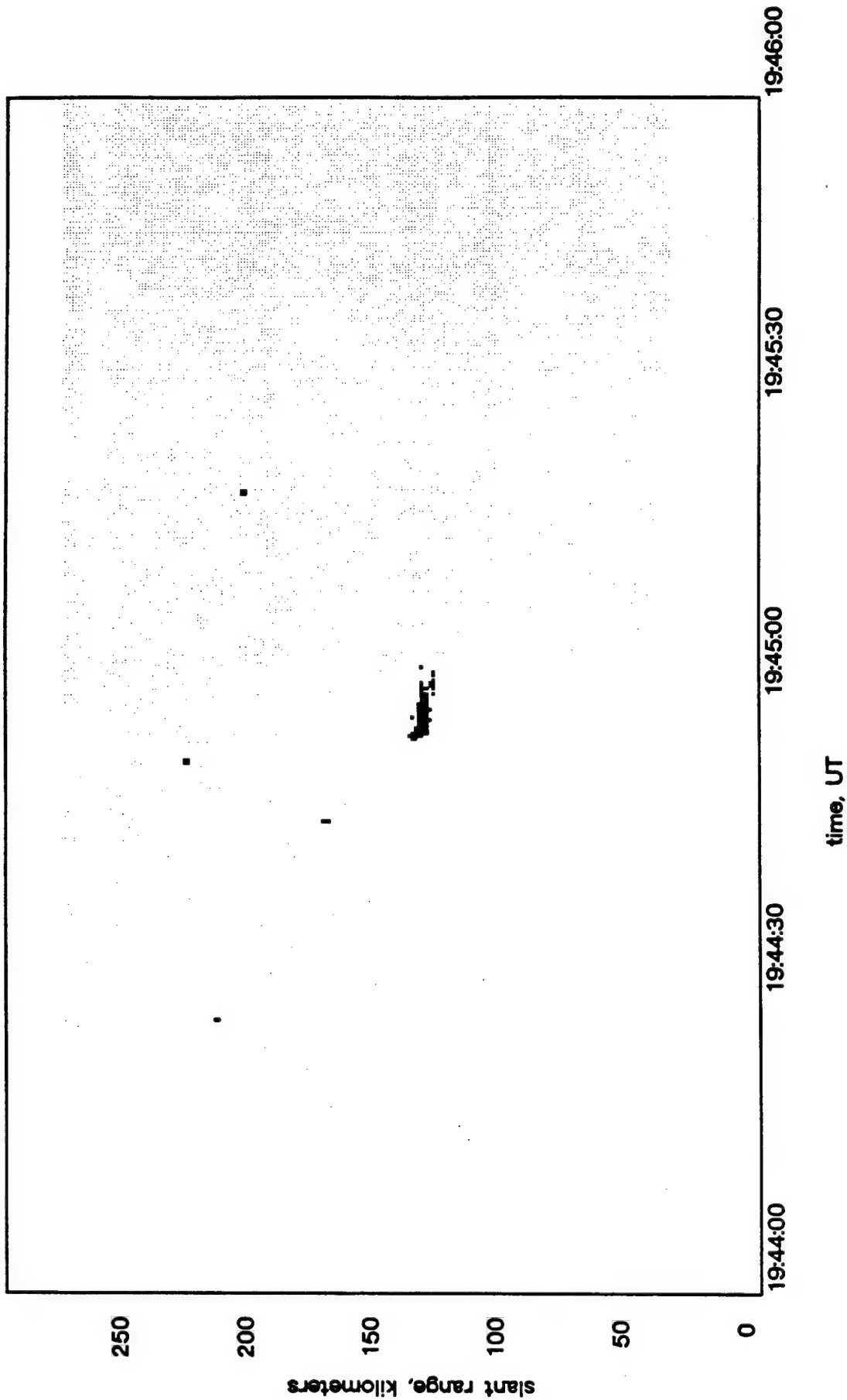


Figure 31. Rev 2 RTI.

49.92 MHz Radar RTI Hawaii 1986 Day: 248

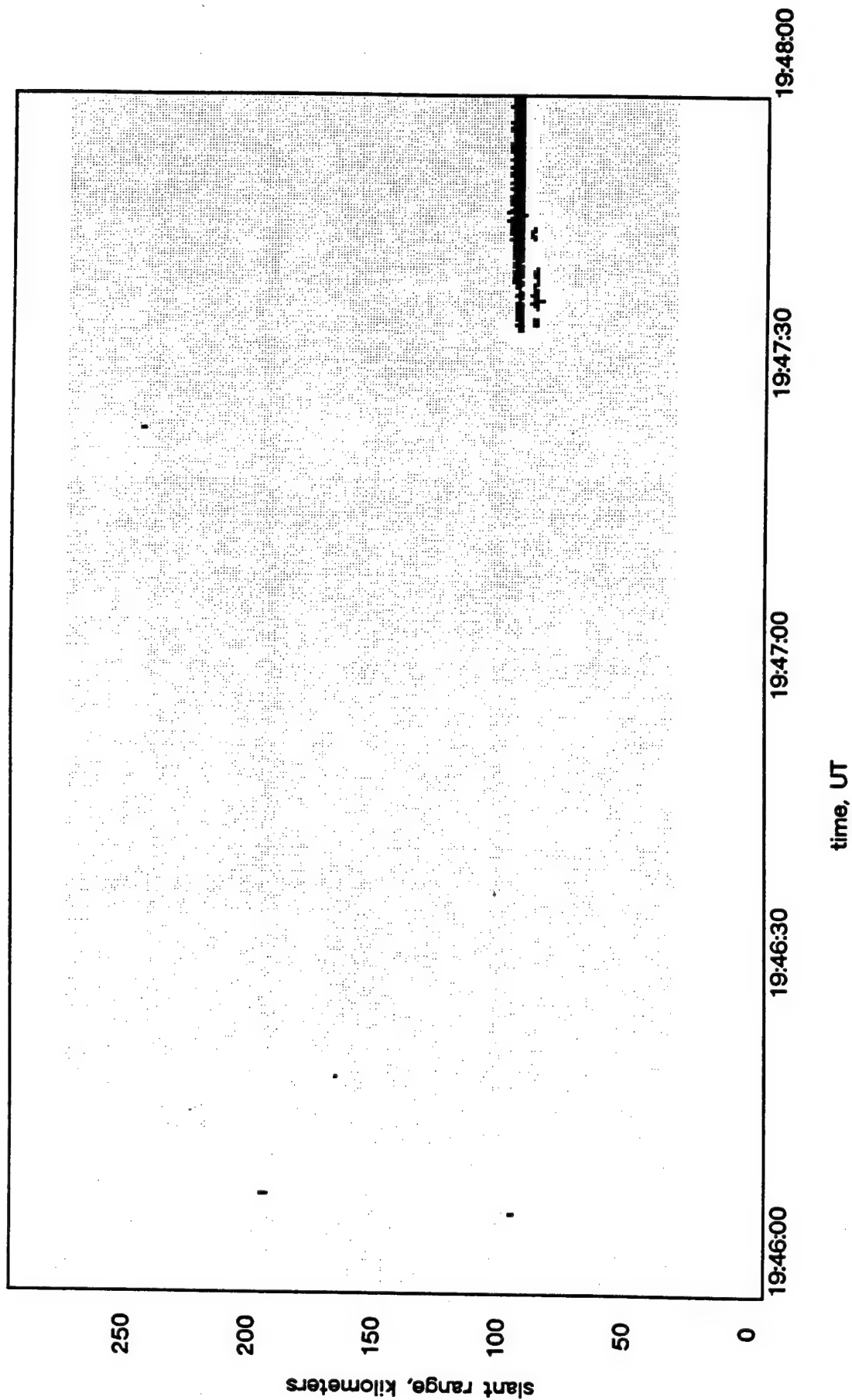


Figure 32. Rev 2 RTI.

49.92 MHz Radar RTI Hawaii 1986 Day: 248

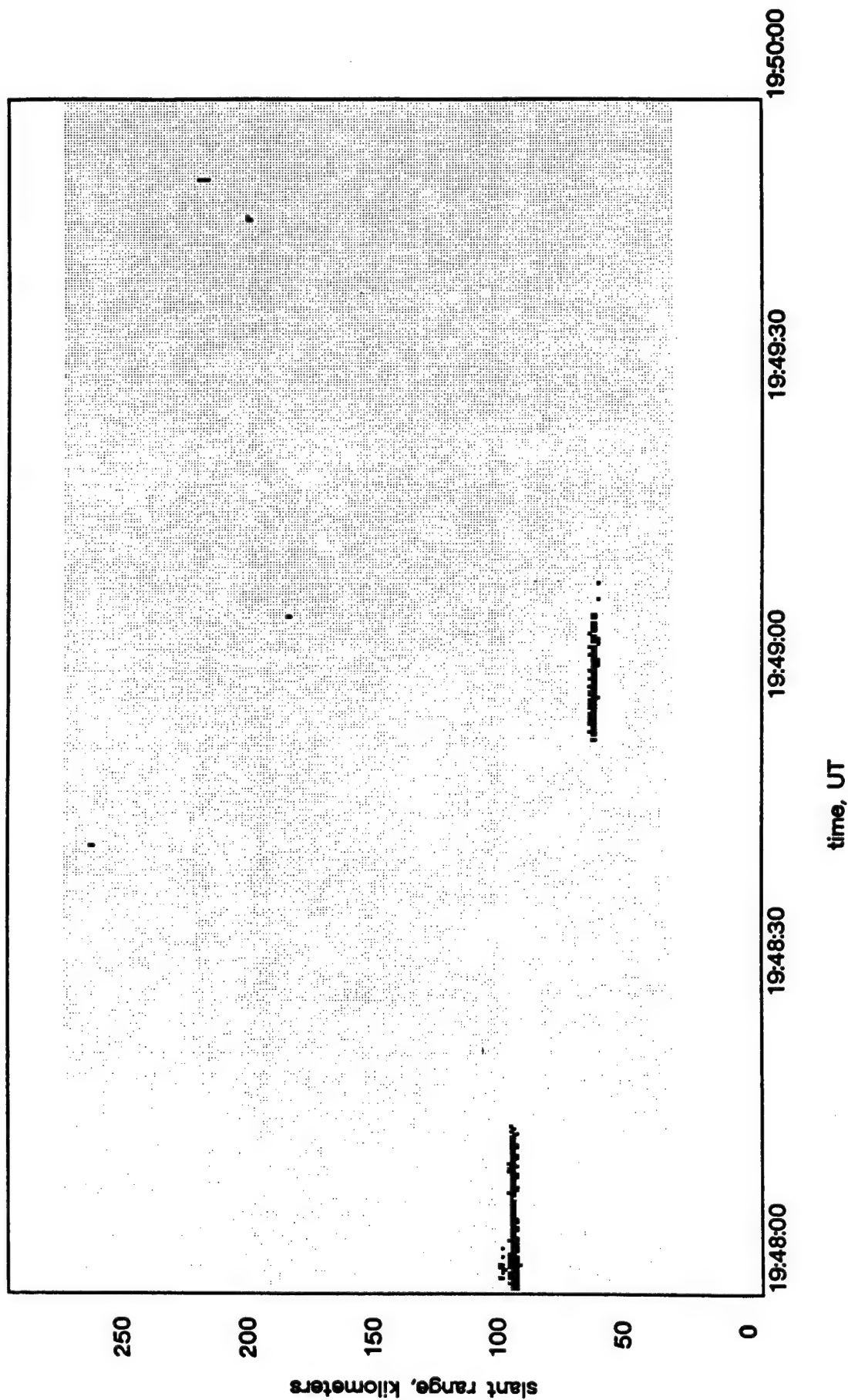


Figure 33. Rev 2 RTI.

49.92 MHz Radar RTI Hawaii 1986 Day: 248

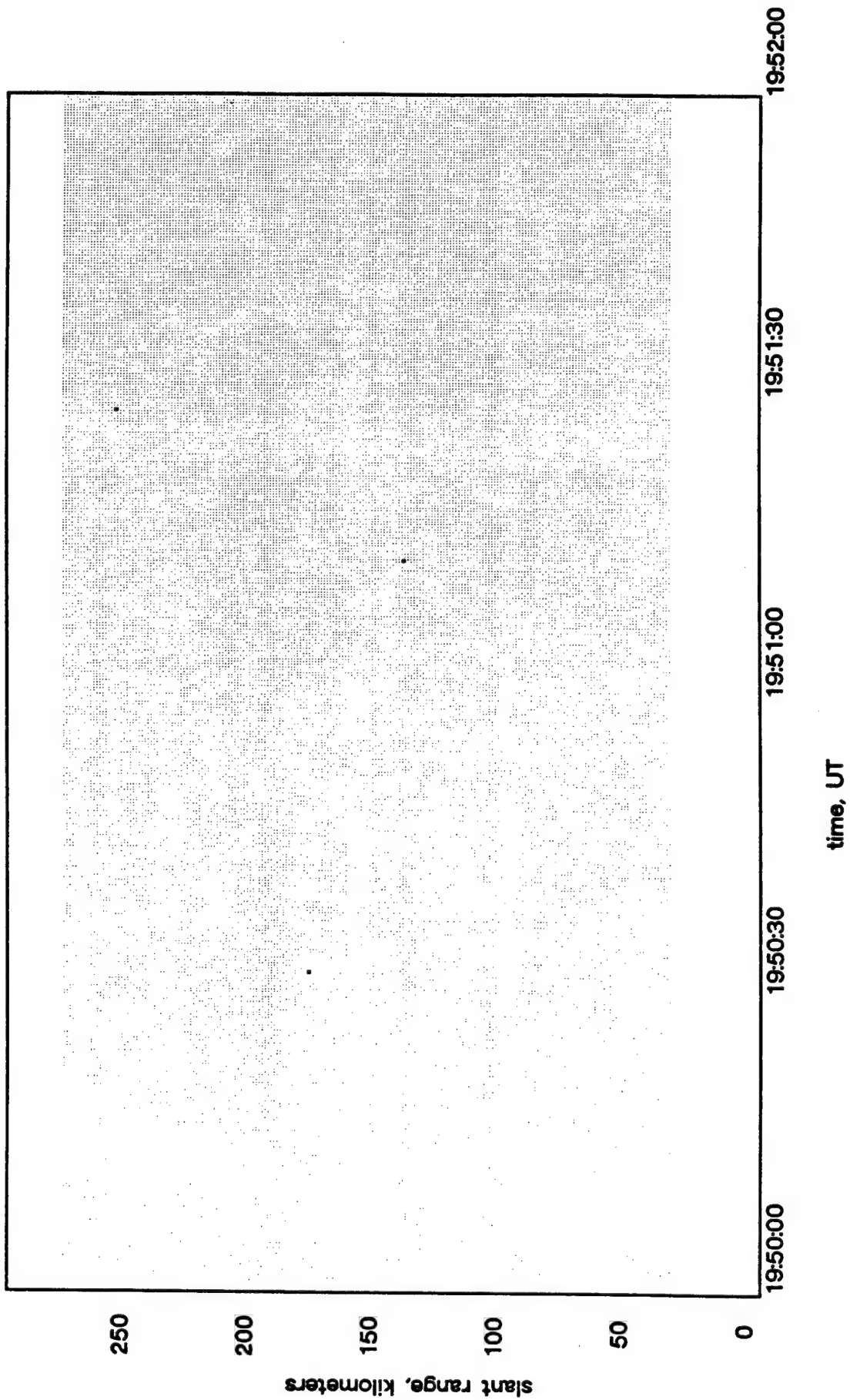


Figure 34. Rev 2 RTI.

49.92 MHz Radar RTI Hawaii 1986 Day: 248

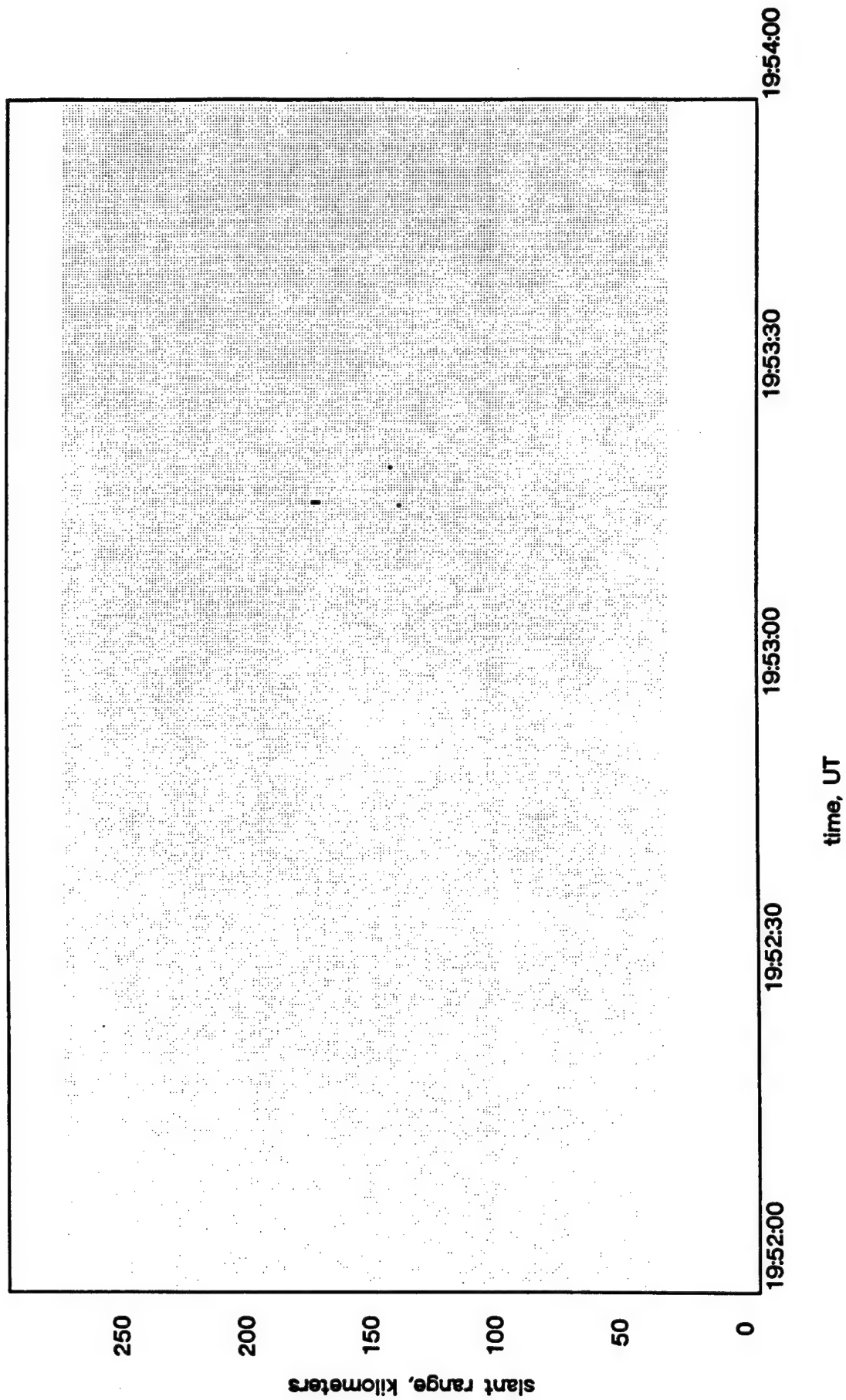


Figure 35. Rev 2 RTI.

49.92 MHz Radar RTI Hawaii 1986 Day: 248

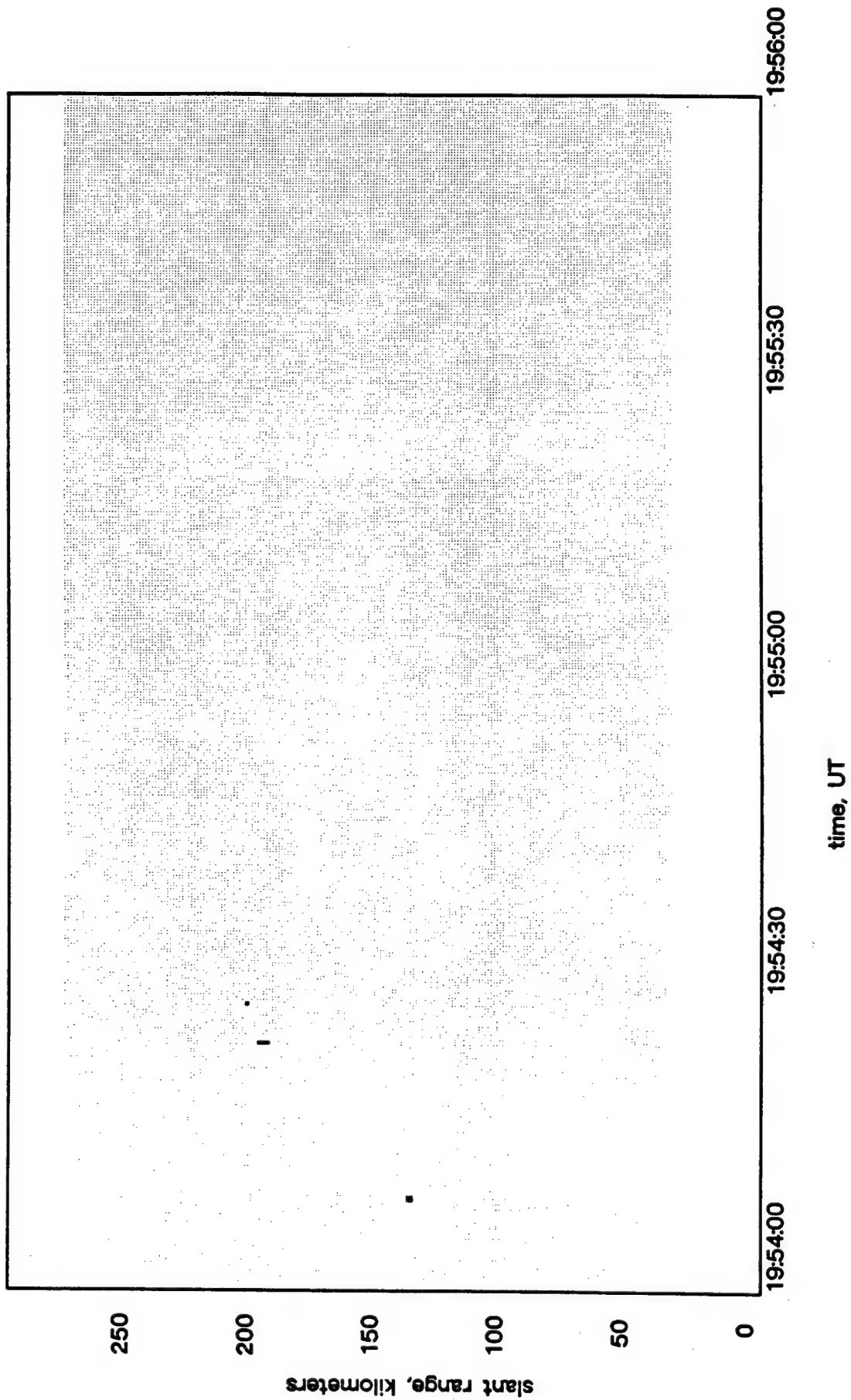


Figure 36. Rev 2 RTI.

49.92 MHz Radar RTI Hawaii 1986 Day: 248

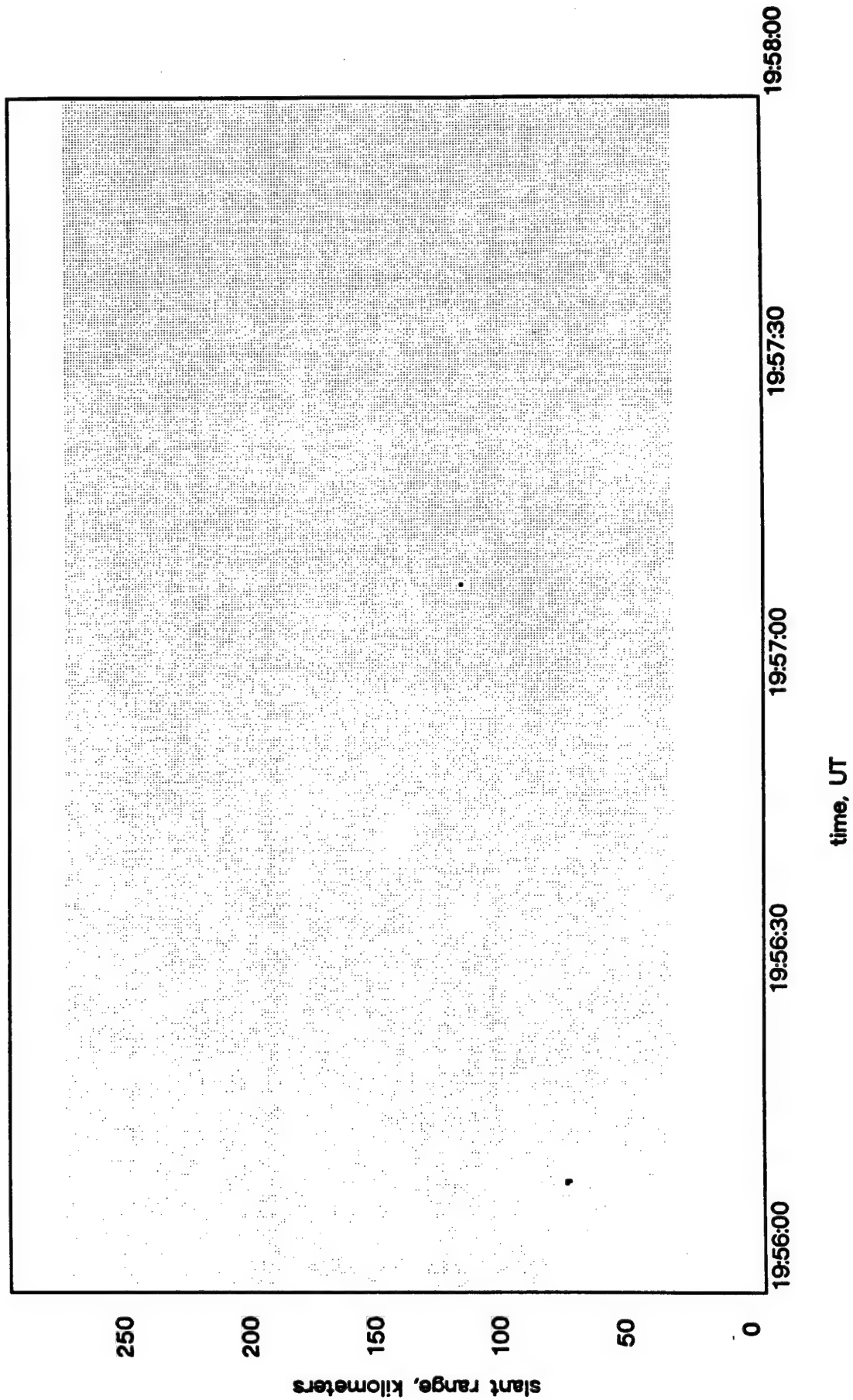


Figure 37. Rev 2 RTI.

49.92 MHz Radar RTI Hawaii 1986 Day: 248

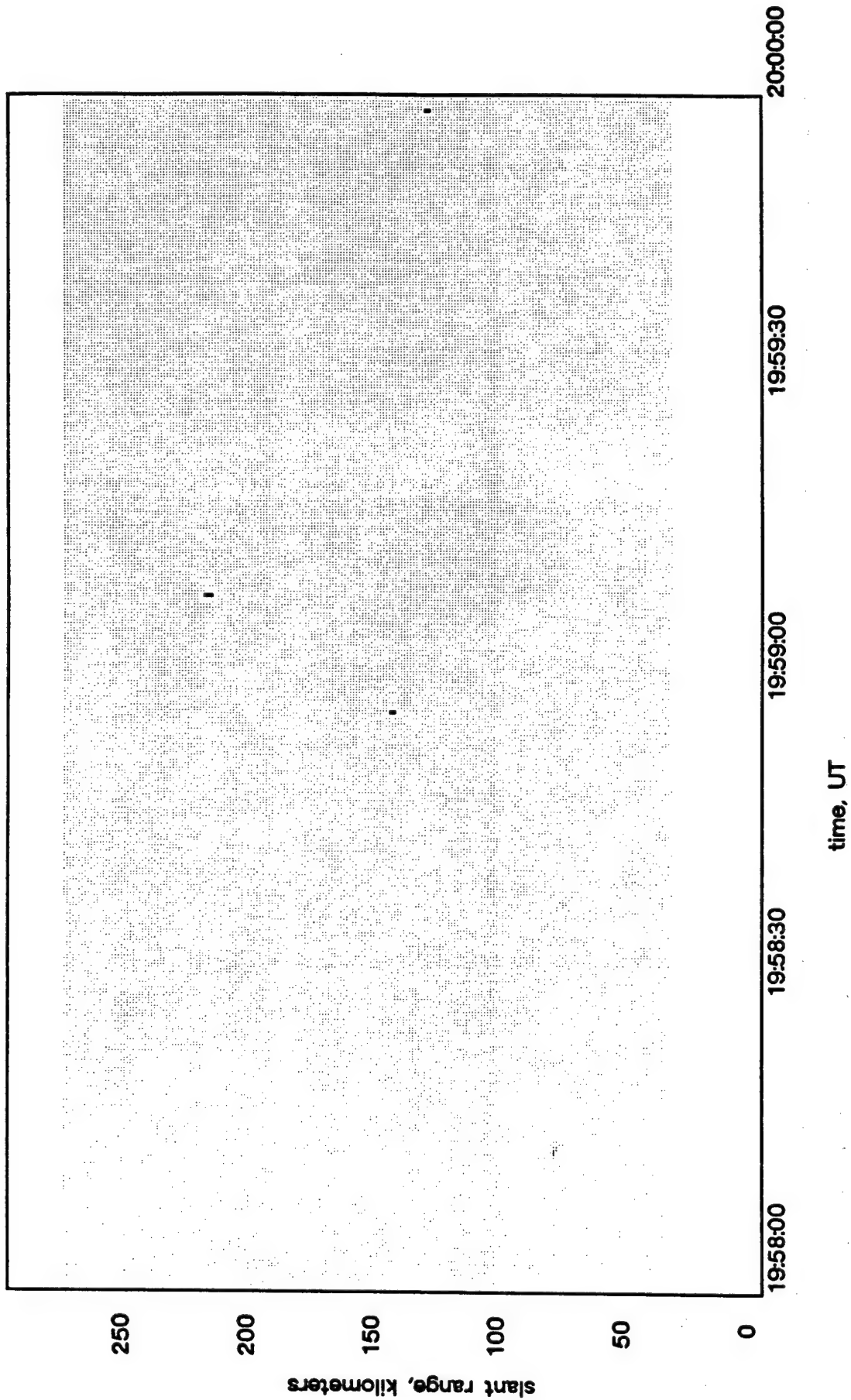


Figure 38. Rev 2 RTI.

Rev 2 - Event Range

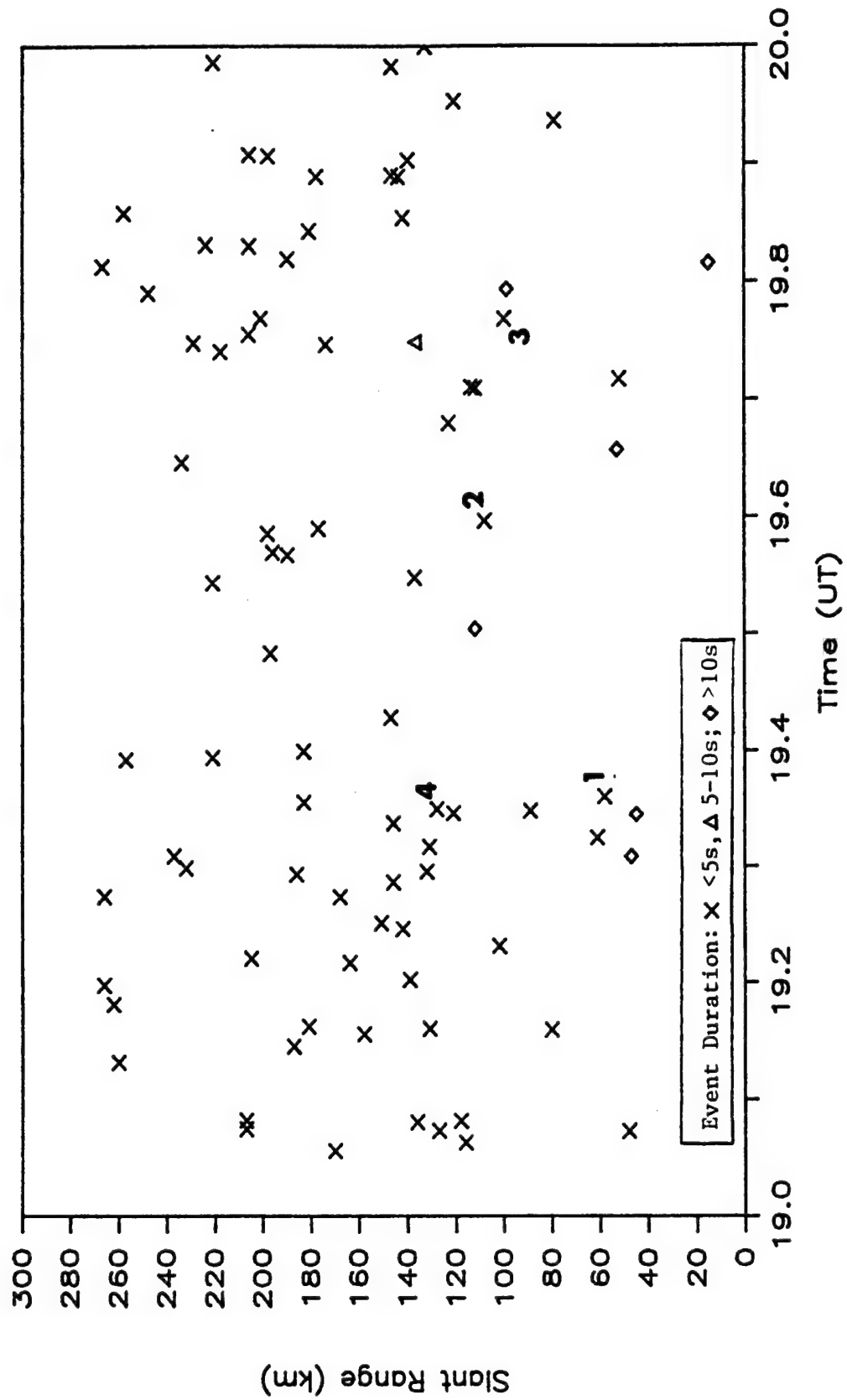


Figure 39. Slant range for each Rev 2 event. Debris candidates are labelled numerically.

Rev 2-Instantaneous Detection Frequency

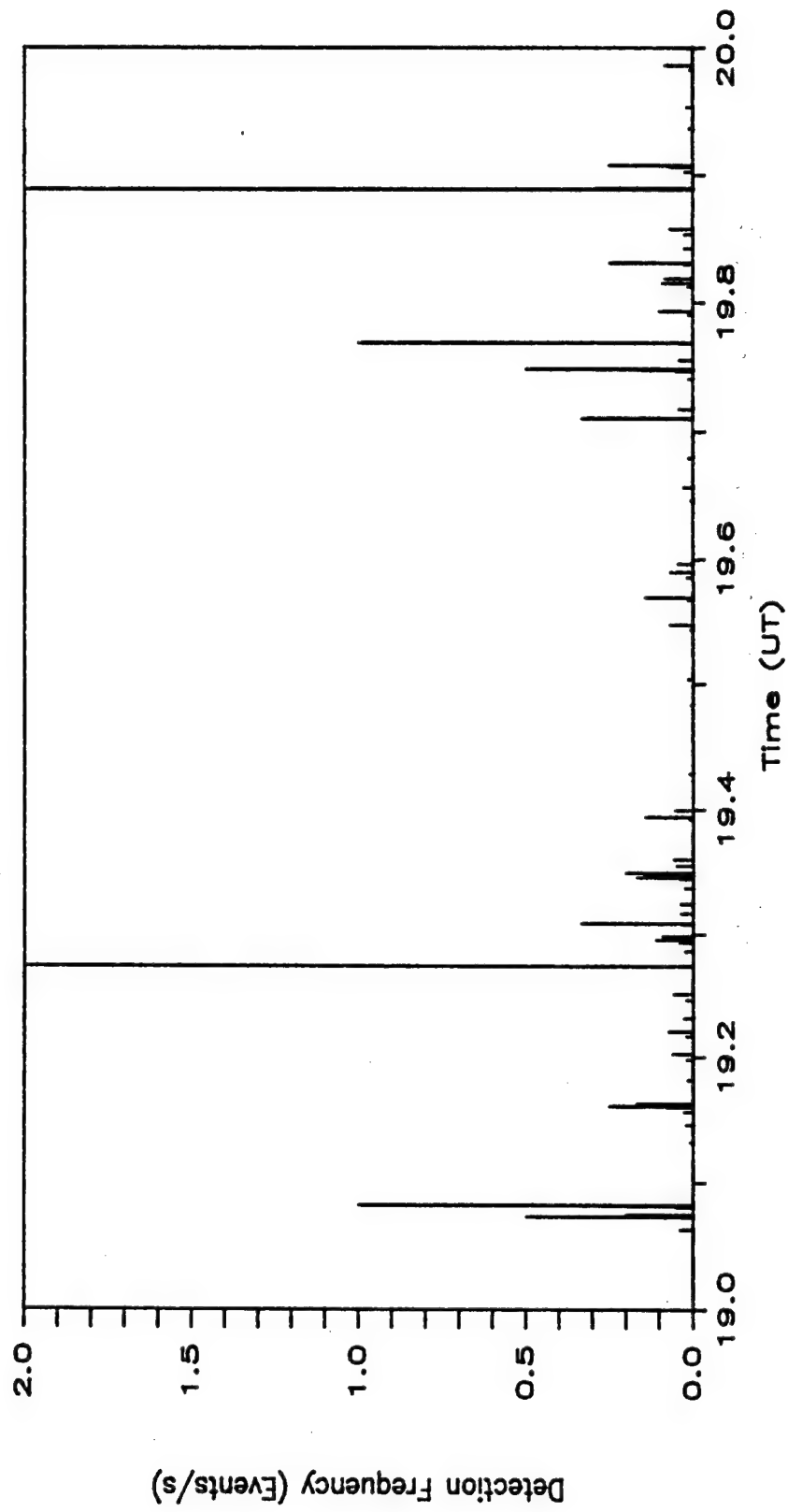


Figure 40. Instantaneous detection frequency for Rev 2 events.

3.2 Debris Particle Velocity (Indirect Measurement)

Since the location and time of payload destruction are known, it is possible to determine the transit velocity from the point of closest approach to the radar detection volume for the events depicted in Figure 8. The total minimum path length between these points can be calculated simply using spherical geometry. It is assumed that a ballistic expansion of the debris cloud along with a spread in velocity accounts for the spread in the arrival times of the detected events and that no "lob" trajectories or other unusual flight paths were associated with the prime data set. Combining the total (minimum) path length for the particles with the time of arrival and location in the radiation pattern gives the minimum exit velocity of the individual debris pieces from the source region. For a given slant range from the radar and time from payload destruction, Appendix B gives the velocity of the debris particles (as well as the software routine used to calculate the time-of-flight velocities).

Velocity contours against the RTI data are shown in Figure 41. All events presented in the figure have an associated velocity in the range of 6.5 - 7.5 km/s, which is less than the initial circular orbital velocity (approximately 7.8 km/s). These data, along with the order-of-magnitude increase in meteor flux, provides irrefutable evidence that the events during this period are associated with the D-180 experiment.

Perhaps the most important information contained in the time-of-flight measurements is that they represent the velocities (at least in part) of the debris particles immediately after the interaction. Direct velocity measurements at a point in the decay-entry process yields information on the particle mass and direction and on the decay process itself, but do not determine the free-space expansion rates from the source event itself.

49.92 MHz Radar RTI Hawaii 1986 Day: 248

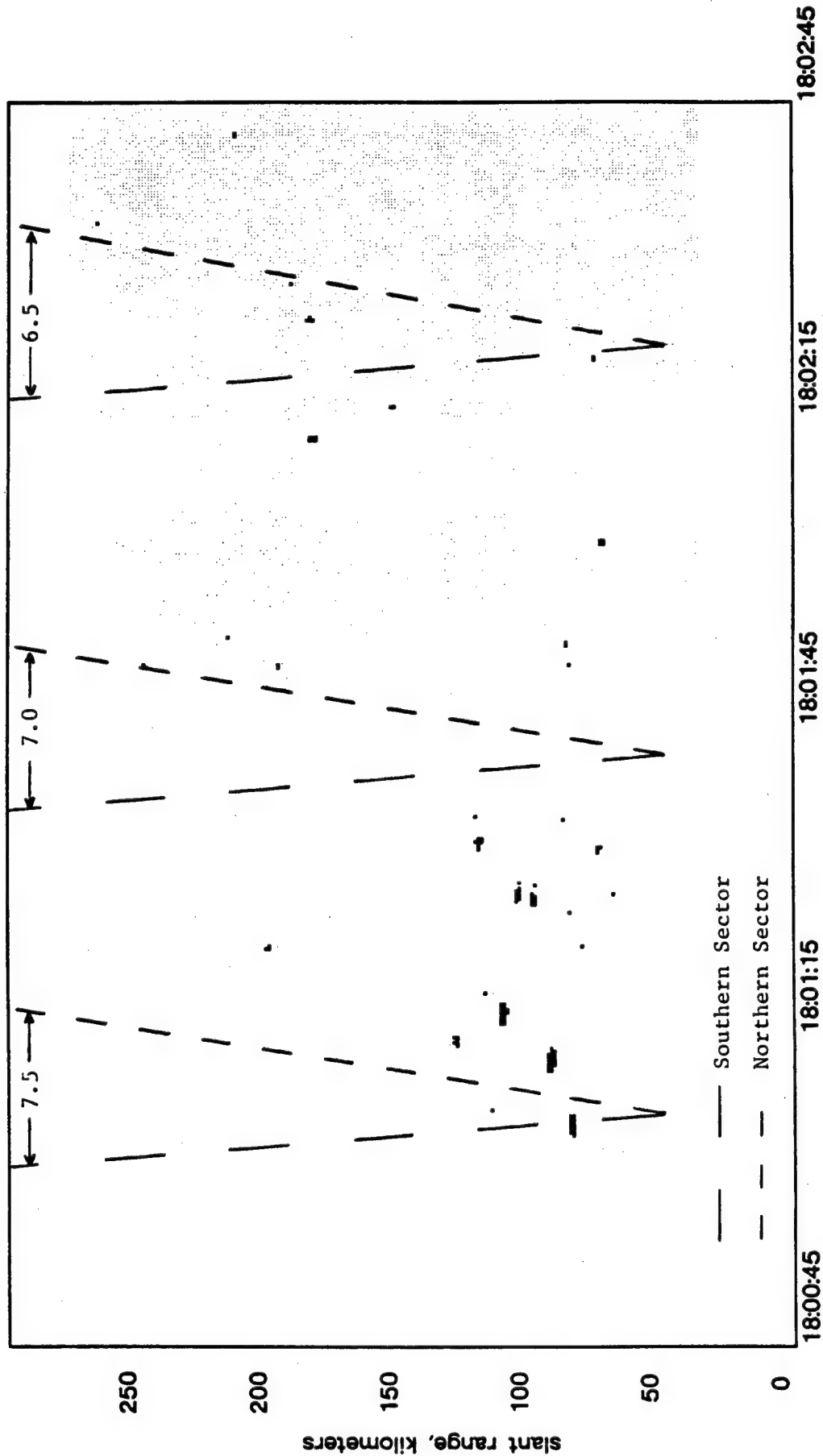


Figure 41. Overlay of time-of-flight velocities on RTI plots for primary 50 MHz events.

3.3 Debris Particle Velocity (Direct Measurement)

There are generally two types of echoes which may be identified with radar techniques -- head echoes and tail echoes. The head echo is attributed to reflections from a cloud of plasma enveloping the entering particle during the formation of the ionized trail. The head echo, therefore, moves with the velocity of the particle (i.e., several km/s). In this case, direct velocity measurements of the particle may be determined through line-of-sight doppler or as a change in range with time.

The tail echo is produced by radar energy reflected from the persistent ionized trail left behind the parent body. Since this trail is relatively stationary, the doppler frequency associated with the echo is small when compared to that from a head echo. Atmospheric winds are the primary contributors to particle trail motions; meteor tail echoes have been used by many researchers as tracers for measuring the neutral wind speeds which are typically less than 100 m/s at 50-100 km. As an example, the doppler velocity obtained for Event 1 is shown in Figure 42. Here the line-of-sight velocity is about 40 m/s (the total velocity is not determined with a single look direction) and has been determined from the fully developed echo. Since this measured line-of-sight velocity is similar to those expected for neutral winds, it is presumed that this particular event is a tail echo. All other events examined to date support the general belief that most (if not all) observed echoes from the debris particles are tail

echoes. Head echo returns, however, would be expected from larger pieces (10's of kilograms) and further processing of all 30+ debris events detected with the 50 MHz system is required to determine the frequency of debris head echoes.

Significantly, the doppler measurements were made on the fully developed echoes and it is reasonable to expect standard, meteor-like tail behavior (e.g. neutral wind line-of-sight doppler velocity). However, a more detailed investigation of the initial "attack" phase of the developing echo indicates that a signature of particle velocity is present in the data.

Direct velocity measurements of Event 1 are indicated in the data presented in Figure 43. In contrast to the 40 m/s doppler measurements of this event, discussed above, these data indicate an average velocity of about 2.3 km/s. This large difference is attributed to the measurement technique and the point in time during the development of the echo that the measurement was made. Both measurements are valid and accurately describe a particular phenomenological observation.

The 2.3 km/s measurement represents the azimuthal (east-west) component of the total particle velocity at the time of detection. This value was determined by the transit-time delays associated with the ionization trail developing across the longest bistatic baseline of the azimuthal interferometer. It should be noted that along with this relatively low apparent

velocity (vs. meteors) the direction of motion is clearly from west to east. Combining the elevation (north-south) and radial velocity components would provide the total velocity vector at the time of detection. For the debris events, the motion of the particles are assumed to be predominately west-to-east with only small velocity components in the other vector directions. With this, 2.3 km/s may be interpreted as the total average velocity of Event 1 through the interferometer radiation pattern.

By comparing the differential time lags between the various baselines there is an apparent slowing of the velocity from an initial 3.3 km/s to 1.3 km/s. Again, only one velocity component of this event has been studied. Also, with these very slow velocities, questions on the ionization mechanism must be raised.

The following section presents a technique for determining the mass of an entering particle. This technique is extremely sensitive to velocity and shows that particle mass cannot be accurately estimated without reliable velocity information.

HAWAII 1986 DAY 248 49.92 MHz 6 AZ
18: 1: 4

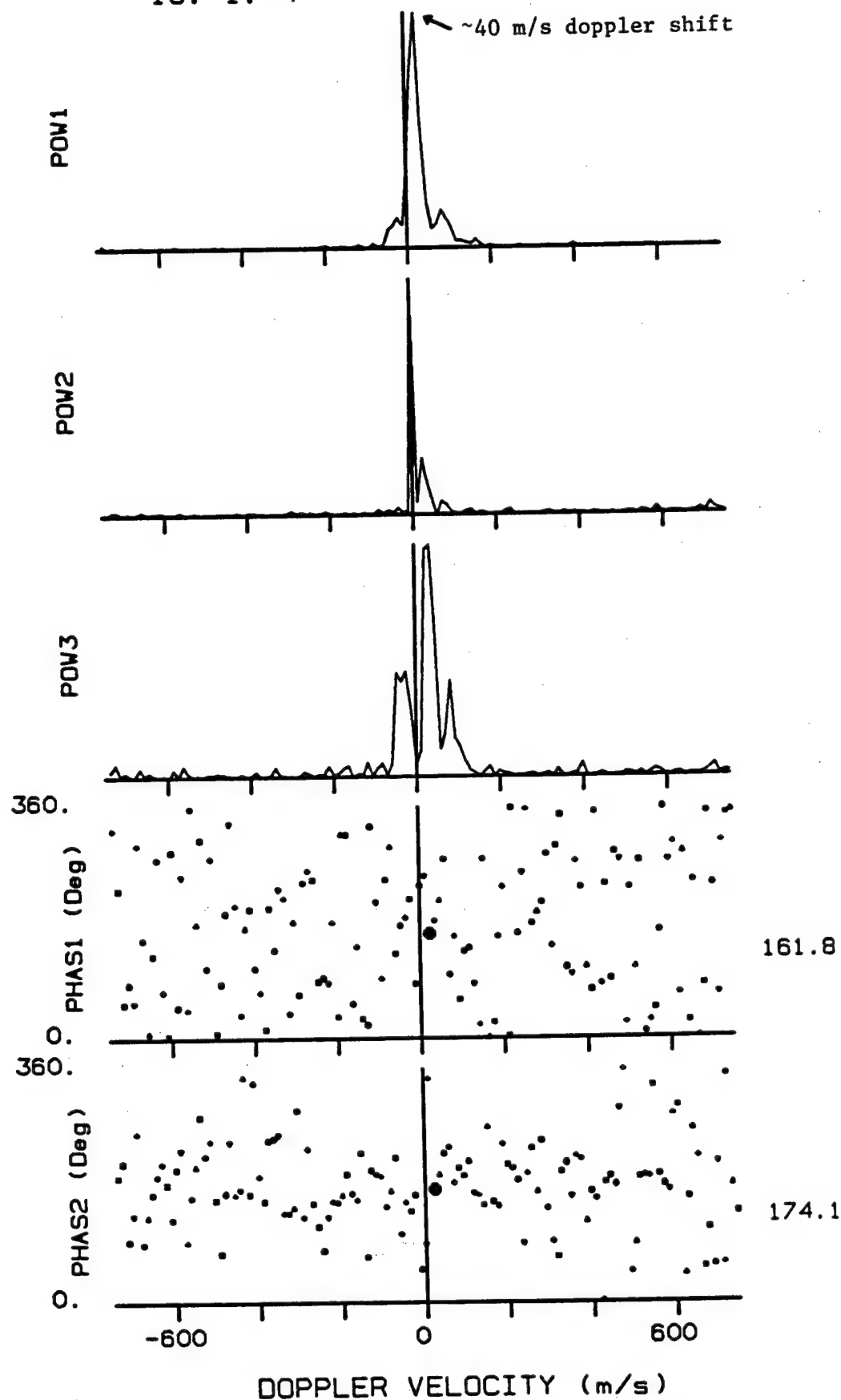


Figure 42. Doppler spectra for Event 1. Line-of-sight velocity equals approximately 40 m/s and is comparable to neutral wind speed.

HAWAII 49.92 MHz DAY= 248, YR 1986 AZ

18: 1: 4 UT

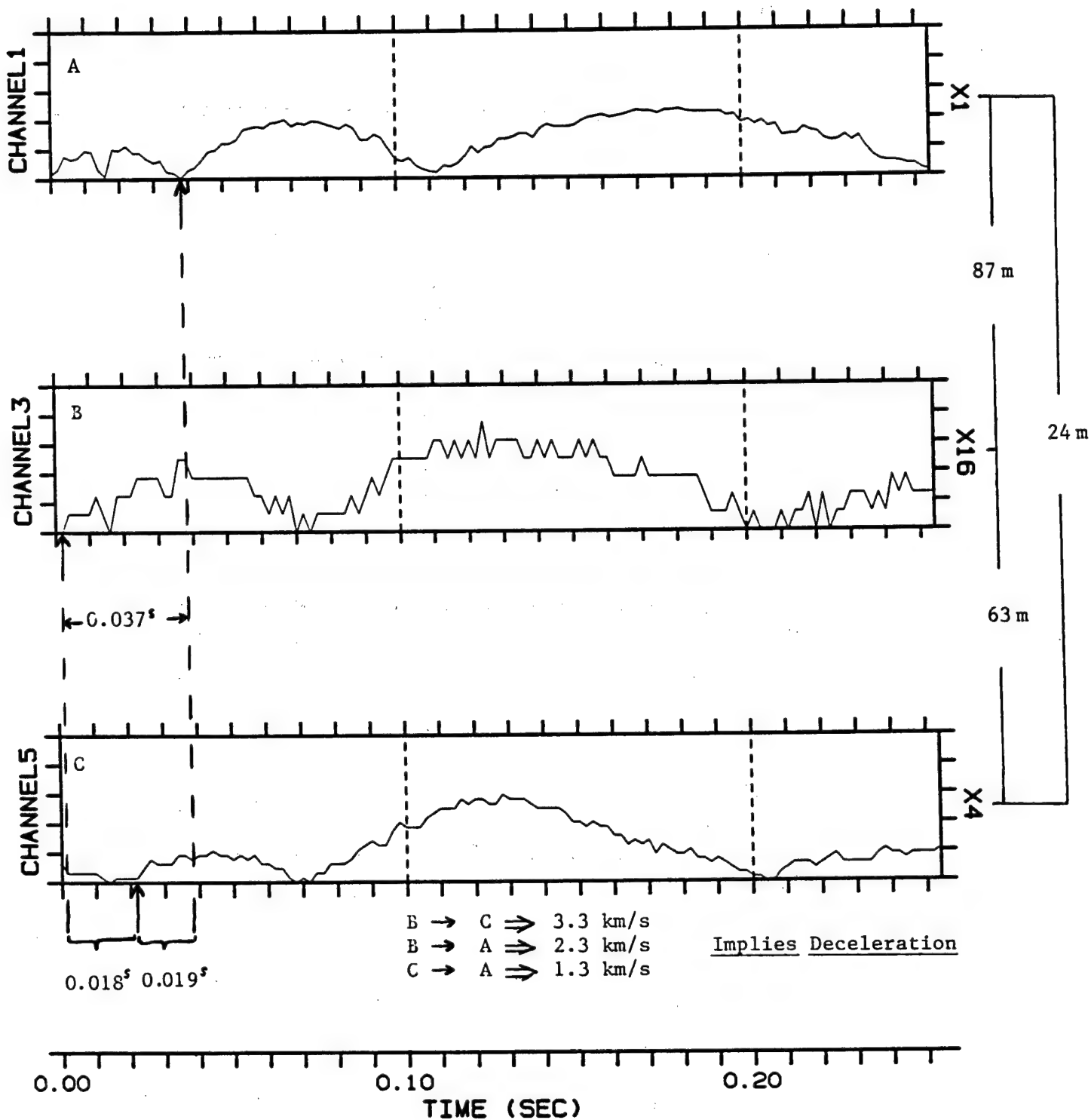


Figure 43. Time shifts in bistatic echoes during development of the echo power profile provide direct velocity measurement.

3.4 Entry Mass

A relationship between the mass of the entering particle, the maximum radar echo strength from its ionization trail, and the measured velocity may be derived. Assume that the rate of loss of mass of the entering object is proportional to the kinetic energy

$$\frac{dm}{dt} = - \frac{\Lambda A}{2\zeta} \left(\frac{m}{\rho_m}\right)^{2/3} \rho_a V^3 \quad (1)$$

where:

- ζ = Heat of ablation
- Λ = Heat transfer coefficient
- A = Shape factor
- ρ_m = Effective object density
- m = Object mass
- ρ_a = Air density at entry altitude
- V = Velocity of object

Now, the power going into the production of ionization is assumed to be proportional to the kinetic "power" loss of the ablated atoms from the surface of the object. If q is the number of electrons produced per unit length and η is the mean ionization potential per atom involved, the energy associated with the ionization process per unit time is

$$qV\eta = - \frac{1}{2} \tau_q \frac{dm}{dt} V^2 \quad (2)$$

where τ_q is the (dimensionless) ionization-efficiency factor.

Substituting the differential mass equation (1) into (2) gives an ionization equation relating mass and velocity to the

resulting line density

$$q = \tau_q \frac{\Lambda A}{4\zeta\eta} \left(\frac{m}{\rho_m}\right)^{2/3} \rho_a V^4 \quad (3)$$

The power returned from an ionization trail in a radar echo can be expressed as a function of the radar wavelength and the trail electron line density. Assuming that the echo returns are from aspect sensitive tail structure (as the doppler data indicate) which fills several Fresnel zones, the return power can be expressed as

$$P_R = \frac{P_T G^2 \lambda^3 \sigma_e}{128 \pi^3 R_0^3} \left(\frac{C^2 + S^2}{2} \right) q^2 \quad (4)$$

Condensing the known constants and isolating q gives

$$q = \frac{6(10^{15})}{G} \left(\frac{R_0}{\lambda}\right)^{3/2} \left(\frac{P_R}{P_T}\right)^{1/2} \quad (5)$$

Cosmic background establishes the noise limit of the receiver system for both radars. Generalizing equation (5) to express the return power in terms of signal-to-noise ratio (S/N) can be done by following Hogg and Mumford (1960) where

$$P_R = (S/N) 100 \lambda^{2.4} \quad (6)$$

Combining equations (3), (5), and (6) produces an expression of mass as function of slant range, signal-to-noise ratio, particle entry velocity, transmitted power, and radar wavelength. The parametric mass relationship is given as

$$m = C_T \left[\frac{R_o^{3/4} (S/N)^{1/4}}{V^2 P_T^{1/4} \lambda^{3/20}} \right]^3 \quad (7)$$

C_T represents a combination of all the constants contained in the previous derivation expressions. The value of this constant has been carefully estimated to enable a first-order measurement of the masses of the detected entering debris particles. For reference, the values used for this determination are presented in Table 1.

Hogg, D. C., and W. W. Mumford, The effective noise temperature of the sky, Microwave Journal, 3, 80, 1960.

TABLE 1.

ENTRY MASS CONSTANTS

PARAMETER	VALUE (cgs units)	RANGE/COMMENTS
Ionization efficiency	$\tau_q = 10^{-2}$	$10^{-1} - 10^{-4}$
Shape factor	$A = 1.0$	$0.6 - 1.7$
Heat of ablation	$\zeta = 10^9$	$10^9 - 10^{10}$
Heat transfer coef.	$\Lambda = 0.15$	$0.1 - 0.6$
Ionization potential	$\eta = 1.6 (10^{-11})$	$0_2 = 10 \text{ eV}$
Atmospheric density	$\rho_a = 10^{-8}$	$0_2 \text{ at } 50\text{-}100 \text{ km}$
Particle density	$\rho_m = 2.7$	Aluminum

Using these parameter values in equation (7) gives the masses of the individual entering particles as a function of radar wavelength, slant range, echo signal strength, transmitted power, and entry velocity. The resulting values for Rev 1 are presented in tabular form in Table 2 and in a mass distribution plot shown in Figure 44. The values for the four debris candidate events from Rev 2 (see Figure 39) are: 1) 2g; (2) 97g; (3) 28g; and (4), 98g.

TABLE 2.

DEBRIS PARTICLE MASS ESTIMATES

EVENT	50 MHZ RADAR *	28 MHZ RADAR
	MASS (grams)	MASS (grams)
1	72	63
2	122	24
3a	48	24
3b	30	15
6	12	
7	18	23
8	17	
12	49	
13	69	
16	10	
17	3.6	
18	9.5	
19	61	31
20	12	
22	88	
23	107	
24	69	88
25	43	44
27	522	505
28	203	133
29	840	537
31	76	379
32	101	
33		38
34	4.3	
35	16	
36	7.1	
37	9.9	
38	12	
39	168	

* Revised November, 1986

These data must be considered preliminary because of the number of assumptions that were associated with deriving the mass equation. It is assumed that the energy loss mechanisms for the relatively slow orbital particles are equivalent (or at least similar) to those for meteors. Also, inspection of the mass equation shows that the strongest controlling variable is the velocity at the time of the measurement. The mass estimates presented were based on the free-space velocities determined from time of arrival in the radar beams. As suggested by the preliminary direct measurement data, at the time an echo is detected, the particle velocity may be considerably slower than its initial entry velocity.

Derivation of the mass equation also neglected the effects of spatial diffusion of the ionized trail. There is a strong wavelength dependence on the signal strength of the return echo for finite width ionization columns. As the width of the trail expands to a scale size approaching a wavelength, destructive interference of reflections from opposite sides of the ionization column quickly quenches the received signal. For the derivation presented, the line density, q , was assumed to be an infinitely thin trail which contains no wavelength dependence.

Generally, the mass data presents an expected functional form in that the low-mass debris strongly dominates the high-mass debris in number density. Refined velocity data will likely cause the mass estimates to increase since mass is inversely dependent

on velocity and it is expected that the velocities will be slower than presently determined. Mass increases are also expected by incorporating the finite tail-width geometry.

Considering the mass-range plot in Figure 45 indicates an altitude dependence on the detected mass. Increasing slant range may be interpreted as increasing altitude to first order. There are a number of possible explanations (and combinations of explanations) that would account for this affect -- (1) range sensitivity of radar system; (2) body kinetic energy dependence on the ionization process; (3) a mass-area (density) dependence; or (4) other unknown processes. Regardless, further investigation is warranted.

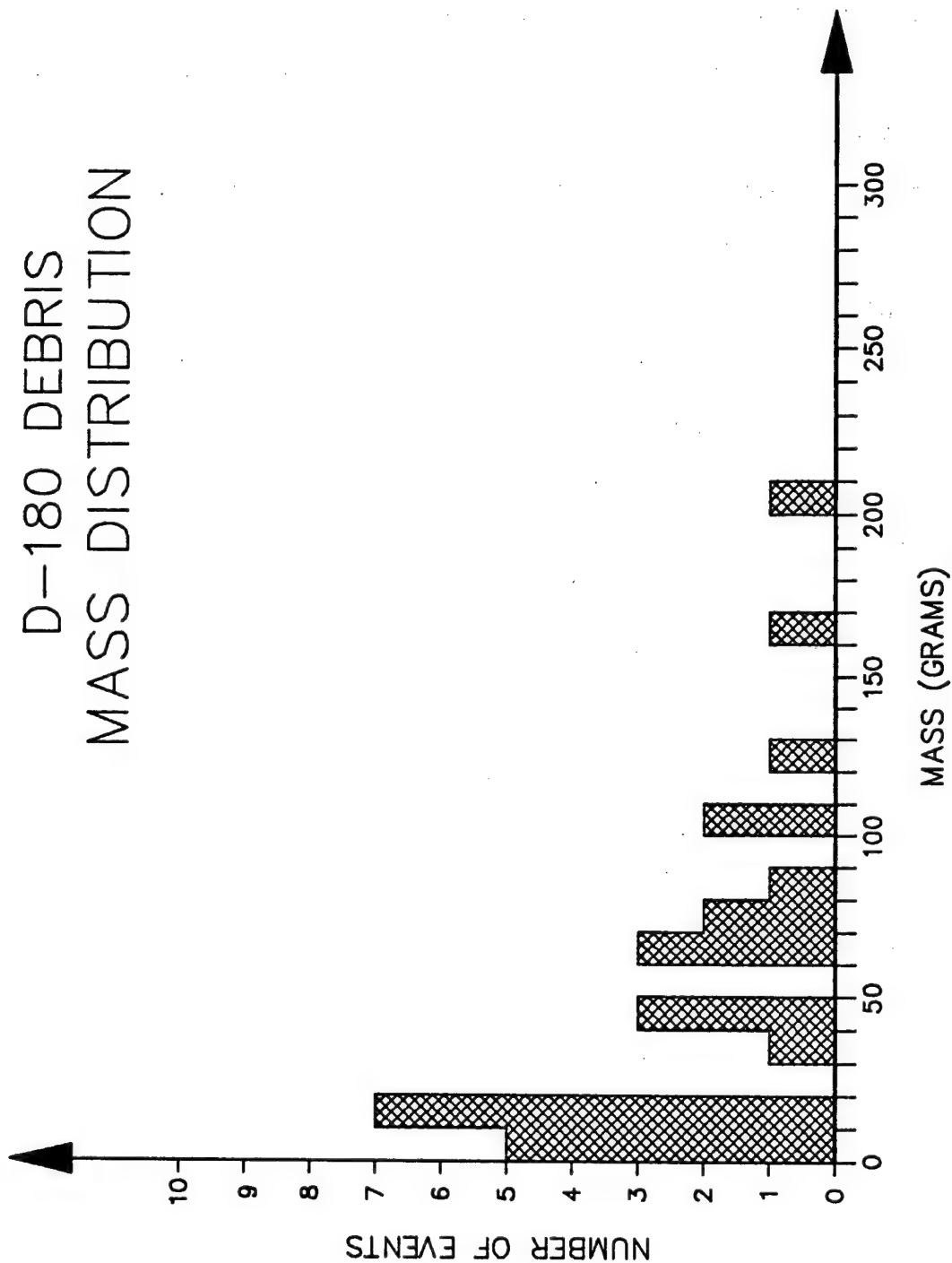


Figure 44. Observed mass distribution for D-180 debris entering over Kauai.
(Revised November 1986)

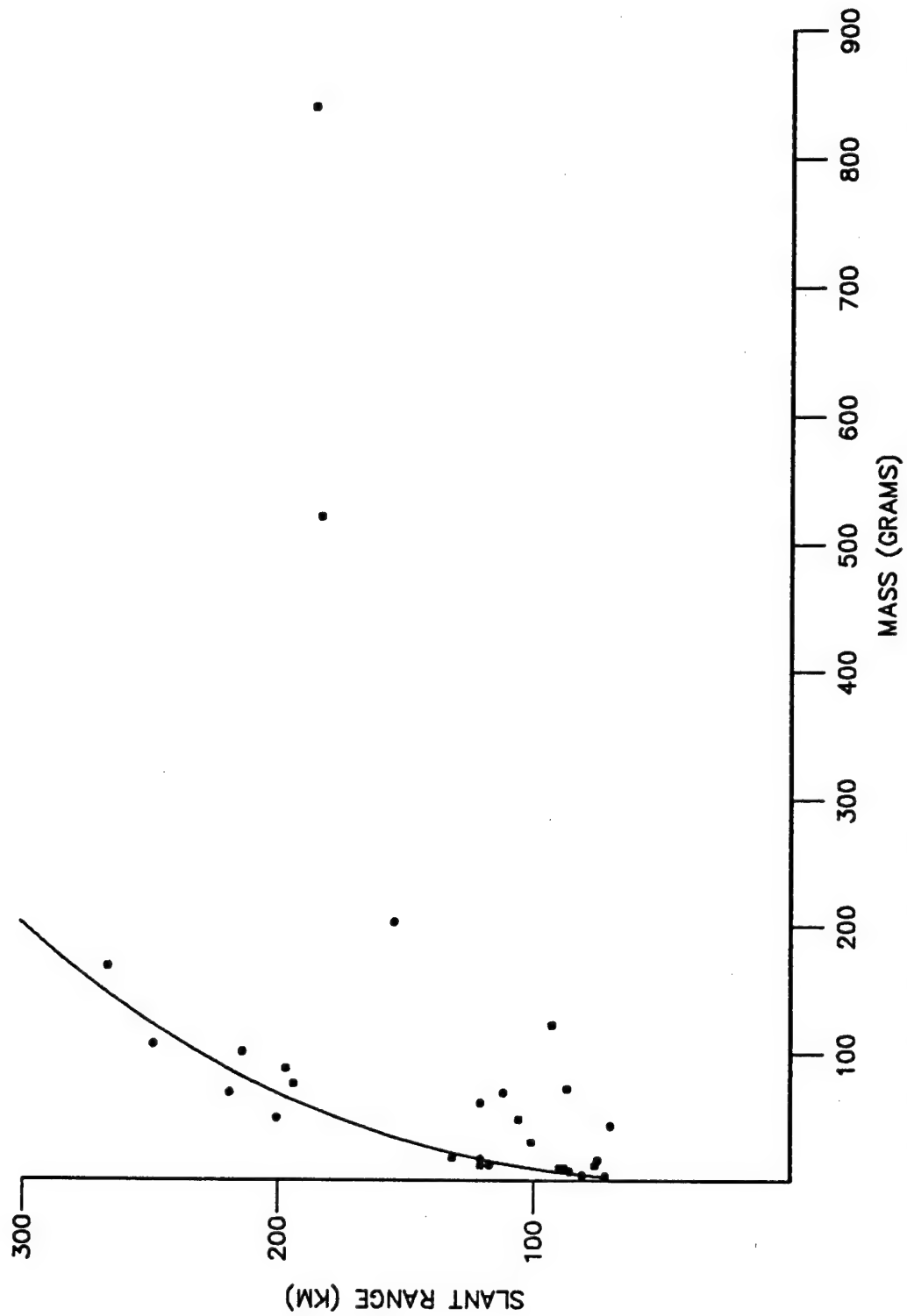


Figure 45. Mass vs. slant range for the 50 MHz debris events. Reference curve suggest an altitude dependence on the maximum ionization vs. mass.
(Revised November 1986)

3.5 Mass Calculation Sensitivity

The problem of evaluating zeroth-order mass estimates is straightforward. However, it is important to understand the variables which comprise equation 7 so that its limitations are known. A large collection of radar meteor literature is available which has been referenced to provide estimates for the parameters used in the debris mass calculation. Thus, meteor related results have been tailored or extended to the debris problem to provide the zeroth-order mass estimate.

Below is a synopsis of each of the parameters listed in Table 1 followed by a description of how the mass equation is affected by the value selected.

Three of the parameters listed in Table 1 have values associated with them which can be relatively easy to determine. These are the particle density, ρ_m , atmospheric density, ρ_a , and the ionization potential, η . In the altitude interval (50-100 km) where debris particles burn up the atmosphere is composed primarily of O_2 . The ionization potential of molecular oxygen is $1.6 \cdot 10^{-11}$ ergs and the peak density encountered by the entering particle is $\sim 10^{-8}$ g/cm³. To first order the ionization potential won't vary significantly from this value. However, particles that burn up higher in the atmosphere will do so at a lower density than those that burn up lower. In general, debris particles, with their inherently lower velocities, burn up at lower altitudes where the densities are greater. In the

mass equation, higher atmospheric densities result in lower mass estimate.

The debris particle is assumed to be composed of aluminum with a density of 2.7 g/cm^3 . Higher particle densities result in larger mass estimates.

The shape factor, A , is a dimensionless quantity which represents the geometry of the decaying particle. For a sphere, $A = 1.2$, and for a cube $A = 1.0 - 1.7$ depending on its orientation relative to the flight path. Values of $A < 1$ are found for long narrow bodies in the streamline aspect and $A > 1$ for the broadside-on aspect. Owing to rotation though, irregularly shaped objects generally have a value close to that of a sphere. For this study the value $A = 1$ is used. Smaller (larger) masses will result for larger (smaller) values of A .

Various processes exist for the ablation of atoms from the entering particle with the mass loss dependence being inversely proportionate to the heat of a ablation, ζ , and directly proportionate to the heat transfer coefficient, Λ . The heat of ablation is usually taken to lie in the range $10^9 - 10^{10}$ ergs/g for meteor particles consisting chiefly of iron. Aluminum with its lower melting point requires less energy to ablate than iron. Consequently, the value selected for use in the mass equation should lie at the lower end of the range given above. In the mass equation, a larger mass will result for larger ζ .

The heat transfer coefficient is a measure of the efficiency of the collision process in converting kinetic energy to heat. From meteor studies, this parameter has values which range from $0.1 - 0.6$.

Speculation maintains that the energy transfer efficiencies of debris particles are less than those for the faster moving meteors.

Consequently, a value near the lower limit of this range is used in the mass calculation. A larger value of Λ would produce a smaller mass according to the mass equation.

The power going into the production of ionization is assumed to be proportional to the kinetic power loss of the ablated atoms. The dimensionless ionization efficiency factor, τ_q , is not easily evaluated for meteor particles and is similarly difficult to evaluate for debris. Past studies suggest that τ_q is slightly to moderately dependent on velocity, e.g., v^n where $n=0-2$, and ranges from $10^{-1} - 10^{-4}$ for meteor particles. A similar range should be expected for debris particles. Smaller τ_q results in larger mass estimations.

The debris particle mass estimates given in Table 2 are based on the values listed in Table 1. As has just been shown, some of the parameters which make up the mass equation have values which are only known approximately. By varying these values a change will be introduced into the mass estimate. The degree of the change is largest when each value is set to its limit in such a way as to either maximize or minimize the mass estimation. Such an exercise, however, certainly would not represent a realistic portrayal of the problem at hand. The values given in Table 1 and used in deriving masses are based on our current understanding of the physics involved.

By taking into account a reasonable range of acceptable values for debris particles for each of the parameters listed in Table 1, the uncertainty in the mass estimate is placed at approximately \pm an order of magnitude. Thus, a 100 g mass could be as large as 1 kg or as small as 10 g.

4. SUMMARY AND RECOMMENDATIONS

4.1 Summary

Several significant results were obtained from the VHF, backscatter radar measurements and resulting analysis for the D-180 debris entry studies:

- 1) Unequivocal detection of ionization trails produced by orbital debris particles entering the upper atmosphere
- 2) Measurement of the free-expansion velocity distribution at immediate post-encounter
- 3) Preliminary demonstration of a direct measurement technique for the velocity for small debris particles during entry
- 4) Preliminary data on rapid deceleration of debris particles during the entry process
- 5) Demonstrated technique for estimating the mass of an entering particle producing detectable ionization
- 6) Evidence for mass-area or kinetic energy effects of the decay process

Some of these results are preliminary estimations while others are complete in themselves. The radar observations clearly provided an invaluable complement of data to aid in the interpretation of the D-180 close encounter.

4.2 Recommendations

The debris radar results, along with providing new information on debris expansion and decay-entry processes, suggest several new areas of research. With these positive results on detection of orbital debris entry, a better understanding of the entry process is required to advance the interpretation of the

data. Proper interpretation and analysis will contribute to the understanding and development of debris math models in general. Demonstration of the measurement technique for the location and velocity of the entering objects could lead to the development of a continuous-operation, automatic system to monitor the general influx of decaying orbital debris. Further work needs to be conducted in the following areas:

- 1) Demonstration of the interferometer technique to determine the vector location of the echo events
- 2) Development of the bistatic determination of vector velocity through the interferometer interference patterns
- 3) Development of the physical model of the ablation and ionization processes associated with the entry of "slow", low-mass debris particles
- 4) Refinement of the mass measurement model and multiple wavelength approach
- 5) Specifically for D-180, extended data reduction for determination of the debris influx on subsequent orbit plane intersection with the Kauai-based radar beams

Continued study of the entry processes should be initiated well ahead of anticipated opportunities to conduct controlled experiments. Improved understanding of the measurement technique and the physics of small body entry will constructively guide field measurements.

APPENDIX A

HAWAII METEOR CAMPAIGN FIELD NOTES

7-4-86

HAWAII METEOR CAMPAIGN

8-28-86 → 9-3-86

- * Joe & Kessler met with Richard Jan at Territorial Savings & Loan in Honolulu to make final request for usage of property at Princeville. The request was denied - no strong rationale was given. They were apparently concerned about liability and interference with the selling of their property. To date (9-4-86) there has been no activity what-so-ever on that land.
- * Noble, Stansbury, & DeMoubrun assembled antennas and checked out matching networks with the network analyzer.
- * The 28 MHz TX was powered-up & tuned at Card 3. Tuning procedure resulted in burning out some components of the T/R switch.

9-1-86/Hawaii

- * Since the prime site was not available, the 1st backup site was selected as the field for the antenna farm. Jost & Noble shot the North star on 8-30-86. On 8-31-86 the field was surveyed and the antenna array was laid-out.
- * The ⁵antennas for the 50 MHz interferometer were raised on 9-1 & 9-2. Some problems with dipole joint failures was experienced. A field test technique was devised to find failed joints & a repair procedure implemented. All antennas were operational (including the 28 MHz) by 9-3-86.

9-4-86 Hawaii

- * 50 MHz TX was Powered up & tuned. A solid-state "booster" stage was added between the exciter & 1st stage to increase the drive level. Output power was kept at about 15 kW for testing purposes
- * After TX tuning and about 30 minutes of operation the matching network for the TX antenna failed. Repairs were completed with starter components & no further problems encountered
- * 28 MHz TX was powered up & tuned into antenna w/ repaired T/R switch. An Operational level of about 12 kW was achieved.

9-4-86 Hawaii

* Early operational tests showed:

- Strong echo returns from (presumably) the ionosphere for the 28 MHz radar - possible sea-state returns in early range gates as well.
- Good meteor echoes were obtained over ranges of $\sim 0.75 - 2.5$ ms. w/ the 28 MHz system
- Ionospheric echo disappeared at sundown.
- 58 MHz echoes are apparent in all five receiver channels
- Echo strength seems a little weak - will use highest TX power for experiment
- Channel 3 (antenna 4) contains strong, intermittent interference. It's believed the interference is coming from a local wireless telephone.

9-4-86 HAWAII

* Check out of Honeywell 101 tape recorder.
15 channels - all direct.

Channel assignment:

<u>Recorder channel</u>	<u>Input</u>
1	50 Rx-0 I
2	50 Rx-0 Q
3	50 Rx-1 I
4	50 Rx-1 Q
5	50 Rx-2 I
6	50 Rx-2 Q
7	50 Rx-3 I
8	50 Rx-3 Q
9	50 Rx-4 I
10	50 Rx-4 Q
11	28 Rx I
12	28 Rx Q
13	SYNC
14	SYNC
15	IRIG-B

9-4-56 HAWAII

- * Test tape was started about 1300 LT to set levels, etc.
- * Tape 2 started ~ 1350 LT w/
all channels of 50 MHz
- * 28 MHz being tested - evidence that high voltage corona or break-down is getting into RX. TX power solid ~ 12 KW
- * 28 MHz $V_F/V_R \approx 8$
- * Visual inspection shows no obvious corona
- * TAPE 2 started ~ ~~1550~~ 1550 LT / 248/0150 UT
- * From here on, all times will be reported in UT
- * Further work on 28 found that RF choke was corona discharging to ground (probably) near its base

9.4.86 HAWAII

248/03:46 Corona started real bad again

* Strong E-region (??) returns observed in 28 RX again. Range ~ 2.5 ms (center); extent ~ 1 ms

* Meteors have been observed on both the 28 & 50 simultaneously for several hours

* Subjectively, the meteor flux seems relatively low

* 248/04:00 \rightarrow $\sim 05:00$ 50 MHz RX & tape recorder were re-configured slightly to improve RX dynamic range & to improve signal quality

* 05:15 : 28 MHz activated at ~ 6 kV (to minimize corona) -- meteor was immediately detected in both systems

* Ionospheric returns have stopped at sun down

* ~~28~~ 28 MHz HV \rightarrow 8 kV - corona noise increases

9-4-86 Hawaii

Pulse configuration:

$$PW = 20 \mu s$$

$$PP = 2 ms$$

+ 50 MHz Directional coupler = 25.5 kW

$$VSWR = V_F / V_R = 7.0 / 0.9 = 7.8 \text{ (50 MHz)}$$

+ 28 MHz (64.5 dB coupler) = 8.8 kW
returning = 10.8 kW

$$* VSWR = 6.2 / 0.6 = 10.3 \text{ (28 MHz)}$$

248:06:20:20 Tape speed increased
7.5 IPS \rightarrow 15 IPS

06:25 Intermittent ionospheric returns
at 0.8 ms (2.0 \pm 0.8 ms) range aligned
very, very weak \sim 2:1 SN; slow Doppler

9.4.86 HAWAII

TAPE 4 END

- 248:06:37 Discovered tape rewinding
- Don't know when finished
 - This tape will not be rewound
 - Anticipate slow changeover

248:06:53 Start TAPE 5

07:00 Continual checking of RX channels indicate that all receivers are working well; no man-made interference; and simultaneous meteor echoes appear in all channels most of the time (depending on amplitude)

07:21 → 07:21 + 15sec Pulse off to check IRIG level

07:24 Discovered that Recorder was in reverse again! Don't know what's going on.

9.4.86 HAWAII

248:07:28 Tape position that reversal occurred was located & tape restarted (in record) from that point (~ 5 min data gap)
It was ~~not~~ noticed that the tape counter was at ~ 2000' when the recorder went into auto rewind. Recorder was difficult to get past the 2000' mark - tape didn't seem stuck - maybe an auto feature that can be reset.

248:07:34 Meteors still appearing in 50 & 28 simultaneously
* Echo strength about the same in most cases (S/N)
* Echo persistence about the same in most cases
* Most echoes appear in all interferometer channels
* Event flux ~ 1 per minute

9.4.86 HAWAII

248:08 END TAPES - START TAPE 6

~ 08:15 Strong interference in 50 MHz System

08:39 Testing Bandwidth select.

08:41 BW set at 20 MHz

Outside interference still very bad w/ 50 MHz

09:05 End TAPE 6

09:09 Start TAPE 7

248:09:12 Interference finally is disappearing

09:25 Pulse width reduced from 20 μ s to 10 μ s; BW \rightarrow 10 μ s (from 20 μ s)

~ 09:28:55^{??} very strong meteor in both systems at 10 μ s

$\frac{SN}{T}$ 10:11: end Tape 7

10:16+: Start Tape 8 Counter = 100'
(15ips)

9-5-86 Hawaiian

248/10:21 bug fried in 50 MHz Tx
10:24 all channels checked and ok

11:16: end Tape 8

11:20 Start Tape 9

11:22 all channels checked and ok.

50 MHz: 3.4 kV / 10 mA

28 MHz: 8 kV / 17 mA

11:54 2500' good event - simultaneous detection; 1 g. ampl. like

12:04:50 3330' good event - s.d.

12:09:40 3690' 28 MHz echo

12:11:30 3820' simultaneous detection

12:22: End Tape 9

12:26: Start Tape 10

12:28 all channels checked and ok
- both Tx's ok.

12:30:00 320' an event

9-5-86 Hawaii

248/12:37:30 875' SUMITE vent

12:46:30 1550' good vent

12:52:25 1990' quick sim. det. vent.

12:58:02 2420' 1/2 arg. vent - in close or closed

J2 Heavy rainfall for ~15min @ ~2:45am LT

248:13:28 END TAPE 10

248:13:33 START TAPE 11 30 IPS

del channels check OK

PS Readings:

28 Final: 8KV/17ma

50 Driver: 3.4KV/10ma

Final: 6.55KV/53ma

PW = 10 μ s

BW = 10 μ s

TAPE speed = 30 IPS

IPP = 2 μ s

248:14:05 END TAPE 11

14:07 START TAPE 12 30 IPS

9.5.86 HAWAII

248:14:38 End TAPE 12

14:41 Start TAPE 13 30 ips

- * System stable - no changes
- * Frequent, good meteor events, all channels

15:45 Tape 14 end

15:48 Tape 15 start 30 ips

16:03:30 30 ips → 60 ips

* Anticipate crossing ~ 06:20 LT
(according to John Stanley)

16:10 Tape 15 end

248/16:13 Tape 16 start 60 ips

9.5.82 HAWAII

General comments during observation
period ~ 0615 - 0630 (1615 - 1630 UT)

- * Very strong persistent echo in both radars at ≈ 0618
- * Strong multiple strike at ≈ 0623
- * Very strong single event at ≈ 0627
- * General background level increased
- * 28 MHz more active than 50 MHz
- * Interferometer channels all operational
- * No outside interference
- * ~~Weather~~ weather excellent
- *

248:16:45 End TAPE 16

248:16:47 Start TAPE 17 30 ips

17:30 30 ips \rightarrow 60 ips

17:33 50 MHz interference returns (weakly)

248:17:37:45 Excellent persistent return
for calibration $\approx 0.3m$

248:17:40 End TAPE 17

17:41 Start TAPE 18 30 ips

9.5.86 HAWAII

248:17:46:50 (approx.) good bistatic echo

47:30 Strong interference

~49:40 interference gone

50:00 Strong meteor 1.8 m/s

248:17:53.6 Nominal impact time

248:18:35 30 → 60 ips

18:11

End TAPE 18

18:14

Start TAPE 19 STOP TAPE 19 @ 18:40

Review of Tape 18 near event time

18:04:55

06:15 6 div quick bath

30 8.5 long med bath

7: 7.8

07

00

8:09 8.5

:18 9.5

:32 8

9:00 no echo

9:42 6.8

50 7.2

10:11

12

15

34

} multiple range

9-5-86 HAWAII

~ 248:18:58 Start TAPE 20 15 ips

248:20 Troubleshooting an RX problem
in 50 MHz channel "0" (Q)

20:26 Back on line - all channels

Total data gap ~ 15 min

21:42 ~~30~~¹⁵ ips \rightarrow ~~30~~³⁰ ips

21:52 Tape 20 end

21:54 Tape 21 Start

22:36 Discovered Q of channel 0 nonoperative

22:37:30 Pulses off

38:00 Pulses on

* 50 MHz output = 25.5 kW

* Problems w/ RX-0 (Q)

* 248:22:42:00 Power Down for today

9.5.86 HAWAII

- * End of data on TAPE 21 at ~ 8200 on tape counter
- * Data review indicates that the Channel "0" receiver was good until about 248:21:30 then went into periodic intermittent operation until EOT.

Discussions w/ Don Kessler

- * Delta launch time 248:15:09:00
- * Interaction 9874.9 sec. later
- * Time of interaction 248:17:53.6 UT
- * Location of interaction from Perseus ground tracks show longitude at $166^{\circ}E$
- * Kauai located at $\approx 159^{\circ}W$
- $\Rightarrow \sim 35^{\circ}$ of orbital rotation; assume ~ 90 min/rev
- $\Rightarrow 8.75$ min after interaction it should be detected at Kauai
- \therefore Time of crossing 248:17:53.6

8.75
248:18:02

9.5.86 HAWAII

249 /

05:23

Start Tape #22

05:54

End TAPE 22

249:05:57

Start TAPE 23

) no echos observed
during tape change
in 28 MHz

06:05 E-region echo growing strong in 28 &
50 MHz systems; all channels

06:08 Range check on E-region echo
2ms \rightarrow 3ms for ≈ 15 sec

06:28 End TAPE 23

End of observations 9.5.86

9.6.86 HAWAII

* Gene Stansbery provided orbital plane
information:

- Ascending ^(plane) pass of high inclination "wand"
cross Kauai ~~15:45~~ \rightarrow 15:45 \rightarrow 16:00

- Peak of low inclination orbit crosses
Kauai once a day for extended period
 \sim 17:00 \rightarrow 19:45

9.6.82 HAWAII

249:17:00 Start TAPE 24

* Channel 2 on 50RX acting up; tape recorder filtering out a high frequency oscillation, however. Data recorded looks fine

~249:18:00 Stop TAPE 24

18:05 Start TAPE 25

19:05 → Stop TAPE 25 30 ips

19:07 Start TAPE 26 (10", 30 ips)

19:40 Stop TAPE 26

19:42 Start TAPE 27 (10", 30 ips)

249:20:00:00 Excellent airplane calibration
in all interferometer channels
and 25 MHz RX

9.6.86 HAWAII

Tape review for impact pass: (Start 17:53) ^{248:}

28 MHz			50 MHz		
Time	Amp**	Range*	Time	Amp**	Range*
17:54:35	med	4.0	53:04	S	6.0
54:47	small	4.5	:15	S	8.0
55:36	S	4.4	:17	S	3.0
56:16	S	2.0	:24	S	7.5
56:28	S	3.5	:47	S	1.5
56:33	S	1.5	:52	M	9.0
56:47	S	9.0	:56	S	5.2
57:15	S	8.0	54:00	S	8.2
57:16	S	2.0	:23	M	5.0
57:31	S	7.5	:36	M	4.0
57:58	S	7.0	:46	S	4.2
58:25	S	5.5	55:36	S	8.0
59:00	S	6.5	55:48	C	
59:10	S	5.0	56:47	L	9.0
59:41	S	8.5	57:15	L	8.0
18:00:07	S	7.2	57:31	L	7.0
00:31	S	5.8	57:58	M	7.0
00:38	S	6.2	58:20	S	3.5
00:47	S	7.2	:24	L	5.2
01:05	S	2.7	:49	M	2.5
:10	S	2.9	59:10	L	5.0
:13	S	4.2	59:40	S	8.5
:26	S	3.2	:49	S	3.5
:31	S	3.3	18:00:05	L	7.0
:47	S	3.5	00:39	S	7.2
:59	S	6.5	00:47	S	7.2
02:10	S	2.2	00:56	S	3.5
:12	S	6.0	01:03	L, S	3.7, 4.5
:21	S	5.0	:10	L, S	3
:24	S	6.0	:10	S	4.2
:36	S	6.0	:15	M	3.5
:43	S	4.0	:17	M	3.5
:48	S	5.0			2.5
03:40	S	6.0			3.2 2
04:38	S	2.8			6
06:32	M	8.5	02:00		4

20 meters

9.6.86 Hawaii

28 MHz

Time	Amp	Range
18:07:00	M	7.5
07:09	M	6.2
08:09	M	8.7
08:35	S	6.0
08:45	M	1.0
09:44	L	6.8
09:52	M	7.2
10:05	S	6.5
11:12	M, M	6.5, 8.5
11:18	S	4.5
11:33	S	4.9
11:35	L	6.2
11:46	M	4.0

50 MHz

Time	Amp	Range
02:09	L	6
12	L	5
18	L	2.5
21	L	6
25	M	6.5
30	M	8.5
38	M	7.0
43	M	5.0
02:49	M	7.8
03:38	L	6.0
05:25	M	7.0
05:42	S	6.5
06:15	M	6.0
06:24	S	4.0
06:32	S	2.0
07:00	M	7.0
07:07	L	5.0
07:13	M	6.2
07:42	S	4.2
08:08	L	8.0
08:12	S	4.5
08:32	M, M	6.0, 8.0
08:45	S	1.5
09:44	S	5.2
09:45	L	6.7
9:52	S	7.2
10:42	M	6.0
11	M	8.2
13	M	4.8
15	L	6
35	L	4
11:16	L	4

9.6.86 HAWAII

Calibration:

Feedline Loss. Power measured at antenna end of feedline. Directional coupler & dummy load placed (connected) to feedline; transmitter operated; and forward power measured.

28 MHz

$$\text{Forward power} = 4.6 \times .2 \text{ volts pp}$$

$$\text{Directional coupler} \Rightarrow 64.5 \text{ dB atten.}$$

$$\therefore \text{Transmitted power} = \underline{\underline{5.96 \text{ kW}}}$$

50 MHz

$$\text{Forward power} = 3 \times .5 \text{ Vpp}$$

$$\text{Directional coupler} \Rightarrow 62.6 \text{ dB atten}$$

$$\therefore \text{Transmitted power} = \underline{\underline{10.2 \text{ kW}}}$$

Phase Calibration

- * All receiver channels driven simultaneously through full length antenna feedlines
- * 249:22:02 Start time
- * Input signal = $49.92 \pm 715 \text{ Hz}$ (approx)
- * 249:22:06 Start test (about 700 ft)
 - :06-08 channel 9 was oscillating
- 249:22:10 Restart test (about 1300 ft)
 - Clipping discovered in channel 5 & 6
- 249:22:12 Restart test (about 1650 ft)
 - 22:16:15 Stop recorder
 - Add $\frac{1}{4} \lambda$ to input of Power divider
 - ~ 22:16:50 Start recorder
 - 22:20:30 Stop
- 22:42 Start pulsed feedline length
Cal.: 40 μs PW 900 μs 1 PP
- 44:45-45:00 go to 500 μs 1 PP

07 Sept 86

250/15:17 UT radar up / recorder on TAPE : 8 START

filter = 100s

50 MHz TX : ~3.5 kV / 10 mA ; ~6.5 / 50

28 MHz TX : ~8 kV / 17 mA.

All channels checked and ok.

PW = 10 μ s

IPP = 200 μ s

Tape speed 30 ips

metres confirmed both radars.

15:30 - 15:48 All channels show meteor activity

15:53 28 MHz dir. cup. checked 8-10:1

50 MHz checked earlier; ok.

15:58:30 good event - both radars, 19 ampl.

16:19 Tape 28 end

16:21 Tape 29 start

All channels checked and ok.

17:23 Tape 29 end

17:25 Tape 30 start

All channels checked and ok.

Txs are also ok.

~18:18 - 18:21 good meteor echoes

07 Sept 86

250/18:27 Tape 30 end

18:29 Tape 31 start

all channels checked and ok

Tx: pulling current as usual

19:23 + good airplane event both channels

19:27:15 good meteor event, both channels

19:31 Tape 31 end

19:33 Tape 32 start

250/20:04 End Tape 32 Run over.

28 Sept '86

Local time = 17:00

251/16:29 UT 28 MHz up START TAPE 33

1/16:40 pulses off

1/16:42 pulses on 50 & 28 MHz systems up

50 MHz direct = 16 V on 5V/div
rf = 1 V on 1V/div



antennas were checked @ 16:00 only 50 MHz Tx out was found to not provide proper freq. response. Further testing indicated that water had entered barrel connector & a trace and checked the line. Barrel was replaced on 50 MHz and came up @ 16:42. The worst weather of this campaign occurred throughout yesterday and last night. Thunderstorms, high winds, and frequent rain storms occurred.

filter = 10 μ s

Transpond = 30 μ s

50 MHz: 3.4 kV / 11 mA ; 0.3 kV / 25 mA

28 MHz: ~5 kV / ~20 mA

28 MHz Rx signal is not as strong as before
all other channels are ok.

1/16:59 Tape 33 end

1/17:01 Tape 34 start

08 Sept 86

251/17:06 echoes confirmed in 50 MHz // 28 MHz still in question.

/17:10 airplane echo in 50 - not observed in 28 MHz
(very lg appl. event in 50 MHz)

/17:15 50 MHz feed line connector @ antenna is moderately warm

/17:32 Tape 34 end

/17:33 Tape 35 start

/18:04 Tape 35 end

/18:06 Tape 36 start

/18:34 airplane event shows in all channels except 28 MHz.

/18:37 Tape 36 end

/18:39 Tape 37 start

heavy rains have returned

/18:53 airplane in all channels X 28 MHz
weak in channels 7 & 8

251/19:10 Tape 37 end Tx off

09 Sept 86

LT=UT-10

252/16:20

50 MHz up
28 MHz down for run

on 1 V/div scale

50 MHz direct, 38 div.
ref 1.4 div.

PS: 3.4 kV/210 mA; 6.6 kV/45 mA

meter echoes confirm radar operation.

Panel connector @ antenna was cleaned prior to turn on.
After 10 min operation this junction is cold
film = 10 μ s

252/16:30

Tape recorder - record on 30ips

Tape 38 START

All channels checked and ok.

/16:54 connector still cold

/17:00 Tape 38 end

/17:02 Tape 39 START

All channels checked and ok.

/17:24 + meters detected

/17:33 Tape 39 end

/17:35 Tape 40 start

all channels ok.

09 Sept 86

252/ 18:06 Type 40 end

/ 18:07 Tape 41 start

/ 18:38 Tape 41 end

/ 18:40 Tape 42 start
meteor detected.
all channels ok.

/ 19:08+ meteor echoes
/ 19:09 all channels look good

/ 19:11 Type 42 end
end exp.

APPENDIX B
TIME-OF-FLIGHT VELOCITY CALCULATIONS

DERIVATION OF TIME-OF-FLIGHT-VELOCITY RELATIONSHIP

Position and time of "event":

14.915 N Lat
165.828 E Long
248:17:52:35.5
Alt = 117.42 NM
= 217.46 km

(1 NM = 6076.12 feet = 1852 meters)

Observer coordinates:

159° 27' W Long = 159.45° W
22° 11' N Lat = 22.18° N

Longitudinal and Latitudinal traversal:

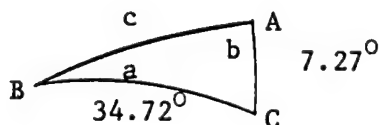
$$\Delta\text{Long} = 180 - 165.828 + 180 - 159.45$$

$\Delta\text{Long} = 34.72^\circ$

$$\Delta\text{Lat}_0 = 22.18 - 14.915 = 7.27^\circ$$

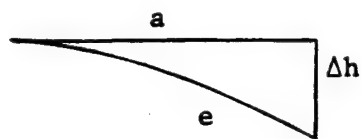
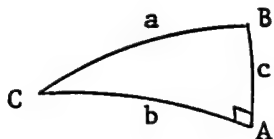
$\Delta\text{Lat} = 7.27^\circ$

Great-Circle Path Length



Law of sines: $\frac{\sin a}{\sin A} = \frac{\sin b}{\sin B} = \frac{\sin c}{\sin C}$

Law of cosines: $\cos a = \cos b \cos c + \sin b \sin c \cos A$



$$b = 34.72^\circ$$

$$c = 7.27^\circ$$

$$A = 90^\circ$$

$$\cos a = \cos(34.72)\cos(7.27) + 0$$

$$a = 35.37^\circ$$

(Orbital angular displacement for zenith of observer)

$$v_e \approx (v_a^2 + v_{\Delta h}^2)^{1/2}$$

Total angular displacement,

$$\cos a = \cos(34.72 - \Omega_E t)\cos(7.27)$$

$$a(t) = \cos^{-1}[\cos(34.72 - \Omega_E t)\cos(7.27)]$$

Considering latitudinal displacement

$$a(\Delta l, t) = \cos^{-1}[\cos(34.72 - \Omega_E t)\cos(7.27 + \Delta l)]$$

again,

$$a(\Delta l, t) = \cos^{-1}[\cos(34.72 - \Omega_E t)\cos(7.27 + \Delta l)]$$

$$\Delta l = \cos^{-1}\left[\frac{a^2 + b^2 - c^2}{2ab}\right]$$

$$b = a + 60$$

$$\Delta l = \cos^{-1}\left[\frac{a^2 + (a + 60)^2 - c^2}{2a(a + 60)}\right]$$

c = slant range

let c = R_s

$$a(R_s, t) = \cos^{-1} \left[\cos(34.72 - \Omega_E t) \cos(7.27 \pm \cos^{-1} \left[\frac{a^2 + (a + 60)^2 - R_s^2}{2a(a + 60)} \right]) \right] \quad (1)$$

$$v_a = \frac{a(R_s, t)}{t} \quad (2)$$

$$v_h = \frac{217-60}{t} \approx 160/t \text{ (km/s)} = 1.6(10^5)/t \quad (3)$$

$$v_t = (v_a^2 + v_h^2)^{1/2} \quad (4)$$

Equations (1), (2), (3), and (4) were evaluated numerically with the following BASIC program. The results provided a velocity dependence on the time-of-arrival (detection) and range of meteor-like echoes.

```

10 '..... TIME-OF-ARRIVAL VELOCITY CALCULATIONS .....
20 '
30 PI=3.1415927#:RE=6357000!:OMEGA=7.2722E-05
40 HT=50000!:ALT=217000!
50 '
60 ' RE = EARTH RADIUS
70 ' OMEGA = EARTH ANGULAR VELOCITY
80 ' ALT = ALTITUDE OF CLOSEST APPROACH
90 ' HT = HEIGHT OF ENTRY
100 ' RS = SLANT RANGE FROM RADAR
110 '
120 FOR IR=1 TO 6
130 RS=IR*50000!
140 '
150 ' .... CALCULATE DIFFERENCE IN LATITUDE WITH SLANT RANGE .....
160 '
170 CAR=(RE^2+(RE+HT)^2-RS^2)/(2*RE*(RE+HT))
180 IF CAR>1 THEN CAR=1!
190 CR=ATN((1-CAR^2)^.5/CAR)
200 FOR I=0 TO 260 STEP 1
210 T=465+I
220 '
230 ' .... CALCULATE FLIGHT PATH LENGTH .....
240 '
250 AA=COS(PI*34.72/180-OMEGA*T)*COS(PI*7.27/180+CR)
260 A=ATN((1-AA^2)^.5/AA)
270 '
280 ' ..... CALCULATE VELOCITIES .....
290 '
300 VA=A*(RE+ALT)/T:VH=(ALT-HT)/T
310 VT=(VA^2+VH^2)^.5/1000
320 PRINT RS,T,VT
330 NEXT I
340 NEXT IR

```

TIME-OF-FLIGHT VELOCITIES

(NORTHERN BEAM)

<u>SLANT RANGE (m)</u>	<u>TIME (sec)</u>	<u>VELOCITY (km/s)</u>
50000	465	8.27162
50000	485	7.91136
50000	505	7.579631
50000	525	7.273178
50000	545	6.989221
50000	565	6.725365
50000	585	6.479556
50000	605	6.250003
50000	625	6.035137
50000	645	5.833597
50000	665	5.644192
50000	685	5.465843
50000	705	5.297611
50000	725	5.138666
100000	465	8.310467
100000	485	7.94872
100000	505	7.615616
100000	525	7.307901
100000	545	7.022765
100000	565	6.757826
100000	585	6.511003
100000	605	6.280505
100000	625	6.064751
100000	645	5.862389
100000	665	5.672195
100000	685	5.493115
100000	705	5.324194
100000	725	5.164598
150000	465	8.336983
150000	485	7.974207
150000	505	7.640172
150000	525	7.331591
150000	545	7.045661
150000	565	6.779979
150000	585	6.532468
150000	605	6.301318
150000	625	6.084966
150000	645	5.882035
150000	665	5.691304
150000	685	5.51173
150000	705	5.342333
150000	725	5.182288
200000	465	8.363621
200000	485	7.999824
200000	505	7.664853
200000	525	7.355407
200000	545	7.068674
200000	565	6.802241
200000	585	6.554025
200000	605	6.322234
200000	625	6.105269
200000	645	5.901773
200000	665	5.710512
200000	685	5.530423
200000	705	5.360562
200000	725	5.200068

NORTHERN BEAM (CONT)

250000	465	8.391094
250000	485	8.026251
250000	505	7.690304
250000	525	7.379962
250000	545	7.0924
250000	565	6.825194
250000	585	6.576271
250000	605	6.343803
250000	625	6.126214
250000	645	5.922126
250000	665	5.730312
250000	685	5.549708
250000	705	5.379347
250000	725	5.218394
300000	465	8.419586
300000	485	8.053638
300000	505	7.716693
300000	525	7.405418
300000	545	7.116994
300000	565	6.84899
300000	585	6.599317
300000	605	6.366159
300000	625	6.147926
300000	645	5.943225
300000	665	5.750841
300000	685	5.569694
300000	705	5.398825
300000	725	5.237394

TIME-OF-FLIGHT VELOCITIES
(SOUTHERN BEAM)

<u>SLANT RANGE (m)</u>	<u>TIME (sec)</u>	<u>VELOCITY (km/s)</u>
50000	465	8.27162
50000	485	7.91136
50000	505	7.579631
50000	525	7.273178
50000	545	6.989221
50000	565	6.725365
50000	585	6.479556
50000	605	6.250003
50000	625	6.035137
50000	645	5.833597
50000	665	5.644192
50000	685	5.465843
50000	705	5.297611
50000	725	5.138666
100000	465	8.23657
100000	485	7.877638
100000	505	7.547153
100000	525	7.241836
100000	545	6.958928
100000	565	6.696061
100000	585	6.451165
100000	605	6.222465
100000	625	6.008399
100000	645	5.807614
100000	665	5.618903
100000	685	5.441218
100000	705	5.273611
100000	725	5.115257
150000	465	8.216361
150000	485	7.858212
150000	505	7.528433
150000	525	7.223773
150000	545	6.941484
150000	565	6.679174
150000	585	6.434806
150000	605	6.206596
150000	625	5.992985
150000	645	5.792634
150000	665	5.604325
150000	685	5.427022
150000	705	5.259772
150000	725	5.10176
200000	465	8.198555
200000	485	7.841079
200000	505	7.511924
200000	525	7.207841
200000	545	6.926083
200000	565	6.664275
200000	585	6.420373
200000	605	6.192597
200000	625	5.9794
200000	645	5.77942
200000	665	5.59147
200000	685	5.414505
200000	705	5.247576
200000	725	5.089859

SOUTHERN BEAM (CONT)

250000	465	8.182421
250000	485	7.825559
250000	505	7.496977
250000	525	7.193428
250000	545	6.912156
250000	565	6.650796
250000	585	6.407314
250000	605	6.179928
250000	625	5.967093
250000	645	5.767463
250000	665	5.579835
250000	685	5.403167
250000	705	5.236525
250000	725	5.079083
300000	465	8.167787
300000	485	7.811497
300000	505	7.48342
300000	525	7.180345
300000	545	6.899516
300000	565	6.638568
300000	585	6.395462
300000	605	6.168427
300000	625	5.955928
300000	645	5.756608
300000	665	5.569278
300000	685	5.392887
300000	705	5.226506
300000	725	5.069306

Appendix D

The Distribution List

Appendix D contains the primary distribution list for this report.

Appendix D

PRIMARY DISTRIBUTION LIST FOR
DELTA 180 FINAL REPORT

Organization w/Distribution and Number of Copies (*)

Office of the Secretary of Defense
The Pentagon
Washington, D.C. 20301-7100

SDIO/T/KE -- (2)
Attn.: Col. Raymond Ross
Attn.: Lt. Col. Michael Rendine

SDIO/D -- (1)
Attn.: Lt. Gen. James Abrahamson
Attn.: Dr. Gordon Smith

SDIO/CS -- (1)
Attn.: Dr. Allan Mense

SDIO/T -- (1)
Attn.: Dr. Louis Marquet
Attn.: Col. William Wisdom

SDIO/T/DE -- (1)
Attn.: Dr. John Hammond
Attn.: Lt. Col. Robert Van Allen

SDIO/T/SN -- (1)
Attn.: Col. Garry Schnelzer
Attn.: Dr. William Frederick
Attn.: Dr. Barry Katz

SDIO/T/SL -- (1)
Attn.: Col. George Hess

SDIO/T/IS -- (1)
Attn.: Dr. James Ionson

SDIO/S -- (1)
Attn.: Brig. Gen. Malcolm O'Neill

SDIO/S/SA -- (1)
Attn.: Col. Jeffrey Schofield

SDIO/S/BM -- (1)
Attn.: Capt. David Hart

SDIO/S/PM -- (1)
Attn.: Dr. Richard Bleach

SDIO/S/SE -- (1)
Attn.: Col. Jim Graham

SDIO/SI -- (1)
Attn.: Dr. Keith Taggart
Attn.: Lt. Col. Marshall Sanders

SDIO/MN -- (1)
Attn.: Col. Thomas Fiorino

SDIO/EA -- (1)
Attn.: Col. Leon DeLorme

McDonnell Douglas Astronautics Company -- (15)
5301 Bolsa Avenue
Huntington Beach, CA 92647

Attn.: L. C. Raburn, Director
Delta Programs

McDonnell Douglas Astronautics Company -- (1)
P.O. Box 516
St. Louis, MO 63166

Attn.: Mr. Howard Anthes

MDAC/Florida Test Center -- (1)
P.O. Box 21007
Kennedy Space Center, FL 32815

Attn.: Mr. Lyle Holloway, Director

The John Hopkins University / Applied Physics Laboratory -- (1)
John Hopkins Road
Laurel, MD 20707

Attn.: Mr. John Dassoulas

NASA/GSFC -- (1)
Greenbelt Road
Greenbelt, MD 20771

Attn.: Mr. W. A. Russell, Jr.
Code 470

ANSER -- (1)
1215 Jefferson Davis Highway
Suite 800
Arlington, VA 22202

Attn.: Ms. Lori Pecht

Hughes Aircraft Company -- (1)
8433 Fallbrook Avenue
Canoga Park, CA 91034

Attn.: Mr. Dennis F. Kaelin
Bldg. 265, M/S X30

ESMC/ROPN -- (1)
Patrick Air Force Base, FL 32925-5512

Attn.: Ms. Sandra Lochman
ESMC Program Manager

USA/Strategic Defense Command -- (1)
DASD-DP
P.O. Box 15280
Arlington, VA 22215-0150

Attn.: Lt. Gen. J. F. Wall

USA/Strategic Defense Command
P.O. Box 1500
Huntsville, AL 35807

DASD-H-L -- (1)
Attn.: Dr. E. L. Wilkinson

DASD-H-HR -- (1)
Attn.: Maj. Frank Grose

DASD-H-TE -- (1)
Attn.: Mr. Barnie Davis

DASD-H-TT -- (1)
Attn.: Mr. W. L. Holman

HQ USAF/RD-D -- (1)
The Pentagon
Washington, D.C. 20330

Attn.: Col. Carol Yarnall

USAF Space Division -- (1)
SD/CNWK
Los Angeles Air Force Station
P.O. Box 92960
Los Angeles, CA 90009

Attn.: Lt. Col. James Simmons

Aerospace Corporation -- (1)
P.O. Box 92957
Los Angeles, CA 90009

Attn.: Dr. Fred Simmons

Chief of Naval Operations -- (1)
Navy Dept. (OP-981 SDI)
Washington, D. C. 20350-2000

Attn.: Capt. Tom Sanders

Lockheed Missiles and Space Company -- (1)
3251 Hanover Street
Palo Alto, CA 94304

Attn.: Mr. Ed McAdams, Bldg. 201

Charles Stark Draper Laboratories -- (1)
555 Technology Square
Cambridge, MA 02139

Attn.: John Elwell, MS 59

Air Force Geophysics Laboratory -- (1)
Hanscom AFB, MA 01731

Attn.: A. T. Stark

Lincoln Laboratories - MIT -- (1)
P.O. Box 73
Lexington, MA 02173-0073

Attn.: Mr. Walter Morrow, Director

Sandia National Laboratory -- (1)
P.O. Box 5800
Albuquerque, NM 87815

Attn.: Mr. Lawton F. Miller
Organization 9142

The Analytic Science Corporation -- (1)
1700 N. Moore Street
Suite 1220
Arlington, VA 22209

Attn.: Mr. Charles Henning

Nichols Research Corporation
Polk Bldg/Westgate Research Park
1764 Old Meadow Lane, Suite 150
McLean, VA 22102-4307

Attn.: Mr. Martin Zlotnick

Titan Systems, Inc. -- (1)
500 W. Cummings Park
Suite 600
Woburn, MA 01801

Attn.: Mr. Richard Ryan

Ball Aerospace Systems Division -- (1)
P.O. Box 1062
Boulder, CO 80306

Attn.: Mr. Lynn R. Lewis

Aeromet, Inc. -- (1)
P.O. Box 70167
Tulsa, OK 74170-1767

Attn.: Mr. D. Ray Booker

Institute for Defense Analysis -- (1)
1801 N. Beauregard St.
Alexandria, VA 22311

Attn.: Control and Distribution, Dr. Hans Wolfhard

Riverside Research Institute -- (1)
1815 N. Fort Meyer Drive
Suite 800
Arlington, VA 22209

Attn.: Document Control/Sensors Library

Air Force Weapons Laboratory (AFWL/AR) -- (1)
Kirtland AFB, NM 87117-6008

Attn.: Col. K. Gilbert

Martin Marietta Denver Aerospace -- (1)
P.O. Box 179
Denver, CO 80201

Attn.: Ms. D. A. Strange

AFSTC/SWK -- (1)
Kirtland AFB, NM 87117-6008

Attn.: Mr. J. Jablonski

Commander USA/ARDEC -- (1)
Attn.: SMCAR: FSP-A
Bldg. 353-North
Picatinney Arsenal, NJ 07806-5000

Attn.: Mr. F. Screbo

Headquarters Space Division/CNA -- (1)
Worldwide Postal Center
P.O. Box 92960
Los Angeles, CA 90009-2960

Attn.: Lt. Col. Dean Bovier

Avco Everett Research Lab -- (6)
P.O. Box 261
Puunene
Maui, HI 96784

Attn.: Tom Reed

Don Midkiff -- (3)
2862 S. Circle Drive
Suite 240
Colorado Springs, CO 80906

Headquarters U.S. Space Command -- (3)
J3SOT
Cheyenne Mountain Complex
Peterson AFB, CO 80914-5601

Attn.: Lt. Col. Stephen Marlow

Air Force Space Command/DOF -- (2)
Peterson AFV, CO 80914

Attn.: Col. Jimmy Morrell

Col. Charles W. Patterson -- (1)
1st Space Wing/DO
Peterson AFB, CO 80914

Major Tom Anderson -- (2)
WTR/DOTR
Vandenberg AFB, CA 93437-6021

J.D. Kraft -- (2)
Code 470.0
Goddard Space Flight Center
Greenbelt, MD 20771

Teledyne Brown Engineering
1250 Academy Park Loop
Suite 240
Colorado Springs, CO 80910

Attn.: Nick Johnson -- (2)
Attn.: David Nauer -- (1)
Attn.: Ron Kling -- (1)

SPS Remote Sensing Corporation -- (2)
4418 Illinois Street
Dickinson, TX 77539

Attn.: Jerry Jost

NASA/JSC

AA/Aaron Cohen -- (1)
Paul Weitz -- (1)
AC/Carolyn Huntoon -- (1)
AT/Joe Loftus -- (1)
SA/Joe Kerwin -- (1)
SN/Mike Duke -- (1)
SN3/A. Potter -- (20)
J. Stanley -- (1)
D. Kessler -- (1)
F. Vilas -- (1)
K. Henize -- (1)
G. Stansbery (1)
BE3/Ghetzler -- (1)

Lockheed-EMSCO/C23

Bob Reynolds -- (5)
Philip Anz-Meador -- (1)
Richard Rast -- (1)
David Talent -- (1)
Jesse Carnes -- (1)
Pat Jones -- (1)